HABITABILITY BEYOND EARTH

EDITED BY: Karen Olsson-Francis, Daniela Billi, Andreas Teske and Jean-Pierre Paul de Vera

PUBLISHED IN: Frontiers in Microbiology

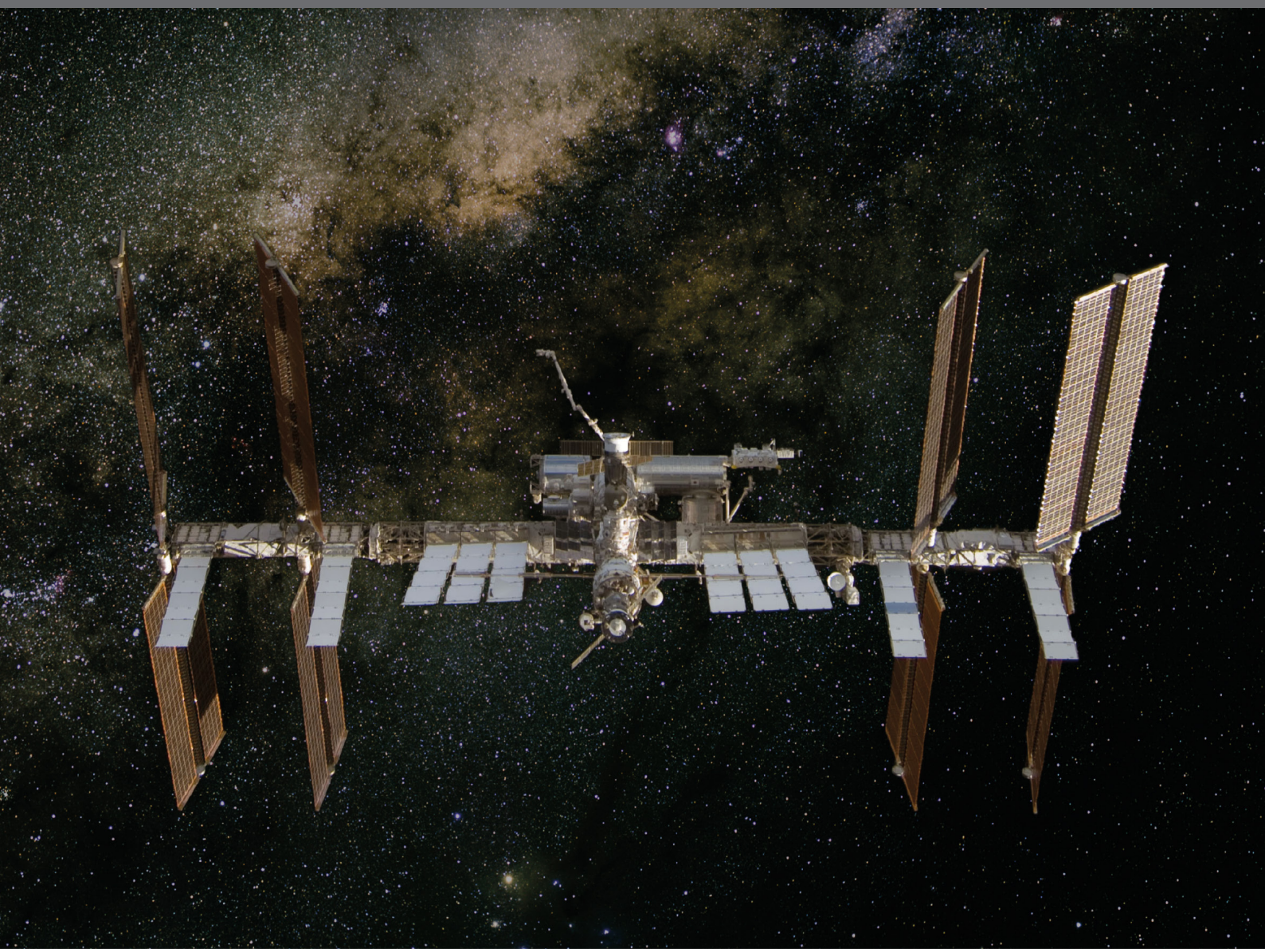

frontiers Research Topics

ISSN 1664-8714
ISBN 978-2-88945-765-6
DOI 10.3389/978-2-88945-765-6

About Frontiers

Frontiers is more than just an open-access publisher of scholarly articles: it is a pioneering approach to the world of academia, radically improving the way scholarly research is managed. The grand vision of Frontiers is a world where all people have an equal opportunity to seek, share and generate knowledge. Frontiers provides immediate and permanent online open access to all its publications, but this alone is not enough to realize our grand goals.

Frontiers Journal Series

The Frontiers Journal Series is a multi-tier and interdisciplinary set of open-access, online journals, promising a paradigm shift from the current review, selection and dissemination processes in academic publishing. All Frontiers journals are driven by researchers for researchers; therefore, they constitute a service to the scholarly community. At the same time, the Frontiers Journal Series operates on a revolutionary invention, the tiered publishing system, initially addressing specific communities of scholars, and gradually climbing up to broader public understanding, thus serving the interests of the lay society, too.

Dedication to Quality

Each Frontiers article is a landmark of the highest quality, thanks to genuinely collaborative interactions between authors and review editors, who include some of the world's best academicians. Research must be certified by peers before entering a stream of knowledge that may eventually reach the public - and shape society; therefore, Frontiers only applies the most rigorous and unbiased reviews.
Frontiers revolutionizes research publishing by freely delivering the most outstanding research, evaluated with no bias from both the academic and social point of view. By applying the most advanced information technologies, Frontiers is catapulting scholarly publishing into a new generation.

What are Frontiers Research Topics?

Frontiers Research Topics are very popular trademarks of the Frontiers Journals Series: they are collections of at least ten articles, all centered on a particular subject. With their unique mix of varied contributions from Original Research to Review Articles, Frontiers Research Topics unify the most influential researchers, the latest key findings and historical advances in a hot research area! Find out more on how to host your own Frontiers Research Topic or contribute to one as an author by contacting the Frontiers Editorial Office: researchtopics@frontiersin.org

HABITABILITY BEYOND EARTH

Topic Editors:
Karen Olsson-Francis, The Open University, United Kingdom
Daniela Billi, University of Rome Tor Vergata, Italy
Andreas Teske, University of North Carolina at Chapel Hill, United States
Jean-Pierre Paul de Vera, DLR Institute of Planetary Research, Germany

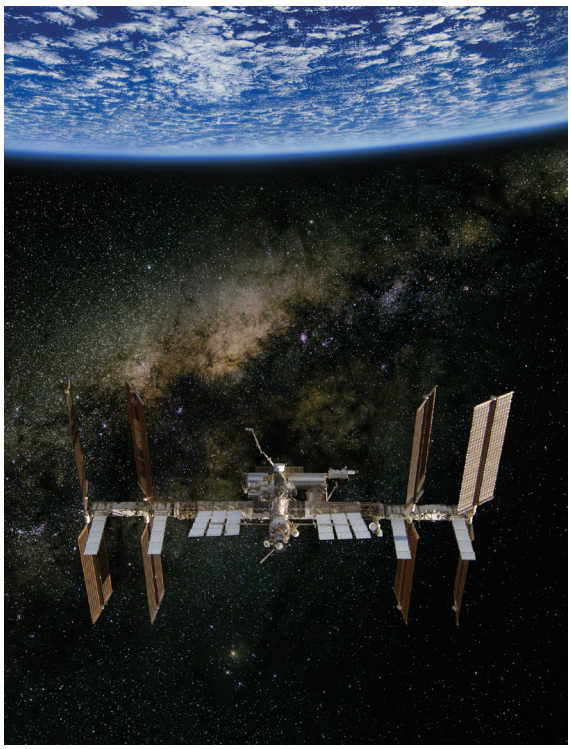

Image: MarcelClemens/Shutterstock.com

Citation: Olsson-Francis, K., Billi, D., Teske, A., de Vera, J.-P. P., eds. (2019). Habitability Beyond Earth. Lausanne: Frontiers Media. doi: 10.3389/978-2-88945-765-6

Table of Contents

frontiers in Microbiology

EDITORIAL
published: 15 November 2018
doi: 10.3389/fmicb.2018.02645

Editorial: Habitability Beyond Earth

Karen Olsson-Francis[1], Daniela Billi[2], Andreas Teske[3] and Jean-Pierre P. de Vera[4]*

[1] School of Environment, Earth and Ecosystem Sciences, The Open University, Milton Keynes, United Kingdom, [2] Deparment of Biology, University of Rome Tor Vergata, Rome, Italy, [3] Department of Marine Sciences, University of North Carolina at Chapel Hill, Chapel Hill, NC, United States, [4] Astrobiological Laboratories, German Aerospace Center (DLR), Institute of Planetary Research, Management and Infrastructure, Berlin, Germany

Keywords: astrobiology, space, habitability, mars, extremophiles, analog sites

Editorial on the Research Topic

Habitability Beyond Earth

The question of whether Earth is a unique location for life remains one of the most enduring questions of our time. Geochemical data suggests that habitable environments may exist, or may have existed, elsewhere in the Solar System with promising targets including Mars and icy bodies where liquid water is believed to exist (Kargel, 2000; Grotzinger et al., 2014; Glein et al., 2015). Furthermore, potential habitable Exoplanets have been discovered where potentially there is sufficient atmospheric pressure to maintain liquid water (Jenkins et al., 2015; Gillon et al., 2017; Orosei et al., 2018). Yet, for life to exist it is not solely dependent on liquid water as it also needs bio-essential elements, an energy source, and the environmental conditions, that are conducive to life (Nixon et al., 2013). To investigate the feasibility of life elsewhere in the Solar System a combination of field and laboratory based studies, *in-situ* space experiments, and theoretical modeling is required. Here, we present 14 original research papers, one mini review, and two hypothesis and theory papers highlighting the novel and diverse methods that are employed to investigate potential life beyond the Earth. The overall focus of this collection of work is to understand if terrestrial life could exist elsewhere in the Solar System, and if so, what evidence (bio-signatures) could be used to support or negate the hypothesis of life.

Our understanding of life in extreme environments on Earth forms the basic concepts of where life could exist elsewhere in the Solar System. Extremophilic microorganisms have adapted to live in environments where parameters, such as, pH, temperature and pressure, and water availability are deemed extreme. Determining the limits of life in regard to these parameters is important for defining the limits of life. As Schulze-Makuch et al. demonstrates the limits of terrestrial life can be used to outline a range of possible habitable environments, some that are present in our Solar System and others that are hypothetical.

Extreme environments on Earth can also be used as terrestrial analog sites. These are sites that exhibit similar environmental conditions, such as pH, pressure, atmosphere composition, and water availability, as environments on other planets or moons (Martins et al., 2017). Historically analog studies have predominantly been focused on Mars. Evidence proposes that conditions on early Mars were clement and less oxidizing than they are today (e.g., Carr and Head, 2010; Mangold et al., 2012). Data from Mars Science Laboratory (MSL) shows that habitable environments may have existed at Gale Crater (Grotzinger et al., 2014). Chemolithotrophy has been recommended ed as a plausible metabolism for life on Mars and using data from MSL, Price et al. suggests the feasibility of iron oxidation-nitrate reduction as a plausible metabolism for life on ancient Mars.

As the conditions on Mars evolved from wet to dry during the Hesperian period ephemeral lakes are thought to have formed. For example, the presence of hydrated magnesium sulfates within the rim of Columbia Crater is ascribed to the existence of a paleolake, which at times must have been hypersaline in nature (Wray et al., 2011). Pontefract et al. shows, using a sulfate rich

OPEN ACCESS

Edited by:
Baolei Jia,
Chung-Ang University, South Korea

Reviewed by:
Mirjam Perner,
GEOMAR Helmholtz Center for Ocean Research Kiel, Germany
Donato Giovannelli,
Tokyo Institute of Technology, Japan

****Correspondence:***
Karen Olsson-Francis
k.olsson-francis@open.ac.uk

Specialty section:
This article was submitted to Extreme Microbiology, a section of the journal Frontiers in Microbiology

Received: *07 September 2018*
Accepted: *17 October 2018*
Published: *15 November 2018*

Citation:
Olsson-Francis K, Billi D, Teske A and de Vera J-PP (2018) Editorial: Habitability Beyond Earth. Front. Microbiol. 9:2645. doi: 10.3389/fmicb.2018.02645

analog site for the ancient hypersaline palolakes, Spotted Lake (British Columbia, Canada) that sulfate salt deposits may have offered periodically habitable environments, and could have concentrated and preserved organic materials or their biomarkers over geologic time.

On modern day Mars, the evaporitic past is evident by the widespread deposition of sulfate, perchlorates and chloride salts observed today on the martian surface (Wanke et al., 2001; Clark et al., 2005). It has been hypothesized that perchlorates may bind water from the atmosphere forming brines, which remain liquid at low temperatures (e.g., Toner and Catling, 2016). Beblo-Vranesevic et al. demonstrates that *Hydrogenothermus marinus*, a desiccation tolerant bacterium, was able to tolerate high concentrations of perchlorates, which highlights the possibility of using this microorganism as a model microorganism in future experiments. Evaporitic deposits on the surface of Mars also suggests that water in the near sub-surface would by saline. Recent work has emphasized that the hypersaline springs on Axel Heiberg are a unique analog to represent putative subsurface aquifers on Mars (e.g., Sapers et al.). Based on the microbial diversity within these hypersaline springs, Sapers et al. shows that even a small chemical variation in propinquities sites in the martian sub-surface would have significant implications for community structure, and resulting bio-signatures.

Increasingly, data suggests that habitable environments may exist in the sub-surface oceans of the icy moons. For example, the Galileo, Cassini-Huygens, and Hubble Space Telescope missions support the theory of a potential briny ocean beneath the outer ice shells of Europa, Ganymede and Enceladus. Using environmental characteristics of icy worlds and terrestrial glaciers and ice sheets, Garcia-Lopez et al. concludes that the icy worlds such as Europa and Enceladus are the most likely locations to harbor life of the Solar System.

Analogue environments can also be used to test and develop new instrumentation for future life detection missions. Ideally these methods are low cost with small mass and energy requirement. Using the Canadian high Artic as an analog, Goordial proposes three techniques: the cryo-iPlate for culturing microorganisms (2) a Microbial Activity Microassay (MAM) plate (BIOLOG Ecoplate) for detecting viable extant microorganisms, and (3) the Oxford Nanopore MinION for nucleic acid detection and sequencing. Additionally, based on work carried out in the hyper-arid Namib Desert, Hinchliffe et al. recommends advanced photogrammetry as a method for future autonomous rovers to detect viable surface colonization on the surface of Mars. However, as Fox and Strasdeit discusses there are problems with misinterpreting bio-signatures on other planets and moons that need to be considered.

In addition to environmental analog studies, laboratory simulation experiments are used to further our understanding of potential processes on Mars. Based on data from past mission, Mars regolith analog material can be prepared and used to study potential biogeochemical cycling on Mars. Using Mars simulants as a source of metals, Kölbl et al. demonstrates that surface bioprocesses on the regolith surface could be used as a bio-signature for future missions. However, laboratory based experiments are short-term and Olsson-Francis et al. shows that combining laboratory based experiments with thermochemical modeling is a feasible method for identifying geochemical bio-signatures that are produced over geological timescales. Laboratory based simulation experiments are also used to determine the effect of the extraterrestrial conditions on microbial survivability and activity. For example, de la Torre Noetzel et al. establishes that lichens can survive 30 days in simulated Mars conditions, but the photobiont was unable to perform photosynthesis under these conditions. Microorganisms have been extensively studied under simulated conditions at the surface of Mars (for review see Olsson-Francis and Cockell, 2010). However, Bak et al. proves for the first time that stress effect induced by silicates abraded in a Mars-like atmosphere would be detrimental to life at the martian surface.

Laboratory simulation experiments have revealed that ionizing radiations represents the major hazard for microbial survival, persistence of detectable biosignatures, and operation of spacecraft equipment (Dartnell, 2011). The international STARLIFE-irradiation campaign studied the response of increased doses of ionizing radiation and heavy ions, mimicking Galactic cosmic rays, on astrobiological relevant microorganisms (Moeller et al., 2017). As part of this study, Pacelli et al. illustrates that exposure of the black fungus *Cryomyces antarcticus* CCFEE 515 showed that the fungus maintained high survival and metabolic activity with no detectable DNA and ultrastructural damage, even after the highest dose irradiation.

However, to fully understand the effect of extraterrestrial conditions on microorganisms and bio-signatures a combination of laboratory based and *in-situ* space experiments are required. Exposure experiments in Low Earth Orbit (LEO) exposes samples to several radiation types, such as ionizing, UV, and cosmic radiation (galactic cosmic rays and solar particle events) combined with other conditions, such as vacuum and dust bombardment, which cannot be simulated on Earth. Long-term exposure experiments are carried out on the outside on the International Space Station (ISS). Exposure facilities include the ESA funded EXPOSE-R and an in-depth description of the facility is described in detail by Rabbowet et al.. The samples are exposed long-term to the conditions of LEO to investigate the effect of exposure on microorganisms and their associated bio-signatures, before returning to Earth for analysis (for review see Cottin et al., 2017). Bio-signatures include biomarkers, such as carotenoid deinixanthin, which can be used as evidence on past life on Mars. Leuko et al. demonstrates that this biomarker is strongly resistant to LEO conditions and simulated Mars conditions (when protected from solar radiation), suggesting that it could be used as a target for future missions.

In future, as technology develops microorganisms could play a key part in space exploration, such as *in-situ* resource utilization, and life support systems. On Earth, previous work has shown that the microorganism C. *metallidurans* CH34 is able to leach bio-essential elements from basaltic material (Olsson-Francis et al., 2010). Building on this work, Byloos et al. investigates the effect of space flight and long-term storage on *C. metallidurans* CH34 and interactions with basaltic material (a lunar-type rock), which was the first step to determining the feasibility of

bio-mining in space. Although more work is needed the results may "open the door future studies and potential application in space."

With future missions planned to Mars and the icy moons, understanding the limits of microbial life and their associated bio-signatures is vital. This Research Topic presents advances in our understanding of habitability and bio-signatures using a suit of state-of-the-art methods. To date research has predominantly focused on Mars, but as our understanding of the icy moons increases, our attention most expands to the outer Solar System.

AUTHOR CONTRIBUTIONS

All authors listed have made a substantial, direct and intellectual contribution to the work, and approved it for publication.

ACKNOWLEDGMENTS

We would like to thank the contributing authors for submission of their papers to the Research Topic. In addition, we would like to thank the reviewers for their time and valuable comments.

REFERENCES

Carr, M. H., and Head, J. W. (2010). Geologic history of Mars. *Earth Planet. Sci. Lett.* 294, 185–203. doi: 10.1016/j.epsl.2009.06.042

Clark, B. C., Morris, R. V., Mclennan, S. M., Gellert, R., Jolliff, B., Knoll, A. H., et al. (2005). Chemistry and mineralogy of outcrops at Meridiani Planum. *Earth Planet. Sci. Lett.* 240, 73–94. doi: 10.1016/j.epsl.2005.09.040

Cottin, H., Kotler, J. M., Billi, D., Cockell, C., Demets, R., Ehrenfreund, P., et al. (2017). Space as a tool for astrobiology: review and recommendations for experimentations in earth orbit and beyond. *Space Sci. Rev.* 209, 83–181. doi: 10.1007/s11214-017-0365-5

Dartnell, L. R. (2011). Ionizing radiation and life. *Astrobiology* 11, 551–582. doi: 10.1089/ast.2010.0528

Gillon, M., Triaud, A. H. M. J., Demory, B.-O., Jehin, E., Agol, E., Deck, K. M., et al. (2017). Seven temperate terrestrial planets around the nearby ultracool dwarf star TRAPPIST-1. *Nature* 542, 456–460. doi: 10.1038/nature21360

Glein, C. R., Baross, J. A., and Waite, J. H. (2015). The pH of Enceladus' ocean. *Geochim. Cosmochim. Acta* 162, 202–219. doi: 10.1016/j.gca.2015.04.017

Grotzinger, J. P., Sumner, D. Y., Kah, L. C., Stack, K., Gupta, S., Edgar, L., et al. and (2014), A.T.M.T. (2014). A habitable fluvio-lacustrine environment at Yellowknife Bay, Gale Crater, Mars. *Science* 343:14. doi: 10.1126/science.1242777

Jenkins, J. M., Twicken, J. D., Batalha, N. M., Caldwell, D. A., Cochran, W. D., Endl, M., et al. (2015). Discovery and validation of Kepler-452b: A 1.6 $R_{\oplus}$ Super Earth Exoplanet in the habitable zone of a G2 Star. *Astronom. J.* 150:56. doi: 10.1088/0004-6256/150/2/56

Kargel, J. S. E. A. (2000). Europa's crust and ocean: origin, composition, and the prospects for life. *Icarus* 148, 226–265. doi: 10.1006/icar.2000.6471

Mangold, N., Kite, E. S., Kleinhans, M. G., Newsom, H., Ansan, V., Hauber, E., et al. (2012). The origin and timing of fluvial activity at Eberswalde crater, Mars. *Icarus* 220, 530–551. doi: 10.1016/j.icarus.2012.05.026

Martins, Z., Cottin, H., Kotler, J. M., Carrasco, N., Cockell, C. S., Noetzel, R. D., et al. (2017). Earth as a tool for astrobiology-a european perspective. *Space Sci. Rev.* 209, 43–81. doi: 10.1007/s11214-017-0369-1

Moeller, R., Raguse, M., Leuko, S., Berger, T., Hellweg, C. E., Fujimori, A., et al. (2017). STARLIFE-an international campaign to study the role of galactic cosmic radiation in astrobiological model systems. *Astrobiology* 17, 101–109. doi: 10.1089/ast.2016.1571

Nixon, S. L., Cockell, C. S., and Cousins, C. R. (2013). Plausible microbial metabolisms on Mars. *Astronomy Geophys.* 54, 13–16. doi: 10.1093/astrogeo/ats034

Olsson-Francis, K., and Cockell, C. S. (2010). Experimental methods for studying microbial survival in extraterrestrial environments. *J. Microbiol. Methods* 80, 1–13. doi: 10.1016/j.mimet.2009.10.004

Olsson-Francis, K., Van Houdt, R., Mergeay, M., Leys, N., and Cockell, C. S. (2010). Microarray analysis of a microbe-mineral interaction. *Geobiology* 8, 446–456. doi: 10.1111/j.1472-4669.2010.00253.x

Orosei, R., Lauro, S. E., Pettinelli, E., Cicchetti, A., Coradini, M., Cosciotti, B., et al. (2018). Radar evidence of subglacial liquid water on Mars. *Science* 361, 490–493. doi: 10.1126/science.aar7268

Toner, J. D., and Catling, D. C. (2016). Water activities of $NaClO_4$, $Ca(ClO_4)_2$, and $Mg(ClO_4)_2$ brines from experimental heat capacities: Water activity $>$ 0.6 below 200 K. *Geochim. Cosmochim. Acta* 181, 164–174. doi: 10.1016/j.gca.2016.03.005

Wanke, H., Bruckner, J., Dreibus, G., Rieder, R., and Ryabchikov, I. (2001). Chemical composition of rocks and soils at the Pathfinder site. *Space Sci. Rev.* 96, 317–330. doi: 10.1023/A:1011961725645

Wray, J. J., Milliken, R. E., Dundas, C. M., Swayze, G. A., Andrews-Hanna, J. C., Baldridge, A. M., et al. (2011). Columbus crater and other possible groundwater-fed paleolakes of Terra Sirenum, Mars. *J. Geophys. Res. Planets* 116:3694. doi: 10.1029/2010JE003694

Conflict of Interest Statement: The authors declare that the research was conducted in the absence of any commercial or financial relationships that could be construed as a potential conflict of interest.

frontiers in Microbiology

HYPOTHESIS AND THEORY
published: 16 October 2017
doi: 10.3389/fmicb.2017.02011

The Adaptability of Life on Earth and the Diversity of Planetary Habitats

Dirk Schulze-Makuch[1,2,3], Alessandro Airo[1]* and Janosch Schirmack[1]**

[1] *Astrobiology Group, Center for Astronomy and Astrophysics, Technical University Berlin, Berlin, Germany,* [2] *Beyond Center, Arizona State University, Tempe, AZ, United States,* [3] *School of the Environment, Washington State University, Pullman, WA, United States*

The evolutionary adaptability of life to extreme environments is astounding given that all life on Earth is based on the same fundamental biochemistry. The range of some physicochemical parameters on Earth exceeds the ability of life to adapt, but stays within the limits of life for other parameters. Certain environmental conditions such as low water availability in hyperarid deserts on Earth seem to be close to the limit of biological activity. A much wider range of environmental parameters is observed on planetary bodies within our Solar System such as Mars or Titan, and presumably even larger outside of our Solar System. Here we review the adaptability of life as we know it, especially regarding temperature, pressure, and water activity. We use then this knowledge to outline the range of possible habitable environments for alien planets and moons and distinguish between a variety of planetary environment types. Some of these types are present in our Solar System, others are hypothetical. Our schematic categorization of alien habitats is limited to life as we know it, particularly regarding to the use of solvent (water) and energy source (light and chemical compounds).

Keywords: extremophiles, habitability, solar system, exoplanets, extraterrestrial environment, ocean planets, desert planets

OPEN ACCESS

Edited by:
Daniela Billi,
Università degli Studi di Roma Tor Vergata, Italy

Reviewed by:
Lena Noack,
Freie Universität Berlin, Germany
Stefan Leuko,
Deutsches Zentrum für Luft- und Raumfahrt (DLR), Germany

****Correspondence:***
Janosch Schirmack
j.schirmack@tu-berlin.de
Dirk Schulze-Makuch
schulze-makuch@tu-berlin.de
Alessandro Airo
airo@tu-berlin.de

Specialty section:
This article was submitted to Extreme Microbiology, a section of the journal Frontiers in Microbiology

Received: *30 June 2017*
Accepted: *29 September 2017*
Published: *16 October 2017*

Citation:
Schulze-Makuch D, Airo A and Schirmack J (2017) The Adaptability of Life on Earth and the Diversity of Planetary Habitats. Front. Microbiol. 8:2011. doi: 10.3389/fmicb.2017.02011

INTRODUCTION

Life on Earth inhabits a broad range of environments and is so ubiquitous that there is hardly any environment near the surface of our planet where no life can exist. Nevertheless, the range of some physicochemical parameters on Earth exceeds the ability of life to adapt, for example with respect to high temperatures. Other parameters such as radiation or pressure remain well within the limits of life on Earth. An example is pressure in the deep oceans which does not seem to affect life's abundance and diversity. Low water activity, on the other hand, appears to be one parameter which is close to the limit of biological activity, as evidenced by research done in the hyperarid Atacama Desert and Antarctica's Dry Valleys (Davila and Schulze-Makuch, 2016; Goordial et al., 2016). This does not mean, however, that all localities are habitats, places where life is actively metabolizing and reproducing. In many localities life simply survives in a dormant state, waiting for environmental conditions to change and become more suitable. Thus, when addressing the physicochemical limits of life on Earth, there is a need to distinguish between physicochemical limits that, if breached, destroy life (e.g., high temperature) and those under which life's activity is terminated, but the organism is capable of surviving (e.g., low temperatures, desiccation).

Life also exists in an amazing diversity on Earth and this despite that all life on Earth has fundamentally the same biochemistry. While archaea and bacteria are mostly the record holder for adapting to a particular kind of extreme environmental stress or a combination of stresses, there are also eukaryotic organisms, even relatively complex animals and plants that can withstand or even

metabolize and reproduce in harsh environments. Examples are tardigrades, which are known for their radiation and temperature tolerance, the Crucian Carp, which can slow its metabolism as an adaptation to low oxygen levels, and resurrection plants, which are specially adapted to desiccation (Islam and Schulze-Makuch, 2007). In assessing life's ability to cope with extreme environmental conditions, we also need to differentiate between the limits of single organisms/cells versus single- and multiple-species communities, since their ability to adapt can change substantially. A particularly intriguing case are lichens, which are symbiotic organisms composed of phototrophs (algae or cyanobacteria) and fungi. This symbiosis makes lichens more resistant to combinations of environmental stresses compared to the individual phototrophs or fungi.

While the diversity of environmental niches and life forms on Earth is impressive, there is likely a much greater diversity of habitats existing on other planets within and especially outside our Solar System, particularly considering their projected immense quantity, with currently more than 3000 exoplanets confirmed and another 5000 awaiting confirmation. Many of the newly discovered planets have no analog in our Solar System such as "Super Earths", presumed terrestrial rocky planets with a mass several times that of Earth.

It can be assumed that a subset of these alien environments will in principle be habitable for some organisms we know on Earth; however, the range of habitable niches could be even much greater for alternative alien biochemistries, which allows one to conjecture that life in the Universe would exhibit a much larger variety of forms and functions than life on Earth (Schulze-Makuch, 2015). Furthermore, if one considers other molecules than water as a solvent for an alien biochemistry, the types of possible habitats becomes highly speculative and increases enormously in quantity and therefore goes beyond the scope of this paper.

Here we review the adaptability of life, especially regarding to temperature, pressure, and water activity. We use this knowledge to outline the range of possible habitable environments on alien planets and moons based on life as we know it on Earth.

PHYSICOCHEMICAL LIMITS OF LIFE

Adaptation to Temperature Extremes

Life on Earth is based on carbon containing molecules as the major building blocks for biomass, water as a solvent and exergonic chemical reactions or light. These are energy sources that are life-sustaining and suitable for Earth (Schulze-Makuch, 2015), a terrestrial planet with a mean surface temperature of 15°C at an atmospheric pressure of 1 bar. Yet, the conditions under which life can persist on Earth are incredibly broad, also in regard to temperature range. Relatively, well-explored is the upper temperature limit of life. The current hyperthermophilic record holder, *Methanopyrus kandleri*, can grow at 122°C (Takai et al., 2008). The survival range is even higher, at least 130°C, as shown for *Geogemma barossii* (Kashefi and Lovley, 2003). Even if yet undiscovered species can thrive under higher temperatures, it can be assumed that no organism on Earth can cope with substantially higher temperatures, since the molecular building blocks of life as we know it, such as DNA, thermally disintegrate above about 150°C under wet conditions (White, 1984; Madigan and Orent, 1999). Conceivably, hyperthermophilic microorganisms could rapidly re-synthesize amino acids such as cysteine and glutamic acid that decompose quickly at higher temperatures, as well as low molecular weight compounds (e.g., NAD and ATP) that hydrolyze rather rapidly (Stetter, 1999). While the DNA within a cell is generally negatively supercoiled, all hyperthermophilic microorganisms studied so far have a reverse gyrase that positively supercoils the DNA (Baross et al., 2007). Daniel et al. (2004) pointed out that the thermal stability of DNA is further increased by the supercoiling when cationic proteins are present. Advantageous are also ether-linked, heat resistant lipids, which are commonly found in hyperthermophilic archaea and some hyperthermophilic bacteria. Beeby et al. (2005) suggested that the increased use of disulfide bonds and amino acid substitutions at high temperatures stabilizes protein structures. The formation of higher-order oligomers, the increase in ion-pair content, and the use of salts of various valence states demonstrates that the proteins of thermophiles have evolved to deal with the higher temperatures, which also enhances the stability of RNA and DNA (Rothschild and Mancinelli, 2001). Holden and Baross (1995) proposed that thermal stability of organic macromolecules is also increased by high pressure conditions such as usually existing at submarine hydrothermal vents, particularly when temperatures are so high that they approach the limit of life. The previous discussion does not only pertain to microorganisms. There are also thermophilic multicellular organisms. The Pompeii worm is one of the outstanding examples of a thermophilic metazoan, because it can withstand temperatures approaching 105°C (Chevaldonné et al., 1992). It does so by using both biochemical and physical means. For example, the worm uses the most thermostable fibrillar collagen known and it circulates cold water over its exterior body.

The lower temperature limit for active life is much less well-explored, since the metabolic activity in principle only ceases entirely, when the aqueous cell plasma freezes. Due to intracellular anti-freeze proteins, metabolic activity can occur well below 0°C and microbial growth has been determined for *Planococcus halocryophilus* down to −15°C (Mykytczuk et al., 2013). Recently, multicellular eukaryotes such as the lichen *Umbilicaria* and the yeast *Rhodotorula glutinis* have been shown to still grow at −17 and −18°C, respectively (De Maayer et al., 2014). However, since metabolic reaction rates are temperature dependent (described by the Arrhenius equation) metabolism and growth become so slow that experimental detection is increasingly difficult. Although, there have been reports of metabolic activity in permafrost soils at −39°C (Panikov et al., 2006), thermodynamic considerations suggest that at −40°C the metabolic turnover of the entire cellular carbon takes 100 million years (Price and Sowers, 2004). Hence, the determination of the lower temperature limit of life on Earth becomes experimentally impossible due to ever decreasing metabolic rates. Clarke et al. (2013) predicted that the limit for growth of psychrophilic organisms is approximately −26°C for microbes and −50°C for

multicellular organisms with advanced organismal adaptations for thermoregulation based on the energetics of metabolic processes. As long as an organism is able to endure the process of freezing and thawing, there is no principle lower temperature limit for survival, since being in a frozen state is equivalent to being dormant. As shown for tardigrades the limit of survival can extend for some species to nearly absolute zero (Jönsson et al., 2008).

While the temperature range from about −40 to +150°C seems to represent the physicochemical limits of active life (with its ability to metabolize and grow) it can be speculated that organisms could be adapted to more extreme values, particularly higher temperatures, if a different biochemistry of putative alien organisms is assumed. However, even any alien organism will be bound to its limits of metabolism and reproduction, because of biochemical and energetic constraints. In principle, life cannot flourish above the critical temperature at which the solvent for life cannot remain anymore in the liquid phase. For water, this value is 374°C at 22 MPa pressure. If some other solvent is used by life such as ammonia, an ammonia-water mixture or methanol (e.g., Schulze-Makuch and Irwin, 2008), these limits will be different. In essence, the absolute limit depends on the major building blocks and the type of solvent used by life. Even if carbon-based building blocks and water pair up (as being the case on Earth), the biochemical diversity may be very different from life as we know it, including life's physicochemical limits. In principle, even in this case the temperature range between 150°C and the critical point of water could still be accessed. The intriguing question is how far the envelope of life can be extended with a different type of biochemistry, and also different types of adaptations.

Adaptations to Pressure Extremes

The physiological limit to pressure is not well-defined for life on Earth. The deepest regions of Earth probed to date seem not to be an obstacle for life. Microbes have been obtained from the Mariana Trench, which is 10,660 m deep with pressures reaching 110 MPa (Yayanos, 1995; Kato et al., 1998; Abe et al., 1999) and temperatures hovering around 2°C. Kato et al. (1998) showed that two species of bacteria apparently related to *Shewanella* and *Moritella* seem to be obligately barophilic, because they grow optimally at 70 MPa, but do not grow at pressures less than 50 MPa. Pledger et al. (1994) reported on archaea that were retrieved from localities near deep-sea hydrothermal vents and that survived at pressures of up to 89 MPa. It appears that the higher pressure at hydrothermal vents has a net effect of stabilizing organic molecules (Marion and Schulze-Makuch, 2006). Sharma et al. (2002) demonstrated with the help of a diamond anvil cell that *Shewanella oneidensis* and also some *Escherichia coli* strains can remain metabolically and physiologically active at pressures in the range of 68 to 1680 MPa for close to 30 h. In the pressure window of 1200 to 1600 MPa, viable bacteria were found in fluid inclusions within Ice VI crystals. One percent of the population stayed viable when pressure was reduced back to 1 bar (Sharma et al., 2002). The critical parameter in these experiments is the rate of pressure change, because organisms are very sensitive to abrupt pressure changes.

The lower limit of pressure for life is not well-determined either, but the main obstacle seems to be rather associated with desiccation and low water activity rather than pressure itself (Diaz and Schulze-Makuch, 2006). Schuerger and Nicholson (2016) exposed many different organisms to Mars surface pressure conditions of about 0.6 kPa, and showed that many species were surviving at this low pressure, even species not known as hypobarophiles. Thus, as a first working assumption we postulate that pressure conditions, at least as experienced on a terrestrial planet, such as Earth, will not constitute a major problem for alien life. Life on Earth seems to adapt relatively well to either high or low pressure conditions, and is only rather sensitive to sudden pressure changes.

Adaptations to Low Water Activity

On Earth, water is the solvent critical to life without which organisms cannot survive. Its presence is so critical, because water provides an environment allowing some chemical bonds to be stable and to maintain macromolecular structure, while at the same time assisting in the dissociation of other chemical bonds. This occurs rather easily and therefore enables frequent chemical interchange and also transformations from one molecular state to another. The solvent is instrumental for dissolving many solutes, but at the same time is enabling certain macromolecules to resist dissolution. This, in turn, provides boundaries, interfaces, surfaces, and stereochemical stability. Further, the solvent's density maintains critical concentrations of reactants and thus constrains their dispersal. The solvent is a medium in which biochemical reactions can operate by providing both a lower and upper limit to prevailing pressures and temperatures. The result is that the solvent funnels the evolution of metabolic pathways into a narrower range that is optimized for multiple interactions. And finally, the solvent is a buffer softening environmental fluctuations (Schulze-Makuch and Irwin, 2008). This kind of properties makes water essential for life's activity. The parameter of water activity (a_w) is usually used in this context to quantify whether a specific medium can provide enough free water to facilitate a microorganism's cellular functions. The water activity of a fresh water lake is about 0.99 and very close to that of pure water of 1.0, because nearly all the water is available for an organism, while in a saturated sodium chloride solution ($a_w \sim 0.75$) much of the water is bound to the hydration sphere of the salt ions, and thus not available for organisms. The lowest water activity measured for active metabolism of a microbial strain is 0.605, which has been reported for xerophilic fungi in a saturated sugar solution (Williams and Hallsworth, 2009). The lowest water activity measured at which halophilic archaea and bacteria were able to metabolize is 0.611, which has been tested in their natural habitat as well as in laboratory experiments, and could be extrapolated from measured growth curves (Stevenson et al., 2015a,b; Yakimov et al., 2015). However, water activities are often measured in bulk, e.g., using a large volume and thus can be misleading. Although a bulk water activity of $a_w = 0.49$ was measured in a liquid asphalt lake, active microorganisms were found in micro-droplets of water within the hydrocarbons

(Meckenstock et al., 2014). Further, water activities fluctuate daily and seasonally, and organisms may be active once a certain threshold of a_w is breached. Stevenson et al. (2015b) suggested that there might be a common water activity limit of about 0.6 for all three domains of life on Earth based on its physicochemical constraints. The key for microorganisms not only to survive, but to remain active under desiccating environmental conditions with low water activity, is facilitated by the stabilization of enough liquid water within the cell or its direct vicinity. Therefore, two major adaption strategies have evolved among microorganisms.

One of the adaptions to desiccating conditions is the formation of extracellular polymeric substances (EPSs). The EPS serve to restrain the evaporation of water molecules in the direct cell surrounding or within cell accumulations (Tamaru et al., 2005; Anderson et al., 2012). Roberson and Firestone (1992) and Roberson et al. (1993) showed that the microstructure of EPS of *Pseudomonas* spp. cells did not change in shape from the normal to the desiccated state, but the EPS matrix was significantly larger and contained less protein. Also, the EPS matrix contained several times of the cells' weight in water compared to the EPS of cells grown at high water activities. Desiccation did not appear to affect the activity of the tested cells, which was explained by a higher water retention potential of the EPS matrix (Roberson et al., 1993). The archaeon *Haloquadratum walsbyi* secrets halomucin, a 9159 amino acids long highly glycosylated and sulfated protein, believed to function analogous to EPS, protecting the cell from desiccation by forming a water-rich capsule (Stan-Lotter and Fendrihan, 2015).

Another adaption strategy is to attract as much water from the environment as possible rather than avoiding the loss of water under desiccating conditions. Davila et al. (2013) showed the use of salt deliquescence by microorganisms in halite nodules. The microbes were able to attract water molecules directly from the atmosphere in the Atacama Desert. This strategy is feasible when the relative humidity of the atmosphere was above 70%, equating to a bulk $a_w > 0.7$. This mechanism creates an ecological niche for microbial metabolism and growth in a hyperarid and otherwise hostile environment (**Figure 1**; Davila et al., 2008; Wierzchos et al., 2012). Jänchen et al. (2016) suggested that the deliquescence of a halite sample obtained from the Atacama Desert in combination with a hydrophilic biofilm formed by the cyanobacterium *Nostoc commune* might be a strategy for getting access to water for putative microorganisms living in environmental niches on Mars. The deliquescence effect of various salts was also implicated as a possible mechanism on Mars for staying longer habitable than previously thought, with the result that microbial communities may still be present in the southern highlands of Mars, where large salt deposits occur (Davila and Schulze-Makuch, 2016).

Areas of low water availability on Earth are often associated with high salt content; thus, organisms that live in desert environments, must be adapted to those as well. Examples are archaea and halophilic bacteria growing in 35% NaCl solution (Rodriguez-Valera et al., 1980; Antón et al., 2002; Asker and Ohta, 2002). Life at high salt concentrations is energetically expensive for microorganisms. The upper limit of physiological feasible salt concentrations is determined by bioenergetic constrains, as the amount of energy gained through the dissimilatory metabolism and how an organism adapts to osmotic stress (Oren, 2011). Any organism, which is capable to thrive in environments with high salt concentration must balance its cytoplasm osmotically to its surrounding medium. Two different basic strategies of adaptation exist: the first is based on the accumulation of ions in the cytoplasm. Mostly K^+ instead of Na^+ is used for this purpose with Na^+ often being actively exported by Na^+/H^+ antiporters located in the cell membrane (Grant, 2004). This process is energetically not very cost intensive, but requires high salt concentrations for most of the cellular proteins to function properly and thus narrows down the adaptive range. This strategy is mainly used by a small group of halophiles (Oren, 2011). The second adaption strategy is the exclusion of salts from the cytoplasm and biosynthesis or accumulation of solutes at the same time, which are compatible with the cell machinery and therefore called compatible solutes (Borowitzka and Brown, 1974; Grant, 2004; Stan-Lotter and Fendrihan, 2013). The intercellular compatible solutes concentration is regulated to match the environmental salt concentration. Examples for compatible solutes are polyols like glycerol, sugars and sugar derivatives, betaines, ectoines and amino acids and their derivatives (Grant, 2004). This adaption process is energetically more cost intensive compared to the ion accumulation strategy mentioned above, but it offers a wider adaption range to different levels of salt concentrations (Oren, 2011).

Another often associated physical limit of life thriving in environments of low water availability on a planetary surface are increased levels of radiation, both ultraviolet (UV) and ionizing radiation. The most common form of harmful radiation on Earth's surface is UV radiation acting frequently as a natural mutagen. Baross et al. (2007) pointed out that UV light can also prevent replication of cells, because of the dimerization of thymidine residues in the DNA. Ionizing radiation such as alpha and beta particles, gamma rays, and X-rays, and part of the ultraviolet spectrum can cause multiple breaks in the double-stranded DNA and is thus quickly detrimental to cells (Obe et al., 1992). Further, reactive oxygen species (ROS) are produced by ionizing radiation that can modify bases and/or cause single and double-strand DNA breaks (Rothschild and Mancinelli, 2001). Organisms evolved effective detoxification and inactivation mechanisms for ROS to counter their effect (Daly et al., 2004, 2007), and these mechanisms are positively correlated to higher internal Mn/Fe concentration ratios (>0.1) (Fredrickson et al., 2008). Most organisms on Earth have evolved protective mechanisms to counter harmful radiation. These include various DNA repair mechanisms and the accumulation of radiation-absorbing pigments. However, if an organism is resistant to one type of radiation is does not mean that it is resistant to some other type (Marion and Schulze-Makuch, 2006). *Deinococcus radiodurans* is best known for its resistance to ionizing radiation and can survive approximately 15,000 Gy, while *Thermococcus gammatolerans* can even survive 30,000 Gy (Hirsch et al., 2004). Mattimore and Battista (1996) suggested that this tolerance has evolved initially as an adaptation to desiccation. Leuko et al. (2015) claimed that experimental evidence indicates that halophilic adaptations may provide tolerance to radiation

FIGURE 1 | Yungay Salar, an analog environment for Mars. The insert on the lower left shows a salt crust populated by microorganisms using salt deliquescence for getting access to water. The dark band (arrow) within the salt crust is the pigment scytonemin.

encountered in space. Fredrickson et al. (2008) argued that the UV and ionizing radiation resistance of soil bacteria is an incidental mechanism evolved to prevent oxidative protein damage induced during cycles of drying and rehydration, since most of the soil bacteria are shielded from such radiation by overlying soil. Surprisingly though, hyperthermophilic archaea recovered, e.g., from submarine hydrothermal vents have been found to withstand radiation levels of nearly 8,000 Gy (Jolivet et al., 2004; Beblo et al., 2011). Some multicellular organisms are also quite resistant to radiation such as the tardigrade *Ramazzottius varieornatus*. In its desiccated anhydrobiotic state it shows a high resistance to UVC (100–280 nm) (Horikawa et al., 2013), and the cockroach *Blattella germanica* can survive levels of ionizing radiation close to 1,000 Gy (Schulze-Makuch and Seckbach, 2013). Organisms limit radiation damage by a variety of microbial protection mechanisms. These include avoidance behavior, excision repair, photorepair, homologous recombinational repair, as well as the production of detoxifying enzymes and antioxidants (Yasui and McCready, 1998; Petit and Sancar, 1999; Rothschild, 1999; Smith, 2004). Other options for organisms to protect themselves from UV irradiation are habitation beneath protective layers of water or soil (Pierson et al., 1987; Wynn-Williams and Edwards, 2000), the development of iron-enriched silica crusts (Phoenix et al., 2001), self-shading (Smith, 1982), shielding by organic compounds that are derived from dead cells (Marchant et al., 1991), and the use of specialized organic pigments including scytonemin and carotenoids (Wynn-Williams et al., 2002). The major source of UV irradiation on Earth is the Sun, which is a yellow dwarf star (G2V). Due to Earth's magnetic field the surface of our planet is relatively well-protected from ionic radiation. On an exoplanet however, the amount and spectrum of radiation it experiences at its surface will depend largely on the type and activity of the host star and whether the planet has a magnetic field.

PLANETARY ENVIRONMENT TYPES (PETs) AND THEIR HABITABILITY

In the following, we consider two major factors constraining the water-based habitability of planetary environment types (PETs): (1) high temperature, where the currently known limit is 122°C (Takai et al., 2008) and (2) low water activity, where the currently known limit is 0.6 (Williams and Hallsworth, 2009). Other factors influencing habitability, such as radiation, pressure, or water chemistry, can be mitigated, e.g., through shielding or adaptation and are not considered for PET classification.

Here, we present a classification of PETs (**Figure 2**) centered on the habitability of three principle aqueous environments: (1) atmospheric water "A" (e.g., clouds/rain), (2) surface water "S" (e.g., morning dew or deep oceans), (3) and/or ground water "G". The relevant factors constraining PET-habitability are temperature and water activity, which are largely dependent on planetary water content, size and age, as well as solar irradiation or the geothermal heat which mostly depends on the planetary composition and amount of radioactive elements. In the context of the here presented PET classification, we use the term 'planet' more broadly that includes moons and other planetary bodies.

Furthermore, we classify three compositional configurations based on the presence or absence of surface water layer(s): PET-0 lacks a surface water layer, while the other types possess different constellations of water layers. The absence of a surface water layer of PET-0 can have the following reasons: (1) The surface of the body lacks inherently water and is dry, which can be the result of a dry formation process or due to subsequent events or processes depleting an initial water content. (2) The atmospheric pressure is below the triple point value for water (<612 kPa), in which case liquid water is thermodynamically not stable. (3) The surface temperature is too low for liquid water to exist, which, if salts such as $CaClO_4$ are present, can be as low as −70°C. (4) The surface temperature is too high at the respective pressure for water to condense.

PET-I and II have a surface water layer, ranging from a thin water film (e.g., morning dew) to massive Earth-like oceans or from water-ice caps to a global water-ice shell. PET-II is characterized by the presence of high-pressure water-ice, which is only possible if the planet is above a certain size and has a sufficiently massive water layer for generating the required pressures (e.g., 632 MPa at 273 K). While PET-I has only one liquid water layer, PET-II has two liquid water layers that are separated by an interstitial high-pressure water-ice layer. Finally, all PETs can host an atmosphere that permits the condensation of liquid water if the atmospheric density and temperature range are adequate.

Water-bearing PET sub-environments (atmosphere, surface, and ground) can be (1) uninhabitable due to the lack of liquid water (dry or frozen) or due to too high temperatures; (2) habitable, but not receiving any sunlight and therefore only permit chemotrophic life, or (3) habitable with access to sunlight allowing additionally phototrophic life to be possible.

Except for recurring slope lineae (RSL) and similar features on Mars, it is generally believed that Mars has no surficial liquid water, making it largely a PET-0 planet, where the polar water-ice caps would classify as PET-I. However, Mars is assumed to have a liquid subsurface water aquifer and consequently would be then classified a PET-0-G and PET-I-G, respectively.

If a PET-0 planet has a sufficient atmosphere for water to condense, microbial life is in principle possible within such air-born water droplets, as it has been suggested for the upper atmosphere of Venus (Schulze-Makuch et al., 2004, 2013), classifying it as PET-0-A. While on Venus the surface and subsurface is too hot for life to be possible, temperatures on other bodies can be low enough for stable liquid water at temperatures suitable for life in the subsurface. Such a PET would be classified as 0-AG and is exemplified by hyperarid deserts on Earth such as the Atacama Desert.

Earth has the greatest diversity of habitats in our Solar System occupying all habitat types (atmosphere, surface, ground) and hosts besides hyperarid deserts (0-AG), three types of PET-I: rivers, lakes, or oceans (I-ASG), continental ice such as the Greenland ice-cap (I-G) and ice-covered water bodies such as Lake Vostok, Antarctica (I-SG).

Under low surface temperatures or for smaller planets prohibiting a stable atmosphere, a surface water layer will be frozen as in the case for the global water-ice shell of Europa (I-SG). PET-II are characterized by a lower high-pressure water-ice layer underlain by a secondary ocean, which is only possible if the surface water layer (frozen and/or liquid) is sufficiently thick and the planet large enough for having high-pressure conditions at depth. For PET-II it is unclear whether the upper ocean layer is subject to nutrient limitation, since the interstitial high-pressure water-ice layer prevents a direct interaction with the silicate surface below. In the case of PET-II-AS/ASG, the upper ocean could receive direct nutrient input from cosmic dust. Such a nutrient input is not efficient for PET-II-S/SG, since the upper ocean is overlain by a water-ice crust.

DISCUSSION AND CONCLUSION

The diversity of planets and moons in our Solar System is astonishing and considering the immense quantity of exoplanets the variability in the Galaxy is presumably even much larger. This is largely due to multiple factors affecting the nature of a planet, such as a planet's size, composition, type of host star, formation scenario and orbital distance. Consequently, a geophysical-based comprehensive planet classification would need to be multi-dimensional and presumably would be highly complex. Also, planets are not static objects, but undergo an evolutionary path during which their habitability parameters can change dramatically. Over the past 4.5 billion years Earth has undergone fundamental changes such as the Moon-forming impact, the development of continental crust, Snowball Earth periods and the Great Oxidation Event. In the case of Mars and Venus, which both might have harbored Earth-like habitats early on, evolutionary changes have been even more dramatic (Schulze-Makuch et al., 2013) and resulted in a partial or possibly total loss of habitability.

While a few decades ago, there was much skepticism whether life could exist in the Solar System beyond Earth, multiple locations have today become sites for the search of life beyond Earth: Mars, Europa and Enceladus, as well as Ceres, Titan, and even Venus. This increase in conceivable potential habitats has led to multiple classification schemes being proposed.

Lammer et al. (2009) classified four planetary types, where their class-I planets are Earth-like planets that allow the evolution of complex multi-cellular life in contrast to class-II planets where life is possible but cannot develop complex forms, exemplified by Mars- and Venus-like bodies. The other two types are ocean-planets, where the ocean is in contact with the silicate surface

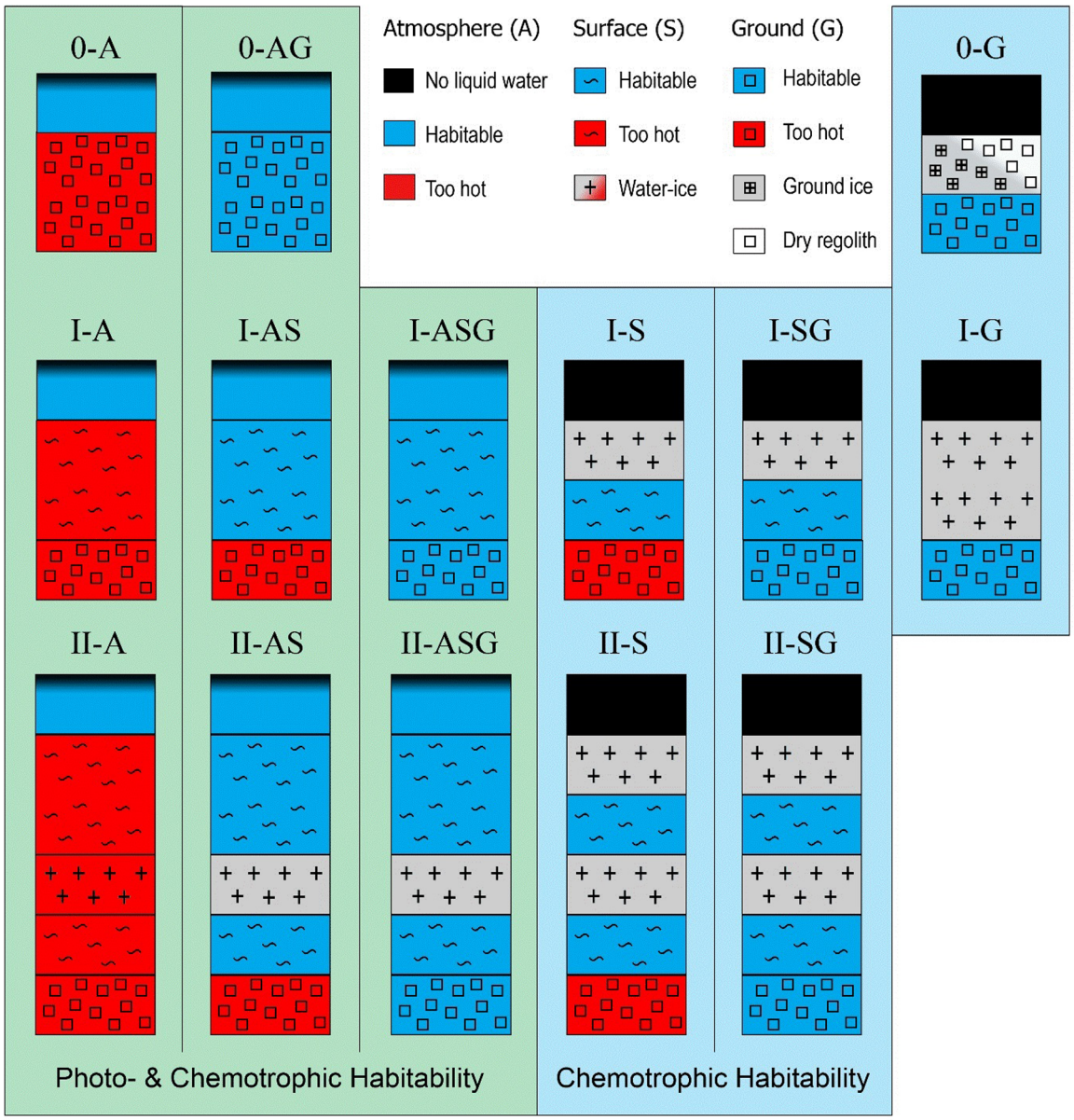

FIGURE 2 | Planetary environment types (PETs) and their water-based habitability. Surface water is here defined as any substantial amount of liquid water residing on top of a solid surface (e.g., silicates, ice).

(class-III) or not (class-IV). Noack et al. (2016) have focused on the classification of ocean-planets, where the H1 type hosts a single ocean layer that is in contact with a silicate surface, the H2 type has two ocean layers where the lower one is in contact with the silicate surface, and the H3 type with only one ocean that is not in direct contact with a silicate surface due to a high-pressure water-ice layer at the bottom.

We here present a classification of water-based PETs that are not necessarily occurring at a global scale and can occur in parallel on a single moon or planet. Although such a classification does not always allow the assignment of one PET to a single planetary body, it provides the possibility to describe the range of habitats on a single planet in more detail. While Lammer et al. (2009) classify Earth as a class-I planet we here require four PETs (0-AG, I-ASG, I-G, I-SG) to describe Earth's habitat diversity. In fact, for an exoplanet to be truly Earth-like or being considered an Earth 2.0 planet, it would have to have multiple environmental habitats and the presence of a sizable biosphere and complex ecosystems, without which Earth, as we experience it, would not exist (Schulze-Makuch and Guinan, 2016). For planetary bodies with only one habitat type the classification is equivalent to other schemes; e.g., Europa is here classified as I-SG while Lammer et al. (2009) classifies such a body as class-III and Noack et al. (2016) as H1 with a surficial water-ice crust.

We have to emphasize that the PET scheme is based on life as we know it, which particularly applies to the use of solvent and energy source. If life's biochemistry is or can be markedly different, for example, as a result of the utilization of a different type of solvent or energy source, this will also alter the results of the habitability assessment. A solvent with a lower liquidity range such as ammonia or an ammonia-water mixture would significantly decrease the temperature range at which life might be viable. If life can utilize a different source of energy such as magnetic fields, thermal or osmotic gradients (e.g., Schulze-Makuch and Irwin, 2008), then this may open up new habitats, that would otherwise not be viable. A test case of the biochemical diversity of life in our Solar System might be Titan, which is partly covered by liquid non-polar hydrocarbons (methane and ethane). If those hydrocarbons can function as a solvent of life, this would require a biochemistry different from the one we are familiar with. A non-polar solvent would mean that the membrane of cells, which on Earth have outer polar ends to interact optimally with a polar solvent (water), would not be suitable on Titan, but would likely have to be hydrophobic. Further, the extremely cold temperatures on the surface of Titan would likely require the utilization of chemical reactions energetic enough to overcome the otherwise low kinetics in this type environment. This might even mean the utilization of radical reactions (Schulze-Makuch and Grinspoon, 2005), which are in general much more energetic than the redox-reaction on which life on Earth is based on. Thus, the PET scheme as outlined above (**Figure 2**) has to be understood as a first attempt to generalize some of the habitats that are possible to support life, but it is unlikely to encompass all possibilities for life in the Universe.

AUTHOR CONTRIBUTIONS

DS-M: concept, acquisition, interpretation, drafting; AA: concept, acquisition, interpretation, drafting; JS: concept, acquisition, interpretation, drafting.

ACKNOWLEDGMENT

This research was supported by the ERC Advanced Grant HOME (#339231).

REFERENCES

Abe, F., Kato, C., and Horikoshi, K. (1999). Pressure-regulated metabolism in microorganisms. *Trends Microbiol.* 7, 447–453. doi: 10.1016/S0966-842X(99)01608-X

Anderson, K. L., Apolinario, E. E., and Sowers, K. R. (2012). Desiccation as a long-term survival mechanism for the archaeon *Methanosarcina barkeri*. *Appl. Environ. Microbiol.* 78, 1473–1479. doi: 10.1128/AEM.06964-11

Antón, J., Oren, A., Benlloch, S., Rodríguez-Valera, F., Amann, R., and Rosselló-Mora, R. (2002). *Salinibacter ruber* gen. nov., sp. nov., a novel, extremely halophilic member of the Bacteria from saltern crystallizer ponds. *Int. J. Syst. Evol. Microbiol.* 52, 485–491. doi: 10.1099/00207713-52-2-485

Asker, D., and Ohta, Y. (2002). *Haloferax alexandrinus* sp. nov., an extremely halophilic canthaxanthin-producing archaeon from a solar saltern in Alexandria (Egypt). *Int. J. Syst. Evol. Microbiol.* 52, 729–738. doi: 10.1099/00207713-52-3-729

Baross, J. A., Benner, S. A., Cody, G. D., Copley, S. D., Pace, N. R., et al. (2007). *The Limits of Organic Life in Planetary Systems*. Washington, DC: National Academies Press.

Beblo, K., Douki, T., Schmalz, G., Rachel, R., Wirth, R., Huber, H., et al. (2011). Survival of thermophilic and hyperthermophilic microorganisms after exposure to UV-C, ionizing radiation and desiccation. *Arch. Microbiol.* 193, 797–809. doi: 10.1007/s00203-011-0718-5

Beeby, M., O'Connor, B. D., Ryttersgaard, C., Boutz, D. R., Perry, L. J., and Yeates, T. O. (2005). The genomics of disulfide bonding and protein stabilization in thermophiles. *PLOS Biol.* 3:e309. doi: 10.1371/journal.pbio.0030309

Borowitzka, L. J., and Brown, A. D. (1974). The salt relations of marine and halophilic species of the unicellular green alga, *Dunaliella*. The role of glycerol as a compatible solute. *Arch. Microbiol.* 96, 37–52. doi: 10.1007/BF00590161

Chevaldonné, P., Desbruyéres, D., and Childress, J. J. (1992). Some like it hot... and some even hotter. *Nature* 359, 593–594. doi: 10.1038/359593b0

Clarke, A., Morris, G. J., Fonseca, F., Murray, B. J., Acton, E., and Price, H. C. (2013). A low temperature limit for life on earth. *PLOS ONE* 8:e66207. doi: 10.1371/journal.pone.0066207

Daly, M. J., Gaidamakova, E. K., Matrosova, V. Y., Vasilenko, A., Zhai, M., Leapman, R. D., et al. (2007). Protein oxidation implicated as the primary determinant of bacterial radioresistance. *PLOS Biol.* 5:e92. doi: 10.1371/journal.pbio.0050092

Daly, M. J., Gaidamakova, E. K., Matrosova, V. Y., Vasilenko, A., Zhai, M., Venkateswaran, A., et al. (2004). Accumulation of Mn(II) in *Deinococcus radiodurans* facilitates gamma-radiation resistance. *Science* 306, 1025–1028. doi: 10.1126/science.1103185

Daniel, R. M., Holden, J. F., van Eckert, R., Truter, J., and Cowan, D. A. (2004). "The stability of biomolecules and the implications for life at high temperatures," in *The Subseafloor Biosphere at Mid-Ocean Ridges*, eds W. Wilcock, E. DeLong, D. Kelley, J. Baross, and S. Cary (Washington DC: American Geophysical Union), 25–39.

Davila, A. F., Gómez-Silva, B., de los Rios, A., Ascaso, C., Olivares, H., McKay, C. P., et al. (2008). Facilitation of endolithic microbial survival in the hyperarid core of the Atacama Desert by mineral deliquescence. *J. Geophys. Res.* 113, G01028. doi: 10.1029/2007JG000561

Davila, A. F., Hawes, I., Ascaso, C., and Wierzchos, J. (2013). Salt deliquescence drives photosynthesis in the hyperarid Atacama Desert. *Environ. Microbiol. Rep.* 5, 583–587. doi: 10.1111/1758-2229.12050

Davila, A. F., and Schulze-Makuch, D. (2016). The last possible outposts for life on Mars. *Astrobiology* 16, 159–168. doi: 10.1089/ast.2015.1380

De Maayer, P., Anderson, D., Cary, C., and Cowan, D. A. (2014). Some like it cold: understanding the survival strategies of psychrophiles. *EMBO Rep.* 15, 508–517. doi: 10.1002/embr.201338170

Diaz, B., and Schulze-Makuch, D. (2006). Microbial survival rates of *Escherichia coli* and *Deinococcus radiodurans* under low temperature, low pressure, and UV-Irradiation conditions, and their relevance to possible Martian life. *Astrobiology* 6, 332–347. doi: 10.1089/ast.2006.6.332

Fredrickson, J. K., Li, S.-M. W., Gaidamakova, E. K., Matrosova, V. Y., Zhai, M., Sulloway, H. M., et al. (2008). Protein oxidation: key to bacterial desiccation resistance? *ISME J.* 2, 393–403. doi: 10.1038/ismej.2007.116

Goordial, J., Davila, A., Lacelle, D., Pollard, W., Marinova, M. M., Greer, C. W., et al. (2016). Nearing the cold-arid limits of microbial life in permafrost of an upper dry valley, Antarctica. *ISME J.* 10, 1613–1624. doi: 10.1038/ismej.2015.239

Grant, W. D. (2004). Life at low water activity. *Philos. Trans. R. Soc. Lond. B Biol. Sci.* 359, 1249–1266. doi: 10.1098/rstb.2004.1502

Hirsch, P., Gallikowski, C. A., Siebert, J., Peissl, K., Kroppenstedt, R., Schumann, P., et al. (2004). *Deinococcus frigens* sp. nov., *Deinococcus saxicola* sp. nov., and *Deinococcus marmoris* sp. nov., low temperature and draught-tolerating,

UV-resistant bacteria from continental Antarctica. *Syst. Appl. Microbiol.* 27, 636–645. doi: 10.1078/0723202042370008

Holden, J. F., and Baross, J. A. (1995). Enhanced thermotolerance by hydrostatic pressure in the deep-sea hyperthermophile *Pyrococcus* strain ES4. *FEMS Microbiol. Ecol.* 18, 27–33. doi: 10.1016/0168-6496(95)00037-B

Horikawa, D. D., Cumbers, J., Sakakibara, I., Rogoff, D., Leuko, S., Harnoto, R., et al. (2013). Analysis of DNA repair and protection in the Tardigrade *Ramazzottius varieornatus* and *Hypsibius dujardini* after exposure to UVC radiation. *PLOS ONE* 8:e64793. doi: 10.1371/journal.pone.0064793

Islam, M. R., and Schulze-Makuch, D. (2007). Adaptations to environmental extremes by multicellular organisms. *Int. J. Astrobiol.* 6, 199–215. doi: 10.1017/S1473550407003783

Jänchen, J., Feyh, N., Szewzyk, U., and de Vera, J.-P. P. (2016). Provision of water by halite deliquescence for *Nostoc commune* biofilms under Mars relevant surface conditions. *Int. J. Astrobiol.* 15, 107–118. doi: 10.1017/S1473550415000018X

Jolivet, E., Corre, E., L'Haridon, S., Forterre, P., and Prieur, D. (2004). *Thermococcus marinus* sp. nov. and *Thermococcus radiotolerans* sp. nov., two hyperthermophilic archaea from deep-sea hydrothermal vents that resist ionizing radiation. *Extremophiles* 8, 219–227. doi: 10.1007/s00792-004-0380-9

Jönsson, K. I., Rabbow, E., Schill, R. O., Harms-Ringdahl, M., and Rettberg, P. (2008). Tardigrades survive exposure to space in low Earth orbit. *Curr. Biol.* 18, R729–R731. doi: 10.1016/j.cub.2008.06.048

Kashefi, K., and Lovley, D. R. (2003). Extending the upper temperature limit for life. *Science* 301, 934. doi: 10.1126/science.1086823

Kato, C., Li, L., Nogi, Y., Nakamura, Y., Tamaoka, J., and Horikoshi, K. (1998). Extremely barophilic bacteria isolated from the Mariana Trench, Challenger Deep, at a depth of 11,000 meters. *Appl. Environ. Microbiol.* 64, 1510–1513.

Lammer, H., Bredehöft, J. H., Coustenis, A., Khodachenko, M. L., Kaltenegger, L., Grasset, O., et al. (2009). What makes a planet habitable? *Astron. Astrophys. Rev.* 17, 181–249. doi: 10.1007/s00159-009-0019-z

Leuko, S., Domingos, C., Parpart, A., Reitz, G., and Rettberg, P. (2015). The survival and resistance of *Halobacterium salinarum* NRC-1, *Halococcus hamelinensis*, and *Halococcus morrhuae* to simulated outer space solar radiation. *Astrobiology* 15, 987–997. doi: 10.1089/ast.2015.1310

Madigan, M. T., and Orent, A. (1999). Thermophilic and halophilic extremophiles. *Curr. Opin. Microbiol.* 2, 265–269. doi: 10.1016/S1369-5274(99)80046-0

Marchant, H. J., Davidson, A. T., and Kelly, G. J. (1991). UV-B protecting compounds in the marine alga *Phaeocystis pouchetii* from Antarctica. *Mar. Biol.* 109, 391–395. doi: 10.1007/BF01313504

Marion, G., and Schulze-Makuch, D. (2006). "Astrobiology and the search for life," in *Physiology and Biochemistry of Extremophiles*, eds C. Gerday and N. Glansdorff (Sterling, VA: ASM Press), 351–358.

Mattimore, V., and Battista, J. R. (1996). Radioresistance of *Deinococcus radiodurans*: functions necessary to survive ionizing radiation are also necessary to survive prolonged desiccation. *J. Bacteriol.* 178, 633–637. doi: 10.1128/jb.178.3.633-637.1996

Meckenstock, R. U., von Netzer, F., Stumpp, C., Lueders, T., Himmelberg, A. M., Hertkorn, N., et al. (2014). Water droplets in oil are microhabitats for microbial life. *Science* 345, 673–676. doi: 10.1126/science.1252215

Mykytczuk, N. C. S., Foote, S. J., Omelon, C. R., Southam, G., Greer, C. W., and Whyte, L. G. (2013). Bacterial growth at -15°C; molecular insights from the permafrost bacterium *Planococcus halocryophilus* Or1. *ISME J.* 7, 1211–1226. doi: 10.1038/ismej.2013.8

Noack, L., Höning, D., Rivoldini, A., Heistracher, C., Zimov, N., Journaux, B., et al. (2016). Water-rich planets: how habitable is a water layer deeper than on Earth? *Icarus* 277, 215–236. doi: 10.1016/j.icarus.2016.05.009

Obe, G., Johannes, C., and Schulte-Frohlinde, D. (1992). DNA double-strand breaks induced by sparsely ionizing radiation and endonucleases as critical lesions for cell death, chromosomal aberrations, mutations and oncogenic transformation. *Mutagenesis* 7, 3–12. doi: 10.1093/mutage/7.1.3

Oren, A. (2011). Thermodynamic limits to microbial life at high salt concentrations. *Environ. Microbiol.* 13, 1908–1923. doi: 10.1111/j.1462-2920.2010.02365.x

Panikov, N. S., Flanagan, P. W., Oechel, W. C., Mastepanov, M. A., and Christensen, T. R. (2006). Microbial activity in soils frozen to below −39°C. *Soil Biol. Biochem.* 38, 785–794. doi: 10.1016/j.soilbio.2005.07.004

Petit, C., and Sancar, A. (1999). Nucleotide excision repair: from *E. coli* to man. *Biochimie* 81, 15–25. doi: 10.1016/S0300-9084(99)80034-0

Phoenix, V. R., Konhauser, K. O., Adams, D. G., and Bottrell, S. H. (2001). Role of biomineralization as an ultraviolet shield: implications for Archean life. *Geology* 29, 823–826. doi: 10.1130/0091-7613(2001)029<0823:ROBAAU>2.0.CO;2

Pierson, B., Oesterle, A., and Murphy, G. L. (1987). Pigments, light penetration, and photosynthetic activity in the multi-layered microbial mats of Great Sippewissett Salt Marsh, Massachusetts. *FEMS Microbiol. Lett.* 45, 365–376. doi: 10.1016/0378-1097(87)90022-X

Pledger, R. J., Crump, B. C., and Baross, J. A. (1994). A barophilic response by two hyperthermophilic, hydrothermal vent Archaea: an upward shift in the optimal temperature and acceleration of growth rate at supra-optimal temperatures by elevated pressure. *FEMS Microbiol. Ecol.* 14, 233–241. doi: 10.1111/j.1574-6941.1994.tb00109.x

Price, P. B., and Sowers, T. (2004). Temperature dependence of metabolic rates for microbial growth, maintenance, and survival. *Proc. Natl. Acad. Sci. U.S.A.* 101, 4631–4636. doi: 10.1073/pnas.0400522101

Roberson, E. B., Chenu, C., and Firestone, M. K. (1993). Microstructural changes in bacterial exopolysaccharides during desiccation. *Soil Biol. Biochem.* 25, 1299–1301. doi: 10.1016/0038-0717(93)90230-9

Roberson, E. B., and Firestone, M. K. (1992). Relationship between desiccation and exopolysaccharide production in a soil *Pseudomonas* sp. *Appl. Environ. Microbiol.* 58, 1284–1291.

Rodriguez-Valera, F., Ruiz-Berraquero, F., and Ramos-Cormenzana, A. (1980). Isolation of extremely halophilic bacteria able to grow in defined inorganic media with single carbon sources. *Microbiology* 119, 535–538. doi: 10.1099/00221287-119-2-535

Rothschild, L. J. (1999). "Microbes and radiation," in *Enigmatic Microorganisms and Life in Extreme Environments*, ed. J. Seckbach (Dordrecht: Springer), 549–562. doi: 10.1007/978-94-011-4838-2_43

Rothschild, L. J., and Mancinelli, R. L. (2001). Life in extreme environments. *Nature* 409, 1092–1101. doi: 10.1038/35059215

Schuerger, A. C., and Nicholson, W. L. (2016). Twenty-three species of hypobarophilic bacteria recovered from diverse ecosystems exhibit growth under simulated Martian conditions at 0.7 kPa. *Astrobiology* 16, 335–347. doi: 10.1089/ast.2015.1394

Schulze-Makuch, D. (2015). "The landscape of life," in *The Impact of Discovering Life Beyond Earth*, ed. S. Dick (Cambridge: Cambridge University Press), 81–94. doi: 10.1017/CBO9781316272480.008

Schulze-Makuch, D., and Grinspoon, D. H. (2005). Biologically enhanced energy and carbon cycling on Titan? *Astrobiology* 5, 560–567. doi: 10.1089/ast.2005.5.560

Schulze-Makuch, D., Grinspoon, D. H., Abbas, O., Irwin, L. N., and Bullock, M. A. (2004). A sulfur-based survival strategy for putative phototrophic life in the Venusian atmosphere. *Astrobiology* 4, 11–18. doi: 10.1089/153110704773600203

Schulze-Makuch, D., and Guinan, E. (2016). Another Earth 2.0? Not so fast. *Astrobiology* 16, 817–821. doi: 10.1089/ast.2016.1584

Schulze-Makuch, D., and Irwin, L. N. (2008). *Life in the Universe: Expectations and Constraints*, 2nd edn. Berlin: Springer.

Schulze-Makuch, D., Irwin, L. N., and Fairén, A. G. (2013). Drastic environmental change and its effects on a planetary biosphere. *Icarus* 225, 775–780. doi: 10.1016/j.icarus.2013.05.001

Schulze-Makuch, D., and Seckbach, J. (2013). "Tardigrades: an example of multicellular extremophiles," in *Polyextremophiles*, eds J. Seckbach, A. Oren, and H. Stan-Lotter (Dordrecht: Springer), 597–607.

Sharma, A., Scott, J. H., Cody, G. D., Fogel, M. L., Hazen, R. M., Hemley, R. J., et al. (2002). Microbial activity at gigapascal pressures. *Science* 295, 1514–1516. doi: 10.1126/science.1068018

Smith, D. W. (1982). "Extreme natural environments," in *Experimental Microbial Ecology*, eds R. G. Burns and H. J. Slater (Oxford: Blackwell Scientific Publications), 555–574.

Smith, K. C. (2004). Recombinational DNA repair: the ignored repair systems. *Bioessays* 26, 1322–1326. doi: 10.1002/bies.20109

Stan-Lotter, H., and Fendrihan, S. (2013). "Survival strategies of halophilic oligotrophic and desiccation resistant prokaryotes," in *Polyextremophiles – Life under Multiple Forms of Stress*, eds J. Seckbach, A. Oren, and H. Stan-Lotter (Dordrecht: Springer), 235–248.

Stan-Lotter, H., and Fendrihan, S. (2015). Halophilic Archaea: life with desiccation, radiation and oligotrophy over geological times. *Life* 5, 1487–1496. doi: 10.3390/life5031487

Stetter, K. O. (1999). Extremophiles and their adaptation to hot environments. *FEBS Lett.* 452, 22–25. doi: 10.1016/S0014-5793(99)00663-8

Stevenson, A., Burkhardt, J., Cockell, C. S., Cray, J. A., Dijksterhuis, J., Fox-Powell, M., et al. (2015a). Multiplication of microbes below 0.690 water activity: implications for terrestrial and extraterrestrial life. *Environ. Microbiol.* 17, 257–277. doi: 10.1111/1462-2920.12598

Stevenson, A., Cray, J. A., Williams, J. P., Santos, R., Sahay, R., Neuenkirchen, N., et al. (2015b). Is there a common water-activity limit for the three domains of life? *ISME J.* 9, 1333–1351. doi: 10.1038/ismej.2014.219

Takai, K., Nakamura, K., Toki, T., Tsunogai, U., Miyazaki, M., Miyazaki, J., et al. (2008). Cell proliferation at 122 degrees C and isotopically heavy CH4 production by a hyperthermophilic methanogen under high-pressure cultivation. *Proc. Natl. Acad. Sci. U.S.A.* 105, 10949–10954. doi: 10.1073/pnas.0712334105

Tamaru, Y., Takani, Y., Yoshida, T., and Sakamoto, T. (2005). Crucial role of extracellular polysaccharides in desiccation and freezing tolerance in the terrestrial cyanobacterium *Nostoc commune*. *Appl. Environ. Microbiol.* 71, 7327–7333. doi: 10.1128/AEM.71.11.7327-7333.2005

White, R. H. (1984). Hydrolytic stability of biomolecules at high temperatures and its implication for life at 250 degrees C. *Nature* 310, 430–432. doi: 10.1038/310430a0

Wierzchos, J., Davila, A. F., Sánchez-Almazo, I. M., Hajnos, M., Swieboda, R., and Ascaso, C. (2012). Novel water source for endolithic life in the hyperarid core of the Atacama Desert. *Biogeosciences* 9, 2275–2286. doi: 10.5194/bg-9-2275-2012

Williams, J. P., and Hallsworth, J. E. (2009). Limits of life in hostile environments: no barriers to biosphere function? *Environ. Microbiol.* 11, 3292–3308. doi: 10.1111/j.1462-2920.2009.02079.x

Wynn-Williams, D. D., Edwards, H., Newton, E. M., and Holder, J. M. (2002). Pigmentation as a survival strategy for ancient and modern photosynthetic microbes under high ultraviolet stress on planetary surfaces. *Int. J. Astrobiol.* 1, 39–49. doi: 10.1017/S1473550402001039

Wynn-Williams, D. D., and Edwards, H. G. M. (2000). Proximal analysis of regolith habitats and protective biomolecules in situ by laser Raman spectroscopy: overview of terrestrial antarctic habitats and Mars analogs. *Icarus* 144, 486–503. doi: 10.1006/icar.1999.6307

Yakimov, M. M., La Cono, V., Spada, G. L., Bortoluzzi, G., Messina, E., Smedile, F., et al. (2015). Microbial community of the deep-sea brine Lake Kryos seawater-brine interface is active below the chaotropicity limit of life as revealed by recovery of mRNA. *Environ. Microbiol.* 17, 364–382. doi: 10.1111/1462-2920.12587

Yasui, A., and McCready, S. J. (1998). Alternative repair pathways for UV-induced DNA damage. *Bioessays* 20, 291–297. doi: 10.1002/(SICI)1521-1878(199804)20:4<291::AID-BIES5>3.0.CO;2-T

Yayanos, A. A. (1995). Microbiology to 10,500 meters in the deep sea. *Annu. Rev. Microbiol.* 49, 777–805. doi: 10.1146/annurev.mi.49.100195.004021

Conflict of Interest Statement: The authors declare that the research was conducted in the absence of any commercial or financial relationships that could be construed as a potential conflict of interest.

frontiers in Microbiology

HYPOTHESIS AND THEORY
published: 20 March 2018
doi: 10.3389/fmicb.2018.00513

Nitrate-Dependent Iron Oxidation: A Potential Mars Metabolism

Alex Price[1], Victoria K. Pearson[1], Susanne P. Schwenzer[1], Jennyfer Miot[2] and Karen Olsson-Francis[1]*

[1] Faculty of Science, Technology, Engineering and Mathematics, The Open University, Milton Keynes, United Kingdom, [2] CNRS, Institut de Minéralogie, de Physique des Matériaux et de Cosmochimie, Muséum National d'Histoire Naturelle, Université Pierre et Marie Curie – Sorbonne Universités, UMR 7590, Paris, France

This work considers the hypothetical viability of microbial nitrate-dependent Fe^{2+} oxidation (NDFO) for supporting simple life in the context of the early Mars environment. This draws on knowledge built up over several decades of remote and *in situ* observation, as well as recent discoveries that have shaped current understanding of early Mars. Our current understanding is that certain early martian environments fulfill several of the key requirements for microbes with NDFO metabolism. First, abundant Fe^{2+} has been identified on Mars and provides evidence of an accessible electron donor; evidence of anoxia suggests that abiotic Fe^{2+} oxidation by molecular oxygen would not have interfered and competed with microbial iron metabolism in these environments. Second, nitrate, which can be used by some iron oxidizing microorganisms as an electron acceptor, has also been confirmed in modern aeolian and ancient sediment deposits on Mars. In addition to redox substrates, reservoirs of both organic and inorganic carbon are available for biosynthesis, and geochemical evidence suggests that lacustrine systems during the hydrologically active Noachian period (4.1–3.7 Ga) match the circumneutral pH requirements of nitrate-dependent iron-oxidizing microorganisms. As well as potentially acting as a primary producer in early martian lakes and fluvial systems, the light-independent nature of NDFO suggests that such microbes could have persisted in sub-surface aquifers long after the desiccation of the surface, provided that adequate carbon and nitrates sources were prevalent. Traces of NDFO microorganisms may be preserved in the rock record by biomineralization and cellular encrustation in zones of high Fe^{2+} concentrations. These processes could produce morphological biosignatures, preserve distinctive Fe-isotope variation patterns, and enhance preservation of biological organic compounds. Such biosignatures could be detectable by future missions to Mars with appropriate instrumentation.

Keywords: iron, nitrate, Mars, astrobiology, chemolithotrophy, NDFO, nitrate-dependent ferrous iron oxidation, anaerobic

OPEN ACCESS

Edited by:
Virginia P. Edgcomb, Woods Hole Oceanographic Institution, United States

Reviewed by:
Trinity L. Hamilton, University of Minnesota Twin Cities, United States
Stephen Brian Pointing, Yale-NUS College, Singapore

****Correspondence:***
Alex Price
alex.price@open.ac.uk

Specialty section:
This article was submitted to Extreme Microbiology, a section of the journal Frontiers in Microbiology

Received: *30 August 2017*
Accepted: *06 March 2018*
Published: *20 March 2018*

Citation:
Price A, Pearson VK, Schwenzer SP, Miot J and Olsson-Francis K (2018) Nitrate-Dependent Iron Oxidation: A Potential Mars Metabolism. Front. Microbiol. 9:513. doi: 10.3389/fmicb.2018.00513

INTRODUCTION

Mars, the red planet, has inspired the search for extraterrestrial life since the early days of the telescope, and continues to do so with perceptions of its habitability—or even inhabitation—changing with advances in exploration capabilities and knowledge of martian environments from images and data (Filiberto and Schwenzer, 2017). The present-day surface of Mars is cold, dry,

and exposed to ionizing and UV radiation, conditions deemed detrimental to life, but evidence in the geological and geomorphological record of Mars confirms warmer, wetter, and potentially more favorable surface conditions during the Noachian period of early Mars (4.1–3.7 Ga) (Carr and Head, 2010). During this period, evidence for a denser atmosphere and less oxidizing conditions suggests that more hospitable surface environments for life may have prevailed (Carr and Head, 2010; Mangold et al., 2012), including: large-scale fluvial systems (Malin and Edgett, 2003; Irwin et al., 2005; Fassett and Head, 2008; Mangold et al., 2012; Williams et al., 2013), lacustrine environments (Grotzinger et al., 2014; Rampe et al., 2017a), and impact-generated hydrothermal systems (Schwenzer and Kring, 2009; Osinski et al., 2013). Evidence for these environments comes from lake bed sediments, such as those identified at Gale Crater, which the NASA Mars Science Laboratory rover (Curiosity) is investigating in detail (e.g., Grotzinger et al., 2015). Phyllosilicates and other hydrated minerals have also been observed from orbit (Gendrin et al., 2005; Bibring et al., 2006; Chevrier et al., 2007) and from the ground (Squyres et al., 2004; Ehlmann et al., 2011). In light of our developing understanding of Mars as a dynamic planet with a complex history, this review appraises the viability of microbial nitrate-dependent iron oxidation as a candidate metabolism with regard to past and present martian environments.

MARS – GEOLOGICAL BACKGROUND

For a better understanding of the contrast between the detrimental conditions on the surface of present-day Mars and the wetter, more clement past of martian surface environments, two specific potentially habitable environments are discussed here: (1) the ancient lake bed investigated by the Curiosity rover at Gale Crater (Grotzinger et al., 2014, 2015; Palucis et al., 2016) and (2) the impact-generated hydrothermal environment discovered in the rim of Endeavour Crater by the MER Opportunity rover (Squyres et al., 2012; Arvidson et al., 2014; Fox et al., 2016).

The ancient lake bed at Gale Crater is likely to be one of many that formed within impact craters on Mars (Cabrol and Grin, 1999). Conglomerates, cross-bedded sandstones, siltstones, and mudstones have been identified by the Curiosity rover, allowing for a detailed understanding of water flow, standing water conditions, and even temporary periods of desiccation (Vaniman et al., 2013; Williams et al., 2013; Grotzinger et al., 2014, 2015; Palucis et al., 2016; Hurowitz et al., 2017). The mineralogy and geochemistry of Gale Crater sediments suggest that the conditions in this ancient lake were temperate and pH-neutral, suitable for the maintenance of life for most of the time (Grotzinger et al., 2014, 2015), although excursions to, or local areas of, acidic conditions are evidenced by the discovery of jarosite (Rampe et al., 2017a,b). Post-depositional diagenetic and alteration processes, such as the dissolution of primary minerals, the formation of calcium-sulfate veins, cementation, desiccation, or even changes to the chemistry of the incoming sediment load due to external silicic volcanism, will have changed the environmental conditions multiple times, leading to a complex association of environmental conditions variable in space and time (Bridges et al., 2015; Johnson et al., 2016; Schwenzer et al., 2016; Frydenvang et al., 2017; Nachon et al., 2017; Rampe et al., 2017a; Yen et al., 2017). Further, Gale Crater sediments are reported to contain bioessential elements such as hydrogen, phosphorus, oxygen, and nitrogen, variable iron and sulfur oxidation states as possible energy sources, and perhaps even complex organic molecules at concentrations that could have supported past life (Vaniman et al., 2013; Grotzinger et al., 2014; Stern et al., 2015; Morris et al., 2016; Sutter et al., 2016).

Orbital observations have shown that many craters bear evidence of impact-generated hydrothermal activity (Marzo et al., 2010; Mangold et al., 2012), and ground-based exploration by the MER rover Opportunity revealed an impact-generated hydrothermal system at Endeavour Crater (Squyres et al., 2012; Arvidson et al., 2014; Fox et al., 2016). Characteristic products of such alteration are clay minerals, with the most complete succession of minerals ascribed to impact-generated hydrothermal activity found in the nakhlite meteorites (Changela and Bridges, 2010; Bridges and Schwenzer, 2012; Hicks et al., 2014). While these meteorites have an unknown geological context, and thus the impact-generated nature of the alteration remains an informed guess, the opportunity to investigate the succession of minerals with Earth-based instrumentation adds significant detail to an understanding of the compositional, reduction–oxidation (redox), and pH evolution of such alteration processes. For example, the alteration reactions evident in the nakhlites indicate a change in the redox conditions from Fe^{2+} precipitates to Fe^{3+} precipitates in the course of the formation of the assemblage (Bridges and Schwenzer, 2012; Hicks et al., 2014). Investigating such details is, to date, beyond the capability of rovers and landers, but provides essential information for assessing the habitability of the site during and after the hydrothermal activity.

Active terrestrial hydrothermal systems observed today are linked to active tectonic processes or volcanism, which drive water circulation on present-day Earth; there is no evidence of a sufficiently large or sufficiently young crater in which an active impact-generated hydrothermal system could exist. However, evidence for past hydrothermal systems is observed in the form of hydrothermal mineral veins around many terrestrial craters, e.g., Chicxulub, Manicouagan, Sudbury, and many others (see Pirajno, 2009; Osinski et al., 2013 for reviews). The difference between impact-generated and volcanic hydrothermal systems is the addition of species from degassing magma in the latter system, mainly HCl, H_2HSO_4, and other volatiles (Pirajno, 2009; Osinski et al., 2013), though fluids in both types of systems dissolve the wall rock and deposit secondary phases as conditions change throughout their lifetime. In both cases, the hydrothermal systems contain abundant bioessential elements (carbon, hydrogen, oxygen, nitrogen, and sulfur) that support diverse microbial communities (Arnold and Sheppard, 1981; Welhan and Craig, 1983; Charlou and Donval, 1993; Wheat et al., 1996; Konn et al., 2009). On Mars, hydrothermal systems caused by large hypervelocity impacts could provide warm water conditions even in periods of cold

climate. With estimated life-times of 150–200k years even for modest craters (100–180 km diameter) the size of Gale, and with cycles of continuous mineral dissolution and precipitation maintaining the availability of redox substrates during that time, impact-generated hydrothermal systems could have provided localized hospitable zones (Abramov and Kring, 2005; Schwenzer and Kring, 2009).

These two examples of martian environments (lacustrine and impact-generated hydrothermal systems) demonstrate the diversity of potentially habitable environments (as we understand them today) on ancient Mars. In early surface environments, where the conditions were less inhospitable than the present-day, both phototrophic (solar energy-driven) and chemotrophic (chemical energy-driven) primary producers may have been viable, possibly producing enough organic carbon for the subsequent development of heterotrophy and a complex web of microbial life. As the environment evolved from "warm and wet" to "cold and dry," life would have likely become limited to the sub-surface environment (Nixon et al., 2012), protected from the adverse surface conditions and, as such, may have become limited to light-independent chemolithotrophic (inorganic chemical energy-driven) metabolisms.

Laboratory-based Mars simulation experiments, using analog regolith or brine, and theoretical modeling have suggested that chemolithotrophic life could persist in the sub-surface martian environment across a wide range of pH, salinity, desiccation, and temperature (Parnell et al., 2004; Amils et al., 2007; Jepsen et al., 2007; Gronstal et al., 2009; Chastain and Kral, 2010; Smith, 2011; Popa et al., 2012; Hoehler and Jørgensen, 2013; Montoya et al., 2013; Summers, 2013; Bauermeister et al., 2014; Oren et al., 2014; King, 2015; Fox-Powell et al., 2016; Schuerger and Nicholson, 2016).

CHEMOLITHOTROPHY ON MARS

Chemolithotrophic microorganisms harvest energy from redox reactions using inorganic substrates that are available in the environment. This metabolic strategy involves the transfer of electrons donated by the inorganic substrate, through the electron transport chain for ATP production, to a final acceptor. Chemolithotrophy is pivotal for biogeochemical cycling on Earth, such as iron, nitrogen, and sulfur cycling, and for rock weathering (Madigan et al., 2009).

The iron-rich nature of Mars raises possibilities regarding the feasibility of iron biogeochemical cycling. Martian crustal geology is dominated by rocks of basaltic composition, which contain abundant FeO in quantities roughly twice those observed in comparable basalts on Earth (McSween et al., 2003, 2009). Though the planet's surface is widely colored by iron oxides, reduced iron, Fe^{2+}, exists as little as a few centimeters beneath the surface (Vaniman et al., 2013). Indeed, Fe^{2+}-bearing minerals such as olivine [$(Mg, Fe^{2+})_2SiO_4$] have been detected across wide areas of the martian surface (Hoefen et al., 2003) and large amounts of basaltic glass (amorphous Fe^{2+}-containing materials) are contained within martian crustal rocks (Morris et al., 2006a,b; McSween et al., 2009). An active hydrological cycle, combined with prevailing reducing conditions during the Noachian period, is likely to have facilitated large-scale transport of iron (**Figure 1**).

On early Earth, iron biogeochemical cycling and the occurrence of iron redox couples were crucial to the biosphere, to provide energy sources and because of the role of iron in many metalloproteins such as cytochromes, nitrogenases, and hydrogenases (Canfield et al., 2006; Hoppert, 2011; Raiswell and Canfield, 2012). Iron can act as either an electron acceptor or donor dependent on its redox state (Miot and Etique, 2016). Iron oxidizing microorganisms have been shown to utilize Fe^{2+} directly after its dissolution from minerals such as olivine (Santelli et al., 2001), and a similar process may have operated within potentially habitable environments on Mars. Conversely, microbial iron reduction commonly utilizes electrons donated from organic substrates, H_2 or S^0, with oxidized Fe^{3+} as the final electron acceptor (Lovley and Phillips, 1988; Lovley et al., 1989).

A hypothetical 'loop' of biologically mediated martian iron cycling (**Figure 2**) was first proposed by Nealson (1997), which included both iron reduction and also phototrophic iron oxidation (Ehrenreich and Widdel, 1994); the plausibility of iron reduction has been appraised previously (Nixon et al., 2012, 2013; Nixon, 2014). However, Nealson's model has limited applications to present-day Mars because of prohibitive conditions for phototrophic life in surface environments that prevent closure of this 'loop' for biogeochemical iron cycling.

Although research suggests that phototrophs may be sufficiently protected inside various micro-habitats within ice, halite, Fe^{3+}-rich sediments, and impact-shocked rocks to withstand modern martian UV flux and remain photosynthetically productive (Cockell and Raven, 2004), the effect of desiccation, in combination with UV irradiation, would prevent dispersal and negatively impact viability (Cockell et al., 2005). Additionally, a lack of liquid water at the surface of Mars would be detrimental to life (Martín-Torres et al., 2015). A plausible alternative to a phototrophic iron oxidizer would be a chemolithotrophic iron oxidizer, which can obtain energy from redox reactions involving inorganic substances. This would allow for a light-independent iron cycle, which could have existed at the surface or in the sub-surface of early Mars and even continue today in deep sub-surface groundwaters (Michalski et al., 2013).

BIOTIC IRON OXIDATION

Abiotic Fe^{2+} oxidation occurs as a function of oxidant concentration, pH, temperature, and Fe^{2+} concentration (Ionescu et al., 2015). On Earth, low pH (<4) prevents the abiotic oxidation of Fe^{2+} by atmospheric O_2, allowing biotic oxidation (using oxygen as the electron acceptor) to dominate (Morgan and Lahav, 2007). Evidence from evaporitic palaeoenvironments on Mars suggests historic low pH (<3.5) conditions existed in certain regions (Gendrin et al., 2005; Squyres and Knoll, 2005; Ming et al., 2006), although neutral–alkaline pH-associated clays are also observed in older terrains (Bibring et al., 2006). The transition to more arid conditions is thought to have coincided with a general shift from widespread clay formation to evaporitic sulfate precipitation at the surface (Bibring et al., 2006;

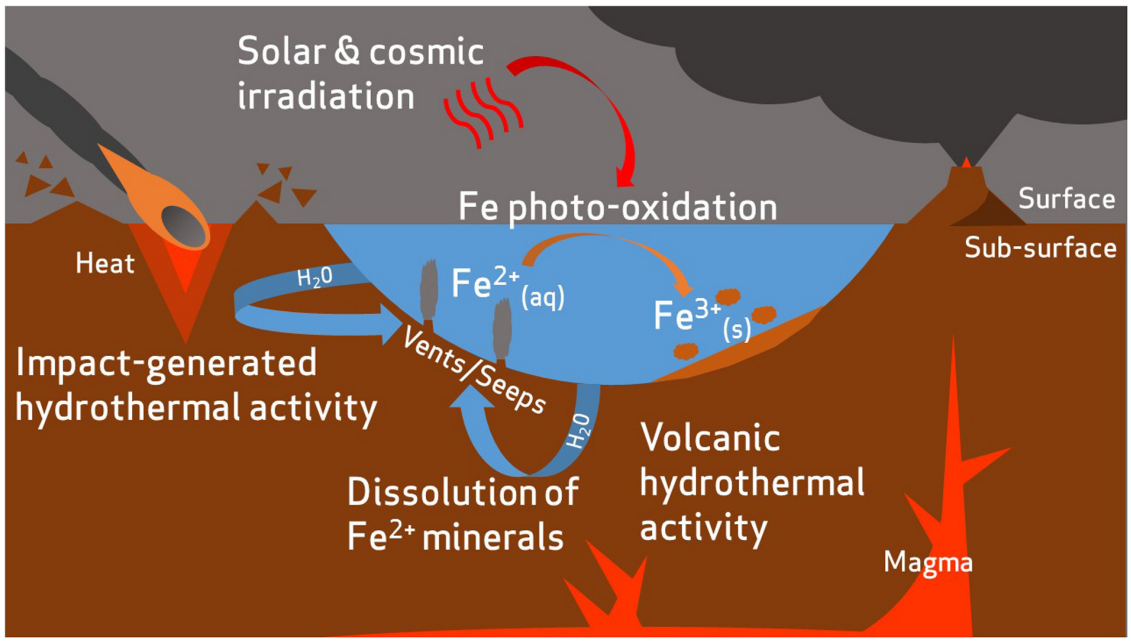

FIGURE 1 | Hypothetical transport of iron on early Mars. Reduced iron is released into aqueous environments by dissolution of ferrous minerals. This process could be accelerated by volcanic or impact-generated hydrothermal activity (McSween et al., 2009). Some dissolved iron may be photo-oxidized by solar UV radiation to ferric compounds and deposited as sediments (Nie et al., 2017).

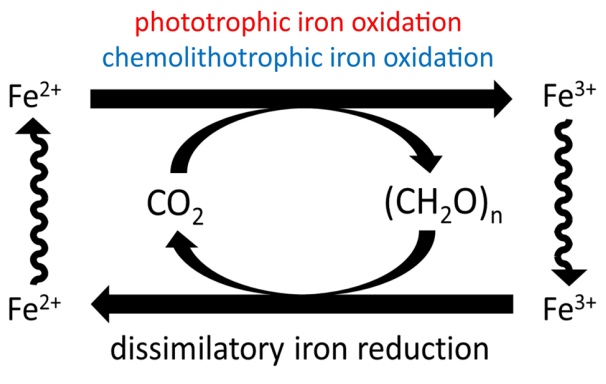

FIGURE 2 | Hypothetical martian biogeochemical cycle of iron. Nealson (1997) suggested combination of phototrophic iron oxidation (Ehrenreich and Widdel, 1994) and heterotrophic iron reduction (Myers and Nealson, 1988) to give a hypothetical iron cycle. Carbon cycles are driven by solar and chemical energy sources. Iron is both the oxidant and the reductant for the cycle. Chemolithotrophic iron oxidation is proposed as an alternative to phototrophic iron oxidation, as the post-Noachian Mars surface environment may restrict opportunities for phototrophy, and any mechanism of iron oxidation in more recent periods may necessarily be light-independent.

Chevrier et al., 2007), resulting in increasingly acidic brines that may promote this form of biotic iron oxidation (Tosca and McLennan, 2006, 2009). However, given that only trace quantities (1450 ppm) of oxygen exist in the modern martian atmosphere (Mahaffy et al., 2013), aerobic, acidophilic iron oxidation is unlikely at the surface today (Bauermeister et al., 2014).

An alternative to aerobic iron oxidizers is microaerophilic neutrophilic iron oxidizers (NFeOs), which are able to compete with abiotic oxidation at near neutral pH. On Earth, this form of metabolism is largely restricted to oxic–anoxic boundary zones, where chemical oxidation is much slower (Roden et al., 2004). Phylogenetic studies have identified NFeOs in a variety of terrestrial environments including arctic tundra, Icelandic streams, deep-ocean vents, iron-rich soils, and temperate ground waters (Emerson and Moyer, 2002; Edwards et al., 2003; Emerson and Weiss, 2004; Cockell et al., 2011; Hedrich et al., 2011; Emerson et al., 2015). Many NFeOs are psychrophilic (Edwards et al., 2003, 2004), which could be linked to the much lower rate of abiotic iron oxidation at low temperatures (Millero et al., 1987).

On Mars, regions of higher partial pressure of oxygen in the modern sub-surface, relative to the surface, have been proposed as tolerable for microaerophiles today (Fisk and Giovannoni, 1999). King (2015) also argued that aerobic activity could be supported by the oxygen concentrations recorded by the Curiosity rover (Mahaffy et al., 2013); however, aerobic metabolism would be restricted, since oxygen diffusion distances in sediments are often limited to a few millimeters (Revsbech et al., 1980; Reimers et al., 1986; Visscher et al., 1991). Furthermore, there is evidence to suggest that redox stratification, seen in standing water bodies on Earth (Comeau et al., 2012), also occurred in martian lakes such as Gale Crater, resulting in an anoxic bottom layer (Hurowitz et al., 2017). Even assuming an oxygen-rich early martian atmosphere such as that suggested by Tuff et al. (2013), deeper waters, sediments, and the sub-surface would have been largely anoxic. As such, whatever the martian atmospheric oxygen concentration, potential habitats

for anaerobically respiring light-independent chemolithotrophs would have been prevalent on ancient and present-day Mars.

Anaerobic chemotrophic iron oxidation is known to occur in terrestrial anoxic waters and sediments of approximately circumneutral pH (Straub et al., 1996; Benz et al., 1998; Kappler and Straub, 2005; Chakraborty and Picardal, 2013). Data from Curiosity at Gale Crater have shown that the Sheepbed mudstone formation at Yellowknife Bay contains abundant clay minerals, indicating a circumneutral pH environment during sedimentation (Vaniman et al., 2013; Grotzinger et al., 2014; Bridges et al., 2015; Schwenzer et al., 2016). The conditions associated with Gale Crater are not unique and can be inferred for other sites on Mars. For example, circumneutral aqueous alteration during both the Noachian and across the Noachian–Hesperian boundary has been proposed based on orbital data of Jezero crater (Ehlmann et al., 2008, 2009), indicating further environments in which anaerobic iron oxidation may have occurred.

AVAILABILITY OF ELECTRON ACCEPTORS

In the absence of molecular oxygen, chemolithotrophic iron oxidizers would be limited by the availability of alternative electron acceptors, such as perchlorates and nitrates, for metabolic redox reactions (Straub et al., 1996; Benz et al., 1998; Kappler and Straub, 2005; Chakraborty and Picardal, 2013).

Studies at multiple locations on Mars have confirmed the presence of perchlorate (Hecht et al., 2009; Navarro-González et al., 2010; Glavin et al., 2013; Kounaves et al., 2014). Perchlorate-reducing bacteria, some able to grow at 0.4 M ClO_4^- (Oren et al., 2014)—concentrations exceeding those found on Mars (Stern et al., 2017)—have been isolated from terrestrial environments. Many are able to promote Fe^{2+} oxidation when perchlorate or nitrate is provided as an electron acceptor (Bruce et al., 1999; Chaudhuri et al., 2001; Lack et al., 2002), though energy conservation leading to growth is yet to be described in the case of perchlorate reduction coupled to Fe^{2+} oxidation.

Nitrate is thus a more feasible electron acceptor for martian iron oxidation, having been observed as the oxidant in iron-oxidizing metabolisms of growth-phase cultures (Hafenbradl et al., 1996; Straub et al., 1996; Benz et al., 1998; Straub and Buchholz-Cleven, 1998). However, until the recent discovery of nitrates on the surface of Mars (Stern et al., 2015), nitrate reducers have been largely overlooked with regard to Mars astrobiology. The following sections discuss the discovery of nitrates on Mars and the feasibility of nitrate-dependent iron oxidation as a plausible metabolism for now closing the biological iron 'loop' on Mars (**Figure 2**).

NITRATES AND NITROGEN CYCLING ON MARS

The geochemical evidence of nitrates on the surface of Mars comes from *in situ* analysis of mudstone at Gale Crater by Curiosity (Stern et al., 2015) and from analysis of the EETA79001 and Nakhla martian meteorites (Grady et al., 1995; Kounaves et al., 2014). It has been proposed that these nitrates may have formed through photochemical processing (Smith et al., 2014) of the low abundance molecular nitrogen (1.9%) in the martian atmosphere (Mahaffy et al., 2013), volcanic-induced lightning, or thermal shock from impacts (Stern et al., 2015), and may have resulted in large accumulated quantities of nitrates during the early history of the planet (Manning et al., 2009; Stern et al., 2017) (**Figure 3**).

Although it is not believed that nitrate deposition currently operates on the martian surface (Stern et al., 2015), interest in the martian nitrogen cycle has been reignited because of recent spacecraft observations of atmospheric nitrogen in the upper atmosphere (Stevens et al., 2015). On Earth, the production of molecular nitrogen is primarily facilitated by microbes through denitrification (Fowler et al., 2013). Biological denitrification on Mars could have contributed to an early nitrogen cycle during the Noachian period, although Mars' atmosphere (including its primordial atmosphere) has long been suspected to have had a low nitrogen abundance relative to Earth (Fox, 1993). Nevertheless, the presence of nitrates as a plausible electron acceptor expands the range of microbial metabolisms that could be considered potentially viable on Mars. Of particular interest is the coupling of nitrate reduction to iron oxidation, which could exploit the vast martian reservoir of Fe^{2+} ions via nitrate-dependent Fe^{2+} oxidation (NDFO).

NITRATE-DEPENDENT Fe^{2+} OXIDATION (NDFO)

Nitrate-dependent Fe^{2+} oxidation metabolism was identified on Earth two decades ago (Straub et al., 1996), yet the detailed biochemical mechanisms involved are still unresolved (e.g., Carlson et al., 2013). Early studies reported Fe^{2+} oxidation balanced with nitrate reduction in mixed cultures and isolates from anaerobic freshwater, brackish water, and marine sediments (Hafenbradl et al., 1996; Straub et al., 1996; Benz et al., 1998). There are only a few known isolates capable of this metabolism (see **Table 1**), but this is likely to be an under-representation of the true diversity and prevalence of these organisms (Straub and Buchholz-Cleven, 1998); NDFO may actually be an innate capability of all nitrate reducers (Carlson et al., 2013; Etique et al., 2014). Enzymatic Fe^{2+} oxidation by NDFO has never been proven and a detailed proteomic study of the NDFO species *Acidovorax ebreus* definitively demonstrated that this strain lacks any specific Fe^{2+} oxidoreductase (Carlson et al., 2013). Alternatively, electrons may transit from Fe^{2+} to other periplasmic enzymes (e.g., enzymes from the nitrate reduction chain) and abiotic side reactions between Fe^{2+} and reactive nitrogen species (NO and NO_2^-) produced upon nitrate reduction could also account for Fe^{2+} oxidation (Carlson et al., 2013; Klueglein et al., 2014, 2015).

Nitrate-dependent Fe^{2+} oxidation microorganisms have to balance (a) a potential energy gain from coupled iron oxidation and nitrate reduction and (b) energy consumption to overcome

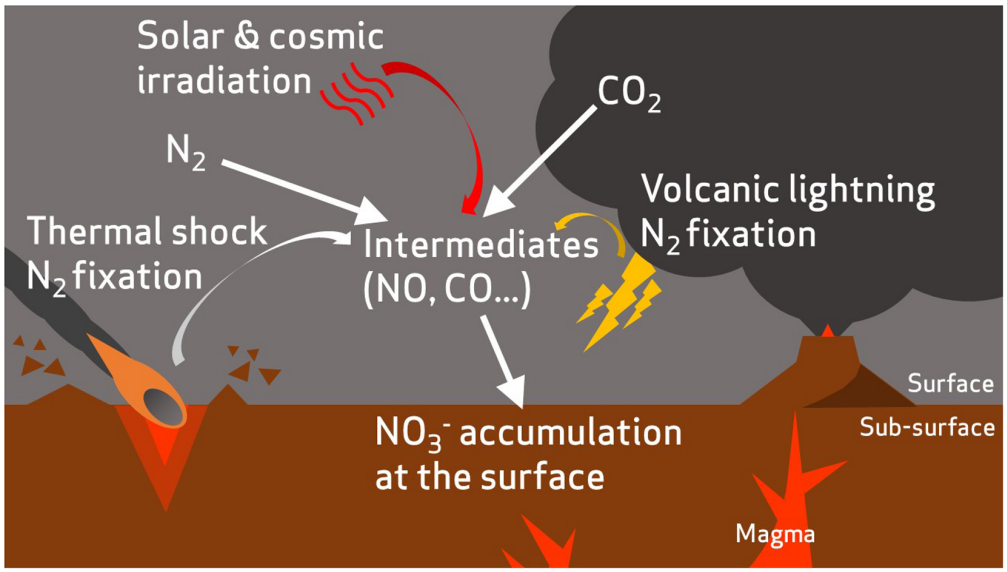

FIGURE 3 | A hypothetical incomplete nitrogen cycle on early Mars. Atmospheric nitrogen is fixed to oxidized nitrogen species via abiotic processes such as volcanic lightning (Stern et al., 2015), thermal shock during impacts (Summers and Khare, 2007), and irradiation from solar and cosmic sources (Smith et al., 2014).

the toxicity of Fe^{2+} and reactive nitrogen species (Carlson et al., 2012, 2013). Although Fe^{2+} oxidation coupled to nitrate reduction to nitrite provides less energy (-481.15 kJ mol^{-1} NO_3^-) than both organotrophic denitrification (-556 kJ mol^{-1} NO_3^-) and organotrophic nitrate ammonification (-623 kJ mol^{-1} NO_3^-) (Strohm et al., 2007), this reaction is exergonic at circumneutral pH (-481.15 kJ mol^{-1} NO_3^-), and may theoretically provide enough energy to sustain growth under mixotrophic (Muehe et al., 2009; Weber et al., 2009) or autotrophic conditions (Laufer et al., 2016). At the same time, ferruginous conditions stimulate metal efflux pumping and stress response pathways (Carlson et al., 2013) and may thus impair the energetic budget of NDFO.

The terrestrial NDFO microbes currently described in the literature are phylogenetically diverse, including an archaeal species, as well as representatives of the alph-, beta-, gamma-, and delta-proteobacteria (Hafenbradl et al., 1996; Kappler et al., 2005; Kumaraswamy et al., 2006; Weber et al., 2009; Chakraborty et al., 2011). The isolation of a member of the euryarchaeota capable of NDFO from a submarine vent system (Hafenbradl et al., 1996) is suggestive that NDFO may have been a very early microbial process on Earth, due to the implication of such environments in the earliest evolution of life (Martin et al., 2008). Ilbert and Bonnefoy (2013) postulated that the mechanisms of biological anaerobic iron oxidation have arisen independently several times on Earth in an example of convergent evolution (i.e., similar strategies are adopted by genetically distant species). This widespread phylogeny, evidence from iron palaeochemistry, physiology, and redox protein cofactors involved in these pathways, suggests that NDFO may be the most ancient iron oxidation pathway in terrestrial life (Ilbert and Bonnefoy, 2013). Indeed, NDFO microbes have been implicated, alongside anoxygenic Fe^{2+}-oxidizing phototrophy, in iron cycling and the production of early banded iron formations prior to the full oxygenation of the atmosphere on Earth (Weber et al., 2006a; Busigny et al., 2013; Ilbert and Bonnefoy, 2013). Thus, NDFO may be relevant to any putative early biosphere on Mars, where the conditions are favorable to this metabolism.

FEASIBILITY OF NDFO ON EARLY MARS

The relevance of NDFO as a plausible metabolism for putative life on Mars had, until recently, been overlooked due to the lack of evidence of nitrogen species on Mars, although the theoretical possibility of NDFO was explored using numerical modeling with hypothetical nitrate sources (Jepsen et al., 2007). The newly found availability of nitrates helps to close the 'loop' of potential chemotrophic iron cycling on Mars (**Figure 2**), since it could provide a ready source of electron acceptors for NDFO organisms (**Figure 4**); the concentration of nitrates detected at Gale Crater (Stern et al., 2015) is consistent with predictions of a 5×10^{15} mol global nitrate reservoir from past impact processing (Manning et al., 2009). It should be noted that the highest nitrate concentrations (1,100 ppm) determined by Curiosity were present in the sedimentary rocks with the least evidence of subsequent alteration, suggesting a period of more active nitrate production during sediment deposition, which was then followed by leaching of some sediments (Stern et al., 2015).

The modern martian atmosphere is 95.9% CO_2 (Mahaffy et al., 2013), and CO_2 is likely to have also formed a major proportion of the denser early Mars atmosphere (Ramirez et al., 2014; Jakosky et al., 2017) (**Figure 5**). Microbes that can utilize inorganic atmospheric carbon would therefore hold an advantage in the Mars environment. Although a low energy-yielding metabolism, a some species (*Pseudogulbenkiania* sp. strain 2002

TABLE 1 | Examples of microbial species capable of nitrate-dependent iron oxidation.

Isolate	Respiration	e^- Donor	e^- Acceptor	Optimum pH	Optimum temperature (°C)	Metabolism	NDFO Growth	Reference
Thiobacillus denitrificans	Obligate anaerobe	S-species/Fe^{2+}	NO_3^-	6.90	30	Autotrophic	Unclear	Straub et al., 1996
Pseudogulbenkiania sp. strain 2002	Facultative aerobe	Fe^{2+}	NO_3^-	6.75–8.00	37	Autotrophic	Yes	Weber et al., 2006b
Paracoccus sp. strain KS1	Facultative aerobe	Organics/S/Fe^{2+}	NO_3^-	7.00	37	Heterotrophic	No	Kumaraswamy et al., 2006
Acidovorax sp. strain BoFeN1	Facultative anaerobe	Organics/Fe^{2+}	NO_3^-	6.80	30	Mixotrophic	Unclear	Kappler et al., 2005
Ferroglobus placidus	Obligate anaerobe	Fe^{2+}/H_2S^{2-}	NO_3^-	7.00	85	Autotrophic	Yes	Hafenbradl et al., 1996
Azospira sp. strain PS	Facultative anaerobe	Fe^{2+}/humic acids	NO_3^-/ClO_4^-	7.00	26	Mixotrophic	No	Lack et al., 2002; Byrne-Bailey and Coates, 2012
Acidovorax sp. strain BrG1	Facultative anaerobe	Organics/Fe^{2+}	NO_3^-	6.70	28–35	Heterotrophic	No	Straub et al., 1996, 2004
Aquabacterium sp. strain BrG2	Facultative anaerobe	Organics/Fe^{2+}	NO_3^-	6.40–6.70	28	Heterotrophic	Unclear	Straub et al., 1996, 2004
Thermomonas sp. strain BrG3	Facultative anaerobe	Organics/Fe^{2+}	NO_3^-	6.70	32–35	Heterotrophic	No	Straub et al., 1996, 2004
Klebsiella mobilis	Facultative aerobe	Organics	NO_3^-	7.00	30	Heterotrophic	No	Etique et al., 2014

and the hyperthermophilic archaeon *Ferroglobus placidus*) have been found to fix carbon autotrophically from CO_2 and other inorganic sources during growth by NDFO (Hafenbradl et al., 1996; Weber et al., 2006b, 2009), providing an alternative carbon assimilatory capability relevant for the early and current Mars environments. Although nitrate reduction can be coupled to anaerobic oxidation of methane (Raghoebarsing et al., 2006; Ettwig et al., 2008), the ability of NDFO strains to use C1 organic compounds as carbon sources has not been investigated. This could prove an important capability when considering the martian environment, given the as yet unexplained detections of methane in the modern atmosphere (Formisano et al., 2004; Webster et al., 2015), and should be investigated further.

Most NDFOs are heterotrophic and require an organic carbon source (Chaudhuri et al., 2001; Kappler et al., 2005; Muehe et al., 2009). Organic carbon has been reported on the martian surface and in martian meteorites (Sephton et al., 2002; Steele et al., 2012; Ming et al., 2014), which may be endogenous (Steele et al., 2012) or have been delivered into the martian crust by meteoritic input ($\sim 2.4 \times 10^5$ kg/year; Yen et al., 2006) (**Figure 5**). Sutter et al. (2016) calculated that <1% of the total carbon detected in sedimentary rocks at Gale Crater would have been sufficient to support 10^5 cells g^{-1} sediment if present as biologically available organics in the earlier lacustrine environment, and hence could well have sustained heterotrophic NDFOs.

Although today's martian atmosphere is oxidizing, even modest levels of volcanism over the last 3.5 billion years are likely to have produced CO_2 at levels that contributed to periodically reducing conditions (Sholes et al., 2017), favoring NDFO by limiting abiotic iron oxidation. However, there has also been a suggestion that certain locations of the ancient surface environment (>3.5 billion years ago) were, at one point, oxidizing (Lanza et al., 2016). In practical terms, oxidizing atmospheric conditions and potential redox stratified water bodies would not preclude the viability of NDFO, but merely restrict it to anoxic sediment and water regions, as is the case on Earth.

Aside from metabolic requirements, life also needs an environment which falls within other sets of physical parameters that are conducive to life. In contrast to phototrophic iron oxidizers, NDFO could have occurred in near-surface ground waters (Straub et al., 1996), which would have protected the microorganisms even if the surface radiation environment of early Mars was as intense as it is today (Dartnell et al., 2007). In addition, cell encrustation by Fe minerals may have protected them against UV irradiation (Gauger et al., 2016). In the deep sub-surface, neutral–alkaline, Fe^{2+}-rich ground waters could have persisted long after the evaporation of most surface bodies (Michalski et al., 2013), greatly extending the period across which NDFO could have been viable, possibly to the present-day.

BIOMINERALIZATION AND PRESERVATION IN THE ROCK RECORD

Under Fe^{2+}-rich (>5 mM) conditions, a major limiting factor for the growth of NDFO populations is the progressive

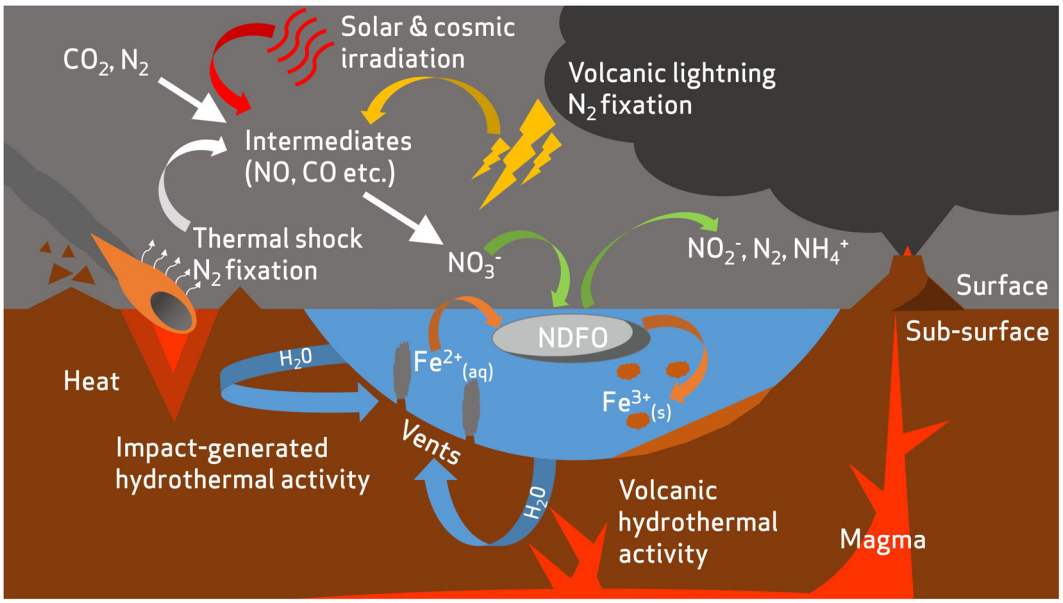

FIGURE 4 | Overview of potential redox substrate sources for nitrate-dependent iron oxidizing microorganisms in the early Mars environment. Nitrates are produced from an early atmospheric nitrogen reservoir by fixation from volcanic lightning (Stern et al., 2015), thermal shock during impacts (Summers and Khare, 2007), and irradiation from solar and cosmic sources (Smith et al., 2014). Reduced iron is released into aqueous environments by mineral dissolution, a process accentuated by hydrothermal activity (Emerson and Moyer, 2002; McSween et al., 2009). A fuller description of abiotic nitrogen fixation pathways is available in Summers et al. (2012).

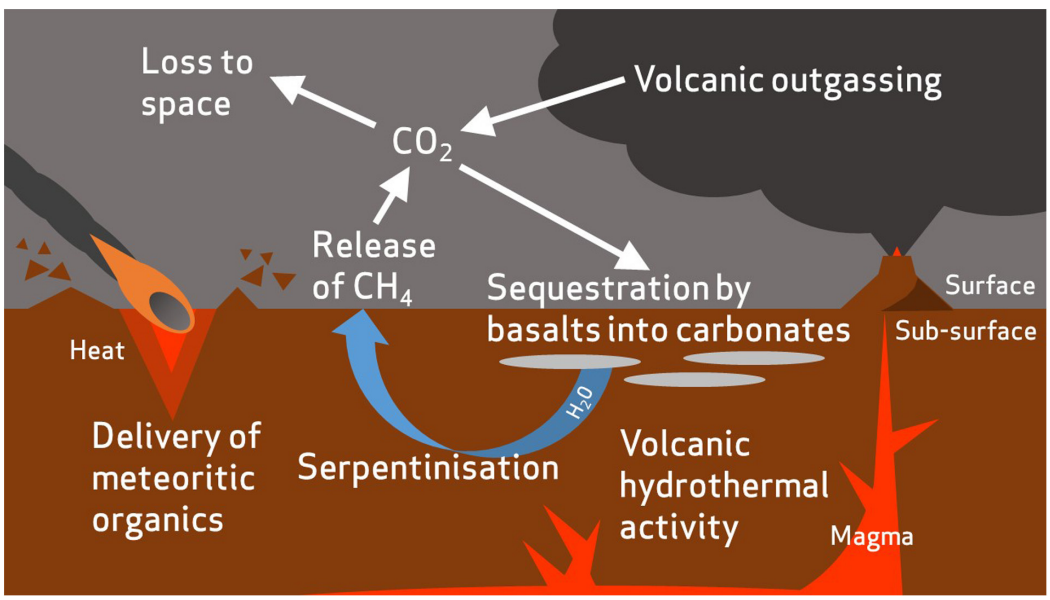

FIGURE 5 | Summary of the proposed processes in carbon cycling on early Mars. Atmospheric carbon dioxide is sequestered by basalts to form carbonate minerals (Edwards and Ehlmann, 2015). The carbon is then remobilized by hydrothermal fluids and incorporated into simple organic compounds, such as methane, by serpentinization reactions (Chassefière and Leblanc, 2011). Carbon dioxide is gradually lost to space due to erosion of the atmosphere by solar winds. Meteorites are also likely to have delivered an inventory of organic carbon to the surface and sub-surface of Mars (Yen et al., 2006).

encrustation of the periplasm and outer membrane by insoluble Fe^{3+} compounds (**Figure 6**), resulting in a decline in individual metabolic activity and cell death (Miot et al., 2015). Even the lithoautotrophic *Pseudogulbenkiania* sp. strain 2002 shows evidence of encrustation after batch culture (Klueglein et al., 2014) (**Figure 6C**). Although the mechanisms remain unexplained, various extracellular Fe^{3+} mineral precipitates also form as by-products of NDFO metabolism, either due to

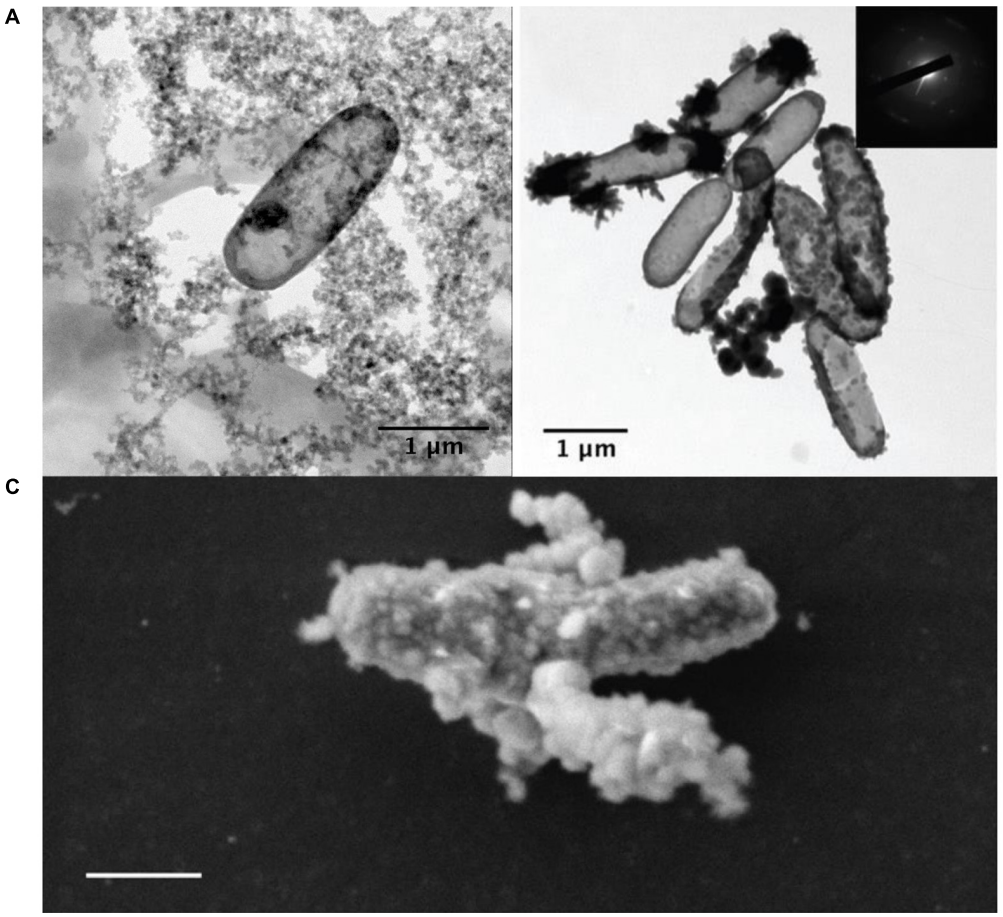

FIGURE 6 | (A) Transmission electron microscopy (TEM) image of an iron-encrusted cell from an NDFO enrichment culture from the anoxic layer of the ferruginous Lake Pavin, France (Jennyfer Miot, personal communication). **(B)** TEM of BoFeN1 cells fully, partially, and non-encrusted with goethite (from Miot et al., 2015). **(C)** SEM of encrusted *Pseudogulbenkiania* sp. 2002 cells (from Klueglein et al., 2014) (scale bar = 500 nm).

the interaction of released Fe^{3+} ions with dissolved phosphate, sulfate, and carbonate ions, or by oxidation of extracellular Fe^{2+}-bearing minerals (Miot et al., 2009). Persistence of a low proportion of cells that escape encrustation ensures the viability of NDFO microorganisms at the population scale, thus accounting for their occurrence in ferruginous habitats on modern Earth (Miot et al., 2016).

The membrane-associated and extracellular mineral precipitates associated with NDFO metabolism may also present plausible biosignatures that may be detectable by future life detection missions, provided that they would persist over geological time. In particular, periplasmic encrustation leads to mineral shells that entrap protein globules and which display a constant thickness (around 40 nm) (Miot et al., 2011). The nature of the minerals has been shown to be dependent on both the local chemical composition and the pH environment. *Acidovorax* sp. strain BoFeN1, one of the best studied NDFO species, has been found to produce either lepidocrocite [γ-FeO(OH)] at pH 7 (Miot et al., 2014b) or a mixture of lepidocrocite and magnetite (Fe_3O_4) at pH 7.6 (Miot et al., 2014a). Likewise, changing the chemical composition of the culture medium at pH 7 results in the precipitation of either Fe^{3+} phosphates (Miot et al., 2009), goethite [α-FeO(OH)] (Kappler et al., 2005; Schädler et al., 2009), or green rust (mixed Fe^{2+}/Fe^{3+} hydroxides) (Pantke et al., 2012).

It is also becoming apparent that encrustation is less likely in environments with low Fe^{2+} concentrations (50–250 µM), i.e., conditions more representative of many terrestrial NDFO sample sites (Chakraborty et al., 2011). Encrustation may occur only when solutions become highly concentrated (millimolar) with Fe^{2+} ions, as may have occurred in hydrothermal and stratified lake settings on early Mars (Hurowitz et al., 2017) or in evaporitic environments during the desiccation of the martian surface (Tosca and McLennan, 2009). Oxide-encrusted cells in both of these contexts could have been deposited and preserved during sedimentation (**Figure 4**). If deposited and lithified as macroscopic flocs or bands within an otherwise generally reducing sedimentary geological context, these oxidized mineral features may be visible in exposed strata and would serve as prime initial targets for further astrobiological investigation. Alternative mineralization processes such as pyritization (saturation and replacement of biological structures

with iron sulfide) or silicification (saturation and replacement of biological structures with silica) could also contribute to non-specific morphological preservation of microbes in iron and sulfur-rich, predominantly basaltic, early martian environments. Microbial silicification has been observed on Earth *in situ* and *in vivo* around hot springs and under simulated conditions as well as in the fossil record (Toporski et al., 2002; Konhauser et al., 2004) whereas microbial pyritization is recognized only in the context of microfossils (Schieber, 2002; Wacey et al., 2013). Given the ability of microbial communities to thrive in conditions which encourage geologically rapid mineralization of biological material, these processes should not be viewed as prohibitive to microbial life on Noachian Mars, and are beneficial to the search for any traces of early life.

Formation of organo-ferric complexes has also been demonstrated to facilitate the preservation of organic molecules in soils and sediment over geological timescales on Earth (Lalonde et al., 2012), raising the possibility that encrustation of NDFO cells by Fe^{3+}-bearing minerals and subsequent complexation may be beneficial to the preservation of organic biosignatures. At the same time, depending on the nature of encrusting minerals and diagenetic (T, P) conditions, Fe minerals may promote the thermal maturation of organic matter and partly erase organic biosignatures (Miot et al., 2017). It may be possible for the Mars Organics Molecule Analyzer (MOMA) mass spectrometer and Raman laser spectrometer (RLS), aboard the ESA ExoMars 2020 rover, to detect biogenic organic molecules in association with Fe^{3+} in iron-rich drill samples and laser targets, respectively (Lopez-Reyes et al., 2013; Arevalo et al., 2015). However, these instruments are not specific enough to distinguish evidence of NDFO microbes from any other potentially biological material encrusted in Fe minerals (e.g., Kish et al., 2016; Mirvaux et al., 2016).

Specific evidence of NDFO metabolism in the geological record on Earth or Mars may, however, come from isotopes. NDFOs have been shown to produce distinctive $^{56}Fe/^{54}Fe$ isotope fractionation patterns, discernible from other processes (Kappler et al., 2010). These variations may be detectable in the rock record, for example, in returned samples, using isotope ratio mass spectrometry (Anand et al., 2006; Czaja et al., 2013). The preservation of isotopic anomalies in martian sediments could provide detectable supporting evidence of NDFO on early Mars.

CONCLUSION

Nitrate-dependent Fe^{2+} oxidation (NDFO) microorganisms oxidase Fe^{2+} compounds while also reducing nitrates under anaerobic, circumneutral conditions. These environments are proposed to have existed on Mars, providing the electron donors and acceptors required for NDFO metabolism. This implies that NDFO is a feasible and logical avenue for investigating hypothetical early martian life.

The discovery of nitrates establishes NDFO as a viable mechanism for hypothetical, biological iron oxidation on present-day Mars. NDFO could help to close a chemotrophic 'loop' of biogeochemical iron cycling on Mars, by providing a potential mechanism for iron oxidation, and allowing chemotrophic iron cycling to occur in both circumneutral ancient surface waters and deep sub-surface waters throughout martian history.

To test the validity of this hypothesis, further research should seek to determine the feasibility of NDFO metabolism under Mars simulation conditions and characterize any associated biomineralization processes. Should the suitability of NDFO to martian environments be supported by the outcomes of these experiments, future life detection missions could be optimized to seek the distinctive mineralized biosignatures of NDFO in the martian rock record.

AUTHOR CONTRIBUTIONS

AP was responsible for writing the manuscript with a large amount of input and revision from KO-F, VP, and SS. JM contributed to the revision, providing experience and expertise in nitrate-dependent iron oxidation and biomineralization processes. The concept for the paper was developed in discussions between AP and KO-F with VP and SS involved from the beginning.

FUNDING

This study was supported by Science and Technology Facilities Council and The Open University. The collaboration was made possible thanks to a Short Term Science Mission (STSM) grant from the EU COST Action ORIGINS TD1308.

REFERENCES

Abramov, O., and Kring, D. A. (2005). Impact-induced hydrothermal activity on early Mars. *J. Geophys. Res. Planets* 110:E12S09. doi: 10.1029/2005JE002453

Amils, R., González-Toril, E., Fernández-Remolar, D., Gómez, F., Aguilera, Á., Rodríguez, N., et al. (2007). Extreme environments as Mars terrestrial analogs: the Rio Tinto case. *Planet. Space Sci.* 55, 370–381. doi: 10.1016/j.pss.2006.02.006

Anand, M., Russell, S., Blackhurst, R., and Grady, M. (2006). Searching for signatures of life on Mars: an Fe-isotope perspective. *Philos. Trans. R. Soc. Lond. B Biol. Sci.* 361, 1715–1720. doi: 10.1098/rstb.2006.1899

Arevalo, R., Brinckerhoff, W., van Amerom, F., Danell, R., Pinnick, V., Xiang, L., et al. (2015). "Design and demonstration of the Mars organic molecule analyzer (MOMA) on the ExoMars 2018 rover," in *Proceedings of the 2015 IEEE Aerospace Conference*, Big Sky, MT, 1–11. doi: 10.1109/AERO.2015.7119073

Arnold, M., and Sheppard, S. M. (1981). East Pacific Rise at latitude 21 N: isotopic composition and origin of the hydrothermal sulphur. *Earth Planet. Sci. Lett.* 56, 148–156. doi: 10.1016/0012-821X(81)90122-9

Arvidson, R. E., Squyres, S. W., Bell, J. F., Catalano, J. G., Clark, B. C., Crumpler, L. S., et al. (2014). Ancient aqueous environments at Endeavour crater, Mars. *Science* 343:1248097. doi: 10.1126/science.1248097

Bauermeister, A., Rettberg, P., and Flemming, H.-C. (2014). Growth of the acidophilic iron–sulfur bacterium *Acidithiobacillus ferrooxidans* under Mars-like geochemical conditions. *Planet. Space Sci.* 98, 205–215. doi: 10.1016/j.pss.2013.09.009

Benz, M., Brune, A., and Schink, B. (1998). Anaerobic and aerobic oxidation of ferrous iron at neutral pH by chemoheterotrophic nitrate-reducing bacteria. *Arch. Microbiol.* 169, 159–165. doi: 10.1007/s002030050555

Bibring, J.-P., Langevin, Y., Mustard, J. F., Poulet, F., Arvidson, R., Gendrin, A., et al. (2006). Global mineralogical and aqueous Mars history derived from OMEGA/Mars express data. *Science* 312, 400–404. doi: 10.1126/science.1122659

Bridges, J. C., and Schwenzer, S. P. (2012). The nakhlite hydrothermal brine on Mars. *Earth Planet. Sci. Lett.* 35, 117–123. doi: 10.1016/j.epsl.2012.09.044

Bridges, J. C., Schwenzer, S. P., Leveille, R., Westall, F., Wiens, R. C., Mangold, N., et al. (2015). Diagenesis and clay mineral formation at Gale Crater, Mars. *J. Geophys. Res. Planets* 120, 1–19. doi: 10.1002/2014JE004757

Bruce, R. A., Achenbach, L. A., and Coates, J. D. (1999). Reduction of (per) chlorate by a novel organism isolated from paper mill waste. *Environ. Microbiol.* 1, 319–329. doi: 10.1046/j.1462-2920.1999.00042.x

Busigny, V., Lebeau, O., Ader, M., Krapež, B., and Bekker, A. (2013). Nitrogen cycle in the Late Archean ferruginous ocean. *Chem. Geol.* 362, 115–130. doi: 10.1016/j.chemgeo.2013.06.023

Byrne-Bailey, K. G., and Coates, J. D. (2012). Complete genome sequence of the anaerobic perchlorate-reducing bacterium *Azospira suillum* strain PS. *J. Bacteriol.* 194, 2767–2768. doi: 10.1128/JB.00124-12

Cabrol, N. A., and Grin, E. A. (1999). Distribution, classification, and ages of Martian impact crater lakes. *Icarus* 142, 160–172. doi: 10.1006/icar.1999.6191

Canfield, D. E., Rosing, M. T., and Bjerrum, C. (2006). Early anaerobic metabolisms. *Philos. Trans. R. Soc. Lond. B Biol. Sci.* 361, 1819–1836. doi: 10.1098/rstb.2006.1906

Carlson, H. K., Clark, I. C., Blazewicz, S. J., Iavarone, A. T., and Coates, J. D. (2013). Fe (II) oxidation is an innate capability of nitrate-reducing bacteria that involves abiotic and biotic reactions. *J. Bacteriol.* 195, 3260–3268. doi: 10.1128/JB.00058-13

Carlson, H. K., Clark, I. C., Melnyk, R. A., and Coates, J. D. (2012). Toward a mechanistic understanding of anaerobic nitrate-dependent iron oxidation: balancing electron uptake and detoxification. *Front. Microbiol.* 3:57. doi: 10.3389/fmicb.2012.00057

Carr, M. H., and Head, J. W. (2010). Geologic history of Mars. *Earth Planet. Sci. Lett.* 294, 185–203. doi: 10.1016/j.epsl.2009.06.042

Chakraborty, A., and Picardal, F. (2013). Neutrophilic, nitrate-dependent, Fe(II) oxidation by a *Dechloromonas* species. *World J. Microbiol. Biotechnol.* 29, 617–623. doi: 10.1007/s11274-012-1217-9

Chakraborty, A., Roden, E. E., Schieber, J., and Picardal, F. (2011). Enhanced growth of *Acidovorax* sp. Strain 2AN during nitrate-dependent Fe(II) oxidation in batch and continuous-flow systems. *Appl. Environ. Microbiol.* 77, 8548–8556. doi: 10.1128/aem.06214-11

Changela, H. G., and Bridges, J. C. (2010). Alteration assemblages in the nakhlites: variation with depth on Mars. *Meteorit. Planet. Sci.* 45, 1847–1867. doi: 10.1111/j.1945-5100.2010.01123.x

Charlou, J. L., and Donval, J. P. (1993). Hydrothermal methane venting between 12° N and 26° N along the Mid-Atlantic Ridge. *J. Geophys. Res. Solid Earth* 98, 9625–9642. doi: 10.1029/92JB02047

Chassefière, E., and Leblanc, F. (2011). Methane release and the carbon cycle on Mars. *Planet. Space Sci.* 59, 207–217. doi: 10.1016/j.pss.2010.09.004

Chastain, B. K., and Kral, T. A. (2010). Zero-valent iron on Mars: an alternative energy source for methanogens. *Icarus* 208, 198–201. doi: 10.1016/j.icarus.2010.02.024

Chaudhuri, S. K., Lack, J. G., and Coates, J. D. (2001). Biogenic magnetite formation through anaerobic biooxidation of Fe (II). *Appl. Environ. Microbiol.* 67, 2844–2848. doi: 10.1128/AEM.67.6.2844-2848.2001

Chevrier, V., Poulet, F., and Bibring, J.-P. (2007). Early geochemical environment of Mars as determined from thermodynamics of phyllosilicates. *Nature* 448, 60–63. doi: 10.1038/nature05961

Cockell, C. S., Kelly, L. C., Summers, S., and Marteinsson, V. (2011). Following the kinetics: iron-oxidizing microbial mats in cold Icelandic volcanic habitats and their rock-associated carbonaceous signature. *Astrobiology* 11, 679–694. doi: 10.1089/ast.2011.0606

Cockell, C. S., and Raven, J. A. (2004). Zones of photosynthetic potential on Mars and the early Earth. *Icarus* 169, 300–310. doi: 10.1016/j.icarus.2003.12.024

Cockell, C. S., Schuerger, A. C., Billi, D., Friedmann, E. I., and Panitz, C. (2005). Effects of a simulated Martian UV flux on the cyanobacterium, *Chroococcidiopsis* sp. 029. *Astrobiology* 5, 127–140. doi: 10.1089/ast.2005.5.127

Comeau, A. M., Harding, T., Galand, P. E., Vincent, W. F., and Lovejoy, C. (2012). Vertical distribution of microbial communities in a perennially stratified Arctic lake with saline, anoxic bottom waters. *Sci. Rep.* 2:604. doi: 10.1038/srep00604

Czaja, A. D., Johnson, C. M., Beard, B. L., Roden, E. E., Li, W., and Moorbath, S. (2013). Biological Fe oxidation controlled deposition of banded iron formation in the ca. 3770Ma Isua Supracrustal Belt (West Greenland). *Earth Planet. Sci. Lett.* 363, 192–203. doi: 10.1016/j.epsl.2012.12.025

Dartnell, L. R., Desorgher, L., Ward, J. M., and Coates, A. J. (2007). Modelling the surface and subsurface Martian radiation environment: implications for astrobiology. *Geophys. Res. Lett.* 34:L02207. doi: 10.1029/2006GL027494

Edwards, C. S., and Ehlmann, B. L. (2015). Carbon sequestration on Mars. *Geology* 43, 863–866. doi: 10.1130/G36983.1

Edwards, K. J., Bach, W., McCollom, T. M., and Rogers, D. R. (2004). Neutrophilic iron-oxidizing bacteria in the ocean: their habitats, diversity, and roles in mineral deposition, rock alteration, and biomass production in the deep-sea. *Geomicrobiol. J.* 21, 393–404. doi: 10.1080/01490450490485863

Edwards, K. J., Rogers, D. R., Wirsen, C. O., and McCollom, T. M. (2003). Isolation and characterization of novel psychrophilic, neutrophilic, Fe-oxidizing, chemolithoautotrophic α-and γ-*Proteobacteria* from the deep sea. *Appl. Environ. Microbiol.* 69, 2906–2913. doi: 10.1128/AEM.69.5.2906-2913.2003

Ehlmann, B. L., Mustard, J. F., Fassett, C. I., Schon, S. C., Head, J. W. III, Des Marais, D. J., et al. (2008). Clay minerals in delta deposits and organic preservation potential on Mars. *Nat. Geosci.* 1, 355–358. doi: 10.1038/ngeo207

Ehlmann, B. L., Mustard, J. F., Murchie, S. L., Bibring, J.-P., Meunier, A., Fraeman, A. A., et al. (2011). Subsurface water and clay mineral formation during the early history of Mars. *Nature* 479, 53–60. doi: 10.1038/nature10582

Ehlmann, B. L., Mustard, J. F., Swayze, G. A., Clark, R. N., Bishop, J. L., Poulet, F., et al. (2009). Identification of hydrated silicate minerals on Mars using MRO-CRISM: geologic context near Nili Fossae and implications for aqueous alteration. *J. Geophys. Res. Planets* 114:E00D08. doi: 10.1029/2009JE003339

Ehrenreich, A., and Widdel, F. (1994). Anaerobic oxidation of ferrous iron by purple bacteria, a new type of phototrophic metabolism. *Appl. Environ. Microbiol.* 60, 4517–4526.

Emerson, D., and Moyer, C. L. (2002). Neutrophilic Fe-oxidizing bacteria are abundant at the Loihi Seamount hydrothermal vents and play a major role in Fe oxide deposition. *Appl. Environ. Microbiol.* 68, 3085–3093. doi: 10.1128/AEM.68.6.3085-3093.2002

Emerson, D., Scott, J. J., Benes, J., and Bowden, W. B. (2015). Microbial iron oxidation in the arctic tundra and its implications for biogeochemical cycling. *Appl. Environ. Microbiol.* 81, 8066–8075. doi: 10.1128/AEM.02832-15

Emerson, D., and Weiss, J. V. (2004). Bacterial iron oxidation in circumneutral freshwater habitats: findings from the field and the laboratory. *Geomicrobiol. J.* 21, 405–414. doi: 10.1080/01490450490485881

Etique, M., Jorand, F. P. A., Zegeye, A., Greìgoire, B., Despas, C., and Ruby, C. (2014). Abiotic process for Fe (II) oxidation and green rust mineralization driven by a heterotrophic nitrate reducing bacteria (*Klebsiella mobilis*). *Environ. Sci. Technol.* 48, 3742–3751. doi: 10.1021/es403358v

Ettwig, K. F., Shima, S., Van de Pas-Schoonen, K. T., Kahnt, J., Medema, M. H., Op Den Camp, H. J. M., et al. (2008). Denitrifying bacteria anaerobically oxidize methane in the absence of *Archaea*. *Environ. Microbiol.* 10, 3164–3173. doi: 10.1111/j.1462-2920.2008.01724.x

Fassett, C. I., and Head, J. W. (2008). The timing of Martian valley network activity: constraints from buffered crater counting. *Icarus* 195, 61–89. doi: 10.1016/j.icarus.2007.12.009

Filiberto, J., and Schwenzer, S. P. (2017). *Volatiles in the Martian Crust*. Amsterdam: Elsevier.

Fisk, M. R., and Giovannoni, S. J. (1999). Sources of nutrients and energy for a deep biosphere on Mars. *J. Geophys. Res. Planets* 104, 11805–11815. doi: 10.1029/1999JE900010

Formisano, V., Atreya, S., Encrenaz, T., Ignatiev, N., and Giuranna, M. (2004). Detection of methane in the atmosphere of Mars. *Science* 306, 1758–1761. doi: 10.1126/science.1101732

Fowler, D., Coyle, M., Skiba, U., Sutton, M. A., Cape, J. N., Reis, S., et al. (2013). The global nitrogen cycle in the twenty-first century. *Philos. Trans. R. Soc. B Biol. Sci.* 368:20130164. doi: 10.1098/rstb.2013.0164

Fox, J. L. (1993). The production and escape of nitrogen atoms on Mars. *J. Geophys. Res. Planets* 98, 3297–3310. doi: 10.1029/92JE02289

Fox, V. K., Arvidson, R. E., Guinness, E. A., McLennan, S. M., Catalano, J. G., Murchie, S. L., et al. (2016). Smectite deposits in Marathon Valley, Endeavour Crater, Mars, identified using CRISM hyperspectral reflectance data. *Geophys. Res. Lett.* 43, 4885–4892. doi: 10.1002/2016GL069108

Fox-Powell, M. G., Hallsworth, J. E., Cousins, C. R., and Cockell, C. S. (2016). Ionic strength is a barrier to the habitability of Mars. *Astrobiology* 16, 427–442. doi: 10.1089/ast.2015.1432

Frydenvang, J., Gasda, P. J., Hurowitz, J. A., Grotzinger, J. P., Wiens, R. C., Newsom, H. E., et al. (2017). Diagenetic silica enrichment and late-stage groundwater activity in Gale crater, Mars. *Geophys. Res. Lett.* 44, 4716–4724. doi: 10.1002/2017GL073323

Gauger, T., Konhauser, K., and Kappler, A. (2016). Protection of nitrate-reducing Fe(II)-oxidizing bacteria from UV radiation by biogenic Fe(III) minerals. *Astrobiology* 16, 301–310. doi: 10.1089/ast.2015.1365

Gendrin, A., Mangold, N., Bibring, J.-P., Langevin, Y., Gondet, B., Poulet, F., et al. (2005). Sulfates in Martian layered terrains: the OMEGA/Mars express view. *Science* 307, 1587–1591. doi: 10.1126/science.1109087

Glavin, D. P., Freissinet, C., Miller, K. E., Eigenbrode, J. L., Brunner, A. E., Buch, A., et al. (2013). Evidence for perchlorates and the origin of chlorinated hydrocarbons detected by SAM at the Rocknest aeolian deposit in Gale Crater. *J. Geophys. Res. Planets* 118, 1955–1973. doi: 10.1002/jgre.20144

Grady, M. M., Wright, I., and Pillinger, C. T. (1995). A search for nitrates in Martian meteorites. *J. Geophys. Res. Planets* 100, 5449–5455. doi: 10.1029/94JE02803

Gronstal, A., Pearson, V., Kappler, A., Dooris, C., Anand, M., Poitrasson, F., et al. (2009). Laboratory experiments on the weathering of iron meteorites and carbonaceous chondrites by iron-oxidizing bacteria. *Meteorit. Planet. Sci.* 44, 233–247. doi: 10.1111/j.1945-5100.2009.tb00731.x

Grotzinger, J. P., Gupta, S., Malin, M. C., Rubin, D. M., Schieber, J., Siebach, K., et al. (2015). Deposition, exhumation, and paleoclimate of an ancient lake deposit, Gale crater, Mars. *Science* 350:aac7575. doi: 10.1126/science.aac7575

Grotzinger, J. P., Sumner, D. Y., Kah, L. C., Stack, K., Gupta, S., Edgar, L., et al. (2014). A habitable fluvio-lacustrine environment at Yellowknife Bay, Gale crater, Mars. *Science* 343:1242777. doi: 10.1126/science.1242777

Hafenbradl, D., Keller, M., Dirmeier, R., Rachel, R., Roßnagel, P., Burggraf, S., et al. (1996). *Ferroglobus placidus* gen. nov., sp. nov., a novel hyperthermophilic archaeum that oxidizes Fe^{2+} at neutral pH under anoxic conditions. *Arch. Microbiol.* 166, 308–314. doi: 10.1007/s002030050388

Hecht, M. H., Kounaves, S. P., Quinn, R. C., West, S. J., Young, S. M. M., Ming, D. W., et al. (2009). Detection of perchlorate and the soluble chemistry of Martian soil at the phoenix Lander site. *Science* 325, 64–67. doi: 10.1126/science.1172466

Hedrich, S., Schlömann, M., and Johnson, D. B. (2011). The iron-oxidizing *Proteobacteria*. *Microbiology* 157, 1551–1564. doi: 10.1099/mic.0.045344-0

Hicks, L. J., Bridges, J. C., and Gurman, S. (2014). Ferric saponite and serpentine in the nakhlite Martian meteorites. *Geochim. Cosmochim. Acta* 136, 194–210. doi: 10.1016/j.gca.2014.04.010

Hoefen, T. M., Clark, R. N., Bandfield, J. L., Smith, M. D., Pearl, J. C., and Christensen, P. R. (2003). Discovery of olivine in the Nili Fossae region of Mars. *Science* 302, 627–630. doi: 10.1126/science.1089647

Hoehler, T. M., and Jørgensen, B. B. (2013). Microbial life under extreme energy limitation. *Nat. Rev. Microbiol.* 11, 83–94. doi: 10.1038/nrmicro2939

Hoppert, M. (2011). "Metalloenzymes," in *Encyclopedia of Geobiology*, eds R. Reitner and V. Thiel (Dordrecht: Springer), 558–563. doi: 10.1007/978-1-4020-9212-1_134

Hurowitz, J. A., Grotzinger, J. P., Fischer, W. W., McLennan, S. M., Milliken, R. E., Stein, N., et al. (2017). Redox stratification of an ancient lake in Gale crater, Mars. *Science* 356:eaah6849. doi: 10.1126/science.aah6849

Ilbert, M., and Bonnefoy, V. (2013). Insight into the evolution of the iron oxidation pathways. *Biochim. Biophys. Acta* 1827, 161–175. doi: 10.1016/j.bbabio.2012.10.001

Ionescu, D., Heim, C., Polerecky, L., Thiel, V., and De Beer, D. (2015). Biotic and abiotic oxidation and reduction of iron at circumneutral pH are inseparable processes under natural conditions. *Geomicrobiol. J.* 32, 221–230. doi: 10.1080/01490451.2014.887393

Irwin, R. P., Howard, A. D., Craddock, R. A., and Moore, J. M. (2005). An intense terminal epoch of widespread fluvial activity on early Mars: 2. Increased runoff and paleolake development. *J. Geophys. Res. Planets* 110:E12S15. doi: 10.1029/2005JE002460

Jakosky, B. M., Slipski, M., Benna, M., Mahaffy, P., Elrod, M., Yelle, R., et al. (2017). Mars' atmospheric history derived from upper-atmosphere measurements of 38Ar/36Ar. *Science* 355, 1408–1410. doi: 10.1126/science.aai7721

Jepsen, S. M., Priscu, J. C., Grimm, R. E., and Bullock, M. A. (2007). The potential for lithoautotrophic life on Mars: application to shallow interfacial water environments. *Astrobiology* 7, 342–354. doi: 10.1089/ast.2007.0124

Johnson, J. R., Bell, J. F., Bender, S., Blaney, D., Cloutis, E., Ehlmann, B., et al. (2016). Constraints on iron sulfate and iron oxide mineralogy from ChemCam visible/near-infrared reflectance spectroscopy of Mt. Sharp basal units, Gale Crater, Mars. *Am. Mineral.* 101, 1501–1514. doi: 10.2138/am-2016-5553

Kappler, A., Johnson, C., Crosby, H., Beard, B., and Newman, D. (2010). Evidence for equilibrium iron isotope fractionation by nitrate-reducing iron (II)-oxidizing bacteria. *Geochim. Cosmochim. Acta* 74, 2826–2842. doi: 10.1016/j.gca.2010.02.017

Kappler, A., Schink, B., and Newman, D. K. (2005). Fe (III) mineral formation and cell encrustation by the nitrate-dependent Fe (II)-oxidizer strain BoFeN1. *Geobiology* 3, 235–245. doi: 10.1128/AEM.03277-13

Kappler, A., and Straub, K. L. (2005). Geomicrobiological cycling of iron. *Rev. Mineral. Geochem.* 59, 85–108. doi: 10.1128/AEM.01151-16

King, G. M. (2015). Carbon monoxide as a metabolic energy source for extremely halophilic microbes: implications for microbial activity in Mars regolith. *Proc. Natl. Acad. Sci. U.S.A.* 112, 4465–4470. doi: 10.1073/pnas.1424989112

Kish, A., Miot, J., Lombard, C., Guigner, J.-M., Bernard, S., Zirah, S., et al. (2016). Preservation of archaeal surface layer structure during mineralization. *Sci. Rep.* 6:26152. doi: 10.1038/srep26152

Klueglein, N., Picardal, F., Zedda, M., Zwiener, C., and Kappler, A. (2015). Oxidation of Fe (II)-EDTA by nitrite and by two nitrate-reducing Fe (II)-oxidizing *Acidovorax* strains. *Geobiology* 13, 198–207. doi: 10.1111/gbi.12125

Klueglein, N., Zeitvogel, F., Stierhof, Y.-D., Floetenmeyer, M., Konhauser, K. O., Kappler, A., et al. (2014). Potential role of nitrite for abiotic Fe (II) oxidation and cell encrustation during nitrate reduction by denitrifying bacteria. *Appl. Environ. Microbiol.* 80, 1051–1061. doi: 10.1128/AEM.03277-13

Konhauser, K. O., Jones, B., Phoenix, V. R., Ferris, G., and Renaut, R. W. (2004). The microbial role in hot spring silicification. *Ambio* 33, 552–558. doi: 10.1579/0044-7447-33.8.552

Konn, C., Charlou, J.-L., Donval, J.-P., Holm, N., Dehairs, F., and Bouillon, S. (2009). Hydrocarbons and oxidized organic compounds in hydrothermal fluids from Rainbow and Lost City ultramafic-hosted vents. *Chem. Geol.* 258, 299–314. doi: 10.1016/j.chemgeo.2008.10.034

Kounaves, S. P., Carrier, B. L., O'Neil, G. D., Stroble, S. T., and Claire, M. W. (2014). Evidence of Martian perchlorate, chlorate, and nitrate in Mars meteorite EETA79001: implications for oxidants and organics. *Icarus* 229, 206–213. doi: 10.1016/j.icarus.2013.11.012

Kumaraswamy, R., Sjollema, K., Kuenen, G., van Loosdrecht, M., and Muyzer, G. (2006). Nitrate-dependent $[Fe(II)EDTA]^{2-}$ oxidation by *Paracoccus ferrooxidans* sp. nov., isolated from a denitrifying bioreactor. *Syst. Appl. Microbiol.* 29, 276–286. doi: 10.1016/j.syapm.2005.08.001

Lack, J. G., Chaudhuri, S. K., Chakraborty, R., Achenbach, L. A., and Coates, J. D. (2002). Anaerobic biooxidation of Fe(II) by *Dechlorosoma suillum*. *Microb. Ecol.* 43, 424–431. doi: 10.1007/s00248-001-1061-1

Lalonde, K., Mucci, A., Ouellet, A., and Gélinas, Y. (2012). Preservation of organic matter in sediments promoted by iron. *Nature* 483, 198–200. doi: 10.1038/nature10855

Lanza, N. L., Wiens, R. C., Arvidson, R. E., Clark, B. C., Fischer, W. W., Gellert, R., et al. (2016). Oxidation of manganese in an ancient aquifer,

Kimberley formation, Gale crater, Mars. *Geophys. Res. Lett.* 43, 7398–7407. doi: 10.1002/2016GL069109

Laufer, K., Røy, H., Jørgensen, B. B., and Kappler, A. (2016). Evidence for the existence of autotrophic nitrate-reducing Fe (II)-oxidizing bacteria in marine coastal sediment. *Appl. Environ. Microbiol.* 82, 6120–6131. doi: 10.1128/AEM.01570-16

Lopez-Reyes, G., Rull, F., Venegas, G., Westall, F., Foucher, F., Bost, N., et al. (2013). Analysis of the scientific capabilities of the ExoMars Raman Laser Spectrometer instrument. *Eur. J. Mineral.* 25, 721–733. doi: 10.1127/0935-1221/2013/0025-2317

Lovley, D. R., Baedecker, M. J., Lonergan, D. J., Cozzarelli, I. M., Phillips, E. J., and Siegel, D. I. (1989). Oxidation of aromatic contaminants coupled to microbial iron reduction. *Nature* 339, 297–300. doi: 10.1038/339297a0

Lovley, D. R., and Phillips, E. J. (1988). Novel mode of microbial energy metabolism: organic carbon oxidation coupled to dissimilatory reduction of iron or manganese. *Appl. Environ. Microbiol.* 54, 1472–1480.

Madigan, M. T., Martinko, J. M., Dunlap, P. V., and Clark, D. P. (2009). *Brock Biology of Microorganisms*, 12th Edn. San Francisco, CA: Pearson Benjamin Cummings.

Mahaffy, P. R., Webster, C. R., Atreya, S. K., Franz, H., Wong, M., Conrad, P. G., et al. (2013). Abundance and isotopic composition of gases in the Martian atmosphere from the Curiosity rover. *Science* 341, 263–266. doi: 10.1126/science.1237966

Malin, M. C., and Edgett, K. S. (2003). Evidence for persistent flow and aqueous sedimentation on early Mars. *Science* 302, 1931–1934. doi: 10.1126/science.1090544

Mangold, N., Carter, J., Poulet, F., Dehouck, E., Ansan, V., and Loizeau, D. (2012). Late Hesperian aqueous alteration at Majuro crater, Mars. *Planet. Space Sci.* 72, 18–30. doi: 10.1016/j.pss.2012.03.014

Manning, C. V., Zahnle, K. J., and McKay, C. P. (2009). Impact processing of nitrogen on early Mars. *Icarus* 199, 273–285. doi: 10.1016/j.icarus.2008.10.015

Martin, W., Baross, J., Kelley, D., and Russell, M. J. (2008). Hydrothermal vents and the origin of life. *Nat. Rev. Microbiol.* 6, 805–814. doi: 10.1038/nrmicro1991

Martín-Torres, F. J., Zorzano, M.-P., Valentín-Serrano, P., Harri, A.-M., Genzer, M., Kemppinen, O., et al. (2015). Transient liquid water and water activity at Gale crater on Mars. *Nat. Geosci.* 8, 357–361. doi: 10.1038/ngeo2412

Marzo, G. A., Davila, A. F., Tornabene, L. L., Dohm, J. M., Fairén, A. G., Gross, C., et al. (2010). Evidence for Hesperian impact-induced hydrothermalism on Mars. *Icarus* 208, 667–683. doi: 10.1016/j.icarus.2010.03.013

McSween, H. Y., Grove, T. L., and Wyatt, M. B. (2003). Constraints on the composition and petrogenesis of the Martian crust. *J. Geophys. Res. Planets* 108:5135. doi: 10.1029/2003JE002175

McSween, H. Y., Taylor, G. J., and Wyatt, M. B. (2009). Elemental composition of the Martian crust. *Science* 324, 736–739. doi: 10.1126/science.1165871

Michalski, J. R., Cuadros, J., Niles, P. B., Parnell, J., Rogers, A. D., and Wright, S. P. (2013). Groundwater activity on Mars and implications for a deep biosphere. *Nat. Geosci.* 6, 133–138. doi: 10.1038/ngeo1706

Millero, F. J., Sotolongo, S., and Izaguirre, M. (1987). The oxidation kinetics of Fe (II) in seawater. *Geochim. Cosmochim. Acta* 51, 793–801. doi: 10.1016/0016-7037(87)90093-7

Ming, D. W., Archer, P. D., Glavin, D. P., Eigenbrode, J. L., Franz, H. B., Sutter, B., et al. (2014). Volatile and organic compositions of sedimentary rocks in Yellowknife Bay, Gale crater, Mars. *Science* 343:1245267. doi: 10.1126/science.1245267

Ming, D. W., Mittlefehldt, D. W., Morris, R. V., Golden, D. C., Gellert, R., Yen, A., et al. (2006). Geochemical and mineralogical indicators for aqueous processes in the Columbia Hills of Gusev crater, Mars. *J. Geophys. Res. Planets* 111:E02S12. doi: 10.1029/2005JE002560

Miot, J., Benzerara, K., Morin, G., Kappler, A., Bernard, S., Obst, M., et al. (2009). Iron biomineralization by anaerobic neutrophilic iron-oxidizing bacteria. *Geochim. Cosmochim. Acta* 73, 696–711. doi: 10.1016/j.gca.2008.10.033

Miot, J., Bernard, S., Bourreau, M., Guyot, F., and Kish, A. (2017). Experimental maturation of *Archaea* encrusted by Fe-phosphates. *Sci. Rep.* 7:16984. doi: 10.1038/s41598-017-17111-9

Miot, J., and Etique, M. (2016). "Formation and transformation of iron-bearing minerals by iron(II)-oxidizing and iron(III)-reducing bacteria," in *Iron Oxides: From Nature to Applications*, ed. D. Faivre (Weinheim: Wiley-VCH), 53–98.

Miot, J., Jézéquel, D., Benzerara, K., Cordier, L., Rivas-Lamelo, S., Skouri-Panet, F., et al. (2016). Mineralogical diversity in lake Pavin: connections with water column chemistry and biomineralization processes. *Minerals* 6:24. doi: 10.3390/min6020024

Miot, J., Li, J., Benzerara, K., Sougrati, M. T., Ona-Nguema, G., Bernard, S., et al. (2014a). Formation of single domain magnetite by green rust oxidation promoted by microbial anaerobic nitrate-dependent iron oxidation. *Geochim. Cosmochim. Acta* 139, 327–343. doi: 10.1016/j.gca.2014.04.047

Miot, J., Maclellan, K., Benzerara, K., and Boisset, N. (2011). Preservation of protein globules and peptidoglycan in the mineralized cell wall of nitrate-reducing, iron(II)-oxidizing bacteria: a cryo-electron microscopy study. *Geobiology* 9, 459–470. doi: 10.1111/j.1472-4669.2011.00298.x

Miot, J., Recham, N., Larcher, D., Guyot, F., Brest, J., and Tarascon, J.-M. (2014b). Biomineralized α-Fe_2O_3: texture and electrochemical reaction with Li. *Energy Environ. Sci.* 7, 451–460. doi: 10.1039/C3EE41767K

Miot, J., Remusat, L., Duprat, E., Gonzalez, A., Pont, S., and Poinsot, M. (2015). Fe biomineralization mirrors individual metabolic activity in a nitrate-dependent Fe (II)-oxidizer. *Front. Microbiol.* 6:879. doi: 10.3389/fmicb.2015.00879

Mirvaux, B., Recham, N., Miot, J., Courty, M., Bernard, S., Beyssac, O., et al. (2016). Iron phosphate/bacteria composites as precursors for textured electrode materials with enhanced electrochemical properties. *J. Electrochem. Soc.* 163, A2139–A2148. doi: 10.1149/2.0101610jes

Montoya, L., Vizioli, C., Rodríguez, N., Rastoll, M. J., Amils, R., and Marin, I. (2013). Microbial community composition of Tirez lagoon (Spain), a highly sulfated athalassohaline environment. *Aquat. Biosyst.* 9:19. doi: 10.1186/2046-9063-9-19

Morgan, B., and Lahav, O. (2007). The effect of pH on the kinetics of spontaneous Fe (II) oxidation by O_2 in aqueous solution–basic principles and a simple heuristic description. *Chemosphere* 68, 2080–2084. doi: 10.1016/j.chemosphere.2007.02.015

Morris, R. V., Klingelhoefer, G., Schröder, C., Rodionov, D. S., Yen, A., Ming, D. W., et al. (2006a). Mössbauer mineralogy of rock, soil, and dust at Gusev crater, Mars: spirit's journey through weakly altered olivine basalt on the plains and pervasively altered basalt in the Columbia Hills. *J. Geophys. Res. Planets* 111:E02S13. doi: 10.1029/2005JE002584

Morris, R. V., Klingelhoefer, G., Schröder, C., Rodionov, D. S., Yen, A., Ming, D. W., et al. (2006b). Mössbauer mineralogy of rock, soil, and dust at Meridiani Planum, Mars: opportunity's journey across sulfate-rich outcrop, basaltic sand and dust, and hematite lag deposits. *J. Geophys. Res. Planets* 111:E12S15. doi: 10.1029/2006JE002791

Morris, R. V., Vaniman, D. T., Blake, D. F., Gellert, R., Chipera, S. J., Rampe, E. B., et al. (2016). Silicic volcanism on Mars evidenced by tridymite in high-SiO_2 sedimentary rock at Gale crater. *Proc. Natl. Acad. Sci. U.S.A.* 113, 7071–7076. doi: 10.1073/pnas.1607098113

Muehe, E. M., Gerhardt, S., Schink, B., and Kappler, A. (2009). Ecophysiology and the energetic benefit of mixotrophic Fe (II) oxidation by various strains of nitrate-reducing bacteria. *FEMS Microbiol. Ecol.* 70, 335–343. doi: 10.1111/j.1574-6941.2009.00755.x

Myers, C. R., and Nealson, K. H. (1988). Microbial reduction of manganese oxides: interactions with iron and sulfur. *Geochim. Cosmochim. Acta* 52, 2727–2732. doi: 10.1016/0016-7037(88)90041-5

Nachon, M., Mangold, N., Forni, O., Kah, L. C., Cousin, A., Wiens, R. C., et al. (2017). Chemistry of diagenetic features analyzed by ChemCam at Pahrump Hills, Gale crater, Mars. *Icarus* 281, 121–136. doi: 10.1016/j.icarus.2016.08.026

Navarro-González, R., Vargas, E., de La Rosa, J., Raga, A. C., and McKay, C. P. (2010). Reanalysis of the Viking results suggests perchlorate and organics at midlatitudes on Mars. *J. Geophys. Res. Planets* 115:E12010. doi: 10.1029/2010JE003599

Nealson, K. H. (1997). The limits of life on Earth and searching for life on Mars. *J. Geophys. Res. Planets* 102, 23675–23686. doi: 10.1029/97JE01996

Nie, N. X., Dauphas, N., and Greenwood, R. C. (2017). Iron and oxygen isotope fractionation during iron UV photo-oxidation: implications for early Earth and Mars. *Earth Planet. Sci. Lett.* 458, 179–191. doi: 10.1016/j.epsl.2016.10.035

Nixon, S. L. (2014). *Microbial Iron Reduction on Earth and Mars*. Ph.D. thesis: The Open University, Milton Keynes.

Nixon, S. L., Cockell, C. S., and Tranter, M. (2012). Limitations to a microbial iron cycle on Mars. *Planet. Space Sci.* 72, 116–128. doi: 10.1016/j.pss.2012.04.003

Nixon, S. L., Cousins, C. R., and Cockell, C. S. (2013). Plausible microbial metabolisms on Mars. *Astron. Geophys.* 54, 1.13–1.16. doi: 10.1093/astrogeo/ats034

Oren, A., Bardavid, R. E., and Mana, L. (2014). Perchlorate and halophilic prokaryotes: implications for possible halophilic life on Mars. *Extremophiles* 18, 75–80. doi: 10.1007/s00792-013-0594-9

Osinski, G. R., Tornabene, L. L., Banerjee, N. R., Cockell, C. S., Flemming, R., Izawa, M. R., et al. (2013). Impact-generated hydrothermal systems on Earth and Mars. *Icarus* 224, 347–363. doi: 10.1038/srep03487

Palucis, M. C., Dietrich, W. E., Williams, R. M., Hayes, A. G., Parker, T., Sumner, D. Y., et al. (2016). Sequence and relative timing of large lakes in Gale crater (Mars) after the formation of Mount Sharp. *J. Geophys. Res. Planets* 121, 472–496. doi: 10.1002/2015JE004905

Pantke, C., Obst, M., Benzerara, K., Morin, G., Ona-Nguema, G., Dippon, U., et al. (2012). Green rust formation during Fe (II) oxidation by the nitrate-reducing *Acidovorax* sp. *strain* BoFeN1. *Environ. Sci. Technol.* 46, 1439–1446. doi: 10.1021/es2016457

Parnell, J., Lee, P., Cockell, C. S., and Osinski, G. R. (2004). Microbial colonization in impact-generated hydrothermal sulphate deposits, Haughton impact structure, and implications for sulphates on Mars. *Int. J. Astrobiol.* 3, 247–256. doi: 10.1017/S1473550404001995

Pirajno, F. (ed.). (2009). "Hydrothermal processes associated with meteorite impacts," in *Hydrothermal Processes and Mineral Systems* (Dordrecht: Springer), 1097–1130. doi: 10.1007/978-1-4020-8613-7_11

Popa, R., Smith, A. R., Popa, R., Boone, J., and Fisk, M. (2012). Olivine-respiring bacteria isolated from the rock-ice interface in a lava-tube cave, a Mars analog environment. *Astrobiology* 12, 9–18. doi: 10.1089/ast.2011.0639

Raghoebarsing, A. A., Pol, A., van de Pas-Schoonen, K. T., Smolders, A. J. P., Ettwig, K. F., Rijpstra, W. I. C., et al. (2006). A microbial consortium couples anaerobic methane oxidation to denitrification. *Nature* 440, 918–921. doi: 10.1038/nature04617

Raiswell, R., and Canfield, D. E. (2012). The iron biogeochemical cycle past and present. *Geochem. Perspect.* 1, 1–322. doi: 10.1038/nature20772

Ramirez, R. M., Kopparapu, R., Zugger, M. E., Robinson, T. D., Freedman, R., and Kasting, J. F. (2014). Warming early Mars with CO_2 and H_2. *Nat. Geosci.* 7, 59–63. doi: 10.1038/ngeo2000

Rampe, E. B., Ming, D. W., Blake, D. F., Bristow, T. F., Chipera, S. J., Grotzinger, J. P., et al. (2017a). Mineralogy of an ancient lacustrine mudstone succession from the Murray formation, Gale crater, Mars. *Earth Planet. Sci. Lett.* 471, 172–185. doi: 10.1016/j.epsl.2017.04.021

Rampe, E. B., Ming, D. W., Grotzinger, J. P., Morris, R. V., Blake, D. F., Vaniman, D. T., et al. (2017b). "Mineral trends in early Hesperian lacustrine mudstone at Gale crater, Mars," in *Proceedings of the 48th Lunar and Planetary Science Conference*, The Woodlands, TX.

Reimers, C. E., Fischer, K. M., Merewether, R., Smith, K., and Jahnke, R. A. (1986). Oxygen microprofiles measured in situ in deep ocean sediments. *Nature* 320, 741–744. doi: 10.1038/320741a0

Revsbech, N. P., Sorensen, J., Blackburn, T. H., and Lomholt, J. P. (1980). Distribution of oxygen in marine sediments measured with microelectrodes. *Limnol. Oceanogr.* 25, 403–411. doi: 10.4319/lo.1980.25.3.0403

Roden, E. E., Sobolev, D., Glazer, B., and Luther, G. W. (2004). Potential for microscale bacterial Fe redox cycling at the aerobic-anaerobic interface. *Geomicrobiol. J.* 21, 379–391. doi: 10.1080/01490450490485872

Santelli, C. M., Welch, S. A., Westrich, H. R., and Banfield, J. F. (2001). The effect of Fe-oxidizing bacteria on Fe-silicate mineral dissolution. *Chem. Geol.* 180, 99–115. doi: 10.1016/S0009-2541(01)00308-4

Schädler, S., Burkhardt, C., Hegler, F., Straub, K., Miot, J., Benzerara, K., et al. (2009). Formation of cell-iron-mineral aggregates by phototrophic and nitrate-reducing anaerobic Fe (II)-oxidizing bacteria. *Geomicrobiol. J.* 26, 93–103. doi: 10.1111/gbi.12088

Schieber, J. (2002). Sedimentary pyrite: a window into the microbial past. *Geology* 30, 531–534. doi: 10.1130/0091-7613(2002)030<0531:SPAWIT>2.0.CO;2

Schuerger, A. C., and Nicholson, W. L. (2016). Twenty species of hypobarophilic bacteria recovered from diverse soils exhibit growth under simulated Martian conditions at 0.7 kPa. *Astrobiology* 16, 964–976. doi: 10.1089/ast.2016.1587

Schwenzer, S. P., Bridges, J. C., Wiens, R. C., Conrad, P. G., Kelley, S. P., Leveille, R., et al. (2016). Fluids during diagenesis and sulfate vein formation in sediments at Gale crater, Mars. *Meteorit. Planet. Sci.* 51, 2175–2202. doi: 10.1111/maps.12668

Schwenzer, S. P., and Kring, D. A. (2009). Impact-generated hydrothermal systems capable of forming phyllosilicates on Noachian Mars. *Geology* 37, 1091–1094. doi: 10.1130/G30340A.1

Sephton, M. A., Wright, I. P., Gilmour, I., de Leeuw, J. W., Grady, M. M., and Pillinger, C. T. (2002). High molecular weight organic matter in Martian meteorites. *Planet. Space Sci.* 50, 711–716. doi: 10.1016/S0032-0633(02)00053-3

Sholes, S. F., Smith, M. L., Claire, M. W., Zahnle, K. J., and Catling, D. C. (2017). Anoxic atmospheres on Mars driven by volcanism: implications for past environments and life. *Icarus* 290, 46–62. doi: 10.1016/j.icarus.2017.02.022

Smith, A. R. (2011). *Subsurface Igneous Mineral Microbiology: Iron-Oxidizing Organotrophs on Olivine Surfaces and the Significance of Mineral Heterogeneity in Basalts*. Master thesis, Portland State University, Portland.

Smith, M. L., Claire, M. W., Catling, D. C., and Zahnle, K. J. (2014). The formation of sulfate, nitrate and perchlorate salts in the Martian atmosphere. *Icarus* 231, 51–64. doi: 10.1016/j.icarus.2013.11.031

Squyres, S. W., Arvidson, R. E., Bell, J., Calef, F., Clark, B., Cohen, B., et al. (2012). Ancient impact and aqueous processes at Endeavour Crater, Mars. *Science* 336, 570–576. doi: 10.1126/science.1220476

Squyres, S. W., Grotzinger, J. P., Arvidson, R. E., Bell, J. F., Calvin, W., Christensen, P. R., et al. (2004). In situ evidence for an ancient aqueous environment at Meridiani Planum, Mars. *Science* 306, 1709–1714. doi: 10.1126/science.1104559

Squyres, S. W., and Knoll, A. H. (2005). Sedimentary rocks at Meridiani Planum: 006Frigin, diagenesis, and implications for life on Mars. *Earth Planet. Sci. Lett.* 240, 1–10. doi: 10.1016/j.epsl.2005.09.038

Steele, A., McCubbin, F. M., Fries, M., Kater, L., Boctor, N. Z., Fogel, M. L., et al. (2012). A reduced organic carbon component in Martian basalts. *Science* 337, 212–215. doi: 10.1126/science.1220715

Stern, J. C., Sutter, B., Freissinet, C., Navarro-González, R., McKay, C. P., Archer, P. D., et al. (2015). Evidence for indigenous nitrogen in sedimentary and aeolian deposits from the Curiosity rover investigations at Gale crater, Mars. *Proc. Natl. Acad. Sci. U.S.A.* 112, 4245–4250. doi: 10.1073/pnas.1420932112

Stern, J. C., Sutter, B., Jackson, W. A., Navarro-González, R., McKay, C. P., Ming, D. W., et al. (2017). The nitrate/(per)chlorate relationship on Mars. *Geophys. Res. Lett.* 44, 2643–2651. doi: 10.1002/2016GL072199

Stevens, M. H., Evans, J., Schneider, N. M., Stewart, A. I. F., Deighan, J., Jain, S. K., et al. (2015). New observations of molecular nitrogen in the Martian upper atmosphere by IUVS on MAVEN. *Geophys. Res. Lett.* 42, 9050–9056. doi: 10.1002/2015GL065319

Straub, K. L., Benz, M., Schink, B., and Widdel, F. (1996). Anaerobic, nitrate-dependent microbial oxidation of ferrous iron. *Appl. Environ. Microbiol.* 62, 1458–1460.

Straub, K. L., and Buchholz-Cleven, B. E. (1998). Enumeration and detection of anaerobic ferrous iron-oxidizing, nitrate-reducing bacteria from diverse European sediments. *Appl. Environ. Microbiol.* 64, 4846–4856.

Straub, K. L., Schönhuber, W. A., Buchholz-Cleven, B. E., and Schink, B. (2004). Diversity of ferrous iron-oxidizing, nitrate-reducing bacteria and their involvement in oxygen-independent iron cycling. *Geomicrobiol. J.* 21, 371–378. doi: 10.1080/01490450490485854

Strohm, T. O., Griffin, B., Zumft, W. G., and Schink, B. (2007). Growth yields in bacterial denitrification and nitrate ammonification. *Appl. Environ. Microbiol.* 73, 1420–1424. doi: 10.1128/AEM.02508-06

Summers, D. P., Basa, R. C., Khare, B., and Rodoni, D. (2012). Abiotic nitrogen fixation on terrestrial planets: reduction of NO to ammonia by FeS. *Astrobiology* 12, 107–114. doi: 10.1089/ast.2011.0646

Summers, D. P., and Khare, B. (2007). Nitrogen fixation on early Mars and other terrestrial planets: experimental demonstration of abiotic fixation reactions to nitrite and nitrate. *Astrobiology* 7, 333–341. doi: 10.1089/ast.2006.0032

Summers, S. (2013). *The Bacterial Ecology and Function from a Sub-surface Critical Zone*. Ph.D. thesis, The Open University, Milton Keynes.

Sutter, B., Eigenbrode, J. L., Steele, A., McAdam, A., Ming, D. W., Archer, D. Jr., et al. (2016). "The sample analysis at Mars (SAM) detections of CO_2 and CO in sedimentary material from Gale crater, Mars: implications for the presence of organic carbon and microbial habitability on Mars," in *Proceedings of the AGU Fall Meeting*, New Orleans, LA.

Toporski, J. K., Steele, A., Westall, F., Thomas-Keprta, K. L., and McKay, D. S. (2002). The simulated silicification of bacteria–new clues to the

modes and timing of bacterial preservation and implications for the search for extraterrestrial microfossils. *Astrobiology* 2, 1–26. doi: 10.1089/153110702753621312

Tosca, N. J., and McLennan, S. M. (2006). Chemical divides and evaporite assemblages on Mars. *Earth Planet. Sci. Lett.* 241, 21–31. doi: 10.1016/j.epsl.2005.10.021

Tosca, N. J., and McLennan, S. M. (2009). Experimental constraints on the evaporation of partially oxidized acid-sulfate waters at the Martian surface. *Geochim. Cosmochim. Acta* 73, 1205–1222. doi: 10.1016/j.gca.2008.11.015

Tuff, J., Wade, J., and Wood, B. (2013). Volcanism on Mars controlled by early oxidation of the upper mantle. *Nature* 498, 342–345. doi: 10.1038/nature12225

Vaniman, D. T., Bish, D. L., Ming, D. W., Bristow, T. F., Morris, R. V., Blake, D. F., et al. (2013). Mineralogy of a mudstone at Yellowknife Bay, Gale crater, Mars. *Science* 343:1243480. doi: 10.1126/science.1243480

Visscher, P. T., Beukema, J., and van Gemerden, H. (1991). In situ characterization of sediments: measurements of oxygen and sulfide profiles with a novel combined needle electrode. *Limnol. Oceanogr.* 36, 1476–1480. doi: 10.4319/lo.1991.36.7.1476

Wacey, D., McLoughlin, N., Kilburn, M. R., Saunders, M., Cliff, J. B., Kong, C., et al. (2013). Nanoscale analysis of pyritized microfossils reveals differential heterotrophic consumption in the 1.9-Ga Gunflint chert. *Proc. Natl. Acad. Sci. U.S.A.* 110, 8020–8024. doi: 10.1073/pnas.1221965110

Weber, K. A., Achenbach, L. A., and Coates, J. D. (2006a). Microorganisms pumping iron: anaerobic microbial iron oxidation and reduction. *Nat. Rev. Microbiol.* 4, 752–764.

Weber, K. A., Hedrick, D. B., Peacock, A. D., Thrash, J. C., White, D. C., Achenbach, L. A., et al. (2009). Physiological and taxonomic description of the novel autotrophic, metal oxidizing bacterium, *Pseudogulbenkiania* sp. strain 2002. *Appl. Microbiol. Biotechnol.* 83, 555–565. doi: 10.1007/s00253-009-1934-7

Weber, K. A., Pollock, J., Cole, K. A., O'Connor, S. M., Achenbach, L. A., and Coates, J. D. (2006b). Anaerobic nitrate-dependent iron (II) bio-oxidation by a novel lithoautotrophic betaproteobacterium, strain 2002. *Appl. Environ. Microbiol.* 72, 686–694.

Webster, C. R., Mahaffy, P. R., Atreya, S. K., Flesch, G. J., Mischna, M. A., Meslin, P.-Y., et al. (2015). Mars methane detection and variability at Gale crater. *Science* 347, 415–417. doi: 10.1126/science.1261713

Welhan, J. A., and Craig, H. (1983). "Methane, hydrogen and helium in hydrothermal fluids at 21 N on the East Pacific Rise," in *Hydrothermal Processes at Seafloor Spreading Centers*, eds P. A. Rona, K. Boström L. Laubier, and K. L. Smith (Berlin: Springer), 391–409. doi: 10.1007/978-1-4899-0402-7_17

Wheat, C. G., Feely, R. A., and Mottl, M. J. (1996). Phosphate removal by oceanic hydrothermal processes: an update of the phosphorus budget in the oceans. *Geochim. Cosmochim. Acta* 60, 3593–3608. doi: 10.1016/0016-7037(96)00189-5

Williams, R. M., Grotzinger, J. P., Dietrich, W. E., Gupta, S., Sumner, D. Y., Wiens, R. C., et al. (2013). Martian fluvial conglomerates at Gale crater. *Science* 340, 1068–1072. doi: 10.1126/science.1237317

Yen, A. S., Ming, D. W., Vaniman, D. T., Gellert, R., Blake, D. F., Morris, R. V., et al. (2017). Multiple stages of aqueous alteration along fractures in mudstone and sandstone strata in Gale Crater, Mars. *Earth Planet. Sci. Lett.* 471, 186–198. doi: 10.1016/j.epsl.2017.04.033

Yen, A. S., Mittlefehldt, D. W., McLennan, S. M., Gellert, R., Bell, J., McSween, H. Y., et al. (2006). Nickel on Mars: constraints on meteoritic material at the surface. *J. Geophys. Res. Planets* 111:E12S11. doi: 10.1029/2006JE002797

Conflict of Interest Statement: The authors declare that the research was conducted in the absence of any commercial or financial relationships that could be construed as a potential conflict of interest.

frontiers in Microbiology

ORIGINAL RESEARCH
published: 26 September 2017
doi: 10.3389/fmicb.2017.01819

Microbial Diversity in a Hypersaline Sulfate Lake: A Terrestrial Analog of Ancient Mars

Alexandra Pontefract[1,2], Ting F. Zhu[1†], Virginia K. Walker[3], Holli Hepburn[2], Clarissa Lui[1], Maria T. Zuber[1], Gary Ruvkun[2,4] and Christopher E. Carr[1,2]*

[1] Department of Earth, Atmospheric and Planetary Sciences, Massachusetts Institute of Technology, Cambridge, MA, United States, [2] Department of Molecular Biology, Massachusetts General Hospital, Boston, MA, United States, [3] Department of Biology, Queens University, Kingston, ON, Canada, [4] Department of Genetics, Harvard Medical School, Boston, MA, United States

Life can persist under severe osmotic stress and low water activity in hypersaline environments. On Mars, evidence for the past presence of saline bodies of water is prevalent and resulted in the widespread deposition of sulfate and chloride salts. Here we investigate Spotted Lake (British Columbia, Canada), a hypersaline lake with extreme (>3 M) levels of sulfate salts as an exemplar of the conditions thought to be associated with ancient Mars. We provide the first characterization of microbial structure in Spotted Lake sediments through metagenomic sequencing, and report a bacteria-dominated community with abundant Proteobacteria, Firmicutes, and Bacteroidetes, as well as diverse extremophiles. Microbial abundance and functional comparisons reveal similarities to Ace Lake, a meromictic Antarctic lake with anoxic and sulfidic bottom waters. Our analysis suggests that hypersaline-associated species occupy niches characterized foremost by differential abundance of Archaea, uncharacterized Bacteria, and Cyanobacteria. Potential biosignatures in this environment are discussed, specifically the likelihood of a strong sulfur isotopic fractionation record within the sediments due to the presence of sulfate reducing bacteria. With its high sulfate levels and seasonal freeze-thaw cycles, Spotted Lake is an analog for ancient paleolakes on Mars in which sulfate salt deposits may have offered periodically habitable environments, and could have concentrated and preserved organic materials or their biomarkers over geologic time.

Keywords: mars analog, extremophiles, hypersaline environments, metagenomic, spotted lake, magnesium sulfate

OPEN ACCESS

Edited by:
Karen Olsson-Francis, The Open University, United Kingdom

Reviewed by:
André Antunes, Edge Hill University, United Kingdom
Melanie R. Mormile, Missouri University of Science and Technology, United States

***Correspondence:**
Christopher E. Carr
chrisc@mit.edu

***Present Address:**
Ting F. Zhu, School of Life Sciences, Tsinghua University, Beijing, China

Specialty section:
This article was submitted to Extreme Microbiology, a section of the journal Frontiers in Microbiology

Received: *12 June 2017*
Accepted: *06 September 2017*
Published: *26 September 2017*

Citation:
Pontefract A, Zhu TF, Walker VK, Hepburn H, Lui C, Zuber MT, Ruvkun G and Carr CE (2017) Microbial Diversity in a Hypersaline Sulfate Lake: A Terrestrial Analog of Ancient Mars. Front. Microbiol. 8:1819. doi: 10.3389/fmicb.2017.01819

INTRODUCTION

Hypersaline environments impose severe stresses on microorganisms, such as high osmotic pressures and potentially low (a_w ~0.75) water activities (Grant, 2004). Despite this, life exists over a wide range of salt concentrations in naturally occurring environments with an unexpected level of diversity (Ley et al., 2006). Hypersaline brines have salinities ranging from 35 g/L to more than 400 g/L. Don Juan Pond, a $CaCl_2$-dominated Antarctic brine is considered one of the most saline bodies of water on Earth (40–45% by mass; Meyer et al., 1962; Marion, 1997; Dickson et al., 2013), surpassed only by the $MgCl_2$-rich Discovery Brine in the Mediterranean, which can reach levels of

up to 500 g/L and with the lowest water activity level, $a_w = 0.382$, recorded for a brine on Earth (Fox-Powell et al., 2016). Brines can also be highly chaotropic, or membrane destabilizing. Strong chaotropes such as Ca^{2+} and Mg^{2+}, when not countered by a suitable kosmotrope (stabilizing ion), prove incredibly hostile to life as evidenced by the apparent lack of viable organisms in both Don Juan Pond and the Discovery Brine. Environments with high levels of kosmotropic sulfate salts however, can sustain life if water activity is sufficiently high (Baldwin, 1996). A saturated $MgSO_4$ solution has an $a_w = 0.85$ (Ha and Chan, 1999), too low for most bacteria to survive but is habitable to some eukaryotes (Stevenson et al., 2015). At such high salinities, the ionic strength of a solution can also become a problem for microorganisms, where a high charge density can perturb cellular activities (Fox-Powell et al., 2016). Thus, the habitability of a saline environment relies heavily on water activity, a function of the ionic composition and concentration of the brine.

Beyond the Earth, orbital and *in situ* observations of Mars have revealed that extensive water flows, as well as saline and acidic fluids, were once present on the planet's surface (Tosca et al., 2008). Ancient Mars transitioned from wet to dry during the Hesperian (beginning 3.7 Ga), a time of ephemeral lakes, resulting in the widespread deposition of sulfate and chloride salts observed today on the Martian surface (Wanke et al., 2001; Clark et al., 2005; Crisler et al., 2012; Goudge et al., 2016). Magnesium sulfate salts ($MgSO_4 \bullet nH_2O$) are common on Mars and are distributed globally, with some sediments containing 10−30% sulfate by weight (Vaniman et al., 2004; Gendrin et al., 2005). The presence of hydrated magnesium sulfates within the rim of Columbia Crater is ascribed to the existence of a paleolake, which at times must have been hypersaline in nature (Wray et al., 2011). Targets for future life-detection missions include such salty environments that could have once been habitable, and are relevant today because of their potential to retain water and generate liquid water brines (McEwen et al., 2011; Möhlmann and Thomsen, 2011; Chevrier and Valentin, 2012; Karunatillake et al., 2016).

Most brine environments on Earth contain Cl^- as the dominant anion, however, some are rich in SO_4-bearing salts, such as the Basque Lakes and Hot Lake, which lie within the Thompson Plateau in British Columbia (Jenkins, 1918; Foster et al., 2010). This region, located within the rain shadow of the Coast and Cascade Mountains, has experienced 20 significant glaciations in the last ∼1 million years (Church and Ryder, 2010), leaving behind a series of drainage basins with no outlets (endhoreic). A subset of these lakes also have a characteristic "spotted" appearance, including Spotted Lake, which has some of the highest magnesium sulfate concentrations in the world. Such high salt concentrations preserve biosignatures and allow organic compounds, and even entire cells, to be preserved on geologic time scales (e.g., Vreeland et al., 2000; Aubrey et al., 2006). Furthermore, organisms have also been shown to exist in fluid inclusions trapped in rapidly forming salt crystals, and viable isolates have been obtained from inclusions that are on the order of 10^5 years old (e.g., Mormile et al., 2003; Fendrihan et al., 2006).

Despite the unique geochemical composition of Spotted Lake, the microbial diversity of the environment has not been well studied. Here we describe, for the first time, the biological diversity within the sediments of Spotted Lake in order to identify the types of biosignatures that may be preserved, of relevance to the search for life on Mars.

METHODS

Field Site

Spotted Lake (**Figure 1A**, Figure S1) is located in Osoyoos, British Columbia, Canada (49°4′40.86″ N, 119°34′3.01″ W) within Carboniferous to Permian green schist facies rocks, along with dolomites, quartzites, marbles and localized deposits of pyrite and pyrrhotite (Jenkins, 1918). Oxidation of these iron sulfides results in the generation of sulfuric acid and the subsequent weathering of the basin dolomites, yielding high levels of Mg^{2+} and SO_4^{2-} that concentrate in the endorheic lake. As a result, Spotted Lake is rich in magnesium and sodium sulfate salts, and with a slightly alkaline pH. Due to low levels of precipitation in this region, summer evaporation leads to the formation of individual brine pools (**Figure 1B**), which are separated by mud mounds (**Figure 1C**) and surficial salt crusts (Jenkins, 1918; Cannon et al., 2012). Samples from Spotted Lake were collected in October 2010 (**Table 1**); in total, 4 individual ponds were surveyed and samples including water and sediment (top 5–10 cm) were aseptically collected in sterile containers. Water samples were collected first (without disturbing the sediment) in autoclaved plastic sterilization units with samples immediately sealed, and subsequently analyzed for pH and ion concentrations following Wilson et al. (2012). Water activity was measured in triplicate from two brine pools in the laboratory using an AquaLab Dew point activity meter 4TE, and on two sediment samples, at a temperature of 25°C. Sediments (45–100 g) from each pond were collected in 50 mL plastic conical tubes and immediately after collection were transferred to glass test tubes, which were sealed with rubber stoppers, purged with nitrogen, and sealed with a crimped metal band before being frozen at −20°C. All tubes were placed in a cooler with freezer packs for shipment, and stored at −80°C upon arrival. Soil samples from each pond were sent for inductively coupled plasma mass spectrometry (ICP MS) analysis, Bureau Veritas, Canada.

Microscopy

For *in situ* imaging of the environment, soil samples were fixed in glutaraldehyde, dehydrated in ethanol and critical-point dried to preserve cell structure using a Tousimis Auto Samdri 815 Series A Critical Point Dryer following Dykstra and Reuss (2003). Samples were then mounted, carbon coated and imaged using a Zeiss Merlin High-resolution Scanning Electron Microscope (SEM) at 1 kV. Soil samples were also imaged to assess viability: soil was stained using Live/Dead Baclight Bacterial Viability Kit (Life Technologies; now Thermo-Fisher Scientific, Waltham, MA) and then imaged on a Zeiss ApoTome 2.

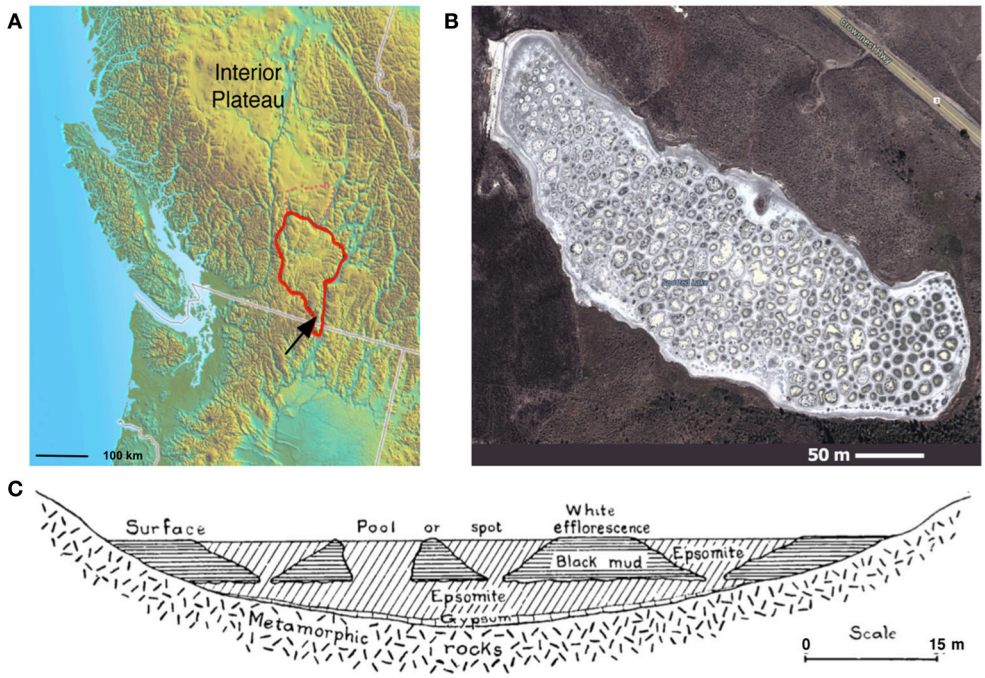

FIGURE 1 | Spotted Lake. **(A)** Spotted Lake (black arrow) is located on the edge of the Thompson Plateau (red line). **(B)** Its hundreds of brine pools are seasonally connected during periods of higher water levels, and separated during periods of low water input and evaporation. **(B)** Imagery © 2014 DigitalGlobe, Map data © 2014 Google. **(C)** During mining of nearby Hot Lake it was discovered that spots represent the bases of inverted cones or cylindrical eposomite masses that connect to a more basal horizontal bed underlain by gypsum. Reprinted from **Figure 4** of Jenkins (1918) with permission from the American Journal of Science.

TABLE 1 | Geochemistry of Spotted Lake water samples.

Major cations	**Concentration (mg/L)**	**Molarity (mM)**
Mg	51,400	2,115
Na	42,600	1,835
K	3,010	77
Ca	214	5
Major anions	**Concentration (mg/L)**	**Molarity (mM)**
SO_4	271,000	2,821
Cl^-	2,700	76
Other	**Concentration (mg/L)**	
Hardness	212,000	
Salinity	370,999	
Water activity	0.98	
Si	8.2	

Values represent an average of four pools.

DNA Extraction and Sequencing

DNA extraction was performed utilizing both a high-input process (MoBio) and a low-input process (Zymo) to explore differences in acquired sequencing data due to extraction protocols (Figure S3). (1) High input method: Genomic DNA (gDNA) was extracted using the MoBio Powersoil DNA isolation kit (Carlsbad, CA), and concentrated with Zymo Research Genomic DNA Clean and Concentrate. Gel electrophoresis and a NanoDrop Spectrophotometer (Thermo Scientific) were used to assess gDNA quality and concentration, respectively. (2) Low input method: gDNA extraction was performed (0.25 g from each of the four samples) using Zymo Research Soil Microbe DNA MicroPrep; eluted gDNA was further subjected to whole genome amplification using phi-29 (GE Healthcare Illustra Ready-To-Go GenomiPhi V3) to produce enough DNA for library construction.

The Ion Torrent PGM system (Rothberg et al., 2011), Ion Xpress Fragment Library and Ion Xpress Template kits were purchased from Ion Torrent Systems (Guilford, CT). Sequencing, library construction and template preparation were performed according to the 200 bp Ion Xpress Fragment Library and Template Preparation protocols, and libraries S1–S4 (high input), and Z1–Z4 (low input) for sediment samples 1–4 were constructed. A single sequencing run was then performed (Table S1) on a 316 chip using 500 flows (equivalent to 125 cycles).

Metagenomic Analysis

Raw sequencing reads were analyzed with Phylosift v1.0.1 (Darling et al., 2014) using default parameters, which included quality trimming of FASTQ data. Microbial community structure was assessed directly from sequencing reads through comparison to reference sequences (37 near-universal single-copy genes,

16S and 18S ribosomal genes, mitochondrial genes, eukaryotic-specific genes, and hundreds of virus-specific genes). Raw reads were also submitted to MG-RAST to confirm Phylosift results, and also for further 16S rRNA phylogenetic and protein functional analyses (Meyer et al., 2008; Glass et al., 2010). For MG-RAST, the default quality control options for quality trimming, dereplication, and screening for common contaminants were used.

In order to compare Spotted Lake metagenomes (Table S2) with previously-analyzed metagenomes, keyword searches for salt-associated metagenomes in addition to a few other sets such as air (in order to include data representing exogenous environmental seeding) were conducted. The resulting list was filtered to exclude virus-specific datasets, contigs/assemblies, and datasets associated with a specific organism, giving a final list of MG-RAST metagenomes for comparison (Table S3). For each of these metagenomes a lowest common ancestor (LCA) analysis was performed at the species level using MG-RAST with the default settings (max *e*-value 10^{-5}, min identity cutoff 60%, min alignment length cutoff 15 bp). An abundance matrix was constructed with one row per metagenome and one column for each unique taxonomic key across all metagenomes. The unique set of taxonomic keys was generated at each taxonomic level and a separate PCA analysis was done for each taxonomic level from domain to species (see Supplementary Material, pg. 2).

RESULTS

Geochemistry

Water pH ranged from 8.0 to 8.3, and a_w was 0.98 for the water column, and ranged from 0.96 to 0.99 within the sediment. Water chemistry measurements revealed brine compositions consisting of SO_4 (2.8 M), Mg (2.1 M), and Na (1.9 M), with minor contributions from K and Cl (**Table 1**), nearly identical to the 1933 historical measurements (McKay, 1935). Total salinity was measured at 37.1% with an approximate molar ratio of $MgSO_4$:Na_2SO_4 of 20:9 consistent with previous identification (Cannon et al., 2012) of minerals including epsomite ($MgSO_4 \bullet 7H_2O$) and mixed Mg-Na salts in various hydration states (**Figure 2A**), e.g., blöedite, konyaite. ICP-MS (**Table 2**) revealed very low silica amounts, <8%, and CaO levels ranging from 17 to 25%. The percentage total for the major oxides ranged from 62 to 66%, which was representative of the fact that a large component of the sediment was comprised of salt and not detectable using the methodology employed. When subtracted from the ideal total of 100%, the remaining ∼33−37% was inferred to be sulfate salt, corresponding with the sulfate concentrations of the water column. Total organic carbon was low, ranging from 1 to 3%.

Metacommunity

Spotted Lake was found to be host to a diverse set of organisms, from macroscopic brine shrimp (**Figure 2B**) to a wide range of bacteria (**Figure 2C**). Imaging of the community through Live/Dead staining revealed a viable population (**Figure 2D**). The abundance assessment of the S1–S4 and Z1–Z4 libraries (representing "high input" vs. "low input" modalities) pooled, revealed respectively 90 and 88% Bacteria, 10 and 4% Eukarya, and 3 and 3% Archaea (**Figure 3**). The S1–S4 and Z1–Z4 libraries varied from each other (**Figures 4A–D**), especially at the sub-domain level. Within the high input libraries, dominant bacterial phyla included Bacteroidetes (33.2%), Proteobacteria (21.4%), and Firmicutes (14.1%). Alternatively, the low-input Z1–Z4 library had a dominant contribution from the Firmicutes (21.3%) only. The highest abundance proteobacterial classes in S1–S4 were δ/ε-proteobacteria (11.2%), γ-proteobacteria (6.1%), and α-proteobacteria (3.2%). While highly diverse at the family to species level, halophiles were well represented, including the genus *Halomonas*, previously found in hypersaline (NaCl) environments, representing 3% of γ-proteobacterial sequences, and the family Rhodobacteraceae (9%), members of which are common in seawater, where they play a key role in marine carbon cycling (Pujalte et al., 2014). Also present were sulfate reducers of the family Desulfobacteraceae (46%), largely comprised of organisms most closely related to the genus *Desulfotignum*, an obligate anaerobe capable of both chemoorganotrophy and chemolithotrophy (Kuever et al., 2001). Sequences belonging to the classes of bacteria lacking a cell wall were also represented: Mollicutes (8%) and Haloplasmatales (1%), the former of which is typically a parasite of eukaryotes (Skennerton et al., 2016), and the latter which is found only in hypersaline environments (Antunes et al., 2008).

Our results underscore the potential for bias in community characterization between "low-input" and "high-input" methodologies, with implications for future Martian expeditions. Not all low-input samples yielded evidence of Archaeal sequences (**Figure 4A**), but consistently demonstrated the presence of β-proteobacteria, which were largely absent in the "high-input" libraries (**Figure 4D**). Utilizing small sample sizes can result in an over- or underrepresentation of species due to the location of the subsample within the larger context, especially where physicochemical boundaries are present, thus care must be taken to extract multiple sub-samples that adequately represent the larger sample of interest. Beyond the issues noted with small sample sizes, whole genome amplification with phi-29 polymerase does result in a preference toward A+T rich genomes (Yilmaz et al., 2010), which may account for the dominance of the Firmicutes in these samples.

Analyses of alpha diversity were abundance weighted and calculated using the Shannon Diversity Index (*H'*). *H'* ranged from 599 to 704, with an average of 666 for high-input samples, and 680 to 1,122, with an average of 802, for low-input samples. To compare species abundance across all metagenomes (**Figure 5A**), a lowest common ancestor (LCA) analysis was performed, using classification down to the species level. This yielded hits in 17,433 unique taxonomic categories, though half of the abundance was captured by only 16 taxonomic categories (**Figure 5B**). Assessment of the metagenomic datasets using these highly abundant taxonomic categories revealed some similarities between Spotted Lake and both hypersaline and Antarctic environments (**Figure 5C**).

Principal components analysis (PCA) on the LCA abundance data (**Figure 6A**) revealed a similar pattern of explanatory power at each level of taxonomic depth: the first three principal

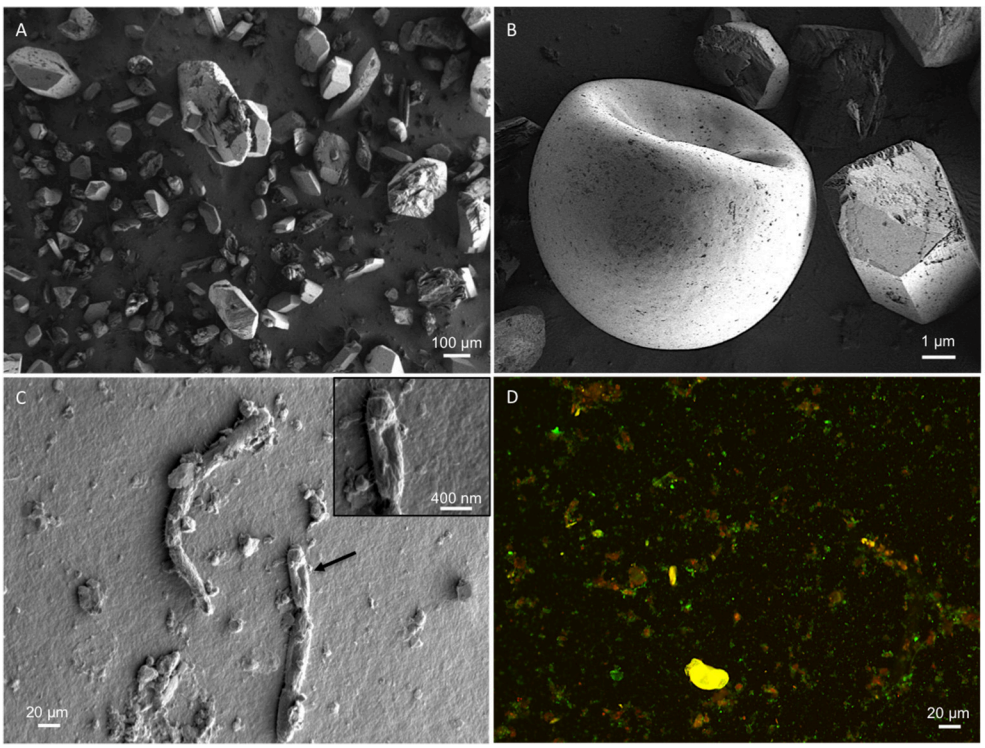

FIGURE 2 | SEM micrographs. Representative micrographs show **(A)** the mineral substrate consisting of sulfate salts; **(B)** a brine shrimp egg (one of many hundreds seen in other micrographs), revealing the presence of higher-order biology in the system; **(C)** presence of *in situ* microbes within the soil samples; **(D)** Sediment-derived microbes, visualized with SYTO 9 and propidium iodide. Original micrographs are available in the Supplementary Material, Figures S4–S8.

TABLE 2 | ICP-MS results for major oxide, total organic carbon, total sulfur composition, and sulfate from the sediment of Spotted Lake.

Sample	Mineral Composition(% Weight)															
	SiO_2	Al_2O_3	Fe_2O_3	MgO	CaO	Na_2O	K_2O	TiO_2	P_2O_5	MnO	Cr_2O_3	LOI	*Total	$*SO_4$	TOC	TOS
SL_1	6.13	1.27	0.64	5.12	17.56	8.42	0.33	0.08	0.06	0.02	<0.002	22.8	62.59	37.41	3.1	15.94
SL_2	7.96	1.72	0.85	4.32	25.01	3.43	0.37	0.12	0.08	0.02	<0.002	20.7	64.78	35.22	2.37	15.52
SL_3	3.23	0.7	0.33	4.32	24.1	3.02	0.25	0.05	0.03	0.01	<0.002	29.3	65.55	34.45	0.99	15.5
SL_4	6.08	1.28	0.68	3.78	25.14	2.03	0.35	0.09	0.05	0.02	<0.002	27	66.76	33.24	1.12	15.36

** Sulfate could not be directly measured by this method and thus is inferred by subtracting the total major oxide percentages from 100. The calculated levels are in keeping with concentrations of sulfate salts measured in the water column, and account for the low Total levels acquired from ICP-MS.*

components (PCs) explained 58–62% of the taxonomic variation from class to species. Thus, we focused on the species level analysis (**Figures 6C–E**), which provides the most specific taxonomic classification at a cost of slightly reduced explained variance for higher-order PCs.

Abundance analysis revealed that the hypersaline environments studied could be distinguished by three main taxonomic signatures: (archaeal) *Halobacteria* (associated with the first principal component, or PC1), unclassified bacterial sequences (PC2), and Cyanobacteria (PC3). These three main directions of variation represent the observed combinations of taxonomic abundances: For example, metagenomes from Chula Vista water samples have moderate to high PC1 scores and are dominated by Halobacteriaceae (**Figure 5C**). Occupying another niche are microbial mat samples from Guerrero Negro, which have low PC1 and range from low to high PC3 scores that are inversely related to PC2, so that high levels of *Microcoleus* are associated with low levels of uncharacterized bacteria, and vice versa (**Figure 5D**); see Table S3 for metagenomic datasets.

To describe the strength between these taxonomic signatures and each PC, a figure of merit (FoM) was defined, which is a score ranging from 0 to 1, where 0 indicates no association with a PC score, and 1 indicates perfect correlation (a PC is uniquely associated with variation of the specified taxonomic signature). Higher-order PCs are similarly associated with specific taxonomic signatures (**Figure 6E**) with high figures of merit. These associations corroborate the patterns of abundance visible in **Figure 5C**. A similar analysis was also carried out using SEED Subsystems database (Overbeek et al., 2005) for functional analysis of protein sequences (**Figure 6B**). Functional

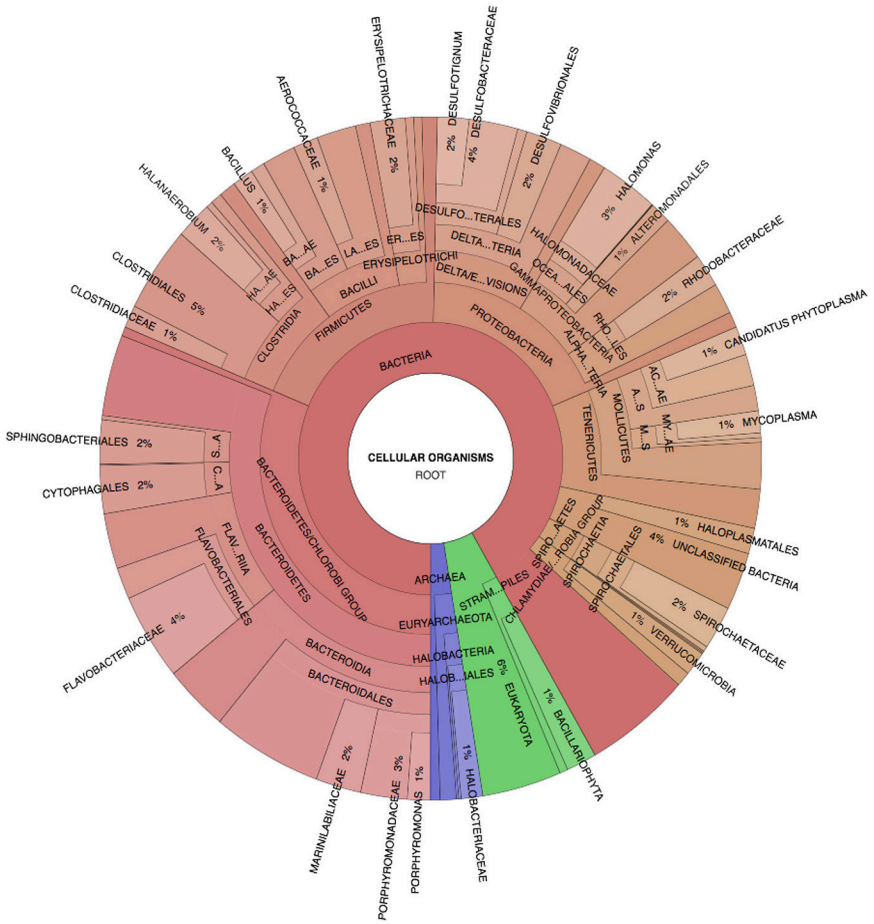

FIGURE 3 | Spotted Lake sediment assemblages**.** Community composition based on Phylosift-estimated abundance within the representative pooled, high-input sample S2, Legend: Eukaryota (blue), Archaea (green), and Bacteria (Red/Orange), with lighter shades indicating lower taxonomic rank (toward species level resolution).

analysis (**Figures 6F,G**) revealed a tighter grouping of hypersaline environments than found based on abundance (**Figures 6C,D**). Functional variation was associated with phages (PC1), protein biosynthesis (PC2), and clustering-based subsystems (PC3). Metagenomes derived from Ace Lake, Antarctica, clustered in a similar fashion to Spotted Lake along PC2 and PC3 (**Figure 6G**), in part due to high abundance of clustering-based subsystems, a label given to genes with unknown function but presumed functional coupling (appearance together within multiple genomes, such as within an operon). The function-based PCs were less associated with specific functions than in the abundance analysis (**Figure 6H**; figure of merit 0.44 ± 0.18 vs. 0.69 ± 0.12 for abundance analysis, mean ± s.d.).

DISCUSSION

The high concentration of sulfates within Spotted Lake makes this one of the most hypersaline environments in the world—yet microbial life is both abundant and diverse, indicating that hypersalinity in and of itself is not a barrier to microorganisms. Rather, habitability is likely more dependent on the water activity and chaotropicity of the brine, controlled by the ionic strength and composition of the solution. Community abundance in the Spotted Lake sediments likely reflect both their geochemical setting (anaerobic organisms such as Firmicutes and Bacteroidetes, sulfate reducers, halophiles) and the integration of exogenously-delivered organisms with microbes transported via aerosols and precipitation on a global scale, seeding populations of facultative anaerobes and aerotolerant organisms. Because salt and other ion levels fluctuate dramatically throughout the year in the water column (Figure S2) with impact on precipitation rates and pore water concentrations in the sediment, we expect that community composition in Spotted Lake sediments may vary seasonally, similar to the archaeal abundances in Lake Tyrrell, Victoria, Australia (Podell et al., 2014) or the relative abundance of Proteobacteria and Cyanobacteria in the waters of nearby Hot Lake, Washington (Crisler et al., 2012; Lindemann et al., 2013).

In comparison to other hypersaline environments, Spotted Lake is notable for its high sequence diversity, reflected in the high abundance of "unclassified bacteria" present, as well

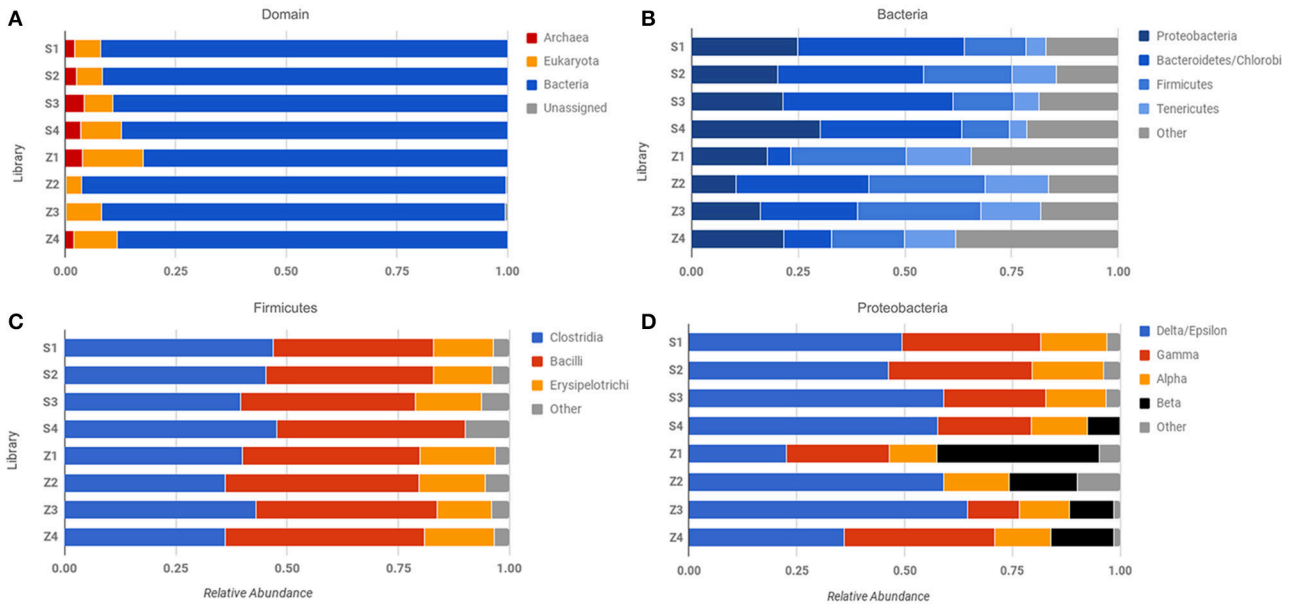

FIGURE 4 | Comparison of abundance across different sequencing libraries and samples. Phylosift-estimated abundance at the level of **(A)** Domain, **(B)** Bacteria, **(C)** Firmicutes, and **(D)** Proteobacteria. Row labels correspond to specific sequencing libraries (see text and Table S1).

as its low levels of Archaea (*Halobacteria*). The latter are aerobes that grow optimally at mesophilic temperatures, and likely their low abundance reflected the anoxic nature of our sediment samples and the temperate environment. The lack of Cyanobacteria, and indeed any phototroph, in our samples was surprising given that they thrive in the water of nearby Hot Lake (Lindemann et al., 2013; Kilmer et al., 2014), and have been observed within the salt crusts of Spotted Lake (Cannon, *pers. comm.*). It is possible that in Spotted Lake these values are indicative of low light levels in the water column, where the situation of the lake (surrounded by hills) limits the amount of direct sunlight received, which is then further mitigated by a large amount of absorbance and scattering of any incident light by the overlying salt layer. Further exploration of the water column will be required to address the absence of detrital eDNA from phototrophs. The tighter grouping of hypersaline environments based on functional analyses emphasizes the number of uncharacterized, but connected genes within these systems. For example, Spotted Lake's taxonomic and functional similarities to Ace Lake, Antarctica may reflect their similar sulfidic, anaerobic environments, which have nearly identical pH (Rankin et al., 1999), though salinity within Spotted Lake is higher by an order of magnitude. However, it is also clear that both extreme environments harbor functionally connected but unknown genes, and thus largely harbor uncharacterized microbes. The extent to which many sequencing reads could not be assigned at the taxonomic levels of family, genus, and species is consistent with the presence of additional uncharacterized extremophiles.

We identified little evidence of representatives from the viral domain of life (phages, eukaryotic viruses, and virophages). In marine environments, phages typically outnumber cells by a factor of 5–25 and represent 5% of biomass (Suttle, 2007). Even in oligotrophic deep sea sediments, characterized by low cell counts and extremely low metabolic rates and turnover, phage to cell ratios can be similar or even higher (Engelhardt et al., 2014), consistent with both active microbial metabolism and viral-induced death; scientists have also found evidence of virophages within Ace Lake, which pray on viruses that infect phototrophic algae (Yau et al., 2011), regulating host-virus interactions and influencing overall carbon flux in the system. If viruses are present in Spotted Lake sediments, we failed to detect them either due to a dominance of RNA viruses to the exclusion of DNA viruses, loss of DNA viruses during extraction despite mechanical disruption techniques known to generally yield viral DNA, or any viral sequences fell within the so-called "dark matter of sequence space" for which we lack suitable marker or reference sequences. We did however, identify sequences belonging to the phylum Tenericutes (class Mollicutes) that lack cell walls and are typically parasites of Eukaryotic organisms (Skennerton et al., 2016). Many members of Mollicutes have been identified in hypersaline environments, though not necessarily associated with a host (Skennerton et al., 2016). Our Mollicute sequences did not relate to any known halophilic organisms, and instead were dominated by the Acholeplasmataceae, which are facultative anaerobes and infectious agents of plants (Stephens et al., 1983). A small portion (1%) of our reads belonged to the class Haloplasmatales, which also lacks a cell wall and is an anaerobic, denitrifying bacterium, unique to hypersaline environments (Antunes et al., 2008, 2011)

Approximately 8% of our Bacterial reads belonged to anaerobic sulfate reducers (Desulfobacterales), with 22% of those belonging to the genus *Desulfotignum*, a group of

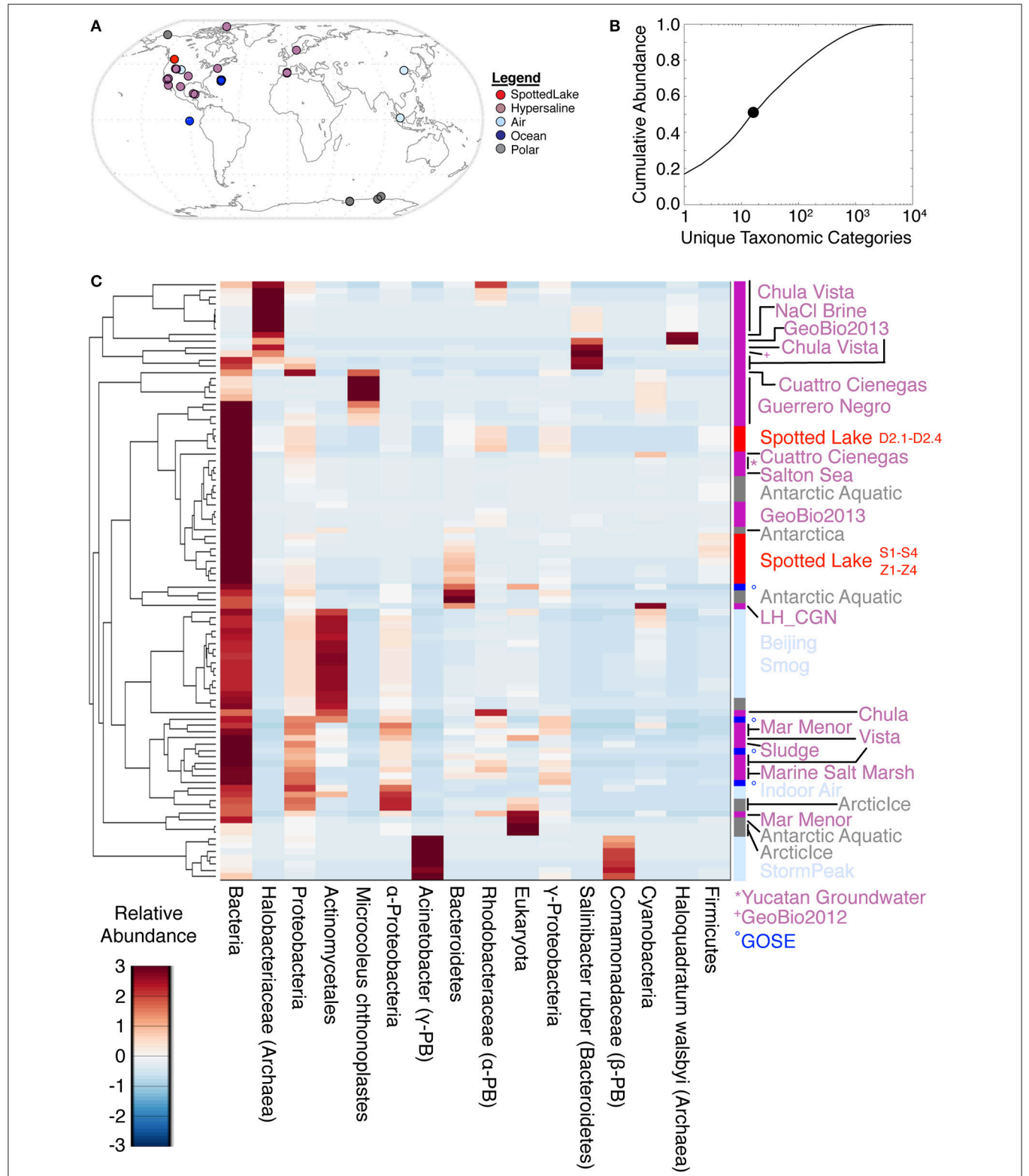

FIGURE 5 | Lowest common ancestor (LCA) abundance comparison of metagenomes. **(A)** Comparator metagenomes (86) were selected from hypersaline, air, polar, and ocean environments representing 20 different sites or projects (Table S3). **(B)** The 16 taxonomic categories of highest abundance capture 50.4% of the cumulative abundance. **(C)** Metagenomes clustered by similarity based on the 16 most abundant taxonomic categories.

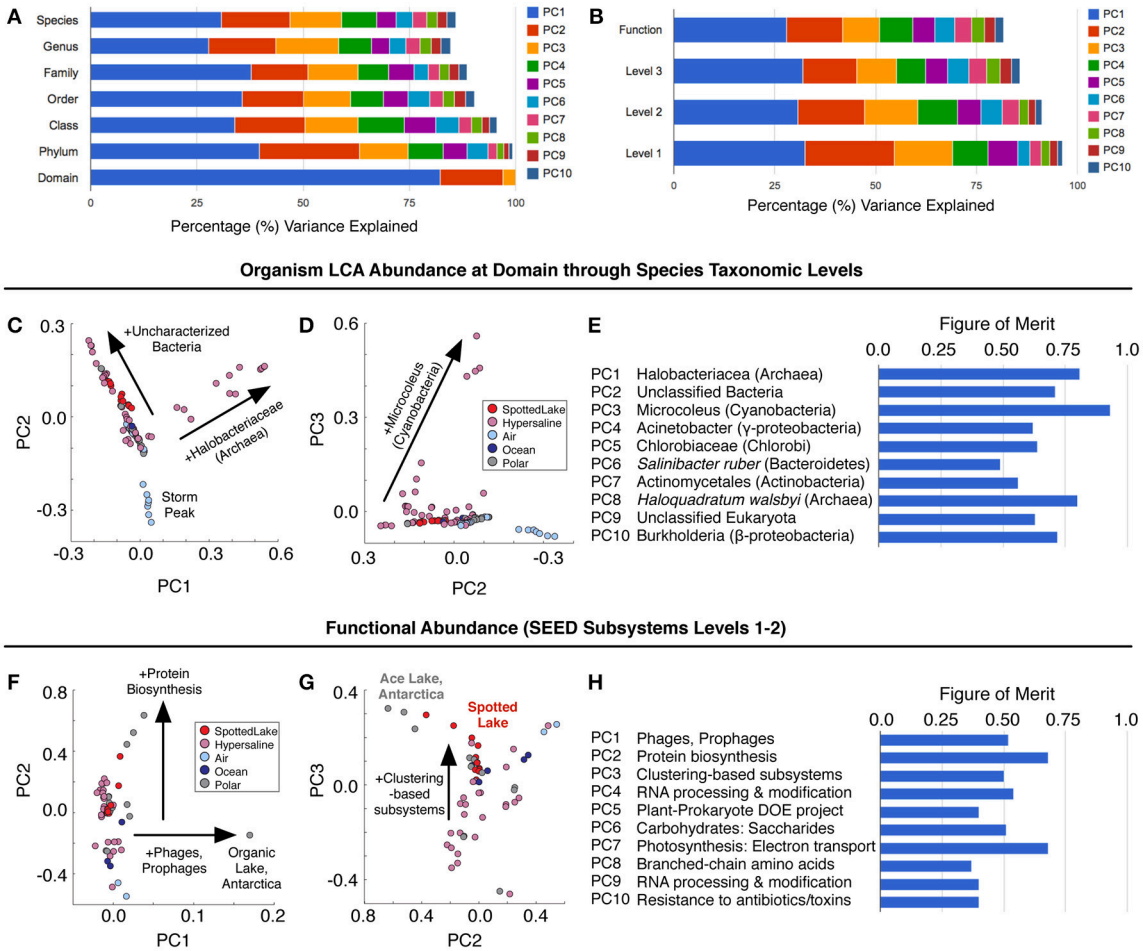

FIGURE 6 | Variation in abundance and function across metagenomes. **(A)** Principal component analysis (PCA) of Lowest Common Ancestor (LCA) -derived abundance at different taxonomic levels. **(B)** PCA of SEED subsystem classification of protein sequences at different functional levels. **(C–E)** Principal components scores based on LCA abundance are associated with specific taxonomic signatures (suggesting a way to classify hypersaline environments). The figure of merit **(E)** indicates the precision of the correlation between a PC score and a specific taxonomic signature (see text and methods for details). **(F–H)** Function-based PCA scores **(F–G)** reveal different variation patterns from abundance-based PCA scores, and lower figures of merit, implying a reduced correlation between PCs and specific functions.

chemoorganotrophs/chemoautotrophs capable of using aromatic compounds as carbon sources or electron donors. In the absence of organic carbon, these organisms are also capable of chemolithoautotrophy, utilizing H_2 as the electron donor, with sulfate, sulfite and thiosulfate all serving as terminal electron acceptors (Kuever et al., 2001). The abundance of sulfate reducers in this system, and the versatility with which some of them can conduct their metabolisms, indicates that the production and preservation of sulfides within this system is likely quite prevalent, similar to Ace Lake (Burton and Barker, 1979), Lake Lisan (Torfstein et al., 2005), and Mono Lake (Stam et al., 2010). In Mono Lake, the low isotope fractionations at low rates of sulfate reduction were thought to be characteristic of halophilic sulfate reducers (Stam et al., 2010). However, Wing and Halevy (2014) suggested that when conditions of low metabolic activity are coupled with high concentrations of environmental sulfate, the kinetic effect of sulfur isotope fractionation is exacerbated, resulting in highly negative values. Thus, it is possible that a strong isotopic signature may exist within the sediments of Spotted Lake; further study is ongoing.

Astrobiological Implications

Hypersaline environments have been shown to preserve biological material on timescales exceeding that of non-saline systems, thus, the presence of paleo-sulfate lakes on Mars is of particular interest for exobiology, as these deposits may retain evidence of previous microbial habitation on the planet. The biological characterization of Spotted Lake is important in order to further delineate the limits to microbial growth in hypersaline environments: do such conditions on present-day or ancient Mars represent potentially habitable, versus merely organic-preserving, environments? On Mars today, climate is mainly regulated by its obliquity (Mischna et al., 2013), which in recent epochs has varied with a 124,000-year cycle. This

cycle alternatively stabilizes and destabilizes ground ice in non-polar regions of Mars, which could alter the probability or frequency of near-surface liquid water brines. While $MgSO_4$ has minimal (−3.6°C) freezing point depression, it can undergo supersaturation allowing for an additional (4–6°C) cooling below this eutectic without precipitation, and at some concentrations can be cooled up to 15°C below the eutectic before becoming solid (Toner et al., 2014). Freezing and salt precipitation events as well as their associated latent heat may help buffer these deposits against low Martian temperatures and diurnal fluctuations. It is plausible that salt precipitation and drying-out events could also result in the entrapment of high molarity fluids that still may maintain transient water activity levels high enough to support microbial activity. Any organisms in such brines would have to cope with osmotic stress, desiccation, and freeze-thaw stresses, as well as cosmic irradiation if within 1–2 m of the surface.

CONCLUSIONS

We have shown that Spotted Lake sediments are inhabited by extremely diverse, mostly anaerobic organisms, with low levels of Archaea and a near absence of detected DNA viruses. This community composition reflects both exogenous delivery of organisms and adaptation to the geochemical environment: the significant presence of anaerobes and extremophiles undoubtedly reflects the capacity of microbes to grow and divide in this extreme environment, characterized by sulfate levels near or at saturation, desiccation, and freeze-thaw stresses. Moreover, analysis of the Spotted Lake genomes in comparison with other hypersaline environments points toward a group of functional genes associated with these brine conditions that have yet to be characterized. Analogous sulfate-rich closed-basin paleolakes on Mars would represent excellent locations to search for preserved organic material and associated biomarkers, which would be concentrated through evaporative processes, entombed in sulfates, and preserved within lake-bed deposits, conserving signatures of ancient life that could persist over geologic time.

AUTHOR CONTRIBUTIONS

AP and CC coordinated and managed the study. VW obtained the samples. VW and AP carried out the geochemical analyses. CC and TZ designed the experiment and CL, TZ, and HR processed the samples. HR performed the sequencing. AP, and CC analyzed the data and wrote the manuscript text. MZ and GR advised on the study and analysis. All authors edited and reviewed the manuscript.

FUNDING

Financial support provided by NASA ASTID (NNX08AX15G) and MatISSE (NNX15AF85G).

ACKNOWLEDGMENTS

We thank the Okanagan Nation Alliance (ONA) and the Osoyoos band office for access to kt̓'lilwˇtˇ (Spotted Lake), which is considered sacred to the ONA. Thank you to the Kinchla Lab, UMass Amherst, for providing the water activity measurements for this work. The authors also thank two reviewers for providing valuable commentary and insights regarding this manuscript. Financial support provided by NASA ASTID (NNX08AX15G) and MatISSE (NNX15AF85G), we also acknowledge support from an NSERC (Canada) Discovery grant. This work was performed in part at the Center for Nanoscale Systems (CNS), a member of the National Nanotechnology Coordinated Infrastructure Network (NNCI), which is supported by the National Science Foundation under NSF award no. 1541959. CNS is part of Harvard University. Metagenomic data sets have been added to the NCBI Sequence Read Archive (SRA) under project PRJNA245804.

SUPPLEMENTARY MATERIAL

The Supplementary Material for this article can be found online at: http://journal.frontiersin.org/article/10.3389/fmicb.2017.01819/full#supplementary-material

REFERENCES

Antunes, A., Alam, I., El Dorry, H., Siam, R., Robertson, A., Bajic, V. B., et al. (2011). Genome sequence of *Haloplasma contractile*, an unusual contractile bacterium from a deep-sea anoxic brine lake. *J. Bacteriol.* 193, 4551–4552. doi: 10.1128/JB.05461-11

Antunes, A., Rainey, F. A., Wanner, G., Taborda, M., Pätzold, J., Nobre, M. F., et al. (2008). A new lineage of halophilic, wall-less, contractile bacteria from a brine-filled deep of the Red Sea. *J. Bacteriol.* 190, 3580–3587. doi: 10.1128/JB.01860-07

Aubrey, A., Cleaves, H. J., Chaimers, J. H., Skelley, A. M., Mathies, R. A., Grunthaner, F. J., et al. (2006). Sulfate minerals and organic compounds on Mars. *Geology* 34, 357−360. doi: 10.1130/G22316.1

Baldwin, R. L. (1996). How Hofmeister ion interactions affect protein stability. *Biophys. J.* 71, 2056−2063.

Burton, H. R., and Barker, R. J. (1979). Sulfur chemistry and microbiological fractionation of sulfur isotopes in a saline Antarctic lake. *Geomicrobiol. J.* 1, 329–340. doi: 10.1080/01490457909377739

Cannon, K. M., Fenwick, L. A., and Peterson, R. C. (2012). "Spotted lake: mineralogical clues for the formation of authigenic sulfates in ancient lakes on Mars," in *LPSC XLIII Abstract* (Kingston), 1989.

Chevrier, V. F., and Valentin, E. R. (2012), Formation of recurring slope lineae by liquid brines on present-day Mars. *Geophys. Res. Lett.* 39:L21202. doi: 10.1029/2012GL054119

Church, M., and Ryder, J. M. (2010). "Physiography of british columbia," in *Compendium of Forest Hydrology and Geomorphology in British Columbia*, Vol. 1 of 2, eds R. G. Pike, T. E. Redding, R. D. D. Moore, R. D. Winkler, and K. D. Bladon (British Columbia Ministry of Forests and Range), 17–45.

Clark, B. C., Morris, R. V., McLennan, S. M., Gellert, R., Jolliff, B., Knoll, A. H., et al. (2005). Chemistry and mineralogy of outcrops at Meridiani Planum. *Earth Planet Sci. Lett.* 240, 73−94. doi: 10.1016/j.epsl.2005.09.040

Crisler, J. D., Newville, T. M., Chen, F., Clark, B. C., and Schneegurt, M. A. (2012). Bacterial growth at the high concentrations of magnesium sulfate found in martian soils. *Astrobiology* 12, 98−106. doi: 10.1089/ast.2011.0720

Darling, A. E., Jospin, G., Lowe, E., Matsen, I. V. R. A., Bik, H. M., and Eisen, J. A. (2014). PhyloSift: phylogenetic analysis of genomes and metagenomes. *PeerJ.* 2:e243. doi: 10.7717/peerj.243

Dickson, J. L., Head, J. W., Levy, J. S., and Marchant, D. R. (2013). Don Juan Pond, Antarctica: near-surface CaCl(2)-brine feeding Earth's most saline lake and implications for Mars. *Sci. Rep.* 3:1166. doi: 10.1038/srep01166

Dykstra, M. J., and Reuss, L. E. (2003). "Biological Electron Microscopy," in *Theory, Techniques and Troubleshooting, 2nd Edn.* (New York, NY: Kluwer Academic/Plenum Publishers), 1–31.

Engelhardt, T., Kallmeyer, J., Cypionka, H., and Engelen, B. (2014). High virus-to-cell ratios indicate ongoing production of viruses in deep subsurface sediments. *ISME J.* 8, 1503–1509. doi: 10.1038/ismej.2013.245

Fendrihan, S., Legat, A., Pfaffenhuemer, M., Gruber, C., Weidler, G., Gerbi, F., et al. (2006). Extremely halophilic archaea and the issue of long-term microbial survival. *Rev. Env. Sci. Bio/Tech.* 5, 203–218. doi: 10.1007/s11157-006-0007-y

Foster, I. S., King, P., Hyde, B. C., and Southam, G. (2010). Characterization of halophiles in natural $MgSO_4$ salts and laboratory enrichment samples: astrobiological implications for Mars. *Planet. Space Sci.* 58, 599–615. doi: 10.1016/j.pss.2009.08.009

Fox-Powell, M. G., Hallsworth, J. E., Cousins, C. R., and Cockell, C. S. (2016). Ionic strength is a barrier to the habitability of Mars. *Astrobiology* 16, 427–442. doi: 10.1089/ast.2015.1432

Gendrin, A., Mangold, N., Bibring, J. P., and Langevin, Y. (2005). sulfates in Martian layered terrains: the OMEGA/Mars express view. *Science* 307, 1587–1591. doi: 10.1126/science.1109087

Glass, E. M., Wilkening, J., Wilke, A., Antonopoulos, D., and Meyer, F. (2010). Using the metagenomics RAST server (MG-RAST) for analyzing shotgun metagenomes. *Cold Spring Harb. Protoc.* 2010:pdb.prot5368. doi: 10.1101/pdb.prot5368

Goudge, T. A., Fassett, C. I., Head, J. W., Mustard, J. F., and Aureli, K. L. (2016). Insights into surface runoff on early Mars from paleolake basin morphology and stratigraphy. *Geol. Soc. Am.* 44, 419–422. doi: 10.1130/G37734.1

Grant, W. D. (2004). Life at low water activity. *Phil. Trans. R. Soc. B Biol. Sci.* 359, 1249–1267. doi: 10.1098/rstb.2004.1502

Ha, Z., and Chan, C. K. (1999). The water activities of $MgCl_2$, $Mg(NO_3)_2$, $MgSO_4$, and their mixtures. *Aerosol. Sci. Tech.* 31, 154–169. doi: 10.1080/027868299304219

Jenkins, O. P. (1918). Spotted lakes of epsomite in Washington and British Columbia. *Am. J. Sci.* 46, 638–644. doi: 10.2475/ajs.s4-46.275.638

Karunatillake, S., Wray, J. J., Gasnault, O., McLenna, S. M., Rogers, A. D., Squyres, S. W., et al. (2016). Sulfates hydrating bulk soil in the Marian low and middle latitudes. *Geophys. Res. Lett.* 41, 7987–7996. doi: 10.1002/2014GL061136

Kilmer, B. R., Eberl, T. C., Cunderla, B., Chen, F., Clark, B. C., and Schneegurt, M. A. (2014). Molecular and phenetic characterization of the bacterial assemblage of Hot Lake, WA, an environment with high concentrations of magnesium sulphate, and its relevance to Mars. *Int. J. Astrobiol.* 13, 69–80. doi: 10.1017/S1473550413000268

Kuever, J., Könneke, M., Galushko, A., and Drzyzga, O. (2001). Reclassification of Desulfobacterium phenolicum as Desulfobacula phenolica comb. nov. and description of strain SaxT as Desulfotignum balticum gen. nov., sp. nov. *Int. J. Syst. Evol. Microbiol.* 51, 171–177. doi: 10.1099/00207713-51-1-171

Ley, R. E., Harris, J. K., Wilcox, J., Spear, J. R., Miller, S. R., Bebout, B. M., et al. (2006). Unexpected diversity and complexity of the Guerrero Negro hypersaline microbial mat. *Appl. Environ. Microbiol.* 72, 3685–3695. doi: 10.1128/AEM.72.5.3685-3695.2006

Lindemann, S. R., Moran, J. J., Stegen, J. C., Renslow, R. S., Hutchison, J. R., Cole, J. K., et al. (2013). The epsomitic phototrophic microbial mat of Hot Lake, Washington: community structural responses to seasonal cycling. *Front. Microbiol.* 4:323. doi: 10.3389/fmicb.2013.00323

Marion, G. M. (1997). A theoretical evaluation of mineral stability in Don Juan Pond, wright valley, victoria land. *Antarct. Sci.* 9, 92–99. doi: 10.1017/S0954102097000114

McEwen, A. S., Ohja, L., Dundas, C. M., Mattson, S. S., Byrne, S., Wray, J. J., et al. (2011). Seasonal flows on warm martian slopes. *Science* 333, 740–743. doi: 10.1126/science.1204816

McKay, E. (1935). Salt tolerance of Ruppia Maritima in lakes of high magnesium sulphate content. *Plant Physiol.* 10, 425–446. doi: 10.1104/pp.10.3.425

Meyer, F., Paarmann, D., D'Souza, M., Olson, R., Glass, E. M., Kubal, M., et al. (2008). The metagenomics RAST server—a public resource for the automatic phylogenetic and functional analysis of metagenomes. *BMC Bioinformatics* 9:386. doi: 10.1186/1471-2105-9-386

Meyer, G. H., Morrow, M. B., Wyss, O., Berg, T. E., and Littlepage, J. L. (1962). Antarctica: the microbiology of an Unfrozen saline pond. *Science* 138, 1103–1104. doi: 10.1126/science.138.3545.1103

Mischna, M. A., Baker, V., and Milliken, R. (2013). Effects of obliquity and water vapor/trace gas greenhouses in the early martian climate. *J. Geophys. Res.* 118, 560–576. doi: 10.1002/jgre.20054

Möhlmann, D., and Thomsen, K. (2011). Properties of cryobrines on Mars. *Icarus* 212, 123–130. doi: 10.1016/j.icarus.2010.11.025

Mormile, M. R., Biesen, M. A., Gutierrez, M. C., Ventosa, A., Pavlovich, J. B., Onstott, T. C., et al. (2003). Isolation of *Halobacterium salinarum* retrieved directly from halite brine inclusions. *Environ. Microbiol.* 5, 1094–1102. doi: 10.1046/j.1462-2920.2003.00509.x

Overbeek, R., Begley, T., Bulter, R. M., Choudhuri, J. V., Chuang, H. Y., Cohoon, M., et al. (2005). The subsystems approach to genome annotation and its use in the project to annotate 1000 genomes. *Nucleic Acids Res.* 33, 5691–5702. doi: 10.1093/nar/gki866

Podell, S., Emerson, J. B., Jones, C. M., Ugalde, J. A., Welch, S., Heidelberg, K. B., et al. (2014). Seasonal fluctuations in ionic concentrations drive microbial succession in a hypersaline lake community. *ISME* 8, 979–990. doi: 10.1038/ismej.2013.221

Pujalte, M. J., Lucena, T., Ruvira, M. A., Arahal, D. R., and Macián, M. C. (2014). "The Family *Rhodobacteraceae*," in *The Prokaryotes – Alphaproteobacteria and Betaproteobacteria*, eds E. Rosenberg, E. F. DeLong, S. Lory, E. Stackebrandt, and F. Thompson (Berlin: Springer-Verlag), 439–512.

Rankin, L. M., Gobson, J. A. E., Franzmann, P. D., and Burton, H. R. (1999). The chemical stratifcation and microbial communities of Ace Lake, Antarctica: a review of the characteristics of a marine-derived meromictic lake. *Polarforschung* 66, 33–52.

Rothberg, J. M., Hinz, W., Rearick, T. M., Schultz, J., Mileski, W., Davey, M., et al. (2011). An integrated semiconductor device enabling non-optical genome sequencing. *Nature* 475, 348–352. doi: 10.1038/nature10242

Skennerton, C. T., Haroon, M. F., Briegel, A., Shi, J., Jensen, G. J., Tyson, G. W., et al. (2016). Phylogenomic analysis of *Candidatus* 'Izimaplasma' species: free-living representatives from a *Tenericutes* clade found in methane seeps. *ISME* 10, 2679–2692. doi: 10.1038/ismej.2016.55

Stam, M. C., Mason, P. R. D., Pallud, C., and Van Cappellen, P. (2010). Sulfate reducing activity and sulfur isotope fractionation by natural microbial communities in sediments of a hypersaline soda lake (Mono Lake, California). *Chem. Geol.* 278, 23–30. doi: 10.1016/j.chemgeo.2010.08.006

Stephens, E. B., Aulakh, D. L. R., Tully, J. G., and Barile, M. F. (1983). Intraspecies genetic relatedness among strains of *Acholeplasma laidlawii* and of *Acholeplasma axanthum* by nucleic acid hybridization. *J. Gen. Microbiol.* 129, 1929–1934. doi: 10.1099/00221287-129-6-1929

Stevenson, A., Cray, J. A., Williams, J. P., Santos, R., Sahay, R., Neuenkirchen, N., et al. (2015). Is there a common water-activity limit for the three domains of life? *ISME* 9, 1333–1351. doi: 10.1038/ismej.2014.219

Suttle, C. A. (2007). Marine viruses — major players in the global ecosystem. *Nat. Rev. Microbio.* 5, 801–812. doi: 10.1038/nrmicro1750

Toner, J. D., Catling, D. C., and Light, B. (2014). The formation of supercooled brines, viscous liquids, and low-temperature perchlorate glasses in aqueous solutions relevant to Mars. *Icarus* 233, 36–47. doi: 10.1016/j.icarus.2014.01.018

Torfstein, A., Gavrieli, I., and Stein, M. (2005). The sources and evolution of sulfur in the hypersaline lake Lisan (paleo-Dead Sea). *Earth Planet. Sci. Lett.* 236, 61–77. doi: 10.1016/j.epsl.2005.04.026

Tosca, N. J., Knoll, A. H., and McLennan, S. M. (2008). Water activity and the challenge for life on early Mars. *Science* 320, 1204–1207. doi: 10.1126/science.1155432

Vaniman, D. T., Bish, D. L., Chipera, S. J., Fialips, C. I., Carey, J. W., and Feldman, W. C. (2004). Magnesium sulphate salts and the history of water on Mars. *Nature* 431, 663–665. doi: 10.1038/nature02973

Vreeland, R. H., Rosenzweig, W. D., and Powers, D. W. (2000). Isolation of a 250 million-year-old halotolerant bacterium from a primary salt crystal. *Nature* 407, 897−900. doi: 10.1038/35038060

Wanke, H., Bruckner, J., Dreibus, G., Rieder, R., and Ryabchikov, I. (2001). Chemical composition of rocks and soils at the Pathfinder site. *Space Sci. Rev.* 96, 317−330. doi: 10.1023/A:1011961725645

Wilson, S. L., Frazer, C., Cumming, B. F., Nuin, P. A. S., and Walker, V. K. (2012). Cross-tolerance between osmotic and freeze-thaw stress in microbial assemblages from temperate lakes. *FEMS Microbio. Ecol.* 82, 405−415. doi: 10.1111/j.1574-6941.2012.01404.x

Wing, B. A., and Halevy, I. (2014). Inracellular metabolite levels shape sulfur isotope fractionation during microbial sulfate respiration. *Proc. Natl. Acad. Sci. U.S.A.* 111, 18116−18125. doi: 10.1073/pnas.14075 02111

Wray, J. J., Miliken, R. E., Dundas, C. M., Swayze, G. A., Andrews-Hanna, J. C., Baldridge, A. M., et al. (2011). Columbus crater and other possible groundwater-fed paleolakes of Terra Sirenum, Mars. *J. Geophys. Res.* 116:E01001. doi: 10.1029/2010JE003694

Yau, S., Lauro, F. M., DeMaere, M. Z., et al. (2011). Virophage control of Antarctic algal host-virus dynamics. *Proc. Natl. Acad. Sci. U.S.A.* 108, 6163−6168. doi: 10.1073/pnas.1018221108

Yilmaz, S., Allgaier, M., and Hugenholtz, P. (2010). Multiple displacement amplification compromises quantitative analysis of metagenomes. *Nat. Methods* 7. 943−944. doi: 10.1038/nmeth1210-943

Conflict of Interest Statement: The authors declare that the research was conducted in the absence of any commercial or financial relationships that could be construed as a potential conflict of interest.

frontiers in Microbiology

ORIGINAL RESEARCH
published: 18 July 2017
doi: 10.3389/fmicb.2017.01369

High Tolerance of *Hydrogenothermus marinus* to Sodium Perchlorate

Kristina Beblo-Vranesevic[1], Harald Huber[2] and Petra Rettberg[1]*

[1] Radiation Biology Division, Institute of Aerospace Medicine, German Aerospace Center (DLR e.V.), Cologne, Germany, [2] Institute for Microbiology and Archaea Center, Faculty of Biology and Preclinical Medicine, University of Regensburg, Regensburg, Germany

On Mars, significant amounts (0.4–0.6%) of perchlorate ions were detected in dry soil by the Phoenix Wet Chemistry Laboratory and later confirmed with the Mars Science Laboratory. Therefore, the ability of *Hydrogenothermus marinus*, a desiccation tolerant bacterium, to survive and grow in the presence of perchlorates was determined. Results indicated that *H. marinus* was able to tolerate concentrations of sodium perchlorate up to 200 mM (≙ 1.6%) during cultivation without any changes in its growth pattern. After the addition of up to 440 mM (≙ 3.7%) sodium perchlorate, *H. marinus* showed significant changes in cell morphology; from single motile short rods to long cell chains up to 80 cells. Furthermore, it was shown that the known desiccation tolerance of *H. marinus* is highly influenced by a pre-treatment with different perchlorates; additive effects of desiccation and perchlorate treatments are visible in a reduced survival rate. These data demonstrate that thermophiles, especially *H. marinus,* have so far, unknown high tolerances against cell damaging treatments and may serve as model organisms for future space experiments.

Keywords: perchlorates, morphology, thermophiles, desiccation, survival

OPEN ACCESS

Edited by:
Karen Olsson-Francis, The Open University, United Kingdom

Reviewed by:
Armando Azua-Bustos, Pontificia Universidad Católica de Chile, Chile
Ivan Glaucio Paulino-Lima, Universities Space Research Association, United States

****Correspondence:***
Kristina Beblo-Vranesevic
kristina.beblo@dlr.de

Specialty section:
This article was submitted to Extreme Microbiology, a section of the journal Frontiers in Microbiology

Received: *10 April 2017*
Accepted: *05 July 2017*
Published: *18 July 2017*

Citation:
Beblo-Vranesevic K, Huber H and Rettberg P (2017) High Tolerance of Hydrogenothermus marinus to Sodium Perchlorate. Front. Microbiol. 8:1369. doi: 10.3389/fmicb.2017.01369

INTRODUCTION

Research on perchlorates has increased over the course of the last 30 years. The natural occurrence of perchlorates is in geographically limited very arid environments such as the Atacama Desert in Chile (Trumpolt et al., 2005; Catling et al., 2010). For example, perchlorate concentrations in nitrate mineral deposits in the Atacama Desert are known to be 0.028 wt % (Michalski et al., 2004).

Not only on Earth, but also on our neighboring planet Mars, perchlorates have been detected, however, in much higher concentrations than on Earth. Significant amounts of perchlorate ions (0.4–0.6%) were first detected by the Phoenix lander in regolith in the northern polar region (Vastitas Borealis) (Hecht et al., 2009). Data from additional studies provide strong evidence that the soil samples analyzed by the Wet Chemical Laboratory on board the Phoenix lander contain calcium perchlorate (Ca-perchlorate) and magnesium perchlorate (Mg-perchlorate) (Kounaves et al., 2014). In general, the data obtained from the Mars Science Laboratory suggests that perchlorates occur throughout the entire surface of Mars (Archer et al., 2013). At distinct craters, different perchlorates were identified. Data from the Compact Reconnaissance Imaging Spectrometer on board the Mars Reconnaissance Orbiter detected a mixture of sodium perchlorate (Na-perchlorate) and Mg-perchlorate in the Palikir and Hale crater (Ojha et al., 2015), at Horowitz

crater, Na-perchlorate can be found (Ojha et al., 2015) and Ca-perchlorate at the Gale Crater (Glavin et al., 2013).

Although the detailed formation mechanism is still unknown, two different formation mechanisms of Martian perchlorates have been proposed to explain their occurrence on the surface of Mars. One explanation suggests that the perchlorates were produced on the surface where Martian surface minerals catalyze the photochemical oxidation of chlorides to perchlorates (Schuttlefield et al., 2011; Kim et al., 2013). It was shown that in chloride containing Martian soil simulants, perchlorates are produced in the presence of ultraviolet light (Carrier and Kounaves, 2015). Another formation mechanism proposes atmospheric formations where Martian perchlorates may have originated are the result of reactivity of atmospheric oxidants in the arid environment on Mars (Catling et al., 2010).

The assessment of the potential habitability of Mars is based on one hand on the state of knowledge of the prevailing environmental conditions on the surface and in the subsurface of Mars and on the other hand on the state of knowledge of the survivability of Earth organisms under extreme Mars-like conditions (Cockell et al., 2016). Potential organisms should survive an exposure to perchlorates or should even able to live in the presence of perchlorates. Since the detection of perchlorates on Mars some years ago, the tolerance of non-perchlorate metabolizing microorganisms against perchlorates has been tested (e.g., Oren et al., 2014; Shcherbakova et al., 2015; Kral et al., 2016; Al Soudi et al., 2017). In general, perchlorate tolerant microorganisms can be affiliated in two groups: organisms that are tolerant to perchlorates without metabolizing them and perchlorate tolerant microorganisms that consume/metabolize perchlorates. Thereby, the perchlorate (ClO_4^-) is reduced in three steps to chloride (Cl^-); the reduction potential is $E^0 = 1.29$ V for the couple ClO_4^-/Cl^- (Logan, 1998; Coates and Achenbach, 2004). More than 40 different strains, mostly belonging to the proteobacterial phylum are known to have the ability to metabolize perchlorates (Coates and Achenbach, 2004; Nerenberg, 2013). Up to now, only a few archaeal perchlorate metabolizing representatives have been identified, namely *Archaeoglobus fulgidus* and several species from the family *Halobacteriaceae* (Liebensteiner et al., 2013; Oren, 2014). Since the metabolizing rates were the focus of these studies, the microorganisms were tested under low metabolic meaningful perchlorate concentrations of up to 0.1 M (Attaway and Smith, 1993). Thereby, the highest metabolic activity is measured at concentrations between 0.02 and 0.04 M. In general, data for the absolute resistance of the strains against high perchlorate concentrations are often missing. In recent times, non-perchlorate metabolizing microorganisms were also tested in their tolerance against perchlorates. Amongst these Archaea and Bacteria, different methanogenic, halophilic, and acidophilic representatives with different tolerance levels could be found: one example of a sensitive organism is the acidophilic iron sulfur bacterium *Acidithiobacillus ferrooxidans,* known to be possibly able to grow under Mars-like geochemical conditions (Bauermeister et al., 2014). *A. ferrooxidans* cannot multiply in the presence of 0.022 M (≙ 0.5%) and 0.044 M (≙ 1%) Mg-perchlorate (Bauermeister, 2012). Different methanogenic Archaea (three *Methanobacterium* strains and two *Methanosarcina* strains) are also influenced in their growth behavior at low concentrations (up to 0.01 M) of Na-perchlorates (Shcherbakova et al., 2015). Spores of *Bacillus subtilis* germinate at a Na-perchlorate concentration of up to 0.1 M (Nagler and Moeller, 2015), a higher concentration (≥0.6 M) of Na-perchlorate and Mg-perchlorate lead to complete inactivation of the germination process (Nagler and Moeller, 2015). It has been reported that several halotolerant strains show only slight alterations in their growth pattern in the presence of perchlorates: nearly all of the halotolerant isolates grew in the presence of 0.05 M Mg-perchlorate. Some exhibited positive growth even in the presence 0.25 M Mg-perchlorate. While some growth may have occurred at levels as high as 0.5 M Mg-perchlorate for certain isolates, the data are limited and inconsistent (Al Soudi et al., 2017).

The identification of perchlorates at different locations on Mars directs the research interest to the investigation of perchlorate tolerance or even perchlorate metabolism in Earth organisms. Since on Earth, natural perchlorates occur mainly in arid areas like desserts, a first thought is that desiccation tolerant microorganisms might be capable to surviving exposures to perchlorates. In previous studies, a variety of Bacteria and Archaea have been screened for their tolerance to desiccation. Because of its desiccation tolerance, the deep-branching microaerophilic bacterium *Hydrogenothermus marinus* proved to be a promising model organism in many respects. *H. marinus* exhibits a unique tolerance to desiccation and to exposure to elevated salt concentrations (Beblo et al., 2009; Beblo-Vranesevic et al., 2017). Therefore, it was hypothesized that this organism would survive and grow in the presence of perchlorates. To test this hypothesis we determined the ability of this organism to replicate after exposure to different perchlorates, even in combination with desiccation. Additionally, the results from *H. marinus* were compared to other well known (model) microorganisms. These well studied organisms, namely *Escherichia coli*, *B. subtilis,* and *Deinococcus radiodurans*, originate from different habitats on Earth and are known to react in different ways to an exposure to cell damaging treatments.

MATERIALS AND METHODS

Strain and Culture Conditions

Hydrogenothermus marinus DSM 12046^T was cultured in microoxic (2% O_2 in 1 bar H_2/CO_2) modified VM1 medium (ZoBell, 1941; Stöhr et al., 2001). Incubated at optimal growth temperatures ($T_{opt.}$: 65°C), a cell density of approximately 10^8 cells per ml was reached after 24 h of incubation. The reference strain, *E. coli* K12 wild-type (DSM No. 498), was cultivated in liquid NB medium (0.5% peptone, 0.3% meat extract) or plated on solidified NB medium (NB medium with 1.5% agar). Incubation temperature was at optimal growth temperature ($T_{opt.}$: 37°C). *B. subtilis* strain NCIB 3610^T (DSM No. 10) and *D. radiodurans* type strain R1^T (DSM No. 20539) were grown in TGY medium in liquid (0.5% tryptone, 0.3% yeast extract, 0.1% glucose) or were plated on solidified TGY medium (TGY medium with 1.5% agar). Incubation temperature was at

organisms' optimal growth temperature (*B. subtilis*: $T_{opt.}$: 37°C; *D. radiodurans*: $T_{opt.}$: 30°C). Additionally, purified *B. subtilis* spores were used for exposure experiments. Isolation of the spores was conducted according to Nagler et al. (2014).

Exposure to Perchlorates

Different concentrations of three perchlorates [Na-perchlorate $NaClO_4$; Mg-perchlorate $Mg(ClO_4)_2$; Ca-perchlorate $Ca(ClO_4)_2$] were added to cells grown at optimal standard conditions. Due to the limited solubility of the perchlorates, concentrations higher than 5 M could not be tested. The solubility of Na-perchlorate hydrate in water is 2090 g per liter at 15°C. But the solubility is noticeably reduced when the perchlorate is dissolved in the modified salty VM-1 medium.

During the shock experiments, the cells were exposed for a specified time (15 min or 96 h) to ascending concentrations of Na-perchlorate at ambient room temperature or at 65°C (only for *H. marinus*). Exposure was disrupted by a dilution step (1:100 and 1:400, respectively) and for analysis of the survivors; either the most probable number assay or standard spread-plate assay was used.

Additionally, *H. marinus* cells were cultivated in the presence of different concentrations of Na-perchlorate.

Desiccation Experiments

Desiccation experiments were performed as described earlier (Beblo et al., 2009). Briefly, cell concentrations were determined by counting in a Thoma chamber (depth: 0.02 mm). The cell suspensions (2 ml) were spread evenly on four glass slides and dried for 24 h under oxic laboratory conditions (room temperature, average relative humidity 33 ± 3.5%).

Determination of the Survival Rate

In general, growth and morphology of the cells was observed by phase-contrast light microscopy (Zeiss® Axiolmager™ M2) with 400× or 1000× magnification.

Desiccated cells on glass slides or non-desiccated control cells were transferred into a culture bottle with culture media. Perchlorate exposed *H. marinus* cells in liquid suspension were subjected to a dilution step (1:100). Since *H. marinus* do not form colonies on solid surfaces with sufficiently high efficiency (see strain references) plating assays on solid media could not be applied. Detection of viable cells was achieved by the most probable number technique via dilution series with 10-fold dilution steps (Franson, 1985).

For *E. coli*, *D. radiodurans*, and *B. subtilis* the stop reaction (1:400) dilution step was performed in sterile PBS buffer solution. Afterward further dilution series were prepared and an aliquot of each dilution was plated.

All experiments were performed at least three times independently, representing biological replicas. The data shown within the graphs represent mean values with standard deviations. The survival rate (S) was calculated as relative survival after treatment (N) compared to the non-treated control (N_0) ($S = N/N_0$). D_{10}-values, giving the dose of perchlorates in Molar (M) which reduces the survival rate by one order of magnitude were calculated from the regression lines of the exponential slopes of the mean survival curves as described by Harm (1980).

RESULTS

Shock exposure (15 min) to Na-perchlorate did not change *H. marinus*' survivability, and can be deduced from the nearly straight line within the dose-survival curve (**Figure 1A**). This is true for concentrations up to 5 M, that corresponds to the maximal solubility limits of perchlorates in salty medium. After long term exposure (96 h), a typical shouldered survival curve was apparent (**Figure 1A**). There was no difference in survivability of *H. marinus* if the shock experiments were performed at ambient room temperature, or at the optimal growth temperature of 65°C. Interestingly, concentrations of Na-perchlorate (500 mM), that is above the growth limit of *H. marinus* (440 mM; see paragraph below), did not lead to a reduction in survivability during long term exposure experiments. Only exposure to 1 M Na-perchlorate for 96 h reduced the survival rate by approximately two orders of magnitude.

For comparison, the survivability of three other, well investigated microorganisms originating from very different environments, namely *E. coli*, *D. radiodurans*, and *B. subtilis* (as vegetative cells or pure spores) was investigated after short term shock exposure to Na-perchlorate (**Table 1**). Differences in sensitivity were obvious (**Figure 1B**): *E. coli* was the most sensitive as determined by the survival curve as well by the calculated D_{10}-value (**Table 1**). Exposure to 2.5 M Na-perchlorate for 15 min reduced the survival of *E. coli* by more than four orders of magnitude. Higher concentrations led to complete loss of viability. Vegetative *B. subtilis* cells showed a medium sensitivity against short term shock exposure to Na-perchlorate and were completely inactivated by concentrations higher than 4 M Na-perchlorate. *D. radiodurans* also reacted significantly to an exposure (15 min) to Na-perchlorates, and exposure of 4 M Na-perchlorate led to a reduction in survivability by three orders of magnitude. Only purified spores were as resistant as *H. marinus* cells and did not react after a treatment with Na-perchlorate up to 5 M (**Table 1**).

Hydrogenothermus marinus was able to replicate in the presence of 440 mM Na-perchlorate. Higher concentration (≥460 mM) led to an inability to replicate. However, the addition of Na-perchlorate during growth led to morphological changes. Under optimal growth conditions *H. marinus* cells usually appear as single motile short rods (**Figure 2A**); in the presence of Na-perchlorate chain formation in combination with a rounding of the single cells within the chain occurred in a concentration dependent manner. The threshold value below which no chain formation could be observed was 100 mM. At concentrations between 100 and 200 mM beside a minor fraction of single cells, short chains up to approximately 10 cells dominated. Concentrations between 200 and 440 mM led exclusively to long almost immobile chains with different lengths up to approximately 80 cells (**Figures 2B–D**). These morphological changes were reversible after the cells were transferred into media and cultivated overnight without perchlorate.

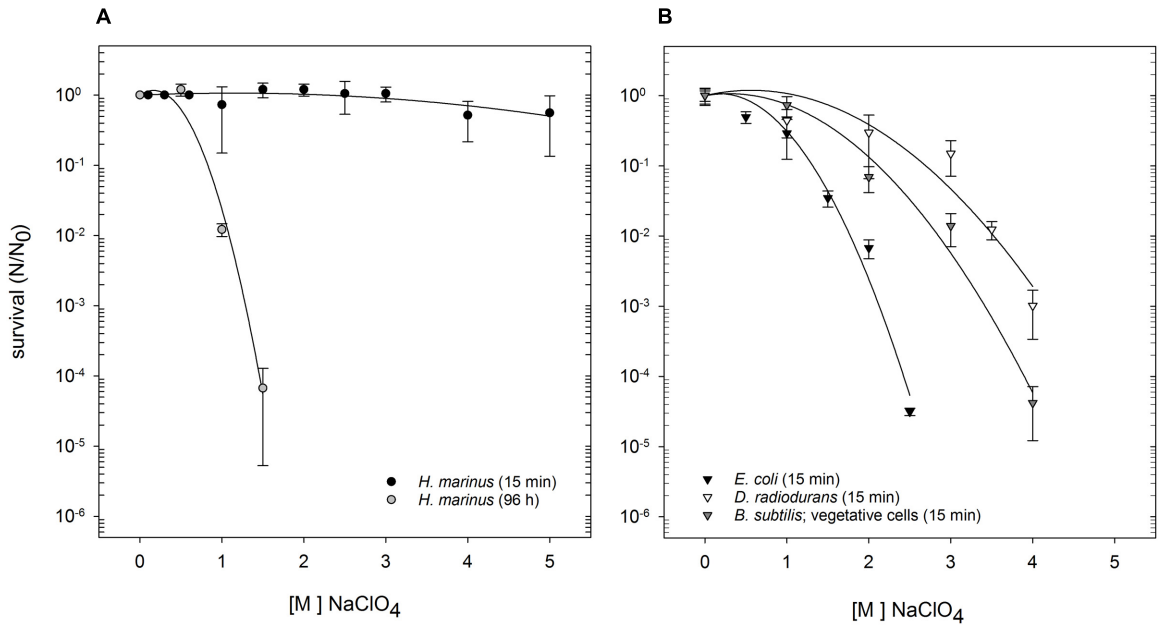

FIGURE 1 | Survival of *H. marinus*, *E. coli*, *B. subtilis* (vegetative cells), and *D. radiodurans* after exposure to Na-perchlorate at room temperature. **(A)** *H. marinus* was either exposed to Na-perchlorate for 15 min (black circles) or for 96 h (gray circles). **(B)** *E. coli* (black triangle), *B. subtilis* (vegetative cells), and *D. radiodurans* were exposed for 15 min to Na-perchlorate.

TABLE 1 | Calculated D_{10}-values of *H. marinus* and reference organisms after treatment with Na-perchlorate.

Strains	D_{10}-value (15 min; $NaClO_4$)
H. marinus	>5 M[a]
B. subtilis (purified spores)	>5 M[a]
B. subtilis (vegetative cells)	1.9 M
E. coli	1.3 M
D. radiodurans	2.7 M

[a]*Not determinable precisely.*

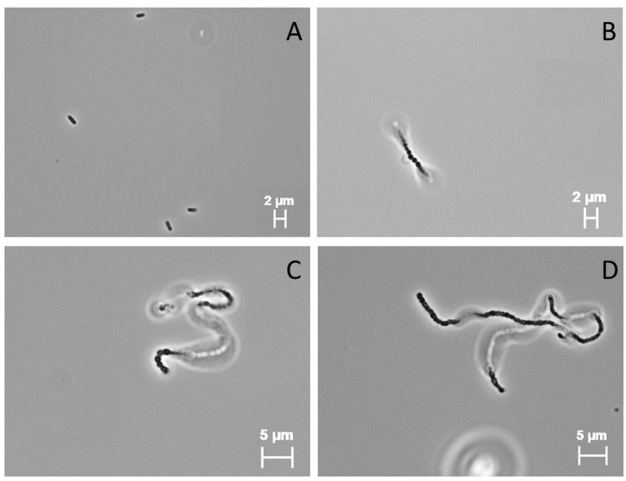

FIGURE 2 | Light microscopic (100×; PH3) images of *H. marinus* under standard cultivation conditions **(A)** and cultivation in the presence of 300 mM Na-perchlorate **(B–D)**.

Hydrogenothermus marinus is tolerant to desiccation under oxic and anoxic conditions is the same way (Beblo et al., 2009). Nevertheless, the desiccation tolerance was negatively influenced by the presence of different perchlorates. Below 100 mM Na-perchlorate during cultivation, only minor effects occurred. In contrast, concentrations of 100 mM and higher had an important influence on desiccation tolerance. Even if *H. marinus* is able to grow in the presence of Na-perchlorate up to 450 mM, perchlorate treated cells showed survival after desiccation only up to a maximum of 200 mM Na-perchlorate [S (24 h, 200 mM $NaClO_4$) = 1×10^{-8}] (**Figure 3A**).

The presence of Mars analogous concentrations (0.5% wt/vol and 1.0% wt/vol, corresponding to 35 mM and 71 mM $NaClO_4$) of different perchlorates (Na-, Mg-, and Ca-perchlorate) during growth also influenced the survival after desiccation treatment. The type of cation of the perchlorate did not have a significant effect on the survival after desiccation. After 24 h of desiccation under oxic conditions, perchlorates in concentration of 0.5% (wt/vol) led to an average survival rate of 3×10^{-4}; concentrations of 1% (wt/vol) entail an additional reduction of the survival rate of one to two orders of magnitude (**Figure 3B**).

DISCUSSION

Halophilic Archaea and Bacteria (e.g., *Halobacterium salinarum*; *Halomonas elongata*) are able to grow to some extent in

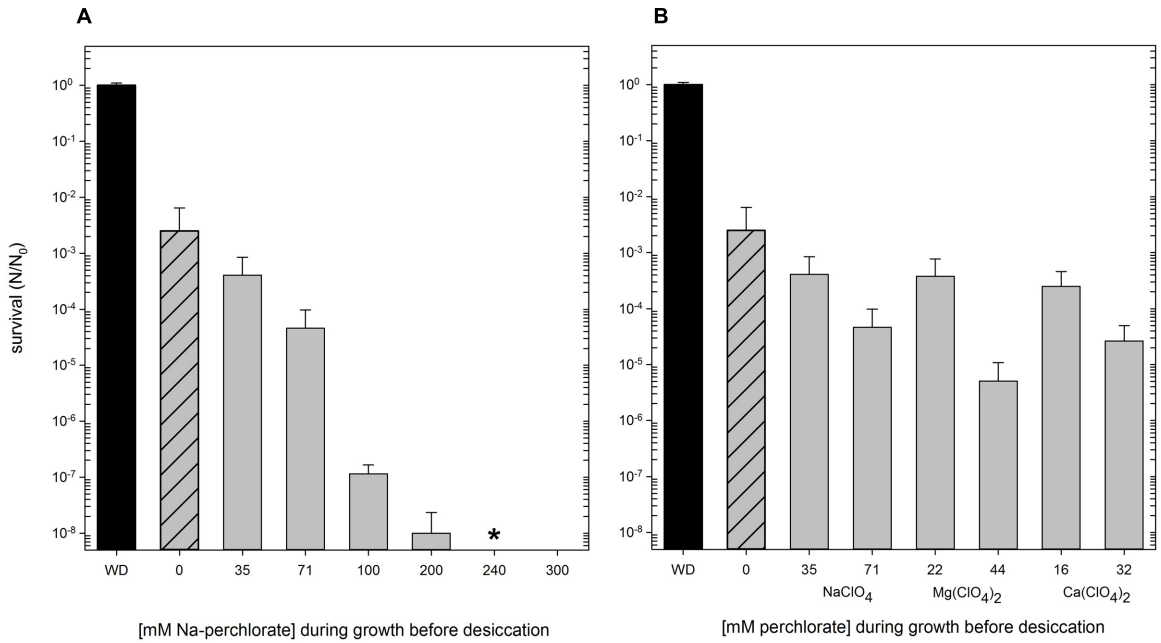

FIGURE 3 | Survival of *H. marinus* after desiccation (24 h, oxic conditions), preceding cultivation of the cells was carried out at the indicated concentrations of perchlorates. Reactivation after desiccation was carried out in standard (perchlorate free) medium. Ascending concentration of Na-perchlorate up to 300 mM **(A)**. Different concentration of different perchlorates [$NaClO_4$, $Mg(ClO_4)_2$, $Ca(ClO_4)_2$] corresponding to 0.5% (wt/vol) and 1.0% (wt/vol), respectively **(B)**. WD: without desiccation; shaded: no perchlorate during cultivation; * no viable cells could be detected after reactivation.

perchlorate containing medium up to 0.4 M Na-perchlorate (Oren et al., 2014; Matsubara et al., 2017). Compared to this, *H. marinus* was as tolerant as the halophilic strains to perchlorates and could grow in the presence of 0.45 M Na-perchlorate. Similar results were obtained for the hyperthermophilic Archaeon *A. fulgidus* where growth was observable up to 0.4 M Na-perchlorate. During the metabolic studies with *A. fulgidus* it could be shown that perchlorates are stable at different cultivation conditions: for example, incubation temperatures of 85°C and high salt concentrations do not lead to a degradation of the perchlorates during cultivation (Liebensteiner et al., 2013; Al Soudi et al., 2017). Therefore, degradation effects for of *H. marinus*, with an incubation temperature of 65°C at moderate salt conditions can be excluded.

The extraordinarily high tolerance of *H. marinus* was obvious in the short term shock exposure experiments where the exposure concentration exceeded by far the concentration where growth is possible: 15 min in 5 M Na-perchlorates at room temperature did not lead to any change in survivability. Only 96 h of exposure resulted in a reduced survivability. The Archaea *Methanothermobacter wolfeii*, and *Methanosarcina barkeri* were able to survive exposure to 5 and 25% perchlorates (Mg-, Ca-, Na-perchlorate) for variable lengths of time with *M. wolfeii* surviving the 25% (≙ 1.1 M Mg-perchlorate) concentration for 72 h (Kral et al., 2016).

In general, modifying size and shape in response to changes in the environmental conditions or to stress factors is known. Filamentation, based on an incomplete cell division process, is one observed shape alteration that can be influenced by several factors such as nutrient deprivation, oxidative stress, DNA damage, exposure to antibiotics and temperatures shifts (Young, 2006; Justice et al., 2008; Perfumo et al., 2014). The presence of perchlorates during growth led to a clearly visible change in *H. marinus*' morphology. At concentrations exceeding 0.2 M, chain formation was observable. When Na-perchlorate was no longer present, the morphological changes were completely reversible and the cells were growing similar to control cells. It seemed that Na-perchlorate triggers the chain formation. Morphological changes due to Na-perchlorate are also described for halophilic and methanogenic microorganisms. Grown at the highest tolerated perchlorate concentrations, *H. salinarum*, *Haloferax mediterranei*, and *Haloarcula marismortui* were unusually swollen and deformed. For instance, *H. elongata* cells looked normal up to 0.2 M Na-perchlorate, but in a medium with 0.4 M Na-perchlorate, the cells had a thin and wrinkled appearance (Oren et al., 2014). One methanogenic strain, *Methanobacterium arcticum,* shows other morphological changes and builds cyst-like cells in the presence of Mg-perchlorate (Shcherbakova et al., 2015). The reason for the morphological change of *H. marinus* is not known. It could be speculated that the chain formation provides an advantage in the survival during cell damaging conditions. Comparable phenomena, including cell aggregation and biofilm formation have already been observed in *Sulfolobus solfataricus* after UV-irradiation and in *A. fulgidus* in various stress conditions (LaPaglia and Hartzell, 1997; Fröls et al., 2008). In addition to these two examples for hyperthermophilic Archaea, filament formation is also known

in Bacteria such as *Listeria monocytogenes* and *Campylobacter jejuni* (Cameron et al., 2012; Jones et al., 2013). In these instances the filamentation is caused by sublethal (e.g., hyperosmotic) stress.

The cellular mechanisms for the morphological changes in *H. marinus* remain speculative. It seemed that the perchlorates ions penetrated the cells and interfere with the cell metabolism. The cells were not able to divide properly in the presence of Na-perchlorate. Which specific part of the cell division mechanism is influenced by perchlorates cannot be clarified so far: possible targets could be proteins used by microorganisms for septum formation and cell separation/division. In this process at least nine proteins (eight Fts proteins and the ZipA protein) are involved (Lutkenhaus and Addinall, 1997). For example, mutants of *E. coli* which have a mutation in the FtsA or the FtsZ protein grow in filaments instead of single cells (Walker et al., 1975; Addinall et al., 1996). Comparable results were obtained for *E. coli* ZipA mutants (Pichoff and Lutkenhaus, 2002). Since the genome sequence and a knock out mutant system for *H. marinus* are lacking, we could not elucidate which proteins are affected, a situation also found for the other microorganisms with morphological changes like *H. salinarum*, *H. mediterranei, H. marismortui*, and *H. elongata*.

Not only morphology was influenced by the presence of perchlorates, but also *H. marinus*' desiccation tolerance was affected by perchlorates. Compared to other vegetative cells, *H. marinus* shows a significant desiccation tolerance and can survive periods of water loss for up to 6 months (Beblo et al., 2009). The combination of exposure to perchlorates during growth followed by desiccation led to a typical additive effect. The additive model may be particularly appropriate when stressors affect different physiological processes (Folt et al., 1999). However, it seemed that only single cells and not the cell chains were tolerant to desiccation. Lower perchlorate concentrations (0.5%; 1%) leading to a mixture of chains and single cells resulted in a reduced survivability after desiccation. Concentrations higher than 0.2 M, lead exclusively to growth in chains, resulted in a complete disappearance of desiccation tolerance.

In general, the question arises whether the perchlorate ions themselves and/or the corresponding counter ions play a role in affecting the cells. Previous studies showed that *H. marinus* is very tolerant to high salinity. The addition of NaCl (up to 1.2 M) during growth leads to formation and accumulation of compatible solutes and an elevation of desiccation tolerance in *H. marinus* (Beblo-Vranesevic et al., 2017). For some halotolerant strains, an influence of the counter ions can be neglected (Al Soudi et al., 2017). For *H. marinus* an influence of the counter ions (Na^+, Ca^{2+}, Mg^{2+}) can nearly be excluded, because all of these ions are also present in the standard cultivation medium (VM-1). VM-1 medium contains 0.4 M of Na^+ ions, 0.13 M of Mg^{2+} ions and 0.01 M of Ca^{2+} ions (Stöhr et al., 2001). These ions are present in lower concentration in the standard medium than during exposures to the corresponding perchlorates in the experiment described above. Nevertheless, *H. marinus* is not only adapted to them and is even dependent on their presence.

On Mars, liquid water may be temporarily available within brines. Perchlorates, as hydroscopic substances, bind water from the atmosphere and contribute to the formation of these brines, which remain liquid at low temperatures prevailing on the surface of Mars (Gough et al., 2011; Toner and Catling, 2016). Martian brines contain high amounts of different dissolved salts, including chlorides, sulfates, and perchlorates (Kounaves et al., 2014; Fox-Powell et al., 2016). Within this transient liquid water on the surface of Mars, a simultaneous appearance of high salt concentrations and perchlorates occur (Martín-Torres et al., 2015). In subsurface of Mars pressure and temperature increases with depth and thereby the probability of liquid, additionally radiation protected, water reservoirs (such as subsurface aquifers) rises, too (Boston et al., 1992; Dartnell et al., 2007). Thinking about Martian habitability these areas could be one option where microbial life could be preserved, survive or even thrive.

In general, *H. marinus* unites some properties which are of essential importance when discussing the past and present habitability of Mars: the organisms can only grow at low oxygen concentrations (down to 0.5 vol % O_2, Stöhr et al., 2001), the Martian atmosphere contains today an average oxygen concentration of 0.13% (Horneck, 2000); the cells are able to grow in the presence of Martian concentrations of perchlorates in combination with an exceptional desiccation tolerance (Beblo et al., 2009); they are tolerant to salt concentrations up to 1.2 M (Stöhr et al., 2001; Beblo-Vranesevic et al., 2017); the organism shows survival after exposure to UV-C and ionizing radiation (Beblo et al., 2011). The radiation dose rate of ionizing radiation on the surface of Mars was measured and calculated to be up to 0.21 mGy per day (Hassler et al., 2014; Matthiä et al., 2016) and is therefore significantly lower than in the applied experiments. In these experiments, viable cells could still be found after a dose of 5 kGy (Beblo et al., 2011). It is assumed that even radiation sensitive organisms, such as *H. marinus*, could survive the radiation occurring on the Martian surface or in the first centimeter of Martian regolith for several years or decades (Dartnell et al., 2007). Altogether, this makes *H. marinus* a promising new model organism for studies in Astrobiology.

AUTHOR CONTRIBUTIONS

KB-V and Kathya Bustamante (KB) performed experiments. KB-V wrote the manuscript. HH and PR contributed to the design of the study and both contributed to the writing and editing of the manuscript.

ACKNOWLEDGMENTS

We want to thank Kathya Bustamante (KB) financed via a DAAD exchange program for performing the experiments with *D. radiodurans*, *E. coli*, and *B. subtilis* at the German Aerospace Center. Purified *B. subtilis* spores were kindly provided by Dr. Ralf Moeller (German Aerospace Center). Additionally, we want to thank Rocco L. Mancinelli (NASA Ames Research Center) for critically reading of the manuscript.

REFERENCES

Addinall, S. G., Bi, E., and Lutkenhaus, J. (1996). FtsZ ring formation in fts mutants. *J. Bacteriol.* 178, 3877–3884. doi: 10.1128/jb.178.13.3877-3884.1996

Al Soudi, A. F., Farhat, O., Chen, F., Clark, B. C., and Schneegurt, M. A. (2017). Bacterial growth tolerance to concentrations of chlorate and perchlorate salts relevant to Mars. *Int. J. Astrobiol.* 16, 229–235. doi: 10.1017/S1473550416000434

Archer, P. D. Jr., Sutter, B., Ming, D. W., McKay, C. P., Navarro-Gonzalez, R., Franz, H. B., et al. (2013). "Possible detection of perchlorates by evolved gas analysis of Rocknest soils: global implications," in *Proceedings of the 44th Lunar and Planetary Science Conference Abstracts* (Houston, TX: Lunar and Planetary Institute).

Attaway, H., and Smith, M. (1993). Reduction of perchlorate by an anaerobic enrichment culture. *J. Ind. Microbiol.* 12, 408–412. doi: 10.1007/BF01569673

Bauermeister, A. (2012). *Characterization of Stress Tolerance and Metabolic Capabilities of Acidophilic Iron-Sulfur-Transforming Bacteria and Their Relevance to Mars*. Doctoral dissertation, University of Duisburg-Essen, Duisburg.

Bauermeister, A., Rettberg, P., and Flemming, H. C. (2014). Growth of the acidophilic iron–sulfur bacterium *Acidithiobacillus ferrooxidans* under Mars-like geochemical conditions. *Planet. Space Sci.* 98, 205–215. doi: 10.1016/j.pss.2013.09.009

Beblo, K., Douki, T., Schmalz, G., Rachel, R., Wirth, R., Huber, H., et al. (2011). Survival of thermophilic and hyperthermophilic microorganisms after exposure to UV-C, ionizing radiation and desiccation. *Arch. Microbiol.* 193, 797–809. doi: 10.1007/s00203-011-0718-5

Beblo, K., Rabbow, E., Rachel, R., Huber, H., and Rettberg, P. (2009). Tolerance of thermophilic and hyperthermophilic microorganisms to desiccation. *Extremophiles* 13, 521–531. doi: 10.1007/s00792-009-0239-1

Beblo-Vranesevic, K., Galinski, E. A., Rachel, R., Huber, H., and Rettberg, P. (2017). Influence of osmotic stress on desiccation and irradiation tolerance of (hyper)-thermophilic microorganisms. *Arch. Microbiol.* 199, 17–28. doi: 10.1007/s00203-016-1269-6

Boston, P. J., Ivanov, M. V., and McKay, C. P. (1992). On the possibility of chemosynthetic ecosystems in subsurface habitats on Mars. *Icarus* 95, 300–308. doi: 10.1016/0019-1035(92)90045-9

Cameron, A., Frirdich, E., Huynh, S., Parker, C. T., and Gaynor, E. C. (2012). Hyperosmotic stress response of *Campylobacter jejuni*. *J. Bacteriol.* 194, 6116–6130. doi: 10.1128/JB.01409-12

Carrier, B. L., and Kounaves, S. P. (2015). The origins of perchlorate in the Martian soil. *Geophys. Res. Lett.* 42, 3739–3745. doi: 10.1002/2015GL064290

Catling, D. C., Claire, M. W., Zahnle, K. J., Quinn, R. C., Clark, B. C., Hecht, M. H., et al. (2010). Atmospheric origins of perchlorate on Mars and in the Atacama. *J. Geophys. Res. Planet.* 115:E00E11. doi: 10.1029/2009je003425

Coates, J. D., and Achenbach, L. A. (2004). Microbial perchlorate reduction: rocket-fuelled metabolism. *Nat. Rev. Microbiol.* 2, 569–580. doi: 10.1038/nrmicro926

Cockell, C. S., Bush, T., Bryce, C., Direito, S., Fox-Powell, M., Harrison, J. P., et al. (2016). Habitability: a review. *Astrobiology* 16, 89–117. doi: 10.1089/ast.2015.1295

Dartnell, L. R., Desorgher, L., Ward, J. M., and Coates, A. J. (2007). Modelling the surface and subsurface Martian radiation environment: implications for astrobiology. *Geophys. Res. Lett.* 34:L02207. doi: 10.1029/2006gl027494

Folt, C. L., Chen, C. Y., Moore, M. V., and Burnaford, J. (1999). Synergism and antagonism among multiple stressors. *Limnol. Oceanogr.* 44, 864–877. doi: 10.4319/lo.1999.44.3_part_2.0864

Fox-Powell, M. G., Hallsworth, J. E., Cousins, C. R., and Cockell, C. S. (2016). Ionic strength is a barrier to the habitability of Mars. *Astrobiology* 16, 427–442. doi: 10.1089/ast.2015.1432

Franson, M. A. H. (ed.). (1985). *Standard Methods for the Examination of Water and Wastewater*, 16th Edn. Washington, DC: American Public Health Association.

Fröls, S., Ajon, M., Wagner, M., Teichmann, D., Zolghadr, B., Folea, M., et al. (2008). UV-inducible cellular aggregation of the hyperthermophilic archaeon *Sulfolobus solfataricus* is mediated by pili formation. *Mol. Microbiol.* 70, 938–952. doi: 10.1111/j.1365-2958.2008.06459.x

Glavin, D. P., Freissinet, C., Miller, K. E., Eigenbrode, J. L., Brunner, A. E., Buch, A., et al. (2013). Evidence for perchlorates and the origin of chlorinated hydrocarbons detected by SAM at the Rocknest aeolian deposit in Gale Crater. *J. Geophys. Res. Planets* 118, 1955–1973. doi: 10.1002/jgre.20144

Gough, R. V., Chevrier, V. F., Baustian, K. J., Wise, M. E., and Tolbert, M. A. (2011). Laboratory studies of perchlorate phase transitions: support for metastable aqueous perchlorate solutions on Mars. *Earth Planet. Sci. Lett.* 312, 371–377. doi: 10.1016/j.epsl.2011.10.026

Harm, W. (1980). *Biological Effects of Ultraviolet Radiation*. Cambridge: Cambridge University Press.

Hassler, D. M., Zeitlin, C., Wimmer-Schweingruber, R. F., Ehresmann, B., Rafkin, S., Eigenbrode, J. L., et al. (2014). Mars' surface radiation environment measured with the Mars Science Laboratory's Curiosity rover. *Science* 343:1244797. doi: 10.1126/science.1244797

Hecht, M. H., Kounaves, S. P., Quinn, R. C., West, S. J., Young, S. M., Ming, D. W., et al. (2009). Detection of perchlorate and the soluble chemistry of Martian soil at the Phoenix lander site. *Science* 325, 64–67. doi: 10.1126/science.1172466

Horneck, G. (2000). The microbial world and the case for Mars. *Planet. Space Sci.* 48, 1053–1063. doi: 10.1089/ast.2012.0833

Jones, T. H., Vail, K. M., and McMullen, L. M. (2013). Filament formation by foodborne bacteria under sublethal stress. *Int. J. Food Microbiol.* 165, 97–110. doi: 10.1016/j.ijfoodmicro.2013.05.001

Justice, S. S., Hunstad, D. A., Cegelski, L., and Hultgren, S. J. (2008). Morphological plasticity as a bacterial survival strategy. *Nat. Rev. Microbiol.* 6, 162–168. doi: 10.1038/nrmicro1820

Kim, Y. S., Wo, K. P., Maity, S., Atreya, S. K., and Kaiser, R. I. (2013). Radiation-induced formation of chlorine oxides and their potential role in the origin of Martian perchlorates. *J. Am. Chem. Soc.* 135, 4910–4913. doi: 10.1021/ja3122922

Kounaves, S. P., Chaniotakis, N. A., Chevrier, V. F., Carrier, B. L., Folds, K. E., Hansen, V. M., et al. (2014). Identification of the perchlorate parent salts at the Phoenix Mars landing site and possible implications. *Icarus* 232, 226–231. doi: 10.1016/j.icarus.2014.01.016

Kral, T. A., Goodhart, T. H., Harpool, J. D., Hearnsberger, C. E., McCracken, G. L., and McSpadden, S. W. (2016). Sensitivity and adaptability of methanogens to perchlorates: implications for life on Mars. *Planet. Space Sci.* 120, 87–95. doi: 10.1016/j.pss.2015.11.014

LaPaglia, C., and Hartzell, P. L. (1997). Stress-induced production of biofilm in the hyperthermophile *Archaeoglobus fulgidus*. *Appl. Environ. Microbiol.* 63, 3158–3163.

Liebensteiner, M. G., Pinkse, M. W., Schaap, P. J., Stams, A. J., and Lomans, B. P. (2013). Archaeal (per)chlorate reduction at high temperature: an interplay of biotic and abiotic reactions. *Science* 340, 85–87. doi: 10.1126/science.1233957

Logan, B. E. (1998). A review of chlorate-and perchlorate-respiring microorganisms. *Bioremed. J.* 2, 69–79. doi: 10.1080/10889869891214222

Lutkenhaus, J., and Addinall, S. G. (1997). Bacterial cell division and the Z ring. *Annu. Rev. Biochem.* 66, 93–116. doi: 10.1146/annurev.biochem.66.1.93

Martín-Torres, F. J., Zorzano, M. P., Valentín-Serrano, P., Harri, A. M., Genzer, M., Kemppinen, O., et al. (2015). Transient liquid water and water activity at Gale crater on Mars. *Nat. Geosci.* 8, 357–361. doi: 10.1038/ngeo2412

Matsubara, T., Fujishima, K., Saltikov, C. W., Nakamura, S., and Rothschild, L. J. (2017). Earth analogues for past and future life on Mars: isolation of perchlorate resistant halophiles from Big Soda Lake. *Int. J. Astrobiol.* 16, 218–228. doi: 10.1017/S1473550416000458

Matthiä, D., Ehresmann, B., Lohf, H., Köhler, J., Zeitlin, C., Appel, J., et al. (2016). The Martian surface radiation environment–a comparison of models and MSL/RAD measurements. *J. Space Weather Space Clim.* 6:A13. doi: 10.1126/science.1244797

Michalski, G., Böhlke, J. K., and Thiemens, M. (2004). Long term atmospheric deposition as the source of nitrate and other salts in the Atacama desert, Chile: new evidence from mass-independent oxygen isotopic compositions. *Geochim. Cosmochim. Acta* 68, 4023–4038. doi: 10.1016/j.gca.2004.04.009

Nagler, K., and Moeller, R. (2015). Systematic investigation of germination responses of *Bacillus subtilis* spores in different high-salinity environments. *FEMS Microbiol. Ecol.* 91:fiv023. doi: 10.1093/femsec/fiv023

Nagler, K., Setlow, P., Li, Y. Q., and Moeller, R. (2014). High salinity alters the germination behavior of *Bacillus subtilis* spores with nutrient and nonnutrient germinants. *Appl. Environ. Microbiol.* 80, 1314–1321. doi: 10.1128/AEM.03293-13

Nerenberg, R. (2013). Breathing perchlorate. *Science* 340, 38–39. doi: 10.1126/science.1236336

Ojha, L., Wilhelm, M. B., Murchie, S. L., McEwen, A. S., Wray, J. J., Hanley, J., et al. (2015). Spectral evidence for hydrated salts in recurring slope lineae on Mars. *Nat. Geosci.* 8, 829–832. doi: 10.1038/ngeo2546

Oren, A. (2014). Halophilic archaea on Earth and in space: growth and survival under extreme conditions. *Philos. Trans. R Soc. Math. Phys. Eng. Sci.* 372:20140194. doi: 10.1098/rsta.2014.0194

Oren, A., Bardavid, R. E., and Mana, L. (2014). Perchlorate and halophilic prokaryotes: implications for possible halophilic life on Mars. *Extremophiles* 18, 75–80. doi: 10.1007/s00792-013-0594-9

Perfumo, A., Elsaesser, A., Littmann, S., Foster, R. A., Kuypers, M. M., Cockell, C. S., et al. (2014). Epifluorescence, SEM, TEM and nanoSIMS image analysis of the cold phenotype of *Clostridium psychrophilum* at subzero temperatures. *FEMS Microbiol. Ecol.* 90, 869–882. doi: 10.1111/1574-6941.12443

Pichoff, S., and Lutkenhaus, J. (2002). Unique and overlapping roles for ZipA and FtsA in septal ring assembly in *Escherichia coli*. *EMBO J.* 21, 685–693. doi: 10.1093/emboj/21.4.685

Schuttlefield, J. D., Sambur, J. B., Gelwicks, M., Eggleston, C. M., and Parkinson, B. A. (2011). Photooxidation of chloride by oxide minerals: implications for perchlorate on Mars. *J. Am. Chem. Soc.* 133, 17521–17523. doi: 10.1021/ja2064878

Shcherbakova, V., Oshurkova, V., and Yoshimura, Y. (2015). The effects of perchlorates on the permafrost methanogens: implication for autotrophic life on Mars. *Microorganisms* 3, 518–534. doi: 10.3390/microorganisms3030518

Stöhr, R., Waberski, A., Völker, H., Tindall, B., and Thomm, M. (2001). *Hydrogenothermus marinus* gen. nov., sp. nov., a novel thermophilic hydrogen-oxidizing bacterium, recognition of *Calderobacterium hydrogenophilum* as a member of the genus *Hydrogenobacter* and proposal of the reclassification of *Hydrogenobacter acidophilus* as *Hydrogenobaculum acidophilum* gen. nov., comb. nov., in thephylum '*Hydrogenobacter/Aquifex*'. *Int. J. Syst. Evol. Microbiol.* 51, 1853–1862. doi: 10.1099/00207713-51-5-1853

Toner, J. D., and Catling, D. C. (2016). Water activities of $NaClO_4$, $Ca(ClO_4)_2$, and $Mg(ClO_4)_2$ brines from experimental heat capacities: water activity > 0.6 below 200K. *Geochim. Cosmochim. Acta* 181, 164–174. doi: 10.1016/j.gca.2016.03.005

Trumpolt, C. W., Crain, M., Cullison, G. D., Flanagan, S. J., Siegel, L., and Lathrop, S. (2005). Perchlorate: sources, uses, and occurrences in the environment. *Remediat. J.* 16, 65–89. doi: 10.1002/rem.20071

Walker, J. R., Kovarik, A. G., Allen, J. S., and Gustafson, R. A. (1975). Regulation of bacterial cell division: temperature-sensitive mutants of *Escherichia coli* that are defective in septum formation. *J. Bacteriol.* 123, 693–703.

Young, K. D. (2006). The selective value of bacterial shape. *Microbiol. Mol. Biol. Rev.* 70, 660–703. doi: 10.1128/MMBR.00001-06

ZoBell, C. E. (1941). Studies on marine Bacteria. The cultural requirements of heterotrophic aerobes. *J. Mar. Res.* 4, 42–75.

Conflict of Interest Statement: The authors declare that the research was conducted in the absence of any commercial or financial relationships that could be construed as a potential conflict of interest.

frontiers in Microbiology

ORIGINAL RESEARCH
published: 22 December 2017
doi: 10.3389/fmicb.2017.02527

Biological Characterization of Microenvironments in a Hypersaline Cold Spring Mars Analog

Haley M. Sapers[1,2,3], Jennifer Ronholm[4,5], Isabelle Raymond-Bouchard[3], Raven Comrey[3], Gordon R. Osinski[1,2,6] and Lyle G. Whyte[3]*

[1] Centre for Planetary Science and Exploration, Faculty of Science, Western Science Centre, Western University, London, ON, Canada, [2] Department of Earth Sciences, University of Western Ontario, London, ON, Canada, [3] Department of Natural Resource Sciences, McGill University, Montreal, QC, Canada, [4] Department of Food Science and Agricultural Chemistry, McGill University, Montreal, QC, Canada, [5] Department of Animal Science, Faculty of Agricultural and Environmental Sciences, McGill University, Montreal, QC, Canada, [6] Department of Physics and Astronomy, University of Western Ontario, London, ON, Canada

While many habitable niches on Earth are characterized by permanently cold conditions, little is known about the spatial structure of seasonal communities and the importance of substrate-cell associations in terrestrial cryoenvironments. Here we use the 16S rRNA gene as a marker for genetic diversity to compare two visually distinct but spatially integrated surface microbial mats on Axel Heiberg Island, Canadian high arctic, proximal to a perennial saline spring. This is the first study to describe the bacterial diversity in microbial mats on Axel Heiberg Island. The hypersaline springs on Axel Heiberg represent a unique analog to putative subsurface aquifers on Mars. The Martian subsurface represents the longest-lived potentially habitable environment on Mars and a better understanding of the microbial communities on Earth that thrive in analog conditions will help direct future life detection missions. The microbial mats sampled on Axel Heiberg are only visible during the summer months in seasonal flood plains formed by melt water and run-off from the proximal spring. Targeted-amplicon sequencing revealed that not only does the bacterial composition of the two mat communities differ substantially from the sediment community of the proximal cold spring, but that the mat communities are distinct from any other microbial community in proximity to the Arctic springs studied to date. All samples are dominated by Gammaproteobacteria: Thiotichales is dominant within the spring samples while Alteromonadales comprises a significant component of the mat communities. The two mat samples differ in their Thiotichales:Alteromonadales ratio and contribution of Bacteroidetes to overall diversity. The red mats have a greater proportion of Alteromonadales and Bacteroidetes reads. The distinct bacterial composition of the mat bacterial communities suggests that the spring communities are not sourced from the surface, and that seasonal melt events create ephemerally habitable niches with distinct microbial communities in the Canadian high arctic. The finding that these surficial complex microbial communities exist in close proximity to perennial springs demonstrates the existence of a transiently habitable niche in an important Mars analog site.

Keywords: cold spring, Mars analog, permafrost, phsycrophile, microbial ecology

OPEN ACCESS

Edited by:
Andreas Teske, University of North Carolina at Chapel Hill, United States

Reviewed by:
Richard Allen White III, Washington State University, United States
Alberto Robador, University of Southern California, United States

****Correspondence:***
Haley M. Sapers
haley.sapers@gmail.com

Specialty section:
This article was submitted to Extreme Microbiology, a section of the journal Frontiers in Microbiology

Received: *26 June 2017*
Accepted: *05 December 2017*
Published: *22 December 2017*

Citation:
Sapers HM, Ronholm J, Raymond-Bouchard I, Comrey R, Osinski GR and Whyte LG (2017) Biological Characterization of Microenvironments in a Hypersaline Cold Spring Mars Analog. Front. Microbiol. 8:2527. doi: 10.3389/fmicb.2017.02527

INTRODUCTION

Despite the dominance of permanently cold environments on Earth (Margesin and Miteva, 2011), the biological significance of the cryosphere has only begun to be recognized over the last decade (e.g., Priscu and Christner, 2004). Terrestrial cryoenvironments in polar regions are characterized by extremely low temperatures, limited water availability, and a thick permafrost layer. Diverse suites of cryophilic microorganisms have successfully colonized these environments and play key ecological roles in carbon and nutrient cycling (Margesin and Miteva, 2011). These extreme environments, characterized by low temperatures and often high salinity are exceptional analogs for putative habitable environments beyond Earth (Fairén et al., 2010; McKay et al., 2012).

The current atmospheric pressure on Mars precludes the formation of standing water at the surface. The presence of past liquid water is evidenced by the association of phyllosilicates with ancient crustal terrains, and subsurface liquid water interacted with the surface environment in catastrophic outflows during the Noachian (Lasue et al., 2013) to as recently as a few million years ago (Burr et al., 2002; Neukum et al., 2010). Liquid water on Mars, if it exists today, is likely in the form of subsurface eutectic brines in a spatially restricted hydrogeological cycle existing in thick permafrost (e.g., Martínez and Renno, 2013). Putative evidence of transient liquid water lies in observations of high-latitude seepage gullies (Malin and Edgett, 2000), recurring slope lineae (RSL) containing evidence of hydrated salts indicating briny water (Ojha et al., 2015) and somewhat more controversially, Martian slope streaks (Bhardwaj et al., 2017). The physiochemical parameters that characterize the cryoenvironments on Axel Heiberg Island, Canada, and specifically, the Gypsum Hill spring system represents a terrestrial analog for putatively habitable subsurface briny aquifers on Mars (Malin and Edgett, 2000; Andersen, 2002; Malin et al., 2006; Rossi et al., 2008; Davila et al., 2010; Fairén et al., 2010; McKay et al., 2012; Battler et al., 2013).

Axel Heiberg Island, in the high Canadian Arctic hosts a series of perennial cold springs (Pollard et al., 1999; Omelon et al., 2001, 2006; Andersen, 2002; Pollard, 2005; Battler et al., 2013) (**Figure 1**) dominated by unique microbial communities (Grasby et al., 2004; Perreault et al., 2007, 2008; Steven et al., 2007; Niederberger et al., 2009, 2010; Lay et al., 2012, 2013; Lamarche-Gagnon et al., 2015) usually associated with deep subsurface or submarine environments. The hypersaline cold springs on Axel Heiberg Island are among the only known perennial springs flowing through thick permafrost on Earth (Andersen, 2002) and comprise a unique opportunity to study microbial diversity in cryoenvironments. Perennial spring activity in regions dominated by permafrost are extremely rare as the permanently frozen layer forms an aquitard effectively separating supra- and sub-permafrost aquifers limiting surficial activity to seasonal melt-associated events (Williams and van Everdingen, 1973). The extensive diapirism characterizing the Expedition Fiord area of Axel Heiberg Island creates a series of chemical talks coupling supra and sub-permafrost reservoirs allowing for continual hypersaline fluid circulation and perennial spring activity (Pollard et al., 1999; Andersen, 2002; Harrison and Jackson, 2014).

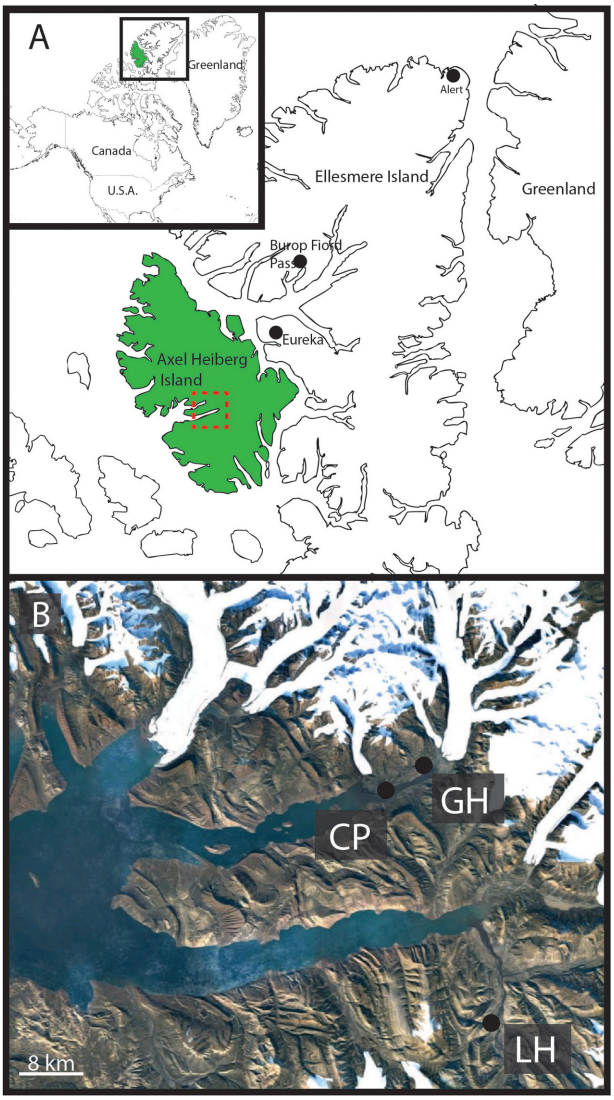

FIGURE 1 | Geographic location of Gypsum Hill spring. **(A)** Axel Heiberg Island (green) and Ellesmere Island, boxed area shown in inset. Expedition Fiord, Axel Heiberg is outlined by the red box. Burop Fiord Pass, Ellesmere Island is indicated. **(B)** Satellite image of Expedition Fiord (red box, **A**). The three main hypersaline cold springs are indicated: LH: Lost Hammer, CP: Color Peak, GH: Gypsum Hill. Landsat-7 image courtesy of the U.S. Geological Survey.

The Gypsum Hill springs, one such system on Axel Heiberg Island, at nearly 80 N, is the only known nonvolcanic, hypersaline, sulphidic, perennial cold spring system on Earth. Detailed studies have characterized the microbial community of Gypsum Hill spring by assessing the diversity of the source sediments and water at four outlets (Perreault et al., 2007, 2008) and snow-covered run-off channels present in the winter (Niederberger et al., 2009). These studies indicate that the springs' microbial community is primarily sustained by

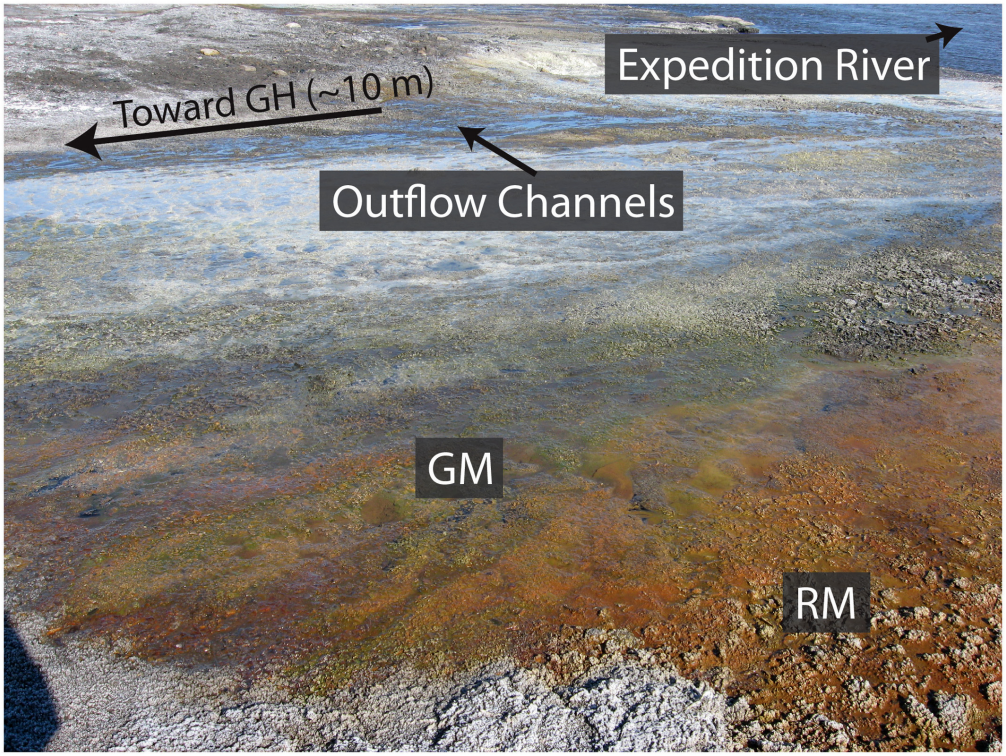

FIGURE 2 | Visually distinct red and green mats forming the Gypsum Hill flood plain. The red (RM) and green (GM) microbial mats sampled in this study are shown relative to the Gypsum Hill (GH) outflow channels proximal to Expedition River. Note the intermixing of the microbial mats with the red mats dominating the areas furthest away from the GH outflow channels.

chemolithoautotrophic primary production performed by sulfur-oxidizing bacteria, with little to no evidence of phototrophic metabolism despite being surface exposed and in continuous illumination during the Arctic summer. To date, ecosystems of this type have been found only in permanently dark hydrothermal vents and sulfidic groundwater (Perreault et al., 2008). A study of streamers growing in snow-covered run-off channels forming during the winter months identified extremely limited microbial diversity again dominated by sulfur-oxidizing bacteria (Niederberger et al., 2009).

The microbial community and metabolic profile of surface waters from the Gypsum Hill springs suggests that the community may be derived from subsurface communities inoculated into the hypersaline fluids upwelling through the underlying Expedition diapir as opposed to seeding by surface-associated microorganisms (e.g., Perreault et al., 2008). Alternatively, the community may be evolved from the source water reservoir, having undergone selection during the residence time of the fluids in the subsurface. A previous study that identified *Marinobacter* within the Gypsum Hill springs suggested its presence may be due to a marine origin of the springs (Perreault et al., 2008). A flood plain hosting red and green microbial mats associated with the Gypsum Hill springs was observed during fieldwork in the summer of 2013 (**Figure 2**). An outstanding question is whether summer flood plains may support ephemeral, seasonal microbial communities colonizing the flood plain and how much diversity these seasonal communities share with the source pool. Such a question is important in understanding the role of perennial fluid flow in permafrost environments in sustaining and/or initiating microbial activity. Here we analyze the bacterial community in visually distinct mats in a proximal flood plain formed during the summer months and compare the results with the sediment-associated bacterial community in Gypsum Hill outlet 4 to assess the potential contribution of surface microorganisms to the spring community. While there are significant limits to using 16S rRNA targeted-amplicon sequencing data to assess microbial community structure, the data highlight compositional differences at high taxonomic levels and provide insight to plausible mechanisms of niche differentiation.

MATERIALS AND METHODS

Gypsum Hill Spring

The Gypsum Hill spring system (79° 25′ N; 90° 45′ W) was originally described by (Beschel, 1963; Pollard et al., 1999) and is discussed in detail by a series of subsequent studies (Pollard et al., 1999; Omelon et al., 2001, 2006; Andersen, 2002; Battler et al., 2013). Gypsum Hill is one of at least 6 identified perennial saline spring systems on Axel Heiberg Island. Gypsum Hill is located in Expedition Fiord approximately 3 km from the White

and Thompson Glaciers on the NE side of Expedition river. The system is comprised of 30–40 small outlets concentrated over an area of approximately 3000 m^2 in a narrow band (∼300 m long × 30 m wide) that perennially discharge a combined average of 15–20 L s^{-1} of anoxic [mean oxido-reduction potential (ORP) ∼325 mV] brines (7.5–8% salts) at the base of Expedition Diapiar (Gypsum Hill). Outlet morphology is highly variable and seasonally dynamic, ranging from well-defined pools, to patches of brine-saturated sediment. Individual outlets discharge microaerophilic (0.05–0.2 ppm dissolved O_2), hypersaline (8–9% salinity), and cold (−0.5–6.6°C) fluids at rates varying from <0.5–1.5 L s^{-1}. The spring waters are near neutral pH (6.9–7.2) characterized by high concentrations of dissolved ions (dominated by Na^+, Cl^-, with lesser K^+, Mg^{2+}, Ca^{2+}, $SO_4{}^{2-}$) and rich in both sulfate (2300–3724 mg^{-1}) and sulfide (25–100 p.p.m.; Andersen, 2002; Pollard, 2005; Perreault et al., 2007). While the temperature of individual outlets vary (–0.5–6.6°C) between one another, fluid temperature (3 or 4°C average) is relatively constant despite significant seasonal changes in air temperature (Pollard, 2005). The physiochemical parameters of the springs have been detailed by others (Pollard et al., 1999; Omelon et al., 2001), and remain largely unchanged from the original chemistry reported by Beschel (1963). It is interesting, as first noted by Beschel (1963), that if all ions are normalized to Na^+, the spring fluids are a chemical match to seawater. Although the physical and chemical characteristics of the fluid discharge have been well characterized, the water source is poorly constrained. It has been hypothesized that the springs originate from subpermafrost salt aquifers and rise to the surface through the permafrost (Andersen, 2002); however, the source aquifer has not been defined and the subsurface hydrogeologic system is largely unknown. An isotopic study by Pollard et al. (1999) found that the Gypsum Hill spring water did not deviate from the established Local Meteoric Water Line suggesting aquifer recharge under climatic conditions similar to modern. While Pollard et al. (1999) had originally presented five possibilities the most favorable including recharge from surface water bodies through tailks, ancient ground water circulation, and deep circulation of glacially pressurized water, Andersen (2002) developed a combined flow and thermal model to demonstrate that the brine discharge may originate in Phantom Lake, a glacially dammed lake several kilometers away.

Field Work

Field work was conducted over two years in July 2013 and July 2014. During the summer of 2013 mats forming in a local flood plain characterized by local patchy color variation over a centimeter scale were identified proximal to outflow channels originating from Gypsum Hill outlet 4 (**Figure 2**). The microbial mats observed were 1–2 mm thick and underlain by dark-black silty water saturated sediments. While surface microbial mat communities are observed on a yearly basis during the summer research season (July–August, personal observations), the extent, appearance (color), range, and location of the mats can change seasonally. Over the course of three field seasons (2013–2015), we observed some mats in different locations, of different sizes, color, and appearance throughout the spring flood plain while other mat areas surrounding the predominant springs (i.e., high continuous flow with little changes over a 15 year observation period) were relatively consistent. During winter the springs become snow covered and it is likely that the flood plains, while not directly visible, are significantly disturbed if not absent. These observations suggest a seasonality and transient nature to the mat communities and a very limited duration of activity during the high Arctic summer months.

Areas dominated with green filamentous streamers (green mat; GM) were observed to be spatially associated with areas of red-brown sediment mats (red mat; RM). Samples of both GM and RM were collected July 10, 2013 by using a sterile 15 ml tube to scoop mat material beneath the air–water interface. Care was taken not to disturb or include the underlying sediment. Samples were frozen in the field and stored at −20°C until DNA extraction. During July 2014, two replicate sediment samples were collected from Gypsum Hill outlet 4 (GH-4, sediment A and sediment B). Sediment samples were frozen in the field and stored at −20°C until DNA extraction. Thus, a total of four samples were selected for downstream analysis, GH4-sediment A and GH4-sediment B from Gypsum Hill outlet 4 (GH-4) and green mats and red mats from the surficial flood plain.

DNA Extraction, Sequencing, and Analysis

Total DNA was extracted from each sample using the RNA PowerSoil Total RNA Kit (MoBio, Carlsbad, CA, United States) and the RNA PowerSoil DNA Elution Accessory Kit (MoBio). Amplicons of partial 16S rRNA (bacteria) were produced for each sample using barcoded primers: forward 27Fmod (5′-AGRGTTTGATCMTGGCTCAG-3′) and reverse 519 (5′-TTACCGCGGCTGCTGGCAC-3′) targeting the V1–V3 hypervariable regions as in (McFrederick et al., 2013). High-throughput targeted-amplicon sequencing was performed by Mr. DNA (Molecular Research LP) (Shallowater, TX, United States) using the GS FLX+ Titanium platform (Roche, Branford, CT, United States) for the outflow channel samples (GM and RM). High-throughput targeted-amplicon sequencing was performed by Genome Quebec using the GS FLX+ Titanium platform for the sediment samples (GH-4).

Sequences were analyzed and classified using the suggested Mothur 454 protocol (Schloss et al., 2009). Briefly,.sff files were separated into.fasta and.qual files using 'sff.info' where flow = T. Sequence error was reduced as per Schloss et al. (2009) RM and GM sequences were trimmed using flowgrams with the 'trim.flows' command with the following parameters: order = A, pdiffs = 5, bdiffs = 2, maxhomop = 8, minflows = 450, maxflows = 450, while spring sediment samples were trimmed with the parameters: order = B, pdiffs = 5, bdiffs = 2, maxhomo = 8, minflows = 650, maxflows = 650. Sequence error was further reduced by 'shhh.flows'. Sequences were reduced to only unique sequences using 'unique.seqs' and unique sequences that passed quality control for the sediment and mat samples were combined. Sequences were aligned to the Mothur-interpreted Silva database (version Silva.nr_v123) with the 'align.seqs' command. Aligned sequences were reduced to

only the overlapping region using 'screen.seqs' and 'filter.seqs' (vertical = T, trump = .). Sequences were again reduced to only unique sequences using 'unique.seqs' then preclustered into OTUs consisting of two or fewer different base pairs using the 'pre.cluster' command (diffs = 2). Chimeras were removed using the uchime program within Mothur. A distance matrix was generated with 'dist.seqs' (cutoff = 0.15) and OTUs were formed based on this distance matrix using 'cluster'. All sequences were classified using the Silva database mentioned above using 'classify.seqs'.

A distance matrix generated of uncorrected pairwise distances between aligned sequences was constructed to compare the molecular diversity between samples. Distance matrices were generated for raw data and rarefied sample sets. The 'count.groups' command was used to determine that GH 4 spring GH4-sediment sample B had the lowest number of sequences, the 'sub.sample' was therefore used to rarefy all samples to only 4670 sequences. OTUs were classified using the 'classify.otu' followed by 'phylotype' and 'make.shared' so that a taxonomic comparison analysis could be completed. A representative sequence with the smallest maximum distance to the other sequences for each OTU was obtained and megaBLAST was used to find the closest uncultured and sequenced organism in the literature. Alpha diversity statistics were calculated on the OTU tables after rarefying all data sets to 4670 sequences.

Taxonomic stacked bar chart were rendered in R using the plot_bar function in phyloseq (McMurdie and Holmes, 2013). A heat map was constructed using the plot_heatmap function in phyloseq (McMurdie and Holmes, 2013) with method = NMDS and distance = bray.

Scanning Electron Microscopy

Initial imaging of samples was conducted at the BioTron advanced imaging facility, Western University, London, Canada. Samples were lightly crushed using a sterile agate mortar and pestle and fragments transferred to carbon tape affixed to titanium TEM stub mounts and imaged at 40 Pa on a Hitachi 3400-N Variable Pressure Scanning Electron Microscope with an accelerating voltage of 10–15 kV at a working distance of 5–10 mm. High resolution imaging was conducted at the Western University Nanofabrication Facility. Samples were mechanically crushed using a mortar and pestle into ∼1 mm fragments under sterile conditions and fixed in 2% glutearalderhyde overnight at room temperature. Following fixation, samples were dehydrated in ethanol by subsequent 15-min immersions in increasing concentrations of ethanol (50, 75, and 100%) followed by a final submersion in 100% ethanol. The dehydrated samples were critical point dried with a Samdri-PVT-3B CP dryer (Tousimis Research Group) in the Biotron imaging facility to preserve cell structure. Samples were then manually transferred to carbon tape (M. E. Taylor Engineering part # DSCC-12) affixed to titanium TEM imaging stubs using a binocular microscope. Each sample was plasma coated with ∼10 nm of amorphous osmium using a Filgen OPC80T Osmium Plasma Coater with an OsO_4 source. High-resolution imaging was carried out under high vacuum on a LEO Zeiss 1540XB FIB/SEM under an accelerating voltage of 1 kV and a working distance of 3.8 mm.

RESULTS

Microbiology GM and RM

Molecular Variance

To determine the microbial composition of the two mat communities standard alpha and beta diversity metrics were calculated. Following preprocessing of sequences, a total of 26,395 16S rRNA sequences were obtained and 1911 of these sequences were unique (**Figure 3**). The sequences were relatively evenly distributed between GH4 samples, GH-4sediment A contained 5849 sequences, GH4-sediment B 4670, green mats 7193, and red mats 8683.

Alpha Diversity

Alpha diversity indices were calculated to assess the diversity within each community. The 1911 unique sequences were assigned to 1113 OTUs with a cutoff value of 0.03. Coverage ranged from 91.7% (GH4-sediment A) to 99.4% (red mat). A higher number of OTUs were observed in the GH4 sediment samples (300–700) compared to the mat samples (60–80); however, measured diversity indices suggest that GH4-sediment A and the red mats had a higher diversity (inverse Simpson = 7.97 and 6.8, Shannon = 4.14, 2.42, respectively) than GH4-sediment B and green mats (inverse Simpson = 2.53, 3.33, Shannon = 2.31, 1.62 respectively; **Table 1**). This suggests that the OTUs accounting for the increased number of OTUs in the sediment samples might be rarely observed and account for a decreased evenness in these samples. This is supported by the high Chao1 values for the sediment samples (1392.7 and 814.5) as Chao1 will inflate species richness with the presence of rare OTUs. Shannon evenness varied from 0.39 (green mats) to 0.62 (GH4-sediment A) suggesting an uneven distribution of OTU abundance. Alpha diversity statistics are summarized in **Table 1**.

Beta Diversity

Beta diversity indices were used to assesses the variation in community structure between the red and green mats. A 4-way Venn diagram summarizes the distribution of the OTUs between samples (**Figure 3**) and the heat map presented in **Figure 4** illustrates major patterns in OUT membership between samples. The total OTU richness at a distance of 0.03 for all samples is 1113, with 803 OTUs observed in GH4-sediment A, 307 in GH4-sediment B, 76 in green mats, 101 in red mats. Only seven OTUs (0.6%) are shared between all samples. The greatest similarity is observed between the two sediment samples which share 94 OTUs or 11.7 and 30.6% of their total respective diversities. GH4-sediment A contains the highest number of unique OTUs (676), this is likely due to the high number of rare OTUs observed in this sample. Nine OTUs are shared only between the two mat samples.

All samples were dominated by Gammaproteobacteria comprising 39, 67, 80, and 49% of each of GH4-sediment A and B, green mats and red mats, respectively (**Figure 5A**). Bacteriodetes is the next most abundant phylum composing 22, 5, 14, and 31% of each respective sample. The composition of Gammaproteobacteria varies between the two groups of samples (**Figure 5B**). The Gammaproteobacteria complement of the GH4

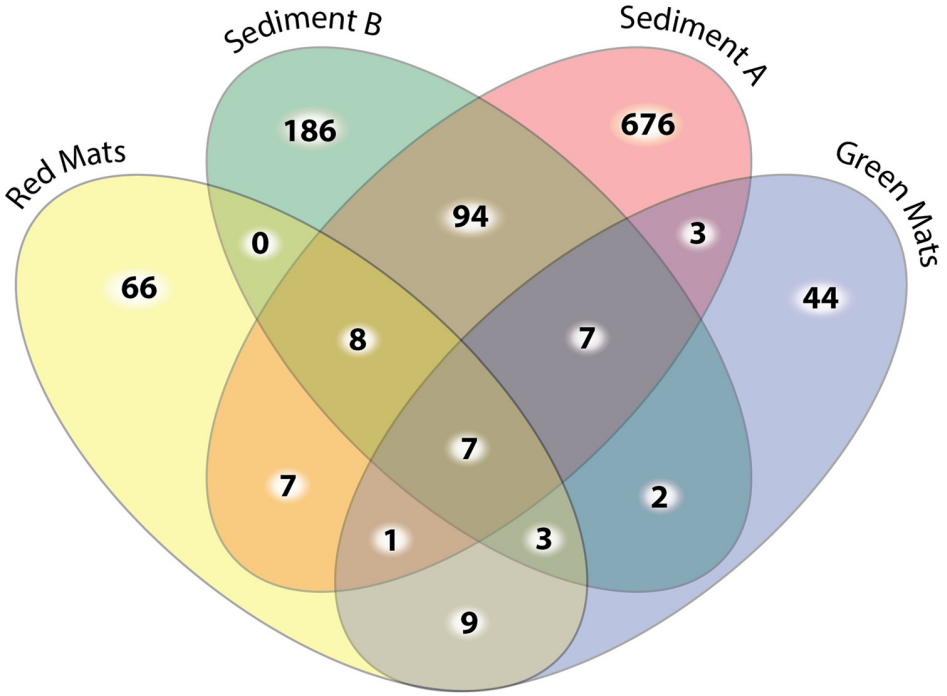

FIGURE 3 | Four-way Venn diagram illustrating the number of shared unique OTUs at the 0.03 cut off level between samples. The sediment samples have the highest number of OTU diversity and the highest number of unique OTUs. Only 9 out of the 177 OTUs observed in the mat samples are observed in both mat communities.

TABLE 1 | Alpha diversity statistics for each sample randomly subsampled to 4760 sequences.

Sample	Coverage	Sobs	invSimpson	Shannon	Evenness	Chao
Sediment A	0.917509	803	7.966514	4.140907	0.630496	1393.740416
Sediment B	0.962527	307	2.530337	2.308351	0.403075	814.5
Green mats	0.993958	76	3.336399	1.623104	0.39232	103.678491
Red mats	0.994138	101	6.800028	2.424413	0.548936	119.404167

Sobs = number of OTUs at a cutoff of 0.03.

sediment samples is almost entirely composed of *Thiotrichales*, (92% and 98% GH4 sediment A and B, respectively) while green mats is 60% *Thiotrichales,* and 37% *Alteromondadales.* The red mats are almost exclusively *Alteromondales* (91%) with subordinate *Oceanosphillales* (3%) and *Thiotrichales* (3%).

Dominant OTUs

To better understand the dominant organisms in each community the most abundant OTUs are discussed. The seven OTUs shared between all samples account for over 40% of the total sequences. This core bacterial community is composed of Gammaproteobacteria (OTUs 0001, 0004, 0016, and 0052) assigned to the genera *Thiomicrospira, Marinobacter,* and *Rhodanobacter* (**Table 2**). The remaining shared OTUs are classified as Bacteroidia (OTU 0008, *Prolixibacter*), Epsilonproteobacteria (OTU 0035, *Sulfurospirillum*), and an unclassified Deltaproteobacteria (OTU 0018). The closest BLASTn representatives in the NCBI database are largely from marine, hypersaline, or psychrophilic environments. *Thiomicrospira* and *Sulfurospirillum* are associated with sulfur metabolism and are consistent with the known microbiology of Gypsum Hill (Perreault et al., 2007).

OTU 0001 classified as *Thiomicrospira* is the dominant taxon in the GH4 sediment samples comprising 34 and 63% of the reads in the Sediment A and Sediment B samples respectively (GH4-sediment A: 2004 reads out of 5849 total sequences; 2920 GH4-sediment B: 2920 reads out of 4670 total sequences). The next most abundant OTU in GH4-sediment A is OTU 0008, Bacteroidia with 335 reads and in GH4-sediment B, OTU 0013, classified as a member of the class Desulfobacterales (**Table 3**). In contrast, the mat samples were not as clearly dominated by a single OTU. OTU 0001 is the most abundant OTU in the green mat with 3464 reads (7193 total sequences), but is only the eighth most abundant in the red mats (8683 total sequences). The most abundant OTU in the red mat sample is OTU 0002, classified as a *Marinobacter* species with 2227 reads. OTU 0002 is the second most abundant OTU in the green mat sample with 1448 reads. The second and third most abundant OTU in the red and green mat samples, respectively is 0003 classified as *Psychroflexus*, with 918 and 1568 reads.

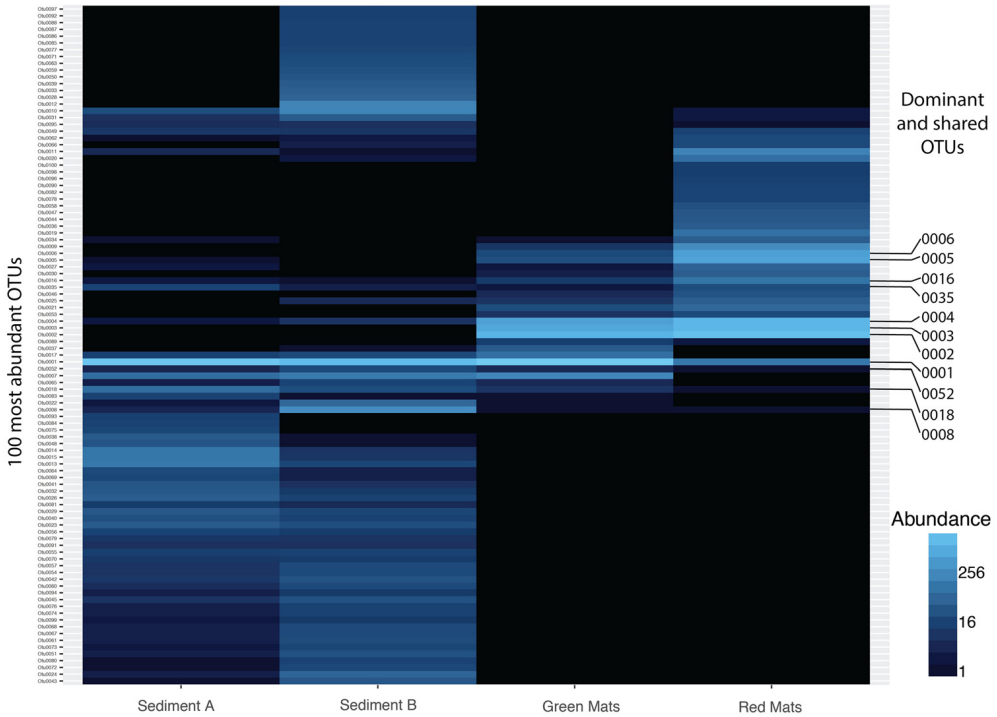

FIGURE 4 | Heatmap illustrating the abundance of the top 50 OTUs across all samples. 7 OTUs are shared across all samples. Dominant (OTU 0001, 0002, 0003, 0004, 0005, 0006) and shared OTUs (0001, 0004, 0008, 0016, 0018, 0035, 0052) are labeled and presented in **Tables 2**, **3**.

Microbe–Substrate Interaction

Secondary electron scanning electron microscopy (SEM) was used to evaluate cell-substrate associations in the mat samples. Imaging of GM samples revealed the presence of completely intact and undamaged diatoms as well as a massive biofilm (**Figures 6A,B**) while specific cell-substrate associations were not observed. As a result of limited samples and the inability to fix immediately in the field, the cells comprising the biofilm are misshapen and desiccated resulting in a puckered, non-canonical morphology despite attempts to preserve cellular morphology using standing fixation and critical point dying protocols prior to electron microscopy. Even though cellular morphology is not adequately preserved for morphological identification, electron microscopy did reveal differences between the red and green mat samples. The dominant bacterial taxon, *Thiomicrospira,* identified through 16S rRNA targeted-amplicon sequencing in the green mat sample is not known to form biofilms (Niederberger et al., 2009) and does not have a known coccoid morphology. The observed biofilm could be formed by algal cells. Algae were not targeted in the by the bacteria-specific primer sets used in the targeted-amplicon sequencing, and would also account for the green color characterizing the GM samples.

Scanning electron microscopy of RM samples revealed intimate associations between cocci and rod-shaped bacteria and the mineral substrate through filament-like extensions of extracellular substance (**Figure 6C**). The dominant rod-shaped cells are consistent with the morphology of *Marinobacter* and *Psychroflexus.* The rough surface texture apparent on the cells imaging in RM is suggestive of mineral precipitation (Ronholm et al., 2014). Cell-coating secondary mineral precipitation can occur through either passive or active biomineralization processes. A cultivation study of a supraglacial spring system Borup Fiord pass on Ellesmere Island, Canada (Gleeson et al., 2011) isolated a psychrophilic, sulfide-oxidizng consortia dominated by *Marinobacter* sp. that precipitated S (0). Subsequent dilution-to-extinction experiments indicated that *Marinobacter* sp. was the dominant sulfide oxidizer. While the majority of *Marinobactor* species are known for their ability to degrade hydrocarbons, the *Marinobacter sp* isolated by Gleeson et al. (2011) is the first known species to oxidize sulfur. This is consistent with a study conducted by Perreault et al. (2008) that identified *soxB*, a thiosulphate oxidation gene, in *Marinobacter* sp. *NP40.* Microscopy showed variably mineralized cells. The mineral coatings of the red mat (RM) cells may have preserved cellular morphology without the need for fixation techniques. The striking morphological difference between the RM and GM communities supports the differences in the genetic diversity as revealed by 16S rRNA targeted-amplicon sequencing. The observation of specific cell-substrate associations in the RM samples suggest that substrate-cell interactions play an important role in the RM communities, and the observation of putative mineral coatings in the RM cells suggests a role for biomineralization processes and perhaps lithoautotrophy involved sulfide oxidation.

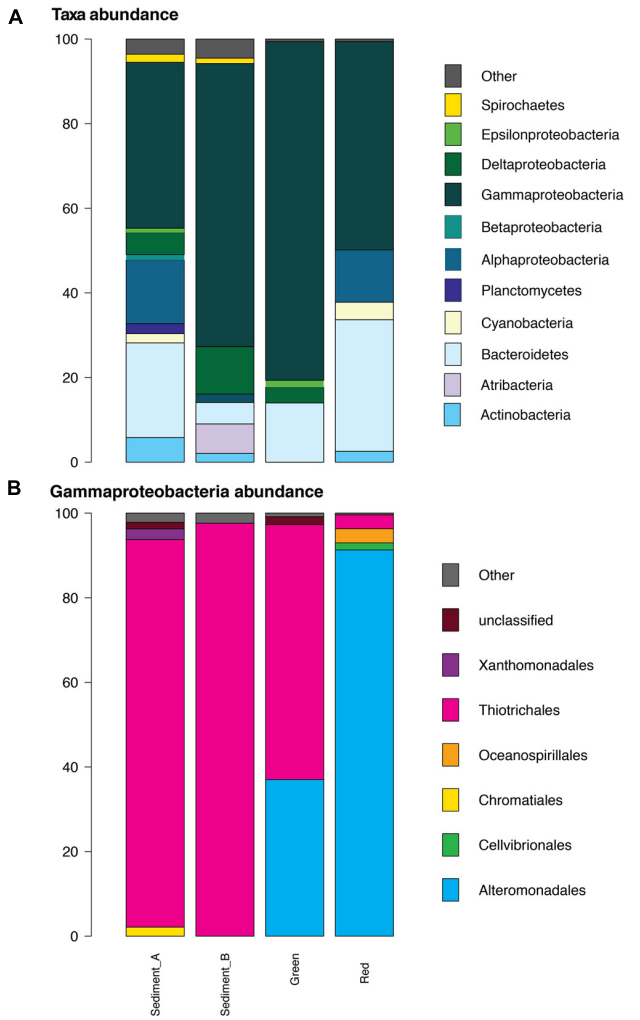

FIGURE 5 | Bacterial composition of classified sequences at the >1% abundance level. **(A)** Phyla and Proteobacteria class. At the phylum level, all samples are dominated by Proteobacteria with the GH4 sediment samples having a higher relative diversity than the matt samples. **(B)** Gammaproteobacteria. Within the Gammaproteobacteria clade, Thiotrichales dominates the two GH4 sediment samples while Alteromonadales comprises a high proportion of the mat sample communities.

DISCUSSION

Flood Plain and Source Pool Bacterial Communities

There are substantial differences between the mat and GH spring sediment communities for classified OTUs at >1% abundance level within the Gammaproteobacteria clade. The Gypsum Hill spring sediment samples are dominated by *Thiotrichales* (>90%), similar to previous studies, while the samples from the mats have a significant *Alteromonadales* component (**Figure 5**). The community composition varies between the visually distinct mats suggesting spatially integrated, yet, biologically distinct bacterial communities. This division may reflect patchy geochemical variation, niche partitioning, or dynamic colonization as discussed in the following sections.

The core bacterial community shared between all samples is consistent with those found in studies comparing the bacterial composition of streamers forming in snow-covered run-off channels during the winter months to the source sediment of Gypsum Hill (Niederberger et al., 2009). The similarity in community structure between the streamers and Gypsum Hill source spring suggests a common source and it can be concluded that the bacterial complement in the runoff channels is, at least in part, derived from the spring outlet. In contrast, the core bacterial community between the mat samples and the source spring reported here comprises less than 1% of the total richness and there was a significant difference in the diversity between the two mat samples and between the mat samples and the source GH4 sediment. Given the significant difference in environment between the GH spring and flood plain, this difference in community structure is not surprising, however, supports the hypothesis that the community within the GH spring is not sourced from surficial microbial communities and is the surficial expression of deeper, subsurface community. We suggest that the seasonal outflow forming the flood plain provides an ephemeral habitat for transient surface microorganisms to colonize.

Marinobacter and *Psychroflexus*, the two most abundant OTUs in the red mat, and second and third most abundant in the green mat, respectively (**Figure 4** and **Table 3**), are not found in the GH4 spring sediment samples in this study, but have been identified previously from the Gypum Hill outlet (Perreault et al., 2008). In this study, the absence of *Marinobacter* and *Psychroflexus* in the GH sediments account for a large degree of the variation between the GH spring sediment samples and the mat samples. The absence of these phyla in the GH sediments in the present study may reflect the large degree of community variation. The top six OTUs, based on relative abundance, are summarized in **Table 3**. The dominant OTU in the green mat is 99% similar to *Marinobacter psychrophilus* at the 16S rRNA level, a nitrite reducer isolated from sea-ice in the Canadian basin (Zhang et al., 2008). The second most dominant, 95% similar to *Psychroflexus sediminis*, isolated from a hypersaline lake in China (Chen et al., 2009), is an obligate aerobic nitrate reducer. It is interesting to note that *Psychroflexus sediminis* produces non-diffusible orange carotenoid pigments (Chen et al., 2009) and this could explain the observable difference in coloration between the red and green mats. *Thiomicrospira*, the dominant taxon in the GH4 sediment samples, is an obligate chemolithoautotrophic sulfur oxidizer (Knittel et al., 2005). The dominance of *Marinobacter* as described here from the RM sample, has not been previously reported from the cold saline springs on AHI and suggests that in contrast to the outflow channels, the mat communities are not sourced directly from the spring. It would be pertinent to assess the microbial diversity in the active layer beneath the surficial mats to assess spatial variation in community structure with respect to changing physical and chemical conditions.

TABLE 2 | Taxonomy of representative sequences from shared OTUs.

	Sample					Closest BLASTn representative			
OTU	**Sediment A**	**Sediment B**	**Green**	**Mixed**	**Taxonomic classification (mothur, Silva V124 database)**	**Isolation location**	***E*-value**	**Identities (%)**	**Acc number**
0001	2004	2920	3464	143	Thiomicrospira	Sediment China: Hai River, northwest of Bohai Bay	8e-134	99	JF806846.1
						GH filament of sulfidic spring, Arctic	8e-130	100	EU430112.1
0004	8	2	700	1535	Marinobacter	Aquatic microbial mat from Antarctica	2e-135	100	FR772219.1
						Antarctic sandy intertidal sediments	2e-135	100	FJ889664.1
0008	335	4	1	1	Prolixibacter	Sediments from Rodas Beach polluted with crude oil	8e-89	90	JQ580434.1
						Guerrero Negro hypersaline microbial mat	8e-89	90	JN459039.1
0016	1	2	11	128	Marinobacter	Aerobic composting reactor	2e-125	98	HE647397.2
						Coastal marine sediment, Melville Harbor, Australia	8e-124	97	JQ032447.1
0018	25	92	8	1	Unclassified Deltaproteobacteria	Intertidal mudflatsediment vegetated by Sueada japonica in Ganghwa Island, Korea	4e-132	97	DQ112467.1
						carbonate-rich metalliferous sediment sample from the Rainbow vent field on the Mid-Atlantic Ridge	8e-129	96	AY354183.1
0035	3	17	2	25	Sulfurospirillum	Psychrophilic thiotrophic bacteria associated with cold seeps of the Barents Sea	2e-105	94	FR875418.1
						Psychrophilic thiotrophic bacteria associated with cold seeps of the Barents Sea	1e-102	93	FR875460.1
0052	22	4	5	1	Rhodanobacter	Shimokita Penninsula offshore drill core sample	1e-136	100	AB806773.1
						Shimokita Penninsula offshore drill core sample	1e-136	100	AB806772.1

TABLE 3 | Taxonomy of representative sequences from dominant OTUs.

	Sample					Closest BLASTn representative			
OTU	**Sediment A**	**Sediment B**	**Green**	**Mixed**	**Taxonomic classification (mothur, Silva V124 database)**	**Isolation location**	***E*-value**	**Identities (%)**	**Acc number**
0001	2004	2920	3464	143	Thiomicrospira (100)	Sediment China: Hai River, northwest of Bohai Bay	8e-134	99	JF806846.1
						Thiomicrospira psychrophila marine arctic sediments Svalbard: Store Jonsfjorden	2e-129	98	NR_042106.1
0002	0	0	1448	2227	Marinobacter (99)	subarctic glacial Fjord, Kongsfjorden	2e-135	100	JQ800125.1
						Marinobacter psychrophilus complete genome isolated from sea-ice of the Canadian Basin	4e-132	99	CP011494.1
0003	0	0	918	1568	Psychroflexus (100)	Tibetan Xiaochaidan Lake	1e-126	98	HM128393.1
						Psychroflexus sediminis haloalkaline soil Qinghai Province, northwest, Qaidam lake basin	1e-111	95	NR_044410.1
0004	8	2	700	1535	Marinobacter (100)	Aquatic microbial mat from Antarctica	2e-135	100	FR772219.1
						Marinobacter antarcticus Antarctic sandy intertidal sediments	2e-135	100	NR_108299.1
0005	0	1	27	787	Sulfitobacter (100)	Aquatic microbial mat from Antarctica	8e-119	100	FR772186.1
						Sulfitobacter japonica	2e-115	99	AB275995.1
0006	0	0	22	685	Psychroflexus (100)	Tibitan lake Xiaochaidan Lake	1e-122	97	HM128393.1
						Psychroflexus gondwanensis isolated from a defective cheese surface	1e-116	96	NR_117200.1

Comparison to Other Microbial Communities

Hypersaline Microbial Mats

The spatial geometry of microbial mats and the physical coupling of diverse metabolisms, niche partitioning, and symbiosis allows mat communities to thrive in extreme environments. In contrast to established mat communities where conditions permit the lithification and growth of thick, cohesive microbial mats, the Gypsum Hill mats are patchy, discontinuous, only a few millimeters thick forming only on the surface of the permafrost active layer within flood plains and do not display any observable structural or community variation with depth. The physical structure of the Gypsum Hill mats make them difficult to compare with other hypersaline mat communities. Wong et al. (2016) reviewed the molecular ecology of 4 model hypersaline mat communities: Guerrero Negro, Shark Bay, S' Avall, and Kiritimati Atoll. Similar to the Axel Heiberg mats, Proteobacteria were a major member in all four communities. Kiritimati Atoll was dominated by Bacteroidetes and Guerro Negro by Chloroflexi. Bacteroidetes contribution to overall diversity was, interestingly, also one of the major differences between the red and green mat communities studied here with the mats having a significantly higher proportion compared to the green mats. In Kiritimati Atoll, Bacteroidetes represented by *Salinibacter* and *Saprospiraceae*, were predominate in the surface layers contributing to photoheterotrophy (Schneider et al., 2013). In contrast, the main taxa contributing to Bacteroidetes in the red mat sample are *Psychroflexus* and *Gillisia*. Wong et al. (2016) suggest niche differentiation as an explanation for the

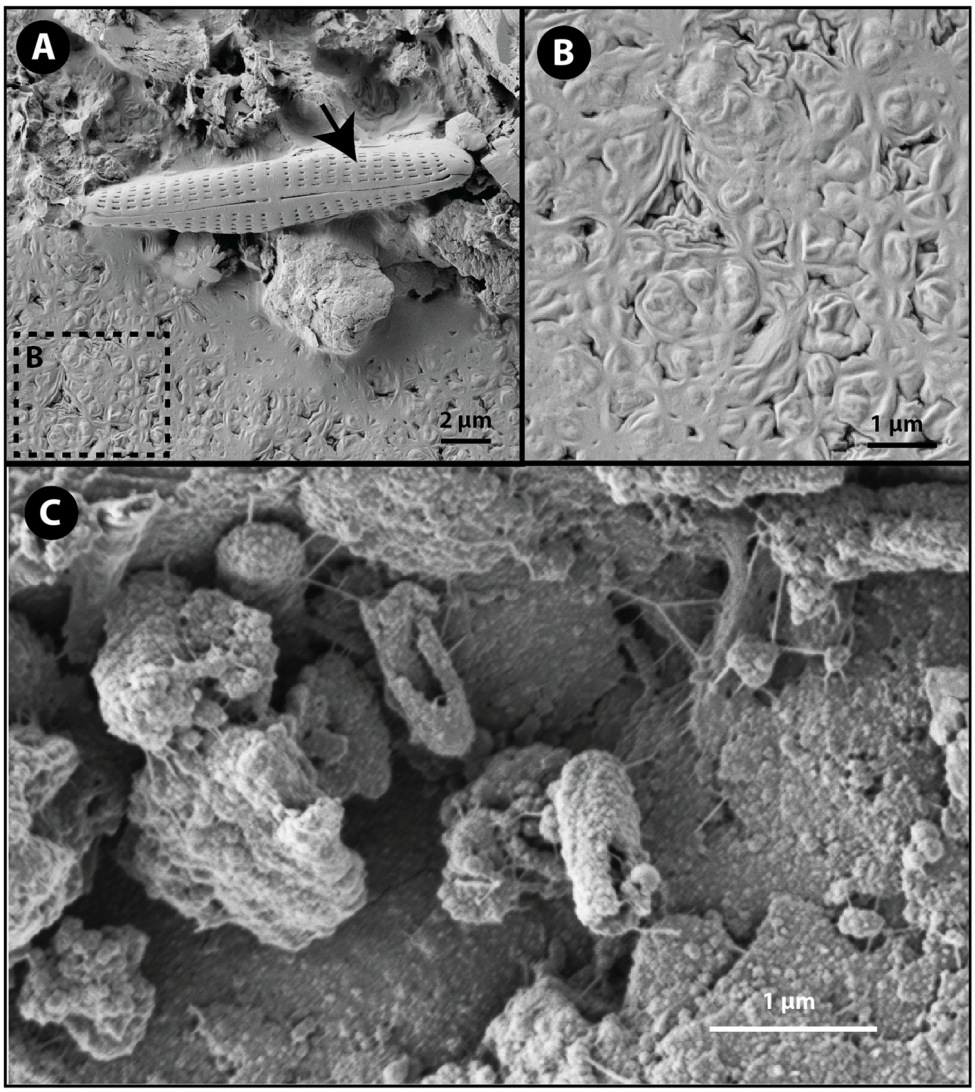

FIGURE 6 | Secondary electron scanning electron microscope images of cell-substrate interaction. **(A)** Intact diatom (black arrow) and a desiccated coccoid biofilm (box B) dominated the GM samples. **(B)** The texture of the biofilm in GM samples is a result of desiccated and puckered coccoid cells. **(C)** Rod shaped cells adhered to the substrate in RM samples. Notice the rough surface textures of the cells consistent with biomineralization processes.

emergent taxonomic structure variations within and between the four model saline mats and is consistent with our observations discussed in section "Hypersaline Microbial Mats". Given the narrow vertical habitable range in the Gypsum Hill flood plain, the spatial organization of mat communities appear to be determined by lateral heterogeneity as compared to vertical stratification as observed in the other hypersaline mat communities.

Bacterial Diversity of AHI Springs

To assess the uniqueness of the mat communities on AHI, we attempted a systematic comparison of bacterial profiles from previous studies. We include datasets from previous studies of three perennial cold spring on AHI, Color Peak (CP), Gypsum Hill (GH), and Lost Hammer (LH), as well as data from a supraglacial spring in Borup Fjord pass on Ellesmere Island (BF).

Over the past two decades, a variety of techniques and approaches have been used to investigate the bacterial diversity of the perennial cold springs at AHI. These studies highlight the advances in microbial ecology: the earliest studies relying on <100 clones while in the last couple of years next generation sequencing technology has allowed for the analysis of tens of 1000s sequences and curation of 1000s of OTUs in a single study. The degree of bias between cloning and sequencing studies and NextGen amplicon sequencing and the increasing amount of information available in reference databases used for classification leads to great difficulty comparing studies. Three perennial cold springs on Axel Heiberg Island, Color Peak (CP), Gypsum Hill (GH), and Lost Hammer (LH), have been studied extensively with respect to their microbial communities. In addition to diversity studies of the main outlets of each spring, surficial run-off channels or outflow from GH and LH have also been examined. To date the bacterial communities characterized have been dominated by members of *Gammaproteobacteria* and *Bacteroidetes* known to be involved in sulfur cycling. Evidence for methanogenesis including the identification of several phylotypes consistent with methanogenesis and anaerobic methane oxidation were identified from LH. Overall the bacterial communities detected to date in the AHI spring systems are consistent with those identified and characterized from psychrophilic Arctic and Antarctic environments such as Antarctic sea ice and quartz sandstone (Nichols et al., 2005), Arctic and Antarctic pack-ice (Brinkmeyer et al., 2003), Arctic sea-ice (Zhang et al., 2008), including representatives from the phylotypes *Halomonas*, *Gillisia*, and *Marinobacter*.

In an attempt to summarize the available information and investigate the most abundant phyla we have recalculated the reported bacterial abundances in each sample in several studies to create a dataset of 26 samples (Supplementary Table S1), each representing bacterial sequences classified at the phylum level, where each phylum is present at >1% abundance. It is important to note that the dynamic nature of reference databases may affect the classification of some OTUs, particularly for older studies. Given that adequate sampling depth requires the generation of thousands of clones and the largest clone library constructed for the AHI spring consisted of 161 clones, it can be assumed that these early studies were biased to detecting only the most abundant species. Therefore, we restrict our comparisons to the phyla level that comprise >1% of the community (**Figure 7**).

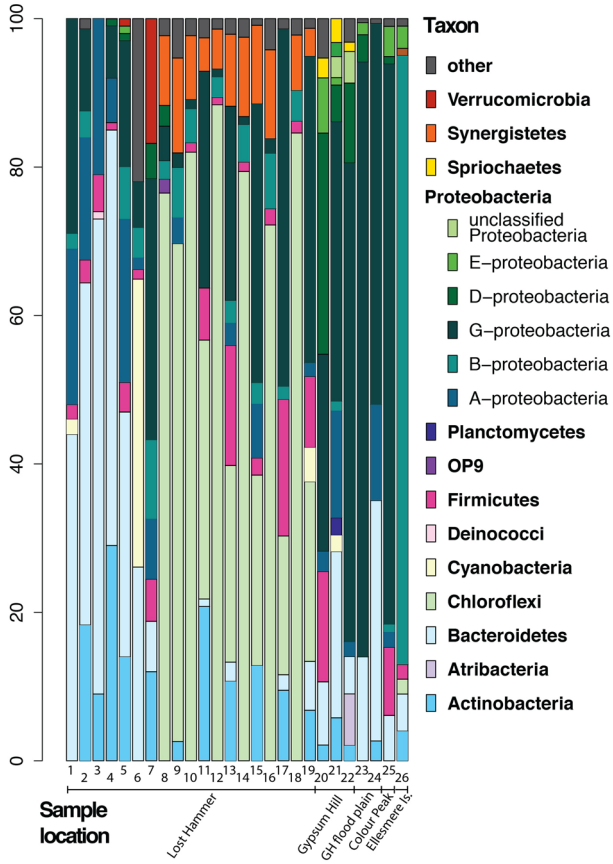

FIGURE 7 | Bacterial composition of high Arctic communities of classified bacterial sequences present at the >1% abundance level. Samples 1, 6–19: Lost Hammer spring outlet, 2–5; Lost Hammer spring outflow, 20–22, Gypsum Hill spring outlet, 23–24 Gypsum Hill (GH) flood plain green mats and red mats, respectively), 25, Color Peak spring, 26, Borup Fjord, Ellesmere Island. Note the predominance of Chloroflexi in Lost Hammer spring samples 8–19, all from one study.

The issues correlating bacterial diversity results between different methods are apparent in the studies of Lost Hammer (LH) Spring (Niederberger et al., 2010; Lay et al., 2012; Lamarche-Gagnon et al., 2015). The distinction between the cDNA and DNA libraries found in both the cloning and sequencing (Niederberger et al., 2010; Lay et al., 2012) and amplicon studies (Lamarche-Gagnon et al., 2015) suggests a background bacterial population not necessarily related to the active community. However, the results of the pyrosequencing study (Lamarche-Gagnon et al., 2015) contrast sharply with the previous data indicating a predominance of Choroflexi, a phyla not previously observed. If all studies are biased to the most abundant phyla, the DNA studies may be recording variation in the dormant/dead population distinguishable over a longer

time frame than the single seasonality studies (Lamarche-Gagnon et al., 2015) as high ionic strength, low temperature fluids increase the long-term stability of DNA (e.g., Lay et al., 2012). The differences may also be a result of changes to reference databases. The availability and quality of the sequence data precluded reclassification using a standard modern database. It is also important to note that sequences represent DNA [16S rRNA gene clone libraries: Niederberger et al., 2010 (LH), Lay et al., 2012 (LH), Perreault et al., 2007 (GH), Perreault et al., 2007 (CP)], 16S rRNA pyrosequencing: [Lamarche-Gagnon et al., 2015 (LH), Gleeson et al., 2011 (BF), this study (GH), cDNA (Lay et al., 2013 (LH), and metagenomic data (Lay et al., 2013 (LH)].

In all samples from all locations, the dominant phyla include Bacteroidetes, Chloroflexi, and Gammaproteobacteria. Notably, when the samples are plotted on a 2 axis NMDS plot, they cluster by site, and not by sequencing technology (**Figure 8**). It is also notable that the two mat samples in this study do not cluster with any particular spring suggesting a unique bacterial community composition at the phylum level. For example, Betaproteobacteria and Bacteroidetes membership better defines the Lost Hammer clusters than the other spring sites that are better described by other Proteobacteria sub-classes and Atribacteria. The red mats cluster closer to the Lost Hammer samples than the green mat samples consistent with a higher proportion of Bacteroidetes in the red mats relative to the green mats dominated by Betaproteobactia. These distinct bacterial communities suggest that the differences in physiochemical parameters between the spring sites play a role in community structure. Metabolic roles cannot adequately be inferred through 16S rRNA targeted-amplicon sequencing studies and detailed paired studies analyzing the spring geochemistries and transciptomic analyses are required to further comment on plausible mechanisms leading to the distinct microbial assemblages observed between sites.

Bacterial Community Structure

Niche Partitioning

Marinobacter, more abundant in the RM sample, is a ubiquitous Gram-negative anaerobic Gammaproteobacteria in marine environments known for its ability to degrade hydrocarbons including aliphatics, polycyclic aromatics and acyclic isoprenoids (Gauthier et al., 1992; Liu et al., 2012). *Marinobacter* spp. lack fermentative metabolism, have a restricted nutritional profile, and respire nitrate. It is interesting to note that *Psychroflexus,* also more abundant in the RM sample, is also capable of nitrate reduction. However, a *Marinobacter sp.* isolated from a cold spring in Borup Fjord was found to be a key sulfide oxidizer, and the first known *Marinobacter* isolate known to biomineralize sulfur. Additionally, the soxB gene for sulfur oxidation was present in Marinobacter previously isolated from GH (Perreault et al., 2008) If the *Marinobacter sp.* in RM is capable of sulfide oxidation, *Thiomicrospira* and *Marinobacter* may be competing for resources and competition could partially explain spatial separation. More work isolating and identifying the dominant *Marinobacter* in RM is required to show sulfide oxidation, if so, the metabolic diversity is consistent with niche partitioning based on resource competition.

Nitrate metabolism could also explain the difference in community structure between the red and green mats, although more detailed studies directed at the metabolic potential and activity of the communities is required. The electron microscopy results suggest that the RM communities are more intimately associated with the physical substrate. It is not clear if the difference in community structure also represents different stages in colonization such as if the development of cohesive mats associated with sulfate reducing bacteria precedes or follows a substrate-associated, sulfide oxidizing community, or if the structure is representative of geochemical heterogeneous distribution of key nutrient and energy sources.

Microbial Source

The source of the microbial communities in the AHI springs remains enigmatic. The dependence on chemolithoautotrophy in the springs and similarity with subsurface and hydrothermal vent communities suggests a subsurface source. The water source is similarly unconstrained. Here we show that there is a difference in the dominant bacterial members between the Gypsum Hill source pool as samples by the Gypsum Hill sediments and surface mats in an associated flood plain suggesting fundamentally different sources. However, deeper sampling including both increased physical and technological replicates is necessary to assess the significance of these observed differences. Dispersal, transport of viable cells over geographic distances resulting in the colonization of new habitats, is one of the most important processes defining the microbial biogeography of cold environments (Margesin and Miteva, 2011). Given the seasonal habitability of the mats, the distinct geochemical parameters and the geographic relationship to the GH outflow, whether the structure of the core bacterial community is a result of endemic or cosmopolitan distribution is still unclear.

Habitat Considerations

Here we show the presence of a microbial niche in summer surface microbial mats associated with flood plains likely fed by Gypsum Hill runoff channels. The microbial composition of these mats is unique with respect to other bacterial communities reported from other Arctic springs on AHI (e.g., Perreault et al., 2007, 2008; Niederberger et al., 2010; Lay et al., 2013; Lamarche-Gagnon et al., 2015). We suggest that seasonal shift produces ephemeral surface habitats that are not populated by through spring runoff channels. The fact that the surface is only habitable in the summer months suggests seasonality to the activity of these communities.

While results from this study are hint at a surficial community active only during the summer months, future metagenomics and metatranscriptomic analyses would lead to a better understanding of the metabolic potential and active members inhabiting these mat communities. A deeper assessment of the mat cyanobacterial diversity would allow for a more thorough comparison to other mat communities and replicate analyses are required to better understand seasonal variability and stability.

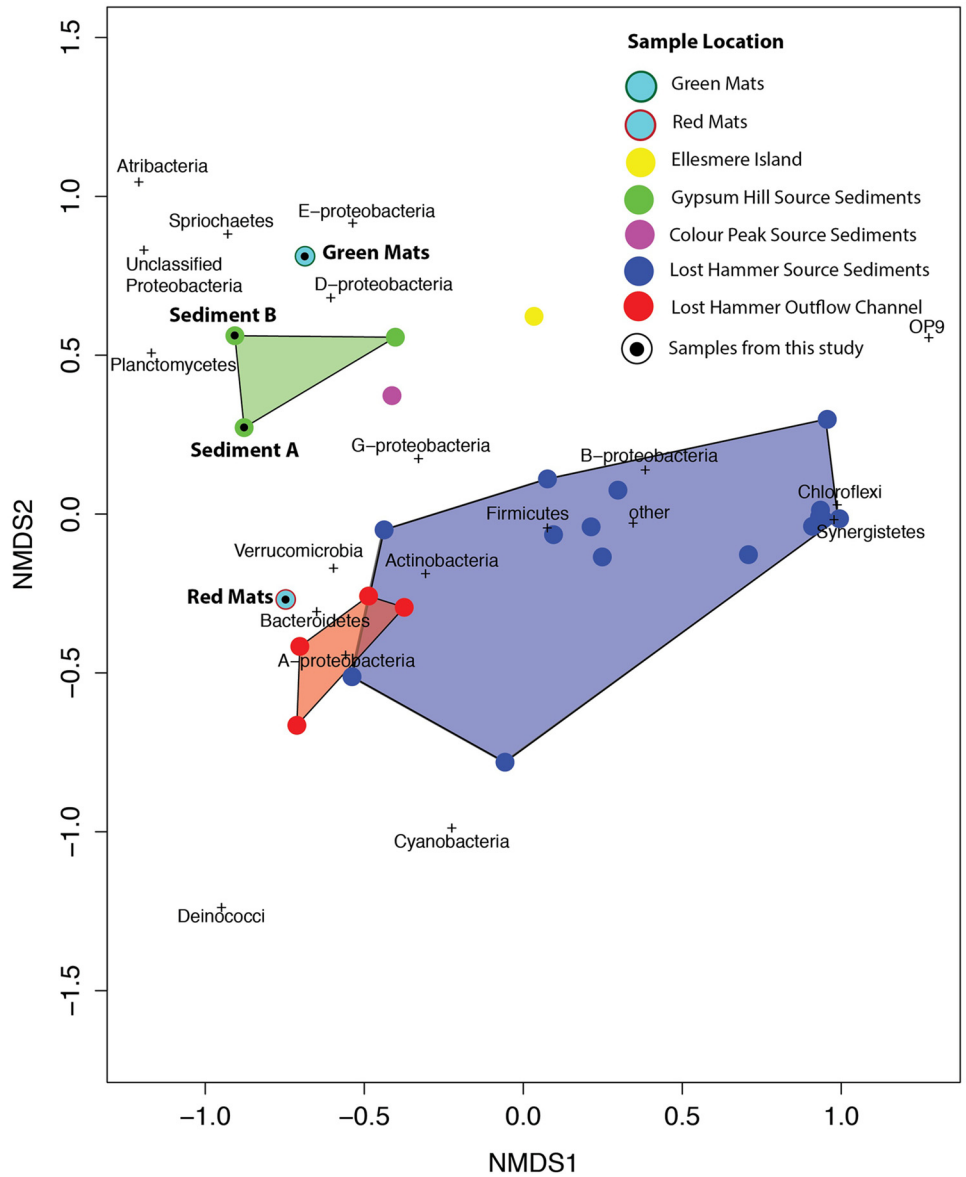

FIGURE 8 | NMDS plot using the Bray–Curtis dissimilarity matrix of bacterial communities in high Arctic environments. Bacterial communities cluster by site. The mat communities studies here do not tightly cluster with any of the previously studied communities.

At present the surface conditions on Mars are inconsistent with the formation of standing bodies of water. The subsurface represents the most temporally extensive habitable and potentially inhabited environment on Mars. Water ice is present in the near Martian subsurface (10 s of cm; Bandfield, 2007) with polar layer deposits upwards of 1 km thick (Picardi et al., 2005). Recent radar observations have demonstrated the existence of large volumes of ground ice in the near surface environment (Stuurman et al., 2016). Modern subsurface water may be present in pockets due to radiogenic heating and lithostatic pressure and the presence of brines depressing the freezing point (Clifford et al., 2010); droplets of salts on the Phoenix lander legs demonstrate the thermodynamic stability of brines on Mars (Rennó et al., 2009). Both recurring slope lineae and (Ojha et al., 2015) Martian slope streaks (Bhardwaj et al., 2017) have been hypothesized as indicators of trainset water activity on the modern Martian surface. If these features represent surface expressions of subsurface briny aquifers (e.g., Stillman et al., 2016), transient liquid water on the surface could potentially transport subsurface microbial communities, or evidence of these communist to the surface. Alternatively, RSL features may be formed in the absence of flowing liquid water through phenomena such as deliquescence (Heinz et al., 2016). The presence of salts depresses the freezing point of water raising the depth at which liquid water could theoretically be stable. However, the presence of salt can also lower the water activity

below that required for life (Tosca et al., 2008). The absence of sulfates and chlorates associated with clay-rich terrains on Mars suggests that liquid water was not always characterized by extreme salinity indicating potentially more habitable conditions in the past.

On Axel Heiberg Island, the perennial cold spring such as Gypsum Hill represent the surface expression of subsurface briny aquifers flowing through thick permafrost. Our results here suggest that the communities within these springs are distinct from the transient surficial communities that form in flood plains during the summer months. Detailed sampling over the course of several consecutive seasons is required to better understand the variability in the surface communities and their persistence through the winter. Understanding the geomicrobiology and microbial activity in hypersaline cold springs like Gypsum Hill shed insight into the potential habitability of putative subsurface Martian brines. The development of the mat communities demonstrates the potential for ephemeral environments linked to seasonal melt events, and/or flooding to host diverse and unique microbial communities.

CONCLUSION

The bacterial diversity, presence of diatoms, cyanobacteria, and coloration described for the first time in the surficial mats associated with the Gypsum Hill summer flood plain is distinct from the source pool. This provides support for the hypothesis that the communities in the Gypsum Hill spring are sourced from the subsurface based on diversity differences between surficial communities as estimated by the 16s rRNA profiling. The mat communities are distinctly different from both the spring outlet and the snow-covered winter streamers suggesting temporal and spatial heterogeneity in community composition. The red mat bacterial community in particular is the first microbial community to be isolated from hypersaline cold spring systems that are not dominated by *Thiomicrospira,* but rather by *Marinobacter* (40.6%). There is a need for studies characterizing extreme environments such as the hypersaline cold springs in the Canadian High Arctic to focus on physical replicates.

We have been able to link macro-scale visual differences to distinct microbial communities that show very different micro-scale cell-substrate associations. The microbial communities of the red and green mats differ also from the reported microbial communities of the Gypsum Hill outlet (Perreault et al., 2007). Our data suggests that minor variations in chemistry, even between propinquitous sites, can have significant implications for community structure. Detailed studies of emerging, transiently habitable niches in Mars analog environments will aid our understanding of the potential for microbial life, and its detection, in putatively habitable environments beyond Earth.

AUTHOR CONTRIBUTIONS

HS prepared the manuscript, isolated the nucleic acids, performed the analyses, electron microscopy, and data reduction. JR greatly assisted with the manuscript preparation, data analyses, and laboratory work. RC, IR-B, and JR conducted the fieldwork, collected the samples and environmental metadata and participated in manuscript and data discussions. GO contributed to the discussion, and made possible the electron microscopy. LW conceived the design, organized the field expeditions, provided all laboratory space and materials, and contributed to the manuscript preparation and discussion.

FUNDING

Financial support was provided by fellowships from the Natural Sciences and Engineering Research Council (NSERC) CREATE Canadian Astrobiology Training Program (CATP) and Canadian Graduate Scholarship to IR-B and RC and CATP postgraduate fellowships to HS and JR, and NSERC Discovery Grant Program, Northern Research Supplement grant, and a Polar Continental Shelf Project grant to LW.

ACKNOWLEDGMENTS

The authors wish to gratefully acknowledge the Nanofabrication Facility and Tim Goldhawk and Dr. Todd Simpson at Western University for assistance with SEM imaging. They also thank Dr. Jacqueline Goordial for discussion and insight.

SUPPLEMENTARY MATERIAL

The Supplementary Material for this article can be found online at: https://www.frontiersin.org/articles/10.3389/fmicb.2017.02527/full#supplementary-material

REFERENCES

Andersen, D. T. (2002). Cold springs in permafrost on Earth and Mars. *J. Geophys. Res.* 107, 5015–5017. doi: 10.1029/2000JE001436

Bandfield, J. L. (2007). High-resolution subsurface water-ice distributions on Mars. *Nature* 447, 64–67. doi: 10.1038/nature05781

Battler, M. M., Osinski, G. R., and Banerjee, N. R. (2013). Mineralogy of saline perennial cold springs on Axel Heiberg Island, Nunavut, Canada and implications for spring deposits on Mars. *Icarus* 224, 364–381. doi: 10.1016/j.icarus.2012.08.031

Beschel, R. E. (1963). *Sulphur Springs at Gypsum Hill*. Preliminary Report 1961–1962. Montreal, QC: McGill University, 183–187.

Bhardwaj, A., Sam, L., Martín-Torres, F. J., Zorzano, M.-P., and Fonseca, R. M. (2017). Martian slope streaks as plausible indicators of transient water activity. *Sci. Rep.* 7:7074. doi: 10.1038/s41598-017-07453-9

Brinkmeyer, R., Knittel, K., Jürgens, J., Weyland, H., Amann, R., and Helmke, E. (2003). Diversity and structure of bacterial communities in Arctic versus Antarctic pack ice. *Appl. Environ. Microbiol.* 69, 6610–6619. doi: 10.1128/AEM.69.11.6610-6619.2003

Burr, D. M., Grier, J. A., McEwen, A. S., and Keszthelyi, L. P. (2002). Repeated aqueous flooding from the Cerberus Fossae: evidence for very recently extant, deep groundwater on Mars. *Icarus* 159, 53–73. doi: 10.1006/icar.2002.6921

Chen, Y. G., Cui, X. L., Wang, Y. X., Tang, S. K., Zhang, Y. Q., Li, W. J., et al. (2009). *Psychroflexus sediminis* sp. nov., a mesophilic bacterium isolated from salt lake sediment in China. *Int. J. Syst. Evol. Microbiol.* 59, 569–573. doi: 10.1099/ijs.0.003269-0

Clifford, S. M., Lasue, J., Heggy, E., Boisson, J., McGovern, P., and Max, M. D. (2010). Depth of the Martian cryosphere: revised estimates and implications for the existence and detection of subpermafrost groundwater. *J. Geophys. Res.* 115:E07001. doi: 10.1029/2009JE003462

Davila, A. F., Duport, L. G., Melchiorri, R., Jänchen, J., Valea, S., de los Rios, A., et al. (2010). Hygroscopic salts and the potential for life on Mars. *Astrobiology* 10, 617–628. doi: 10.1089/ast.2009.0421

Fairén, A. G., Davila, A. F., Lim, D., Bramall, N., Bonaccorsi, R., Zavaleta, J., et al. (2010). Astrobiology through the ages of Mars: the study of terrestrial analogues to understand the habitability of Mars. *Astrobiology* 10, 821–843. doi: 10.1089/ast.2009.0440

Gauthier, M. J., Lafay, B., Christen, R., Fernandez, L., Acquaviva, M., Bonin, P., et al. (1992). *Marinobacter hydrocarbonoclasticus* gen. nov., sp. nov., a new, extremely halotolerant, hydrocarbon-degrading marine bacterium. *Int. J. Syst. Evol. Microbiol.* 42, 568–576. doi: 10.1099/00207713-42-4-568

Gleeson, D. E., Williamson, C., Grasby, S. E., Pappalardo, R. T., Spear, J. R., and Templeton, A. S. (2011). Low Temperature S0 biomineralization at a supraglacial spring system in the Canadian High Arctic. *Geobiology* 9, 360–375. doi: 10.1111/j.1472-4669.2011.00283.x

Grasby, S. E., Allen, C. C., Longazo, T. G., Lisle, J. T., Griffin, D. W., and Beauchamp, B. (2004). Supraglacial sulfur springs and associated biological activity in the Canadian high arctic—signs of life beneath the ice. *Astrobiology* 3, 583–596. doi: 10.1089/153110703322610672

Harrison, J. C., and Jackson, M. P. A. (2014). Exposed evaporite diapirs and minibasins above a canopy in central Sverdrup Basin, Axel Heiberg Island, Arctic Canada. *Basin Res.* 26, 567–596. doi: 10.1111/bre.12037

Heinz, J., Schulza-Makuch, D., and Kounaves, S. P. (2016). Deliquescence-induced wetting and RSL-like darkening of a Mars analogue soil containing various perchlorate and chloride salts. *Geophys. Res. Lett.* 43, 4880–4884. doi: 10.1002/2016GL068919

Knittel, K., Kuever, J., Meyerdierks, A., Meinke, R., Amann, R., and Brinkhoff, T. (2005). *Thiomicrospira arctica* sp. nov. and *Thiomicrospira psychrophila* sp. nov., psychrophilic, obligately chemolithoautotrophic, sulfur-oxidizing bacteria isolated from marine Arctic sediments. *Int. J. Syst. Evol. Microbiol.* 55, 781–786. doi: 10.1099/ijs.0.63362-0

Lamarche-Gagnon, G., Comery, R., Greer, C. W., and Whyte, L. G. (2015). Evidence of in situ microbial activity and sulphidogenesis in perennially sub-0 °C and hypersaline sediments of a high Arctic permafrost spring. *Extremophiles* 19, 1–15. doi: 10.1007/s00792-014-0703-4

Lasue, J., Mangold, N., Hauber, E., Clifford, S., Feldman, W., Gasnault, O., et al. (2013). Quantitative assessments of the Martian hydrosphere. *Space Sci. Rev.* 174, 155–212. doi: 10.1007/s11214-012-9946-5

Lay, C.-Y., Mykytczuk, N. C. S., Niederberger, T. D., Martineau, C., Greer, C. W., and Whyte, L. G. (2012). Microbial diversity and activity in hypersaline high Arctic spring channels. *Extremophiles* 16, 177–191. doi: 10.1007/s00792-011-0417-9

Lay, C.-Y., Mykytczuk, N. C. S., Yergeau, E., Lamarche-Gagnon, G., Greer, C. W., and Whyte, L. G. (2013). Defining the functional potential and active community members of a sediment microbial community in a high-arctic hypersaline subzero spring. *Appl. Environ. Microbiol.* 79, 3637–3648. doi: 10.1128/AEM.00153-13

Liu, C., Chen, C. X., Zhang, X. Y., Yu, Y., Liu, A., Li, G. W., et al. (2012). *Marinobacter antarcticus* sp. nov., a halotolerant bacterium isolated from Antarctic intertidal sandy sediment. *Int. J. Syst. Evol. Microbiol.* 62, 1838–1844. doi: 10.1099/ijs.0.035774-0

Malin, M. C., and Edgett, K. S. (2000). Evidence for recent groundwater seepage and surface runoff on Mars. *Science* 288, 2330–2335. doi: 10.1126/science.288.5475.2330

Malin, M. C., Edgett, K. S., Posiolova, L. V., McColley, S. M., and Dobrea, E. Z. N. (2006). Present-day impact cratering rate and contemporary gully activity on Mars. *Science* 314, 1573–1577. doi: 10.1126/science.1135156

Margesin, R., and Miteva, V. (2011). Diversity and ecology of psychrophilic microorganisms. *Res. Microbiol.* 162, 346–361. doi: 10.1016/j.resmic.2010.12.004

Martínez, G. M., and Renno, N. O. (2013). Water and brines on Mars: current evidence and implications for MSL. *Space Sci. Rev.* 175, 29–51. doi: 10.1007/s11214-012-9956-3

McFrederick, Q. S., Cannone, J. J., Gutell, R. R., Kellner, K., Plowes, R. M., and Mueller, U. G. (2013). Specificity between lactobacilli and hymenopteran hosts is the exception rather than the rule. *Appl. Environ. Microbiol.* 79, 1803–1812. doi: 10.1128/AEM.03681-12

McKay, C., Mykytczuk, N., and Whyte, L. (2012). "Life in ice on other worlds," in *Polar Microbiology: Life in a Deep Freeze*, eds R. Miller and L. Whyte (Washington, DC: ASM Press), 290–304. doi: 10.1128/9781555817183

McMurdie, P. J., and Holmes, S. (2013). phyloseq: an R package for reproducible interactive analysis and graphics of microbiome census data. *PLOS ONE* 8:e61217. doi: 10.1371/journal.pone.0061217

Neukum, G., Basilevsky, A. T., Kneissl, T., Chapman, M. G., van Gasselt, S., Michael, G., et al. (2010). The geologic evolution of Mars: episodicity of resurfacing events and ages from cratering analysis of image data and correlation with radiometric ages of Martian meteorites. *Earth Planet. Sci. Lett.* 294, 204–222. doi: 10.1016/j.epsl.2009.09.006

Nichols, C. A. M., Guezennec, J., and Bowman, J. P. (2005). Bacterial exopolysaccharides from extreme marine environments with special consideration of the southern ocean, sea ice, and deep-sea hydrothermal vents: a review. *Mar. Biotechnol.* 7, 253–271. doi: 10.1007/s10126-004-5118-2

Niederberger, T. D., Perreault, N., Lawrence, J. R., Nadeau, J. L., Mielke, R. E., Greer, C. W., et al. (2009). Novel sulfur-oxidizing streamers thriving in perennial cold saline springs of the Canadian high Arctic. *Environ. Microbiol.* 11, 616–629. doi: 10.1111/j.1462-2920.2008.01833.x

Niederberger, T. D., Perreault, N., Tille, S., Lollar, B. S., Lacrampe-Couloume, G., Andersen, D. T., et al. (2010). Microbial characterization of a subzero, hypersaline methane seep in the Canadian High Arctic. *ISME J.* 4, 1326–1339. doi: 10.1038/ismej.2010.57

Ojha, L., Wilhelm, M. B., Murchie, S. L., McEwen, A. S., Wray, J. J., Hanley, J., et al. (2015). Spectral evidence for hydrated salts in recurring slope lineae on Mars. *Nat. Geosci.* 8, 829–832. doi: 10.1038/ngeo2546

Omelon, C. R., Pollard, W. H., and Andersen, D. T. (2006). A geochemical evaluation of perennial spring activity and associated mineral precipitates at Expedition Fjord, Axel Heiberg Island, Canadian High Arctic. *Appl. Geochem.* 21, 1–15. doi: 10.1016/j.apgeochem.2005.08.004

Omelon, C. R., Pollard, W. H., and Marion, G. M. (2001). Seasonal formation of ikaite (caco3 · 6h 2o) in saline spring discharge at Expedition Fiord, Canadian High Arctic: assessing conditional constraints for natural crystal growth. *Geochim. Cosmochim. Acta* 65, 1429–1437. doi: 10.1016/S0016-7037(00)00620-7

Perreault, N., Andersen, D. T., Pollard, W. H., Greer, C. W., and Whyte, L. G. (2007). Characterization of the prokaryotic diversity in cold saline perennial springs of the Canadian high Arctic. *Appl. Environ. Microbiol.* 73, 1532–1543. doi: 10.1128/AEM.01729-06

Perreault, N., Greer, C. W., Andersen, D. T., Tille, S., Lacrampe-Couloume, G., Lollar, B. S., et al. (2008). Heterotrophic and autotrophic microbial populations in cold perennial springs of the high arctic. *Appl. Environ. Microbiol.* 74, 6898–6907. doi: 10.1128/AEM.00359-08

Picardi, G., Plaut, J. J., Biccari, D., Bombaci, O., Calabrese, D., Cartacci, M., et al. (2005). Radar soundings of the subsurface of Mars. *Science* 310, 1925–1928. doi: 10.1126/science.1122165

Pollard, W., Omelon, C., Andersen, D., and McKay, C. (1999). Perennial spring occurrence in the Expedition Fiord area of western Axel Heiberg Island, Canadian High Arctic. *Can. J. Earth Sci.* 36, 105–120. doi: 10.1139/e98-097

Pollard, W. H. (2005). Icing processes associated with high Arctic perennial springs, Axel Heiberg Island, Nunavut, Canada. *Permafrost Periglac. Process.* 16, 51–68. doi: 10.1002/ppp.515

Priscu, J. C., and Christner, B. C. (2004). "Earth's icy biosphere," in *Microbial Diversity and. Bioprospecting*, ed. A. Bull (Washington, DC: ASM Press), 130–145. doi: 10.1128/9781555817770.ch13

Rennó, N. O., Bos, B. J., Catling, D., Clark, B. C., Drube, L., Fisher, D., et al. (2009). Possible physical and thermodynamical evidence for liquid water at the Phoenix landing site. *J. Geophys. Res.* 114:E00E03. doi: 10.1029/2009JE003362

Ronholm, J., Schumann, D., Sapers, H. M., Izawa, M., Applin, D., Berg, B., et al. (2014). A mineralogical characterization of biogenic calcium carbonates precipitated by heterotrophic bacteria isolated from cryophilic polar regions. *Geobiology* 12, 542–556. doi: 10.1111/gbi.12102

Rossi, A. P., Neukum, G., Pondrelli, M., van Gasselt, S., Zegers, T., Hauber, E., et al. (2008). Large-scale spring deposits on Mars? *J. Geophys. Res.* 113, 1978–2012. doi: 10.1029/2007JE003062

Schloss, P. D., Westcott, S. L., Ryabin, T., Hall, J. R., Hartmann, M., Hollister, E. B., et al. (2009). Introducing mothur: open-source, platform-independent, community-supported software for describing and comparing microbial communities. *Appl. Environ. Microbiol.* 75, 7537–7541. doi: 10.1128/AEM.01541-09

Schneider, D., Arp, G., Reimer, A., Reitner, J., and Daniel, R. (2013). Phylogenetic analysis of a microbialite-forming microbial mat from a hypersaline lake of the Kiritimati atoll, Central Pacific. *PLOS ONE* 8:e66662. doi: 10.1371/journal.pone.0066662

Steven, B., Niederberger, T. D., Bottos, E. M., Dyen, M. R., and Whyte, L. G. (2007). Development of a sensitive radiorespiration method for detecting microbial activity at subzero temperatures. *J. Microbiol. Methods* 71, 275–280. doi: 10.1016/j.mimet.2007.09.009

Stillman, D. E., Michaels, T. I., Grimm, R. E., and Hanley, J. (2016). Observations and modeling of northern mid-latitude recurring slope lineae (RSL) suggest recharge by a present-day Martian briny aquifer. *Icarus* 265, 125–138. doi: 10.1016/j.icarus.2015.10.007

Stuurman, C. M., Osinski, G. R., Holt, J. W., Levy, J. S., Brothers, T. C., Kerrigan, M., et al. (2016). SHARAD detection and characterization of subsurface water ice deposits in Utopia Planitia, Mars. *Geophys. Res. Lett.* 43, 9484–9491. doi: 10.1002/2016GL070138

Tosca, N. J., Knoll, A. H., and McLennan, S. M. (2008). Water activity and the challenge for life on early Mars. *Science* 320, 1204–1207. doi: 10.1126/science.1155432

Williams, J. R., and van Everdingen, R. O. (1973). "Ground water investigations in permafrost regions of North America: a review," in *Proceedings of the 2nd International Conference, on Permafrost, North American Contribution, Yakutsk* (Washington, DC: National Academy of Sciences), 435–446.

Wong, H. L., Ahmed-Cox, A., and Burns, B. P. (2016). Molecular ecology of hypersaline microbial mats: current insights and new directions. *Microorganisms* 4:6. doi: 10.3390/microorganisms4010006

Zhang, D. C., Li, H. R., Xin, Y. H., Chi, Z. M., Zhou, P. J., and Yu, Y. (2008). *Marinobacter psychrophilus* sp. nov., a psychrophilic bacterium isolated from the Arctic. *Int. J. Syst. Evol. Microbiol.* 58, 1463–1466. doi: 10.1099/ijs.0.65690-0

Conflict of Interest Statement: The authors declare that the research was conducted in the absence of any commercial or financial relationships that could be construed as a potential conflict of interest.

frontiers in Microbiology

REVIEW
published: 28 July 2017
doi: 10.3389/fmicb.2017.01407

Glaciers and Ice Sheets As Analog Environments of Potentially Habitable Icy Worlds

*Eva Garcia-Lopez and Cristina Cid**

Microbial Evolution Laboratory, Centro de Astrobiología (Consejo Superior de Investigaciones Cientificas-Instituto Nacional de Técnica Aeroespacial), Madrid, Spain

Icy worlds in the solar system and beyond have attracted a remarkable attention as possible habitats for life. The current consideration about whether life exists beyond Earth is based on our knowledge of life in terrestrial cold environments. On Earth, glaciers and ice sheets have been considered uninhabited for a long time as they seemed too hostile to harbor life. However, these environments are unique biomes dominated by microbial communities which maintain active biochemical routes. Thanks to techniques such as microscopy and more recently DNA sequencing methods, a great biodiversity of prokaryote and eukaryote microorganisms have been discovered. These microorganisms are adapted to a harsh environment, in which the most extreme features are the lack of liquid water, extremely cold temperatures, high solar radiation and nutrient shortage. Here we compare the environmental characteristics of icy worlds, and the environmental characteristics of terrestrial glaciers and ice sheets in order to address some interesting questions: (i) which are the characteristics of habitability known for the frozen worlds, and which could be compatible with life, (ii) what are the environmental characteristics of terrestrial glaciers and ice sheets that can be life-limiting, (iii) What are the microbial communities of prokaryotic and eukaryotic microorganisms that can live in them, and (iv) taking into account these observations, could any of these planets or satellites meet the conditions of habitability? In this review, the icy worlds are considered from the point of view of astrobiological exploration. With the aim of determining whether icy worlds could be potentially habitable, they have been compared with the environmental features of glaciers and ice sheets on Earth. We also reviewed some field and laboratory investigations about microorganisms that live in analog environments of icy worlds, where they are not only viable but also metabolically active.

Keywords: glaciers, ice sheets, habitability, analog environments, icy worlds, cold adaptation, extremophiles, psychrophiles

OPEN ACCESS

Edited by:
Karen Olsson-Francis,
The Open University, United Kingdom

Reviewed by:
Sophie Nixon,
University of Manchester,
United Kingdom
Tatiana A. Vishnivetskaya,
University of Tennessee, Knoxville,
United States
Louisa Jane Preston,
Birkbeck University of London,
United Kingdom

***Correspondence:**
Cristina Cid
cidsc@cab.inta-csic.es

Specialty section:
This article was submitted to Extreme Microbiology, a section of the journal Frontiers in Microbiology

Received: *16 March 2017*
Accepted: *11 July 2017*
Published: *28 July 2017*

Citation:
Garcia-Lopez E and Cid C (2017) Glaciers and Ice Sheets As Analog Environments of Potentially Habitable Icy Worlds. Front. Microbiol. 8:1407. doi: 10.3389/fmicb.2017.01407

INTRODUCTION

Although possible life elsewhere may be different than it is on Earth, several minimum conditions of habitability have been defined: a solvent (water), a source of energy, a group of biologically essential elements (on Earth they are H, C, N, O, S, and P) and some physicochemical conditions (temperature, pH, water activity, etc.) (Hoehler, 2007; Priscu and Hand, 2012; Cockell et al., 2016).

Water on Earth was originated from innumerable collisions with icy comets and asteroids and from volcanic outgassing of the planet's interior (Madigan et al., 2012). At that time, due to the intense heat, water would have been present only as water vapor. Then, Earth cooled down, forming a solid crust and condensing water into oceans around 4.5 billion years ago (Bada et al., 1994). The presence of liquid water implies that conditions could have been compatible with life within a couple of hundred million years after Earth was formed (Madigan et al., 2012). A similar scenario could be the one observed nowadays in icy worlds from our solar system.

The icy worlds of the solar system and beyond meet these conditions of habitability, but their magnitudes are different. It is necessary to know what the intervals of these values are to make them habitable. To know the limits of life, we must first establish what these limits are on Earth, since it is the only case we know. One of the most life limiting features on Earth is low temperature. Actually, the Earth can be considered a cold place. For instance, 90% of the Earth's oceans have a temperature of 5°C or less (Russell, 1990). When terrestrial habitats are included, over 80% of the Earth's biosphere is permanently cold. Among terrestrial environments, 85% of Alaska, 55% of Russia and Canada, 20% of China, and the majority of Antarctica are permanently cold (Pewe, 1995). In our solar system, six of the other eight planets are permanently cold, and hence understanding life's adaptations to cold environments on our planet should be useful in the search for and understanding of life on other planets (Rodrigues and Tiedje, 2008). Living organisms that inhabit the more extreme environments on Earth are microorganisms. Among them, microorganisms inhabiting glaciers and ice sheets could be those that support the environment more similar to the conditions found in icy worlds.

THE CHARACTERISTICS OF HABITABILITY KNOWN FOR THE ICY WORLDS

Insights returned by the solar system planetary missions, and the research in terrestrial extreme environments have widened the concept of habitability in the universe. Many of the potentially habitable places in the universe have cold temperatures. That is why it is important to know the lower limit of temperature in which life is possible. After the successful missions Galileo and Cassini-Huygens to the Jupiter and Saturn systems respectively, this priority has focused on the research of environments potentially habitable in some icy worlds such as Europa, Enceladus, and Titan (Alcazar et al., 2010). It has been hypothesized that life on Earth could have arrived in a process of lithopanspermia. Similarly, such transfers were most likely to occur when these satellites were warmer and meteorites could reach their liquid inner oceans through a thinner ice shell (Worth et al., 2013). Below the most interesting icy worlds are reviewed (**Table 1**), since they are potentially habitable.

TABLE 1 | The characteristics of habitability known for the icy worlds of the solar system.

	Mars	Europa	Ganymede	Callisto	Titan	Rhea	Enceladus	Triton
Solvent	Brines (Martin-Torres et al., 2015)	Briny ocean (Stevenson, 2000)	Water ocean? (Dalton et al., 2010)	Water ocean? (Cooper et al., 2001)	Methane, ethane ocean (Stofan et al., 2007; Béghin et al., 2010)	Water ice (Dalton et al., 2010)	Briny ocean (Kite and Rubin, 2016)	Sub-surface ocean? (Dalton et al., 2010)
Source of energy	Solar radiation (Cockell et al., 2016); Chemical (Westall et al., 2013, 2015)	Cryovolcanism (Dalton, 2010); Hydrothermal processes (Price, 2007)	Cryovolcanism (Schenk et al., 2001)	Cryovolcanism? (Dalton, 2010)	Cryovolcanism (Fortes et al., 2007)	Radioactive elements, tidal interactions (Dalton et al., 2010)	Geochemical (Sekine et al., 2015); Hydrothermal processes (Waite et al., 2017)	Radiogenic heating (Dalton et al., 2010)
Essential elements (identified or predicted)	C, H, N, O, P, S (McGlynn et al., 2012)	C, H, O, S (Dalton, 2010)	C, H, O, S (Calvin et al., 1995; Cooper et al., 2001)	C, H, O, S (Cooper et al., 2001)	C, H, N (Teolis et al., 2010)	C, H, O (Dalton et al., 2010)	C, H, N, O, Ar (Kite and Rubin, 2016)	C, H, N, O (Tyler et al., 1989; Dalton, 2010)
Physico-chemical conditions	Temperature −60°C (Aerts et al., 2014). In winter at the poles −125°C (Forget et al., 1995)	Temperature −187°C to −141°C Possible in interior ocean −3°C (Spencer et al., 1999; Dalton, 2010)	Temperature −183°C to −113°C (Dalton, 2010)	Temperature −193°C to −115°C (Dalton, 2010)	Rainfall, pressure~Earth (Rahm et al., 2016) Temperature −203°C to −73°C	Temperature −220°C to −174°C (Dalton, 2010)	Temperature −240°C to −50°C (Dalton, 2010)	Temperature −237°C to −234°C (Dalton, 2010)
Habitability potential	Low	High	Low	Low	Low	Low	High	Low

Mars

Mars can be considered an icy world because of its low temperatures (Aerts et al., 2014). On average, the temperature on Mars is about −60°C (**Table 1**). And, in winter, temperatures can get down to −125°C at the poles (Forget et al., 1995). Several present and future missions -Curiosity, ExoMars, and possibly Mars 2020- have been equipped with the necessary instrumentation to detect habitable environments *in situ* (Westall et al., 2015). The exploration of Mars has revealed some of the atmospheric and surface properties (Westall et al., 2013). Important gasses have been detected in the Martian atmosphere such as carbon monoxide (96%) and nitrogen (1.9%) (Kaplan et al., 1969). Furthermore, there is an increasing number of reports about superficial water in the past. This has been suggested by the numerous alluvial fans observed in craters (di Achille and Hynek, 2010; Hurowitz et al., 2017), and by the detection of phyllosilicate minerals, which likely represent surface weathering profiles produced by aqueous alteration of the basaltic crust (Fairén et al., 2010). The lack of an ozone layer and the low atmospheric pressure on Mars result in an environment with an intense UV radiation. UVC and UVB daily fluence at 200–315 nm on Mars at present day has been calculated as ∼361 kJ/m^2, while this value is ∼39 kJ/m^2 on Earth (Cockell et al., 2000). This characteristic along with the low temperature contribute to the biologically inhospitable nature of the present Martian surface (Cockell et al., 2000). However, the existence of traces of methane in the Martian atmosphere has been hypothesized to be a plausible evidence for life (Holm et al., 2015). Recent spacecraft-based and Earth ground-based studies have calculated methane values of 10 – 60 ppbv in the Martian atmosphere (Formisano et al., 2004; Mumma et al., 2009; Geminale et al., 2011; Holm et al., 2015). Afterward, the Curiosity rover registered seasonally and regionally variable values around 0.69 ppbv at Gale crater, with episodically elevated levels reaching 7.2 ppbv (Webster et al., 2015). One of the most important discoveries in the exploration of Mars has been the detection of putative hydrothermal phases, including serpentine and phyllosilicates, a weathering product of rocks due to water-rock interactions (Michalski et al., 2013). Serpentinization, a geological low-temperature metamorphic process in which rocks are oxidized and hydrolyzed into serpentinite, has been proposed as an alternative abiotic source for the observed methane low traces.

Satellites of Jupiter

Jupiter has 67 known moons with confirmed orbits. Among them, the Galilean moons Europa, Ganymede and Callisto, are the most interesting from an astrobiological point of view (**Table 1**). The main research about the icy satellites' surface composition have been carried out by the missions Pioneers 10 and 11, Voyagers I and II, Galileo, Cassini and the New Horizons missions (Grundy et al., 2007; Dalton et al., 2010). Future missions such as JUICE (JUpiter ICy moons Explorer) mission from ESA, will perform detailed investigations of Jupiter with a particular focus on the these three satellites.

Europa

Europa is one of the icy worlds in the solar system where potential habitability is more plausible (**Table 1**). Its surface, perhaps geologically active, presents a rigid icy crust that is up to several kilometers thick (Schmidt et al., 2011). The putative ocean of Europa has drawn a remarkable interest (Chyba, 2000; Grundy et al., 2007), as it could be a similar environment to the hydrothermal vents or to the Antarctic Lake Vostok on Earth (**Figure 1**).

Space missions have obtained some data about its temperature distribution (Spencer et al., 1999) and the radiation at surface (Cooper et al., 2001). Temperature on the surface of Europa is around −180°C, but the possible interior ocean can have a much warmer temperature up to −3°C. Observations from Earth have lead to the suggestions that atmospheric oxygen could come from reactions in which water molecules were broken to give rise to molecular hydrogen and oxygen (Hall et al., 1995; Shematovich and Johnson, 2001); through processes related to serpentinization and ice-derived oxidants. On the icy crust of

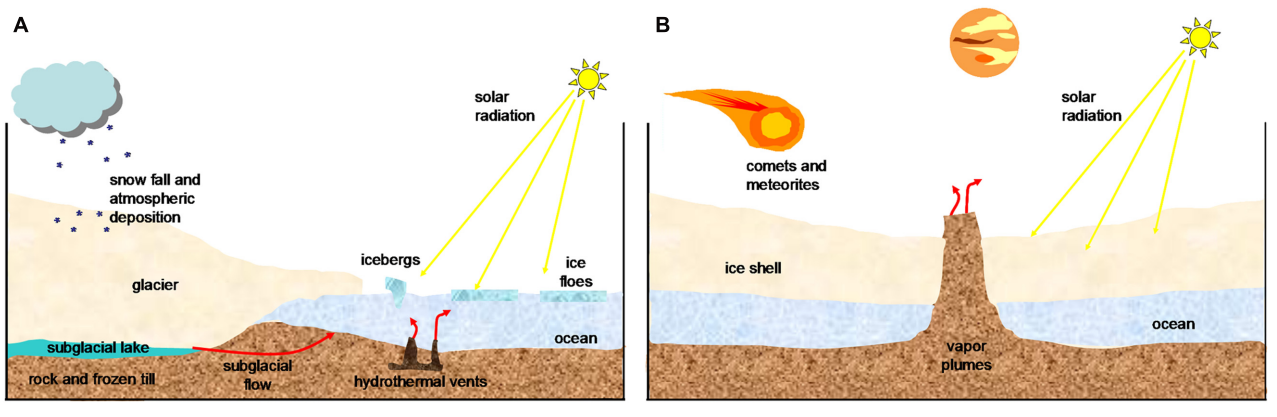

FIGURE 1 | A schematic diagram of cold environments. Surface layers of **(A)** a terrestrial glacier and **(B)** an icy satellite such as Europa. (Adapted from Marion et al., 2003; Priscu and Hand, 2012; Garcia-Lopez and Cid, 2017).

Europa, phyllosilicates have also been detected (Marion et al., 2003); these minerals are often associated with organic matter on Earth. The possible collision with comets and asteroids could be the source of minerals on Europa's surface (Chyba and Phillips, 2001).

As mentioned before, the JUICE mission is planned to explore some icy moons and its potential habitability. For Europa, the focus is on the chemistry essential to life, including the characterization of the surface organic and inorganic chemistry, and on understanding the formation of surface features. If life exists in Europa's ocean, it would be difficult to detect, since it would be necessary to drill the ice before finding the liquid ocean in which the living forms could be preserved. However, it would also be plausible that some convection processes facilitated their rise to the surface (Marion et al., 2003). Life in Europa could exist around hydrothermal vents on the ocean floor. However, some reports have demonstrated that microorganisms could also exist inside ice, as they live in the terrestrial glaciers (Price, 2007). Although temperatures in Europa can be as low as −180°C, the lower limit of temperature at which microbial activity has been detected in laboratory cultures seems to be around −196°C (Junge et al., 2006). Since the environment must be extremely cold and saline, only microorganisms hypothetically analogous to psychrophiles and halophiles could be the ones living in Europa (Marion et al., 2003).

Ganymede

Ganymede's surface has a high number of craters and is mainly composed of silicate rock and water ice. This surface also presents bright, smooth terrains that could be formed by cryovolcanic flows (Schenk et al., 2001). A water ocean (**Table 1**) is believed to exist nearly 200 km below its surface, included between layers of ice (Dalton et al., 2010).

The moon is surrounded by a thin atmosphere composed of O, O_2, O_3, and some H_2 (Calvin et al., 1995; Cooper et al., 2001).

Callisto

Callisto is mainly composed of rock and ice. It may contain an ocean of liquid water beneath its cratered surface (**Table 1**). The atmosphere on Callisto is composed of CO_2 and may probably contain molecular oxygen (Cooper et al., 2001). The likely presence of an ocean within Callisto indicates that it can or could harbor life. Although Callisto is the furthest from the intense radiation of Jupiter, life is considered to be less likely than on Europa.

Satellites of Saturn

Among the more than sixty Saturn moons, only Rhea and Titan have enough mass to hold an atmosphere. However, Titan's atmosphere is mostly nitrogen and methane, with only little amounts of O_2 and CO_2 (Teolis et al., 2010).

Titan

The surface of Titan is thought to be made largely of ice, with oceans of liquid methane and possibly ethane (Stofan et al., 2007; Béghin et al., 2010). Its climate produces wind and rain, which generate fields of dunes in the dark equatorial regions of Titan, rivers, lakes and seas (Rahm et al., 2016) (**Table 1**). Its atmosphere is composed of nitrogen, methane and complex hydrocarbon compounds. The existence of cryovolcanism on the moon's surface has been suggested (Fortes et al., 2007). Cryovolcanism is a very important phenomenon from an astrobiological point of view, because it allows the mixing of organic molecules such as hydrocarbons, nitriles and cyanides with water, giving rise to oxidized more complex prebiotic molecules (Neish et al., 2006; Marin-Yaseli et al., 2017). Titan appears to be very Earth-like in its geology, despite the very different surface conditions and composition. Complex carbon compounds named tholins exist on Titan, as in comets and in the atmospheres of the outer planets (Dalton et al., 2010). Theoretically, tholins might interact with water in a process of hydrolysis to produce complex molecules similar to those found on the early Earth.

Rhea

Rhea is around 527,000 km from Saturn and orbits within its magnetic field. Its average surface temperature is estimated to be −180°C. This moon is characterized by divisions between the leading and trailing hemisphere. The leading hemisphere is uniformly bright, while the trailing hemisphere displays networks of bright stripes on a dark background that overlaps with craters. Cassini observations have established that these lineaments created by tectonic fractures are rich in water ice (Dalton et al., 2010). The moon is surrounded by a thin atmosphere composed of 70% O_2 and 30% CO_2. The O_2 is believed to be formed when water molecules are split by energetic particles in a process of radiolysis (Dalton et al., 2010).

Enceladus

Saturn's moon Enceladus harbors a global ocean of salty water under its icy crust (Kite and Rubin, 2016). Recently, the Cassini-Huygens mission detected significant amounts of hydrogen in the plume, and a warm subsurface region with prominent thermal anomalies that had not been identified before (Le Gall et al., 2017). These observations imply the presence of a broadly distributed heat production and transport system below the south polar terrain with 'plate-like' features, and suggest that a liquid reservoir could exist some kilometers beneath the ice crust (Le Gall et al., 2017). From previous flybys, Cassini determined that nearly 98% of the gas in the plume was water, and the rest was a mixture of other molecules, including carbon dioxide, methane and ammonia (Kite and Rubin, 2016). And recent observations made by the Cassini spacecraft, have found molecular hydrogen in the Enceladus plume, an important finding that represents an evidence for hydrothermal processes (Waite et al., 2017). The existence of serpentinization reactions in Enceladus, which would generate hydrogen, has been suggested. Under particular conditions, this hydrogen could supply chemical energy to support chemoautotrophic life (Sekine et al., 2015). A sample return mission to Enceladus has been proposed, Life Investigation For Enceladus (LIFE), in order to study its high astrobiological potential (Tsou et al., 2012).

Satellites of Neptune

Neptune is one of the coolest places in the solar system. Life is unlikely unless geological activity made it possible. However, its satellites with volcanic activity are interesting for astrobiological exploration.

Triton

Voyager 2 discovered that Triton had a volcanic activity, which consists of the melting of ice water and nitrogen, and perhaps methane and ammonia (Tyler et al., 1989). The atmosphere is composed of nitrogen and methane, the same compounds that exist on Saturn's largest moon, Titan. Nitrogen is also the main compound of the Earth's atmosphere, and methane on Earth is normally associated with life. Nevertheless, like Titan, Triton is extremely cold. If that were not the case, these two components of the atmosphere would be considered signs of life. However, due to the geological activity and possible internal warming, it has been suggested that Triton could harbor primitive life forms in liquid water below the surface, in the same way that it has been suggested for Jupiter's moon Europa (Dalton et al., 2010). Evidence of the detection of the HCN ice has also been presented. HCN is a product of the photolytic processing of nitrogen and carbon bearing molecules, and represents an intermediate step in the production of macromolecules of astrobiological interest (Dalton et al., 2010; Marin-Yaseli et al., 2017).

Habitability Beyond the Solar System. Exoplanets

It is considered that any exoplanet that rotates around its star in an area not too hot and not too cold, allowing the existence of liquid water, could contain some form of life (Kasting et al., 1993). In addition to temperature, another of the conditions of habitability is the radiation emitted by the star. Red dwarfs are considered excellent candidates. These are small stars, with less than half the mass of our Sun and with surface temperatures below 4,000°C (Anglada-Escude et al., 2016). The discovery of thousands of exoplanets that are very different from our own solar system could completely change several aspects of the planetary sciences as we know them today (Seager and Bains, 2015).

Beyond our Solar System, Proxima Centauri b, a planet similar to Earth in size, provides an exciting opportunity to learn about the evolution of terrestrial planets orbiting M dwarfs. This planet is located in the habitable zone away from its star, and might even contain an ocean; thus it has been considered as potentially habitable. However, red dwarfs are also prone to have stellar eruptions much more frequent and powerful than those of our Sun. These eruptions generate bursts of high-energy radiation that break the molecules in their constituent atoms and ionize them; so electrons are easily lost in the space. Over time, positively charged particles are sent away from the surface of the planet (Airapetian et al., 2017). Hydrogen, essential for water and the lightest element, is the most vulnerable to this process. In all likelihood, Proxima Centauri b must have also lost most of its atmospheric O_2 during the first ten million years of its existence. This is frontally opposed to the idea that Proxima Centauri b could harbor a vast ocean. The addition of frequent solar storms and intense magnetic activity also places it far from being the ideal place to shelter any kind of life (Anglada-Escude et al., 2016).

Some recent researches have found other exoplanets, such as LHS 1140b, transiting a small cool star (LHS 1140), within the liquid water habitable zone (Dittmann et al., 2017). Moreover, recent observations revealed that seven planets similar to Earth rotate around their host star named TRAPPIST-1 (Gillon et al., 2017). Their surface temperatures are low enough to enable the existence of liquid water (Stevenson, 1999; Kopparapu et al., 2013; Leconte et al., 2013). Upcoming observations with large ground and space-based telescopes may help to illuminate the intriguing environment of our nearest exoplanetary neighbor.

ENVIRONMENTAL LIFE-LIMITING CHARACTERISTICS OF TERRESTRIAL GLACIERS AND ICE SHEETS

Several reviews have been published with the aim of evaluating the key sites that are contributing most to our understanding of potential extraterrestrial habitable environments in the solar system (Preston and Dartnell, 2014). Studies aimed at detecting life beyond Earth have inevitably been centered on Earth life because this is the only example of life that we know. Therefore, it is necessary to study environments on Earth that are analog to those in other planets and satellites. It is also important to consider that many terrestrial environments in which life exists today may not be adequate for the life that originated 1000s of years ago.

Several common habitability conditions have been defined (Priscu and Hand, 2012), but the environmental conditions of the extraterrestrial systems we know are very different from each other and very different from those on Earth. A potentially habitable location needs to meet a number of requirements. The abovementioned requirements -solvent, energy, essential elements and physicochemical conditions- must be present in limited quantities. However, which are those limits that determine life? To know the limits of life on Earth, we have to consider the extremophile organisms. These can be defined as organisms living in physical or geochemical conditions that are incompatible with the life of most organisms. Thus, they live to the limit. These organisms (usually microorganisms, as they are simpler) collectively define the physiochemical limits to life. Extremophiles are able to live in harsh environments such as volcanic hot springs, glaciers, extremely salty environments, in waters having a pH as low as 0 or as high as 12, or in the deep sea under extreme pressure (Pikuta et al., 2007). Interestingly, these prokaryotes do not only tolerate their particular environmental extreme conditions, but they require it in order to grow (Madigan et al., 2012). **Table 2** summarizes some examples among extremophiles, the especial conditions these microorganisms support, the type of habitats in which they reside, and the extraterrestrial environments to which they are analog.

TABLE 2 | Extremophiles on Earth with similar environments to the icy worlds of the solar system.

Extremophile	Conditions	Earth habitat	Analog environments	Examples of microorganisms
Psychrophiles	Low temperature	Glaciers, sea ice	Ice shells of Europa and Enceladus; poles of Mars	*Psychrobacter*[b]
Acidophiles	Low pH	Mines, volcanoes	Surface of Mars	*Acetobacter*[b]
Alkaliphiles	High pH	Soda lakes	Ocean of Enceladus	*Bacillus firmus*[b]
Halophiles	High salinity	Salterns, sea ice inclusions	Subsurface oceans of Europa, Titan and Enceladus	*Halobacterium*[a]
Barophile or Piezophiles	High pressure	Deep ocean	Ocean floors of Europa	*Moritella*[b]
Xerophiles	Low water activity	Deserts, rock surfaces	Surface of Mars	*Bacillus megaterium*[b]
Radiotolerant	High radiation	Nuclear reactor water	Surface of Europa	*Deinococcus*[b]

[a]*Archaea.* [b]*Bacteria.*

On Earth, three environments maintain very low temperatures throughout the year: poles, oceans and glaciers. Considering that a great diversity of microorganisms belonging to the three main domains (Bacteria, Eucarya, and Archaea) has been discovered inhabiting glaciers (Garcia-Lopez and Cid, 2017), they have been considered biomes that should be recognized as such in their own right (Hodson et al., 2008; Anesio and Laybourn-Parry, 2012).

The inhabitants of the glaciers have to be polyextremophiles, due to the diverse extreme conditions in which they live (**Table 2**). Most of the microorganisms isolated from cold environments are psychotolerant (also called psychrotrophs) and psychrophiles. Psychotolerant organisms can grow at temperatures close to 0°C but have their optimum growth temperature at about 20°C. However, psychrophiles have their optimal growth temperature at 15°C or less (Cavicchioli et al., 2002). In addition to the low temperatures, microorganisms from glaciers generally tolerate high solar radiation -radiophiles- (Martin-Cerezo et al., 2015), scarce availability of water -xerophiles- (Imshenetsky et al., 1973), and sometimes they can also bear extremely acidic media -acidophiles- (Cid et al., 2010).

MICROBIAL COMMUNITIES LIVING IN GLACIERS AND ICE SHEETS

All the organisms are composed of nearly the same macromolecules, but the environments and physical–chemical conditions in which they live are very different. Some organisms can cope with very extreme conditions, and the knowledge of this versatility of life on Earth can help the understanding of a hypothetical life in other worlds (Des Marais et al., 2008).

The discovery of cold-tolerant microorganisms in glaciated and permanently frozen environments has broadened the known range of environmental conditions that support microbial life. In glaciers and ice sheets, three different ecosystems have been considered: the supraglacial ecosystem, the subglacial system and the englacial ecosystem (Hodson et al., 2008; Boetius et al., 2015) (**Figure 2**). These three ecosystems differ in terms of their solar radiation, water content, nutrient abundance and redox potential (Hodson et al., 2008).

The supraglacial ecosystem is characterized by the absorption of solar radiation, which causes ice melting yielding liquid water.

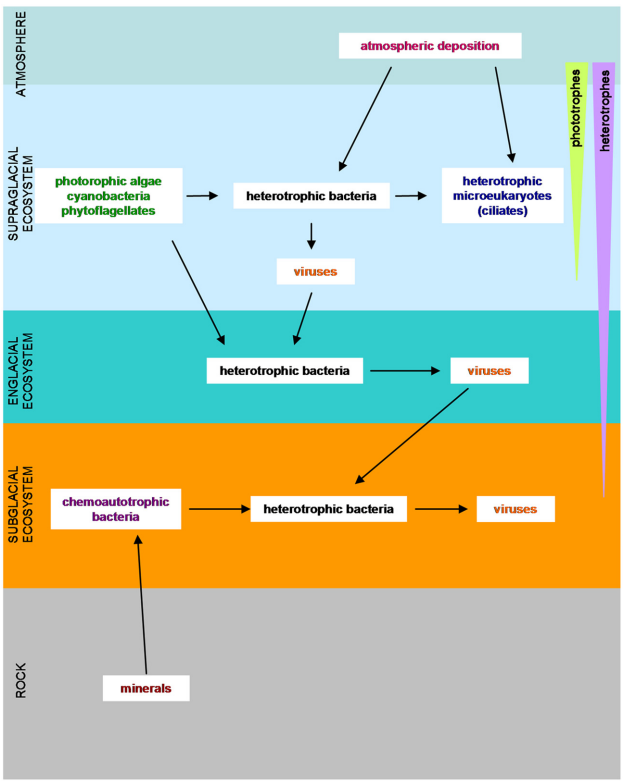

FIGURE 2 | Overview of the microorganisms in glaciers and ice sheets with their food requirements. (Adapted from Hodson et al., 2008; Anesio and Laybourn-Parry, 2012; Garcia-Lopez and Cid, 2017).

Meltwater dissolves nutrients from adjacent rocks, and even directly from the atmosphere (Tranter et al., 1993). This facilitates the growth of microbial colonies (Maccario et al., 2015) of autotrophic microorganisms such as microalgae and diatoms. The supraglacial surface is also populated by chemolitotrophic bacteria, which feed on inorganic sand particles, by heterotrophic bacteria and by microeukaryotes (Mieczen et al., 2013). Cryoconite holes, cylindrical melt holes in a glacier surface (Fountain et al., 2008), have recently gained attention because they may be a refuge similar to the one that could be inhabited by

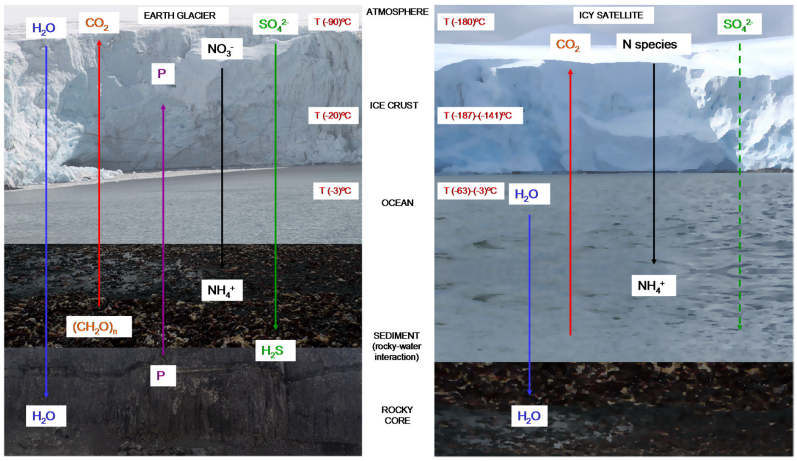

FIGURE 3 | Stratification of nutrients and temperatures in cold habitats. Microbial metabolism in terrestrial glaciers (left) is driven by coupling surface oxidants with reductants associated with the subglacial rocks (Rankin et al., 1999; Hodson et al., 2008; Murray et al., 2012). The same mechanism could be possible in icy worlds (right), in which come of this nutrients have been detected (Cockell et al., 2016). Temperature on the surface of Europa is around −180°C, but the interior ocean can have a much warmer temperature that reaches −3°C (Spencer et al., 1999). At the coldest point of the Earth's surface (Base Vostok, Antartica) temperatures can reach −90°C, but inside the Antarctic Lake Vostok the temperature is also around −3°C (Priscu and Hand, 2012).

the microorganisms in the frozen worlds (Vincent and Howard-Williams, 2000; Nisbet and Sleep, 2001) or on planet Earth during the glaciations (Hoffman et al., 1998; Priscu and Christner, 2004).

The englacial ecosystem presents a minor impact upon nutrient dynamics (Hodson et al., 2008), but it is the most analogous to the environment that could be found in icy worlds. Biomass is low in the englacial ecosystem, and microorganisms live in places that protect them against radiation and dehydration (Aerts et al., 2014). Inside glacier ice, bacteria live at clay particles or at grain boundaries, and other interstices like triple point junctions, brine channels and gas bubbles. Mineral substrates provide nutrients and a supply of water for microorganisms (Price, 2007). Englacial ecosystems are mainly inhabited by chemoautotrophs; but they can also be heterotrophic bacteria that feed on solubilized organic products. At great depth, anaerobic respiration and methanogens can take place (Tung et al., 2005; Price, 2007; Hodson et al., 2008).

The subglacial ecosystem is composed of sediments and bedrock. These environments are isolated by the upper deposits of glacial ice, which decreases temperature fluctuations and make them suitable for microbial life (Sharp et al., 1999). For example, beneath a High Arctic Glacier, aerobic chemoheterotrophs and anaerobic nitrate reducers, sulfate reducers, and methanogens have been identified (Skidmore et al., 2000; Phillips and Parnell, 2006; Harrold et al., 2016). Underneath the glaciers, microorganisms can persist in a quiescent way for years at subfreezing temperatures (Sharp et al., 1999; Skidmore et al., 2000). When conditions are favorable, and partial melting of the ice occurs by a temperature rise, microorganisms may be reactivated. The presence of liquid water, favored by the high pressure exerted by overlying layers of ice is a good solvent for the organic and inorganic nutrients from dissolved particulate material and gasses. Some ingredients necessary for life such as the organic carbon, derive from soil and decaying plants overridden by glacial advance. There is evidence that some redox reactions like sulfide oxidation (Raiswell, 1984), denitrification (Tranter et al., 1994), iron reduction (Nixon et al., 2017) and oxidation of organic carbon (Fairchild et al., 1993) can occur at subglacial sediments. Furthermore, some microbial communities are able to live nearly isolated from the atmosphere in subglacial environments, thanks to their chemolithotrophic metabolism (Boyd et al., 2014).

Subglacial water can be very abundant in subglacial rivers and lakes such as the Blood Falls (Mikucki et al., 2009) or Lake Vostok (Christner et al., 2006; Rogers et al., 2013) in Antarctica. These environments have been studied with great interest because they can be considered analogs of the underground oceans of some icy satellites (**Figure 3**). High pressures and high salinity of water running through subsurface or ice depositions lower the freezing point of water and thus provide liquid water available for biochemical processes (Aerts et al., 2014). These subglacial ecosystems harbor diverse communities of heterotrophic and lithotrophic microorganisms over extended periods of time. They are dominated by bacteria and viruses in basal bedrock and subglacial lakes, and they also contain, metabolically active archaeal, bacterial and fungal species (Butinar et al., 2007). At this depth, a diversity of metabolic mechanisms may be expected, but processes such as serpentinization (Michalski et al., 2013) could possibly provide energy for microorganisms in subglacial ecosystems. For instance, the permanent ice covered Lake Vida (Antarctica) contains a cryogenic, aphotic and anoxic ecosystem in which active bacteria live under very high levels of reduced metals, ammonia, dissolved organic carbon; as well as high concentrations of oxidized species

of nitrogen and sulfur (Rankin et al., 1999; Murray et al., 2012).

In icy satellites such as Europa, a similar environment could exist. Liquid water could be present in the subsurface ocean, containing materials derived from the original formation of the satellite (Dalton et al., 2010). In addition, new compounds may have been produced by chemical reactions in the interior, reaching the surface by endogenic processes such as cryovolcanism or extensional tectonics. Additional material may be brought by comets or meteorites (Dalton et al., 2010). N species could come from the surface crust; and CO_2, SO_4^{2-} and organic compounds could be expected due to meteoritic delivery (Cockell et al., 2016). Other compounds such as HCN have been detected in other icy satellites such as Enceladus, Triton and Titan (Dalton et al., 2010; Cockell et al., 2016; Marin-Yaseli et al., 2017) (**Figure 3**).

Molecular Mechanisms of Adaptation to Cold Environments

Inside glaciers and ice sheets, ice veins provide a liquid microenvironment, which may serve as a habitat for microbial life (Thomas and Dieckmann, 2002). However, microorganisms in the ice veins support a variety of physiochemical stresses including low water activity, low pH, reduced solute diffusion rates and membrane damaging due to ice crystal formation. To grow efficiently at low temperatures, microorganisms have developed complex structural and functional strategies for their adaptation (D'Amico et al., 2006). The study of these adaptation strategies aims to identify the limits of life at these temperatures (**Table 3**). Adaptations include: (i) the synthesis of catalytically efficient enzymes that are functional at low temperatures with a high efficiency (Feller and Gerday, 2003); (ii) the synthesis of specialized unsaturated fatty acids in the cell membrane to increase its fluidity (Los and Murata, 2004; Nichols et al., 2004); (iii) the production of extracellular polymeric substances (Krembs et al., 2011) which affect ice crystal structure and allow the cell to protect itself from frostbite (e.g., sugars, polysaccharides, antifreeze proteins) (Alcazar et al., 2010; Garcia-Descalzo et al., 2012a); (iv) the synthesis of certain proteins that allow synthesizing others at low temperatures (Garcia-Descalzo et al., 2011); (v) the reorganization of protein networks (Garcia-Descalzo et al., 2014); (vi) the use pigments to obtain energy, stress resistance and for ultraviolet light protection (Garcia-Lopez and Cid, 2016). For instance, colored glacier surfaces are caused by snow algae or melanized fungi. Additionally, some cold-adapted bacteria produce pigments such as xanthins, carotenes and cytochromes (Garcia-Descalzo et al., 2014).

In recent years, a few studies have been published on the recovery of live microorganisms from ancient ice, where they have survived for 100s of millions of years (Bidle et al., 2007). The endurance of these microorganisms depends on their ability to persist in a dormant, metabolically inert state. This means that glaciers and ice sheets are inhabited by microorganisms, which maintain active biochemical processes to preserve their cellular integrity and a minimal metabolism (Dieser et al., 2013). The long-term survival does not imply a very active functional metabolism, but it is at least necessary that the microorganisms can recover the damaged molecules, such as the DNA that breaks because of background radiation in the permafrost (Johnson et al., 2007).

TABLE 3 | Mechanisms of adaptation to extreme environments.

Extremophile	Challenges	Mechanisms of adaptation
Psychrophiles	Reduced enzyme activity Decreased membrane fluidity and altered transport Decreased rates of transcription, translation and cell division Protein cold denaturation, inappropriate protein folding	Active enzymes at low temperature Cold shock proteins Fats that allow membrane fluidity Antifreeze compounds
Acidophiles	Alteration in the cellular membrane and transport	H^+ transport pumps Active enzymes at low pH
Alkaliphiles	Alteration in the cellular membrane and transport	Active enzymes at high pH
Halophiles	Water loss and desiccation	Synthesis of compounds such as betaine, glycerol, etc. Active enzymes at high salinity
Barophile or Piezophiles	Decreases the ability of the subunits of proteins to interact Protein synthesis, DNA synthesis, and nutrient transport are sensitive to high pressure	Higher proportion of unsaturated fatty acids in cytoplasmic membranes Special membrane proteins
Xerophiles	Water loss and desiccation	They live inside rocks to use water condensation
Radiotolerant	DNA mutations	Multiple copies of DNA Various mechanisms of DNA repair

Detection of Microbial Activity at Subzero Temperature

Due to techniques such microscopy, and more recently DNA sequencing methods, a great biodiversity of prokaryote and eukaryote microorganisms have been discovered inhabiting glaciers and ice sheets (**Table 4**).

Morphology and motility of microbial cells observed by *in situ* microscopy have been used as a technique for the detection of biosignatures in the liquid brines that persist in ice (Lindensmith et al., 2016; Nadeau et al., 2016). Microbial metabolism in glaciers and ice sheets is driven by coupling surface oxidants with reductants associated with the subglacial rocks (**Figure 3**). The incorporation of radio labeled compounds has been used to detect cellular respiration (Panikov et al., 2006), to investigate DNA, lipid or protein synthesis and to reveal CH_4 production (Doyle et al., 2012, 2013; Murray et al., 2012). Using these methods, it has been shown that snow and firn contain bacteria able to maintain low rates of DNA and protein synthesis, and different microorganisms able to metabolize at subzero temperatures (−12°C to −17°C) (Carpenter et al., 2000; Siddiqui and Cavicchioli, 2006).

TABLE 4 | Evidence for activity in microorganisms at subzero temperatures.

Sample	Temperature (°C)	Activity	Technique	Reference
Lake microbial community	0	Carbon fixation Fermentation Methanogenesis Methane oxidation CO oxidation Nitrogen assimilation Denitrification Nitrogen fixation Sulfate reduction Sulfide oxidation	Proteomics	Lauro et al., 2011
Antarctic sea bacterioplankton	−0.92	Ammonia oxidation Reverse tricarboxylic acid cycle	Proteomics	Williams et al., 2012
Methanococcoides burtonii	−2	EPS production Oxidative stress Quality control of protein folding	Proteomics	Williams et al., 2011
Greenland sea ice	−4	Morphology and motility	Microscopy	Lindensmith et al., 2016
Ice-sealed Antarctic lake	−13	Macromolecular Synthesis	^{3}H-leucine incorporation	Murray et al., 2012
Basal glacier ice	−15	Macromolecular Synthesis	^{3}H-thymidine and ^{3}H-leucine incorporation	Doyle et al., 2013
Snow	−17	Macromolecular Synthesis	^{3}H-thymidine and ^{3}H-leucine incorporation	Carpenter et al., 2000
Sea ice	−20	Respiration	5-cyano-2,3-ditolyl tetrazolium chloride reduction	Junge et al., 2004
Permafrost	−39	Respiration	[^{14}C]Glucose uptake	Panikov et al., 2006
Psychrobacter cryohalolentis K5	−80	Metabolism	ATP and ADP levels	Amato and Christner, 2009
Environmental isolates from sea ice	−196	Protein synthesis	^{3}H-leucine incorporation	Junge et al., 2006

Other analytical techniques such as the measurement of ATP and ADP concentrations demonstrated the existence of metabolism in the psychrophilic bacteria *Psychrobacter cryohalolentis* K5 cultured at −80°C (Amato and Christner, 2009); although, the lower limit of temperature at which microbial activity has been detected in laboratory culture seems to be −196°C (Junge et al., 2006). Additionally, measurement of nitrate and ammonium has been performed to detect N mineralization and nitrification. The reduction of some chemical compounds such as 5-cyano-2, 3-ditolyl tetrazolium chloride (CTC) has been used to detect cellular respiration (Junge et al., 2004).

Recently, the diversity of life forms and mechanisms of adaptation to extreme conditions, and the characterization of the specific signs of their biological activity on glaciers have been investigated with other approaches such as Fourier Transform Infrared Spectroscopy (FTIR), Raman spectroscopy, and "omics" technologies (genomics, transcriptomics, proteomics or metabolomics).

Specifically, proteomic techniques have identified proteins that are active at cold temperatures, showing that microorganisms are alive and metabolically active inside glaciers (**Table 4**). For example, in the cold-adapted microorganism *Methanococcoides burtonii* transcription and translational mechanisms are compromised at −2°C, which enables very low growth rates (Williams et al., 2011). The advantage of using proteomic techniques over other analytical techniques, is that proteomics can simultaneously detect various activities of microorganisms by the identification of specific proteins involved in each cellular process. When combined with genomic techniques, proteomics can identify the activity of complete microbial communities. Another advantage of studying proteins is that they are molecules that actually work in the cell. By determining which proteins have been synthesized by microorganisms, metaproteomics enables the reconstruction of microbial processes and metabolic pathways that are central to the functioning of the ecosystem (Williams et al., 2012). This is especially interesting in the study of microbial communities from glaciers and ice sheets, where cell motility is lower than it is in aqueous media such as lakes and oceans (Lauro et al., 2011). Therefore, proteomics presents an attractive alternative for the direct identification of biosignatures in analog environments of icy worlds (Garcia-Descalzo et al., 2012b; Martin-Cerezo et al., 2015).

It has also been shown that microbial proteins take part in complexes, which are modulated by the environment (Garcia-Descalzo et al., 2014). Therefore, the molecular machinery in cold-adapted microorganisms is very adaptable through the interaction network they establish. Proteins that take part in networks are dependent on environmental conditions. For instance, it has been demonstrated that the protein HSP90 and HSP90-associated proteins from microorganisms inhabiting analogous environments conserve similar HSP90 interactors in opposition to phylogenetically closely related microorganisms living in different environments (Garcia-Descalzo et al., 2011).

CONCLUDING REMARKS

Icy worlds have attracted a remarkable attention in the search for habitability beyond Earth.

Here we have compared the environmental characteristics of icy worlds and the environmental characteristics of terrestrial glaciers and ice sheets in order to address some interesting questions. Firstly, which are the characteristics of habitability known for the frozen worlds, and which could be compatible with life? Secondly, what are the environmental characteristics of terrestrial glaciers that can be life-limiting, and which are the microbial communities that can live in them? And finally, taking into account all of these observations, could any of these planets or satellites meet the conditions of habitability? After comparing the characteristics of habitability of icy worlds and Earth glaciers, it can be concluded that the icy worlds of the solar system most likely to harbor life are Europa and Enceladus (**Table 1**). Other icy worlds could also contain a water ocean below the surface, but it would be included between layers of ice (Dalton et al., 2010). Nevertheless, Europa and Enceladus are the only two recognized moons where liquid water could be in contact with rocks. This conclusion is supported by the recent observations made by the Cassini spacecraft, which found molecular hydrogen in the Enceladus' plume, suggesting the possible existence of hydrothermal processes (Waite et al., 2017).

In the pursuit of life in other planets, it is widely recognized that the presence of liquid water is requirement for habitability. And it has been demonstrated not only that life is possible inside glaciers and ice sheets, but also that ice could constitute a shelter to protect microorganisms from solar radiation. The existence in Earth glaciers of microbial communities that maintain active biochemical routes in englacial and subglacial ecosystems can broaden the scenarios in which life might be possible.

These findings open new questions to research: (i) as the studies of enzymatic activity at very low temperatures (up to −196°C) have mostly been carried out in the laboratory, could these metabolic activities be detected *in situ* in the coldest regions of Earth?, (ii) are we using the best techniques to detect biosignatures on icy worlds?, (iii) what will we find in upcoming missions to Europa and Enceladus?, (iv) are there other new potential candidate worlds to be habitable?, (iv) what characteristics of habitability can be found in exoplanets? The future space exploration of these icy worlds will be challenging.

AUTHOR CONTRIBUTIONS

CC: wrote the manuscript, reviewed the literature on microbiology of glaciers, and edited figures. EG-L: reviewed the literature on astrobiology and habitability and wrote the first part of the manuscript.

FUNDING

This research was supported by grants CTM/2008-00304/ANT, CTM 2010-12134-E/ANT and CTM2011-16003-E from the Spanish Ministerio de Economía, Industria y Competitividad (MINECO). EG-L is recipient of a MINECO Fellowship (Grant PTAT2010-03424, Programa Nacional de Contratación e Incorporación de RRHH).

ACKNOWLEDGMENT

We are indebted to Paula Alcazar for her technical assistance.

REFERENCES

Aerts, J. W., Röling, W. F., Elsaesser, A., and Ehrenfreund, P. (2014). Biota and biomolecules in extreme environments on Earth: implications for life detection on Mars. *Life* 4, 535–565. doi: 10.3390/life4040535

Airapetian, V. S., Glocer, A., Khazanov, G. V., Loyd, R. O. P., France, K., Sojka, J., et al. (2017). How hospitable are space weather affected habitable zones? The role of ion escape. *Astrophys. J. Lett.* 836:L3. doi: 10.3847/2041-8213/836/1/L3

Alcazar, A., Garcia-Descalzo, L., and Cid, C. (2010). "Microbial evolution and adaptation in icy worlds," in *Astrobiology: Physical Origin, Biological Evolution and Spatial Distribution*, eds S. Hegedûs and J. Csonka (New York, NY: Springer Verlag Inc), 81–95.

Amato, P., and Christner, B. C. (2009). Energy metabolism response to low-temperature and frozen conditions in *Psychrobacter cryohalolentis*. *Appl. Environ. Microbiol.* 75, 711–718. doi: 10.1128/AEM.02193-08

Anesio, A. M., and Laybourn-Parry, J. (2012). Glaciers and ice sheets as a biome. *Trends Ecol. Evol.* 27, 219–225. doi: 10.1016/j.tree.2011.09.012

Anglada-Escude, G., Amado, P. J., Barnes, J., Berdiñas, Z. M., Butler, R. P., Coleman, G., et al. (2016). A terrestrial planet candidate in a temperate orbit around Proxima Centauri. *Nature* 7617, 437–440. doi: 10.1038/nature19106

Bada, J. L., Bigham, C., and Miller, S. L. (1994). Impact melting of frozen oceans on the early Earth: implications for the origin of life. *Proc. Natl. Acad. Sci. U.S.A.* 91, 1248–1250. doi: 10.1073/pnas.91.4.1248

Béghin, C., Sotin, C., and Hamelin, M. (2010). Titan's native ocean revealed beneath some 45 km of ice by a Schumann-like resonance. *C. R. Geosci.* 342, 425–433. doi: 10.1016/j.crte.2010.03.003

Bidle, K. D., Lee, S., Marchant, D. R., and Falkowski, P. G. (2007). Fossil genes and microbes in the oldest ice on Earth. *Proc. Natl. Acad. Sci. U.S.A.* 104, 13455–13460. doi: 10.1073/pnas.0702196104

Boetius, A., Anesio, A. M., Deming, J. W., Mikucki, J. A., and Rapp, J. Z. (2015). Microbial ecology of the cryosphere: sea ice and glacial habitats. *Nat. Rev. Microbiol.* 13, 677–690. doi: 10.1038/nrmicro3522

Boyd, E. S., Hamilton, T. L., Havig, J. R., Skidmore, M. L., and Shock, E. L. (2014). Chemolithotrophic primary production in a subglacial ecosystem. *Appl. Environ. Microbiol.* 80, 6146–6153. doi: 10.1128/AEM.01956-14

Butinar, L., Spencer-Martins, I., and Gunde-Cimerman, N. (2007). Yeasts in high Arctic glaciers: the discovery of a new habitat for eukaryotic microorganisms. *Antonie van Leeuwenhoek* 91, 277–289. doi: 10.1007/s10482-006-9117-3

Calvin, W. M., Clark, R. N., Brown, R. H., and Spencer, J. R. (1995). Spectra of the icy Galilean satellites from 0.2 to 5 mm: a compilation, new observations, and a recent summary. *J. Geophys. Res.* 100, 19041–19048. doi: 10.1029/94JE03349

Carpenter, E. J., Lin, S., and Capone, D. G. (2000). Bacterial activity in South Pole snow. *Appl. Environ. Microbiol.* 66, 4514–4517. doi: 10.1128/AEM.66.10.4514-4517.2000

Cavicchioli, R., Siddiqui, K. S., Andrews, D., and Sowers, K. R. (2002). Low-temperature extremophiles and their applications. *Curr. Opin. Biotechnol.* 13, 253–261. doi: 10.1016/S0958-1669(02)00317-8

Christner, B. C., Royston-Bishop, G., Foreman, C. M., Arnold, B. R., Tranter, M., Welch, K. A., et al. (2006). Limnological conditions in subglacial Lake

Vostok, Antarctica. *Limnol. Oceanogr.* 51, 2485–2501. doi: 10.4319/lo.2006.51.6.2485

Chyba, C. F. (2000). Energy for microbial life on Europa. *Nature* 403, 381–382. doi: 10.1038/35000281

Chyba, C. F., and Phillips, C. B. (2001). Possible ecosystems and the search for life on Europa. *Proc. Natl. Acad. Sci. U.S.A.* 98, 801–804. doi: 10.1073/pnas.98.3.801

Cid, C., Garcia-Descalzo, L., Casado-Lafuente, V., Amils, R., and Aguilera, A. (2010). Proteomic analysis of the response of an acidophilic strain of *Chlamydomonas* sp. (Chlorophyta) to natural metal-rich water. *Proteomics* 10, 2026–2036. doi: 10.1002/pmic.200900592

Cockell, C. S., Bush, T., Bryce, C., Direito, S., Fox-Powell, M., Harrison, J. P., et al. (2016). Habitability: a review. *Astrobiology* 16, 89–117. doi: 10.1089/ast.2015.1295

Cockell, C. S., Catling, D. C., Davis, W. L., Snook, K., Kepner, R. L., Lee, P., et al. (2000). The UV environment of Mars: biological implications past, present, and future. *Icarus* 146, 343–359. doi: 10.1006/icar.2000.6393

Cooper, J. F., Johnson, R. E., Mauk, B. H., Garrett, H. B., and Gehrels, N. (2001). Energetic ion and electron irradiation of the icy Galilean satellites. *Icarus* 149, 133–159. doi: 10.1006/icar.2000.6498

Dalton, J. B. (2010). Spectroscopy of Icy Moon surface materials. *Space Sci. Rev.* 153, 219–247. doi: 10.1007/s11214-010-9658-7

Dalton, J. B., Cruikshank, D. P., Stephan, K., McCord, T. B., Coustenis, A., Carlson, R. W., et al. (2010). Chemical composition of icy satellite surfaces, Space. *Sci. Rev.* 153, 113–154. doi: 10.1007/s11214-010-9665-8

D'Amico, S., Collins, T., Marx, J. C., Feller, G., and Gerday, C. (2006). Psychrophilic microorganisms: challenges for life. *EMBO Rep.* 7, 385–389. doi: 10.1038/sj.embor.7400662

Des Marais, D. J., Nuth, J. A., Allamandola, L. J., Boss, A. P., Hoehler, T. M., Jakosky, B. M., et al. (2008). The NASA astrobiology roadmap. *Astrobiology* 8, 715–730. doi: 10.1089/ast.2008.0819

di Achille, G., and Hynek, B. M. (2010). Ancient ocean on Mars supported by global distribution of deltas and valleys. *Nat. Geosci.* 3, 459–463. doi: 10.1038/ngeo891

Dieser, M., Battista, J. R., and Christner, B. C. (2013). DNA double-strand break repair at −15°C. *Appl. Environ. Microbiol.* 79, 7662–7668. doi: 10.1128/AEM.02845-13

Dittmann, J. A., Irwin, J. M., Charbonneau, D., Bonfils, X., Astudillo-Defru, N., Haywood, R. D., et al. (2017). A temperate rocky super-Earth transiting a nearby cool star. *Nature* 544, 333–336. doi: 10.1038/nature22055

Doyle, S. M., Dieser, M., Broemsen, E., and Christner, B. C. (2012). "General characteristics of cold-adapted microorganisms," in *Polar Microbiology: Life in a Deep Freeze*, eds L. Whyte and R. V. Miller (Washington, DC: ASM Press), 103–125.

Doyle, S. M., Montross, S. N., Skidmore, M. L., and Christner, B. C. (2013). Characterizing microbial diversity and the potential for metabolic function at −15°C in the basal ice of Taylor Glacier, Antarctica. *Biology* 2, 1034–1053. doi: 10.3390/biology2031034

Fairchild, I. J., Bradby, L., and Spiro, B. (1993). Carbonate diagenesis in ice. *Geology* 21, 901–904. doi: 10.1130/0091-7613(1993)021<0901:CDII>2.3.CO;2

Fairén, A. G., Chevrier, V., Abramov, O., Marzoe, G. A., Gavin, P., Davila, A. F., et al. (2010). Noachian and more recent phyllosilicates in impact craters on Mars. *Proc. Natl. Acad. Sci. U.S.A.* 107, 12095–12100. doi: 10.1073/pnas.1002889107

Feller, G., and Gerday, C. (2003). Psychrophilic enzymes: hot topics in cold adaptation. *Nat. Rev. Microbiol.* 1, 200–208. doi: 10.1038/nrmicro773

Forget, F., Hansen, G. B., and Pollack, J. B. (1995). Low brightness temperatures of Martian polar caps: CO_2 clouds or low surface emissivity? *J. Geophys. Res.* 100, 21219–21234. doi: 10.1029/95JE02378

Formisano, V., Atreya, S., Encrenaz, T., Ignatiev, N., and Giuranna, M. (2004). Detection of methane in the atmosphere of Mars. *Science* 306, 1758–1761. doi: 10.1126/science.1101732

Fortes, A. D., Grindrod, P. M., Tricketta, S. K., and Vocadloa, L. (2007). Ammonium sulfate on Titan: possible origin and role in cryovolcanism. *Icarus* 188, 139–153. doi: 10.1016/j.icarus.2006.11.002

Fountain, A. G., Nylen, T. H., Tranter, M., and Bagshaw, E. (2008). Temporal variations in physical and chemical features of cryoconite holes on Canada Glacier, McMurdo Dry Valleys, Antarctica. *J. Geophys. Res. Biogeosci.* 113:G01S92. doi: 10.1029/2007jg000430

Garcia-Descalzo, L., Alcazar, A., Baquero, F., and Cid, C. (2011). Identification of in vivo HSP90-interacting proteins reveals modularity of HSP90 complexes is dependent on the environment in psychrophilic bacteria. *Cell Stress Chaperones* 16, 203–218. doi: 10.1007/s12192-010-0233-7

Garcia-Descalzo, L., Alcazar, A., Baquero, F., and Cid, C. (2012a). "Biotechnological applications of cold-adapted bacteria," in *Extremophiles: Sustainable Resources and Biotechnological Implications*, ed. O. V. Singh (Hoboken, NJ: Wiley-Blackwell), 159–174. doi: 10.1002/9781118394144.ch6

Garcia-Descalzo, L., Garcia-Lopez, E., Alcazar, A., Baquero, F., and Cid, C. (2014). Proteomic analysis of the adaptation to warming in the Antarctic bacteria *Shewanella frigidimarina*. *Biochim. Biophys. Acta.* 1844, 2229–2240. doi: 10.1016/j.bbapap.2014.08.006

Garcia-Descalzo, L., García-López, E., Moreno, A. M., Alcazar, A., Baquero, F., and Cid, C. (2012b). Mass spectrometry for direct identification of biosignatures and microorganisms in Earth analogs of Mars. *Planet. Space Sci.* 72, 138–145. doi: 10.1016/j.pss.2012.08.009

Garcia-Lopez, E., and Cid, C. (2016). "Color producing extremophiles," in *Bio-Pigmentation and Biotechnological Implementations*, ed. O. V. Singh (Hoboken, NJ: Wiley-Blackwell).

Garcia-Lopez, E., and Cid, C. (2017). "The role of microbial ecology in glacier retreat analysis," in *Glaciers*, ed. W. V. Tangborn (Rijeka: InTech).

Geminale, A., Formisano, V., and Sindoni, G. (2011). Mapping methane in Martian atmosphere with PFS-MEX data. *Planet. Space Sci.* 59, 137–148. doi: 10.1016/j.pss.2010.07.011

Gillon, M., Triaud, A. H., Demory, B., Jehin, E., Agol, E., Deck, K. M., et al. (2017). Seven temperate terrestrial planets around the nearby ultracool dwarf star TRAPPIST-1. *Nature* 542, 456–460. doi: 10.1038/nature21360

Grundy, W. M., Buratti, B. J., Cheng, A. F., Emery, J. P., Lunsford, A., McKinnon, W. B., et al. (2007). New Horizons mapping of Europa and Ganymede. *Science* 318, 234–237. doi: 10.1126/science.1147623

Hall, D. T., Strobel, D. F., Feldman, P. D., McGrath, M. A., and Weaver, H. A. (1995). Detection of an oxygen atmosphere on Jupiter's moon Europa. *Nature* 373, 677–681. doi: 10.1038/373677a0

Harrold, Z. R., Skidmore, M. L., Hamilton, T. L., Desch, L., Amada, K., van Gelder, W., et al. (2016). Aerobic and anaerobic thiosulfate oxidation by a cold-adapted, subglacial chemoautotroph. *Appl. Environ. Microbiol.* 82, 1486–1495. doi: 10.1128/AEM.03398-15

Hodson, A., Anesio, A. M., Tranter, M., Fountain, A., Osborn, M., Priscu, J., et al. (2008). Glacial ecosystems. *Ecol. Monogr.* 78, 41–67. doi: 10.1890/07-0187.1

Hoehler, T. M. (2007). An energy balance concept for habitability. *Astrobiology* 7, 824–838. doi: 10.1089/ast.2006.0095

Hoffman, P. F., Kaufman, A. J., Halverson, G. P., and Schrag, D. P. (1998). A Neoproterozoic snowball Earth. *Science* 281, 1342–1346. doi: 10.1126/science.281.5381.1342

Holm, N. G., Oze, C., Mousis, O., Waite, J. H., and Guilbert-Lepoutre, A. (2015). Serpentinization and the formation of H_2 and CH_4 on celestial bodies (planets, moons, comets). *Astrobiology* 15, 587–600. doi: 10.1089/ast.2014.1188

Hurowitz, J. A., Grotzinger, J. P., Fischer, W. W., McLennan, S. M., Milliken, R. E., Stein, N., et al. (2017). Redox stratification of an ancient lake in Gale Crater, Mars. *Science* 356:eaah6849. doi: 10.1126/science.aah6849

Imshenetsky, A. A., Kouzyurina, L. A., and Jakshina, V. M. (1973). On the multiplication of xerophilic micro-organisms under simulated Martian conditions. *Life Sci. Space Res.* 11, 63–66.

Johnson, S. S., Hebsgaard, M. B., Christensen, T. R., Mastepanov, M., Nielsen, R., Munch, K., et al. (2007). Ancient bacteria show evidence of DNA repair. *Proc. Natl. Acad. Sci. U.S.A.* 104, 14401–14405. doi: 10.1073/pnas.0706787104

Junge, K., Eicken, H., and Deming, J. W. (2004). Bacterial activity at −2 to −20°C in Arctic wintertime sea ice. *Appl. Environ. Microbiol.* 70, 550–557. doi: 10.1128/AEM.70.1.550-557.2004

Junge, K., Eicken, H., Swanson, B. D., and Deming, J. W. (2006). Bacterial incorporation of leucine into protein down to −20°C with evidence for potential activity in sub-eutectic saline ice formations. *Cryobiology* 52, 417–429. doi: 10.1016/j.cryobiol.2006.03.002

Kaplan, L. D., Connes, J., and Connes, P. (1969). Carbon monoxide in the Martian atmosphere. *Astrophys. J.* 157, 187–192. doi: 10.1086/180416

Kasting, J. F., Whitmire, D. P., and Reynolds, R. T. (1993). Habitable zones around main sequence stars. *Icarus* 101, 108–128.

Kite, E. S., and Rubin, A. M. (2016). Sustained eruptions on Enceladus explained by turbulent dissipation in tiger stripes. *Proc. Natl. Acad. Sci. U.S.A.* 113, 3972–3975. doi: 10.1073/pnas.1520507113

Kopparapu, R. K., Ramirez, R., Kasting, J. F., Eymet, V., Robinson, T. D., Mahadevan, S., et al. (2013). Habitable zones around main-sequence stars: new estimates. *Astrophys. J.* 765:131. doi: 10.1088/0004-637x/765/2/131

Krembs, C., Eicken, H., and Deming, J. W. (2011). Exopolymer alteration of physical properties of sea ice and implications for ice habitability and biogeochemistry in a warmer Arctic. *Proc. Natl. Acad. Sci. U.S.A.* 108, 3653–3658. doi: 10.1073/pnas.1100701108

Lauro, F. M., DeMaere, M. Z., Yau, S., Brown, M. V., Ng, C., Wilkins, D., et al. (2011). An integrative study of a meromictic lake ecosystem in Antarctica. *ISME J.* 5, 879–895. doi: 10.1038/ismej.2010.185

Le Gall, A., Leyrat, C., Janssen, M. A., Choblet, G., Tobie, G., Bourgeois, O., et al. (2017). Thermally anomalous features in the subsurface of Enceladus's south polar terrain. *Nat. Astron.* 1:0063. doi: 10.1038/s41550-017-0063

Leconte, J., Forget, F., Charnay, B., Wordsworth, R., Selsis, F., Millour, E., et al. (2013). 3D climate modeling of close-in land planets: circulation patterns, climate moist instability, and habitability. *Astron. Astrophys.* 554:A69. doi: 10.1051/0004-6361/201321042

Lindensmith, C. A., Rider, S., Bedrossian, M., Wallace, J. K., Serabyn, E., Showalter, G. M., et al. (2016). A submersible, off-axis holographic microscope for detection of microbial motility and morphology in aqueous and icy environments. *PLoS ONE* 11:e0147700. doi: 10.1371/journal.pone.0147700

Los, D. A., and Murata, N. (2004). Membrane fluidity and its roles in the perception of environmental signals. *Biochim. Biophys. Acta* 1666, 142–157. doi: 10.1016/j.bbamem.2004.08.002

Maccario, L., Sanguino, L., Vogel, T. M., and Larose, C. (2015). Snow and ice ecosystems: not so extreme. *Res. Microbiol.* 166, 782–795. doi: 10.1016/j.resmic.2015.09.002

Madigan, M. T., Martinko, J. M., Stahl, D. A., and Clark, D. P. (2012). *Brock Biology of Microorganisms*, 13th Edn. San Francisco, CA: Pearson Education.

Marin-Yaseli, M. R., Cid, C., Yagüe, A. I., and Ruiz-Bermejo, M. (2017). Detection of macromolecular fractions in HCN polymers using electrophoretic and ultrafiltration techniques. *Chem. Biodivers.* 14:e1600241. doi: 10.1002/cbdv.201600241

Marion, G. M., Fritsen, C. H., Eicken, H., and Payne, M. C. (2003). The search for life on Europa: limiting environmental factors, potential habitats, and Earth analogues. *Astrobiology* 3, 785–811. doi: 10.1089/153110703322736105

Martin-Cerezo, M. L., Garcia-Lopez, E., and Cid, C. (2015). Isolation and identification of a red pigment from the Antarctic bacterium *Shewanella frigidimarina*. *Protein Pept. Lett.* 22, 1076–1082. doi: 10.2174/0929866522666150915122247

Martin-Torres, J., Zorzano, M. P., Valentin-Serrano, P., Harri, A. M., Genzer, M., Kemppainen, O., et al. (2015). Transient liquid water and water activity at Gale Crater on Mars. *Nat. Geosci.* 8, 357–361. doi: 10.1038/ngeo2412

McGlynn, I. O., Fedo, C. M., and McSween, H. Y. (2012). Soil mineralogy at the Mars Exploration Rover landing sites: an assessment of the competing roles of physical sorting and chemical weathering. *J. Geophys. Res.* 117:E01006. doi: 10.1029/2011JE003861

Michalski, J. R., Cuadros, J., Niles, P. B., Parnell, J., Rogers, A. D., and Wright, S. P. (2013). Groundwater activity on Mars and implications for a deep biosphere. *Nat. Geosci.* 6, 133–138. doi: 10.1038/ngeo1706

Mieczen, T., Gorniak, D., Swiatecki, A., Zdanowski, M., Tarkowska-Kukuryk, M., and Adamczuk, M. (2013). Vertical microzonation of ciliates in cryoconite holes in Ecology Glacier, King George Island. *Pol. Polar Res.* 34, 201–212. doi: 10.2478/popore-2013-0008

Mikucki, J. A., Pearson, A., Johnston, D. T., Turchyn, A. V., Farquhar, J., Schrag, D. P., et al. (2009). A contemporary microbially maintained subglacial ferrous "ocean". *Science* 324, 397–400. doi: 10.1126/science.1167350

Mumma, M. J., Villanueva, G. L., Novak, R. E., Hewagama, T., Bonev, B. P., DiSanti, M. A., et al. (2009). Strong release of methane on Mars in northern summer 2003. *Science* 323, 1041–1045. doi: 10.1126/science.1165243

Murray, A. E., Kenig, F., Fritsen, C. H., McKay, C. P., Cawley, K. M., Edwards, R., et al. (2012). Microbial life at −13°C in the brine of an ice-sealed Antarctic lake. *Proc. Natl. Acad. Sci. U.S.A.* 109, 20626–20631. doi: 10.1073/pnas.1208607109

Nadeau, J., Lindensmith, C., Deming, J. W., Fernandez, V., and Stocker, R. (2016). Microbial morphology and motility as biosignatures for outer planet missions. *Astrobiology* 16, 755–774. doi: 10.1089/ast.2015.1376

Neish, C. D., Lorenz, R. D., and O'Brien, D. P. (2006). The potential for prebiotic chemistry in the possible cryovolcanic dome Ganesa Macula on Titan. *Int. J. Astrobiol.* 5, 57–65. doi: 10.1017/S1473550406002898

Nichols, D. S., Miller, M. R., Davies, N. W., Goodchild, A., Raftery, M., and Cavicchioli, R. (2004). Cold adaptation in the Antarctic archaeon *Methanococcoides burtonii* involves membrane lipid unsaturation. *J. Bacteriol.* 186, 8508–8515. doi: 10.1128/JB.186.24.8508-8515.2004

Nisbet, E. G., and Sleep, N. H. (2001). The habitat and nature of early life. *Nature* 409, 1083–1091. doi: 10.1038/35059210

Nixon, S. L., Telling, J. P., Wadham, J. L., and Cockell, C. S. (2017). Viable cold-tolerant iron-reducing microorganisms in geographically diverse subglacial environments. *Biogeosciences* 14, 1445–1455. doi: 10.5194/bg-14-1445-2017

Panikov, N., Flanagan, P., Oechel, W., Mastepanov, M., and Christensen, T. (2006). Microbial activity in soils frozen to below −39°C. *Soil Biol. Biochem.* 38, 785–794. doi: 10.1016/j.soilbio.2005.07.004

Pewe, T. (1995). *Permafrost*, Vol. 20. New York, NY: Chapman and Hall.

Phillips, S. J. M., and Parnell, J. (2006). The detection of organic matter in terrestrial snow and ice: implications for astrobiology. *Int. J. Astrobiol.* 10, 353–359. doi: 10.1017/S1473550406003430

Pikuta, E. V., Hoover, R. B., and Tang, J. (2007). Microbial extremophiles at the limits of life. *Crit. Rev. Microbiol.* 33, 183–209. doi: 10.1080/10408410701451948

Preston, L. J., and Dartnell, L. R. (2014). Planetary habitability: lessons learned from terrestrial analogues. *Int. J. Astrobiol.* 13, 81–98. doi: 10.1017/S1473550413000396

Price, P. B. (2007). Microbial life in glacial ice and implications for a cold origin of life. *FEMS Microbiol. Ecol.* 59, 217–231. doi: 10.1111/j.1574-6941.2006.00234.x

Priscu, J. C., and Christner, B. C. (2004). "Earth's icy biosphere," in *Microbial Diversity and Bioprospecting*, ed. A. Bull (Washington, DC: ASM Press), 130–145. doi: 10.1128/9781555817770.ch13

Priscu, J. C., and Hand, K. P. (2012). Microbial habitability of icy worlds. *Microbe* 7, 167–172. doi: 10.1073/pnas.1208607109

Rahm, M., Lunine, J. I., Usher, D. A., and Shalloway, D. (2016). Polymorphism and electronic structure of polyimine and its potential significance for prebiotic chemistry on Titan. *Proc. Natl. Acad. Sci. U.S.A.* 113, 8121–8126. doi: 10.1073/pnas.1606634113

Raiswell, R. (1984). Chemical models of solute acquisition in glacial meltwaters. *J. Glaciol.* 30, 49–57. doi: 10.1017/S0022143000008480

Rankin, L. M., Gibson, J. A. E., Franzrnann, P. D., and Burton, H. R. (1999). The chemical stratification and microbial communities of Ace Lake, Antarctica: a review of the characteristics of a marine-derived meromictic lake. *Polarforschung* 66, 33–52.

Rodrigues, D. F., and Tiedje, J. M. (2008). Coping with our cold planet. *Appl. Environ. Microbiol.* 74, 1677–1686. doi: 10.1128/AEM.02000-07

Rogers, S. O., Shtarkman, Y. M., Koçer, Z. A., Edgar, R., Veerapaneni, R., and D'Elia, T. (2013). Ecology of subglacial Lake Vostok (Antarctica) based on metagenomic/metatranscriptomic analyses of accretion ice. *Biology* 2, 629–650. doi: 10.3390/biology2020629

Russell, N. J. (1990). Cold adaptation of microorganisms. *Philos. Trans. R. Soc. Lond. B. Biol. Sci.* 326, 595–611. doi: 10.1098/rstb.1990.0034

Schenk, P. M., McKinnon, W. B., Gwynn, D., and Moore, J. M. (2001). Flooding of Ganymede's bright terrains by low-viscosity water-ice lavas. *Nature* 410, 57–60. doi: 10.1038/35065027

Schmidt, B. E., Blankenship, D. D., Patterson, G. W., and Schenk, P. M. (2011). Active formation of 'chaos terrain' over shallow subsurface water on Europa. *Nature* 479, 502–505. doi: 10.1038/nature10608

Seager, S., and Bains, W. (2015). The search for signs of life on exoplanets at the interface of chemistry and planetary science. *Sci. Adv.* 1:e1500047. doi: 10.1126/sciadv.1500047

Sekine, Y., Shibuya, T., Postberg, F., Hsu, H. W., Suzuki, K., Masaki, Y., et al. (2015). High-temperature water-rock interactions and hydrothermal environments in the chondrite-like core of Enceladus. *Nat. Commun.* 6:8604. doi: 10.1038/ncomms9604

Sharp, M., Parkes, J., Cragg, B., Fairchild, I. J., Lamb, H., and Tranter, M. (1999). Widespread bacterial populations at glacier beds and their relationship to rock weathering and carbon cycling. *Geology* 27, 107–110. doi: 10.1130/0091-7613(1999)027<0107:WBPAGB>2.3.CO;2

Shematovich, V. I., and Johnson, R. E. (2001). Near-surface oxygen atmosphere at Europa. *Adv. Space Res.* 27, 1881–1888. doi: 10.1016/S0273-1177(01)00299-X

Siddiqui, K. S., and Cavicchioli, R. (2006). Cold-adapted enzymes. *Annu. Rev. Biochem.* 75, 403–433. doi: 10.1146/annurev.biochem.75.103004.142723

Skidmore, M. L., Foght, J. M., and Sharp, M. J. (2000). Microbial life beneath a high arctic glacier. *Appl. Environ. Microbiol.* 66, 3214–3220. doi: 10.1128/AEM.66.8.3214-3220.2000

Spencer, J. R., Tamppari, L. K., Martin, T. Z., and Travis, L. D. (1999). Temperatures on Europa from Galileo photopolarimeter-radiometer: nighttime thermal anomalies. *Science* 284, 1514–1516. doi: 10.1126/science.284.5419.1514

Stevenson, D. (2000). Europa's ocean - the case strengthens. *Science* 289, 1305–1307. doi: 10.1126/science.289.5483.1305

Stevenson, D. J. (1999). Life-sustaining planets in interstellar space? *Nature* 400:32. doi: 10.1038/21811

Stofan, E. R., Elachi, C., Lunine, J. I., Lorenz, R. D., Stiles, B., Mitchell, K. L., et al. (2007). The lakes of Titan. *Nature* 445, 61–64. doi: 10.1038/nature05438

Teolis, B. D., Jones, G. H., Miles, P. F., Tokar, R. L., Magee, B. A., Waite, J. H., et al. (2010). Cassini finds an oxygen-carbon dioxide atmosphere at Saturn's icy moon Rhea. *Science* 330, 1813–1815. doi: 10.1126/science.1198366

Thomas, N. D., and Dieckmann, G. S. (2002). Antarctic sea ice -a habitat for extremophiles. *Science* 295, 641–644. doi: 10.1126/science.1063391

Tranter, M., Brown, G. H., Hodson, A., Gurnell, A. M., and Sharp, M. (1994). Variations in the nitrate concentration of glacial runoff in alpine and subpolar environments. *Int. Assoc. Hydrol. Sci. Publ.* 223, 299–310.

Tranter, M., Brown, G. H., Raiswell, R., Sharp, M. J., and Gurnell, A. M. (1993). A conceptual model of solute acquisition by Alpine glacial meltwaters. *J. Glaciol.* 39, 573–581. doi: 10.1017/S0022143000016464

Tsou, P., Brownlee, D. E., McKay, C. P., Anbar, A. D., Yano, H., Altwegg, K., et al. (2012). LIFE: Life Investigation for Enceladus. A sample return mission concept in search for evidence of life. *Astrobiology* 12, 730–742. doi: 10.1089/ast.2011.0813

Tung, H. C., Bramall, N. E., and Price, B. P. (2005). Microbial origin of excess methane in glacial ice and implications for life on Mars. *Proc. Natl. Acad. Sci. U.S.A.* 102, 18292–18296. doi: 10.1073/pnas.0507601102

Tyler, G. L., Sweetnam, D. N., Anderson, J. D., Borutzki, S. E., Campbell, J. K., Eshleman, V. R., et al. (1989). Voyager radio science observations of Neptune and Triton. *Science* 246, 1466–1473. doi: 10.1126/science.246.4936.1466

Vincent, W. F., and Howard-Williams, C. (2000). Life on snowball Earth. *Science* 287:2421. doi: 10.1126/science.287.5462.2421b

Waite, J. H., Glein, C. R., Perryman, R. S., Teolis, B. D., Magee, B. A., Miller, G., et al. (2017). Cassini finds molecular hydrogen in the Enceladus plume: evidence for hydrothermal processes. *Science* 356, 155–159. doi: 10.1126/science.aai8703

Webster, C. R., Mahaffy, P. R., Atreya, S. K., Flesch, G. J., Mischna, M. A., Meslin, P. Y., et al. (2015). Mars atmosphere. Mars methane detection and variability at Gale crater. *Science* 347, 415–417. doi: 10.1126/science.1261713

Westall, F., Foucher, F., Bost, N., Bertrand, M., Loizeau, D., Vago, J. L., et al. (2015). Biosignatures on Mars: What, where, and how? Implications for the search for Martian life. *Astrobiology* 15, 998–1029. doi: 10.1089/ast.2015.1374

Westall, F., Loizeau, D., Foucher, F., Bost, N., Betrand, M., Vago, J., et al. (2013). Habitability on Mars from a microbial point of view. *Astrobiology* 13, 887–897. doi: 10.1089/ast.2013.1000

Williams, T. J., Lauro, F. M., Ertan, H., Burg, D. W., Poljak, A., Raftery, M. J., et al. (2011). Defining the response of a microorganism to temperatures that span its complete growth temperature range (−2°C to 28°C) using multiplex quantitative proteomics. *Environ. Microbiol.* 13, 2186–2203. doi: 10.1111/j.1462-2920.2011.02467.x

Williams, T. J., Long, E., Evans, F., Demaere, M. Z., Lauro, F. M., Raftery, M. J., et al. (2012). A metaproteomic assessment of winter and summer bacterioplankton from Antarctic Peninsula coastal surface waters. *ISME J.* 6, 1883–1900. doi: 10.1038/ismej.2012.28

Worth, R. J., Sigurdsson, S., and House, C. H. (2013). Seeding life on the moons of the outer planets via lithopanspermia. *Astrobiology* 13, 1155–1165. doi: 10.1089/ast.2013.1028

Conflict of Interest Statement: The authors declare that the research was conducted in the absence of any commercial or financial relationships that could be construed as a potential conflict of interest.

frontiers in Microbiology

ORIGINAL RESEARCH
published: 20 December 2017
doi: 10.3389/fmicb.2017.02594

In Situ Field Sequencing and Life Detection in Remote (79°26′N) Canadian High Arctic Permafrost Ice Wedge Microbial Communities

J. Goordial[1,2]*, *Ianina Altshuler*[1], *Katherine Hindson*[1], *Kelly Chan-Yam*[1], *Evangelos Marcolefas*[1] *and Lyle G. Whyte*[1]*

[1] *Department of Natural Resource Sciences, McGill University, Ste. Anne-de-Bellevue, QC, Canada,* [2] *Bigelow Laboratory for Ocean Sciences, East Boothbay, ME, United States*

OPEN ACCESS

Edited by:
Karen Olsson-Francis, Open University, United Kingdom

Reviewed by:
Richard Allen White III, Washington State University, United States
Alfonso Benítez-Páez, Instituto de Agroquímica y Tecnología de Alimentos (CSIC), Spain

***Correspondence:**
J. Goordial
jacqueline.goordial@mail.mcgill.ca
Lyle G. Whyte
lyle.whyte@mcgill.ca

Specialty section:
This article was submitted to Extreme Microbiology, a section of the journal Frontiers in Microbiology

Received: *06 September 2017*
Accepted: *12 December 2017*
Published: *20 December 2017*

Citation:
Goordial J, Altshuler I, Hindson K, Chan-Yam K, Marcolefas E and Whyte LG (2017) In Situ Field Sequencing and Life Detection in Remote (79°26′N) Canadian High Arctic Permafrost Ice Wedge Microbial Communities. Front. Microbiol. 8:2594. doi: 10.3389/fmicb.2017.02594

Significant progress is being made in the development of the next generation of low cost life detection instrumentation with much smaller size, mass and energy requirements. Here, we describe *in situ* life detection and sequencing in the field in soils over laying ice wedges in polygonal permafrost terrain on Axel Heiberg Island, located in the Canadian high Arctic (79°26′N), an analog to the polygonal permafrost terrain observed on Mars. The life detection methods used here include (1) the cryo-iPlate for culturing microorganisms using diffusion of in situ nutrients into semi-solid media (2) a Microbial Activity Microassay (MAM) plate (BIOLOG Ecoplate) for detecting viable extant microorganisms through a colourimetric assay, and (3) the Oxford Nanopore MinION for nucleic acid detection and sequencing of environmental samples and the products of MAM plate and cryo-iPlate. We obtained 39 microbial isolates using the cryo-iPlate, which included several putatively novel strains based on the 16S rRNA gene, including a *Pedobacter* sp. (96% closest similarity in GenBank) which we partially genome sequenced using the MinION. The MAM plate successfully identified an active community capable of L-serine metabolism, which was used for metagenomic sequencing with the MinION to identify the active and enriched community. A metagenome on environmental ice wedge soil samples was completed, with base calling and uplink/downlink carried out via satellite internet. Validation of MinION sequencing using the Illumina MiSeq platform was consistent with the results obtained with the MinION. The instrumentation and technology utilized here is pre-existing, low cost, low mass, low volume, and offers the prospect of equipping micro-rovers and micro-penetrators with aggressive astrobiological capabilities. Since potentially habitable astrobiology targets have been identified (RSLs on Mars, near subsurface water ice on Mars, the plumes and oceans of Europa and Enceladus), future astrobiology missions will certainly target these areas and there is a need for direct life detection instrumentation.

Keywords: life detection, astrobiology, nanopore MinION, polar microbiology, permafrost

INTRODUCTION

The search for life on other solar system bodies is and will be a major focus of planetary exploration in the coming decades. The primary targets for astrobiology investigations of other solar system bodies are Mars, in the short term, as well as Europa and Enceladus, in the mid to longer term (Hays et al., 2015). Extremely cold temperatures characterize these primary astrobiology targets, and, as such, the best terrestrial analogs may be the Earth's polar regions. Based on our current knowledge of extremophile microbiology, these targets are potentially capable of hosting microbial life and ecosystems either currently or in the past. For example, considerable evidence has been found on Mars indicating that, before ∼3.5 bya, the planet was warmer and wetter (Golombek, 1999). The Mars Science Laboratory (MSL) mission has reported ample evidence of past fluvial, deltaic, and lacustrine environments within Gale Crater (Grotzinger et al., 2014); However, the recent report of surface brine water at several reoccurring slope linaea (RSL) locations on Mars (Ojha et al., 2015) now opens up the possibility that extant microbial life (which would be most likely cold-adapted and halophilic) could be present at these sites and will almost certainly be the targets of future missions in the mid-2020s and beyond, including potential sample return missions. Similarly, exciting discoveries over the last 5–10 years point to the existence of cold, salty oceans under the ice covers of Europa and Enceladus (Kargel et al., 2000; Melosh et al., 2004; Waite et al., 2006; McKay et al., 2008; Roth et al., 2014) which could also support extant microbial ecosystems based on our knowledge of similar salty cryoenvironments on Earth (Goordial et al., 2013).

Currently, the scientific instruments available for astrobiology space missions are focused on identification of habitable environments or on detection of biosignatures. To date, these instruments remain high mass, large in size, and have high energy requirements. Such instruments are entirely unsuited for missions to locations such as Europa or Enceladus for which lander packages are likely to be tightly constrained. Even for Mars missions, there are advantages to utilizing multiple small scientific instruments over fewer larger instruments. Additionally, the difficulties in defining biomarkers attest to the need for more specific astrobiological instruments to be deployed (Brasier et al., 2004). Though life detection is a primary driver of planetary exploration, no direct life detection instrumentation has been included on an astrobiology mission payload since the Viking missions to Mars in the 1970's (Levin, 1997; Davila et al., 2010; Schulze-Makuch et al., 2015).

In the present study, we utilized pre-existing, low mass, low cost, and robust next generation miniaturized scientific instrumentation for biosignature detection, and microbiology techniques in a novel context for biosignature identification and characterization of viable microbial life in a high fidelity analog environment in the Canadian high Arctic. Such a MICRObial life detection platform attached to surface rover platforms and/or penetrators could conceptually be used in future missions to Mars, Europa, Enceladus or any other planetary target. Additionally, such a platform also has clear applications for quick analysis of community metagenomics and assessment of microbial activity in environmental field sites, including extreme sites such as the high Arctic and Antarctic (Edwards et al., 2016; Johnson et al., 2017).

The conceptual life detection platform we developed and tested here is modular, and it is envisioned that as new technologies and methodologies emerge that they can be "swapped out" or added to such a platform. The life detection platform components tested here includes: (Hays et al., 2015) the cryo-iPlate for culturing microorganisms using diffusion of *in situ* nutrients on a solid media based on the recently described innovative ichip method (Golombek, 1999; Nichols et al., 2010) a microbial activity microassay (MAM) (Ecolog plate) for detection of viable microoganisms through a colourimetric assay, and (Grotzinger et al., 2014) the Oxford Nanopore MinION for biosignature detection (DNA, RNA, and in the near future proteins) which can be used for environmental samples, as well as for positive results from the cryo-iPlate and positive wells in the microbial activity assay (**Figure 1**).

MATERIALS AND METHODS

Study Site and Sampling

The analog study site is located near the McGill Arctic Research Station (MARS) on Axel Heiberg Island in the Canadian High Arctic (79°26′N, 90°46′W). MARS is located in a polar desert and is located in proximity to a number of high fidelity Mars analog sites of interest to astrobiology, including cold saline springs arising through permafrost, gypsum cryptoendoliths and extensive polygonal permafrost terrain underlain with ice wedges similar in structure to those observed on Mars (Pollard et al., 2009; Fairén et al., 2010). Soils are a low carbon mineral cryosol, with a mean annual temperature of −15.2°C (Doran, 1993; Lau et al., 2015). The active soil layer that overlays the permafrost ranges 60-73 cm in depth during the summer and is completely frozen over during winter and spring months. For this study, soil samples overlaying the ice-wedges were aseptically collected using an ethanol-sterilized metal sampling spoon to scrape the frozen trough soils into sterile 50 mL falcon tubes.

DNA Extraction

Ice-wedge soil: DNA was extracted from two 0.5 cc of thawed ice wedge soil using the PowerLyzer (MoBio Laboratories, Inc., Carlsbad, CA) according to manufacturer's protocol. The two replicates were pooled prior to sequencing. This required the use of a vortex and centrifuge in the field, in addition to pipettors and consumables. *Biolog plate: Three* replicate wells which showed microbial metabolism on L-serine were chosen for extraction. The three wells were pooled (total 600 µl), and added directly to a bead tube from the MoBio PowerLyzer kit, and processed according to manufacturer's instruction. The DNA extractions for the Biolog plate and Cryo-iplate were quantified in the field using a Qubit 2.0 Fluorometer (Life Technologies) per the manufacturer's instruction, and measured to be 13.3 and 4.6 ng/µL (total volume extracted 90 ul). *Cryo-iplate Pedobacter isolate*: The *Pedobacter* sp. was isolated as described below. In the lab, the strain was grown in R2A broth for 1 week, and the culture pelleted and resuspended in 500 µL water for

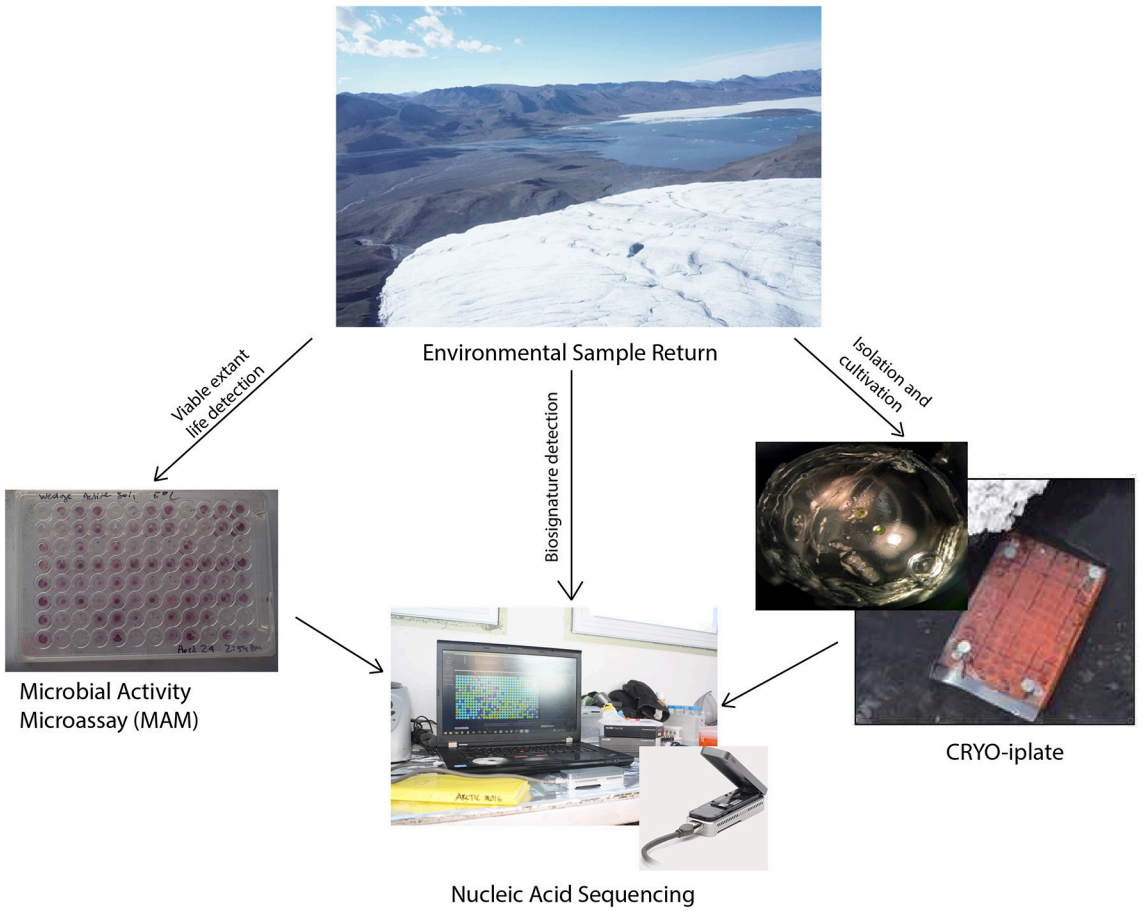

FIGURE 1 | MICRO life detection platform components tested.

use with the PowerLyzer kit. DNA extracted was 307 ng/μL (90 μL volume) measured on a NanoDrop instrument (Thermo Scientific, Wilmington, MA).

MinION Sequencing and Analysis

All reagents were stored in a cooler with blue ice for transportation from McGill University (Montreal, Canada) to the McGill Arctic Research Station. *DNA Library Preparation:* At MARS we used the MinION MK1 device for sequencing with the Nanopore Sequencing Kit (SQK- MAP006) combined with the with EXP-LWI001(Low Input Expansion Kit). These kits were used according to manufacturer's instruction, but with the omission of the DNA shearing step. Briefly, 46 μL of DNA extract was used for a DNA repair step using NEBNext FFPE Repair Mix (New England Biolabs, Ipswich, MA), followed by clean-up using AMPure XP beads incubated with mixing at room temperature for 5 min. Samples were ethanol cleaned while on a magnetic rack. Water was then added to beads, and the 45 μL eluate used for end repair and dA-tailing of DNA using NEBNext Ultra II End-repair/dA tailing kit (New England Biolabs). The end repaired DNA was washed again on a magnetic rack with ethanol, and eluted with 10 μL nuclease free water. The 10 μL of eluate was used for adapter ligation using the NEB Blunt/TA Ligase Master Mix (New England Bioloabs) with the Low Input Hairpin Tether from the low input expansion pack (EXP-LWI001). The adapted and tethered DNA library was subsequently bound to purified MyOne C1 Streptavidin beads and suspended in resuspension buffer provided with the library prep kit. The beads were loaded onto MinION Flow Cells (R7.3) according to protocol, and sequenced for 12 h powered by a laptop, with intermittent battery charging power supplied through a generator. In the lab, we used the MinION rapid library prep kit (SQK-RAD001), in conjunction with the MinION MK1b device for library preparation according to manufacturer's instruction, and using MinION Flow Cells (R9), again omitting the DNA shearing step. Samples were sequenced over 48 h. *Sequence Analysis:* Base-calling was performed using Metrichor software (Oxford Nanopore). Fasta files were extracted from the generated fast5 files using PoreTools (Loman and Quinlan, 2014). Passed 2D and 1D reads from the ice-wedge soil sample and Biolog plate were uploaded to MG-RAST (Meyer et al., 2008), and sequences additionally quality trimmed using the default settings for dynamic trimming (sequences contain <5 bp below a phred score

of 15). Any human or chordata contaminants were removed from the dataset. To determine taxonomy/functional genes, we used RefSeq annotated proteins in MG-RAST (*e*-value $\leq 10^{-5}$, 60% protein similarity, alignment length >15). We removed reads identified as belonging to *E. Coli* from further analysis (6,131, 55, 3 genes identified in the rapid kit ice-wedge metagenome, low input kit ice-wedge metagenome, and Biolog plate metagenome respectively). Metagenome sequences are deposited in MG-RAST under accession numbers mgm4705800.3, mgm4705797.3, mgm4735353.3, and mgm4718581.3. The *Pedobacter* isolate genome sequence was base called and the fastq sequences extracted as for the metagenomes. 9050 reads were assembled into 87 contigs using the long read assembler Canu (release 1.4) (Koren et al., 2017) using an assumed genome size of 5 Mb, based on the average genome sizes of closely related *Pedobacter* sp. genomes on the JGI Integrated microbial genomes (IMG) database. Assembled reads have been deposited at DDBJ/ENA/GenBank under the accession PEIM00000000. The version described in this paper is version PEIM01000000. Assembled contigs were annotated using MyRast (Overbeek et al., 2013), and those annotations scanned for genes associated with cold adaptation.

Illumina Sequencing

Community bacterial 16S rRNA amplicon sequencing was performed using an Illumina MiSeq (Illumina, San Diego, CA, USA) following the 16S rRNA gene sample preparation protocol. Amplicon primers targeted the V3 and V4 regions with the Illumina adapter overhand sequences (forward: 5′-TCGTCGGC AGCGTCAGATGTGTATAAGAGACAGCCTACGGGNGGC WGCAG-3′; reverse: 5′-GTCTCGTGGGCTCGGAGATGTGT ATAAGAGACAGGACTACHVGGGTATCTAATCC-3′) from Integrated DNA Technologies (Coralville, IA, USA). For the amplicon PCR, each 25 μL reaction contained 2.5 μL sample, 8.5 μL PCR-grade water, 12.5 μL 2× KAPA HiFi HotStart ReadyMix (KAPA, Wilmington, MA, USA), and 0.75 μL of 20 μM forward and reverse primers. PCR was performed with a 95°C initialization for 5 min, followed by 30 cycles of 95°C for 30 s, 55°C for 30 s, 72°C for 45 s, and a final 72°C extension for 10 min. The results were then verified on a gel. For the Index PCR step, index primers from the Nextera XT Index Kit for 24 samples (Illumina, San Diego, CA, USA) were used. The 25 μL sequencing reaction contained 12.5 μL2× KAPA HiFi HotStart ReadyMix, 2.5 μL PCR-grade water, 2.5 μL of each primer 1 and 2, and 5 μL purified amplicon. Indexing PCR was performed with a 95°C initialisation for 5 min, followed by 8 cycles of 95°C for 30 s, 55°C for 30 s, 72°C for 30 s, and a final 72°C extension for 5 min. After clean-up, the PCR products were quantified by Qubit fluorometric quantification with the Qubit dsDNA BR Assay Kit (Thermo Fisher Scientific, Waltham, MA, USA). The indexed library was pooled to about 4 nM and the quality was checked with an Agilent DNA 1000 kit and Agilent 2100 Bioanalyzer (Agilent Technologies, Santa Clara, CA, USA). The pooled library was run on the Illumina MiSeq platform with the MiSeq Reagent Kit v3, 600 cycles. The pooled denatured library was diluted to 4 pM as recommended by the protocol.

Isolation of Permafrost Bacteria Using a Prototype Cryo-iplate Methodology

The design of the cryo-iplate used in this study was largely inspired by Nichols et al.'s isolation chip (ichip) methodology (Nichols et al., 2010). Semi-permeable hydrophilic polycarbonate membranes with 0.03 μm pores (Whatman plc GE Healthcare Life Sciences, Mississauga, ON, Canada) were glued with silicon to the bottom of 96 well trays, obtained by disassembling a 200 μl-pipette-tip boxes (FroggaBio, North York, ON, Canada)—providing a barrier between the plate wells and the external environment. The assembly was then autoclaved to sterilize. The 96 wells of the sterilized tray were then filled with 2% w/v gellan gum (Alfa Aesar, Haverhill, Massachusetts, USA) in the laboratory prior to field deployment. In the field, the top of each gellan-filled well of the central tray was inoculated with an estimated ∼1 microbial cell using 10 μL of a 10^{-8} diluted ice wedge soil solution based on our previous study of this polygon site (Wilhelm et al., 2011, 2012). Once inoculated, the cryo-iplate assembly was sealed with a sterile 96 well plate film. One cryo-iplate was incubated *in situ* at the study site in the wedge soil for 14 days in May 2016. A second cryo-iplate was incubated at room temperature in a whirlpak bag filled with thawed ice-wedge soil. Both cryo-iplates were transported back to McGill in a cooler and held at 5°C, until processing within 1 month. In the laboratory, gellan plugs were removed from trays of both cryo-iplates using sterile toothpicks and were then observed under a dissecting microscope for microcolony formation. Observable colonies were picked using a toothpick and streaked onto ½ R2A broth media (Difco, USA) supplemented with 2% w/v gellan and incubated for 14 days at 10°C. Successive rounds of subcultivation at 20°C on solid ½ R2A media were conducted to isolate distinct morphotypes.

Isolate Identification

For colonies isolated from the Cryo-iPlate that were subcultivatable, cell lysates were prepared by placing biomass from agar plates in 250 μL of molecular grade dH_20 (ThermoFisher Scientific). Lysis was achieved through vortexing and heating in a microwave oven for 3 min before centrifugation for 30 s at 10.0 RCF. Each PCR reaction consisted of a final volume of 20 μL containing: 200 μM dNTP, 0.5 μM of each primer (27F/1492R for bacterial lysates and ITS1F/R for 18S amplification of fungal lysates), 2.5 U/reaction of *HotStarTaq Plus* DNA Polymerase (Qiagen), ∼1 μg template DNA, and 1.5 mM $MgCl_2$. The final concentrations above followed Qiagen's HotStartTaq Kit instructions. The sequence of the 27F (forward) bacterial primer consisted of: 5′-AGAGTTACCTTGTTACGACTT-3′. The sequence of the 1492R (reverse) bacterial primer was: 5′-GGTTACCTTGTTACGACTT-3′. The 16S rDNA amplification PCR reaction cycling program consisted of: (1) 95°C for 7 min, (2) 94°C for 45 s, (3) 55°C for 45 s, (4) 72°C for 1 min, (where steps 2–4 were repeated 30 times), (5) 72°C for 10 min. Amplification of the 16S rRNA gene was confirmed on an agarose gel. Sanger sequencing using the 27F primer was conducted at the Plate-forme d'Analyses Génomiques sequencing center at Laval University. For quality control, chromatograms were first

manually curated using 4Peaks software (http://nucleobytes.com/4peaks/) where sequence segments with an average Q>40 was used as a query against the NCBI non-redundant database (https://blast.ncbi.nlm.nih.gov/). The 16S rRNA gene sequences are publicly available on GenBank with accession numbers MG266397–MG266429.

Biolog Characterization of Microbial Communities

We used Eco-plates (Biolog, Hayward, CA, USA) for colourimetric evaluation of community metabolic activity. Wedge soil was added to a 50 mL falcon tube up to a 5 mL volume. The tube was filled to 45 mL with sterile water. The tube was vortexed for 30 s and particles allowed to settle for 10 min. The supernatant was used to inoculate wells of the Ecoplate (150 μL per well), as well as to inoculate iplates. Eco-plates were incubated at 20° and 5°C for 10 days, and color formation monitored daily based on visualization and photographed with a Sony ILCE-6000. After 3 days of incubation, L-serine wells from the 20°C incubation were pooled, cells pelleted at 10,000 × g for 5 min, and resuspended in 500 μL of water. The re-suspended cells were then used for a DNA extraction as described above.

RESULTS

Nucleic Acid Life Detection in Ice-Wedge Soils

Two metagenomes were sequenced from a single ice-wedge soil DNA extract using the MinION rapid library prep kit (SQK-RAD001) and the MinION low input library prep kit (SQK-NSK007 combined with the Low Input Expansion Kit; EXP-LWI001). The MinION rapid library preparation kit requires fewer consumables, and took ∼20 min to complete, but requires ∼200–1,000 ng/μL of DNA. The MinION low input library preparation kit required much lower amounts of DNA (∼20–100 ng), took ∼160 min and required more instrumentation (a microcentrifuge, magnetic beads, additional enzymes, ligation of a hairpin adapter etc.) Both methods generated single molecule reads without the need for PCR amplification and resulted in similar functional and taxonomic profiles of the ice-wedge soil community (**Figure 2**). Sequencing results are summarized in Table S1, the low input kit generated 6,348 sequences with a mean length of 3,811 ± 2,704, and the rapid kit generated 9,530 sequences of 3,018 ± 2,015 bp in length. The ice wedge soil was dominated by bacteria (∼96%) using both library preparation kits, with low, but detectable sequences belonging to Archaea (0.3–05% of reads). The MinION rapid kit detected more reads annotated as viral in origin (3% of reads), and less Eukaryotic sequences (1%) than the MinION low input kit on the same DNA extract (0.2 and 3% respectively). The McGill Arctic research station (MARS) is equipped with satellite internet, that works intermittently and is highly weather dependent. Due to the stochastic nature of internet access and poor weather during the latter half of the expedition at MARS we were only able to carry out one data transfer of a MinION sequencing run in which raw data was uplinked to the cloud-based base calling service, Metrichor (Oxford Nanopore), and the base called nucleic acid sequences downlinked back to MARS. A local base calling program that was provided by Oxford Nanopore upon request was used in the Arctic for the other sequencing runs carried out at MARS. To evaluate the accuracy of the MinION sequencing data obtained in the field, we extracted only Bacterial reads from the MinION metagenomic data sets and compared the assigned taxa with Bacterial 16S rRNA gene amplicon sequences (Illumina MiSEQ) generated from the same DNA extract used in the field with the MinION. At the phyla level, similar taxonomic groups were identified from Illumina sequencing and with the MinION (**Figure 3**), however the relative abundances varied between the two library preparation kits, as well as the amplicon sequencing. There was a larger number of unclassified reads associated with the amplicon dataset, possibly attributable to the longer read lengths derived from the MinION. *Alphaproteobacteria, Actinobacteria, Acidobacteria*, and *Bacteriodetes* were the prominent phyla present in all three datasets, consistent with previous molecular surveys in permafrost ice-wedge soils at this site (Wilhelm et al., 2011). The metagenomes derived from the MinION identified proteins clustered into 22 COG categories, which similarly varied in relative abundance between library preparation kits (**Figure 2**). We used the MinION generated ice-wedge soil metagenomes to identify functional genes and pathways in the microbial communities. For example, we were able to observe all of the genes in the (ubiquitous) citric acid cycle (TCA) (Figure S1). We also identified genes known to be associated with cold adaptation in permafrost microorganisms (Goordial et al., 2016b, 2017) (ie-genes for osmotic stress response mediated through compatible solutes like glycine betaine and choline, cold shock proteins, oxidative stress) (Table S2).

Viable Microbial Activity Assay Using the Biolog Ecoplate

Colorimetric assays such as those employed in the Biolog Ecoplate enable easy and fast visualization of microbial growth based on a colorimetric reaction when a carbon substrate is reduced for growth. Such assays can be miniaturized, and made to be high throughput, with community level physiological profile (CLPP) interpreted on a basic level via visualization alone and quantified via a spectrometer (Weber and Legge, 2009; Rutgers et al., 2016). Slurries of ice wedge soil and sterilized water were used as inocula for the Biolog Ecoplate, CLPP were obtained at 20° and 5°C. We attempted to incubate Ecoplates in the field however all wells froze. While not tested here, the use of freezing point depressants such as NaCl or glycerol in the wells could enable identification and enrichment of active, cold-tolerant and osmo-tolerant microorganisms *in situ*. Wells were assessed visually alone as we did not have access to a spectrophotometer in the field. Substrate utilization patterns were faster at 20°C for all substrates that tested positive (**Figure 4**), color formation was visible in the 20°C plate after 24 h incubation, and only visible in the 5°C plate after 3 days. There were no substrates which could be utilized by a cold adapted community incubated at 5°C that did could not be utilized by a community capable of

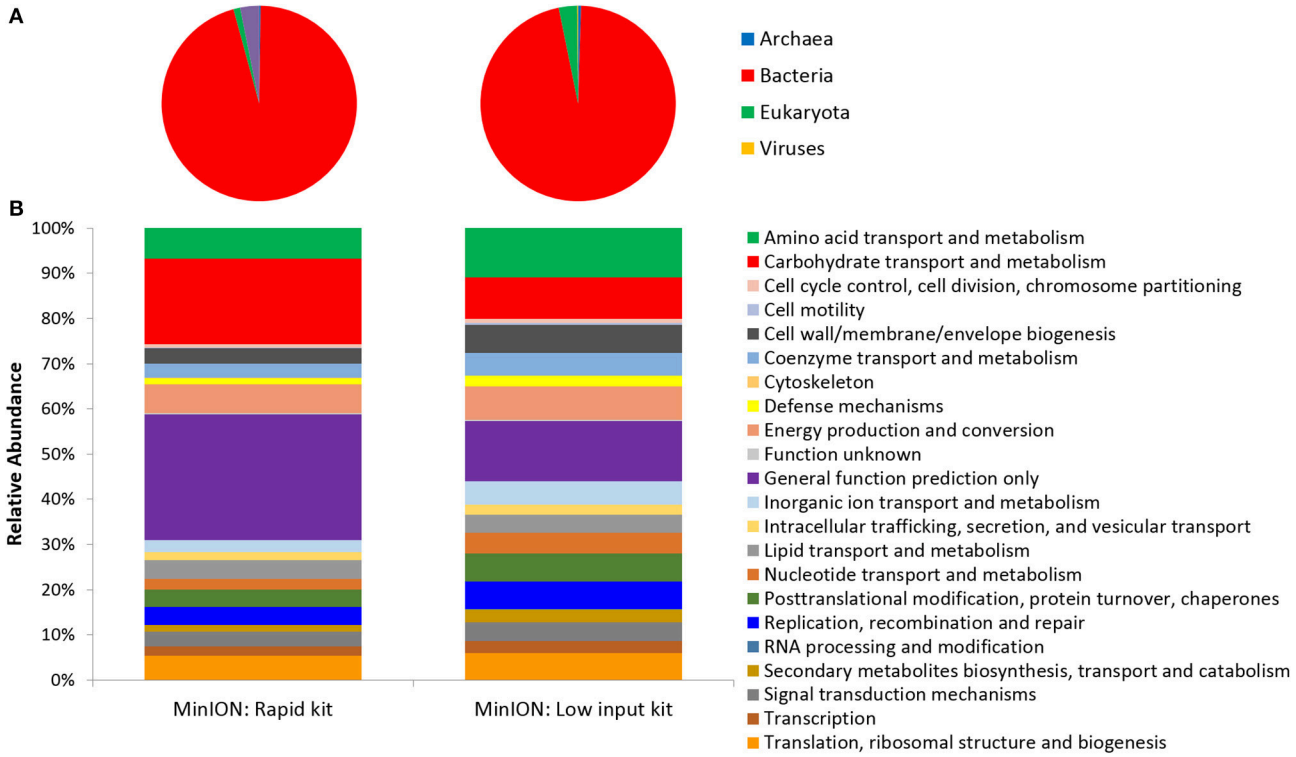

FIGURE 2 | Function and Taxonomy of Ice Wedge soil. Ice wedge soil metagenomes sequenced using the MinION rapid and low input kit **(A)** Taxonomy at the domain level **(B)** Clusters of Orthologous Groups (COG) categories (level 2).

metabolism at 20°C (**Table 1**), the order of substrate utilization over time was not the same for both communities. For example, L-serine, L-arginine, 2-hydroxy benzoic acid, 4-hydroxy benzoic acid were among the first substrates to be visibly reduced in the 5°C incubation, occurring nearly simultaneously (4 days); In the 20°C incubation L-serine was visibly used almost immediately (8 h), while L-arginine, 2-hydroxy benzoic acid, 4-hydroxy benzoic acid proceeded relatively slowly after that (3 days). These differences are likely attributable to different metabolically active microbial communities with different temperature tolerances and optima in the ice wedge soil. We selected reduced wells containing the amino acid L-serine due to the speed and intensity of color formation in these wells after 2 days at 20°C. The wells were pooled together, and DNA extracted using a conventional DNA extraction kit (MoBIO power soil) before sequencing with the MinION low input kit. These wells generated no "passed" sequences which were above the default quality cut-offs generated by the Nanopore Metrichor software after a 6 h sequencing run. Post-deployment, the same DNA extract was sequenced successfully using the MinION rapid library prep. The reason for this is not clear, it is possible that inhibitors associated with the redox dye chemistry disrupted sequencing with the low input kit due to the use of direct binding of beads to the nanopores, compared with the rapid kit which does not employ beads. The L-serine wells were composed almost entirely (∼90%) of a *Pseudomonas*, results which were confirmed via Illumina sequencing of the 16S rRNA gene (**Figure 5**). The MinION generated metagenome of the L-serine ecolog well included full ORFs which encoded for proteins related to conversion of serine to amino acids cysteine, glycine, and methionine. We identified a serine transporter on a single molecule read (ORF 90% similar to an ORFs found in *Pseudomonas antarctica* PAMC27494; Genbank accension CP015600.1) and searched the GenBank database against the entire read. This single molecule read was 5005 bp in length with 89% similarity to the *P. antarctica* PAMC 27494 genome across 95% of the query; only the last 202 bp of the read did not match to the *P antarctica* genome. This included homology to 3 hypothetical proteins in *P. Antarctica* PAMC27494, 5 intergenic regions, and a partial serine dehydratase ORF (Figure S2). Another single molecule read with serine metabolism related hits (3,606 bp) had 87% similarity to the *P. Antarctica* genome (97% query cover), this single molecule read alignment included homology to 3 intergenic regions.

Cryo-iPlate Culturing and Analyses

From the cryo-iPlates 33 bacterial isolates were successfully sub-cultured and chosen for sequencing based on differences in morphology and color (**Table 2**). Most of these isolates were related to strains previously cultured, and 3 isolates were candidates for novel species based on 16S rRNA gene sequence (<98% similarity to anything in GenBank database). It is quite probable that a higher number of slow-growing novel microorganisms would be isolated if longer incubation times

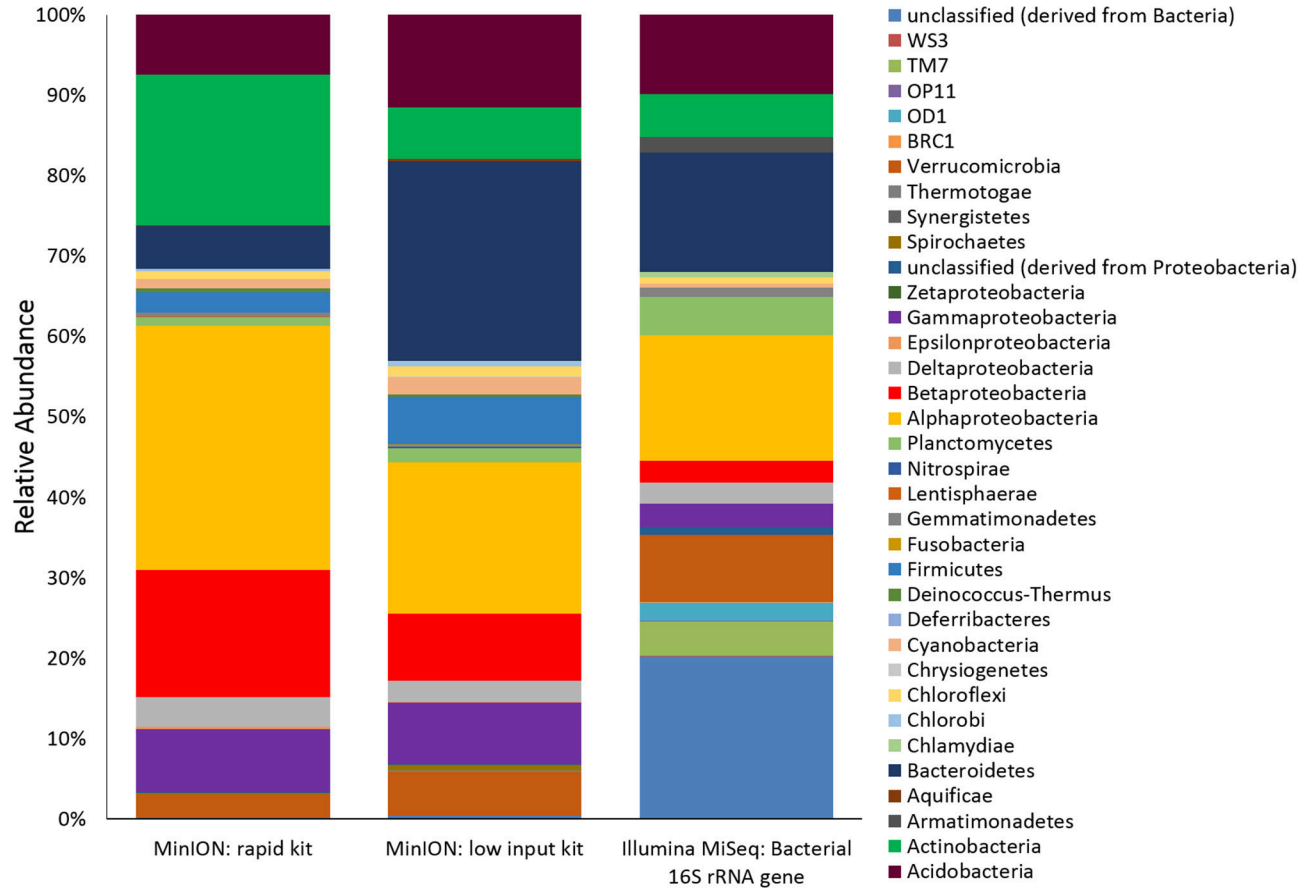

FIGURE 3 | Ice Wedge soil bacterial community composition detected by the MinION. Bacterial reads from ice wedge soil metagenomes sequenced using the MinION rapid and low input kit compared with Bacterial composition inferred from amplicon sequencing of 16S rRNA gene.

for the cryo-iPlates were included in this study (greater than 2 weeks) based on in-laboratory incubations of cryo-iPlates with environmental samples from other Arctic environments (ex-saline sprig sediments) (data not shown). Based on the initial 16S rRNA gene sequencing results, one of the isolates, a *Pedobacter* sp. Str. IW39 (closest cultured representative similarity 96%) was sequenced using the MinION on a single flow cell over 48 h. Genome sequencing was carried out in the laboratory post-field deployment, while the initial colony on a cryo-iplate was in hand in the field. A partial genome was obtained, consisting of 9050 reads, and the majority of reads were <2,000 bp in length, and the longest read was 31,623 bp in length (Figure S3). The longest read was found to be most similar (77%) to *Pedobacter cryoconitis* PAMC 27485, a soil isolate from King George Island, Antarctica (GenBank: CP014504.1). Using Canu, a long read assembler (Koren et al., 2017), we assembled the *Pedobacter* genome into 87 contigs. We were able to identify several genes associated with cold adaptation/osmotic stress regulation such as two glycerol uptake facilitator proteins, a glycerol kinase, and glycerol 3-phosphate dehydrogenase occurring in close proximity to each other. Glycerol is a known compatible solute that depresses freezing point, protects cells from damage caused by freezing, and is synthesized in cultures grown at subzero temperatures (Bore et al., 2017).

DISCUSSION

Our results demonstrate biomarker detection (nucleic acids) in environmental samples, as well as in conjunction with active microbial life detection methods through cultivation of microorganisms and a colourimetric microbial activity assay. The MinION generated metagenomic and genomic sequences identifying organisms across the 3 domains (Bacteria, Archaea, Eukaryotes) from environmental, enriched and an active-layer soil isolate (most closely related to *Pedobacter cryoconitis)* in a platform that was highly portable and robust in the highly remote and relatively extreme conditions in the Canadian high Arctic. The MinION sequencer is driven by Nanopore technology for real-time biological analysis where biomolecules are drawn through nanopore channels blocking and reducing the ionic current through the pore. The ionic current drop and transport duration provides discrimination between different nucleic acids, including base modifications such as methylation

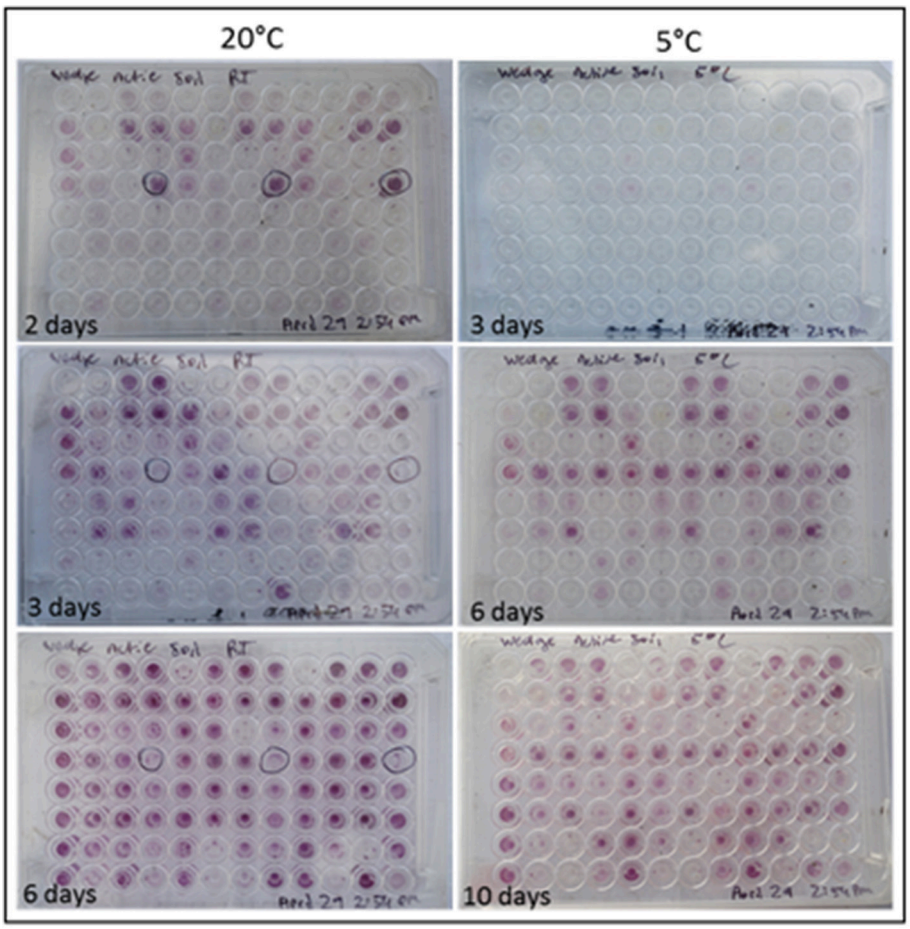

FIGURE 4 | Colorimetric microbial metabolic activity assay (Ecolog). Ecolog plates over several days incubation at 20° and 5°C. Colored wells in Ecolog plates are indicative of microbial activity.

(Simpson et al., 2017). Nanopore technology offers considerable promise for low-resource overhead, miniaturized but robust astrobiology instruments. Because of these traits, it was used as the first DNA sequencer in space, on the ISS in 2016 (Castro-Wallace et al., 2016). In this study, we used the MinION to identify microorganisms across 3 domains based on nucleic acid sequences (**Figure 2**) in the Canadian high Arctic. We have not attempted to quantify error rates in this study, though high error rates in basecalling remains a serious concern with the Nanopore MinION (Deschamps et al., 2016) with current base calling error rates of 13–15% (Boža et al., 2017). Nevertheless, we found the data from MinION to be comparable with Illumina sequencing in environmental and enriched samples (**Figure 3**) with similar proportions of phyla detected using both technologies. Similarly, Brown et al. (2017) were able to correctly assign MinION generated reads from synthetic metagenomes (a mixture of genomic DNA from 20 bacterial strains) to the correct bacterial species up to 98% of the time using the high quality 2D reads (Brown et al., 2017).

Overall, both advances in the nanopore sequencing hardware technology and better bioinformatics tools for MinION-generated sequences should continue to improve sequencing accuracy in the coming years (Boža et al., 2017; Brown et al., 2017). For example, the Oxford Nanopore is currently developing and testing the SmidgION, using MinION sequencing technology and approximately the size of a standard USB memory stick and requiring less energy. While astrobiology life detection *per se* may not need highly accurate reads as opposed to the ability to recognize biogenically produced patterns, a certain level of sequence accuracy will be required in order to discern between earth microbial contaminants from extant alien organisms which share an origin with or from organisms on Earth. In addition, the detection of an unambiguous complex molecular biomarker such as DNA or RNA in samples from Mars, Europa and/or Enceldadus would in itself be a revolutionary scientific discovery if the platform can be designed with the proper controls (i.e., with blank samples) and protocols to detect terrestrial contamination.

The relatively very low weight and low energy requirements of the Nanopore MinION platform for in situ nucleic acid sequencing is beneficial for life detection missions elsewhere, but also to address planetary protection concerns—both for

TABLE 1 | Carbon substrate usage in ice wedge soils (6 day incubation).

Carbon substrate	20°C	5°C
2-Hydroxy Benzoic Acid	+	–
4-Hydroxy Benzoic Acid	++	++
D-Galacturonic Acid	+++	++
D-Glucosaminic Acid	+++	+
D,L-α-Glycerol Phosphate	+	–
D-Cellobiose	+++	–
D-Galactonic Acid γ-Lactone	+++	++
D-Malic Acid	+++	–
D-Mannitol	++	++
D-Xylose	+++	–
Glucose-1-Phosphate	++	–
Glycogen	+++	–
Glycyl-L-Glutamic Acid	+++	–
i-Erythritol	+	–
Itaconic Acid	+++	++
L-Phenylalanine	+	–
L-Arginine	+++	++
L-Asparagine	+++	++
L-Serine	+++	++
L-Threonine	++	–
N-Acetyl-D-glucosamine	++	+
Phenylethylamine	+	++
Putrescine	+	+
Pyruvic Acid Methyl Ester	+++	–
Tween 40	+++	++
Tween 80	+++	++
Water	+	–
α-Cyclodextrin	+++	–
α-D-Lactose	+++	–
α-Ketobutyric Acid	++	–
β-Methyl-D-glucoside	+++	–
γ-Hydroxybutyric Acid	++	+

"forward" contamination in future robotic missions within our solar system, and to assess the potential for "backward" contamination prior to sample return to Earth (Race et al., 2015). The lower limits of biomass detection in environmental samples remains to be tested with the MinION. The current 2017 Nanopore MinION low input kit (SQK-RLB001) requires a minimum of 1 ng of DNA for successful sequencing which would require ∼2.5–5 × 10^5 cells per gram or ml environmental sample based on a 4–2 Mbp microbial genome mass of ∼2.5–5 fg per genome. In most cases this limit will be determined by the efficiency of nucleic acid extraction protocols which is often sample specific. Nonetheless, robust DNA extraction and nucleic acid sequencing has been successfully carried out on a number of low biomass/analog samples on Earth (Navarro-González et al., 2003; Direito et al., 2012; Goordial et al., 2016a; Mojarro et al., 2017) and can be used to inform biomarker extraction elsewhere. Ideally however, nanopore or other novel future novel sequencing technologies that can successfully sequence even lower amounts of DNA [0.1 (= ∼10^4 cells/g or ml) to 0.01 ng (= ∼10^3 cells/g or ml)] from extremely low biomass samples would be more desired for astrobiology life detection instrument platforms given the expected very low concentrations that would probably exist in Mars, Europa or Enceladus samples. Current and future such technologies should be field and lab tested in extremely low biomass terrestrial analog samples such as Antarctic high elevation dry valley permafrost soils (Weber and Legge, 2009) or Atacama extremely dry desert soils (Goordial et al., 2017). In principle, the MinION methodology as outlined here could be automated, which has not been explored here. SetG is an example system which uses the MinION in conjunction with a custom Claremont BioSolutions SimplePrep X1 Automated Lysis and Nucleic Acid Extraction Platform (Mojarro et al, 2016). There are several promising technologies and instruments for such an application including the Voltrax from Oxford Nanopore, or the SOLID-SPU associated with the SOLID life detection instrument (Parro et al., 2011; Manchado et al., 2015).

In this study, we also showed how wells from a Biolog plate resulting in growth can be enriched for extant microbial communities and subsequently have nucleic acids extracted and the communities sequenced—which offers many possibilities for substrate utilization experiments for life detection and ecological studies. The redox dye chemistry employed by the Biolog Ecoplate can be made high throughput, miniaturized, and a number of substrates can be simultaneously tested including chiral forms of sugars and amino acids. Additionally, tolerance and resistance to a number of different environmental conditions such as pH, salinity, metals, antibiotics etc. can be tested simultaneously to probe the CLPP of any extant life encountered amenable to enrichment in this manner. Since positive wells are indicative of metabolism and possibly growth, each positive well represents an enrichment of active microorganisms that can then be used for further analysis—for sequencing, or possibly isolation. The NASA Biosentinel mission, projected to launch in November 2018 as a secondary payload mission on the new Space Launch System, will have a similar microfluidic microbial activity assay (using LED detection system and the metabolic indicator dye alamarBlue, similar to Biolog chemistry) to test the effects of radiation on a targeted yeast strain viability in (see https://www.nasa.gov/centers/ames/engineering/projects/biosentinel.html).

While molecular techniques (ex. metagenomic sequencing) provide some information independent of our ability to culture microorganisms, it is essentially impossible to confirm new gene and pathway functions from pure sequence data. A true understanding of the adaptations, physiology, and metabolic capacities of the bacteria inhabiting the extreme cryoenvironment analog sites requires their cultivation in the laboratory. Recently developed procedures, such as the iChip method can grow up to 20–30% of the microbes, many of which have been found to be novel (Nichols et al., 2010). One such recently discovered organism first cultured with the ichip, *Eleftheria terrae* is the first in 25 years capable of producing a new class of antibiotic (teixobactin) (Ling et al., 2015). The cryo-iplate is modeled off of the ichip method, utilizing diffusion of *in situ* nutrients across a 0.03 membrane into a solid media (gellan gum) to form a medium that more closely mimics in situ

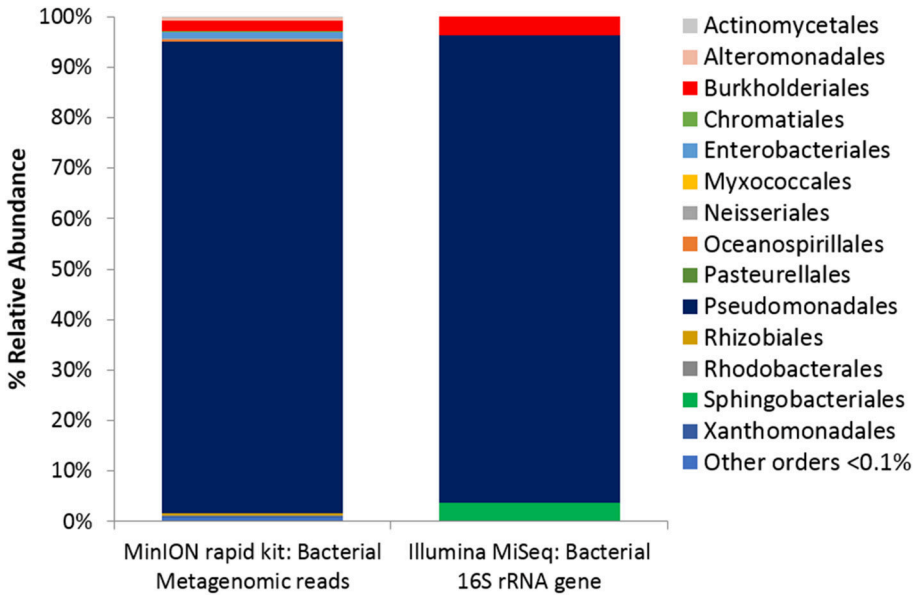

FIGURE 5 | Microbial Activity Microassay (Ecolog plate) Bacterial diversity. Bacterial reads from Ecolog metagenome sequenced using the MinION rapid kit compared with Bacterial composition inferred from amplicon sequencing of 16S rRNA gene.

conditions. Using this methodology, the majority of the isolates from the ice wedge soil were related to organisms previously isolated (**Table 2**); though few candidates for novel strains and species were identified, one of which we sequenced. While there is utility in isolating microorganisms, and a culturable isolate would be an unambiguous sign of life if proven not to be a contaminant, this methodology would be very difficult to robotocize, and may be limited to future human missions, for example to Mars. The small volume involved for each of these modules (Biolog plate, MinION, cryo-iplate) used in this study means that a single sample (for example a core segment or scoop full of soil) can be split for multiple analyses occurring in parallel.

The methods in this study were used in a life detection/astrobiology context, however all methodology presented here has clear application to microbial ecology work, especially *in situ*. The single molecule long reads generated by the MinION proved to be a valuable tool to probe the microbial ecology of analog permafrost samples at the single organism level, offering the ability able to place individual functional genes in genomic context. The long reads from the metagenome allows single functional genes to be placed in genomic context within the organism it was sequenced from, without any potential bias from assembling methodology (Alkan et al., 2011; English et al., 2012; Koren and Phillippy, 2015). Long read sequencing technologies (ex- Moleculo, PacBIO) have been recently applied to generate soil (White et al., 2016) and skin (Tsai et al., 2016) metagenomes, and have proven advantageous to address the challenges of assembly and genomic binning in samples with low coverage regions or with diverse microbial communities. Similarly, other long read generating technology such as PacBIO have been found to be especially advantageous resolving genomic context when multiple replicons and large repetitive elements are present that make it inherently difficult to assemble by short read sequencing technologies (Ricker et al., 2016). Though not the focus of this paper, we were able to identify such a repetitive sequence (15 bp long) associated with an integron integrase in a 2,850 bp single molecule read from the MinION-generated ice wedge soil metagenome. This technology also allows comparison of long stretches of DNA from environmental metagenomic samples to known isolate genomic DNA, such as the homology found in this study between an enriched *Pseudomonas*, and *P. Antarctica* PAMC27294 (Figure S1). This enables science such as genomic comparisons with related isolates in the database to examine questions sensitive to single amino acid differences such as looking at cold adaptation traits which aid activity in the permafrost environment (Goordial et al., 2016b) providing an invaluable window into single organism genomes when single cell methodologies are not feasible, or when isolating microorganisms is not possible. Real-time DNA sequencing has been carried out in the field previously in polar environments (Edwards et al., 2016; Johnson et al., 2017); for example, in the Antarctic Dry Valleys where hand warmers and insulating materials were used to run the device for 2 h outside of shelter (Johnson et al., 2017). The use of fast, simple and reliable tools for detection and identification of microbial life will help researchers respond to rapidly changing conditions and communities, or help direct hypothesis while in the field instead of post analysis in the lab. This is especially important in remote and hard to sample areas.

CONCLUSIONS

Our results demonstrated successful biosignature detection (DNA) using nanopore sequencing on Mars analog

TABLE 2 | Cryo-iplate subcultured isolates.

Strain ID #	GenBank accession no.	Closest cultured BLAST match	% Identity	Isolation source [Accession no.]	Closest BLAST match	% Identity	Isolation source
IW5	MG266397	Flavobacterium sp. UA-JF1530	96	glacial river Iceland: Jokulsa a Fjollum [KC108930.1]	Flavobacterium sp. UA-JF1530	96	glacial river Iceland: Jokulsa a Fjollum [KC108930.1]
IW39	MG266398	Pedobacter sp. UYP1	96	Endolythic, Antarctica: King George Island [KU060818.1]	Pedobacter sp. UYP1	96	Endolith, Antarctica: King George Island [KU060818.1]
IW28	MG266399	Flavobacterium sp. NBRC 101333	98	stream water, Yakushima Island, Kagoshima, Japan[AB681458.1]	Uncultured bacterium clone W201e10_12765	98	Free Air CO2 Enrichment (FACE) field soil USA [JQ375009.2]
IW2	MG266400	Pseudomonas antarctica PAMC 27494	99	Freshwater Antarctica: King George Island[CP015600.1]	Pseudomonas antarctica strain PAMC 27494	99	Freshwater Antarctica: King George Island[CP015600.1]
IW4	MG266401	Pseudomonas antarctica PAMC 27494	99	Freshwater Antarctica: King George Island [CP015600.1]	Pseudomonas antarctica strain PAMC 27494	99	Freshwater Antarctica: King George Island [CP015600.1]
IW6	MG266402	Pseudomonas antarctica PAMC 27494	99	Freshwater Antarctica King George Island[CP015600.1]	Pseudomonas antarctica strain PAMC 27494	99	Freshwater Antarctica: King George Island[CP015600.1]
IW7	MG266403	Pseudomonas antarctica PAMC 27494	99	Freshwater Antarctica: Barton Peninsula, King George Island[CP015600.1]	Pseudomonas antarctica strain PAMC 27494	99	Freshwater Antarctica: Barton Peninsula, King George Island[CP015600.1]
IW8	MG266404	Pseudomonas yamanorum, TSA20	99	deep sea sediment Southern Indian Ocean[LT673850.1]	Pseudomonas yamanorum, strain TSA20	99	deep sea sediment Southern Indian Ocean[LT673850.1]
IW9	MG266405	Flavobacterium sp. HP11M	99	Amphibian skin, host:Pseudacris crucifer, USA [KM187393.1]	Uncultured bacterium clone	99	Human skin [HM263969.1]
IW10	MG266406	Janthinobacterium lividum TJ-1-35	99	Garden in Hamburg, Germany, HH100–HH107) [MF157598.1]	Uncultured bacterium clone	99	pit from Kuytun 51 Glacier, Tianshan Mountains, China [EU267871.1]
IW12	MG266407	Pseudomonas antarctica PAMC 27494	99	Freshwater Antarctica: Barton Peninsula, King George Island[CP015600.1]	Pseudomonas antarctica strain PAMC 27494	99	Freshwater Antarctica: Barton Peninsula, King George Island[CP015600.1]
IW13	MG266408	Pedobacter cryoconitis A37	99	bacteria in a wall crust in lava tube cave Iceland: [KF577526.1]	Pedobacter cryoconitis strain A37	99	bacteria in a wall crust in lava tube cave Iceland: [KF577526.1]
IW14	MG266409	Plantibacter sp. AK20-4	99	bacterial communities in alpine forest soils Austria [KP899147.1]	Plantibacter sp. AK20-4	99	bacterial communities in alpine forest soils Austria [KP899147.1]
IW15	MG266410	Flavobacterium collinsii 983-08	99	Farmed Fish (Oncorhynchus mykiss) liver [NR_145952.1]	Flavobacterium collinsii strain 983-08	99	Farmed Fish (Oncorhynchus mykiss) liver [NR_145952.1]
IW16	MG266411	Duganella sp. JH16	99	agricultural field frozen soil in winter, South Korea [KF424273.1]	Uncultured bacterium isolate 1112842459844	99	loamy sand of Eucalyptus forest in La Jolla, CA [HQ119381.1]
IW17	MG266412	Pseudomonas antarctica strain PAMC 27494	99	Freshwater Antarctica: King George Island [CP015600.1]	Pseudomonas antarctica strain PAMC 27494	99	Freshwater Antarctica: King George Island [CP015600.1]
IW18	MG266413	Variovorax paradoxus strain SL37	99	Endophyte in the circumpolargrass, Finland[KJ529023.1]	Variovorax paradoxus strain SL37	99	Endophyte in the circumpolargrass, Finland[KJ529023.1]
IW20	MG266414	Frondihabitans sp. BAR42	99	Water/rock samples Dry Valleys, Antarctica [KP717942.1]	Frondihabitans sp. BAR42	99	Water/rock samples Dry Valleys, Antarctica [KP717942.1]
IW21	MG266415	Pseudomonas fluorescens strain S18	99	Atlantic Salmon Eggs [KT223386.1]	Pseudomonas fluorescens strain S18	99	Atlantic Salmon Eggs [KT223386.1]
IW22	MG266416	Pseudomonas antarctica strain PAMC 27494	99	Freshwater Antarctica: King George Island [CP015600.1]	Pseudomonas antarctica strain PAMC 27494	99	Freshwater Antarctica: King George Island [CP015600.1]
IW23	MG266417	Pedobacter sp. R20-57	99	Alpine forest soil, Austria [KP899225.1]	Pedobacter sp. R20-57	99	Alpine forest soil, Austria [KP899225.1]
IW24	MG266418	Duganella sp. JH16	99	agricultural field frozen soil in winter, South Korea [KF424273.1]	Uncultured bacterium isolate	99	loamy sand of Eucalyptus forest in La Jolla, CA [HQ119381.1]

(Continued)

TABLE 2 | Continued

Strain ID #	GenBank accession no.	Closest cultured blast match	% identity	Isolation source [Accession no.]	Closest blast match	% Identity	Isolation source
IW25	MG266419	Oxalobacteraceae bacterium PDD-69b-39	99	cloud water collected at the puy de Dome, 1465 m, France [KR922302.1]	Uncultured bacterium clone bar-b48	99	temperate highland grassland [JN024091.1]
IW27	MG266420	Pseudomonas fluorescens strain S18	99	Atlantic Salmon Eggs [KT223386.1]	Pseudomonas fluorescens strain S18	99	Atlantic Salmon Eggs [KT223386.1]
IW29	MG266421	Sphingomonas sp. strain ANT_H46B	99	soil sample from Arctowski Polish Antarctic Station [KY405918.1]	Uncultured Clostridium sp. clone ABLBf53	99	atmospheric boundary layer at 1500 feet [JF269141.1]
IW30	MG266422	Pseudomonas fluorescens strain S18	99	Atlantic Salmon Eggs [KT223386.1]	Pseudomonas fluorescens strain S18	99	Atlantic Salmon Eggs [KT223386.1]
IW31	MG266423	Pseudomonas yamanorum, strain TSA20	99	deep sea sediment Southern Indian Ocean [LT673850.1]	Pseudomonas yamanorum, strain TSA20	99	deep sea sediment Southern Indian Ocean [LT673850.1]
IW32	MG266424	Pseudomonas yamanorum, strain TSA20	99	deep sea sediment Southern Indian Ocean [LT673850.1]	Pseudomonas yamanorum, strain TSA20	99	deep sea sediment Southern Indian Ocean [LT673850.1]
IW33	MG266425	Sphingomonas aurantiaca strain MA101b	99	air- and dustborne Antarctic [NR_042128.1]	Sphingomonas aurantiaca strain MA101b	99	air- and dustborne Antarctic [NR_042128.1]
IW34	MG266426	Pseudomonas sp. BT-A-S4	99	isolated from Arctic, China (unpublished no further info) [KU671225.1]	Pseudomonas sp. BT-A-S4	99	isolated from Arctic, China (unpublished no further info) [KU671225.1]
IW35	MG266427	Pseudomonas fluorescens strain S18	99	Atlantic Salmon Eggs [KT223386.1]	Pseudomonas fluorescens strain S18	99	Atlantic Salmon Eggs [KT223386.1]
IW36	MG266428	Janthinobacterium sp. 1_2014MBL_MicDiv	99	Soil, Woods Hole, MA [CP011319.1]	Janthinobacterium sp. 1_2014MBL_MicDiv	99	Soil, Woods Hole, MA [CP011319.1]
IW38	MG266429	Pseudomonas frederiksbergensis strain AS1	99	arsenic-contaminated soil, South Korea: Gwangju, Kyunggi-Do [CP018319.1]	Pseudomonas frederiksbergensis strain AS1	99	arsenic-contaminated soil, South Korea: Gwangju, Kyunggi-Do [CP018319.1]

environmental samples, in conjunction with active life detection methods through cultivation of microorganisms and a colorimetric microbial activity assay in a highly remote and extreme terrestrial environment. The platforms and methods outlined here are highly portable and offer the possibility to examine microbial ecology in real-time, in dynamic, and remote environments. Future planetary exploration life detection missions will likely not rely on a single instrument, rather a suite of instruments will need to be used in concert to confirm whether extant or relic life is present. The tools presented here are pre-existing, relatively low weight, have relatively low energy requirements, and relatively low cost. While Nanopore MinION sequencing technology has considerable promise and potential as an unambiguous biosignature detection platform for future planetary exploration missions, a number of significant hurdles remain. To optimize these tools for a flight mission further work needs to be done; for example, the lifetime of protein based nanopores are currently not suitable for the long duration space flights necessary for targets like Mars, Europa or Enceladus; however, synthetic solid state nanopore sequencers are currently being developed through the NASA ColdTech Program (Whyte personal communication). It will also be crucial to develop miniaturized robust, robotic nucleic acid extraction platforms capable of extracting sufficient nucleic acids from a variety of very low biomass Mars and Icy moon analog samples for successful nanopore sequencing technologies, current and future.

AUTHOR CONTRIBUTIONS

JG carried out field work, lab work, analysis, and writing, IA carried out field work and writing, KC-Y carried out Illumina Sequencing, EM and KH carried out isolation and sanger sequencing and analysis, and LW advised and contributed significantly to writing and analysis.

FUNDING

Funding for this project was provided from a Canadian Space Agency Mars Sample Return (MSR) and FAST grant, a McGill Space Institute (MSI) PDF to JG, NSERC Discovery, Northern

Research Supplement, Polar Continental Shelf Project (676-16), and Northern Research Supplement Grants to LW.

ACKNOWLEDGMENTS

The authors would like to thank Dat Buoi, Isabelle Raymond-Bouchard for their assistance with the cryo-iPlate, to Richard Ronan at Oxford Nanopore Technologies for his help with MinION sequencing, especially the logistics of local base calling in the field, and to Slava Epstein (North Eastern University, USA) for his guidance in helping us develop the cryo-iPlate prototype used in this study. The authors also thank the two reviewers who improved this manuscript. The authors are grateful for support from the Canadian Space Agency (CSA) for this project.

SUPPLEMENTARY MATERIAL

The Supplementary Material for this article can be found online at: https://www.frontiersin.org/articles/10.3389/fmicb.2017.02594/full#supplementary-material

REFERENCES

Alkan, C., Sajjadian, S., and Eichler, E. E. (2011). Limitations of next-generation genome sequence assembly. *Nat. Methods* 8, 61–65. doi: 10.1038/nmeth.1527

Bore, E. K., Apostel, C., Halicki, S., Kuzyakov, Y., and Dippold, M. A. (2017). Microbial metabolism in soil at subzero temperatures: adaptation mechanisms revealed by position-specific (13)C labeling. *Front. Microbiol.* 8:946. doi: 10.3389/fmicb.2017.00946

Boža, V., Brejová B., and Vinar, T. (2017). DeepNano: deep recurrent neural networks for base calling in MinION nanopore reads. *PLoS ONE* 12:e0178751. doi: 10.1371/journal.pone.0178751

Brasier, M. D., Green, O. R., and McLoughlin, N. (2004). Characterization and critical testing of potential microfossils from the early Earth: the Apex 'microfossil debate' and its lessons for Mars sample return. *Int. J. Astrobiology*. 3, 139–150. doi: 10.1017/S1473550404002058

Brown, B. L., Watson, M., Minot, S. S., Rivera, M. C., and Franklin, R. B. (2017). MinION^{TM} nanopore sequencing of environmental metagenomes: a synthetic approach. *Gigascience* 6, 1–10. doi: 10.1093/gigascience/gix007

Castro-Wallace, S. L., Chiu, C. Y., John, K. K., Stahl, S. E., Rubins, K. H., McIntyre, A. B. R., et al. (2016). Nanopore DNA sequencing and genome assembly on the international space station. *bioRxiv*. doi: 10.1101/077651

Davila, A. F., Skidmore, M., Fairén, A. G., Cockell, C., and Schulze-Makuch, D. (2010). New priorities in the robotic exploration of Mars: the case for in situ search for extant life. *Astrobiology* 10, 705–710. doi: 10.1089/ast.2010.0538

Deschamps, S., Mudge, J., Cameron, C., Ramaraj, T., Anand, A., Fengler, K., et al. (2016). Characterization, correction and de novo assembly of an Oxford Nanopore genomic dataset from *Agrobacterium tumefaciens*. *Sci. Rep.* 6:28625. doi: 10.1038/srep28625

Direito, S. O., Marees, A., and Röling, W. F. (2012). Sensitive life detection strategies for low-biomass environments: optimizing extraction of nucleic acids adsorbing to terrestrial and Mars analogue minerals. *FEMS Microbiol. Ecol.* 81, 111–123. doi: 10.1111/j.1574-6941.2012.01325.x

Doran, P. T. (1993). Sedimentology of Colour Lake, a nonglacial high Arctic lake, Axel Heiberg Island, NWT, Canada. *Arctic Alpine Res.* 25, 353–367. doi: 10.2307/1551918

Edwards, A., Debbonaire, A. R., Sattler, B., Mur, L. A., and Hodson, A. J. (2016). Extreme metagenomics using nanopore DNA sequencing: a field report from Svalbard, 78 N. *bioRxiv* 073965. doi: 10.1101/073965

English, A. C., Richards, S., Han, Y., Wang, M., Vee, V., Qu, J., et al. (2012). Mind the gap: upgrading genomes with Pacific Biosciences RS long-read sequencing technology. *PLoS ONE* 7:e47768. doi: 10.1371/journal.pone.0047768

Fairén, A. G., Davila, A. F., Lim, D., Bramall, N., Bonaccorsi, R., Zavaleta, J., et al. (2010). Astrobiology through the ages of Mars: the study of terrestrial analogues to understand the habitability of Mars. *Astrobiology* 10, 821–843. doi: 10.1089/ast.2009.0440

Golombek, M. P. (1999). A message from warmer times. *Science* 283, 1470–1471. doi: 10.1126/science.283.5407.1470

Goordial, J., Davila, A., Greer, C. W., Cannam, R., DiRuggiero, J., McKay, C. P., et al. (2017). Comparative activity and functional ecology of permafrost soils and lithic niches in a hyper-arid polar desert. *Environ. Microbiol.* 19, 443–458. doi: 10.1111/1462-2920.13353

Goordial, J., Davila, A., Lacelle, D., Pollard, W., Marinova, M. M., Greer, C. W., et al. (2016a). Nearing the cold-arid limits of microbial life in permafrost of an upper dry valley, Antarctica. *ISME J.* 10, 1613–1624. doi: 10.1038/ismej.2015.239

Goordial, J., Lamarche-Gagnon, G., Lay, C.-Y., and Whyte, L. (2013). "Left out in the cold: life in cryoenvironments," in *Polyextremophiles. Cellular Origin, Life in Extreme Habitats and Astrobiology*, Vol. 27, eds J. Seckbach, A. Oren, and H. Stan-Lotter (Dordrecht: Springer), 335–363.

Goordial, J., Raymond-Bouchard, I., Zolotarov, Y., de Bethencourt, L., Ronholm, J., Shapiro, N., et al. (2016b). Cold adaptive traits revealed by comparative genomic analysis of the eurypsychrophile Rhodococcus sp. JG3 isolated from high elevation McMurdo Dry Valley permafrost, Antarctica. *FEMS Microbiol. Ecol.* 92:fiv154. doi: 10.1093/femsec/fiv154

Grotzinger, J. P., Sumner, D., Kah, L., Stack, K., Gupta, S., Edgar, L., et al. (2014). A habitable fluvio-lacustrine environment at Yellowknife Bay, Gale Crater, Mars. *Science* 343:1242777. doi: 10.1126/science.1242777

Hays, L., Archenbach, L., Bailey, J., Barnes, R., Barros, J., Bertka, C., et al. (2015). NASA Astrobiology *Strategy.* Available online at: https://nai.nasa.gov/media/medialibrary/2015/10/NASA_Astrobiology_Strategy_2015_151008.pdf

Johnson, S. S., Zaikova, E., Goerlitz, D. S., Bai, Y., and Tighe, S. W. (2017). Real-Time DNA sequencing in the antarctic dry valleys using the oxford nanopore sequencer. *J. Biomol. Tech.* 28, 2–7. doi: 10.7171/jbt.17-2801-009

Kargel, J. S., Kaye, J. Z., Head, J. W., Marion, G. M., Sassen, R., Crowley, J. K., et al. (2000). Europa's crust and ocean: origin, composition, and the prospects for life. *Icarus* 148, 226–265. doi: 10.1006/icar.2000.6471

Koren, S., and Phillippy, A. M. (2015). One chromosome, one contig: complete microbial genomes from long-read sequencing and assembly. *Curr. Opin. Microbiol.* 23, 110–120. doi: 10.1016/j.mib.2014.11.014

Koren, S., Walenz, B. P., Berlin, K., Miller, J. R., Bergman, N. H., and Phillippy, A. M. (2017). Canu: scalable and accurate long-read assembly via adaptive k-mer weighting and repeat separation. *Genome Res.* 27, 722–736. doi: 10.1101/gr.215087.116

Lau, M. C., Stackhouse, B., Layton, A. C., Chauhan, A., Vishnivetskaya, T., Chourey, K., et al. (2015). An active atmospheric methane sink in high Arctic mineral cryosols. *ISME J.* 9, 1880–1891. doi: 10.1038/ismej.2015.13

Levin, G. V. (1997). The Viking labeled release experiment and life on Mars. *Optical Sci. Engineer. Instrum.* 97, 146–161.

Ling, L. L., Schneider, T., Peoples, A. J., Spoering, A. L., Engels, I., Conlon, B. P., et al. (2015). A new antibiotic kills pathogens without detectable resistance. *Nature* 5177535, 455–459. doi: 10.1038/nature14098

Loman, N. J., and Quinlan, A. R. (2014). Poretools: a toolkit for analyzing nanopore sequence data. *Bioinformatics* 30, 3399–3401. doi: 10.1093/bioinformatics/btu555

Manchado, J., Sebastián, E., Romeral, J., Sobrado-Vallecillo, J., Herrero, P., Compostizo, C., (eds.). et al. (2015). "SOLID SPU: a TRL 5–6 sample preparation instrument for wet chemistry analysis on mars," in *Lunar and Planetary Science Conference* (Woodlands, TX).

McKay, C. P., Porco, C. C., Altheide, T., Davis, W. L., and Kral, T. A. (2008). The possible origin and persistence of life on Enceladus and detection of biomarkers in the plume. *Astrobiology* 8, 909–919. doi: 10.1089/ast.2008.0265

Melosh, H., Ekholm, A., Showman, A., and Lorenz, R. (2004). The temperature of Europa's subsurface water ocean. *Icarus* 168, 498–502. doi: 10.1016/j.icarus.2003.11.026

Meyer, F., Paarmann, D., D'Souza, M., Olson, R., Glass, E., Kubal, M., et al. (2008). The metagenomics RAST server - a public resource for the automatic phylogenetic and functional analysis of metagenomes. *BMC Bioinform.* 9:386. doi: 10.1186/1471-2105-9-386

Mojarro, A., Hachey, J., Tani, J., Smith, A., Bhattaru, S., Pontefract, A., (eds.). et al. (2016). "SETG: nucleic acid extraction and sequencing for in situ life detection on Mars," in *3rd International Workshop on Instrumentation for Planetary Mission* (Pasadena, CA).

Mojarro, A., Ruvkun, G., Zuber, M. T., and Carr, C. E. (2017). Nucleic acid extraction from synthetic mars analog soils for in situ life detection. *Astrobiology* 17, 747–760. doi: 10.1089/ast.2016.1535

Navarro-González, R., Rainey, F. A., Molina, P., Bagaley, D. R., Hollen, B. J., de la Rosa, J., et al. (2003). Mars-like soils in the Atacama Desert, Chile, and the dry limit of microbial life. *Science* 302, 1018–1021. doi: 10.1126/science.1089143

Nichols, D., Cahoon, N., Trakhtenberg, E., Pham, L., Mehta, A., Belanger, A., et al. (2010). Use of ichip for high-throughput in situ cultivation of "uncultivable" microbial species. *Appl. Environ. Microbiol.* 76, 2445–2450. doi: 10.1128/AEM.01754-09

Ojha, L., Wilhelm, M. B., Murchie, S. L., McEwen, A. S., Wray, J. J., Hanley, J., et al. (2015). Spectral evidence for hydrated salts in recurring slope lineae on Mars. *Nat. Geosci.* 8, 829–832. doi: 10.1038/ngeo2546

Overbeek, R., Olson, R., Pusch, G. D., Olsen, G. J., Davis, J. J., Disz, T., et al. (2013). The SEED and the Rapid Annotation of microbial genomes using Subsystems Technology (RAST). *Nucleic Acids Res.* 42, D206–D214. doi: 10.1093/nar/gkt1226

Parro, V., de Diego-Castilla, G., Rodríguez-Manfredi, J. A., Rivas, L. A., Blanco-López, Y., Sebastián, E., et al. (2011). SOLID3: a multiplex antibody microarray-based optical sensor instrument for in situ life detection in planetary exploration. *Astrobiology* 11, 15–28. doi: 10.1089/ast.2010.0501

Pollard, W., Haltigin, T., Whyte, L., Niederberger, T., Andersen, D., Omelon, C., et al. (2009). Overview of analogue science activities at the McGill Arctic research station, axel heiberg island, canadian high arctic. *Planet. Space Sci.* 57, 646–659. doi: 10.1016/j.pss.2009.01.008

Race, M. S., Johnson, J. E., Spry, J. A., Siegel, B., and Conley, C. A. (2015). *Planetary Protection Knowledge Gaps for Human Extraterrestrial Missions*. Workshop Report. Mountain View: NASA.

Ricker, N., Shen, S. Y., Goordial, J., Jin, S., and Fulthorpe, R. R. (2016). PacBio SMRT assembly of a complex multi-replicon genome reveals chlorocatechol degradative operon in a region of genome plasticity. *Gene* 586, 239–247. doi: 10.1016/j.gene.2016.04.018

Roth, L., Retherford, K. D., Saur, J., Strobel, D. F., Feldman, P. D., McGrath, M. A., et al. (2014). Orbital apocenter is not a sufficient condition for HST/STIS detection of Europa's water vapor aurora. *Proc. Nat. Acad. Sci. U.S.A.* 111, E5123–E5132. doi: 10.1073/pnas.1416671111

Rutgers, M., Wouterse, M., Drost, S. M., Breure, A. M., Mulder, C., Stone, D., et al. (2016). Monitoring soil bacteria with community-level physiological profiles using Biolog^{TM} ECO-plates in the Netherlands and Europe. *Appl. Soil Ecol.* 97, 23–35. doi: 10.1016/j.apsoil.2015.06.007

Schulze-Makuch, D., Rummel, J. D., Benner, S. A., Levin, G., Parro, V., and Kounaves, S. (2015). Nearly forty years after viking: are we ready for a new life-detection mission? *Astrobiology* 15, 413–419. doi: 10.1089/ast.2015.1336

Simpson, J. T., Workman, R. E., Zuzarte, P., David, M., Dursi, L., and Timp, W. (2017). Detecting DNA cytosine methylation using nanopore sequencing. *Nat. Methods* 14, 407–410. doi: 10.1038/nmeth.4184

Tsai, Y.-C., Conlan, S., Deming, C., Segre, J. A., Kong, H. H., Korlach, J., et al. (2016). Resolving the complexity of human skin metagenomes using single-molecule sequencing. *MBio* 7:e01948-15. doi: 10.1128/mBio.01948-15

Waite, J. H., Combi, M. R., Ip, W.-H., Cravens, T. E., McNutt, R. L., Kasprzak, W., et al. (2006). Cassini ion and neutral mass spectrometer: enceladus plume composition and structure. *Science* 311, 1419–1422. doi: 10.1126/science.1121290

Weber, K. P., and Legge, R. L. (2009). One-dimensional metric for tracking bacterial community divergence using sole carbon source utilization patterns. *J. Microbiol. Methods.* 79, 55–61. doi: 10.1016/j.mimet.2009.07.020

White, R. A., Bottos, E. M., Roy Chowdhury, T., Zucker, J. D., Brislawn, C. J., Nicora, C. D., et al. (2016). Moleculo long-read sequencing facilitates assembly and genomic binning from complex soil metagenomes. *mSystems* 1:e00045-16. doi: 10.1128/mSystems.00045-16

Wilhelm, R. C., Niederberger, T. D., Greer, C., and Whyte, L. G. (2011). Microbial diversity of active layer and permafrost in an acidic wetland from the Canadian High Arctic. *Can. J. Microbiol.* 57, 303–315. doi: 10.1139/w11-004

Wilhelm, R. C., Radtke, K. J., Mykytczuk, N. C., Greer, C. W., and Whyte, L. G. (2012). Life at the wedge: the activity and diversity of Arctic ice wedge microbial communities. *Astrobiology* 12, 347–360. doi: 10.1089/ast.2011.0730

Conflict of Interest Statement: JG received a $1000 travel bursary from Oxford Nanopore to aid attendance costs at the Astrobiology Science conference (AbSciCon) in Mesa, Arizona, April 23–27th, 2017, where she gave an oral presentation on these results. ONT have generously provided free-of-charge reagents and technical support for this project. No authors were/are financially compensated by ONT, hold stocks, shares or options.

The other authors declare that the research was conducted in the absence of any commercial or financial relationships that could be construed as a potential conflict of interest.

frontiers in Microbiology

ORIGINAL RESEARCH
published: 27 October 2017
doi: 10.3389/fmicb.2017.02083

Advanced Photogrammetry to Assess Lichen Colonization in the Hyper-Arid Namib Desert

Graham Hinchliffe[1], Barbara Bollard-Breen[1], Don A. Cowan[2], Ashray Doshi[1], Len N. Gillman[1], Gillian Maggs-Kolling[3], Asuncion de Los Rios[4] and Stephen B. Pointing[5]**

[1] Institute for Applied Ecology New Zealand, School of Science, Auckland University of Technology, Auckland, New Zealand, [2] The Genomics Research Institute, University of Pretoria, Pretoria, South Africa, [3] Gobabeb Research and Training Centre, Gobabeb, Namibia, [4] Departamento de Biogeoquímica y Ecología Microbiana, Museo Nacional de Ciencias Naturales, Madrid, Spain, [5] Division of Science, Yale-NUS College, National University of Singapore, Singapore, Singapore

The hyper-arid central region of the Namib Desert is characterized by quartz desert pavement terrain that is devoid of vascular plant covers. In this extreme habitat the only discernible surface covers are epilithic lichens that colonize exposed surfaces of quartz rocks. These lichens are highly susceptible to disturbance and so field surveys have been limited due to concerns about disturbing this unusual desert feature. Here we present findings that illustrate how non-destructive surveys based upon advanced photogrammetry techniques can yield meaningful and novel scientific data on these lichens. We combined 'structure from motion analysis,' computer vision and GIS to create 3-dimensional point clouds from two-dimensional imagery. The data were robust in its application to estimating absolute lichen cover. An orange *Stellarangia* spp. assemblage had coverage of 22.8% of available substrate, whilst for a black *Xanthoparmelia* spp. assemblage coverage was markedly lower at 0.6% of available substrate. Hyperspectral signatures for both lichens were distinct in the near-infra red range indicating that *Xanthoparmelia* spp. was likely under relatively more moisture stress than *Stellarangia* spp. at the time of sampling, and we postulate that albedo effects may have contributed to this in the black lichen. Further transformation of the data revealed a colonization preference for west-facing quartz surfaces and this coincides with prevailing winds for marine fog that is the major source of moisture in this system. Furthermore, a three-dimensional 'fly through' of the lichen habitat was created to illustrate how the application of computer vision in microbiology has further potential as a research and education tool. We discuss how advanced photogrammetry could be applied in astrobiology using autonomous rovers to add quantitative ecological data for visible surface colonization on the surface of Mars.

Keywords: astrobiology, computer vision, desert, GIS, lichen, microbial ecology, Namib Desert, photogrammetry

OPEN ACCESS

Edited by:
Andreas Teske, University of North Carolina at Chapel Hill, United States

Reviewed by:
Armando Azua-Bustos, Pontificia Universidad Católica de Chile, Chile
Thomas L. Kieft, New Mexico Institute of Mining and Technology, United States

****Correspondence:***
Asuncion de Los Rios
arios@mncn.csic.es
Stephen B. Pointing
stephen.pointing@yale-nus.edu.sg

Specialty section:
This article was submitted to Extreme Microbiology, a section of the journal Frontiers in Microbiology

Received: *27 July 2017*
Accepted: *11 October 2017*
Published: *27 October 2017*

Citation:
Hinchliffe G, Bollard-Breen B, Cowan DA, Doshi A, Gillman LN, Maggs-Kolling G, de Los Rios A and Pointing SB (2017) Advanced Photogrammetry to Assess Lichen Colonization in the Hyper-Arid Namib Desert. Front. Microbiol. 8:2083. doi: 10.3389/fmicb.2017.02083

INTRODUCTION

Deserts are the largest terrestrial biome (Thomas, 2011) and are characterized by prolonged moisture stress and also significant UV and thermal stress (UNEP, 1992; Peel and Finlayson, 2007). These factors limit animal and vascular plant occurrence and in the most extreme desert landscapes they may be virtually absent, with microbial communities forming the dominant biological cover

(Pointing and Belnap, 2012). In semi-arid and arid regions biological soil crusts are common and these comprise a complex association of bacteria, fungi, algae, lichen, and mosses (Belnap et al., 2003). Their diversity and ecological role have been comprehensively studied (Gundlapally and Garcia-Pichel, 2006; Elbert et al., 2012; Rajeev et al., 2013; Colesie et al., 2014; Rutherford et al., 2017) and they are critical to desert ecosystem stability (Pointing and Belnap, 2014). In the most extreme hyper-arid deserts more severe environmental conditions limit the occurrence of biological soil crusts and refuge communities account for much of the standing biomass. Colonization includes hypolithic cyanobacterial communities beneath quartz rocks (Warren-Rhodes et al., 2006, 2007; Pointing et al., 2007; Stomeo et al., 2013) as well as cryptoendolithic cyanobacterial and lichen communities within porous rocks (Lee et al., 2016; Archer et al., 2017) and mineral substrates (Wierzchos et al., 2006, 2012). A high degree of niche filtering between such communities has been observed, reflecting the strong selective forces involved in shaping these communities (Lee et al., 2016). Open soil in desert systems is relatively depauperate and largely supports low-biomass bacterial communities (Makhalanyane et al., 2015).

In the most extreme hyper-arid regions of the central Namib Desert additional surface biological cover comprises epilithic lichens that colonize exposed rocky surfaces (Nash et al., 1977; Lange and Green, 2008; Wirth, 2010). Lichen associations colonize the exposed quartz surfaces of desert pavement and strikingly lichens appear to thrive where no other surface colonization occurs. Whilst subsurface refuge communities rely on a mineral layer for protection from environmental extremes (Pointing and Belnap, 2012), the epilithic lichens are fully exposed and so have developed extraordinary desiccation tolerance (Kranner et al., 2008) and UV protective pigmentation strategies (Wierzchos et al., 2015). Namib Desert lichens are thought to derive their moisture from coastal fog and this is assumed to influence their colonization such that they appear visually to preferentially colonize elevated ground and exposed rock surfaces (Lange and Green, 2008).

The extreme and isolated environment of the Namib Desert makes ecological surveys challenging, and traditional ground-based estimates of lichen cover are limited in their application to meaningful landscape scales. In addition, the fragile nature and slow recovery rate for desert landscapes makes disturbance during scientific surveys a serious concern (Belnap and Eldridge, 2003; Kuske et al., 2012). For this reason, there is growing interest in field techniques that minimize environmental harm such as photogrammetry and remote sensing. These techniques are also a key component of remote sensing for other planetary surfaces in the field of astrobiology, the science of identifying whether life exists or has existed on other planets (Grady, 2001). A major focus for astrobiology has been our closest planetary neighbor Mars, and extreme deserts on Earth such as the Namib Desert are geologically and climatically the closest analogs available to Mars' current surface environment (Fairén et al., 2010). The future search for extant microbial colonization on Mars' surface will benefit from multiple approaches, and advanced photogrammetry techniques proven in desert analog environments on Earth may prove a powerful tool in this regard.

Here we report results from a field photogrammetry survey of Namib Desert lichens using RGB and hyper-spectral cameras. We report findings that demonstrate how advanced photogrammetry applied to standard photographic imagery can be used to accurately map colonization, discriminate between major taxa, create 3D renderings that inform colonization preference and azimuth, and be combined with hyper-spectral imagery to infer lichen health.

MATERIALS AND METHODS

Field Location and Manual Sampling

The sampling location (S 23° 03.383′, E14° 38.071′; 105 m above sea level) was typical of the central Namib Desert terrain comprising desert pavement with quartz rocks embedded in a mineral soil substrate. This area is internationally renowned for its 'lichen fields', large areas where exposed quartz is colonized largely by orange and black lichens to form a spectacular and unusual microbial landscape. The field survey was made in April 2016 during an expedition hosted by the Gobabeb Research and Training Centre[1]. Lichen colonization comprised either orange or black-pigmented lichen thalli. Both types of lichen thalli comprised multiple species of a single genus co-existing on the quartz substrate. The orange lichens all belonged to *Stellarangia* spp. and the black lichens were *Xanthoparmelia* spp. (Wirth, 2010; Arup et al., 2013).

Equipment and Photography

The camera used for the terrestrial photography was a Nikon D7200 24.2MP DSLR, a high-end prosumer model, combined with an 18–200 mm f/3.5–5.6 lens. The photographs for this survey were taken in bright afternoon direct sun with focal lengths between 48 and 50 mm (equivalent to 72–75 mm on a 35 mm camera). Images were captured using ISO 100 and f/8 to ensure minimal image noise and a wide depth of field. In total, 95 images were acquired in 3 passes, each a circle around the target mound at differing height and angle to ensure a high level of photographic overlap. Hyperspectral measurements were acquired using an ASD Handheld2 VNIR Spectroradiometer. This instrument allowed for readings across 325–1075 nm covering the visible and near-infrared portion of the spectrum. This was employed to measure the reflectance spectrum of light from lichens for a given pixel, as well as background substrate measurements. Wavelengths included the UV and near-UV wavelengths typically associated with photo-protective pigments, visible light including photosynthetically active wavelengths, as well as near-infra red range associated with water molecules. Calibration measurements were obtained against a Spectrolon reference disk prior to each sampling.

Structure from Motion Photogrammetry

Structure from Motion (SfM) is a process for obtaining 3D information from a series of 2D images. It is seen as a revolution in the field of geospatial science, as compared to traditional

[1]http://www.gobabebtrc.org/

photogrammetry techniques which require detailed *a priori* camera position. The SfM approach solves the geometric location of features in a scene and those of camera positions and orientations simultaneously (Westoby et al., 2012).

Recent developments in the field computer vision have resulted in the release of a number of commercial and open-source software packages. This project utilized RealityCapture[2] for the photogrammetric reconstruction of the Lichen field, including the initial camera alignment and sparse point cloud generation followed by densification and 3D meshing. The resulting model comprised 78.5 million triangles and 39.4 million points, exported as a colourised point cloud for further analysis.

Geospatial Analysis

Point data over the site were analyzed using an open source point cloud visualization software CloudCompare[3] for the discrimination of lichen species based on color. Classification raster and Digital Surface Model (DSM) raster datasets were further exported to ESRI ArcGIS software for additional processing including slope and aspect analysis.

RESULTS AND DISCUSSION

Visual characterization of microbial habitats and colonization using advanced photogrammetry is an emerging and potentially powerful tool in microbial ecology. This approach has particular relevance in fragile or poorly accessible habitats such as deserts and has several advantages over conventional field sampling surveys that involve physical displacement or removal of samples, since recovery of disturbed desert microbial communities may occur on decadal or even longer timescales (Belnap and Eldridge, 2003). Furthermore, the technique may have important applications in the search for extant life on the surface of Mars (Fairén et al., 2010). Here we report a proof of concept study that demonstrates how advanced photogrammetry can be applied to accurately determine colonization and identity of desert lichens without disturbance.

The quartz pavement study site was characterized by numerous elevated mounds up to several meters in diameter where colonization was more pronounced than at elevations several centimeteres lower. We focused our activity on a single mound with the intention to demonstrate the feasibility of photogrammetry for lichen surveys (**Figure 1a**). This area was colonized by orange *Stellarangia* spp. and black *Xanthoparmelia* spp. (**Figures 1b,c**). Initially lichens were classified within the 3D point cloud based on spectral properties measured using the RGB camera, the distinctive orange color of *Stellarangia* spp. was identified through a simple threshold for the ratio of red to blue and green. The point cloud was also visualized showing relative local elevation (**Figure 2**). This revealed that exposed quartz surfaces were the most elevated parts of the micro-habitat. This supports field observations that lichens colonize these surfaces in order to access moisture from coastal fog events

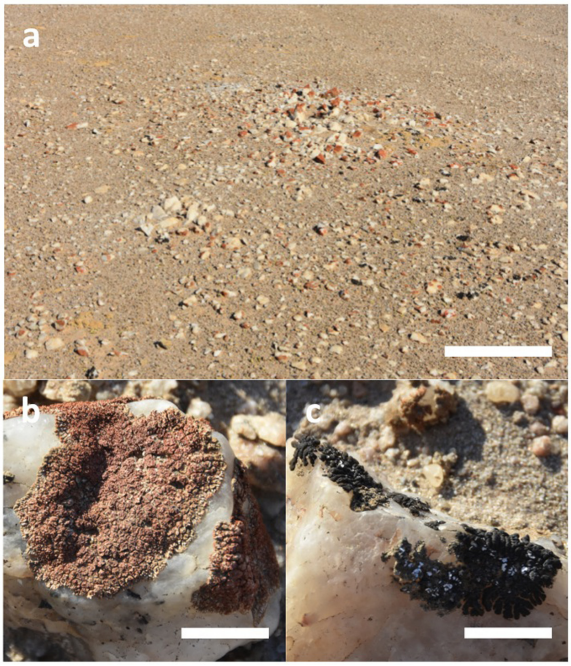

FIGURE 1 | (a) Elevated mound supporting epilithic lichens on quartz pavement in the Namib Desert (scale bar 1 m). **(b)** Orange lichen *Stellarangia* spp. (scale bar 10 mm). **(c)** Black lichen *Xanthoparmelia* spp. (scale bar 10 mm). Each genus was encountered as multiple morphospecies co-existing within the same quartz fragments.

(Lange and Green, 2008), a strategy that has also been proposed for hypolithic microbial communities beneath quartz (Warren-Rhodes et al., 2006, 2007; Azúa-Bustos et al., 2011) and those colonizing deliquescent substrates in other deserts (Davila et al., 2008; Wierzchos et al., 2015). Interestingly the exploitation of deliquescent substrates has been postulated as a potential strategy for any extant life on the surface of Mars in order to access moisture that would otherwise be biologically unavailable as well as during stochastic moisture events (Davila et al., 2010). Our findings further suggest that a consideration of local terrain is also likely to be a key predictor in the search for habitable refuges on Mars, since colonization by Namib Desert lichens clearly occurred on surface features that facilitated marginal gains in moisture availability. The quartz substrate itself may also be important, since they display a generally cooler thermal regime than surrounding soil and so may act as condensation water collectors during fog events (Lange and Green, 2008; Azúa-Bustos et al., 2011).

Transforming the 3D model to a 2D orthographic projection allowed an estimate of lichen coverage on quartz surfaces (**Figure 3**). The orange *Stellarangia* spp. had coverage of 22.8% of available substrate, whilst for the black *Xanthoparmelia* spp. coverage was markedly lower at 0.6% of available substrate. This difference may reflect several unmeasured factors such as adaptation to micro-climate and habitat and/or duration of colonization. It is interesting to speculate that an albedo effect may result in hotter temperatures for the black lichen

[2]www.capturingreality.com

[3]http://www.cloudcompare.org/

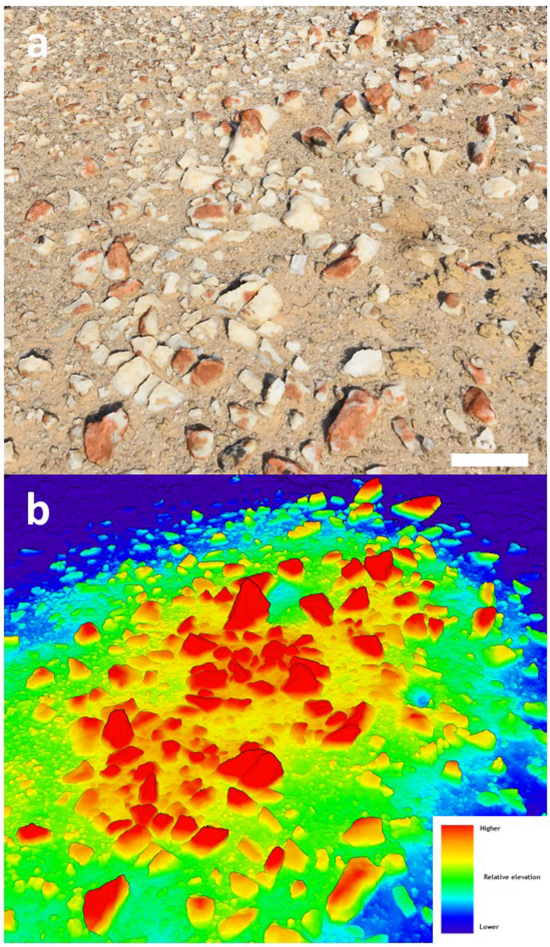

FIGURE 2 | (a) Photograph of elevated mound section showing colonized quartz (scale bar 10 cm); **(b)** heat-map based upon the 3D point cloud showing relative elevation above surface.

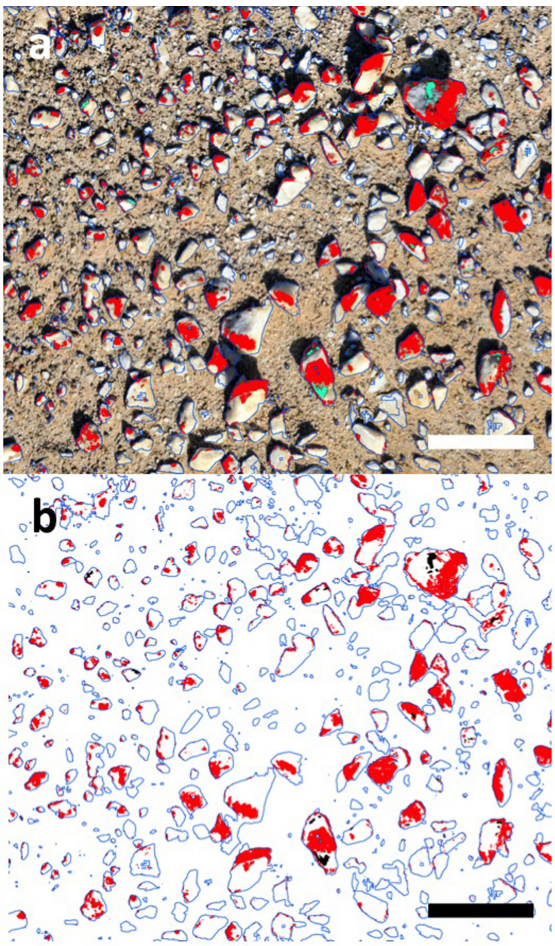

FIGURE 3 | Coverage estimates for lichen based upon transformed 2D mosaic imagery using Eye Dome Lighting. **(a)** Original image, red = orange lichen, green = black lichen (scale bar 10 cm); **(b)** transformed digital image, red = orange lichen, 22.8% cover of available substrate; green = black lichen, 0.6% cover of available substrate (scale bar 10 cm).

and this may be a factor limiting colonization in hot deserts where irradiance and ambient temperatures are extremely high. It is worth noting that the orthographic transformation used in the coverage estimates relies on creation of a 2-dimensional image from 3-dimensional imagery and so the 'top down' view that is used for this does introduce a degree of bias into coverage estimates for the 3-dimensional substrate. Further refinement of this approach will allow this bias to be better understood and addressed, although for comparative studies it is unlikely to present a major issue. This method of coverage assessment can readily be scaled up to broader spatial scales (several km^2) using both rotary and fixed wing unmanned aerial vehicles (UAV) and we have recently applied the technique to airborne surveys of microbial mats on landscape spatial scales in terrestrial Antarctic deserts (Bollard-Breen et al., 2015). In deserts the UAV approach could also be applied to vascular plants that display characteristic patterns of colonization related to resource limitation (Rietkerk et al., 2004), since although satellite multispectral imaging has been used to map vascular plants in deserts the resolution remains limited (Adam et al., 2017).

A further data set was captured using a hyper-spectral sensor that recorded reflectance from orange and black lichens from 325 to 1066 nm (**Figure 4**), and this mirrored observations for other microbially dominated biological covers in drylands (Weber et al., 2008; Chamizo et al., 2011). The curves for both lichens were distinct from that of the quartz substrate and showed characteristic dips in reflectance in the chlorophyll wavelengths (approximately 700 and 750 nm). The lower reflectance at near UV and UV wavelengths for both lichens likely occurred due to absorbance by melanised pigments and/or depisdones that are commonly produced by lichen mycobionts (Solhaug et al., 2003). At higher wavelengths anthraquinone-like compounds that account for the characteristic orange-yellow color of some lichens and are produced as photo-protective accessory pigments for chlorophyll typically absorb strongly at blue wavelengths (Solhaug and Gauslaa, 1996). Reflectance in the near infra-red

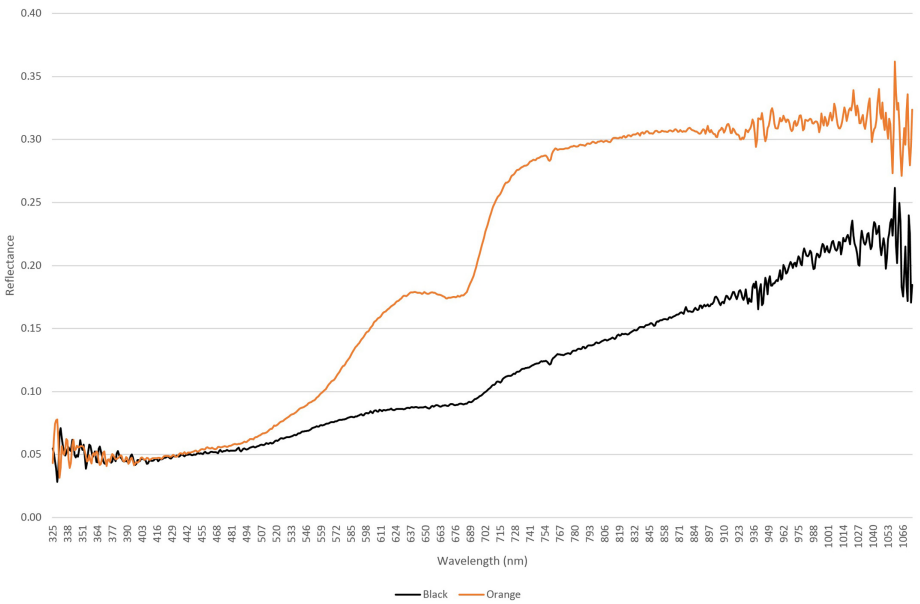

FIGURE 4 | Hyperspectral reflectance curves for orange lichen *Stellarangia* spp. and black lichen *Xanthoparmelia* spp.

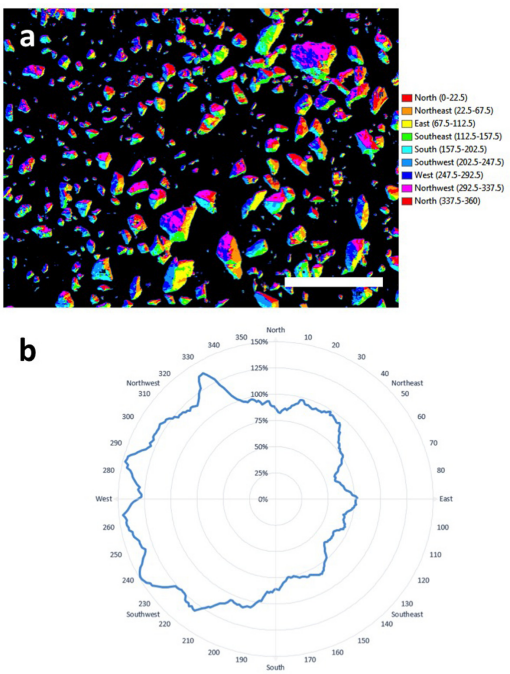

FIGURE 5 | (a) Aspect-map showing azimuth for colonized surfaces on quartz (scale bar 10 cm); **(b)** plot of azimuth for colonization showing a clear preference by lichens for west-facing surfaces.

region is associated with plant cell moisture status and can indicate plant health (Peñuelas and Filella, 1998). The near threefold difference between lichens in this range could therefore indicate that the orange lichen thalli supported a relatively more hydrated photoautotrophic biomass compared with the black lichens.

An important aspect of lichen ecology in extreme deserts is their source of moisture since this is the major limiting factor to survival in deserts (Pointing and Belnap, 2012). Further transformation of the data and assignment of surfaces to a given azimuth allowed creation of an aspect map showing azimuth for colonized surfaces on quartz (**Figure 5**). The polar plot showed that at the micro-habitat scale both orange and black lichens displayed a clear preference for colonization of west-facing surfaces. This is consistent with prevailing sources of coastal fog in this desert and so the data adds strong empirical support to the proposal that fog is the major driver of lichen colonization in the Namib Desert (Lange and Green, 2008). The thallus structure of lichens colonizing elevated substrates can be envisaged as effective water collectors, in contrast to refuge communities beneath rocky substrates that rely on an indirect moisture transfer mechanism from substrate to biomass (Pointing, 2016).

The computer vision techniques applied to these data have clear applications in the search for traces of life on the surface of Mars. Whilst there is a strong argument that any extant life today is likely to be chemotrophic and anaerobic (Westall et al., 2015) and thus comprise simple prokaryotic cells, the symbiotic relationship within lichens evolved as an adaptation to environmental stress and was likely ancestral to many extant free-living fungal taxa (Lutzoni et al., 2001). As such lichens are a useful model for any potential symbiotic associations on other planetary surfaces and both cryptoendolithic and epiphytic lichens have been demonstrated as capable of surviving extended periods in outer space (Sancho et al., 2007; Onofri et al., 2012) and simulated Mars-like conditions (de Vera et al., 2004;

de Vera et al., 2010). The image capture data presented here could feasibly be acquired from surface rover-mounted cameras on Mars surface and used to identify biological colonization as well as important supporting ecological data such as substrate and aspect preference.

A further value for photogrammetry data in microbial ecology lies in its potential value in education and outreach. We created a 3-dimensional 'fly through' video (**Supplementary Video File**) to illustrate how lichen colonization occurs at the micro-habitat scale[4] and this has clear value in allowing learners and the general public to visualize fundamentals of microbial colonization in desert research and visualize concepts in astrobiology. Ongoing refinement with user interface options such as interactive callouts and transferring 3D data to virtual reality environments will undoubtedly see the rapid emergence of new resources for many habitats and applications.

CONCLUSION

We have demonstrated the feasibility of using advanced photogrammetry to accurately map lichen coverage and discriminate between lichen taxa in the central Namib Desert. The method also allows important micro-habitat related information to be determined such as the micro-topography of colonization on the quartz substrate. The imaging systems could readily be carried as payload by fixed wing and rotary UAV to provide important landscape scale low-impact ecological surveys for deserts.

[4] https://youtu.be/aoUsJRxnV84

AUTHOR CONTRIBUTIONS

SP, AdLR, and DC conceived the study. BB-B, DC, AD, LG, AdLR, and SP conducted the fieldwork. GM-K provided fieldwork logistical support and local knowledge. GH conducted computer vision and GIS analysis. AdLR conducted lichen identifications. SBP wrote the manuscript. All authors read and commented on the draft manuscript.

ACKNOWLEDGMENTS

The authors wish to acknowledge the excellent logistical and field support provided by the Gobabeb Research and Training Centre, Gobabeb, Namibia. AdLR thanks the support of the grant CTM2015-64728-C2-2-R from the Spanish Ministry of Economy, Industry and Competitiveness.

SUPPLEMENTARY MATERIAL

FILE | 3D video fly-through of elevated mound showing quartz pavement colonised by orange and black lichens. Accessible online: https://youtu.be/aoUsJRxnV84

REFERENCES

Adam, E., Mureriwa, N., and Newete, S. (2017). Mapping Prosopis glandulosa (mesquite) in the semi-arid environment of South Africa using high-resolution WorldView-2 imagery and machine learning classifiers. *J. Arid Environ.* 145, 43–51. doi: 10.1016/j.jaridenv.2017.05.001

Archer, S. D. J., de los Ríos, A., Lee, K. C., Niederberger, T. S., Cary, S. C., Coyne, K. J., et al. (2017). Endolithic microbial diversity in sandstone and granite from the McMurdo Dry Valleys, Antarctica. *Polar Biol.* 40, 997–1006. doi: 10.1007/s00300-016-2024-9

Arup, U., Søchting, U., and Frödén, P. (2013). A new taxonomy of the family Teloschistaceae. *Nord. J. Bot.* 31, 016–083. doi: 10.1016/j.ympev.2012.01.012

Azúa-Bustos, A., González-Silva, C., Mancilla, R., Salas, L., Gómez-Silva, B., McKay, C., et al. (2011). Hypolithic cyanobacteria supported mainly by fog in the coastal range of the atacama desert. *Microb. Ecol.* 61, 568–581. doi: 10.1007/s00248-010-9784-5

Belnap, J., Büdel, B., and Lange, O. L. (2003). "Biological soil crusts: characteristics and distribution," in *Biological Soil Crusts: Structure, Function, and Management*, eds J. Belnap and O. L. Lange (Berlin: springer-Verlag), 3–30.

Belnap, J., and Eldridge, D. (2003). "Disturbance and recovery of biological soil crusts," in *Biological Soil Crusts: Structure, Function, and Management*, eds J. Belnap and O. L. Lange (Berlin: Springer-Verlag), 363–384. doi: 10.1007/978-3-642-56475-8

Bollard-Breen, B., Brooks, J. D., Jones, M. R. L., Robertson, J., Betschart, S., Kung, O., et al. (2015). Application of an unmanned aerial vehicle in spatial mapping of terrestrial biology and human disturbance in the McMurdo Dry Valleys, East Antarctica. *Polar Biol.* 38, 573–578. doi: 10.1007/s00300-014-1586-7

Chamizo, S., Cantón, Y., Lázaro, R., Solé-Benet, A., and Domingo, F. (2011). Crust composition and disturbance drive infiltration through biological soil crusts in semiarid ecosystems. *Ecosystems* 15, 148–161. doi: 10.1007/s10021-011-9499-6

Colesie, C., Allan Green, T. G., Haferkamp, I., and Büdel, B. (2014). Habitat stress initiates changes in composition, CO2 gas exchange and C-allocation as life traits in biological soil crusts. *ISME J.* 8, 2104–2115. doi: 10.1038/ismej.2014.47

Davila, A. F., Duport, L. G., Melchiorri, R., Jänchen, J., Valea, S., de Los Rios, A., et al. (2010). Hygroscopic salts and the potential for life on Mars. *Astrobiology* 10, 617–628. doi: 10.1089/ast.2009.0421

Davila, A. F., Gómez-Silva, B., de los Rios, A., Ascaso, C., Olivares, H., McKay, C. P., et al. (2008). Facilitation of endolithic microbial survival in the hyperarid core of the Atacama Desert by mineral deliquescence. *J. Geophys. Res.* 113:G01028. doi: 10.1029/2007JG000561

de Vera, J.-P., Horneck, G., Rettberg, P., and Ott, S. (2004). The potential of the lichen symbiosis to cope with the extreme conditions of outer space II: germination capacity of lichen ascospores in response to simulated space conditions. *Adv. Space Res.* 33, 1236–1243. doi: 10.1016/j.asr.2003.10.035

de Vera, J.-P., Möhlmann, D., Butina, F., Lorek, A., Wernecke, R., and Ott, S. (2010). Survival potential and photosynthetic activity of lichens under mars-like conditions: a laboratory study. *Astrobiology* 10, 215–227. doi: 10.1089/ast.2009.0362

Elbert, W., Weber, B., Burrows, S., Steinkamp, J., Büdel, B., Andreae, M. O., et al. (2012). Contribution of cryptogamic covers to the global cycles of carbon and nitrogen. *Nat. Geosci.* 5, 459–462. doi: 10.1038/ngeo1486

Fairén, A. G., Davila, A. F., Lim, D., Bramall, N., Bonaccorsi, R., Zavaleta, J., et al. (2010). Astrobiology through the ages of mars: the study of terrestrial analogues to understand the habitability of mars. *Astrobiology* 10, 821–843. doi: 10.1089/ast.2009.0440

Grady, M. (2001). *Astrobiology*. Washington, DC: Smithsonian.

Gundlapally, S. R., and Garcia-Pichel, F. (2006). The community and phylogenetic diversity of biological soil crusts in the Colorado Plateau studied by molecular fingerprinting and intensive cultivation. *Microb. Ecol.* 52, 345–357. doi: 10.1007/s00248-006-9011-6

Kranner, I., Beckett, R., Hochman, A., and Thomas, H. (2008). Desiccation-tolerance in lichens: a review desiccation-tolerance in lichens: a review. *Bryologist* 111, 576–593. doi: 10.1639/0007-2745-111.4.576

Kuske, C. R., Yeager, C. M., Johnson, S., Ticknor, L. O., and Belnap, J. (2012). Response and resilience of soil biocrust bacterial communities to chronic physical disturbance in arid shrublands. *ISME J.* 6, 886–897. doi: 10.1038/ismej.2011.153

Lange, O., and Green, T. (2008). Epilithic lichens in the namib fog desert: field measurements of water relations and carbon dioxide exchange epilithische flechten in der namib-nebelwüste: freilandmessungen von wassergehalt und. *Sauteria* 15, 283–302.

Lee, K. C., Archer, S. D. J., Boyle, R. H., Lacap-Bugler, D. C., Belnap, J., and Pointing, S. B. (2016). Niche filtering of bacteria in soil and rock habitats of the colorado plateau desert, Utah, USA. *Front. Microbiol.* 7:1489. doi: 10.3389/fmicb.2016.01489

Lutzoni, F., Pagel, M., and Reeb, V. (2001). Major fungal lineages are derived from lichen symbiotic ancestors. *Nature* 411, 937–940. doi: 10.1038/35082053

Makhalanyane, T. P., Valverde, A., Gunnigle, E., Frossard, A., Ramond, J.-B., and Cowan, D. A. (2015). Microbial ecology of hot desert edaphic systems. *FEMS Microbiol. Rev.* 39, 203–221. doi: 10.1093/femsre/fuu011

Nash, T. H. I. I. I., White, S. L., and Marsh, J. E. (1977). Lichen and moss distribution and biomass in hot desert ecosystems. *Bryologist* 80, 470–479. doi: 10.2307/3242022

Onofri, S., de la Torre, R., de Vera, J.-P., Ott, S., Zucconi, L., Selbmann, L., et al. (2012). Survival of rock-colonizing organisms after 1.5 years in outer space. *Astrobiology* 12, 508–516. doi: 10.1089/ast.2011.0736

Peel, M. C., and Finlayson, B. L. (2007). Updated world map of the Köppen-Geiger climate classification. *Hydrol. Earth Syst. Sci.* 11, 1633–1644. doi: 10.5194/hess-11-1633-2007

Peñuelas, J., and Filella, L. (1998). Visible and near-infrared reflectance techniques for diagnosing plant physiological status. *Trends Plant Sci.* 3, 151–156. doi: 10.1039/c3em00388d

Pointing, S. (2016). "Hypolithic microbial communities," in *Biological Soil Crusts: An Organising Principle in Drylands*, eds B. Weber, B. Budel, and J. Belnap (Berlin: Springer), 199–214. doi: 10.1007/978-3-319-30214-0_11

Pointing, S. B., and Belnap, J. (2012). Microbial colonization and controls in dryland systems. *Nat. Rev. Microbiol.* 10, 551–562. doi: 10.1038/nrmicro2831

Pointing, S. B., and Belnap, J. (2014). Disturbance to desert soil ecosystems contributes to dust-mediated impacts at regional scales. *Biodivers. Conserv.* 23, 1659–1667. doi: 10.1007/s10531-014-0690-x

Pointing, S. B., Warren-Rhodes, K. A., Lacap, D. C., Rhodes, K. L., and McKay, C. P. (2007). Hypolithic community shifts occur as a result of liquid water availability along environmental gradients in China's hot and cold hyperarid deserts. *Environ. Microbiol.* 9, 414–424. doi: 10.1111/j.1462-2920.2006.01153.x

Rajeev, L., da Rocha, U. N., Klitgord, N., Luning, E. G., Fortney, J., Axen, S. D., et al. (2013). Dynamic cyanobacterial response to hydration and dehydration in a desert biological soil crust. *ISME J.* 7, 2178–2191. doi: 10.1038/ismej.2013.83

Rietkerk, M., Dekker, S. C., de Ruiter, P. C., and van de Koppel, J. (2004). Self-organized patchiness and catastrophic shifts in ecosystems. *Science* 305, 1926–1929. doi: 10.1126/science.1101867

Rutherford, W. A., Painter, T. H., Ferrenberg, S., Belnap, J., Okin, G. S., Flagg, C., et al. (2017). Albedo feedbacks to future climate via climate change impacts on dryland biocrusts. *Sci. Rep.* 7:44188. doi: 10.1038/srep44188

Sancho, L. G., de la Torre, R., Horneck, G., Ascaso, C., de los Rios, A., Pintado, A., et al. (2007). Lichens survive in space: results from the 2005 LICHENS experiment. *Astrobiology* 7, 443–454. doi: 10.1089/ast.2006.0046

Solhaug, K. A., and Gauslaa, Y. (1996). Parietin, a photoprotective secondary product of the lichen *Xanthoria parietina*. *Oecologia* 108, 412–418. doi: 10.1007/BF00333715

Solhaug, K. A., Gauslaa, Y., Nybakken, L., and Bilger, W. (2003). UV-induction of sun-screening pigments in lichens. *New Phytol.* 158, 91–100. doi: 10.1046/j.1469-8137.2003.00708.x

Stomeo, F., Valverde, A., Pointing, S. B., McKay, C. P., Warren-Rhodes, K. A., Tuffin, M. I., et al. (2013). Hypolithic and soil microbial community assembly along an aridity gradient in the Namib Desert. *Extremophiles* 17, 329–337. doi: 10.1007/s00792-013-0519-7

Thomas, D. S. G. (2011). "Arid environments: their nature and extent," in *Arid Zone Geomorphology: Process, Form and Change in Drylands*, ed. D. S. G. Thomas (Hoboken, NJ: Wiley-Balckwell), 3–16. doi: 10.1002/9780470710777

UNEP (1992). *World Atlas of Desertification*. London: Edward Arnold.

Warren-Rhodes, K. A., Rhodes, K. L., Boyle, L. N., Pointing, S. B., Chen, Y., Liu, S., et al. (2007). Cyanobacterial ecology across environmental gradients and spatial scales in China's hot and cold deserts. *FEMS Microbiol. Ecol.* 61, 470–482. doi: 10.1111/j.1574-6941.2007.00351.x

Warren-Rhodes, K. A., Rhodes, K. L., Pointing, S. B., Ewing, S. A., Lacap, D. C., Gomez-Silva, B., et al. (2006). Hypolithic cyanobacteria, dry limit of photosynthesis, and microbial ecology in the hyperarid Atacama Desert. *Microb. Ecol.* 52, 389–398. doi: 10.1007/s00248-006-9055-7

Weber, B., Olehowski, C., Knerr, T., Hill, J., Deutschewitz, K., Wessels, D. C. J., et al. (2008). A new approach for mapping of biological soil crusts in semidesert areas with hyperspectral imagery. *Remote Sens. Environ.* 112, 2187–2201. doi: 10.1016/j.rse.2007.09.014

Westall, F., Foucher, F., Bost, N., Bertrand, M., Loizeau, D., Vago, J. L., et al. (2015). Biosignatures on mars: what, where, and how? Implications for the search for martian life. *Astrobiology* 15, 998–1029. doi: 10.1089/ast.2015.1374

Westoby, M. J., Brasington, J., Glasser, N. F., Hambrey, M. J., and Reynolds, J. M. (2012). 'Structure-from-Motion' photogrammetry: a low-cost, effective tool for geoscience applications. *Geomorphology* 179, 300–314. doi: 10.1016/j.geomorph.2012.08.021

Wierzchos, J., Ascaso, C., and McKay, C. P. (2006). Endolithic cyanobacteria in halite rocks from the hyperarid core of the Atacama Desert. *Astrobiology* 6, 415–422. doi: 10.1089/ast.2006.6.415

Wierzchos, J., DiRuggiero, J., Vítek, P., Artieda, O., Souza-Egipsy, V., Škaloud, P., et al. (2015). Adaptation strategies of endolithic chlorophototrophs to survive the hyperarid and extreme solar radiation environment of the Atacama Desert. *Front. Microbiol.* 6:934. doi: 10.3389/fmicb.2015.00934

Wierzchos, J., Ríos, A. D. L., and Ascaso, C. (2012). Microorganisms in desert rocks: the edge of life on Earth. *Int. Microbiol.* 15, 173–183.

Wirth, V. (2010). *Lichens of the Namib Desert: A Guide to their Identification*. Göttingen: Klaus Hess Verlag.

Conflict of Interest Statement: The authors declare that the research was conducted in the absence of any commercial or financial relationships that could be construed as a potential conflict of interest.

frontiers in Microbiology

MINI REVIEW
published: 25 August 2017
doi: 10.3389/fmicb.2017.01622

Inhabited or Uninhabited? Pitfalls in the Interpretation of Possible Chemical Signatures of Extraterrestrial Life

Stefan Fox and Henry Strasdeit**

Department of Bioinorganic Chemistry, Institute of Chemistry, University of Hohenheim, Stuttgart, Germany

The "Rare Earth" hypothesis—put forward by Ward and Brownlee in their 2000 book of the same title—states that prokaryote-type organisms may be common in the universe but animals and higher plants are exceedingly rare. If this idea is correct, the search for extraterrestrial life is essentially the search for microorganisms. Various indicators may be used to detect extant or extinct microbial life beyond Earth. Among them are chemical biosignatures, such as biomolecules and stable isotope ratios. The present minireview focuses on the major problems associated with the identification of chemical biosignatures. Two main types of misinterpretation are distinguished, namely false positive and false negative results. The former can be caused by terrestrial biogenic contaminants or by abiotic products. Terrestrial contamination is a common problem in space missions that search for biosignatures on other planets and moons. Abiotic organics can lead to false positive results if erroneously interpreted as biomolecules, but also to false negatives, for example when an abiotic source obscures a less productive biological one. In principle, all types of putative chemical biosignatures are prone to misinterpretation. Some, however, are more reliable ("stronger") than others. These include: (i) homochiral polymers of defined length and sequence, comparable to proteins and polynucleotides; (ii) enantiopure compounds; (iii) the existence of only a subset of molecules when abiotic syntheses would produce a continuous range of molecules; the proteinogenic amino acids constitute such a subset. These considerations are particularly important for life detection missions to solar system bodies such as Mars, Europa, and Enceladus.

Keywords: false positives, false negatives, contaminants, abiotic organics, biomolecules, inorganic metabolites, Mars, icy moons

OPEN ACCESS

Edited by:
Karen Olsson-Francis,
The Open University, United Kingdom

Reviewed by:
Jens Kallmeyer,
Helmholtz-Zentrum Potsdam Deutsches GeoForschungsZentrum (GFZ), Germany
Amy Michele Grunden,
North Carolina State University, United States

****Correspondence:***
Stefan Fox
stefan.fox@uni-hohenheim.de
Henry Strasdeit
henry.strasdeit@uni-hohenheim.de

Specialty section:
This article was submitted to Extreme Microbiology, a section of the journal Frontiers in Microbiology

Received: *02 June 2017*
Accepted: *09 August 2017*
Published: *25 August 2017*

Citation:
Fox S and Strasdeit H (2017) Inhabited or Uninhabited? Pitfalls in the Interpretation of Possible Chemical Signatures of Extraterrestrial Life. Front. Microbiol. 8:1622. doi: 10.3389/fmicb.2017.01622

INTRODUCTION

Life can leave different kinds of signatures. Fossil evidence of microorganisms, for example, can be morphological (e.g., fossilized cells) or chemical (organic, mineralogical, elemental, isotopic; Westall and Cavalazzi, 2011). Biosignatures by definition are of biological origin. However, even the discrimination between fossilized cells and abiogenic structures, which might be expected to be straightforward, can require special methods and sophisticated instrumentation (Westall et al., 2011). A cautionary example is the erroneous interpretation of filamentous structures in 3.46 Ga

old rocks from the Pilbara Craton of northwestern Australia. These structures were originally believed to be cyanobacterial microfossils (Schopf, 1993). This view was later challenged ("Schopf–Brasier controversy"; see Hazen, 2005). Strong evidence against the biogenicity of these structures comes from chemistry. Chemical analysis by Raman spectroscopy revealed that morphologically similar structures from the same locality as the original specimens were in fact quartz and haematite-filled fractures (Marshall et al., 2011; Marshall and Marshall, 2013). Interestingly, carbonaceous material, though not associated with these structures, occurs disseminated in the surrounding mineral matrix. It could be a degradation product of biomolecules, in other words, a chemical biosignature.

Searching for chemical constituents of organisms and other chemical fingerprints of life is not only important in studies of ancient traces of life on Earth but is also a promising approach to establish whether other planets and moons are, or were, inhabited. Currently, the Sample Analysis at Mars (SAM) suite of instruments on NASA's Curiosity rover performs chemical analyses on Mars to assess the planet's habitability and to possibly find evidence of extant or extinct life (Mahaffy et al., 2012). In the near future, ESA's ExoMars rover and NASA's Mars 2020 rover will join the search for chemical biosignatures on the red planet (Beegle et al., 2015; Goetz et al., 2016). Chemical analyses of the (sub)surfaces and plumes of icy moons, such as Enceladus and Europa, could answer the question of whether these moons' subsurface oceans harbor life. Several studies on missions to Enceladus and Europa have been proposed. Many include the search for chemical biosignatures—for example, "Enceladus Life Finder" (ELF; Lunine et al., 2015), "Testing the Habitability of Enceladus's Ocean" (THEO; MacKenzie et al., 2016), "Enceladus Explorer" (EnEx; Konstantinidis et al., 2015), and "Europa Lander" (Hand et al., 2017). The realization of such missions, however, is still some way off.

Among the advantages of chemical biosignatures is that often well-established analytical methods such as Raman spectroscopy and gas chromatography/mass spectrometry can be used for detection and identification (Rodier et al., 2005; Villar and Edwards, 2006; Poinot and Geffroy-Rodier, 2015). Furthermore, certain "biomarkers"—a term that in a narrow sense refers to biomolecules or specific degradation products thereof—can persist over long periods of time. Examples of such "molecular fossils" are 1.64 Ga old carotenoid derivatives (Lee and Brocks, 2011) and degradation products of chlorophylls and hemes (geoporphyrins; Callot and Ocampo, 2000) which have been reported, for example, from ∼500 Ma old oil shales (Serebrennikova and Mozzhelina, 1994). Hence, the extraordinary stability of certain molecular fossils opens the prospect of detecting chemical traces of life on other planets and moons even if it became extinct a long time ago. Accurate dating, however, can be difficult because the molecules need not necessarily be of the same age as the surrounding geological matrix. A good example is 2-methylhopanes and steranes from 2.7 Ga old shales from Australia. These molecules, which derive from membrane lipids, are regarded as characteristic biomarkers for bacteria and eukaryotes, respectively. Therefore, it was originally concluded that eukaryotes and possibly oxygen-producing cyanobacteria already existed 2.7 Ga ago (Brocks et al., 1999). This conclusion was refuted by Rasmussen et al. (2008) who demonstrated that the biomarkers were not indigenous but entered the rock at least ∼0.5 Ga later.

It is often difficult to identify chemical biosignatures unambiguously because they are prone to various types of misinterpretation. In this context, two main categories can be distinguished, namely (i) chemical compounds and properties that are mistakenly considered as products of extraterrestrial life ("false positives") and (ii) chemical biosignatures of extraterrestrial origin that are not recognized as such ("false negatives"). The category of false positive biosignatures may be further subdivided into terrestrial biogenic contaminants and products of non-biological processes. This minireview gives examples of potential pitfalls in the search for extraterrestrial chemical biosignatures. It is not meant to be comprehensive. Accordingly, some aspects of the topic are not addressed—for example, unusual concentrations of elements that may or may not result from biological processing.

FALSE POSITIVES I: TERRESTRIAL CONTAMINANTS

Terrestrial biological contaminants could be unambiguously identified in some meteorites. For example, Brinton et al. (1998) found that all five samples of Antarctic micrometeorites they studied contained terrestrial amino acids. Similarly, in some Apollo lunar regolith samples the amino acids alanine, aspartic acid, glutamic acid, serine, threonine, and valine showed a clear L-enantiomeric excess, implying at least a contribution from terrestrial biology (Elsila et al., 2016). The contaminants were present despite the fact that the samples had been stored under NASA curation since their collection. Such terrestrial biological contamination of samples from space bears the risk of false positive detection of extraterrestrial molecules (or even biosignatures). However, it is necessary to ascertain that the suspicious molecules are really of terrestrial origin. In the case of meteorites, this has been accomplished, for example, by comparing the meteoritic amino acid composition with that of the environment from which the meteorite was collected (Brinton et al., 1998; Kminek et al., 2002).

In a certain sense, the contamination of extraterrestrial objects on Earth is related to the contamination of other planets and moons by spacecrafts. The latter process, called "forward contamination," is an important aspect of planetary protection (Race, 1995; Rummel, 2001) and a persistent problem in space missions (Debus, 2006). Although the main goal is to protect extraterrestrial environments against viable organisms from Earth, terrestrial extracellular biomolecules may also be deleterious, at least to the scientific exploration of these environments. Adenosine triphosphate (ATP), for example, may stay intact for 100s of sols in martian UV climate under certain conditions such as shielding by the spacecraft or in global dust storms (Schuerger et al., 2008). Thus, ATP and possibly other

terrestrial biomolecules could remain detectable on the surface of a spacecraft throughout the entire duration of a mission. Again, here is a possible source of false positives.

In addition to biological contaminants, man-made substances may also be critical. These include chemicals used in production and cleaning processes and in onboard analyses (e.g., reagents for GC–MS). They can be difficult to discern from indigenous organics or products thereof. For example, the source of the chlorinated methane derivatives CH_xCl_y that have been detected in the martian soil by the Viking Landers and more recently by the Mars Science Laboratory (MSL) rover Curiosity is unclear. They may originate from anthropogenic sources, meteoritic organics in the regolith or indigenous martian molecules (Leshin et al., 2013; Ming et al., 2014). There is a comprehensive paper by Summons et al. (2014) that deals with possible organic contaminations of martian samples with special regard to NASA's Mars 2020 rover mission, which is planned to cache samples for a future return to Earth.

FALSE POSITIVES II: ABIOTIC ORGANICS

Abiotically formed organic molecules are another potential source of false positive biosignatures. A huge number of them have been found in carbonaceous meteorites (Cronin and Chang, 1993; Schmitt-Kopplin et al., 2010), in the interstellar medium (Irvine, 1998; Kwok, 2012) and in laboratory simulations of early Earth chemistry (Miller, 1993, 1998). This diversity shows that natural abiotic pathways exist to "simple" organic compounds from virtually all classes. Porphyrins, for example, were originally regarded as "ideal biomarkers" (Suo et al., 2007), partly because no experimental evidence for their abiotic formation existed. In recent years, however, abiotic routes to these molecules have been discovered, so that we now need to look more critically at the role of porphyrins as biosignatures (Fox and Strasdeit, 2013).

There are different approaches that can help to distinguish biotic from abiotic molecules. One is to look at the relative abundances of monomers of the same compound class, such as amino acids ["monomer abundance distribution biosignature" (MADB); Dorn et al., 2011]. This approach is based on the idea that "abiotic synthesis forms the compounds that are *easy to make*. Organisms, on the other hand, make the compounds *that they need* in order to survive and compete" (Dorn, 2005). If this holds universally, which seems to be a reasonable assumption, then the differences in the distribution patterns would be a powerful tool to identify extraterrestrial chemical biosignatures.

Another approach uses the fact that abiotic synthesis yields a continuous range of members of a compound class, while organisms synthesize only a subset of the possible molecules ("Lego Principle"; McKay, 2004). The α-amino acids of the type $(^+H_3N)CHR(CO_2^-)$ are a good example. In Miller-Urey type spark discharge experiments, the members with R = Me, Et, *n*-Pr, and *iso*-Pr form together (Johnson et al., 2008). In addition to these four, the amino acids with R = *n*-Bu, *iso*-Bu, *sec*-Bu, *tert*-Bu, and the eight pentyl isomers were detected in the Murchison meteorite (Meierhenrich, 2008). However, only four out of these 16 homologs occur in proteins, namely alanine (R = Me), valine (R = *iso*-Pr), leucine (R = *iso*-Bu), and isoleucine (R = *sec*-Bu). In the Lego Principle, the mere fact that a discontinuous instead of a continuous distribution pattern exists is indicative of a biological origin. Details of the subset play a subordinate role (Davies et al., 2009). This is advantageous because an extraterrestrial organism may use subsets different from those of terrestrial organisms. Nevertheless, knowing the exact nature of the subset may be important to exclude terrestrial biological contamination. Biological homochirality also fits into the Lego Principle (see below).

In addition to the chemical structures, stable isotope ratios have been used to infer the source of organic compounds. A strong depletion in ^{13}C, for example, is often interpreted as an indication of biogenic origin. However, results of laboratory experiments suggest that abiotic Fischer–Tropsch-type syntheses in hydrothermal settings can produce degrees of ^{13}C depletion similar to those found in organisms (McCollom and Seewald, 2006). Therefore, the carbon isotope ratio alone may not be particularly suitable to identify biological carbon and may lead to false positive identification of biomolecules in extraterrestrial samples. An actual case is the methane that has been detected in trace concentrations in the martian atmosphere. The release of this gas from carbonaceous meteorites by ultraviolet radiation—a possible source on Mars—has been studied experimentally by Keppler et al. (2012). The authors found that the deuterium isotopic signature clearly confirmed the extraterrestrial origin of methane released from the Murchison meteorite. In contrast, the $\delta^{13}C$ values were in the range of the carbon isotopic signatures of methane from terrestrial biogenic sources. Some of the $\delta^{13}C$ data from NOMAD might be similarly misleading. NOMAD is part of the ExoMars Trace Gas Orbiter payload and designed to spectroscopically determine isotope ratios in atmospheric molecules such as methane and carbon dioxide (Vandaele et al., 2015). Fortunately, the combined measurement of different isotopologs (for example, $^{13}CH_4$, CH_3D and $^{13}CO_2$, ^{17}OCO, ^{18}OCO, $C^{18}O_2$) is planned. This will certainly reduce the danger of misinterpretation of results.

FALSE NEGATIVES

Situations are conceivable where a substantial risk of false negative chemical biosignatures exists. For example, when a molecule simultaneously has a biotic and an abiotic source and the biotic production rate is low, the partially biological origin of this molecule may be overlooked. This situation might occur for methane on other planets and moons. In fact, on Earth, methane is not only produced by archaea and by decomposition of organic matter but also by magmatic processes and gas–water–rock interactions (Horita and Berndt, 1999; Etiope and Sherwood Lollar, 2013). Terrestrial hydrothermal systems are typical environments where both biological and non-biological methane sources coexist (Bradley, 2016). In this context, it is

interesting to note that hydrothermal activity probably also occurs on the ocean floor of Saturn's moon Enceladus (Hsu et al., 2015). Other compounds that have biotic and abiotic sources are the oxalate minerals, such as whewellite ($CaC_2O_4 \cdot H_2O$). Oxalates on Mars, for example, may originate from meteoritic organic material as well as from extant or extinct martian life (Applin et al., 2015).

Some structural criteria that are useful in identifying molecules of terrestrial biological origin may fail when applied to extraterrestrial samples. For example, the odd-over-even predominance found in many sedimentary *n*-alkanes indicates an origin from biomolecules, namely fatty acids with even numbers of C atoms. It is routinely regarded as diagnostic of a biological origin (for example, of a 3.5 Ga old kerogen; Derenne et al., 2008). Rare cases of even-over-odd predominance in *n*-alkanes have been reported (Nishimura and Baker, 1986). Nevertheless, according to the Lego Principle (see above), the mere existence of a predominance is a strong biosignature—at least in terrestrial samples. Fatty acids of an extraterrestrial organism, however, may be neither preferentially even- nor odd-chain. Thus, their biological origin can remain unrecognized if the even–odd pattern is the only criterion used. This false negative may possibly be avoided by searching for structural features that can occur in biological fatty acids, such as unsaturation, chain branching, and others (Georgiou and Deamer, 2014). In general, an alien biochemistry, even if carbon-based, could be very different from the one we know (Schulze-Makuch and Irwin, 2008). Therefore, its molecules may not be readily recognized as biosignatures.

Extensive destruction of biomolecules by heat and/or pressure (for example, in diagenesis; Hatcher and Clifford, 1997; Killops and Killops, 2005; Wakeham and Canuel, 2006; Vandenbroucke and Largeau, 2007; Arndt et al., 2013) or by energetic radiation (Ward, 1985; Garrison, 1987; Kempner, 1993) can lead to inconclusive or even false negative results because the decomposition products may not reveal their origin. Unfavorable properties could make some decomposition products difficult to detect. The glycine thermomelanoid may be a good example. Its composition is not well-defined and depends on the formation temperature, the material has a low solubility, and its spectra are not particularly informative (Fox et al., 2015).

Recently, a promising technique for the detection of viable microorganisms has been described (Kasas et al., 2015). It is based on the nanoscale fluctuations that a living cell shows due to its metabolic activity. This method is independent of specific biomolecules because it observes a physical manifestation of the *overall* metabolism. Therefore, it avoids the problem of false negatives that can occur with identifying extraterrestrial biomolecules (see above). Of course, this technique can only detect sufficiently metabolically active cells, but not dead or dormant ones.

Finally, it is important to emphasize that negative results in the detection of a chemical biosignature should not be equated with its absence. The biosignature may be present but in concentrations below the analytical detection limit, or the respective environment may prevent its detection. Here, the sentence "Absence of evidence is not evidence of absence" applies (Sagan, 1995).

BIOPOLYMERS

It is highly unlikely that a natural abiotic process generates long chain molecules that have precisely defined lengths, ordered sequences, and homochiral building blocks. Therefore, proteins and nucleic acids can certainly be regarded as strong chemical biosignatures. Alien life forms, too, will probably be built on ordered polymers, but not necessarily on polypeptides and polynucleotides (Schulze-Makuch and Irwin, 2008).

Biopolymers break down more or less rapidly outside of living organisms. The decomposition often proceeds until the ultimately biological origin is no longer identifiable (false negatives, see above). In exceptional cases, however, larger fragments can still be intact after very long periods of time. With respect to long-term stability, proteins are more promising than DNA (Cappellini et al., 2014). An intriguing example of very old protein fragments is collagen peptides that have been detected in bone matrix from a ∼80 Ma old *Brachylophosaurus canadensis* specimen (Schroeter et al., 2017). Hence, it is perhaps not over-optimistic to assume that biopolymer fragments can have long lifetimes on other planetary bodies, too, if the conditions are favorable. However, even on Earth unambiguous identification is difficult, as shown by a recent example (Arnaud, 2017; Lee et al., 2017).

HOMOCHIRALTY AND ENANTIOPURITY

Homochiral and enantiopure molecules each form "subsets" in terms of the Lego Principle (see above). Homochirality and, in the case of individual compounds, enantiopurity represent powerful chemical biosignatures. No natural non-biological processes that generate them have been observed in nature, but there are some indications that, at least in rare instances, natural abiotic compounds might be enantiopure. For example, there is a single case where, under laboratory conditions, a small enantiomeric excess of an amino acid was amplified to near enantiopurity (>99%; Klussmann et al., 2006). This amino acid was serine under solid–liquid equilibrium conditions in water at the eutectic point. However, for all other amino acids tested, enantiopurity was not achieved. Also, this mechanism will not work with chiral compounds that crystallize as conglomerates (i.e., mixtures of pure L and pure D crystals). Because of the special conditions and compounds necessary, it is unclear if this physical process is relevant to the generation of enantiopurity (i.e., enantiomeric excesses near 100%) in extraterrestrial environments.

In addition, as-yet-undiscovered abiotic chemical reactions that yield enantiopure products might exist in nature. In fact, a laboratory reaction is known that can amplify enantiomeric excesses as low as 10^{-5} % to virtual enantiopurity (>99.5%; Soai and Kawasaki, 2008). This so-called Soai reaction is, however, highly water-sensitive and therefore not relevant to habitable environments.

Low to moderate enantiomeric excesses, as they occur, for example, in meteoritic α,α-dialkyl amino acids (Pizzarello and Cronin, 2000), are definitely not indicative of a biological origin. On the other hand, a lack of enantiopurity can be a false-negative

result because the initial enantiopurity could have been lost by racemization, a process well-known for the proteinogenic L-amino acids (Bada and Schroeder, 1975; Bada, 1985). Furthermore, one should not discard the possibility that an extraterrestrial organism synthesizes both enantiomers. In fact, terrestrial bacteria produce diverse D-amino acids (e.g., D-Ala, D-Glu, D-Leu, D-Met, D-Phe, and D-Tyr) which have effects on the peptidoglycan of the cell wall, both directly by incorporation into the polymer and indirectly by regulating enzymes that synthesize and modify peptidoglycan (Höltje, 1998; Lam et al., 2009). Another intriguing example from terrestrial life is the simultaneous presence of L- and D-isovaline in some fungal peptides (Degenkolb et al., 2007).

INORGANIC METABOLIC PRODUCTS

Certain inorganic compounds—mainly biominerals and some simple gasses—can also serve as indicators of biological activity. They may, however, face the same problem of ambiguity as organic biosignatures. A well-known example is the magnetite crystals in the martian meteorite ALH84001. They have been interpreted as a biomineral similar to the magnetosome crystals of terrestrial magnetotactic bacteria (McKay et al., 1996). Although this interpretation cannot be excluded, it remains inconclusive (Weiss et al., 2004). Other features of ALH84001 which were originally taken as evidence for former life on Mars appear to be even less conclusive (Jakosky et al., 2007). These include (i) ovoid structures that were interpreted as microbial fossils but appear to be too small for bacterial cells, do not meet the criteria for microbial fossils (Westall and Cavalazzi, 2011) and can be explained as products of aqueous corrosion of carbonates; and (ii) organic compounds that were regarded as chemical biosignatures but were mainly of terrestrial origin, and those of martian origin could have been formed by non-biological processes.

Chemical disequilibria that would rapidly disappear if the input from metabolic activity ceases can be relatively robust biosignatures. For example, considering the O_2 concentration, the methane concentration in the terrestrial atmosphere appears to be several orders of magnitude too high (Sagan, 1970). A high O_2 concentration, if discovered in the atmosphere of a rocky exoplanet with moderate surface temperature, is often regarded as a good indicator of biological photosynthesis (Léger et al., 2011). This view, however, has been challenged by the argument that abiotic water photolysis on a habitable-zone planet can also produce an oxygen-dominated atmosphere and thus may result in a false positive for life (Wordsworth and Pierrehumbert, 2014). According to Stüeken et al. (2016), it is unlikely that high levels of *abiotic* O_2 can coexist with high levels of N_2. In other words, the simultaneous presence of large amounts of both O_2 and N_2 indicates an aerobic biosphere and reduces the risk of false positives.

CONCLUDING REMARKS

In summary, it can be said that no putative chemical biosignature is inherently safe from misinterpretation. In the coming years, life-detection missions will focus on Mars and the icy moons of Jupiter and Saturn. Spacecrafts going to these destinations should not only be capable of performing sophisticated chemical analyses but also provide as much as possible contextual information, which is essential to identify chemical biosignatures. Returning extraterrestrial samples to Earth for analysis would be a major step forward. Indeed, sample return from the surface of Mars or the plumes of Enceladus is now within the realm of the technologically feasible.

AUTHOR CONTRIBUTIONS

SF and HS conceived, wrote and edited the minireview, and approved it for publication.

REFERENCES

Applin, D. M., Izawa, M. R. M., Cloutis, E. A., Goltz, D., and Johnson, J. R. (2015). Oxalate minerals on Mars? *Earth Planet. Sci. Lett.* 420, 127–139. doi: 10.1016/j.epsl.2015.03.034

Arnaud, C. (2017). Collagen found in 195 million-year-old dinosaur bone, perhaps. *Chem. Eng. News* 95, 6.

Arndt, S., Jørgensen, B. B., LaRowe, D. E., Middelburg, J. J., Pancost, R. D., and Regnier, P. (2013). Quantifying the degradation of organic matter in marine sediments: a review and synthesis. *Earth Sci. Rev.* 123, 53–86. doi: 10.1016/j.earscirev.2013.02.008

Bada, J. L. (1985). "Racemization of amino acids," in *Chemistry and Biochemistry of the Amino Acids*, ed. G. C. Barrett (London: Chapman and Hall), 399–414.

Bada, J. L., and Schroeder, R. A. (1975). Amino acid racemization reactions and their geochemical implications. *Naturwissenschaften* 62, 71–79. doi: 10.1007/BF00592179

Beegle, L., Bhartia, R., White, M., DeFlores, L., Abbey, W., Wu, Y.-H., et al. (2015). "SHERLOC: scanning habitable environments with Raman & luminescence for organics & chemicals," in *Proceedings of the 2015 IEEE Aerospace Conference*, Big Sky, MT, 1–11. doi: 10.1109/aero.2015.7119105

Bradley, A. S. (2016). The sluggish speed of making abiotic methane. *Proc. Natl. Acad. Sci. U.S.A.* 113, 13944–13946. doi: 10.1073/pnas.1617103113

Brinton, K. L. F., Engrand, C., Glavin, D. P., Bada, J. L., and Maurette, M. (1998). A search for extraterrestrial amino acids in carbonaceous Antarctic micrometeorites. *Orig. Life Evol. Biosph.* 28, 413–424. doi: 10.1023/A:1006548905523

Brocks, J. J., Logan, G. A., Buick, R., and Summons, R. E. (1999). Archean molecular fossils and the early rise of eukaryotes. *Science* 285, 1033–1036. doi: 10.1126/science.285.5430.1033

Callot, H. J., and Ocampo, R. (2000). "Geochemistry of porphyrins," in *The Porphyrin Handbook*, Vol. 1, eds K. M. Kadish, K. M. Smith, and R. Guilard (San Diego, CA: Academic Press), 349–398.

Cappellini, E., Collins, M. J., and Gilbert, M. T. P. (2014). Unlocking ancient protein palimpsests. *Science* 343, 1320–1322. doi: 10.1126/science.1249274

Cronin, J. R., and Chang, S. (1993). "Organic matter in meteorites: molecular and isotopic analyses of the Murchison meteorite," in *The Chemistry of Life's Origins*, eds J. M. Greenberg, C. X. Mendoza-Gómez, and V. Pirronello (Dordrecht: Springer), 209–258.

Davies, P. C. W., Benner, S. A., Cleland, C. E., Lineweaver, C. H., McKay, C. P., and Wolfe-Simon, F. (2009). Signatures of a shadow biosphere. *Astrobiology* 9, 241–249. doi: 10.1089/ast.2008.0251

Debus, A. (2006). The European standard on planetary protection requirements. *Res. Microbiol.* 157, 13–18. doi: 10.1016/j.resmic.2005.06.013

Degenkolb, T., Kirschbaum, J., and Brückner, H. (2007). New sequences, constituents, and producers of peptaibiotics: an updated review. *Chem. Biodivers.* 4, 1052–1067. doi: 10.1002/cbdv.200790096

Derenne, S., Robert, F., Skrzypczak-Bonduelle, A., Gourier, D., Binet, L., and Rouzaud, J.-N. (2008). Molecular evidence for life in the 3.5 billion year old Warrawoona chert. *Earth Planet. Sci. Lett.* 272, 476–480. doi: 10.1016/j.epsl.2008.05.014

Dorn, E. D. (2005). *Universal Biosignatures for the Detection of Life*. Ph.D. thesis, California Institute of Technology, Pasadena, CA.

Dorn, E. D., Nealson, K. H., and Adami, C. (2011). Monomer abundance distribution patterns as a universal biosignature: examples from terrestrial and digital life. *J. Mol. Evol.* 72, 283–295. doi: 10.1007/s00239-011-9429-4

Elsila, J. E., Callahan, M. P., Dworkin, J. P., Glavin, D. P., McLain, H. L., Noble, S. K., et al. (2016). The origin of amino acids in lunar regolith samples. *Geochim. Cosmochim. Acta* 172, 357–369. doi: 10.1016/j.gca.2015.10.008

Etiope, G., and Sherwood Lollar, B. (2013). Abiotic methane on Earth. *Rev. Geophys.* 51, 276–299. doi: 10.1002/rog.20011

Fox, S., Dalai, P., Lambert, J.-F., and Strasdeit, H. (2015). Hypercondensation of an amino acid: synthesis and characterization of a black glycine polymer. *Chem. Eur. J.* 21, 8897–8904. doi: 10.1002/chem.201500820

Fox, S., and Strasdeit, H. (2013). A possible prebiotic origin on volcanic islands of oligopyrrole-type photopigments and electron transfer cofactors. *Astrobiology* 13, 578–595. doi: 10.1089/ast.2012.0934

Garrison, W. M. (1987). Reaction mechanisms in the radiolysis of peptides, polypeptides, and proteins. *Chem. Rev.* 87, 381–398. doi: 10.1021/cr00078a006

Georgiou, C. D., and Deamer, D. W. (2014). Lipids as universal biomarkers of extraterrestrial life. *Astrobiology* 14, 541–549. doi: 10.1089/ast.2013.1134

Goetz, W., Brinckerhoff, W. B., Arevalo, R. Jr., Freissinet, C., Getty, S., Glavin, D. P., et al. (2016). MOMA: the challenge to search for organics and biosignatures on Mars. *Int. J. Astrobiol.* 15, 239–250. doi: 10.1017/S1473550416000227

Hand, K. P., Murray, A. E., Garvin, J. B., Brinckerhoff, W. B., Christner, B. C., Edgett, K. S., et al. (2017). *Report of the Europa Lander Science Definition Team*. Available at: http://solarsystem.nasa.gov/docs/Europa_Lander_SDT_Report_2016.pdf [accessed March 23, 2017].

Hatcher, P. G., and Clifford, D. J. (1997). The organic geochemistry of coal: from plant materials to coal. *Org. Geochem.* 27, 251–274. doi: 10.1016/S0146-6380(97)00051-X

Hazen, R. M. (2005). *Genesis: The Scientific Quest for Life's Origin*. Washington, DC: Joseph Henry Press, 37–44.

Höltje, J.-V. (1998). Growth of the stress-bearing and shape-maintaining murein sacculus of *Escherichia coli*. *Microbiol. Mol. Biol. Rev.* 62, 181–203.

Horita, J., and Berndt, M. E. (1999). Abiogenic methane formation and isotopic fractionation under hydrothermal conditions. *Science* 285, 1055–1057. doi: 10.1126/science.285.5430.1055

Hsu, H.-W., Postberg, F., Sekine, Y., Shibuya, T., Kempf, S., Horányi, M., et al. (2015). Ongoing hydrothermal activities within Enceladus. *Nature* 519, 207–210. doi: 10.1038/nature14262

Irvine, W. M. (1998). Extraterrestrial organic matter: a review. *Orig. Life Evol. Biosph.* 28, 365–383. doi: 10.1023/A:1006574110907

Jakosky, B. M., Westall, F., and Brack, A. (2007). "Mars," in *Planets and Life: The Emerging Science of Astrobiology*, eds W. T. Sullivan III and J. A. Baross (Cambridge: Cambridge University Press), 357–387.

Johnson, A. P., Cleaves, H. J., Dworkin, J. P., Glavin, D. P., Lazcano, A., and Bada, J. L. (2008). The Miller volcanic spark discharge experiment. *Science* 322, 404. doi: 10.1126/science.1161527

Kasas, S., Ruggeri, F. S., Benadiba, C., Maillard, C., Stupar, P., Tournu, H., et al. (2015). Detecting nanoscale vibrations as signature of life. *Proc. Nat. Acad. Sci. U.S.A.* 112, 378–381. doi: 10.1073/pnas.1415348112

Kempner, E. S. (1993). Damage to proteins due to the direct action of ionizing radiation. *Q. Rev. Biophys.* 26, 27–48. doi: 10.1017/S0033583500003954

Keppler, F., Vigano, I., McLeod, A., Ott, U., Früchtl, M., and Röckmann, T. (2012). Ultraviolet-radiation-induced methane emissions from meteorites and the martian atmosphere. *Nature* 486, 93–96. doi: 10.1038/nature11203

Killops, S., and Killops, V. (2005). *Introduction to Organic Geochemistry*, 2nd Edn. Malden, MA: Blackwell, 117–165.

Klussmann, M., Iwamura, H., Mathew, S. P., Wells, D. H. Jr., Pandya, U., Armstrong, A., et al. (2006). Thermodynamic control of asymmetric amplification in amino acid catalysis. *Nature* 441, 621–623. doi: 10.1038/nature04780

Kminek, G., Botta, O., Glavin, D. P., and Bada, J. L. (2002). Amino acids in the Tagish Lake meteorite. *Meteorit. Planet. Sci.* 37, 697–701. doi: 10.1111/j.1945-5100.2002.tb00849.x

Konstantinidis, K., Flores Martinez, C. L., Dachwald, B., Ohndorf, A., Dykta, P., Bowitz, P., et al. (2015). A lander mission to probe subglacial water on Saturn's moon Enceladus for life. *Acta Astronaut.* 106, 63–89. doi: 10.1016/j.actaastro.2014.09.012

Kwok, S. (2012). *Organic Matter in the Universe*. Weinheim: Wiley-VCH.

Lam, H., Oh, D.-C., Cava, F., Takacs, C. N., Clardy, J., de Pedro, M. A., et al. (2009). D-amino acids govern stationary phase cell wall remodeling in bacteria. *Science* 325, 1552–1555. doi: 10.1126/science.1178123

Lee, C., and Brocks, J. J. (2011). Identification of carotane breakdown products in the 1.64 billion year old Barney Creek Formation, McArthur Basin, northern Australia. *Org. Geochem.* 42, 425–430. doi: 10.1016/j.orggeochem.2011.02.006

Lee, Y.-C., Chiang, C.-C., Huang, P.-Y., Chung, C.-Y., Huang, T. D., Wang, C.-C., et al. (2017). Evidence of preserved collagen in an Early Jurassic sauropodomorph dinosaur revealed by synchrotron FTIR microspectroscopy. *Nat. Commun.* 8:14220. doi: 10.1038/ncomms14220

Léger, A., Fontecave, M., Labeyrie, A., Samuel, B., Demangeon, O., and Valencia, D. (2011). Is the presence of oxygen on an exoplanet a reliable biosignature? *Astrobiology* 11, 335–341. doi: 10.1089/ast.2010.0516

Leshin, L. A., Mahaffy, P. R., Webster, C. R., Cabane, M., Coll, P., Conrad, P. G., et al. (2013). Volatile, isotope, and organic analysis of martian fines with the Mars Curiosity rover. *Science* 341:1238937. doi: 10.1126/science.1238937

Lunine, J. I., Waite, J. H., Postberg, F., Spilker, L., and Clark, K. (2015). *Enceladus Life Finder: The Search for Life in a Habitable Moon*. Available at: http://www.hou.usra.edu/meetings/lpsc2015/pdf/1525.pdf [accessed March 23, 2017].

MacKenzie, S. M., Caswell, T. E., Phillips-Lander, C. M., Stavros, E. N., Hofgartner, J. D., Sun, V. Z., et al. (2016). THEO concept mission: testing the habitability of Enceladus's Ocean. *Adv. Space Res.* 58, 1117–1137. doi: 10.1016/j.asr.2016.05.037

Mahaffy, P. R., Webster, C. R., Cabane, M., Conrad, P. G., Coll, P., Atreya, S. K., et al. (2012). The sample analysis at mars investigation and instrument suite. *Space Sci. Rev.* 170, 401–478. doi: 10.1007/s11214-012-9879-z

Marshall, A. O., and Marshall, C. P. (2013). Comment on "Biogenicity of Earth's earliest fossils: a resolution of the controversy" by J. W. Schopf and A. B. Kudryavtsev, Gondwana Research, volume 22, issue 3–4, pages 761–771. *Gondwana Res.* 23, 1654–1655. doi: 10.1016/j.gr.2012.12.006

Marshall, C. P., Emry, J. R., and Marshall, A. O. (2011). Haematite pseudomicrofossils present in the 3.5-billion-year-old Apex Chert. *Nat. Geosci.* 4, 240–243. doi: 10.1038/ngeo1084

McCollom, T. M., and Seewald, J. S. (2006). Carbon isotope composition of organic compounds produced by abiotic synthesis under hydrothermal conditions. *Earth Planet. Sci. Lett.* 243, 74–84. doi: 10.1016/j.epsl.2006.01.027

McKay, C. P. (2004). What is life—and how do we search for it in other worlds? *PLoS Biol.* 2:e302. doi: 10.1371/journal.pbio.0020302

McKay, D. S., Gibson, E. K. Jr., Thomas-Keprta, K. L., Vali, H., Romanek, C. S., Clemett, S. J., et al. (1996). Search for past life on Mars: possible relic biogenic activity in martian meteorite ALH84001. *Science* 273, 924–930. doi: 10.1126/science.273.5277.924

Meierhenrich, U. (2008). *Amino Acids and the Asymmetry of Life*. Berlin: Springer, 204–205.

Miller, S. L. (1993). "The prebiotic synthesis of organic compounds on the early Earth," in *Organic Geochemistry – Principles and Applications*, eds M. H. Engel and S. A. Macko (New York, NY: Plenum Press), 625–637. doi: 10.1007/978-1-4615-2890-6_30

Miller, S. L. (1998). "The endogenous synthesis of organic compounds," in *The Molecular Origins of Life*, ed. A. Brack (Cambridge: Cambridge University Press), 59–85.

Ming, D. W., Archer, P. D. Jr., Glavin, D. P., Eigenbrode, J. L., Franz, H. B., Sutter, B., et al. (2014). Volatile and organic compositions of sedimentary rocks in Yellowknife Bay, Gale crater, Mars. *Science* 343:1245267. doi: 10.1126/science.1245267

Nishimura, M., and Baker, E. W. (1986). Possible origin of n-alkanes with a remarkable even-to-odd predominance in recent marine sediments. *Geochim. Cosmochim. Acta* 50, 299–305. doi: 10.1016/0016-7037(86)90178-X

Pizzarello, S., and Cronin, J. R. (2000). Non-racemic amino acids in the Murray and Murchison meteorites. *Geochim. Cosmochim. Acta* 64, 329–338. doi: 10.1016/S0016-7037(99)00280-X

Poinot, P., and Geffroy-Rodier, C. (2015). Searching for organic compounds in the universe. *Trends Anal. Chem.* 65, 1–12. doi: 10.1016/j.trac.2014.09.009

Race, M. S. (1995). Societal issues as Mars mission impediments: planetary protection and contamination concerns. *Adv. Space Res.* 15, 285–292. doi: 10.1016/S0273-1177(99)80099-4

Rasmussen, B., Fletcher, I. R., Brocks, J. J., and Kilburn, M. R. (2008). Reassessing the first appearance of eukaryotes and cyanobacteria. *Nature* 455, 1101–1104. doi: 10.1038/nature07381

Rodier, C., Sternberg, R., Szopa, C., Buch, A., Cabane, M., and Raulin, F. (2005). Search for organics in extraterrestrial environments by in situ gas chromatography analysis. *Adv. Space Res.* 36, 195–200. doi: 10.1016/j.asr.2004.12.072

Rummel, J. D. (2001). Planetary exploration in the time of astrobiology: protecting against biological contamination. *Proc. Natl. Acad. Sci. U.S.A.* 98, 2128–2131. doi: 10.1073/pnas.061021398

Sagan, C. (1970). *Planetary Exploration: Condon Lectures*. Eugene, OR: Oregon State System of Higher Education, 31.

Sagan, C. (1995). *The Demon-Haunted World: Science as a Candle in the Dark*. New York, NY: Random House, 213.

Schmitt-Kopplin, P., Gabelica, Z., Gougeon, R. D., Fekete, A., Kanawati, B., Harir, M., et al. (2010). High molecular diversity of extraterrestrial organic matter in Murchison meteorite revealed 40 years after its fall. *Proc. Natl. Acad. Sci. U.S.A.* 107, 2763–2768. doi: 10.1073/pnas.0912157107

Schopf, J. W. (1993). Microfossils of the Early Archean Apex Chert: new evidence of the antiquity of life. *Science* 260, 640–646. doi: 10.1126/science.260.5108.640

Schroeter, E. R., DeHart, C. J., Cleland, T. P., Zheng, W., Thomas, P. M., Kelleher, N. L., et al. (2017). Expansion for the *Brachylophosaurus canadensis* collagen I sequence and additional evidence of the preservation of Cretaceous protein. *J. Proteome Res.* 16, 920–932. doi: 10.1021/acs.jproteome.6b00873

Schuerger, A. C., Fajardo-Cavazos, P., Clausen, C. A., Moores, J. E., Smith, P. H., and Nicholson, W. L. (2008). Slow degradation of ATP in simulated martian environments suggests long residence times for the biosignature molecule on spacecraft surfaces on Mars. *Icarus* 194, 86–100. doi: 10.1016/j.icarus.2007.10.010

Schulze-Makuch, D., and Irwin, L. N. (2008). *Life in the Universe: Expectations and Constraints*, 2nd Edn. Berlin: Springer.

Serebrennikova, O. V., and Mozzhelina, T. K. (1994). Features of porphyrin compounds in Cambrian oil shales from Yakutiya, Siberia. *Org. Geochem.* 21, 891–895. doi: 10.1016/0146-6380(94)90048-5

Soai, K., and Kawasaki, T. (2008). Asymmetric autocatalysis with amplification of chirality. *Top. Curr. Chem.* 284, 1–33. doi: 10.1007/128_2007_138

Stüeken, E. E., Kipp, M. A., Koehler, M. C., Schwieterman, E. W., Johnson, B., and Buick, R. (2016). Modeling pN2 through geological time: implications for planetary climates and atmospheric biosignatures. *Astrobiology* 16, 949–963. doi: 10.1089/ast.2016.1537

Summons, R. E., Sessions, A. L., Allwood, A. C., Barton, H. A., Beaty, D. W., Blakkolb, B., et al. (2014). Planning considerations related to the organic contamination of martian samples and implications for the Mars 2020 rover. *Astrobiology* 14, 969–1027. doi: 10.1089/ast.2014.1244

Suo, Z., Avci, R., Schweitzer, M. H., and Deliorman, M. (2007). Porphyrin as an ideal biomarker in the search for extraterrestrial life. *Astrobiology* 7, 605–615. doi: 10.1089/ast.2006.0120

Vandaele, A. C., Neefs, E., Drummond, R., Thomas, I. R., Daerden, F., Lopez-Moreno, J.-J., et al. (2015). Science objectives and performances of NOMAD, a spectrometer suite for the ExoMars TGO mission. *Planet. Space Sci.* 119, 233–249. doi: 10.1016/j.pss.2015.10.003

Vandenbroucke, M., and Largeau, C. (2007). Kerogen origin, evolution and structure. *Org. Geochem.* 38, 719–833. doi: 10.1016/j.orggeochem.2007.01.001

Villar, S. E. J., and Edwards, H. G. M. (2006). Raman spectroscopy in astrobiology. *Anal. Bioanal. Chem.* 384, 100–113. doi: 10.1007/s00216-005-0029-2

Wakeham, S. G., and Canuel, E. A. (2006). "Degradation and preservation of organic matter in marine sediments," in *Marine Organic Matter: Biomarkers, Isotopes and DNA (The Handbook of Environmental Chemistry*, Vol. 2N, ed. J. K. Volkman (Berlin, Germany: Springer), 295–321.

Ward, J. F. (1985). Biochemistry of DNA lesions. *Radiat. Res.* 104, S103–S111. doi: 10.2307/3576637

Weiss, B. P., Kim, S. S., Kirschvink, J. L., Kopp, R. E., Sankaran, M., Kobayashi, A., et al. (2004). Magnetic tests for magnetosome chains in martian meteorite ALH84001. *Proc. Natl. Acad. Sci. U.S.A.* 101, 8281–8284. doi: 10.1073/pnas.0402292101

Westall, F., and Cavalazzi, B. (2011). "Biosignatures in rocks," in *Encyclopedia of Geobiology*, eds J. Reitner and V. Thiel (Dordrecht: Springer), 189–201. doi: 10.1007/978-1-4020-9212-1_36

Westall, F., Foucher, F., Cavalazzi, B., de Vries, S. T., Nijman, W., Pearson, V., et al. (2011). Volcaniclastic habitats for early life on Earth and Mars: a case study from ∼3.5 Ga-old rocks from the Pilbara, Australia. *Planet. Space Sci.* 59, 1093–1106. doi: 10.1016/j.pss.2010.09.006

Wordsworth, R., and Pierrehumbert, R. (2014). Abiotic oxygen-dominated atmospheres on terrestrial habitable zone planets. *Astrophys. J. Lett.* 785:L20. doi: 10.1088/2041-8205/785/2/L20

Conflict of Interest Statement: The authors declare that the research was conducted in the absence of any commercial or financial relationships that could be construed as a potential conflict of interest.

frontiers in Microbiology

ORIGINAL RESEARCH
published: 09 October 2017
doi: 10.3389/fmicb.2017.01918

Exploring Fingerprints of the Extreme Thermoacidophile *Metallosphaera sedula* Grown on Synthetic Martian Regolith Materials as the Sole Energy Sources

*Denise Kölbl[1], Marc Pignitter[2], Veronika Somoza[2], Mario P. Schimak[3], Oliver Strbak[4], Amir Blazevic[1] and Tetyana Milojevic[1]**

[1] Extremophiles Group, Department of Biophysical Chemistry, University of Vienna, Vienna, Austria, [2] Department of Nutritional and Physiological Chemistry, Faculty of Chemistry, University of Vienna, Vienna, Austria, [3] Department of Symbiosis, Max Planck Institute for Marine Microbiology, Bremen, Germany, [4] Biomedical Center Martin, Jessenius Faculty of Medicine in Martin, Comenius University in Bratislava, Martin, Slovakia

The biology of metal transforming microorganisms is of a fundamental and applied importance for our understanding of past and present biogeochemical processes on Earth and in the Universe. The extreme thermoacidophile *Metallosphaera sedula* is a metal mobilizing archaeon, which thrives in hot acid environments (optimal growth at 74°C and pH 2.0) and utilizes energy from the oxidation of reduced metal inorganic sources. These characteristics of *M. sedula* make it an ideal organism to further our knowledge of the biogeochemical processes of possible life on extraterrestrial planetary bodies. Exploring the viability and metal extraction capacity of *M. sedula* living on and interacting with synthetic extraterrestrial minerals, we show that *M. sedula* utilizes metals trapped in the Martian regolith simulants (JSC Mars 1A; P-MRS; S-MRS; MRS07/52) as the sole energy sources. The obtained set of microbiological and mineralogical data suggests that *M. sedula* actively colonizes synthetic Martian regolith materials and releases free soluble metals. The surface of bioprocessed Martian regolith simulants is analyzed for specific mineralogical fingerprints left upon *M. sedula* growth. The obtained results provide insights of biomining of extraterrestrial material as well as of the detection of biosignatures implementing in life search missions.

Keywords: *Metallosphaera sedula*, Martian regolith simulants, EPR spectroscopy, microbe–mineral interactions, biosignatures

OPEN ACCESS

Edited by:
Karen Olsson-Francis, The Open University, United Kingdom

Reviewed by:
Trinity L. Hamilton, University of Minnesota Twin Cities, United States
James A. Coker, University of Maryland University College, United States

****Correspondence:***
Tetyana Milojevic
tetyana.milojevic@univie.ac.at

Specialty section:
This article was submitted to Extreme Microbiology, a section of the journal Frontiers in Microbiology

Received: *30 June 2017*
Accepted: *20 September 2017*
Published: *09 October 2017*

Citation:
Kölbl D, Pignitter M, Somoza V, Schimak MP, Strbak O, Blazevic A and Milojevic T (2017) Exploring Fingerprints of the Extreme Thermoacidophile Metallosphaera sedula Grown on Synthetic Martian Regolith Materials as the Sole Energy Sources. Front. Microbiol. 8:1918. doi: 10.3389/fmicb.2017.01918

INTRODUCTION

Chemolithoautotrophy has been indicated as the most primordial form of microbial metabolism on the early Earth (Blöchl et al., 1992; Wächtershäuser, 1992; Stetter, 2006) and proposed as a possible metabolic form for other iron-mineral-rich planets like Mars (Grotzinger et al., 2014; Hurowitz et al., 2017). Recent Mars exploration missions have provided a comprehensive analysis of the physical and geochemical environment of Mars (Grotzinger, 2013; Grotzinger et al., 2014; Hurowitz et al., 2017) aiming to identify potential habitats that bear the energy sources available on this planet to support chemolithotrophic life. The rich content of iron and sulfur minerals on Mars makes iron and sulfur transforming microorganisms the prime candidates for considering as models for putative Martian extant or extinct life forms

(Amils et al., 2007; Nixon et al., 2012). In the hydrogeological and atmospheric oxygen-rich past of Mars (>3 Ga ago), such metabolically similar microorganisms might have contributed in redox cycling of elements from Martian regolith and deposition of the mineral sediments of hydrated sulfates and ferric oxide content (Amils et al., 2007). The detection of a stable redox-stratified water body along with recent mineralogical, geochemical and sedimentological investigations point to an ancient habitable fluvio-lacustrine environment at Yellowknife Bay in the Gale crater of Mars that would have been suited to harbor a Martian biosphere based on chemolithoautotrophy (Grotzinger, 2013; Grotzinger et al., 2014; Hurowitz et al., 2017). The present atmosphere of Mars contains traces of oxygen at a concentration of 0.146% (Mahaffy et al., 2013), ruling out the consideration of Mars as an environment where only anaerobic metabolism can be expected, while mineralogical analysis points to a plausible redox couple for prokaryotic respiration (Grotzinger, 2013; Grotzinger et al., 2014). In this context metal transforming extremophiles represent an exciting field of research for the study of microbe–mineral interactions in order to find the unique biosignatures of life in extreme conditions.

A rock-eating archaeon *Metallosphaera sedula*, originally isolated from a geothermal environment, flourishes in hot and acidic conditions (optimal growth at 74°C and pH 2.0) and exhibits unusual heavy-metal resistance (Huber et al., 1989; Peeples and Kelly, 1995; Auernik et al., 2008; McCarthy et al., 2014). This facultative chemolithotroph is capable of bioleaching, and the key to its chemical attack of metal ores is the redox regeneration of Fe^{3+} from Fe^{2+}. Apart from Fe-oxidizing properties, metabolically versatile *M. sedula* has the ability to use a variety of electron donors, including reduced inorganic sulfur compounds, uranium ores, as well as molecular hydrogen under microaerobic conditions (Auernik and Kelly, 2008, 2010a; Maezato et al., 2012; Mukherjee et al., 2012; Wheaton et al., 2016).

In light of future perspectives of space exploration and *in situ* resource utilization (ISRU) programs, the possible implications of the extreme thermoacidophile *M. sedula* have been already suggested for asteroid biomining (Reed, 2015). A deeper investigation of the physiology of metal transforming microorganisms and mineral–microbial interactions facilitates our understanding of the possible energy production mechanisms of early life forms. Further, it extends our understanding of putative biosignatures that can be detected during missions aiming to uncover evidence of past habitability on planetary bodies.

The main goal of this work was to explore the growth potential and metal extraction capacity of the extremely thermoacidophilic archeon *M. sedula* cultivated on four different types of Mars regolith simulants – JSC Mars 1A, P-MRS, S-MRS, and MRS07/52 as the sole energy sources, as well as to investigate the possible biosignatures of mineral–microbial interactions associated with these cases. The different simulants were used to mimic the Martian regolith composition from different locations and historical periods of Mars: a palagonitic tephra (JSC Mars 1A as a close spectral analog to the bright regions of Mars); Early Hydrous or Phyllosilicatic Mars Regolith Simulant (P-MRS, characterized by high clay content); Late Acidic or Sulfatic Mars Regolith Simulant (S-MRS, characterized by the gypsum); the highly porous Mars Regolith Simulant (MRS07/52 that simulate sediments of the Martian surface). Due to its metal oxidizing metabolic activity, when given an access to these Martian regolith simulants, *M. sedula* released soluble metal ions into the leachate solution and altered their mineral surface leaving behind specific signatures of life.

MATERIALS AND METHODS

Strain and Media Composition

Metallosphaera sedula (DSMZ 5348) cultures were grown aerobically in DSMZ88 Sulfolobus medium containing 1.3 g $(NH_4)_2SO_4$, 0.28 g KH_2PO_4, 0.25 g $MgSO_4{\cdot}7\ H_2O$, 0.07 g $CaCl_2{\cdot}2\ H_2O$ and 0.02 g $FeCl_3{\cdot}6\ H_2O$ dissolved in 1 L of water. After autoclaving, Allen's trace elements solution was added to 1 L media resulting in 1.80 mg $MnCl_2{\cdot}4\ H_2O$, 4.50 mg $Na_2B_4O_7{\cdot}10\ H_2O$, 0.22 mg $ZnSO_4{\cdot}7\ H_2O$, 0.05 mg $CuCl_2{\cdot}2\ H_2O$, 0.03 mg $Na_2MoO_4{\cdot}2\ H_2O$, 0.03 mg $VSO_4{\cdot}2\ H_2O$, and 0.01 mg $CoSO_4$ final concentration. The pH was adjusted to 2.0 with 10 N H_2SO_4. Chemicals of high purity grade were used for media preparation.

Composition of Synthetic Martian Regolith Analogs

In this study, four mineral mixtures of Mars regolith simulants (MRS) were used to examine whether these minerals could provide nutrients/energy sources necessary for lithoautotrophic growth of *M. sedula* (**Tables 1**, **2**). The mineral mixtures of synthetic Martian regolith analogs were assembled in accordance

TABLE 1 | Chemical composition of the synthetic Martian regolith analogs used in this study.

Major chemical composition	JSC Mars-1A[1]	P-MRS[2]	S-MRS[3]	MRS07/52[4]
	Wt %	Wt %	Wt %	Wt %
Silicon dioxide (SiO_2)	34.5–44	43.6	30.6	34.6
Aluminum oxide (Al_2O_3)	18.5–23.5	11.9	9.2	14.1
Titanium dioxide (TiO_2)	3–4	0.36	0.05	0.1
Ferric oxide (Fe_2O_3)	9–12	19.6	14.9	20.6
Iron oxide (FeO)	2.5–3.5	–	–	–
Magnesium oxide (MgO)	2.5–3.5	4.52	10.3	3.4
Calcium oxide (CaO)	5–6	4.74	17.8	6.1
Sodium oxide (Na_2O)	2–2.5	0.32	1.09	2.5
Potassium oxide (K_2O)	0.5–0.6	1.04	0.13	0.2
Manganese oxide (MnO)	0.2–0.3	0.16	0.3	–
Diphosphorus pentoxide (P_2O_5)	0.7–0.9	0.55	0.05	–
Sulfur trioxide (SO_3)	–	0.2	9.1	5.1
LOI	–	11.8	5.4	–

[1]*Data for JSC Mars-1A obtained from Orbital Technologies Corporation, Madison, WI, United States;* [2,3]*Data for P-MRS and S-MRS were obtained from Boettger et al. (2012);* [4]*Data for MRS07/52 were obtained from Moeller et al. (2008).*

TABLE 2 | Mineral composition of the synthetic Martian regolith analogs used in this study.

Mineral component	JSC 1A[1]	P-MRS[2]	S-MRS[3]	MRS07/52[4]
	Wt %	Wt %	Wt %	Wt %
Plagioclase Feldspar	64	–	–	–
Olivine	12	–	–	-
Magnetite	11	–	–	–
Pyroxene and/or glass	9	–	–	–
Gabbro		3	32	–
Dunite		2	15	–
Quartz		10	3	1
Hematite	5	5	13	20
Montmorillonite		45	–	48
Chamosite		20	–	–
Kaolinite		5	–	10
Siderite		5	–	–
Hydromagnesite		5	–	–
Goethite		–	7	–
Gypsum		–	30	–
Anhydrite		–	–	13
$MgSO_4$		–	–	7
Halite		–	–	1

[1]*Data for JSC Mars-1A were obtained from Morris et al. (1993);* [2,3]*Data for P-MRS and S-MRS were obtained from Boettger et al. (2012);* [4]*Data for MRS07/52 were obtained from Moeller et al. (2008).*

to data on the structural and chemical composition of Martian minerals identified in meteorites (McSween, 1994) and by recent orbiter and rover missions (Bibring et al., 2005; Poulet et al., 2005; Chevrier and Mathé, 2007; Mustard et al., 2009; Morris et al., 2010) reflecting current knowledge of environmental changes on Mars (Boettger et al., 2012). JSC Mars-1A Martian Regolith Simulant is a palagonitic tephra (volcanic ash altered at low temperatures), produced by Orbital Technologies Corporation, Madison, WI, United States. The only phases detected by x-ray diffraction are plagioclase feldspar and minor magnetite. Iron Mossbauer spectroscopy also detected traces of hematite, olivine, pyroxene and/or glass (Morris et al., 1993). One of the Mars regolith simulants was phyllosilicate-rich (Phyllosilicate Mars Simulant, P-MRS), containing a high percentage of smectite clays like montmorillonite, kaolinite, and chamosite, as well as carbonates (siderite, hydromagnesite). The other mixture (Sulfatic Mars Simulant, S-MRS) was characterized by its high gypsum and goethite content. Both mineral mixtures consist also of pyroxene and plagioclase (gabbro), olivine, quartz, and the anhydrous ferric oxide hematite (Gooding, 1978; Boettger et al., 2012). The mineral composition of P-MRS is modeled based on the phyllosilicate-rich sites on Mars, which formed during an aqueous weathering regime with neutral to alkaline conditions in the Noachian epoch (>3.7 Ga), either on the surface or in the subsurface at hydrothermal areas (**Tables 1**, **2**) (Bibring et al., 2006; Chevrier and Mathé, 2007; Halevy et al., 2007; Bishop et al., 2008; Ehlmann et al., 2011). S-MRS represents the Martian sediments with a high sulfate content that presumably correspond to the acidic conditions in the Hesperian epoch (3.7–3.0 Ga) (Bibring et al., 2006; Bullock and Moore, 2007; Chevrier and Mathé, 2007). The final inorganic mineral mixture investigated in this study was the Martian soil simulate MRS07/52. This sample was supplied by German Aerospace Center and was produced to have comparable constituents to that of the soil on Mars (Moeller et al., 2008) (**Tables 1**, **2**).

Cultivation Setup

Chemolithoautotrophic cultivation of *M. sedula* was performed in DSMZ88 Sulfolobus medium described above in 1 L glassblower modified Schott-bottle bioreactors (Duran DWK Life Sciences GmbH, Wertheim/Main, Germany), equipped with a thermocouple connected to a heating and magnetic stirring plate (IKA RCT Standard/IKA C-MAG HS10, Lab Logistics Group GmbH, Meckenheim, Germany) for temperature and agitation control. Each bioreactor was equipped with three 10 mL graduated glass pipettes, permitting carbon dioxide and air gassing (with the gas flow of 9 mL min^{-1}, adjusted to five bubbles s^{-1} by using 8 mm valves (Serto, Frauenfeld, Switzerland)) and sampling of culture, respectively (Supplementary Figure 1). The graduated pipettes used for gassing were connected by silicon tubing to sterile 0.2 μm filters (Millex-FG Vent filter unit, Millipore, Billerica, MA, United States). The graduated pipettes used for sampling were equipped with a Luer-lock system in order to permit sampling with sterile syringes (Soft-Ject, Henke Sass Wolf, Tuttlingen, Germany). The offgas was forced to exit via a water-cooled condenser (Ochs GmbH, Bovenden, Germany). For the cultivations of *M. sedula* at 73°C the temperature inside the bioreactors was controlled by electronic thermocouple via the heating and magnetic stirring plates. *M. sedula* inocula were obtained by resuspending a chemolithoautotrophically grown cell pellet formed by centrifugation at 6000 × *g* for 15 min in DSMZ88 media without organic carbon source and inorganic metals/metalloids as energy sources. For chemolithoautotrophic growth cultures with initial pH of 2.0 were supplemented with 1 g/liter Martian regolith simulants, no further pH adjustments were introduced during the cultivation. The minerals were temperature sterilized at 180°C in a heating chamber for a minimum of 24 h prior to autoclaving at 121°C for 20 min. Abiotic controls consisting of uninoculated culture media supplemented with MRSs were included in all the experiments. Growth of cells was monitored by phase contrast/epifluorescence microscopy and metal release. Precise cell enumeration was found to be difficult due to the interference with mineral particles of similar size and round shaped morphology and shielding of *M. sedula* by iron mineral precipitates, especially at later stages of the growth. To visualize wiggling cells on solid particles, a modified "DAPI" (4′-6′- Diamidino-2-phenylindole) staining was used (Huber et al., 1985); afterward the cells were observed and recorded with ProgRes® MF cool camera (Jenoptik) mounted on Nikon eclipse 50i microscope, equipped with F36-500 Bandpass Filterset (ex, 377/50 nm; em, 447/60 nm).

Multi-Labeled-Fluorescence *In Situ* Hybridization (MiL-FISH)

Cultures of *M. sedula* grown on Martian Regolith Simulants (Supplementary Figure 2) were fixed in 2% paraformaldehyde

(PFA) at room temperature for 1 h and subsequently washed three times in 1x PBS (phosphate buffer saline) with centrifugation steps of 3000 × *g* for 5 min between each exchange. Cells were extracted from sediment after Braun et al. (2016) as follows: 1 ml sediment from each sample was centrifuged at 5000 × *g* for 5 min, the supernatant discarded, re-suspended in 1.5 ml Mili-Q that included 0.2 ml methanol and 0.2 ml detergent mix (100 mM EDTA, 100 mM sodium pyrophosphate decahydrate and 1% v:v Tween 80) and shaken at 750 rpm for 60 min. To separate cells from sediment particles samples were sonicated at 30% power three times for 15 s using an ultrasonic probe. Finally, a gradient centrifugation was applied consisting of three 2 ml Nycodenz layers of 30, 50, and 80% on top of a 2 ml sodium polytungstate solution with a 2.23 g per ml density and centrifuged at 5000 × *g* for 2 h at 4°C. The microbial fraction contained within the supernatant above the sodium polytungstate was extracted with a glass pipette. To further clean the samples from fine sediment particles the gradient centrifugation was repeated a second time in the same manner. *M. sedula* 16S rRNA phylotype specific probe was designed with the software package ARB (Ludwig et al., 2004) and labeled with 4x Atto488 via Click chemistry (biomers.net GmbH, Ulm, Germany) (see **Table 3**). Cells were mounted on 10 well Diagnostica glass slides (Thermo Fisher Scientific Inc. Waltham, MA, United States) and MiL-FISH conducted directly on slides with 30% formamide and a 3 h hybridization time (Schimak et al., 2015). Positive control for the specificity of the phylotype specific probe M.sedula_174 was provided by use of the same *M. sedula* DSM5348 culture published in Schimak et al. (2015). After hybridization, slides were washed for 15 min at 48°C according to Manz et al. (1992) (14 to 900 mM NaCl, 20 mM Tris-HCl [pH 8], 5 mM EDTA [pH 8], and 0.01% SDS) at a stringency adjusted to the formamide concentration used (Manz et al., 1992). DNA staining with DAPI (4 = ,6-diamidino-2-phenylindole) followed (10 mg/ml) for 10 min after which slides were rinsed in distilled water three times. Vectashield (Vector Laboratories, Burlingame, CA, United States) mounting medium was applied and slides closed with a coverslip. Fluorescence images were taken with an AxioCam Mrm camera mounted on an Nikon Eclipse 50i illuminated by a Nikon Intensilight C-HGFI light source and equipped with a F36-525 Alexa 488 (ex, 472/30 nm; em, 520/35 nm) filter cube. Images were recorded with the Windows based AxioVision (release 4.6.3 SP1) imaging software and any image-level adjustments made either therein or using the Mac OS X based Adobe Photoshop version 12.0.4. The figure table depicted was composed using Mac OS X based Adobe Illustrator version 15.0.2 and images cropped by use of clipping masks.

Scanning Electron Microscopy

The mineral precipitates (Supplementary Figure 3) were examined with a Zeiss Supra 55 VP scanning electron microscope (SEM), equipped with a spectroscope of dispersive energy (EDS), which was used for imaging and elemental analysis of precipitates. The samples were coated with a thin Au/Pd layer (Laurell WS-650-23 spincoater). The acceleration voltage applied was 5 kV and the EDS analyses were performed with a 120 μm aperture and a counting time of 50 s. In order to control the beam parameters, cobalt was used as a standard. Conventional ZAF matrix correction was used to calculate the final composition from the measured X-ray intensities. All the sample spots investigated by EDS were chosen randomly and each spot was measured three times. **Table 4** represents the chemical composition of aluminum/chlorine containing microspheroids, which was taken as the average of the measurements from 20 randomly chosen spots.

Metal Analysis

To determine the extracellular concentrations of metal ions mobilized from the Martian regolith simulants, culture samples were clarified by centrifugation. Samples of the resulting supernatants were filtered (0.44 μm pore size) and analyzed by inductively coupled plasma-optical emission spectrometer (ICP-OES) Perkin Elmer Optima 5300 DV. All reported values are averages from duplicate samples.

Electron Paramagnetic Resonance (EPR)

The Electron Paramagnetic Resonance (EPR) spectra were recorded on an X-Band Bruker Elexsys-II E500 CW-EPR spectrometer (Bruker Biospin GmbH, Rheinstetten, Germany) at 90 ± 1 and 293 ± 1 K using a high sensitivity cavity (SHQE1119). Solid state EPR measurements were performed setting microwave frequency to 9 GHz, modulation frequency to 100 kHz, center field to 6000 G, sweep width to 12000 G, sweep time to 335.5 s, modulation amplitude to 20.37 G, microwave power to 15 mW, conversion time to 81.92 ms and resolution to 4096 points. The samples were put in EPR quartz tubes (Wilmad-LabGlass, Vineland, NJ, United States) and scanned three times, of which the average was used for analysis. The spectrum of an empty control tube was subtracted from all sample spectra. All spectra were analyzed with the Bruker Xepr software.

Statistical Analysis

For the statistical analysis and graphical representation of the data the Excel 2016 (version 7.0) and Sigma plot (version 13.0) software packages were used.

TABLE 3 | Oligonucleotide probes used in this study.

Probe	Sequence 5′–3′ (reverse complementary)	Target gene	Label	Synthesis	Taxon	Target species	FA %	Colour
M. sedula_174_17mer	AGA UUC CCU UGC CCG CU	16S rRNA	Atto488	Click chemistry	Archaea	*Metallosphaera sedula*	30%	Green

Probe name, nucleotide sequence - underscore indicates nucleotide:fluorochrome conjugates, target gene, label type, label synthesis, target taxon or higher, target species and probe color during imaging.

TABLE 4 | Average metal composition (%) of microhemispheroids detected in mineral precipitates withdrawn from cultures of *Metallosphaera sedula* grown on JSC Mars 1A, P-MRS, and S-MRS.

	C	O	Al	Cl
Mean % (± standard deviation) *n = 20*	6.41 ± 5.01	20.33 ± 7.71	18.18 ± 10.47	7.10 ± 3.85

RESULTS

Chemolithotrophic Growth on Synthetic Martian Regolith

Metallosphaera sedula was grown under chemolithoautotrophic conditions on MRSs (**Table 5**), and interaction of cells with the mineral particles was examined. After 21 days of CO_2-supplemented cultivation on MRSs as the sole energy source, phylogenetic identification and visualization of *M. sedula* cells was achieved with Multi-Labeled fluorescence *in situ* hybridization (MiL-FISH). For this purpose a newly designed phylotype specific probe targeting the 16S rRNA (**Table 3**) was used. The cultures of *M. sedula* grown on all four investigated in this study MRSs (JSA 1A, P-MRS, S-MRS, and MRS07/52) resulted in positive fluorescent signal with Atto488 labeled probes at a 30% formamide concentration (**Figure 1**). Only cells that show both DAPI and fluorescent signal were considered as positive hybridization with the target organism. Additionally, it was noted that cells of S-MRS and MRS07/52 cultures occur in mucus bound aggregates which can be inferred as extracellular polysaccharide substances (EPS) known for *M. sedula* (Auernik et al., 2008) (**Figures 1G–L**).

Metal Release

Inductively coupled plasma-optical emission spectrometer analysis of composition of major elements mobilized from all tested Martian regolith simulants showed the elevated levels of released S, K, Ca, Mg, Si, and Na in the growth medium (leachate solution) (**Figure 2**). A further change in trace elements (higher released Mn) occurred in cultures of *M. sedula* grown on JSA 1A, P-MRS, and S-MRS. Additionally, in case with MRS07/52 leachate solution was characterized by elevated levels of Fe, Ni, and to lesser extent Al in comparison to abiotic control (**Figure 2D**). The increased level of released Ni ions was also detected in S-MRS grown cultures. The elevated levels of Sr ions were measured in culture supernatants of *M. sedula* grown on P-MRS, S-MRS, and MRS07/52, while increased soluble Zn was represented in JSC 1A and MRS07/52 grown cultures. The drop in P concentrations was detected in leachate solutions of all the tested MRS. The decrease of total iron observed in *M. sedula* cultures grown on JSC 1A, P-MRS, and S-MRS could be possibly attributed to the formation of insoluble iron oxyhydroxides which form precipitated mineral phase and therefore are not included in the samples of leachate solution used for the ICP-OES analysis. This phenomenon of 'lost iron' has been already previously reported in case of microbial cultivation on extraterrestrial material (Gronstal et al., 2009).

TABLE 5 | Cell densities of *M. sedula* cultures grown on the synthetic Martian regolith analogs at "0" time point and after 21 days of cultivation.

Cultivation time	0 day	21 days
	Cell density [cells/ml]	
JSC 1A	4,93E+06 ± 6,49E+05	1,24E+08 ± 7,40E+07
P-MRS	5,98E+06 ± 3,19E+06	4,77E+08 ± 3,74E+08
S-MRS	5,57E+06 ± 3,10E+06	3,06E+08 ± 3,07E+08
MRS07/52	4,34E+06 ± 2,25E+06	2,02E+08 ± 1,32E+08
Pyrite	9,80E+06 ± 9,45E+05	1,50E+09 ± 2,50E+08
No MRSs added	6,95E+06 ± 7,85E+05	1,48E+05 ± 8,73E+03

Mean and standard deviation of n = 3 biological replicates are represented. When no MRSs were added, cultivation medium was inoculated with cells of M. sedula without additional energy source.

SEM-EDS Investigation of Solid Mineral Phase

To further study the interactions of *M. sedula* with the Martian regolith simulants, the surface of these minerals was examined for possible alterations upon *M. sedula* growth. Inspection by SEM of solid mineral phase in cultures of *M. sedula* grown on synthetic Martian regolith revealed the presence of sphere-like particles of variable size (0.3–3 μm). These microhemispheroids were represented in cultures of *M. sedula* grown on JSC 1A, P-MRS, and S-MRS and absent in the corresponding abiotic controls (**Figure 3**). The results of SEM-EDS analysis indicate that these hemispheroidal morphologies are mainly composed of oxygen, aluminum and chlorine and with no or low carbon content (**Table 4** and Supplementary Figure 4). The solid mineral phase withdrawn from S-MRS grown cultures of *M. sedula* was especially enriched with aluminum/chlorine containing microspheroids, while both biotransformed JSC 1A and P-MRS had a minor occurrence of these particles. **Figure 3C** and Supplementary Figure 4 show budding microspheroids represented on biotransformed surface of S-MRS. SEM assisted investigations of a solid phase of biotransformed MRS07/52 showed the biofilm layer distributed over the mineral surface (**Figure 3G**). Such a deposited biofilm layer was absent in the corresponding abiotic control of MRS07/52 incubated in the growth medium at 73°C but without *M. sedula* (**Figure 3H**).

EPR Investigation of Solid Mineral Phase

Electron Paramagnetic Resonance measurements were performed to (1) identify paramagnetic species of manganese and iron in the different MRSs samples and to (2) investigate the impact of *M. sedula* on MRSs with a possible effect on the oxidative state of manganese and iron. The four different MRSs mineral mixtures were incubated in cultivation medium in the presence (biotic) or absence (abiotic) of *M. sedula*. The spectra

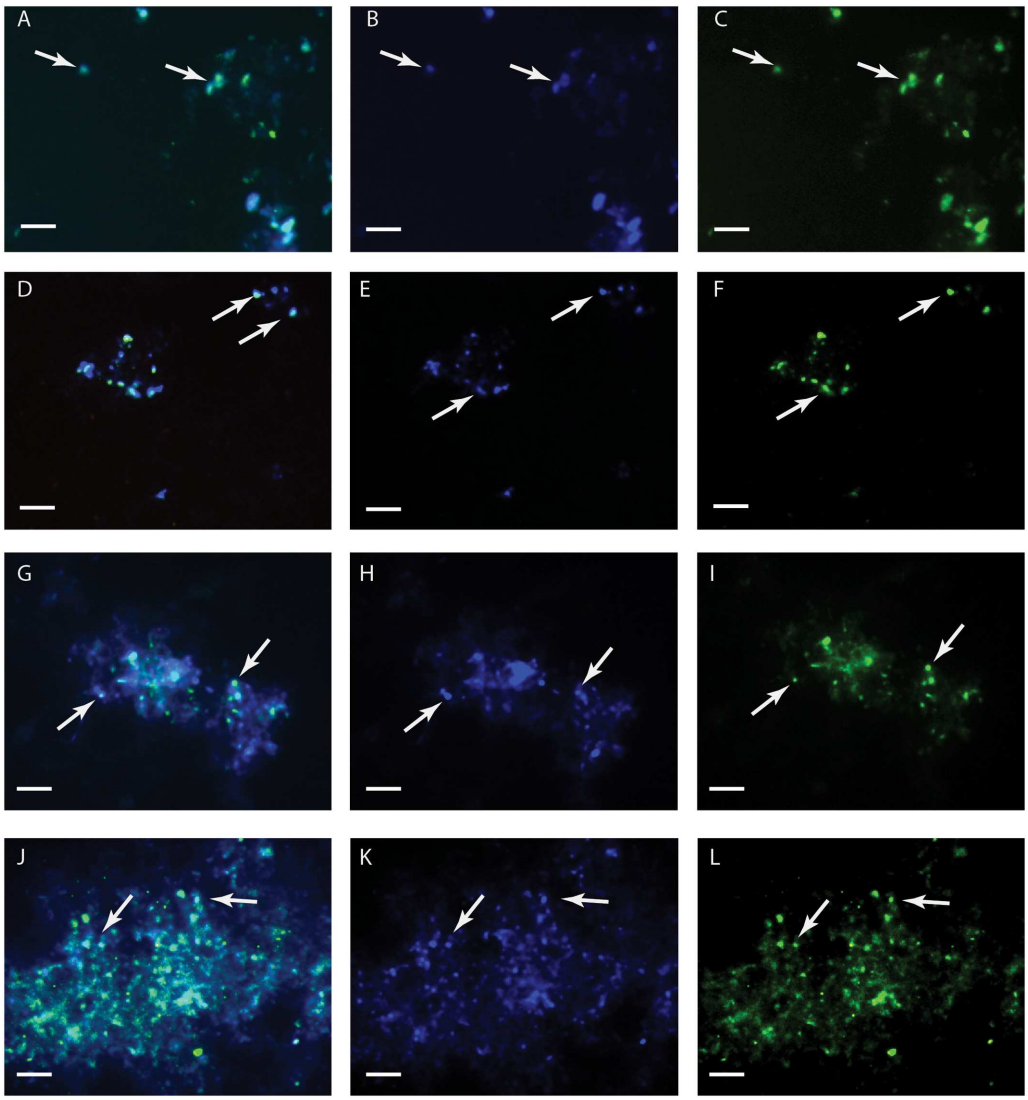

FIGURE 1 | Multi-Labeled-Fluorescence *in situ* Hybridization (MiL-FISH) of *Metallosphaera sedula* cells grown on synthetic Martian regolith materials as the sole energy sources. **(A,D,G,J)** Overlaid epifluorescence images, showing overlap of the specific oligonucleotide probe targeting *M. sedula* with DAPI signals. **(B,E,H,K)** DAPI staining of the same field (blue). **(C,F,I,L)** MiL-FISH images of cells (green) after hybridization with the specific oligonucleotide probe targeting *M. sedula*. Cultures of *M. sedula* were examined with MiL-FISH conducted after Schimak et al. (2015) after 21 days of cultivation with JSC Mars 1A **(A–C)**, P-MRS **(D–F)**, S-MRS **(G–I)**, and MRS07/52 **(J–L)**.

of untreated (raw) MRSs were investigated as well. The abiotic samples of JSC 1A and P-MRS contained Mn^{2+} as evident by a prominent signal at $g = 2.4$ with a broad linewidth of >1200 G (**Figure 4** and Supplementary Tables 1, 2) typical for abiotic Mn^{2+} samples (Kim et al., 2011; Ivarsson et al., 2015). For JSC 1A, the biotic sample revealed an almost complete decline of the Mn^{2+} signal, while for P-MRS an alteration of the $g = 2.4$ signal in the biotic sample resulted to the appearance of a broad signal with $g = 3.3$, indicating dipolar interactions of mixed ionic states (Mn^{3+} and Mn^{4+}) (Ivarsson et al., 2015). In biotic and abiotic samples of JSC 1A and P-MRS, Fe^{3+} could be identified by the characteristic $g = 4.3$ and $g = 9$ signals. A high spin d5 configuration of the Fe^{3+} can be inferred from the positions of these resonance signals. **Figure 4B** shows that the amplitude of high spin Fe^{3+} $g = 4.3$ signal is slightly lower in biotic P-MRS than in the corresponding abiotic sample, while the signals $g = 11.5$ and $g = 9.9$ measured at 90 and 293 K, respectively, are clearly diminished after *M. sedula* cultivation. Independent of the incubation conditions, the EPR spectra of all four MRSs samples recorded at 90 K revealed small signals with g-values in the range of 2.0 and 2.7, which were assigned to Fe^{3+} with low spin electron configuration. No significant changes were detected between the biotic and abiotic samples measured at 90 K with regard to the Fe^{3+} in the low spin state. In opposite, a continuously narrowing resonance signal $g = 2$ was recorded at 293 K in JSC 1A samples after cultivation

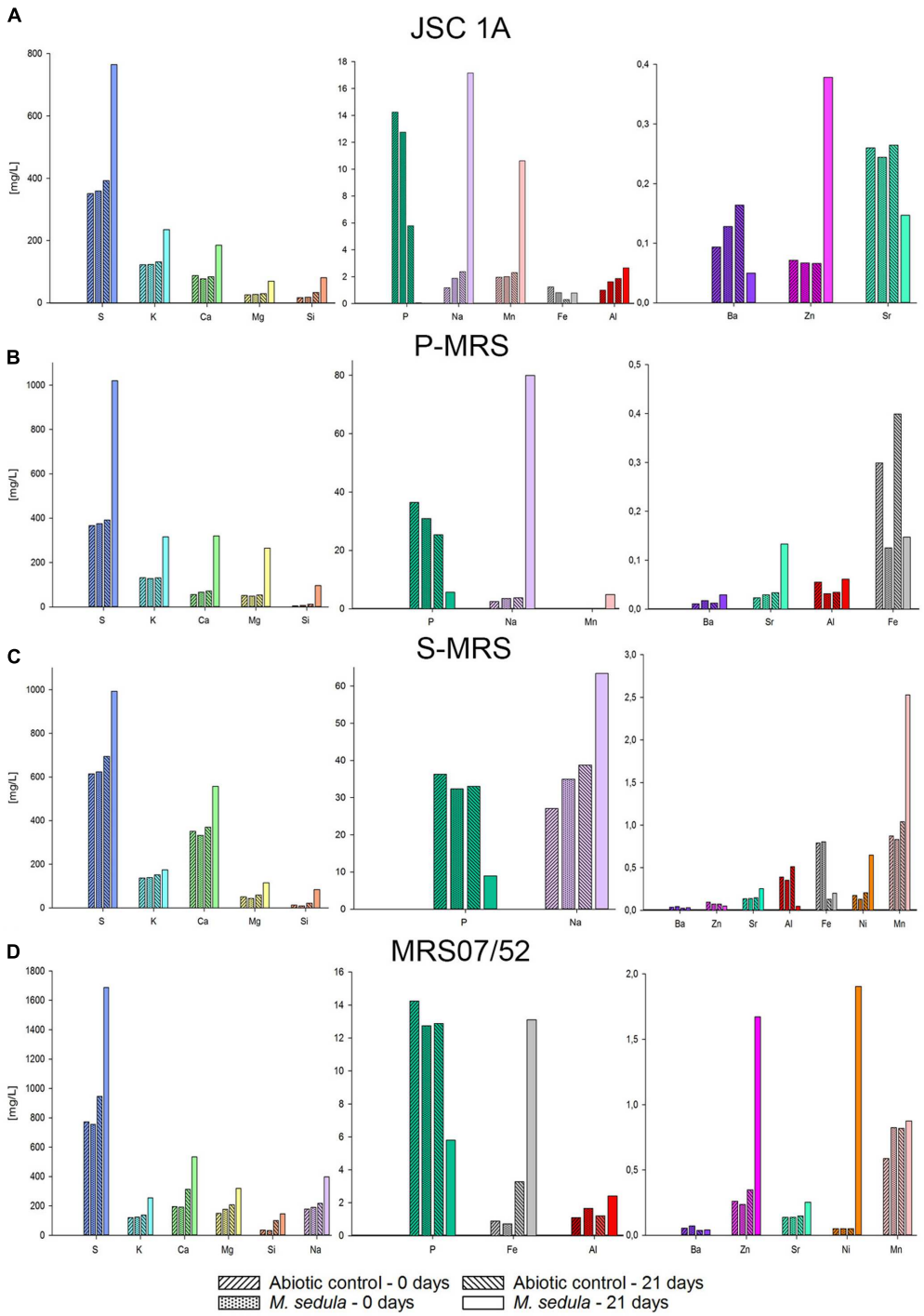

FIGURE 2 | Inductively coupled plasma-optical emission spectrometer (ICP-OES) analysis of released metal ions in supernatant of *M. sedula* cultures grown on the Martian regolith simulants [JSC Mars 1A **(A)**; P-MRS **(B)**; S-MRS **(C)**; MRS07/52 **(D)**] as the sole energy sources. Samples were taken at "0" time point and after 21 days of cultivation of *M. sedula* on the Martian regolith simulants and from corresponding abiotic controls.

with *M. sedula*. The linewidth (ΔH) remained unaltered for raw and abiotic JSC 1A (732 G) and decreased to 600 G after the cultivation with *M. sedula* (**Figure 4** and Supplementary Table 2).

The EPR spectrum of the abiotic S-MRS sample exhibits a prominent resonance at $g = 3.2$ with a broad linewidth of 2061 G, which is absent in the EPR spectra of all the other MRSs samples measured at 90 K. This specific resonance is obtained from

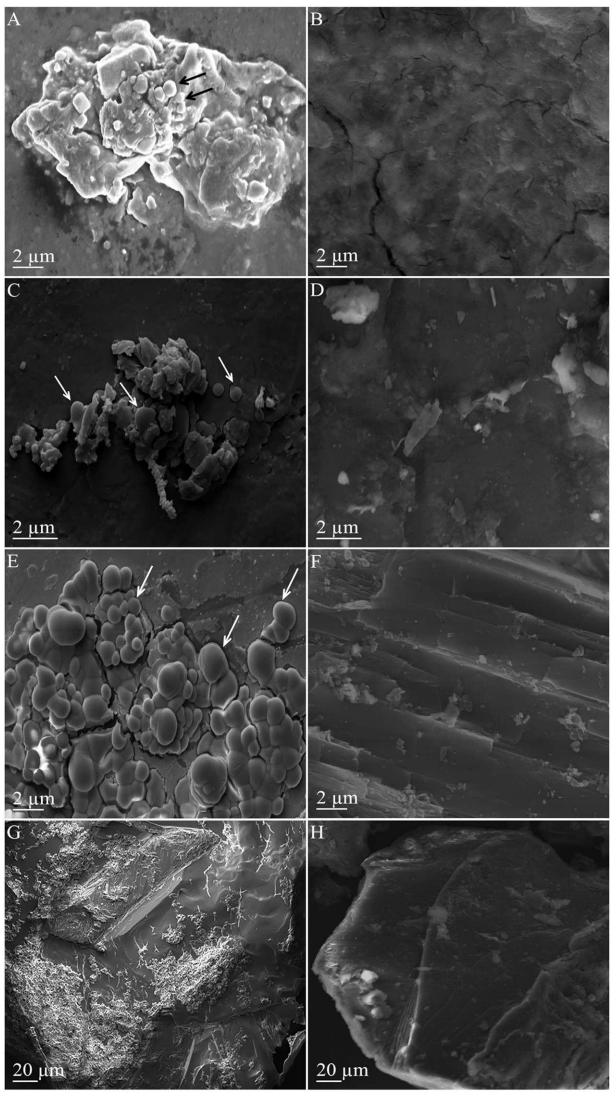

FIGURE 3 | Scanning electron microscopy (SEM) images of the mineral surfaces of synthetic Martian regolith materials. **(A)** Scanning electron image showing a surface of mineral precipitate obtained after the cultivation of *M. sedula* on JSC 1A. **(C)** Scanning electron image showing a surface of mineral precipitate obtained after the cultivation of *M. sedula* on P-MRS. **(E)** Scanning electron image showing a surface of mineral precipitate obtained after the cultivation of *M. sedula* on S-MRS. **(G)** Scanning electron image showing a surface of mineral precipitate obtained after the cultivation of *M. sedula* on JSC 1A. Cultures of *M. sedula* were examined with SEM after 21 days of cultivation on the Martian regolith simulants. Aluminum/chlorine containing microspheroids occurred in mineral precipitates of JSC Mars 1A, P-MRS, and S-MRS after *M. sedula* growth, are depicted with arrows. Images **(B,D,F,H)** represent the corresponding abiotic controls.

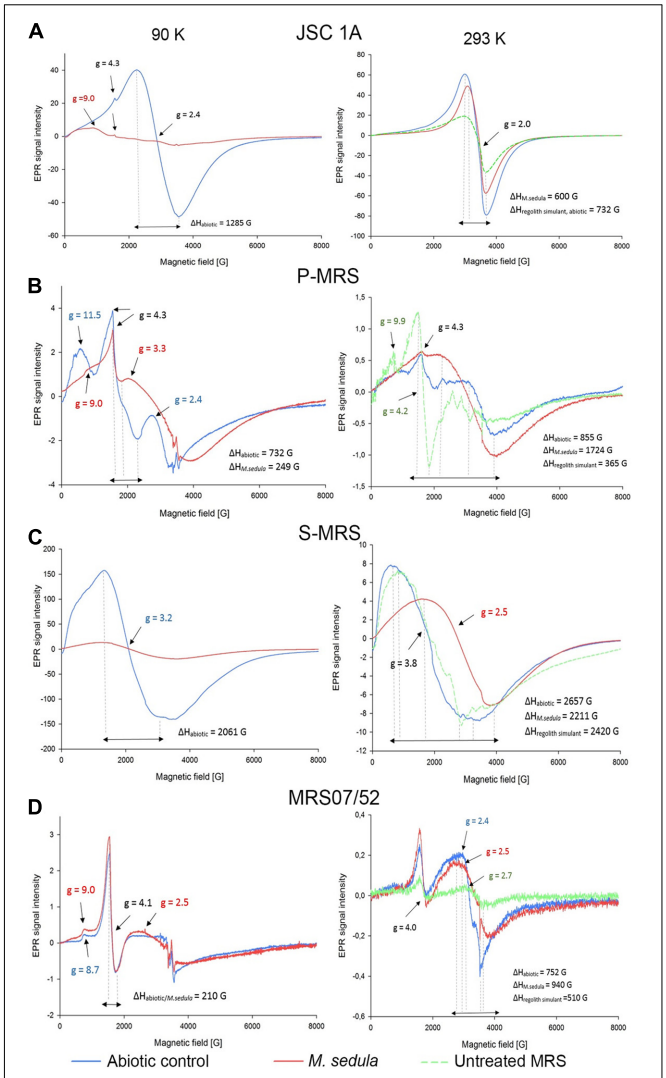

FIGURE 4 | Electron Paramagnetic Resonance (EPR) spectra of raw synthetic Martian regolith materials (green line), synthetic Martian regolith materials bioprocessed by *M. sedula* (red line), and synthetic Martian regolith materials after the treatment with cultivation medium, but without *M. sedula* (abiotic control, blue line). **(A)** EPR spectra of JSC Mars 1A; **(B)** EPR spectra of P-MRS; **(C)** EPR spectra of S-MRS; **(D)** EPR spectra of MRS07/52). Spectra recorded at 90 and 293 K are represented in left and right columns, respectively. *g*- values are depicted with the color code corresponding to the spectra; identical *g*-values are represented in black color. The EPR *g*-values recorded at 90 and 293 K are grouped in Supplementary Table 1. The corresponding EPR Linewidths (ΔH) values are provided in Supplementary Table 2.

samples containing tetrahedral Mn^{2+} species (Xu et al., 1999). A pronounced decrease of the $g = 3.2$ resonance signal could be demonstrated for the biotic sample of S-MRS compared to the corresponding abiotic sample. In MRS07/52, Fe^{3+} species in the low and high spin state were identified based on the characteristic EPR signals as mentioned above. No manganese could be detected in MRS07/52. The minor difference in biotic and abiotic MRS07/52 samples occurred at the area of low spin Fe^{3+}, which is even more detectable in spectra recorded at 293 K (**Figure 4D**). The slightly increased amplitude of high spin Fe^{3+} signal along with the shift of *g*-value from 8.7 for abiotic to 9 for biotic samples was also observed at 90 K. The strong resonance line at $g = 4.1$ which can be assigned to Fe^{3+} located in orthorhombic positions (Polikreti and Maniatis,

2002) is not altered in biotic and abiotic MRS07/52 samples (**Figure 4D**).

DISCUSSION

Evolutionally diversified metal-solubilizing microorganisms with their fascinating metabolic pathways have developed an exquisite set of capabilities for manipulating minerals by dissolving them to access useful metals. We tested the ability of *M. sedula* to grow chemolithoautotrophically in four different types of synthetic Martian regolith. As growth was detected in all four MRS, we concluded that *M. sedula* is capable of chemolithotrophic growth using the synthetic Martian regolith as the sole energy source. Further, our results indicated that *M. sedula* is able to solubilize metals from the synthetic Martian regolith (e.g., S, K, Ca, Na, Mg, Si, Mn, Fe, Zn, Ni, and Sr) into the growth medium (leachate solution). Interestingly, in all four tested MRSs, the amount of detected phosphorus decreased in the biogenic samples after 21 days of cultivation, possibly indicating phosphorous consumption by *M. sedula* in order to maintain the growing population of the cells, which can explain a decreased amount of P in leachate solutions (**Figure 2**). The observed metabolic activity coupled to the release of free soluble metals from the synthetic Martian regolith can certainly pave the way to asteroid biomining, launching the biologically assisted exploitation of raw materials from asteroids, meteors and other celestial bodies.

However, insufficient evidence exists to confidently identify which metal/or metals in all tested MRSs serve as electron donors utilized by *M. sedula* to satisfy its bioenergetics needs. Due to its versatile metal-oxidizing capacities (Huber et al., 1989; Auernik and Kelly, 2010a,b; Maezato et al., 2012; Mukherjee et al., 2012; Wheaton et al., 2016), the fact that *M. sedula* can potentially respire on a combination of different elements represented in MRSs cannot be ruled out. It would seem beneficial for *M. sedula* to attach preferentially to those minerals containing useable substrates such as reduced iron or sulfur compounds. Fe^{2+} as a constitutive element is represented in variety of minerals, including olivine [$(Mg, Fe^{2+})_2SiO_4$] (11% in JSC 1A, 2% in P-MRS, 15% in S-MRS), and siderite [$Fe(CO_3)$, 5% in P-MRS], or bound to the smectite clay chamosite [$(Fe^{2+}, Mg)_5Al_2Si_3O_{10}(OH)_8$, 20% in P-MRS] (**Table 2**). The comparison of the obtained EPR spectra of raw and abiotic samples (**Figure 4**, green and blue lines, correspondingly) with the mineralogy and chemical composition of all MRSs we tested suggested that the recorded signals are most likely due to Mn^{2+} and Fe^{3+} ions. The obvious alteration of the width of EPR signals $g = 2$ detected in JSC 1A samples at 293 K after *M. sedula* growth might well reflect the oxidation of Fe^{2+} into Fe^{3+} (Presciutti et al., 2005; Mangueira et al., 2011). Interestingly, no ΔH alteration of $g = 2$ signal was observed for abiotically treated JSC 1A compared to raw JSC 1A material (**Figure 4A** and Supplementary Table 2). The slight increase of the signal amplitude of high spin Fe^{3+} $g = 4.1$ and $g = 9$ signals along with the appearance of $g = 2.5$ signal in biotic samples of MRS07/52 suggest the accumulation of Fe^{3+} in mineral phase, which also speaks on the account of Fe^{2+} oxidation mediated by *M. sedula* (**Figure 4D**). Interestingly, MRS07/52 is the only simulant among all tested MRSs, where Fe ions were detected to be released from after 21 days of cultivation with *M. sedula*. In biotic samples of Mn-bearing MRSs (JSC 1A, P-MRS, and S-MRS) the increased signals of mixed ionic states Mn^{3+} and Mn^{4+} and the decrease of Mn^{2+} in tetrahedral positions were observed pointing to a plausible redox couple for *M. sedula* respiration. The accumulation of redox heterogeneous Mn species may occur in the mineral phase due to *M. sedulas* oxidative metabolism, analogously to microbial mediated sulfur oxidation with the wide variety of redox heterogeneous intermediate sulfur compounds (Schippers et al., 1996) and serve as a fingerprint of chemolithoautotrophic life. However, to which extent Mn^{2+} is oxidized to Mn^{3+} and Mn^{4+} by *M. sedula* cannot be elucidated by EPR.

The signal $g \cong 4$ assigned for high spin energy Fe^{3+} is well preserved within JSC 1A, P-MRS, and MRS07/52 abiotic and biotic samples, with only small variations in amplitude. This situation indicates that the Fe^{3+} remained associated to orthorhombic positions in the structure of mineral precipices upon *M. sedula* growth. Such an observation is also in line with EPR-characterization of iron-bearing multi-mineral materials under the oxidative conditions of firing temperatures, suggesting that a biologically mediated oxidative effect does not differ from abiotic physical–chemical oxidation in this spectral area. However, changes were detected at signals $g = 9$ (**Figures 4A,B,D** and Supplementary Table 1) originating from high-spin rhombic Fe^{3+} centers, supporting the microbial mediated alteration of Fe^{3+} complexes in axial symmetry.

The different composition of mineral phases of MRSs has to be taken into account when assigning a certain resonance signal and the formation of different environments in response to abiotic and biologically mediated oxidation. Nevertheless, the EPR data should be supported by other observations such as synchrotron assisted X-ray absorption techniques, to obtain a deeper insight into the microbial mediated mineralogical alterations.

The development of the microspheroids described here that overgrow mineral surface of Martian regolith simulants was one of the features mediated by *M. sedula*. Most of the microspheroids were observed in the range of 0,3 to 3 μm in size, with the majority in between 0,5 and 1 μm. Frequently, the microspheroids were characterized by very low carbon content, which did not exceed the background carbon level in surrounding mineral surface according to our EDS analysis and suggested the non-cellular nature of these morphologies (Supplementary Figure 4). Chlorine and aluminum content of the microspheroids has been constantly detected by EDS analysis, with chlorine represented solely in microspheroid structures and absent in the mineral background (Supplementary Figure 4 and **Table 4**). These microspheroid structures tend to cluster into aggregates, which overgrow the mineral surfaces while forming assemblages on underlying structures (**Figure 3E** and Supplementary Figure 4).

Occurring as single particles (**Figures 3A,B**), these microstructures expose correctly shaped hemispherical surface. When grouped into aggregates, overgrowing the surface of S-MRS and competing with each other in restricted size area,

microspheroids expose overlapping conjoined boundary sides, which results in a distorted hemispherical morphology and "overcrowded" appearance (**Figure 3C**). The neoformed opaline microhemispheroids of similar morphology were previously described as a part of possibly microbial mediated diagenesis of marine sediments (Monty et al., 1991). Massively deposited chlorine/aluminum microspheroids can be inferred to be self-assembled aggregated clusters that form new nuclei and mineral intermediates as a part of new mineral formation process biologically mediated by *M. sedula*. This fine-scale morphological signature along with leaching of elements as the signs of metabolic activity may serve as indication of chemolithotrophic life in extreme environments.

CONCLUSION

The mineralogical composition of the synthetic Martian regolith analogs supports the chemolithotrophic growth of *M. sedula*, when Martian regolith simulants are used as the sole energy sources. Acquisition of Fe^{2+} and/or Mn^{2+} from these simulants seems to satisfy the bioenergetic needs of *M. sedula*. The obtained results highlight metallophilic life in extreme environments and reveal unique fingerprints of life in the extreme conditions.

AUTHOR CONTRIBUTIONS

DK, MS, MP, OS, AB, and TM performed experiments. DK and MP planned, performed, and interpreted EPR experiments; all authors provided editorial input. All authors made substantial contributions to the acquisition, analysis, and interpretation of data described in this perspective. All authors critically reviewed the report and approved the final version.

FUNDING

This work was supported by the Austrian Science Fund (FWF) through an Elise-Richter Research fellowship V333 "Iron- and Sulfur-oxidizing Machinery of the bioleaching Archaeon Metallosphaera sedula". OS was supported by COST Action STSM fellowship: "Understanding the metal oxidation machinery in archeon *M. sedula*" Nr. TD1308.

ACKNOWLEDGMENTS

We warmly thank R. Moeller (German Aerospace Center (DLR), Cologne) for providing the synthetic Martian regolith analogs used in this study. We would like to acknowledge T. Hofmann and W. Obermaier (University of Vienna, Department of Environmental Geosciences) for help with ICP-OES and Dr. Pelin Yilmaz for ARB 16S rRNA probe design. The support of Stephan Puchegger (University of Vienna, Physics Faculty Center for Nano Structure Research) with electron microscopy investigations is greatly appreciated. TM would also like to thank Frances Westall for fruitful discussions.

SUPPLEMENTARY MATERIAL

The Supplementary Material for this article can be found online at: https://www.frontiersin.org/articles/10.3389/fmicb.2017.01918/full#supplementary-material

REFERENCES

Amils, R., González-Toril, E., Fernández-Remolar, D., Gómez-Gómez, F., Aguilera, Á, Rodríguez, N., et al. (2007). Extreme environments as Mars terrestrial analogs: the rio tinto case. *Planet. Space Sci.* 55, 370–381. doi: 10.1016/j.pss.2006.02.006

Auernik, K. S., and Kelly, R. M. (2008). Identification of components of electron transport chains in the extremely thermoacidophilic crenarchaeon *Metallosphaera sedula* through iron and sulfur compound oxidation transcriptomes. *Appl. Environ. Microbiol.* 74, 7723–7732. doi: 10.1128/AEM.01545-08

Auernik, K. S., and Kelly, R. M. (2010a). Impact of molecular hydrogen on chalcopyrite bioleaching by the extremely thermoacidophilic archaeon *Metallosphaera sedula*. *Appl. Environ. Microbiol.* 76, 2668–2672. doi: 10.1128/AEM.02016-09

Auernik, K. S., and Kelly, R. M. (2010b). Physiological versatility of the extremely thermoacidophilic archaeon *Metallosphaera sedula* supported by transcriptomic analysis of heterotrophic, autotrophic, and mixotrophic growth. *Appl. Environ. Microbiol.* 76, 931–935. doi: 10.1128/AEM.01336-09

Auernik, K. S., Maezato, Y., Blum, P. H., and Kelly, R. M. (2008). The genome sequence of the metal- mobilizing, extremely thermoacidophilic archaeon *Metallosphaera sedula* provides insights into bioleaching-associated metabolism. *Appl. Environ. Microbiol.* 74, 682–692. doi: 10.1128/AEM.02019-07

Bibring, J.-P., Langevin, Y., Gendrin, A., Gondet, R., Poulet, F., Berthe, M., et al. (2005). Mars surface diversity as revealed by the OMEGA/Mars express observations. *Science* 307, 1576–1581. doi: 10.1126/science.1108806

Bibring, J. P., Langevin, Y., Mustard, J. F., Poulet, F., Arvidson, R., Gendrin, A., et al. (2006). Global mineralogical and aqueous mars history derived from OMEGA/mars express data. *Science* 312, 400–404. doi: 10.1126/science.1122659

Bishop, J. L., Dobrea, E. Z., McKeown, N. K., Parente, M., Ehlmann, B. L., Michalski, J. R., et al. (2008). Phyllosilicate diversity and past aqueous activity revealed at Mawrth Vallis, Mars. *Science* 321, 830–833. doi: 10.1126/science.1159699

Blöchl, E., Keller, M., Wachtershäuser, G., and Stetter, K. O. (1992). Reactions depending on iron sulfide and linking geochemistry with biochemistry. *Proc. Natl. Acad. Sci. U.S.A.* 89, 8117–8120. doi: 10.1073/pnas.89.17.8117

Boettger, U., de Vera, J. P., Fritz, J., Weber, I., Hübers, H. W., and Schulze-Makuch, D. (2012). Optimizing the detection of carotene in cyanobacteria in a martian regolith analogue with a Raman spectrometer for the ExoMars mission. *Planet. Space Sci.* 60, 356–362. doi: 10.1016/j.pss.2011.10.017

Braun, S., Morono, Y., Becker, K. W., Hinrichs, K.-U., Kjeldsen, K. U., Jørgensen, B. B., et al. (2016). Cellular content of biomolecules in sub-seafloor microbial communities. *Geochim. Cosmochim. Acta* 188, 330–351. doi: 10.1016/j.gca.2016.06.019

Bullock, M. A., and Moore, J. M. (2007). Atmospheric conditions on early Mars and the missing layered carbonates. *Geophys. Res. Lett.* 34, L19201. doi: 10.1029/2007GL030688

Chevrier, V., and Mathé, P. E. (2007). Mineralogy and evolution of the surface of Mars: a review. *Planet. Space Sci.* 55, 289–314. doi: 10.1016/j.pss.2006.05.039

Ehlmann, B. L., Mustard, J. F., Murchie, S. L., Bibring, J. P., Meunier, A., Fraeman, A. A., et al. (2011). Subsurface water and clay mineral formation during the early history of Mars. *Nature* 479, 53–60. doi: 10.1038/nature10582

Gooding, J. L. (1978). Chemical weathering on Mars thermodynamic stabilities of primary minerals (and their alteration products) from mafic igneous rocks. *Icarus* 33, 483–513. doi: 10.1016/0019-1035(78)90186-0

Gronstal, A., Pearson, V., Kappler, A., Dooris, C., Anand, M., Poitrasson, F., et al. (2009). Laboratory experiments on the weathering of iron meteorites and carbonaceous chondrites by iron-oxidizing bacteria. *Meteorit. Planet. Sci.* 44, 233–247. doi: 10.1111/j.1945-5100.2009.tb00731.x

Grotzinger, J. P. (2013). Analysis of surface materials by the Curiosity Mars rover. *Science* 341:1475. doi: 10.1126/science.1244258

Grotzinger, J. P., Sumner, D. Y., Kah, L. C., Stack, K., Gupta, S., Edgar, L., et al. (2014). A habitable fluvio-lacustrine environment at Yellowknife Bay, Gale crater, Mars. *Science* 343:1242777. doi: 10.1126/science.1242777

Halevy, I., Zuber, M. T., and Schrag, D. P. (2007). A sulfur dioxide climate feedback on early Mars. *Science* 318, 1903–1907. doi: 10.1126/science.1147039

Huber, G., Spinnler, C., Gambacorta, A., and Stetter, K. O. (1989). *Metallosphaera sedula* gen. and sp. nov. represents a new genus of aerobic, metal-mobilizing, thermoacidophilic archaebacteria. *Syst. Appl. Microbiol.* 12, 38–47. doi: 10.1016/S0723-2020(89)80038-4

Huber, H., Huber, G., and Stetter, K. O. (1985). A modified DAPI fluorescence staining procedure suitable für the visualization of lithotrophic bacteria. *Syst. Appl. Microbiol.* 6, 105–106. doi: 10.1016/S0723-2020(85)80021-7

Hurowitz, J. A., Grotzinger, J. P., Fischer, W. W., McLennan, S. M., Milliken, R. E., Stein, N., et al. (2017). Redox stratification of an ancient lake in Gale crater, Mars. *Science* 356:eaah6849. doi: 10.1126/science.aah6849

Ivarsson, M., Broman, C., Gustafsson, H., and Holm, N. G. (2015). Biogenic Mn-Oxides in Subseafloor Basalts. *PLOS ONE* 10:e0128863. doi: 10.1371/journal.pone.0128863

Kim, S. S., Bargar, J. R., Nealson, K. H., Flood, B. E., Kirschvink, J. L., Raub, T. D., et al. (2011). Searching for biosignatures using electron paramagnetic resonance (EPR) analysis of manganese oxides. *Astrobiology* 11, 775–786. doi: 10.1089/ast.2011.0619

Ludwig, W., Strunk, O., Westram, R., Richter, L., Meier, H., Yadhukumar, et al. (2004). ARB: a software environment for sequence data. *Nucleic Acids Res.* 32, 1363–1371. doi: 10.1093/nar/gkh293

Maezato, Y., Johnson, T., McCarthy, S., Dana, K., and Blum, P. (2012). Metal resistance and lithoautotrophy in the extreme thermoacidophile *Metallosphaera sedula*. *J. Bacteriol.* 194, 6856–6863. doi: 10.1128/JB.01413-12

Mahaffy, P. R., Webster, C. R., Atreya, S. K., Franz, H., Wong, M., Conrad, P. G., et al. (2013). Abundance and isotopic composition of gases in the martian atmosphere from the curiosity rover. *Science* 341, 263–266. doi: 10.1126/science.1237966

Mangueira, G. M., Toledo, R., Teixeira, S., and Franco, R. W. A. (2011). A study of the firing temperature of archeological pottery by X-ray diffraction and electron paramagnetic resonance. *J. Phys. Chem. Solids* 72, 90–96. doi: 10.1016/j.jpcs.2010.11.005

Manz, W., Amann, R., Ludwig, W., and Amann, R. I. (1992). Phylogenetic oligodeoxynucleotide probes for the major subclasses of proteobacteria: problems and solutions. *Syst. Appl. Microbiol.* 15, 593–600. doi: 10.1016/S0723-2020(11)80121-9

McCarthy, S., Ai, C., Wheaton, G., Tevatia, R., Eckrich, V., Kelly, R., et al. (2014). Role of an archaeal PitA transporter in the copper and arsenic resistance of *Metallosphaera sedula*, an extreme thermoacidophile. *J. Bacteriol.* 196, 3562–3570. doi: 10.1128/JB.01707-14

McSween, H. Y. J. (1994). What have we learned about Mars from the SNC meteorites. *Meteoritics* 29, 757–779. doi: 10.1111/j.1945-5100.1994.tb01092.x

Moeller, R., Horneck, G., Rabbow, E., Reitz, G., Meyer, C., Hornemann, U., et al. (2008). Role of DNA protection and repair in resistance of *Bacillus subtilis* spores to ultrahigh shock pressures simulating hypervelocity impacts. *Appl. Environ. Microbiol.* 74, 6682–6689. doi: 10.1128/AEM.01091-08

Monty, C., Westall, F., and Van Der Gaast, S. (1991). Diagenesis of siliceous particles in subantarctic sediments. Hole 699A: possible microbial mediation. *Proc. ODP Sci. Res.* 114, 685–710. doi: 10.2973/odp.proc.sr.114.121.1991

Morris, R. V., Golden, D. C., Bell, J. F. I. I. I., Lauer, H. V. Jr., and Adams, J. B. (1993). Pigmenting agents in martian soils: inferences from spectral, Mössbauer, and magnetic properties of nanophase and other iron oxides in Hawaiian palagonitic soil PN-9. *Geochim. Cosmochim. Acta* 57, 4597–4609. doi: 10.1016/0016-7037(93)90185-Y

Morris, R. V., Ruff, S. W., Gellert, R., Ming, D. W., Arvidson, R. E., Clark, B. C., et al. (2010). Identification of carbonate-rich outcrops on Mars by the Spirit rover. *Science* 329, 421–424. doi: 10.1126/science.1189667

Mukherjee, A., Wheaton, G. H., Blum, P. H., and Kelly, R. M. (2012). Uranium extremophily is an adaptive, rather than intrinsic, feature for extremely thermoacidophilic Metallosphaera species. *Proc. Natl. Acad. Sci. U.S.A.* 109, 16702–16707. doi: 10.1073/pnas.1210904109

Mustard, J. F., Ehlmann, R. L., Murchie, S. L., Poulet, F., Mangold, N., Head, J. W., et al. (2009). Composition, morphology, and stratigraphy of noachian crust around the Isidis basin. *J. Geophys. Res.* 114:EOOD12. doi: 10.1029/2009JE003349

Nixon, S. L., Cockell, C. S., and Tranter, M. (2012). Limitations to a microbial iron cycle on Mars. *Planet. Space Sci.* 72, 116–128. doi: 10.1016/j.pss.2012.04.003

Peeples, T. L., and Kelly, R. M. (1995). Bioenergetic response of the extreme thermoacidophile *Metallosphaera sedula* to thermal and nutritional stress. *Appl. Environ. Microbiol.* 61, 2314–2321.

Polikreti, K., and Maniatis, Y. (2002). A new methodology for the provenance of marble based on EPR spectroscopy. *Archaeometry* 44, 1–21. doi: 10.1111/1475-4754.00040

Poulet, F., Bibring, J.-P., Mustard, J. F., Gendrin, A., Mangold, N., Langevin, Y., et al. (2005). Phyllosilicates on Mars and implications for early martian climate. *Nature* 438, 623–627. doi: 10.1038/nature04274

Presciutti, F., Capitani, D., Sgamellotti, A., Brunetti, B. G., Costantino, F., Viel, S., et al. (2005). Electron paramagnetic resonance, scanning electron microscopy with energy dispersion X-ray spectrometry, X-ray powder diffraction, and NMR characterization of iron-rich fired clays. *J. Phys. Chem. B* 109, 22147–22158. doi: 10.1021/jp0536091

Reed, C. (2015). Earth microbe prefers living on meteorites. *Science*. doi: 10.1126/science.aab2499

Schimak, M. P., Kleiner, M., Wetzel, S., Liebeke, M., Dubilier, N., and Fuchs, B. M. (2015). MiL-FISH: Multilabeled oligonucleotides for fluorescence in situ hybridization improve visualization of bacterial cells. *Appl. Environ. Microbiol.* 82, 62–70. doi: 10.1128/AEM.02776-15

Schippers, A., Jozsa, P., and Sand, W. (1996). Sulfur chemistry in bacterial leaching of pyrite. *Appl. Environ. Microbiol.* 62, 3424–3431.

Stetter, K. O. (2006). History of discovery of the first hyperthermophiles. *Extremophiles* 10, 357–362. doi: 10.1007/s00792-006-0012-7

Wächtershäuser, G. (1992). Groundworks for an evolutionary biochemistry: the iron-sulphur world. *Prog. Biophys. Mol. Biol.* 58, 85–201. doi: 10.1016/0079-6107(92)90022-X

Wheaton, G. H., Mukherjee, A., and Kelly, R. M. (2016). Metal 'shock' transcriptomes of the extremely thermoacidophilic archaeon *Metallosphaera sedula* reveal generic and specific metal responses. *Appl. Environ. Microbiol.* 82, 4613–4627. doi: 10.1128/AEM.01176-16

Xu, J., Luan, Z., Hartmann, M., and Kevan, L. (1999). Synthesis and characterization of Mn-containing cubic mesoporous MCM-48 and AlMCM-48 molecular sieves. *Chem. Mater.* 11, 2928–2936. doi: 10.1021/cm990300j

Conflict of Interest Statement: The authors declare that the research was conducted in the absence of any commercial or financial relationships that could be construed as a potential conflict of interest.

frontiers in Microbiology

ORIGINAL RESEARCH
published: 08 September 2017
doi: 10.3389/fmicb.2017.01668

Determination of Geochemical Bio-Signatures in Mars-Like Basaltic Environments

Karen Olsson-Francis[1], Victoria K. Pearson[2], Elisabeth D. Steer[2,3] and Susanne P. Schwenzer[1]*

[1] School of Environment, Earth and Ecosystem Sciences, Open University, Milton Keynes, United Kingdom, [2] School of Physical Sciences, Open University, Milton Keynes, United Kingdom, [3] Nanoscale and Microscale Research Centre, University of Nottingham, Nottingham, United Kingdom

Bio-signatures play a central role in determining whether life existed on early Mars. Using a terrestrial basalt as a compositional analog for the martian surface, we applied a combination of experimental microbiology and thermochemical modeling techniques to identify potential geochemical bio-signatures for life on early Mars. Laboratory experiments were used to determine the short-term effects of biota on the dissolution of terrestrial basalt, and the formation of secondary alteration minerals. The chemoorganoheterotrophic bacterium, *Burkholderia* sp. strain B_33, was grown in a minimal growth medium with and without terrestrial basalt as the sole nutrient source. No growth was detected in the absence of the basalt. In the presence of basalt, during exponential growth, the pH decreased rapidly from pH 7.0 to 3.6 and then gradually increased to a steady-state of equilibrium of between 6.8 and 7.1. Microbial growth coincided with an increase in key elements in the growth medium (Si, K, Ca, Mg, and Fe). Experimental results were compared with theoretical thermochemical modeling to predict growth of secondary alteration minerals, which can be used as bio-signatures, over a geological timescale. We thermochemically modeled the dissolution of the basalt (in the absence of biota) in very dilute brine at 25°C, 1 bar; the pH was buffered by the mineral dissolution and precipitation reactions. Preliminary results suggested that at the water to rock ratio of 1×10^7, zeolite, hematite, chlorite, kaolinite, and apatite formed abiotically. The biotic weathering processes were modeled by varying the pH conditions within the model to adjust for biologic influence. The results suggested that, for a basaltic system, the microbially-mediated dissolution of basalt would result in "simpler" secondary alteration, consisting of Fe-hydroxide and kaolinite, under conditions where the abiotic system would also form chlorite. The results from this study demonstrate that, by using laboratory-based experiments and thermochemical modeling, it is possible to identify secondary alteration minerals that could potentially be used to distinguish between abiotic and biotic weathering processes on early Mars. This work will contribute to the interpretation of data from past, present, and future life detection missions to Mars.

Keywords: bio-signatures, Mars, life detection, thermochemical modeling, microbial weathering, basalt

OPEN ACCESS

Edited by:
Philippe M. Oger, UMR CNRS 5240 Institut National des Sciences Appliquées, France

Reviewed by:
Aude Picard, Harvard University, United States
Jennifer Ronholm, McGill University, Canada

****Correspondence:***
Karen Olsson-Francis
karen.olsson-francis@open.ac.uk

Specialty section:
This article was submitted to Extreme Microbiology, a section of the journal Frontiers in Microbiology

Received: *11 May 2017*
Accepted: *17 August 2017*
Published: *08 September 2017*

Citation:
Olsson-Francis K, Pearson VK, Steer ED and Schwenzer SP (2017) Determination of Geochemical Bio-Signatures in Mars-Like Basaltic Environments. Front. Microbiol. 8:1668. doi: 10.3389/fmicb.2017.01668

INTRODUCTION

The surface of present-day Mars is cold, dry, highly oxidized, and exposed to ultraviolet (UV) and ionizing radiation. These conditions are considered inhospitable; yet early Mars may have had surface conditions more conducive to life, with a possible warmer climate and a denser atmosphere that could provide protection from UV and cosmic radiation (Molina-Cuberos et al., 2001; Bibring et al., 2006; Fairen et al., 2009; Tian et al., 2009). Geological, geochemical, and geomorphological observations made by orbiting spacecraft have provided definitive evidence of more clement and less oxidizing conditions in early martian history (e.g., Carr and Head, 2010; Mangold et al., 2012). Globally and locally, large ancient fluvial systems (including channels and fans) are observed, which may have been habitable (e.g., Malin and Edgett, 2003; Irwin et al., 2005; Mangold et al., 2012; Williams et al., 2013; Fassett and Head, 2015). On Mars' surface, Curiosity has detected complex lake bed stratigraphy, which are reported to contain nitrogen and carbon compounds, including complex organic molecules (Andeer et al., 2013; Williams et al., 2013; Vaniman et al., 2014; Grotzinger et al., 2015; Stern et al., 2015). As a second, independent, strand of evidence for a more hospitable past, the NASA Mars Exploration Rover Opportunity also found evidence for an impact-generated hydrothermal system at Endeavour crater (Arvidson et al., 2014; Fox et al., 2016); impact-generated hydrothermal systems could have provided habitable conditions even during periods of very cold climate (Abramov and Kring, 2005; Schwenzer and Kring, 2009). Mineralogical and geochemical observations of clay minerals, and the detection of carbonates and sulfates, reveal a complex set of environmental conditions ranging from weathering to evaporation, and from cold surface to elevated subsurface temperature conditions, occurring in complex succession (Filiberto and Schwenzer, 2013; Arvidson et al., 2014; Grotzinger et al., 2014, 2015).

On Mars, the surface rocks are dominated by basaltic compositions, but range from ultramafic to basaltic to potentially even more evolved compositions (Nyquist et al., 2001; Christensen et al., 2005; Filiberto, 2008; Treiman and Filiberto, 2015; Morris et al., 2016; Sautter et al., 2016; Mangold et al., 2017). Alteration is known to range from open-system (with and without acidic influence) to closed system conditions, and as a consequence, the resultant rock chemistry may or may not reflect the basaltic source rocks; the products of weathering can be influenced by location, environmental conditions, geological time, and permeability of the rocks at the time of weathering (see Schwenzer and Kring, 2009; Ehlmann et al., 2013; Bridges et al., 2015; Carter et al., 2015; Zolotov and Mironenko, 2016 for example of the wide variety of alteration conditions found on Mars to date). Extensive laboratory based work has demonstrated that microorganisms can use olivine-pyroxene-plagioclase-bearing rocks as a source of bio-essential elements and can enhance the weathering rates (e.g., Berthelin and Belgy, 1979; Vandevivere et al., 1994; Barker et al., 1998; Rogers et al., 1998; Kalinowski et al., 2000; Liermann et al., 2000; Bennett et al., 2001; Welch et al., 2002; Uroz et al., 2009).

The mechanisms employed by microorganisms in basaltic environments are variable and range from the production of excess protons, to the production of low molecular weight organic acids and siderophores (highly specific $Fe^{(III)}$ ligands), and, in some cases, and the production of extracellular polysaccharides and enzymes (Welch and Ullman, 1993; Vandevivere et al., 1994; Barker et al., 1998; Bennett et al., 2001; Wu et al., 2007; Olsson-Francis et al., 2015). These mechanisms may occur in the bulk phase or in local microenvironments, where concentrations would be much higher (Bennett et al., 2001). For example, in terrestrial systems, solutions of organic acids in concentrations comparable to, or slightly higher than, ground water show an increase in dissolution rates of less than one magnitude. In contrast, in local microenvironments the concentration of acid may be much higher (Banfield et al., 1999). If life had once existed on early Mars, it may have left a record of these processes within the martian rock record (Banfield et al., 2001) and recognizing microbially-induced minerals, which could have potentially formed in an early Mars environment, would identify important bio-signatures for use in future life detection efforts.

To ensure unequivocal identification of bio-signatures, comparison with abiotic processes is necessary. Terrestrial abiotic basalt weathering has been extensively studied and characterized using field observations, laboratory-based experiments and thermochemical modeling (e.g., Gislason and Eugster, 1987a,b; Oelkers and Schott, 2001; Wolff-Boenisch et al., 2006). In contrast, to date, stand-alone laboratory experiments have been the only way to investigate the influence that biota has on basalt dissolution and the growth and evolution of secondary alteration minerals (e.g., Wu et al., 2007; Olsson-Francis et al., 2012, 2015). From these experiments alone it is difficult to predict what would happen over years-long or even geological time scales, for example, on early Mars, when the rock is fully dissolved or, more likely, subject to the effects of incongruent dissolution. In these circumstances, the formation of amorphous and leached layers, and secondary mineral precipitation, may occur, influencing the availability of cations for use in biological metabolism.

Themochemical modeling is a powerful tool that aids the prediction of mineral assemblage formation by assessing reaction pathways and studying the formation of secondary minerals in a gas-fluid-rock system (e.g., Reed, 1982; Kühn, 2004) and this has been applied to studies of secondary mineral formation and fluid compositions on Mars (Bridges and Schwenzer, 2012; Filiberto and Schwenzer, 2013; Schwenzer and Kring, 2013; Bridges et al., 2015). In biotic experiments, geochemical models such as Geochemist's workbench are routinely used to characterize mineral precipitation during laboratory-based experiments (e.g., Orcutt et al., 2011; Olsson-Francis et al., 2012), and to characterize redox reactions in water-rock environments (Posth et al., 2008). However, there have been limited, if any, studies that have combined laboratory-based experiments and thermochemical modeling to compare biotically and abiotically generated secondary alteration mineralization over geological time scales.

In this paper, we present preliminary work carried out to investigate the feasibility of coupling microbial dissolution experiments with thermochemical modeling in order to identify mineralogical bio-signatures that could be used

as evidence of life on early Mars. The experiments invoke chemoorganoheterotrophic metabolism as a plausible metabolism on early Mars because of the availability of suitable energy sources (electron donors) (Cockell, 2014; Westall et al., 2015). For example, organic carbon at Gale Crater has been predicted to be between 800 and 2,400 ppm. Even if 1% or less of this carbon was bio-available on early Mars this could sustain a chemoorganoheterotrophic community of 10^5 cells/g of sediment (Sutter et al., 2016). Further, if life had evolved on early Mars, either by photosynthesis or chemolithotrophy, their organic remnants could be used as an electron donor for this metabolism. Finally, chemoorganoheterotrophic metabolism is known to enhance silicate dissolution, predominantly by the production of excess protons and organic acids (Wu et al., 2007; Olsson-Francis et al., 2015).

For microorganisms that only utilize minerals as essential micronutrients and macronutrients (i.e., they are not respired), acidification is the most common, and straightforward, mechanism for silicate dissolution and is generally universal (for review see Uroz et al., 2009). Our understanding of basaltic weathering is predominately based on aerobic metabolism (e.g., Welch and Ullman, 1993; Vandevivere et al., 1994; Blake and Walter, 1996; Drever and Stillings, 1997). On Mars, aerobic metabolism may have been feasible, Curiosity data indicates that there is sufficient molecular oxygen (∼1,450 ppm; Mahaffy et al., 2013) in the martian atmosphere to support aerobic activity (King, 2015). In addition, inorganic alteration reactions that are expected to happen due to water-rock interactions have been shown to shift the redox environment to more oxidizing conditions (e.g., Bridges and Schwenzer, 2012). Therefore, traditional experiments in anoxic conditions (e.g., Schirmack et al., 2014, 2015) are complemented by the experiments in this study, conducted in a more oxidizing milieu.

Step by step titrations were modeled to investigate the effect that microbially-mediated acidification has on the aqueous environment and the precipitation of secondary alteration minerals during microbial-mediated basalt weathering. In parallel, abiotic alteration at different pH are investigated to understand the effects of biota by contrasting the two systems. Secondary alteration minerals uniquely produced by microbial-mediated weathering could be used as a geochemical bio-signature for life. The findings of this study are important for further developing geochemical models that could be used to predict bio-signatures for life on early Mars.

MATERIALS AND METHODS

Water to Rock Ratios

For this study, it is critically important to clearly define three different water to rock ratios: we use subscripts E (experiment), D (dissolved), and M (model) to denote the exact meaning of W/R in each context. $(W/R)_E$ is the experimental water to rock ratio, simply referring to the ratio of the amount of rock and the amount of water weighed out and mixed for the experiment. This is distinct from $(W/R)_D$, which is the amount of rock actually dissolved during the experiment. These two water to rock ratios are different, because, even though dissolution of rock in water is slow, a very small amount of rock will dissolve during the experiment. We assess $(W/R)_D$ by looking at the most soluble elements in the fluids resulting from the experiment. $(W/R)_M$ is the water to rock ratio used in the model, and assumes complete dissolution of all rock. We compared the $(W/R)_D$ and $(W/R)_M$ values at the concentration where the most soluble elements are similar.

Characterization and Preparation of Mars Analog Rock

Basalt from Skye was purchased from Richard Tayler minerals (United Kingdom) as an analog for martian basalts. A polished thin section of the rock was prepared for microprobe analysis. The remaining rock was broken with a hammer and pieces devoid of visible weathering were ground using a Tema swing mill, for 8 min. The crushed rock was sieved to select for a fraction size between 250 and 500 μm. Fine particles were removed by ultrasonication in MiliQ water (Olsson-Francis et al., 2010, 2012). The rock was then dried for 24 h, at 80°C. The specific surface area of the ground rock samples was measured using multi-point BET (Brunauer, Emmett and Teller analysis at Imperial College London) with N_2 and yielded a surface area of $0.976\,m^2\,g^{-1}$.

Petrological analysis was carried out on thin sections of the sample using reflective and transmitted microscopy and a FEI Quanta 3D dual beam scanning electron microscope (SEM) fitted with an Oxford Instruments 80 mm X-Max energy dispersive X-ray spectrometer (EDS), which was operated with an accelerating voltage of 20 kV and a 10–15 mm working distance. The major elemental composition of the basalt was obtained using an ARL 8,420+ dual goniometer wavelength dispersive X-ray Fluorescence (XRF) spectrometer (Applied Research Laboratories, Ecublens, Switzerland). Mineral analysis was obtained from a Cameca SX100 electron microprobe (EMPA) at The Open University using a spot size of 10 μm, accelerated voltage of 20 kV and a beam current of 20 nA.

Basalt Mineralogy

The sample was an altered amygdaloidal basalt from the Skye Tertiary Province. The amygdales were filled with zeolites, which were removed from the sample before experimentation commenced. The sample was fine grained with a groundmass of augite and plagioclase with an accessory phase of Ti-spinel. Much of the original mineralogy had been altered at low temperature to form clays and the general mineralogy was characterized as: 20–25% augite, 30% plagioclase, 50% clays. The amount of Ti-spinel was <1%. The plagioclase was present as laths up to 1 mm in size; the augite crystals were largely anhedral and below 0.5 mm in size, as shown in **Figure 1**. Anhedral grains of Ti-spinel below 100 μm occured throughout the sample. The size and shape of Ti-spinel crystals was prohibitive of EMPA analysis. Representative analyses of the minerals present are detailed in **Table 1**.

The clays present in the sample were vermiculite and saponite. These are similar in composition to clays found by the Curiosity rover on Mars by XRD (Vaniman et al., 2014) and to those modeled by Bridges et al. (2015) to be present in Gale Crater. As a comparison, analyses from this study have been plotted with clay

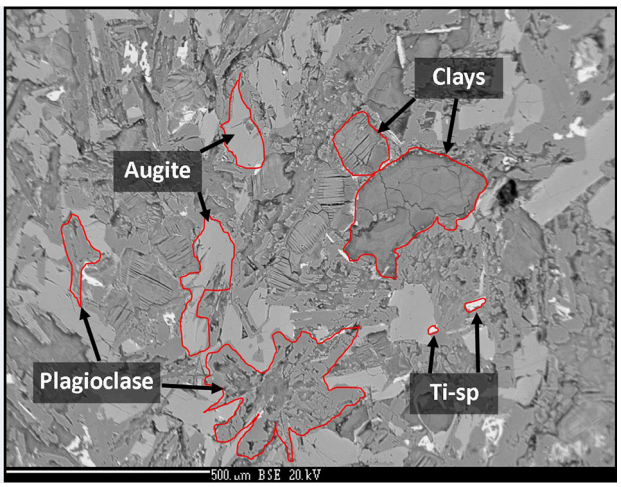

FIGURE 1 | Back-scatter electron image of the analog basalt used in this experiment. Augite, plagioclase, clay, and Ti-spinel are observed. Image width is ~1.5 mm.

TABLE 1 | Representative analyses of minerals in the basalt (wt %).

	SiO_2	Al_2O_3	TiO_2	MgO	CaO	MnO	FeO	Na_2O	K_2O	Total
Augite	50.63	3.25	1.11	14.51	20.59	0.20	8.83	0.33	0.00	99.45
Plagioclase	58.27	25.63	0.11	0.10	8.45	0.00	0.74	6.68	0.52	100.50
Zeolite	50.69	23.49	0.00	0.01	10.63	0.01	0.02	1.63	0.47	86.95
Vermiculite	34.97	11.84	0.00	13.04	1.45	0.32	20.78	0.09	0.04	82.53
Saponite	41.10	11.54	0.00	17.65	0.71	0.25	13.13	0.09	0.04	84.51

compositions modeled to exist on Mars by Bridges et al. (2015) and with clays measured in the martian Lafayette meteorite by Hicks et al. (2014). **Figure 2** shows that the vermiculites and saponite identified in this study form a tight cluster that overlaps with the martian clays as well as the clays modeled here. However, the range of terrestrial clays extends beyond the narrow range of isochemical alteration, showing more Si and Al rich endmembers and clays depleted in those two elements. The latter could be due to an oxidizing reaction causing microcrystalline Fe-oxides and hydroxides intermixed with the clay. The mixture of clay and pristine mineral remnants makes this basalt a proxy for the recently discovered "mudstones" (Vaniman et al., 2014), of basaltic origin, on Mars.

Model Bacterium

The microbiological experiments were conducted using the bacterium *Burkholderia* sp. strain B_33, which has previously been isolated from nutrient limiting soil, in Snowdonia National Park, United Kingdom (Olsson-Francis et al., 2015). A *Burkholderia* sp. was selected because long-term experiments in nutrient poor soils have shown a correlation between the abundance of this genus and specific minerals, such as plagioclase and a mix of phlogopite and quartz (Uroz et al., 2009; Lepleux et al., 2012). It also exhibits chemoorganoheterotrophy, a plausible metabolism for life on past Mars.

Routine growth was carried out in a modified minimal medium, which contained the following (mg L^{-1}): 10 of $FeCl_3$, 150 of $MgSO_4 \bullet 6H_2O$, 20 of $CaCl_2$; 20 of KCl, 65 of NH_4Cl, 100 of $NaNO_3$, 70 of K_2HPO_4, 60 of KH_2PO_4, 20 of glucose. All of the reagents, except the $MgSO_4 \bullet 6H_2O$ and the $FeCl_3$ were added and the pH was adjusted to pH 7.0. After the medium was autoclaved (20 min at 121°C), filtered sterilized $MgSO_4 \bullet 6H_2O$ and $FeCl_3$ were added (this did not alter the pH).

Basalt Dissolution Experiment

The dissolution experiments were carried out in batch culture. The growth medium contained the following: 2 g L^{-1} of glucose, 0.06 g L^{-1} of NH_4Cl, and 200 g L^{-1} of basalt. Twenty grams of the crushed basalt (0.5–1 mm) was placed in an acid-washed 125 ml glass Erlenmeyer culture flask and autoclaved at 121°C for 15 min. Two g L^{-1} of glucose was added ensure that growth was not limited by the amount of carbon. One hundred milliliters of autoclaved liquid medium was added to the flask and the pH was adjusted to pH 7.0 with filtered sterilized 10 mM NaOH. The experiments were conducted with a water to rock $(W/R)_E$ ratio of 100/20 (BET surface area of 0.976 m^2 g^{-1}).

Prior to inoculating the flasks, cells were washed to remove any excess growth medium. Ten milliliters of exponentially grown cells were harvested by centrifugation at 4,000 × g, for 5 min. The cell pellet was washed three times with sterilized 50 mM Tris buffer (pH 7.0) and re-suspended to a final cell density of 10^7–10^8 cell mL^{-1}. A 0.5% inoculum was used to inoculate the flasks. The flasks were incubated, without shaking, at 25°C for 28 days. Each of the experiments were carried out in triplicate. The biotic experiments were designated B1, B2, and B3, and the abiotic controls were designated C1, C2, and C3. Abiotic controls were prepared in an identical manner to the biotic flasks.

At day 1, 4, 7, 11, 14, 21, and 28, 5.5 mL aliquots were aseptically removed from the flask and transferred to a 10 mL acid-washed bottle. Each aliquot was immediately processed as follows: 4.5 mL was passed through a 0.2 µm nylon syringe filter and acidified with concentrated HNO_3 (final 5% acid) for elemental concentration measurements and 1 mL was left unfiltered and used to measure microbial growth and pH.

Measuring Bacterial Growth

Cells were stained with the nucleic acid-binding dye SYBR Green I DNA (0.1% w/v stock; Life Technologies, Paisley, UK) and 1 mL of culture was filtered through a 0.2 µm black polycarbonate filter and then washed with 100 µL of sterile dd H_2O. The cells on the filter were enumerated using a Leica DMRP microscope equipped with epifluorescence, as previously described (Summers et al., 2013). The growth rate constant (k) for the log phase of growth was determined (Pirt, 1978).

Siderophore Production

To determine the ability of the isolates to produce siderophores, the Chrome Azurol S liquid assay (CAS) was used (Schwyn and Neilands, 1987). As a control we used *Cupriavidus metallidurans* CH34, which has previously been shown to produce siderophores

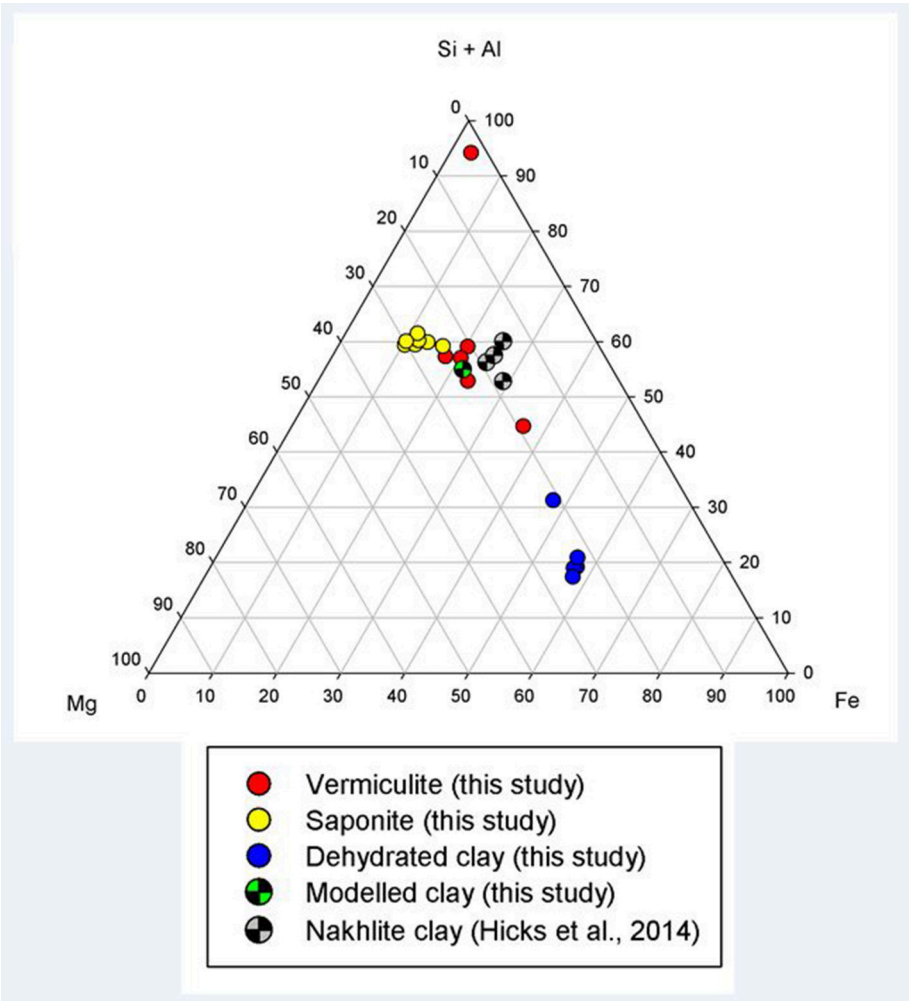

FIGURE 2 | Ternary plot of (Si+Al)–Mg–Fe showing the clay mineral compositions observed in this study (filled circles), in the models of this study (checkered green circle), and in the nakhlite martian meteorites (checkered gray circle; Hicks et al., 2014).

under iron limiting conditions (Olsson-Francis et al., 2010). The detection of siderophores was quantified and defined, as previously described (Payne, 1994). The isolates were grown in the minimal medium, without iron (i.e., they were iron-limited), and siderophore production was measured in stationary stage cells.

Chemical Analyses

The pH was measured using an Orion 3-Star Thermo Scientific bench top meter with an uncertainty of 0.01 pH unit. The total elemental concentration of dissolved elements in the growth medium was measured using Inductively Coupled Plasma–Mass Spectrometry (ICP-MS; Agilent 7500s ICP-MS with New Wave 213 laser system). Detection limits for the ICP-MS were as follows: Ca (39.89 nmol L^{-1}), Mg (2.81 nmol L^{-1}), P (236.64 nmol L^{-1}), Fe (41.83 nmol L^{-1}), Na (7.59 nmol L^{-1}), Si (236.63 nmol L^{-1}), and Al (2.03 nmol L^{-1}). Each of the measurements were conducted in triplicate and the mean was reported; the standard deviation was <5%. The data was corrected for the decrease in fluid volume and the loss of elemental mass during sampling, as previously described (Wu et al., 2007). Glucose concentration was measured using the Amplex red glucose kit (Invitrogen). The absorbance was measured at 595 nm and compared with a calibration curve of known glucose concentrations. Oxalate was measured using an oxalate oxidase assay (Trinity Biotech), at 590 nm, as per manufacturer's instructions.

FEG-SEM Analysis

After 28 d, rocks were removed from the flasks for Field Emission Gun (FEG)-SEM analysis. The rocks were air dried and carbon coated (15–20 nm thickness) on aluminum stubs. The surface of the rocks was examined using a using a FEG-SEM with an EDS detector (ZEISS Supra; 55-VP; Zeiss Microimaging, Göttingen, Germany), which was operated with an accelerating voltage of 2–15 kV and a 7–10 mm working distance.

Elemental Release Rates

The kinetics of elemental release were calculated using the linear release rate (R_i^l), as previously described (Wu et al., 2007). Any significant difference between the biotic and abiotic dissolution kinetics were identified using a Student's *t*-test.

Elemental Uptake

The intracellular elemental concentration was measured at day 28. Twenty milliliters of liquid culture was aseptically taken from the biotic experiments and centrifuged at 13,000 × *g* for 20 min. The resulting cell pellet was washed three times in sterilized 0.5% HNO_3. The cells were washed to ensure that no elements from the experimental solution were analyzed; however, we cannot rule out that elements that were loosely bound to the cells were not lost during this step. The pellet was dried at 80°C overnight, and digested in 1 mL concentrated HNO_3 (final 5% acid) and the resulting solution was analyzed by ICP-MS, as previously described (Olsson-Francis et al., 2012).

Thermochemical Modeling

In order to assess the inorganic reaction pathways possible in the rock-fluid system, we used thermochemical modeling, specifically the code CHIM-XPT (previously CHILLER Reed and Spycher, 2006; Reed et al., 2010). This code has been used extensively in terrestrial basaltic environments (e.g., Reed, 1982) and applied to basaltic rocks of martian compositions (e.g., Debraal et al., 1993; Schwenzer and Kring, 2009; Filiberto and Schwenzer, 2013; Bridges et al., 2015; Schwenzer et al., 2016). We carried out stepwise titration simulations from the initial fluid to a $(W/R)_M$ of 1 to assess dissolution of the rock in the fluid without biotic activity, starting at a very high $(W/R)_M$ of over 10^8, modeling titration to a low $(W/R)_M$ of 1. We report data from $(W/R)_M$ of 1 Mio ensuring that constant conditions independent of any starting mineral choices had been reached at this point. Input data included the rock composition as derived by XRF, and the fluid composition of the minimal growth medium (**Table 2**). Note that the fluid composition is summarized in **Table 2** as one species per element, but elements will be partitioned between several species as relevant to the pH and Eh conditions in the fluid during the modeling. For example, Fe is partitioned between Fe^{2+} and Fe^{3+} species according to redox conditions in the respective modeling step, and compound species, e.g., FeOH or FeCl-bearing ions, are also considered important in this respect. Overall, a set of ∼80 different ionic species are typically used to represent the fluid chemistry in each calculation iteration within the modeling steps. We model at 1 bar and 25°C, which closely mimics the pressure and temperature conditions of the growth experiment and investigate three model experiments: In the first experiment, pH varies, and is treated as a free parameter. In two subsequent experiments, pH is set to 7 and 4, respectively, to simulate the conditions during the stationary and exponential phases in the growth experiment. The Cl-anion is used for charge balance, which is especially important for the pH 4 model, because additional Cl^- is required to set the initial pH.

In the model, we assumed complete dissolution of the rock into solution, which is a simplification many codes make (for an explanation and overview of the diversity of thermochemical rate modeling see Kühn, 2004; Ganguly, 2008; Rimstidt, 2014). To account for a more complex natural system, e.g., varying dissolution rates of the minerals in the rock and/or incongruent dissolution of minerals, the input parameters were varied systematically and with close reference to available thermodynamic data, and experimental and natural observations and data. This results in a parameter space that can be reduced to the most likely approximation of the natural system.

TABLE 2 | Input data for the model.

Rock composition [wt. %]		Fluid composition [10^{-7} moles]	
SiO_2	51.81	Cl^-	51.7
Al_2O_3	14.21	$SiO_{2\ (aq)}$	0.34
Fe_2O_3	13.09	Al^{3+}	0.37
MgO	4.79	Ca^{2+}	0.21
CaO	4.97	Mg^{2+}	0.38
Na_2O	3.83	Fe^{2+}	0.01
K_2O	0.19	K^+	0.24
MnO	0.22	Na^+	49.8
P_2O_5	0.38	HPO_4^{2-}	0.32

Species in the fluid are summarized in the table as one species, but during the modeling were partitioned into several dissolved species (for details see text).

RESULTS

Bacterial Growth

The bacterium, *Burkholderia* sp. strain B_33 was able to grow in the minimal medium with basalt as the sole source of bio-essential elements. No growth was detected in the growth medium without basalt. The bacterium utilized the glucose within the growth medium as a source of carbon and within 7 days the concentration of glucose decreased to ∼20%, as shown in **Figure 3A.** As the bacterium utilized the glucose, the metabolite oxalate was produced. The concentration of oxalate in the growth medium increased steadily until day 7 and then plateaued (**Figure 3B**). There was no significant difference between the triplicate flasks.

The initial cell counts, immediately after inoculation, were between 9.23×10^4 (B3) and 2.92×10^5 (B2) cell mL^{-1}. Within 7 days, the number of cells had increased to a maximum of between 1.53×10^8 (B2) and 2.82×10^8 (B3) cell mL^{-1} (exponential growth) and then remained relatively steady until the end of the experiment (stationary phase), as shown in **Figure 4A**. Coinciding with exponential growth, the pH decreased rapidly and at day 4 the pH was between 3.5 (B2) and 3.6 (B3) (**Figure 4B**). As the cells reached late exponential stage the pH values gradually increased to a steady-state equilibrium of between pH 6.8 and 7.1. In contrast, the pH in the abiotic controls remained near neutral pH (between pH 6.6 and 7.1) throughout the experiment (**Figure 4B**). No cells were observed in the abiotic controls.

Siderophore Production

Burkholderia sp. strain B_33 was screened for siderophore production using the Chrome Azurol S assay. In the minimal

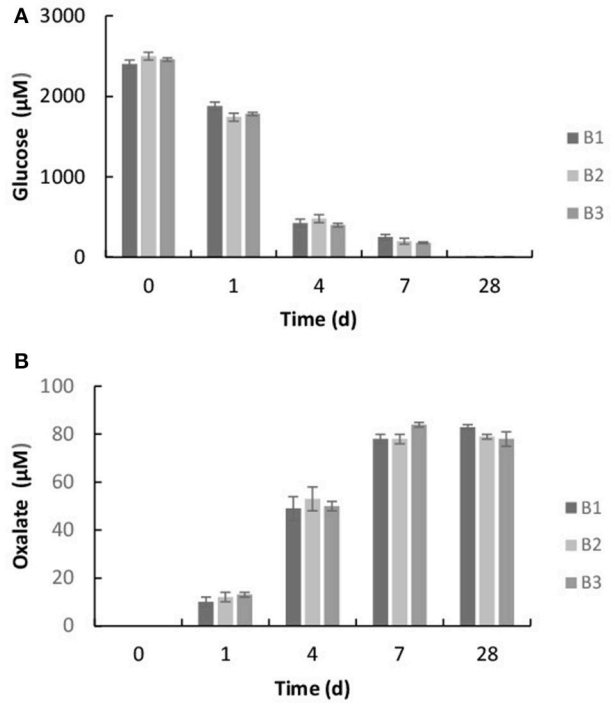

FIGURE 3 | Concentration of glucose **(A)** and oxalic acid **(B)** in the growth medium after 1, 4, 7, and 28 days. The values reported are the means of three independent experiments, and the standard error associated with these determinations is shown.

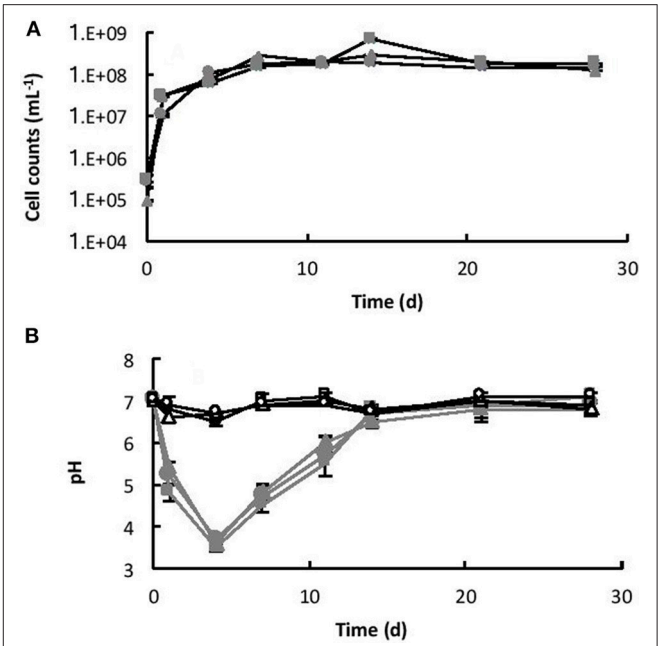

FIGURE 4 | (A) Growth of *Burkholderia* sp. strain B_33 in a minimal medium with basalt as the sole source of bio-essential elements. **(B)** Change in pH of the medium over time. The values reported are the means of three independent biotic [B1 (■), B2 (▲), B3 (●)] and abiotic [C1 (□), C2 (△), C3 (○)] experiments, and the standard error associated with these determinations is shown. Cell counts demonstrated that there was no bacterial contamination in the abiotic controls after 28 days.

medium, without iron, siderophores were produced. The amount varied between 1.20 and 2.10 μmol L^{-1} EDTA equivalent. However, when basalt was added to the growth medium, siderophores were not detected (data not shown).

Basalt Dissolution

Dissolution was measured by the concentration of key elements (Si, K, Ca, P, Mg, and Fe) within the growth medium. All of the values were corrected for the decrease in fluid volume and the loss of elemental mass during sampling. Without the basalt, the concentrations of Si, K, Ca, Mg, Na, Fe, and P in the growth medium were 0.034, 0.024, 0.021, 0.038, 0.018, and 0.01 μmol L^{-1}, respectively. **Figure 5** shows the elemental concentrations in the dissolution experiments as a function of time. The presence of *Burkholderia* sp. strain B_33 enhanced the release of Si, Ca, Mg, Al, K, Na, P, and Fe into the growth medium. In general, the concentration increased linearly until day 4–11 (depending on the element) and then they either reached or began to approach steady-state conditions.

The initial linear release rates were calculated to compare the dissolution kinetics in the abiotic and biotic flasks, as demonstrated in **Table 3**. The presence of *Burkholderia* sp. strain B_33 had a significant ($p < 0.05$) effect on the release rates of Si, Ca, Mg, Al, and Fe (there was no significant effect on the release of P, Na, and K). For example, for B1, the R_i^l value for Ca was approximately eight-fold higher than the abiotic controls. Plotting the $\log R_i^l$ values for Mg, Ca, Si, and K against the average pH of the initial growth phase (day 1–7, which corresponds to the period used to determine the R_i^l values) suggests that the release rates were dependent on pH (**Figure 6**).

Cellular Element Uptake

The intracellular elemental concentration was measured in bacteria collected from day 28. The values in **Table 4** are reported as the elemental concentration per cell. This data was used to determine if elemental uptake was significant with respect to the solute concentrations at day 28. The values reported in **Table 3** were multiplied by the number of cells measured at day 28 and the values were corrected for the decrease in fluid volume during sampling, as previously described (Wu et al., 2007; Olsson-Francis et al., 2012). The intracellular elemental concentrations were <1% of the final fluid concentrations.

Secondary Alteration Minerals

The surface of the basaltic rock was examined for secondary alteration products with FEG-SEM and EDS analysis. Where possible, EDS analysis was performed on areas of the rock where secondary alteration was visible on the surface (**Figure 7**) i.e., where there was a positive relief and evident morphological differences to the crystalline basalt and the clay minerals already contained within the basalt. However, there was limited evidence of alteration on any mineral surfaces; mineral grains

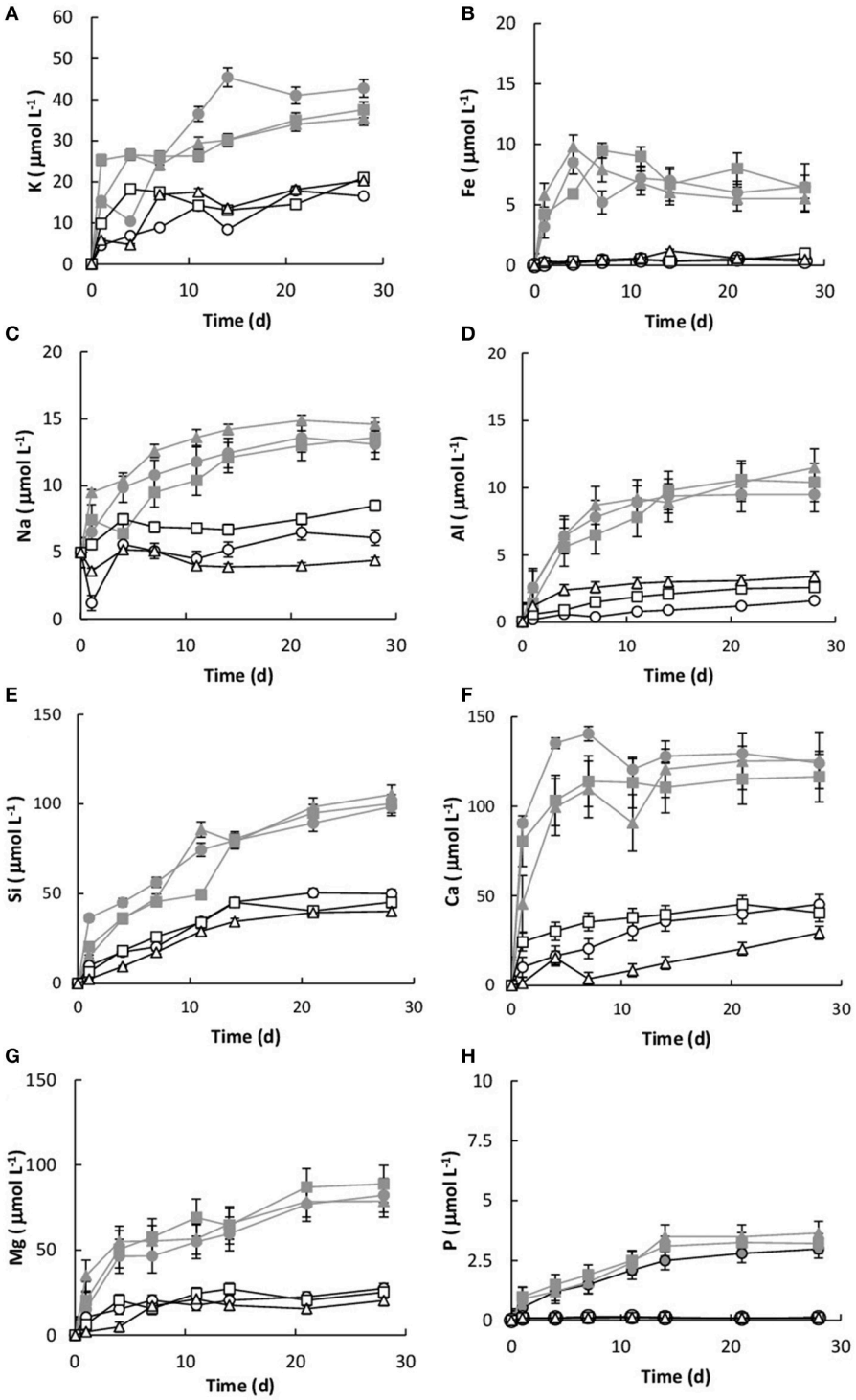

FIGURE 5 | Concentration of K **(A)**, Fe **(B)**, Na **(C)**, Al **(D)**, Si **(E)**, Ca **(F)**, Mg **(G)**, and P **(H)** over time for both the biotic [B1 (■), B2 (▲), B3 (●)] and abiotic flasks [C1 (□), C2 (△), C3 (○)]. The values reported are the means of three independent experiments, and the standard error associated with these determinations is shown.

from the biotic and abiotic flasks showed predominantly pristine surfaces with the exception of dissolution pits and an amorphous silicate layer on the surface of the rocks in the biotic flasks. **Figure 7** also shows small pockets of alteration products in the biotic flasks, which are remarkably diverse (**Table 5**).

The mineral assemblage labeled "spectrum 20" is dominated by Si, with minor Al, Na, Fe, S, and Cl. Dividing this analysis

TABLE 3 | Linear elemental release rates R_i^l calculated from the linear rate law (Wu et al., 2007).

	R_i^l (10^{-12} mol m^{-2} s^{-1})							
	P	**Si**	**Al**	**Mg**	**Ca**	**Na**	**K**	**Fe**
BIOTIC								
B1	0.52	2.68	0.38	2.75	8.02	0.28	0.62	0.51
B2	0.45	2.16	0.21	2.98	6.12	0.08	1.57	0.39
B3	0.42	2.13	0.38	3.26	5.90	0.32	1.56	0.58
ABIOTIC								
C1	0.35	1.04	0.03	0.91	0.98	0.03	0.41	0.01
C2	0.32	1.08	0.05	1.22	1.79	0.01	1.08	0.02
C3	0.41	0.56	0.01	0.29	0.92	0.01	0.28	0.01

into element-oxides results in a "high total," >100%. Even if it is assumed that Cl is more likely to be bound in CaCl, and all Fe is FeS, the total remains above 100%. Inspection of **Figure 7** and knowledge from our models (see below) allows us to assume that kaolinite [$Al_2Si_2O_5(OH)_4$] might be present, and if this accounts for all of the Al, the "high total" is reduced further (**Table 5**). Therefore, it is likely that the alteration assemblage on "spectrum 20" contains silica and kaolinite with minor FeS and NaCl. Alternatively, instead of NaCl, some minor amount of carbonate could take up the excess cations, but is considered unlikely in this partitioning exercise because of the Si-dominance of the precipitate and the amounts of Cl in solution.

The adjacent alteration mineral assemblage has a different composition, since it is even more dominated by Si and Fe, has around 4% Cl, P, and Al, and minor Na and S. The total, after partitioning into oxides, is only slightly above 100%, but is within 2% error of 100% if all Na is assumed to be NaCl and all S is FeS. According to our models, the remaining Fe could be in nontronite [$(CaO_{0.5},Na)_{0.3}Fe_2^{3+}(Si,Al)_4O_{10}(OH)_2{\cdot}nH_2O$]. This analysis also has P (**Table 5**), which could explain the high Cl; there is significantly Cl more than would be taken by NaCl suggesting the presence of another phase that could take both of these elements. We considered Cl-apatite, which also occurs in our models of this system. Unfortunately, Ca was not evident in our analyses. But with the very small grain size used in the experiments, precision of such results is limited. We therefore note the similarity of some of those results with the models, but do not wish to over-interpret them (which is why we have not balanced the amount of kaolinite to result in a 100% analysis total for point 20 in **Table 5**).

Any differences between the mineralogy before and after the experiment were below the detection limits for such changes with XRD, which is readily explained by the very small amounts of dissolution and volume of alteration phases observed.

Thermochemical Models—Three Cases

A set of thermochemical models was used to simulate rock dissolution without bacteria (with pH as free parameter), and to better understand the reactions at the pH conditions invoked by the presence of bacteria during the growth phase (pH 4 and 7; see Section Materials and Methods). We have shown that our model runs within a range of 1,000 > $(W/R)_M$ > 2 Mio, but focus our results and discussion on the range between 100,000 and 1 Mio. This water to rock ratio range is considered to be representative of all $(W/R)_D$ observed in the biotic experiments. Note, that the overall amounts of precipitated minerals in all modeled scenarios are very small and are typically in the order of 0.1–0.3 mg L^{-1} solution at $(W/R)_M$ of 1 Mio and reach ∼1 g at $(W/R)_M$ of 1,000. Variation in the amount of precipitated phases results from the varying solubility of species under different conditions, but also from structurally bound water in the precipitating phases. Further, we use "quartz" for the precipitation of any of the SiO_2 polymorphs: quartz, amorphous silica, and chalcedony.

Abiotic Modeling—pH as Free Parameter

If pH is not held constant in the modeling run, it is calculated together with the other parameters from the dissolution and precipitation processes in the system. The fluid invoked has a neutral pH, which is maintained in the very initial dissolution steps but over the course of the titration changes to alkaline (**Figure 8**). At $(W/R)_M$ of 1 Mio, a mixture of diaspore [α-AlO(OH)] and goethite [FeO(OH)] precipitate. With increasing rock dissolution, Al is no longer precipitated as hydroxide but instead consumed by sheet silicate formation. Chlorite [$(Mg,Fe^{2+},Mn)_5Al(AlSi_3O_{10})(OH)_8$] and kaolinite form alongside goethite, while diaspore is no longer part of the precipitate. Phosphorus is precipitated as chlorapatite [$Ca_5(PO_4)_3Cl$] as soon as the concentrations of Ca and P are sufficiently high in the fluid for to reach the saturation of apatite. With further dissolution, zeolite [mainly stilbite, $NaCa_4(Si_{27}Al_9)O_{72}{\cdot}28(H_2O)$] formation sets in, resulting in a zeolite–hematite–chlorite–kaolinite–apatite assemblage at $(W/R)_M$ of 100,000. With further dissolution, the smectite-group silicate non-tronite is added to the assemblage. As shown above, some of those minerals have been observed in the biotic alteration assemblages, which supports the model results. To observe the full alteration assemblage or fully quantify it using mineralogical methods rather than chemistry, a longer experimental run with more progressive alteration mineral formation would be needed, because quantities are very low. In theory, ∼0.05 g of kaolinite would be expected to form at a W/R of 1,000 per 1 g of dissolved basalt in the model, translating to very small amounts of material expected in the experiment. Given the total amount of basalt in the experiment (20 g) and the very limited dissolution observed, we expect alteration phases to be in the ng range, distributed over 20 g of basaltic grains.

Biotic Simulation—pH Buffered at pH 7

If pH is held constant at pH 7, the resulting precipitates look somewhat similar to the abiotic model with pH as a free parameter, except chlorite does not form at all, and quartz formation begins at around $(W/R)_M$ of 100,000 (**Figure 9**). In detail, at $(W/R)_M$ of >1 Mio, diaspore and goethite precipitate. With increasing rock dissolution Al is no longer precipitated as hydroxide but increasingly consumed by the formation of kaolinite, which forms alongside goethite. In contrast to the previous model, the smectite-group silicate nontronite is added to the assemblage next, together with chlorapatite, while the relative abundance of goethite decreases and eventually

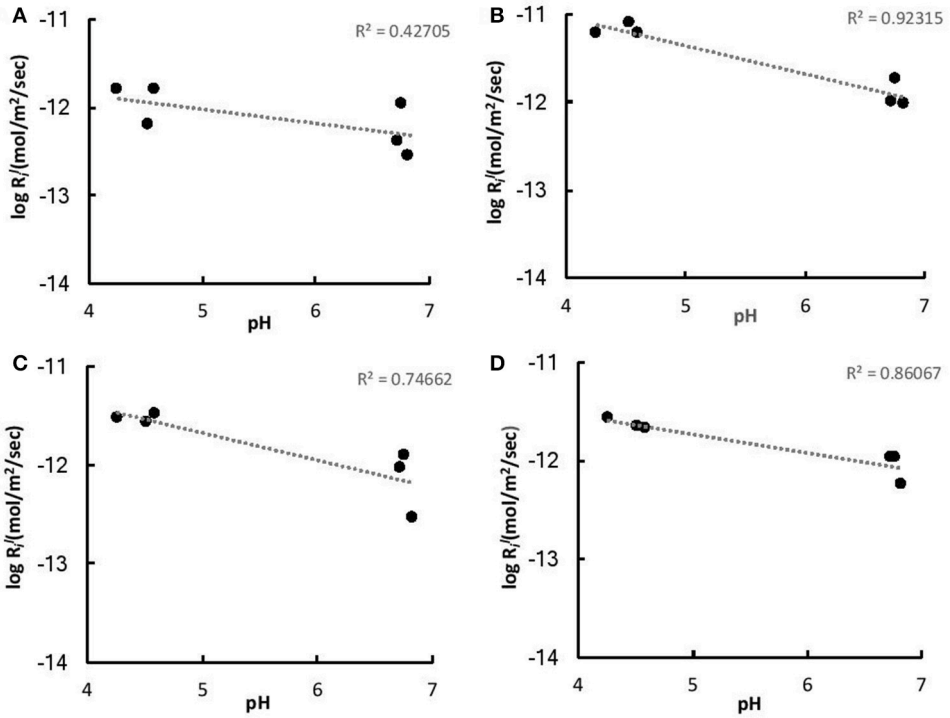

FIGURE 6 | LogR_i^I values of K **(A)**, Ca **(B)**, Mg **(C)**, and Fe **(D)** vs. the average pH of the initial growth phase (days 1–7).

TABLE 4 | Chemical composition of bacterial cells after 28 days.

	Chemical composition [10^{-10} μmol/cell]						
	Si	**Al**	**Mg**	**Ca**	**Na**	**K**	**Fe**
B1	0.02	B.D	0.12	0.01	0.01	0.09	B.D
B2	0.04	B.D	0.09	0.02	0.02	0.08	0.03
B3	B.D	B.D	0.13	0.05	B.D	0.10	0.01

B.D is below the detection limits.

becomes unstable. With further increasing dissolution, zeolite (mainly stilbite) formation begins. In summary, many of the same minerals form in both experiments, but the absence of chlorite and the formation of nontronite are important differences between the assemblages that form under the different conditions.

Biotic Simulation—pH Buffered at pH 4

If pH is held constant at pH 4, which is the pH during exponential growth, the resulting precipitates have a much simpler composition than in the neutral to alkaline parameter space (**Figure 10**). In detail, at $(W/R)_M$ of >1 Mio, only goethite precipitates while Al stays in solution. Al-precipitation begins with the formation of kaolinite, which forms alongside goethite. In contrast to the previous model, apatite does not form at any $(W/R)_M$, but the smectite-group silicate nontronite is added to the assemblage at $(W/R)_M$ below 100,000. Again, the relative abundance of goethite sharply decreases and goethite finally becomes unstable at which point quartz forms. Zeolites do not form at low pH.

DISCUSSION

Microbially-Mediated Basalt Dissolution

Traditionally, martian analog studies have predominantly focused on chemolithoautotrophic microorganisms from extreme environments (e.g., Fernández-Remolar et al., 2004). However, these lack relevance to the large ancient fluvial systems, which are known to exist on Mars (e.g., Malin and Edgett, 2003; Irwin et al., 2005; Mangold et al., 2012; Williams et al., 2013; Fassett and Head, 2015). Although, chemolithoautotrophic metabolism may have occurred within these fluvial systems, more recent data suggests that chemoorganoheterotrophy was also feasible (Mahaffy et al., 2013; Sutter et al., 2016). Based on the data from Curiosity and our extensive understanding of their role in mineral weathering a chemoorganoheterophic microorganisms (e.g., see review Uroz et al., 2009) was selected for this preliminary study.

Consistent with previous studies, microbial growth enhanced the rate of basalt dissolution in batch culture experiments (e.g., Berthelin and Belgy, 1979; Welch and Ullman, 1993; Wu et al., 2007; Olsson-Francis and Cockell, 2010). The results suggest that, specifically, acidification of the experimental fluid had a positive effect on basalt dissolution, also in agreement with prior studies (e.g., Gislason and Eugster, 1987a,b; Oelkers and Schott, 2001). Acidification is likely to have been caused by the presence of both excess protons and organic acids produced as a by-product of

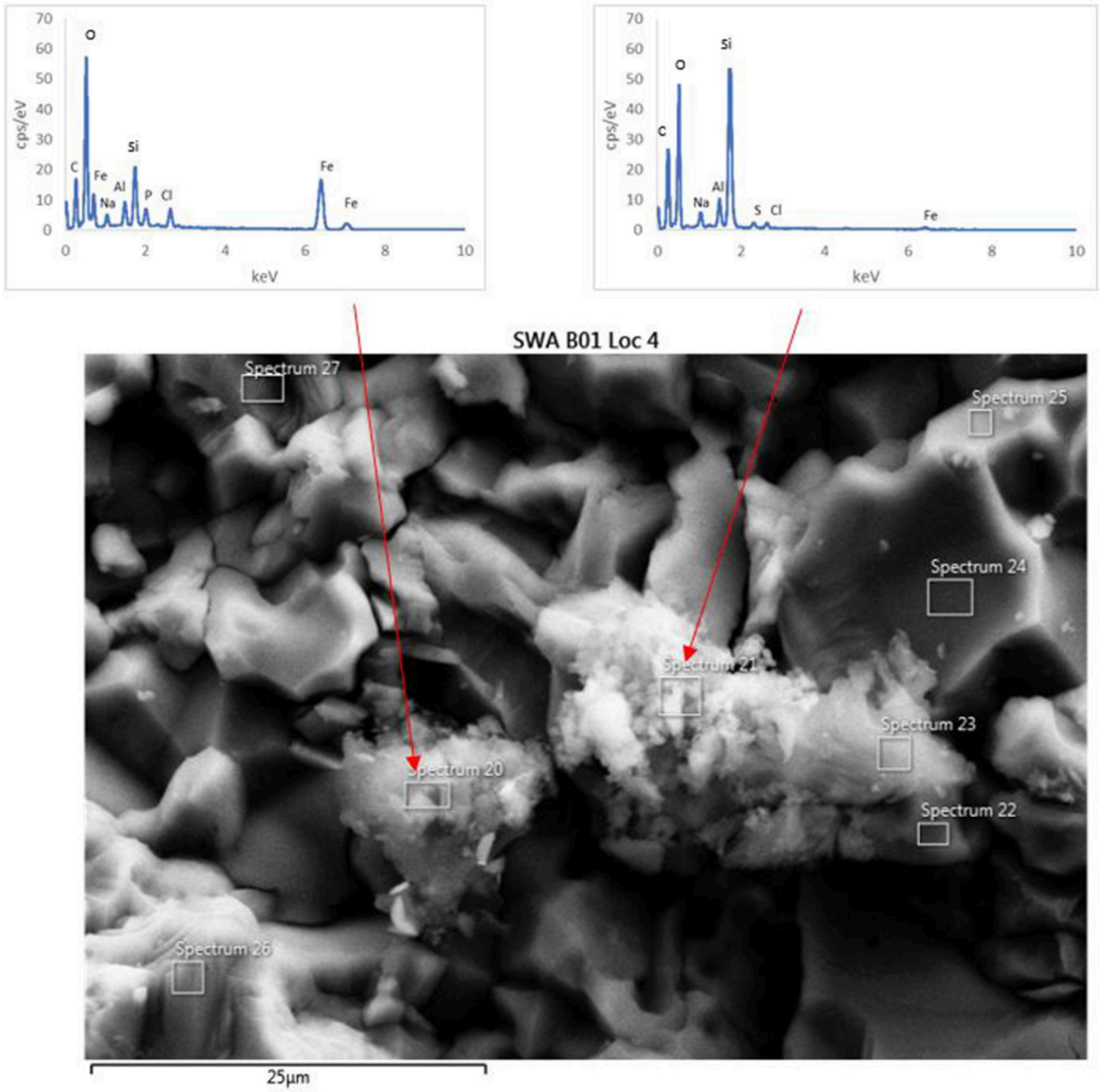

FIGURE 7 | FEG-SEM micrograph of a typical secondary minerals produced in the biological flasks after 28 days. No secondary minerals were observed in the abiotic controls.

chemoorganoheterophic metabolism (Welch and Ullman, 1993; Vandevivere et al., 1994; Blake and Walter, 1996; Drever and Stillings, 1997). Although, it is difficult to distinguish between organic ligand and proton-mediated dissolution, organic acids have been shown to increase the rate of plagioclase dissolution up to 10 times that achieved in the presence of inorganic acids at the same pH (Welch and Ullman, 1993). At acidic pH, organic acids are more likely to be in the protonated form and thus the proton enhanced pathways of weathering are more favorable, consistent with abiotic inorganic aqueous systems (Buffle, 1990).

Burkholderia sp. strain B_33, produced siderophores in the minimal medium, which contained limited iron [the concentration was below the detection limits of the analysis ($1\,\mu mol\ L^{-1}$)]. However, siderophores were not detected in the medium with the basalt. This is in agreement with previous studies, which were unable to measure siderophore production in the presence of silicate rocks, under laboratory conditions (Frey et al., 2010; Olsson-Francis et al., 2010, 2015). The Fe released from the Fe-bearing minerals (augite, clay) in the rock during dissolution may have inhibited siderophore production.

TABLE 5 | EDS analysis of two alteration mineral assemblages (refer to spectra 20 and 21 as shown in **Figure 7**).

Wt. % element measured[a,b,c]			Wt. % oxide[a,b,c]			Wt. % species partitioned[a,b,c]		
	20	21		20	21		20	
O	43.6	30.3						
Na	3.5	2.3	Na_2O	4.7	3.1	Na_2O	2.9	N.D
Al	5.6	3.8	Al_2O_3	10.6	7.2	Al_2O_3	10.6	7.2
Si	40.1	10.1	SiO_2	85.8	21.6	SiO_2	85.8	21.6
Fe	2.9	45.1	FeO	3.7	58.0	FeO	N.D	57.1
Ti	0.6	N.D	TiO_2	1.0	N.D	TiO_2	1.0	N.D
P	N.D	3.5	P_2O_5	N.D	8.0	P_2O_5	N.D	8.0
S	1.7	0.4	SO_2	3.4	0.8	SO_2	0.1	N.D
Cl	2.1	4.4	Cl	2.1	4.4	NaCl	3.5	5.8
						FeS	4.6	1.1
						Cl	N.D	0.9
						$Al_2Si_2O_5(OH)_4$	N.D	N.D
						Na_2O	N.D	N.D
Sum	100.1	99.9	Sum	111.3	103.1	Sum	108.3	101.7

[a] *All Cl is calculated as NaCl, all Fe as FeS, and the remainder of the S as SO2.*

[b] *All Na is calculated as NaCl with the remaining Cl as element. This analysis has significant P, which could form apatite and host Cl.*

[c] *In addition to the partitioning in a, Al is calculated as kaolinite. N.D is not detected.*

Data are given as measured weight % of element converted to oxides, or partitioned into more likely phases, for example, NaCl (for details see text). Zero refers to partitioning results, where an element is calculated as a different species and therefore zero by calculation.

In this study, the basalt contained both augite (8.83% FeO) and vermiculite (20.78% Fe), and ICP-MS data demonstrated that after 1 day the concentration of Fe in the medium was between 3.2 and 5.8 μmol L^{-1}. Based on previous work, this is sufficient to inhibit siderophore expression (Olsson-Francis et al., 2010).

Thermochemical Modeling of Microbial Dissolution

The focus of the thermochemical modeling was the initial stage of the weathering experiments, where supersaturation and the likelihood of secondary phase precipitation was lower; this also reflects the fact that microbial and inorganic weathering in the natural environment often happens in an open system or at least a system open to fluid and the most soluble elements. To compare the experimental and model results, the amount of actual dissolved basalt $(W/R)_D$ in the experimental dissolution experiments needed to be deduced. This value was directly comparable to the model water to rock ratio, $(W/R)_M$ (**Figure 8B**). The $(W/R)_D$ represented by the vertical lines in **Figure 8B** was calculated based on the element K, because it is not incorporated into any of the expected mineral precipitates and the intracellular concentration was <2%. Mass balance calculations based on K demonstrate that very little rock dissolution happened over the course of the experiment in either the abiotic [$(W/R)_D$ value of ∼877,000] or biotic [$(W/R)_D$ value of 230,000] experiments. The elemental abundances of the major cations, in the abiotic experiment, were compared with the model at the $(W/R)_D$ value of 230,000 [the $(W/R)_D$ value determined under biotic conditions].

The abundance of K indicated that dissolution in both the biotic and abiotic experiments was higher than expected from the mass balance calculated from the model. In fact, comparing the measured K abundances with fluid composition of the model indicates that the actual $(W/R)_M$ in the biotic experiment would lie in the range of 2,000–2,500. Fe and Ca concentrations predicted by the model are in the range of the measured values, which indicates their precipitation in the minerals and only a small uptake by the bacteria. In contrast, Na, Al, and Si are higher in solution in the experiment than in the model, which indicates inhibition of precipitation. This could occur due to utilization of bio-essential elements required for precipitation, such as oxygen or phosphate, or complexation of the ions by inorganic or organic species produced by the bacterium. The former would reduce the concentration of another component of the precipitating phase, preventing solubility limits to be reached. This shows that, despite the similarities in detected alteration mineral assemblages and the modeled mineral assemblage [compare **Figure 7** and **Table 5** (experiment) to **Figures 8–10** (model)], biological activity changes precipitation characteristics significantly.

The analog rock used here was a naturally occurring basalt, which included clay minerals. This is in accordance with the "mudstones" found by the Curiosity rover at Gale Crater (Vaniman et al., 2014). The observed alteration minerals—detectable through their position on the surface (**Figure 7**)—agree with the modeled minerals, especially for the low-pH case, where kaolinite forms.

Bio-Signatures and Life Detection

Field studies have suggested a variety of bio-signatures of past life can be found in basaltic material on Earth. These

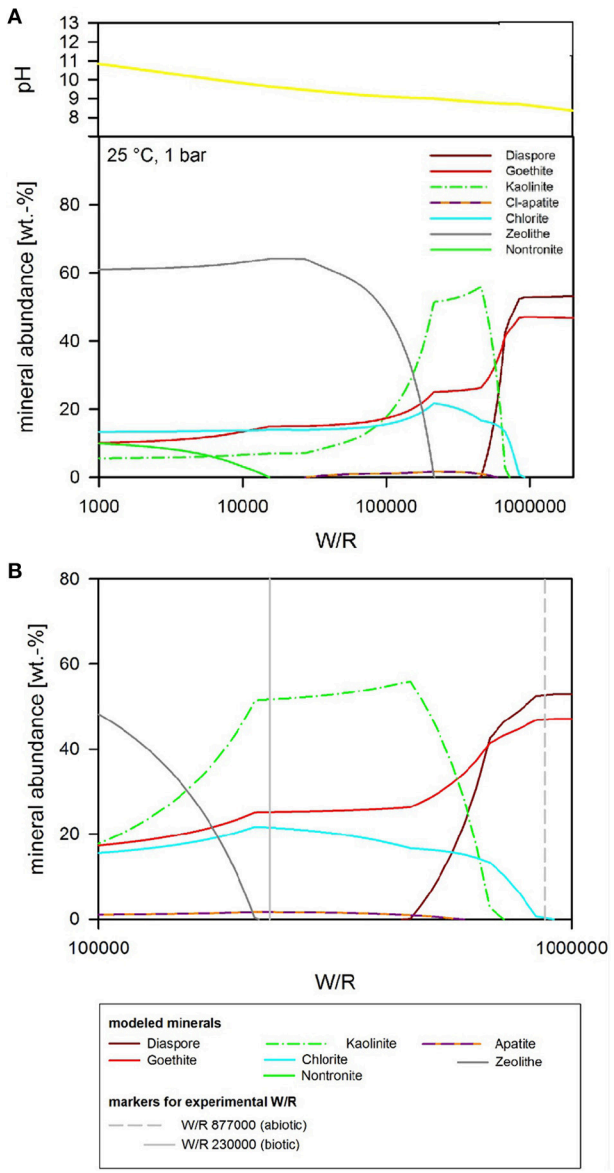

FIGURE 8 | (A) Secondary minerals predicted from the dissolution of analog basalt at 25°C with pH as a free parameter. The diagram shows the formation of diaspore, goethite, kaolinite, Cl-apatite, chlorite, zeolite, and nontronite. **(B)** Secondary minerals predicted from the dissolution of analog basalt at 25°C with pH as a free parameter [at a higher resolution than **(A)**]. The $(W/R)_D$, represented by the vertical lines, was calculated based on the element potassium because it is not incorporated into any of the expected mineral precipitates and the intracellular concentration was <2%.

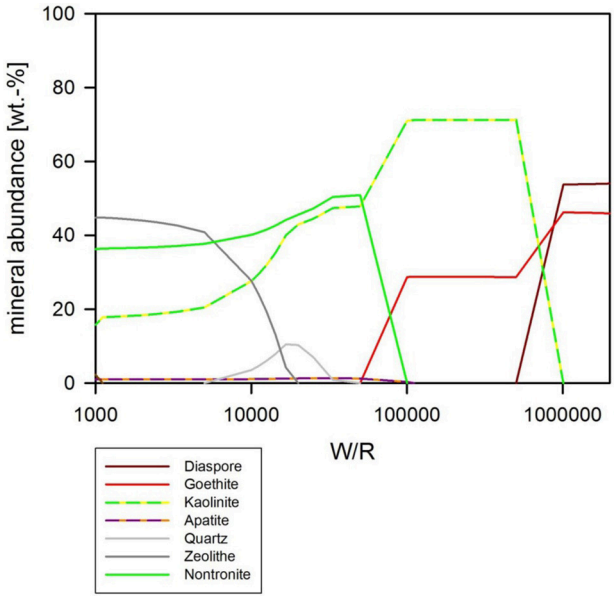

FIGURE 9 | Secondary minerals predicted from the dissolution of analog basalt at 25°C, pH fixed at 7. The mineral precipitates can be divided into three principal assemblages. At low W/R (below about 10,000) zeolites become increasingly important and below about 7,000 are the dominant species. Between about W/R = 10,000 and 900,000, clay minerals (kaolinite and nontronite) are dominating, whereby kaolinite is more prominent at the higher W/R end of that bracket and nontronite at the lower W/R range. At the highest W/R (over 1 Mio) the assemblage contains hydroxides (diaspore and goethite) only.

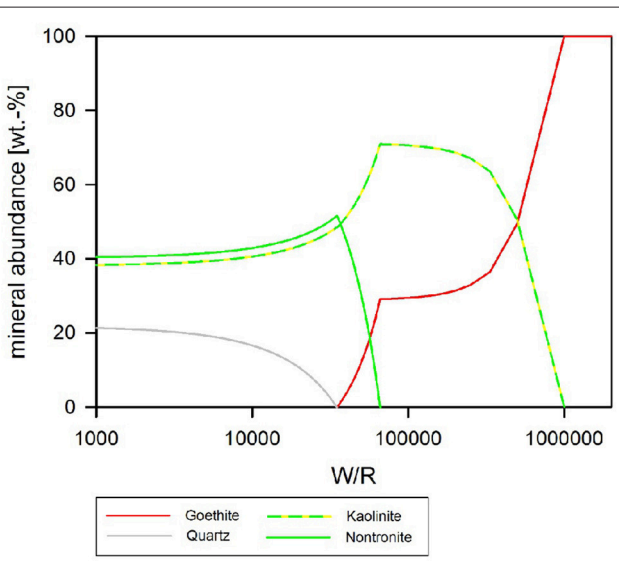

FIGURE 10 | Secondary minerals predicted from the dissolution of analog basalt at 25°C, pH fixed at 4. The precipitated secondary minerals can be grouped in two assemblages: at the highest W/R goethite is the sole precipitate. At lower W/R clays dominate, whereby kaolinite predominantly precipitates at the hither W/R compared to nontronite. Note that quartz starts to precipitate at W/R below about 50,000, but never becomes the dominating species.

include morphological fossils in basaltic amygdales and veins (e.g., Schumann et al., 2004; Cavalazzi, 2007), evidence of isotope fractionation in minerals, such as carbonates and sulfides (Demény and Harangi, 1996; Rouxel et al., 2008), or bio-alteration textures, such as potential biogenic tubulars or pitting (Thoreseth et al., 1991; Fisk et al., 1998). Analyses of the Columbia River basalts revealed organic structures, which were interpreted to be bacteria, intermingled with secondary

iron oxyhydroxides and ferrous smectites, which suggested that the secondary minerals were caused by microbial activity (McKinley and Stevens, 2000). This study has similarly focused on determining the secondary alteration minerals that could form due to microbially-mediated dissolution of basalt in a Mars-like environment.

A small number of laboratory studies have investigated microbially-mediated basaltic weathering. For example, McKinley and Stevens (2000) studied geochemical modeling in sea water. They showed saturation with respect to Fe(OH)2.7Cl0.3, goethite (α-FeOOH), lepidocrocite (δ-FeOOH) schwertmannite ($Fe_8O_8(OH)_5.9(SO_4)_{1.05}$), and K-jarosite ($KFe_3(SO_4)2(OH)_6$ (Daughney et al., 2004). This is broadly consistent with our findings at the highest water to rock ratio (i.e., the formation of kaolinite, and goethite/lepidocrocite), but we note that our system did not contain enough K to form the jarosite modeled by McKinley and Stevens (2000).

Our findings are important for planning and interpreting investigations carried out by rover-based instrumentation currently active on Mars (e.g., CheMin and MastCam and ChemCam passive spectral investigations on Curiosity) and for the selection of future landing sites, e.g., Mawrth Vallis and Oxia Planum currently under discussion for the ESA ExoMars rover (http://exploration.esa.int/mars/53845-landing-site/). Potentially habitable environments may reveal secondary alteration minerals that require the origins (abiotic or biotic) to be unequivocally determined; the combination of thermochemical modeling with simulation studies enables the identification of mineral assemblages that can be used as potential indicators of biotic origin.

Although, the secondary mineral yield was not large enough for detection by XRD in our weeks-to-month long experiments, in a natural martian environment, subsequent generations of microbes would enhance this yield, enabling detection by spacecraft instrumentation.

CONCLUSION

In this study, a novel approach was applied combining both laboratory-based experiments and thermochemical modeling to investigate the feasibility of identifying mineralogical bio-signatures that can be used as evidence of life on early Mars. The modeled basalt–fluid reactions resulted in secondary mineral precipitates, which are comparable with the alteration mineralogy found in the rock after the dissolution experiments and the thermochemical models. This confirms the viability of this methodological approach.

The bacterium-enhanced rock dissolution by acidification was likely to be caused by both organic and inorganic acids. The bulk pH of the growth medium may simulate the micro-environment in the natural environment, which is thought to contain concentrated acids and solutes. Comparison of a carefully selected indicator element (K) in the model allowed the deduction of the actual $(W/R)_D$. This comparison was used to follow individual element paths to understand how secondary mineral precipitation would differ in biotic and abiotic systems over geological time scales. This approach suggests that biologically-mediated secondary alteration is expected to be "simpler," consisting of Fe-hydroxide and kaolinite whereas the abiotic system would form chlorite in addition to Fe-hydroxide and kaolinite. This difference is due to differences in chemical diversity and mineralogical complexity; kaolinite has a 1:1 structure containing only Si, Al, and O, whereas chlorite, as a clay mineral, has a 2:1 structure with Si, Al, and O and additional cations (Fe, Mg, Ca). This is important, because most planetary exploration—in terms of spatial coverage—is from orbit using spectral investigations. Those techniques are capable of distinguishing the different groups of clays, but not necessarily subtle variations within a group that might be indicative of the presence or absence of life.

Therefore, due to the different mineral formation pathways utilized in abiotic and biotic systems, deciphering the chemical and mineralogical details necessary for identifying the presence of life is expected to be a task for rover-based investigation. Small sample size, detailed investigations, such as those possible with the rover-based instrumentation currently active on Mars (e.g., CheMin and MastCam and ChemCam passive spectral investigations on MSL), can make use of the fact that, under bacterially-mediated conditions, a less mineralogically and less chemically diverse precipitate is expected. Therefore, this study highlights the differences to look for when investigating a habitable environment for the presence of past life.

Future work will utilize a fresh basalt to minimize the difficulties that the presence of clay minerals had on the model system, e.g., from recent eruptions on Hawaii or Iceland, with polished surfaces singling out grains for pre- and post-experiment mineralogical investigations. The analysis will include instrumentation relevant to past and present life detection missions, including XRD, FTIR, and Raman, to determine whether bio-signatures are detectable. Furthermore, organic molecules will be included in the thermochemical modeling, for example using the program SOLMINEQ88, to investigate whether they inhibit precipitation (Kharaka et al., 1988). This work will further help to specify and quantify the secondary mineralogy that has the potential to serve as inorganic, radiation, and desiccation resistant biosignatures detectable by instruments such as the CheMin Instrument (Blake et al., 2012) on the Mars Exploration rover Curiosity (Blake et al., 2012).

AUTHOR CONTRIBUTIONS

KOF: Designed the lab experiment, carried out the microbiology analyses, and wrote the manuscript. VP: Carried out the FEG-SEM work. ES: Carried out the geochemical analyses. SS: Ran the models.

ACKNOWLEDGMENTS

This work was supported by a personal fellowship awarded by the UK Space Agency. We would like to thank Gordon Imlach for the support he provided with the FEG-SEM analysis.

REFERENCES

Abramov, O., and Kring, D. A. (2005). Impact-induced hydrothermal activity on early Mars. *J. Geophys. Res.* 110:E12SE09. doi: 10.1029/2005JE002453

Andeer, P., Stahl, D. A., Lillis, L., and Strand, S. E. (2013). Identification of microbial populations assimilating nitrogen from RDX in munitions contaminated military training range soils by high sensitivity stable isotope probing. *Environ. Sci. Technol.* 47, 10356–10363. doi: 10.1021/es401729c

Arvidson, R. E., Squyres, S. W., Bell, J. F., Catalano, J. G., Clark, B. C., Crumpler, L. S., et al. (2014). Ancient aqueous environments at Endeavour Crater, Mars. *Science* 343:1248097. doi: 10.1126/science.1248097

Banfield, J. F., Barker, W. W., Welch, S. A., and Taunton, A. (1999). Biological impact on mineral dissolution: application of the lichen model to understanding mineral weathering in the rhizosphere. *Proc. Natl. Acad. Sci. U.S.A.* 96, 3404–3411. doi: 10.1073/pnas.96.7.3404

Banfield, J. F., Moreau, J. W., Chan, C. S., Welch, S. A., and Little, B. (2001). Mineralogical biosignatures and the search for life on Mars. *Astrobiology* 1, 447–465. doi: 10.1089/153110701753593856

Barker, W. W., Welch, S. A., Chu, S., and Banfield, J. F. (1998). Experimental observations of the effects of bacteria on aluminosilicate weathering. *Am. Mineral.* 83, 1551–1563. doi: 10.2138/am-1998-11-1243

Bennett, P. C., Rogers, J. R., and Choi, W. J. (2001). Silicates, silicate weathering, and microbial ecology. *Geomicrobiol. J.* 18, 3–19. doi: 10.1080/01490450151079734

Berthelin, J., and Belgy, G. (1979). Microbial-degradation of phyllosilicates during simulated podozolization. *Geoderma* 21, 297–310. doi: 10.1016/0016-7061(79)90004-1

Bibring, J. P., Langevin, Y., Mustard, J. F., Poulet, F., Arvidson, R., Gendrin, A., et al. (2006). Global mineralogical and aqueous mars history derived from OMEGA/Mars express data. *Science* 312, 400–404. doi: 10.1126/science.1122659

Blake, D., Vaniman, D., Achilles, C., Anderson, R., Bish, D., Bristow, et al. (2012). Characterization and calibration of the CheMin mineralogical instrument on Mars Science Laboratory. *Space Sci. Rev.* 170, 341–399. doi: 10.1007/s11214-012-9905-1

Blake, R. E., and Walter, L. M. (1996). Effects of organic acids on the dissolution of orthoclase at 80°C and pH 6. *Chem. Geol.* 132, 91–102. doi: 10.1016/S0009-2541(96)00044-7

Bridges, J. C., and Schwenzer, S. P. (2012). The nakhlite hydrothermal brine on Mars. *Earth Planet. Sci. Lett.* 359–360, 117–123. doi: 10.1016/j.epsl.2012.09.044

Bridges, J. C., Schwenzer, S. P., Leveille, R., Westall, F., Wiens, R. C., Mangold, N., et al. (2015). Diagenesis and clay mineral formation at Gale Crater, Mars. *J. Geophys. Res.* 120, 1–19. doi: 10.1002/2014JE004757

Buffle, J. (1990). *Complexation Reactions in Aquatic Systems; Analytical Approach*. New York, NY: Wiley.

Carr, M. H., and Head, J. W. (2010). Geologic history of Mars. *Earth Planet. Sci. Lett.* 294, 185–203. doi: 10.1016/j.epsl.2009.06.042

Carter, D. L., Mangold, N., Poulet, F., and Bibring, J. P. (2015). Widespread surface weathering on early Mars: a case for a warmer and wetter climate. *Icarus* 248, 373–382. doi: 10.1016/j.icarus.2014.11.011

Cavalazzi, B. (2007). Chemotrophic filamentous microfossils from the Hollard Mound (Devonian, Morocco) as investigated by focused ion beam. *Astrobiology* 7, 402–415. doi: 10.1089/ast.2005.0398

Christensen, P. R., McSween, H. Y., Bandfield, J. L., Ruff, S. W., Rogers, A. D., Hamilton, V. E., et al. (2005). Evidence for magmatic evolution and diversity on Mars from infrared observations. *Nature* 436, 882–882. doi: 10.1038/nature04075

Cockell, C. S. (2014). Trajectories of martian habitability. *Astrobiology* 14, 182–203. doi: 10.1089/ast.2013.1106

Daughney, C. J., Rioux, J. P., Fortin, D., and Pichler, T. (2004). Laboratory investigation of the role of bacteria in the weathering of basalt near depp sea hydrothermal vents. *Geomicrobiol. J.* 21, 21–31. doi: 10.1080/01490450490253437

Debraal, J. D., Reed, M. H., and Plumlee, G. S. (1993). "Calculated mineral precipitation upon evaporation of a model Martian groundwater near 0°C," in *MSATT Workshop on Chemical Weathering on Mars* (Lunar and Planetary Inst),10–11.

Demény, A., and Harangi, S. (1996). Stable isotope studies and processes of carbonate formation in Hungarian alkali basalts and lamprophyres: Evolution of magmatic fluids and magma-sediment interactions. *Lithos* 37, 335–349. doi: 10.1016/0024-4937(95)00029-1

Drever, J. I., and Stillings, L. L. (1997). The role of organic acids in mineral weathering. *Colloid. Surf. A* 120, 167–181. doi: 10.1016/S0927-7757(96)03720-X

Ehlmann, B. L., Berger, G., and Mangold, N. (2013). Geochemical consequences of widespread clay mineral formation in Mars' ancient crust. *Space Sci. Rev.* 174, 329–364. doi: 10.1007/s11214-012-9930-0

Fairen, A. G., Davila, A. F., Gago-Duport, L., Amils, R., and McKay, C. P. (2009). Stability against freezing of aqueous solutions on early Mars. *Nature* 459, 401–404. doi: 10.1038/nature07978

Fassett, C. I., and Head, J. W. (2015). Fluvial sedimentary deposits on Mars: ancient deltas in a crater lake in the Nili Fossae region. *Geophys. Res. Lett.* 32. doi: 10.1029/2005GL023456

Fernández-Remolar, D., Gómez-Elvira, J., Gómez, F., Sebastian, E., Martíin, J., Manfredi, J., et al. (2004), The Tinto 273 River, an extreme acidic environment under control of iron, as an analog of the Terra Meridiani hematite site of Mars', Planet. *Space Sci.* 52, 239–248. doi: 10.1016/j.pss.2003.08.027

Filiberto, J. (2008). Similarities between the shergottites and terrestrial ferropicrites. *Icarus* 197, 52–59. doi: 10.1016/j.icarus.2008.04.016

Filiberto, J., and Schwenzer, S. (2013). Alteration mineralogy of Home Plate and Columbia Hillså Formation conditions in context to impact, volcanism, and fluvial activity. *Meteor. Planet. Sci.* 48, 1937–1957. doi: 10.1111/maps.12207

Fisk, M. R., Giovannoni, S. J., and Thorseth, I. H. (1998). Alterations of oceanic volcanic glass, textural evidence of microial activity. *Science* 281, 978–979. doi: 10.1126/science.281.5379.978

Fox, V. K., Arvidson, R. E., Guinness, E. A., McLennan, S. M., Catalano, J. G., Murchie, S. L., et al. (2016). Smectite deposits in Marathon Valley, Endeavour Crater, Mars, identified using CRISM hyperspectral reflectance data. *Geophys. Res. Lett.* 43, 4885–4892. doi: 10.1002/2016GL069108

Frey, B., Rieder, S. R., Brunner, I., Plotze, M., Koetzsch, S., Lapanje, A., et al. (2010). Weathering-associated bacteria from the Damma Glacier forefield: physiological capabilities and impact on granite dissolution. *Appl. Environ. Microbiol.* 76, 4788–4796. doi: 10.1128/AEM.00657-10

Ganguly, J. (2008). "Third Law and Thermochemistry," in *Thermodynamics in Earth and Planetary Sciences* (Berlin; Heidelberg: Springer), 73–90.

Gislason, S. R., and Eugster, H. P. (1987a). Meteoric water-basalt interactions. I: A laboratory study. *Geochim. Cosmochim. Acta* 51, 2827–2840. doi: 10.1016/0016-7037(87)90161-X

Gislason, S. R., and Eugster, H. P. (1987b). Meteoric water: basalt interactions. II.: A field-study in N.E. Iceland. *Geochim. Cosmochim. Acta* 51, 2841–2855. doi: 10.1016/0016-7037(87)90162-1

Grotzinger, J. P., Gupta, S., Malin, M. C., Rubin, D. M., Schieber, J., Siebach, K., et al. (2015). *Deposition, Exhumation, and Paleoclimate of an Ancient Lake Deposit, Gale Crater, Mars*. *Science* 350:aac7575. doi: 10.1126/science.aac7575

Grotzinger, J. P., Sumner, D. Y., Kah, L. C., Stack, K., Gupta, S., Edgar, L., et al. (2014). A habitable fluvio-lacustrine environment at Yellowknife Bay, Gale Crater, Mars. *Science* 343:14. doi: 10.1126/science.1242777

Hicks, L. J., Bridges, J. C., and Gurman, S. J. (2014). Ferric saponite and serpentine in the nakhlite martian meteorites. *Geochim. Cosmochim. Acta* 136, 194–210. doi: 10.1016/j.gca.2014.04.010

Irwin, R. P., Howard, A. D., Craddock, R. A., and Moore, J. M. (2005). An intense terminal epoch of widespread fluvial activity on early Mars: 2. Increased runoff and paleolake development. *J. Geophys. Res.* 110. doi: 10.1029/2005JE002460

Kalinowski, B. E., Liermann, L. J., Givens, S., and Brantley, S. L. (2000). Rates of bacteria-promoted solubilization of Fe from minerals: a review of problems and approaches. *Chem. Geol.* 169, 357–370. doi: 10.1016/S0009-2541(00)00214-X

Kharaka, Y. K., Debraal, J. D., and Ambats, G. (1988). Reactive organic-species in subsurface waters- implications for geochemical modelling. *Am. Chem. Soc.* 196:88.

King, G. (2015). Carbon monoxide as a metabolic energy source for extremly halophilic microbes: Implications for micrbial activity in Mars regolith. *Proc. Natl. Acad. Sci. U.S.A.* 112, 4465–4470. doi: 10.1073/pnas.1424989112

Kühn, M. (2004). *Reactive Flow Modeling of Hydrothermal Systems*. Lecture Notes in Earth Sciences (Berlin: Springer).

Lepleux, C., Turpault, M. P., Oger, P., Frey-Klett, P., and Uroz, S. (2012). Correlation of the abundance of betaproteobacteria on mineral surfaces with mineral weathering in forest soils. *Appl. Environ. Microbiol.* 78, 7114–7119. doi: 10.1128/AEM.00996-12

Liermann, L. J., Barnes, A. S., Kalinowski, B. E., Zhou, X. Y., and Susan, L. (2000). Microenvironments of pH in biofilms grown on dissolving silicate surfaces. *Chem. Geol.* 171, 1–16. doi: 10.1016/S0009-2541(00)00202-3

Mahaffy, P. R., Webster, C. R., Atreya, S. K., Franz, H., and the, M. S. L., Science Team (2013). Abundance and isotopic composition of gases in the martian atmosphere from the Curiosity Rover. *Science* 341, 263–266. doi: 10.1126/science.1237966

Malin, M. C., and Edgett, K. S. (2003). Evidence for persistent flow and aqueous sediments on early Mars. *Science* 302, 1931–1934. doi: 10.1126/science.1090544

Mangold, N., Adeli, S., Conway, S., Ansan, V., and Langlais, B. (2012). A chronology of early Mars climatic evolution from impact crater degradation. *J. Geophys. Res. Planets* 117. doi: 10.1029/2011JE004005

Mangold, N., Schmidt, M. E., Fisk, M. R., Forni, O., McLennan, S. M., Ming, D. W., et al. (2017). Classification scheme for sedimentary and igneous rocks in Gale crater, Mars. *Icarus* 284, 1–17. doi: 10.1016/j.icarus.2016.11.005

McKinley, J. P., and Stevens, T. O. (2000). Microfossils and paleoenvironments in deep subsurface basalt samples. *Geomicrobiol. J.* 17, 43–54. doi: 10.1080/014904500270486

Molina-Cuberos, G. J., Stumptner, W., Lammer, H., and Komle, N. I. (2001). Cosmic ray and UV radiation models on the ancient martian surface. *Icarus* 154, 216–222. doi: 10.1006/icar.2001.6658

Morris, R. V., Vaniman, D. T., Blake, D. F., Gellert, R., Chipera, S. J., Rampe, E. B., et al. (2016). Silicic volcanism on Mars evidenced by tridymite in high-SiO2 sedimentary rock at Gale crater. *Proc. Natl. Acad. Sci. U.S.A.* 113, 7071–7076. doi: 10.1073/pnas.1607098113

Nyquist, L. E., Bogard, D. D., Shih, C. Y., Greshake, A., Stoffler, D., and Eugster, O. (2001). Ages and geologic histories of martian meteorites. *Space Sci. Rev.* 96, 105–164. doi: 10.1023/A:1011993105172

Oelkers, E. H., and Schott, J. (2001). An experimental study of enstatite dissolution rates as a function of pH, temperature, and aqueous Mg and Si concentration, and the mechanism of pyroxene/pyroxenoid dissolution. *Geochim. Cosmochim. Acta* 65, 1219–1231. doi: 10.1016/S0016-7037(00)00564-0

Olsson-Francis, K., and Cockell, C. (2010). Use of cyanobacteria for *in-situ* resource use in space applications. *Planet. Space Sci.* 58, 1279–1285. doi: 10.1016/j.pss.2010.05.005

Olsson-Francis, K., Pearson, V., Boardman, C., Schofield, P., and Summers, S. (2015). A culture-independent and culture-dependent study of the bacteria community from the bedrock soil interface. *Adv. Microbiol.* 5, 842–857. doi: 10.4236/aim.2015.513089

Olsson-Francis, K., Simpson, A. E., Wolff-Boenisch, D., and Cockell, C. S. (2012). The effect of rock composition on cyanobacterial weathering of crystalline basalt and rhyolite. *Geobiology* 10, 434–444. doi: 10.1111/j.1472-4669.2012.00333.x

Olsson-Francis, K., Van Houdt, R., Mergeay, M., Leys, N., and Cockell, C. S. (2010). Microarray analysis of a microbe-mineral interaction. *Geobiology* 8, 446–456. doi: 10.1111/j.1472-4669.2010.00253.x

Orcutt, B. N., Bach, W., Becker, K., Fisher, A. T., Hentscher, M., Toner, B. M., et al. (2011). Colonization of subsurface microbial observatories deployed in young ocean crust. *ISME J.* 5, 692–703. doi: 10.1038/ismej.2010.157

Payne, S. M. (1994). Detection, isolation, and characterization of siderophores. *Methods Enzymol.* 235, 329–344. doi: 10.1016/0076-6879(94)35151-1

Pirt, S. J. (1978). *Principles of Microbe and Cell Cultivation*. Oxford: Blackwell.

Posth, N. R., Hegler, F., Konhauser, K. O., and Kappler, A. (2008). Alternating Si and Fe deposition caused by temperature fluctuations in Precambrian oceans. *Nat. Geosci.* 1, 703–708. doi: 10.1038/ngeo306

Reed, M. H. (1982). Calculation of multicomponent chemical equilibria and reaction processes in systems involving minerals, gases and an aqueous phase. *Geochim. Cosmochim. Acta* 46, 513–528. doi: 10.1016/0016-7037(82)90155-7

Reed, M. H., and Spycher, N. F. (2006). *User Guide for CHILLER: A Program for Computing Water-Rock Reactions, Boiling, Mixing and Other Reaction Processes in Aqueous-Mineral-Gas Systems and Minplot Guide*. Eugene, OR: University of Oregon.

Reed, M. H., Spycher, N. F., and Palandri, J. (2010). *Users Guide for CHIM-XPT: A Program for Computing Reaction Processes in Aquous-Mineral Gas Systems and MINITAB Guide.* Eugene, OR: University of Oregon.

Rimstidt, J. D. (2014). *Geochemical Rate Models: An Introduction to Geochemical Kinetics*. Cambridge, UK: Cambridge University Press.

Rogers, J. R., Bennett, P. C., and Choi, W. J. (1998). Feldspars as a source of nutrients for microorganisms. *Am. Mineral.* 83, 1532–1540. doi: 10.2138/am-1998-11-1241

Rouxel, O., Ono, S., Alt, J., Rumble, D., and Ludden, J. (2008). Sulfur isotope evidence for microbial sulphate reduction in altered oceanic basalts at ODP Site 801. *Earth Planet. Sci. Lett.* 268, 110–123. doi: 10.1016/j.epsl.2008.01.010

Sautter, V., Toplis, M. J., Beck, P., Mangold, N., Wiens, R., Pinet, P., et al. (2016). Magmatic complexity on early Mars as seen through a combination of orbital, *in-situ* and meteorite data. *Lithos* 254, 36–52. doi: 10.1016/j.lithos.2016.02.023

Schirmack, J., Alawi, M., and Wagner, D. (2015). Influence of martian regolith analogs on the activity and growth of methanogenic archaea, with special regard to long-term desiccation. *Front. Microbiol.* 6:210. doi: 10.3389/fmicb.2015.00210

Schirmack, J., Böhm, M., Brauer, C., Löhmannsröben, H. G., de Vera, J. P., Möhlmann, D., et al. (2014). Laser spectroscopic real time measurements of methanogenic activity under simulated Martian subsurface analog conditions. *Planet. Space Sci.* 98, 198–204. doi: 10.1016/j.pss.2013.08.019

Schumann, G., Manz, W., Reitner, J., and Lustrino, M. (2004). Ancient fungal life in north pacific oceanic crust. *Geomicrobiol. J.* 21, 241–246. doi: 10.1080/01490450490438748

Schwenzer, S. P., Bridges, J. C., Wiens, R. C., Conrad, P. G., Kelley, S. P., Leveille, R., et al. (2016). Fluids during diagenesis and sulfate vein formation in sediments at Gale crater, Mars. *Meteor. Planet. Sci.* 51, 2175–2202. doi: 10.1111/maps.12668

Schwenzer, S. P., and Kring, D. A. (2009). Impact-generated hydrothermal systems capable of forming phyllosilicates on Noachian Mars. *Geology* 37, 1091–1094. doi: 10.1130/G30340A.1

Schwenzer, S. P., and Kring, D. A. (2013). Alteration minerals in impact-generated hydrothermal systems - Exploring host rock variability. *Icarus* 226, 487–496. doi: 10.1016/j.icarus.2013.06.003

Schwyn, B., and Neilands, J. B. (1987). Universal chemical assay for the detection and determination of siderophores. *Anal. Biochem.* 160, 47–56. doi: 10.1016/0003-2697(87)90612-9

Stern, J. C., Sutter, B., Freissinet, C., Navarro-Gonzalez, R., McKay, C. P., Archer, P. D., et al. (2015). Evidence for indigenous nitrogen in sedimentary and aeolian deposits from the Curiosity rover investigations at Gale crater, Mars. *Proc. Natl. Acad. Sci. U.S.A.* 112, 4245–4250. doi: 10.1073/pnas.1420932112

Summers, S., Whiteley, A. S., Kelly, L., and Cockell, C. S. (2013). Land coverage influences the bacterial community composition in the critical zone of a sub-Artic basaltic environment. *FEMS Microbiol. Ecol.* 86, 381–391. doi: 10.1111/1574-6941.12167

Sutter, B., McAdam, A. C., Mahaffy, P. R., Ming, D. W., Edgett, K. S., Rampe, E. B., et al. (2016). Evolved gas analyses of sedimentary rocks and eolian sediment in gale crater, mars: results of the curiosity Rover's Sample Analysis at Mars (SAM) instrument from Yellowknife Bay to the Namib Dune. *J. Geophys. Res.* 2169–9100. doi: 10.1002/2016JE005225

Thoreseth, I. H., Furnes, H., and Tumyr, O. (1991). A textrual and chemical study of Iceland palagonite of vared composition and its bearing on the mechanism of glass-palagonite transformation. *Geochim. Cosmochim. Acta* 55, 731–749. doi: 10.1016/0016-7037(91)90337-5

Tian, F., Kasting, J. F., and Solomon, S. C. (2009). Thermal escape of carbon from the early Martian atmosphere. *Geophys. Res. Lett.* 36. doi: 10.1029/2008GL036513

Treiman, A. H., and Filiberto, J. (2015). Geochemical diversity of shergottite basalts: mixing and fractionation, and their relation to Mars surface basalts. *Meteorit. Planet. Sci.* 50, 632–648. doi: 10.1111/maps.12363

Uroz, S., Calvaruso, C., Turpault, M. P., and Frey-Klett, P. (2009). Mineral weathering by bacteria: ecology, actors and mechanisms. *Trend. Microbiol.* 17, 378–387. doi: 10.1016/j.tim.2009.05.004

Vandevivere, P., Welch, S. A., Ullman, W. J., and Kirchman, D. L. (1994). Enhanced dissoluton of silicate minerals by bacteria at near-neutral pH. *Microb. Ecol.* 27, 241–251. doi: 10.1007/BF00182408

Vaniman, D. T., Bish, D. L., Ming, D. W., Bristow, T. F., Morris, R. V., Blake, D. F., et al. (2014). Mineralogy of a mudstone at Yellowknife Bay, Gale crater, Mars. *Science* 343:1243480. doi: 10.1126/science.1243480

Welch, S. A., Taunton, A. E., and Banfield, J. F. (2002). Effect of microorganisms and microbial metabolites on apatite dissolution. *Geomicrobiol. J.* 19, 343–367. doi: 10.1080/01490450290098414

Welch, S. A., and Ullman, W. J. (1993). The effect of organic acids on plagioclase dissolution rates and stoichiometry. *Geochim. Cosmochim. Acta* 57, 2725–2736. doi: 10.1016/0016-7037(93)90386-B

Westall, F., Foucher, F., Bost, N., Bertrand, M., Loizeau, D., Vago, J. L., et al. (2015). Biosignatures on Mars: what, where, and how? Implications for the search for martian life. *Astrobiology* 15, 998–1029. doi: 10.1089/ast.2015.1374

Williams, R. M., Grotzinger, J. P., Dietrich, W. E., Gupta, S., Sumner, D. Y., Wiens, R. C., et al. (2013). Martian fluvial conglomerates at Gale Crater. *Science* 340, 1068–1072. doi: 10.1126/science.1237317

Wolff-Boenisch, D., Gislason, S. R., and Oelkers, E. H. (2006). The effect of crystallinity on dissolution rates and CO2 consumption capacity of silicates. *Geochim. Cosmochim. Acta* 70, 858–870. doi: 10.1016/j.gca.2005.10.016

Wu, L., Jacobson, A. D., Chen, H.-C., and Hausner, M. (2007). Characterization of elemental release during microbe-basalt interactions at T=28°C. *Geochim. Cosmochim. Acta* 71, 2224–2239. doi: 10.1016/j.gca.2007.02.017

Zolotov, M. Y., and Mironenko, M. V. (2016). Chemical models for martian weathering profiles: Insights into formation of layered phyllosilicate and sulfate deposits. *Icarus* 275, 203–220. doi: 10.1016/j.icarus.2016.04.011

Conflict of Interest Statement: The authors declare that the research was conducted in the absence of any commercial or financial relationships that could be construed as a potential conflict of interest.

frontiers in Microbiology

ORIGINAL RESEARCH
published: 05 March 2018
doi: 10.3389/fmicb.2018.00308

Cellular Responses of the Lichen *Circinaria gyrosa* in Mars-Like Conditions

Rosa de la Torre Noetzel[1]†, Ana Z. Miller[2†], José M. de la Rosa[2], Claudia Pacelli[3], Silvano Onofri[3], Leopoldo García Sancho[4], Beatriz Cubero[2], Andreas Lorek[5], David Wolter[5] and Jean P. de Vera[5]*

[1] Departamento de Observación de la Tierra, Instituto Nacional de Técnica Aeroespacial, Madrid, Spain, [2] Instituto de Recursos Naturales y Agrobiología de Sevilla, Consejo Superior de Investigaciones Científicas, Sevilla, Spain, [3] Department of Ecological and Biological Sciences, University of Tuscia, Viterbo, Italy, [4] Departamento de Biología Vegetal II, Universidad Complutense, Madrid, Spain, [5] German Aerospace Center (DLR) Berlin, Institute of Planetary Research, Berlin, Germany

Lichens are extremely resistant organisms that colonize harsh climatic areas, some of them defined as "Mars-analog sites." There still remain many unsolved questions as to how lichens survive under such extreme conditions. Several studies have been performed to test the resistance of various lichen species under space and in simulated Mars-like conditions. The results led to the proposal that *Circinaria gyrosa* (Lecanoromycetes, Ascomycota) is one of the most durable astrobiological model lichens. However, although *C. gyrosa* has been exposed to Mars-like environmental conditions while in a latent state, it has not been exposed in its physiologically active mode. We hypothesize that the astrobiological test system "*Circinaria gyrosa,*" could be able to be physiologically active and to survive under Mars-like conditions in a simulation chamber, based on previous studies performed at dessicated-dormant stage under simulated Mars-like conditions, that showed a complete recover of the PSII activity (Sánchez et al., 2012). Epifluorescence and confocal laser scanning microscopy (CLSM) showed that living algal cells were more abundant in samples exposed to niche conditions, which simulated the conditions in micro-fissures and micro-caves close to the surface that have limited scattered or time-dependent light exposure, than in samples exposed to full UV radiation. The medulla was not structurally affected, suggesting that the niche exposure conditions did not disturb the lichen thalli structure and morphology as revealed by field emission scanning electron microscopy (FESEM). In addition, changes in the lichen thalli chemical composition were determined by analytical pyrolysis. The chromatograms resulting from analytical pyrolysis at 500°C revealed that lichen samples exposed to niche conditions and full UV radiation consisted primarily of glycosidic compounds, lipids, and sterols, which are typical constituents of the cell walls. However, specific differences could be detected and used as markers of the UV-induced damage to the lichen membranes. Based on its viability responses after rehydration, our study shows that the test lichen survived the 30-day incubation in the Mars chamber particularly under niche conditions. However, the photobiont was not able to photosynthesize under the Mars-like conditions, which indicates that the surface of Mars is not a habitable place for *C. gyrosa*.

Keywords: Mars environment, extremotolerance, lichens, *Circinaria gyrosa*, photosynthetic activity, analytical pyrolysis

OPEN ACCESS

Edited by:
Masahiro Ito,
Toyo University, Japan

Reviewed by:
Henrik R. Nilsson,
University of Gothenburg, Sweden
Lyle Whyte,
McGill University, Canada

****Correspondence:***
Rosa de la Torre Noetzel
torrenr@inta.es

† These authors have contributed equally to this work.

Specialty section:
This article was submitted to Extreme Microbiology, a section of the journal Frontiers in Microbiology

Received: *12 September 2017*
Accepted: *09 February 2018*
Published: *05 March 2018*

Citation:
de la Torre Noetzel R, Miller AZ, de la Rosa JM, Pacelli C, Onofri S, García Sancho L, Cubero B, Lorek A, Wolter D and de Vera JP (2018) Cellular Responses of the Lichen Circinaria gyrosa in Mars-Like Conditions. Front. Microbiol. 9:308. doi: 10.3389/fmicb.2018.00308

INTRODUCTION

Lichens are structurally complex organisms resulting from a symbiotic relationship of algae, also known as cyanobacteria (photobiont), and ascomycetes, also known as basidiomycetes (mycobiont). Some lichens may also be composed of a third partner consisting of a specific basidiomycete yeast, which forms the cortex of the lichen thallus (Spribille et al., 2016). When exposed to environmental stress (such as extreme temperatures, desiccation, and UV radiation), lichens develop photoprotective mechanisms, including light scattering, radiation screening, thermal dissipation, antioxidant defense, membrane repair, and macromolecular production (Nguyen et al., 2013).

Lichens may produce several secondary metabolites as adaptive mechanisms for growing in harsh living conditions. Direct gas chromatography (GC)–mass spectroscopy (MS) analysis of a solvent extract is not straightforward because of non-volatile residues, which remain undetected because they are trapped in the chromatographic system (Stojanovic et al., 2011). Thus, we propose direct analyses of the samples by analytical pyrolysis (Py-GC/MS), which is defined as the thermochemical decomposition of organic materials at elevated temperatures in the absence of oxygen. The pyrolysis products (pyrolysates) are amenable to chromatographic separation, which in combination with an MS detector (GC/MS), provide a fingerprint for the molecular structure, including complex mixtures of macromolecular substances (De la Rosa et al., 2009). Pyrolytic techniques have additional well-known advantages such as the requirement of small sample sizes and minimal, if any, sample preparation. Thus, Py-GC/MS has become an important tool for analytical characterization of a wide spectrum of complex carbonaceous matrices including fossil organic matter, algal and vascular plants, sediments, and urban dust (Lee et al., 2005; De la Rosa et al., 2008; Pereira de Oliveira et al., 2011; Braovaca et al., 2016). This technique has already been successfully used to determine changes in lichens' chemical composition under different environmental conditions (MacGillivray and Helleur, 2001). It is based on the fact that lichens often react to stress factors by changing their acids as the result of a defense- or stress-induced metabolism. Rikkinen (1995) studied lichens' response to UV light. It has been reported that lichens under harmful stress condition will alter their composition, either as a chemical defense or in response to damage (Treshow and Anderson, 1989; Richardson, 1992).

Several studies have been performed to test the response of various lichen species to harsh conditions in space and Mars-like conditions on board space missions. Space is an extremely hostile environment, which is characterized by a high vacuum (10^{-7}–10^{-4} Pa), an intense field of ionizing radiation of solar and galactic origin, unfiltered solar ultraviolet (UV) radiation, and extreme temperatures (−120 to +120°C). Among the tested organisms, bacterial spores of *Bacillus subtilis* (Firmicutes, Bacillales) (Horneck et al., 1984, 2001; Horneck, 1993; Rettberg et al., 2002), the lichens *Rhizocarpon geographicum*, *Xanthoria elegans* (Sancho et al., 2007), and *Circinaria gyrosa* (De la Torre et al., 2010), and adults and eggs of the tardigrades *Richtersius coronifer* and *Milnesium tardigradum* (Jönsson et al., 2008) turned out to be the most resistant to these conditions. About 70% of the *B. subtilis* spores survived 2,107 days in space on board the National Aeronautics and Space Administration Long Duration Exposure Facility after being shielded from solar UV (Horneck et al., 1994). However, direct exposure to the solar extra-terrestrial UV radiation, as experienced in space, reduced their survival by orders of magnitude. So far, lichens are the only organisms that were able to survive under space conditions, which included solar extraterrestrial UV radiation as tested during the 2-week flight of BIOPAN-5 and -6 (Sancho et al., 2007; De los Ríos et al., 2009; De la Torre et al., 2010). Other studies were performed to concurrently test the response of lichen species under space and Mars-simulated conditions on board two space missions, EXPOSE-E and -R2 (Onofri et al., 2012; 2014–2016 mission), on the International Space Station. Laboratory studies using a simulated Mars environment and space-relevant ionizing radiation have also been conducted (Sánchez et al., 2012; De la Torre et al., 2017; Meeßen et al., 2017). The results showed that the species most resistant to space and Mars conditions was the vagrant lichen species *C. gyrosa* in a latent state. *Circinaria gyrosa* (formerly *Aspicilia fruticulosa*, Sohrabi et al., 2013) is a vagrant fruticose lichen with a crustose growth form. It does not grow while attached to a substrate. It is from the steppes and shrub lands with outliers in Southwest Asia and the Mediterranean area of Spain (Sohrabi et al., 2013). This lichen is characterized by a coralloid thallus with dichotomous branching and a compact internal structure (Sancho et al., 2000; Meeßen et al., 2013). Externally, it is limited by a thick cortex that provides efficient shielding against the hostile parameters of outer space (Sancho et al., 2007) and planetary conditions such as those seen on Mars. Yet, physiologically active *C. gyrosa* has not been exposed to Mars' environmental conditions. For this reason, our aim was to perform a first-time multidisciplinary assessment of *C. gyrosa*'s viability and morphological changes after exposure to the Mars conditions. Lichen viability was assessed by fluorescence microscopy as chlorophyll-induced red autofluorescence is used as an indicator of cell viability such as seen with intact chlorophyll molecules, which display red fluorescence in living cells. This method has been used to assess terrestrial phototrophic microorganisms' and marine phytoplanktons' viability in addition to a plant's ability to tolerate stress factors (Hense et al., 2008; Osticioli et al., 2013) since the red color of photosynthetic cells under UV light (Gausla and Ustvedt, 2003) is related to optimal photosynthetic activity that produces colored light or absence of light in cases of cell damage. Recently, this technique has been introduced in the field of astrobiology for examination of the viability of lichens exposed to simulated space conditions in order to help to distinguish intact cells from cells injured by high-dose ionizing radiation (De la Torre et al., 2017). In addition, changes in the chemical composition of the lichen thalli were determined by analytical pyrolysis (Py-GC/MS).

MATERIALS AND METHODS

Sample Preparation and Irradiation

We chose the lichen species *C. gyrosa* (Sohrabi et al., 2013) for the Mars simulation experiment. It is characterized by a

coralloid thallus with dichotomous branching and a compact internal structure (Sancho et al., 2000; Meeßen et al., 2013). All samples were collected from clay soils of the Central Spain steppic highlands, which are characterized by extreme insolation, high temperature contrasts, and arid summers (Crespo and Barreno, 1978). In the presence of these extremely harsh environmental conditions, *C. gyrosa* will enter a desiccated state in the form of a metabolic suspension or stasis (known as cryptobiosis or latent state), in which the cells of the lichen symbionts are dehydrated, and most biochemical activity ceases.

Replicate samples of *C. gyrosa* with 10 mm diameter were used and classified into two groups: (i) the first was composed of eight exemplars for exposure to simulated Mars environmental conditions (Cg1–Cg8; **Figure 1**), and (ii) the second, also formed with eight samples, was used as laboratory control (Cg9–Cg16). Samples for the Mars simulation experiment were again classified into two sets, each composed of four samples: (i) the first set was used for niche-led conditions (Cg1–Cg4), and (ii) the second set included samples that were exposed to full UV radiation (Cg5–Cg8). Before the Mars experiment, all samples were activated (as described below), and the photosynthetic activity was measured.

Description of Experiment Equipment

The experiment was carried out at the Mars Simulation Facility (MSF) of the DLR Institute of Planetary Research in Berlin (Lorek and Koncz, 2013, **Figure 2A**). The main part of the MSF is a climate chamber (CC) with inside dimensions of 80 cm height, 60 cm depth, and 50 cm width. The experiment was performed in an experimental chamber (EC), a vacuum sealed stainless steel chamber with a volume of 10.3 L inside the CC (**Figure 2B**). The EC has electrical connectors, connectors for gas in and output, four fibers for xenon light, and one fiber for photosynthetic activity measurements obtained with a photosynthesis yield analyzer (MiniPAM, Walz GmbH, Germany) as described by Sancho et al. (2007). Inside the chamber is a turntable with eight sample holders, a LED unit for the illumination of one sample with visible light and UV-radiation, and two humidity sensors close to the samples (approximately 1 cm) calibrated for the Martian atmosphere, each equipped with a Pt100-sensor. The gas flow through the EC is generated by a gas mixing system, which can control up to five gases and EC humidification. The pressure inside is controlled by a membrane vacuum pump. The radiation dose is measured with an X92-optometer and a RCH-106-4 probe (Gigahertz-Optik GmbH, Germany) at wavelengths ranging from 250 to 400 nm.

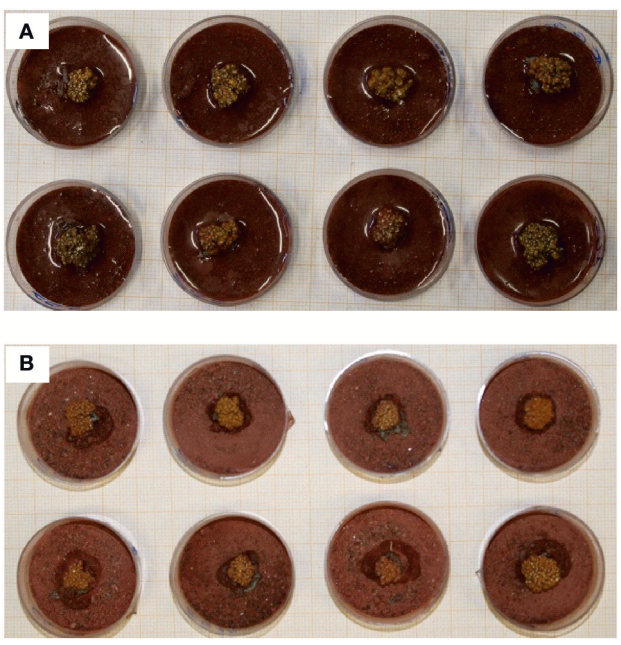

FIGURE 1 | Samples of *Circinaria gyrosa* used in this work. **(A)** Before Mars simulation experiment. **(B)** After Mars simulation experiment.

Experimental Conditions

Over the complete experimental time course, the EC had a continuous gas flow of 20 L h^{-1} (at 101,325 Pa). The gas consisted of 95% CO_2 and 5% air (4% N_2, 1% O_2). The pressure inside the EC was approximately 750 Pa, the temperature varied diurnally between −50°C (night) and 20°C (day), whereas the relative humidity (with respect to ice) ranged between approximately 75% (night) and near 0% (day). **Table 1** summarizes the experimental conditions used in the chamber in comparison with environmental conditions on the surface of Mars.

Four samples of *C. gyrosa* were illuminated with xenon light (full UV-radiation), and four samples were exposed to niche-led conditions. The LED lamp produces photosynthetic active radiation (PAR) and is used in addition to scattered UV-radiation produced by the xenon lamp. This allowed us to approach as closely as possible the conditions that could be faced in micro-fissures and micro-caves (so-called micro-niches) in rocks and the Martian soil. In these fissures and caves, only a short exposure period of scattered or direct light for a few minutes depending on the angle of the sun could be measured (Schuerger et al., 2003; de Vera et al., 2014). The LED unit was active for 16 h and switched off 8 h daily to simulate the Sun's diurnal cycle. During the same time period, the xenon-lamp was switched on and off with the exception that on weekends the UV-lamp remained off because only manual operation was possible. The resulting average radiation doses were 5.19 KJ m^{-2} for niche-led conditions (samples 1–4) and 127.52 KJ m^{-2} for full UV-radiation (samples 5–8). **Figure 3** shows the environmental conditions.

Chlorophyll *a* Fluorescence Analysis

To assess photosynthetic activity of the lichen photobiont after a 4-week exposure to simulated Mars conditions, the maximum quantum yield (QY) calculated as Fv/Fm (Schreiber et al., 1994), of the photosystem II (PS II) was measured in pre-activated samples by chlorophyll *a* fluorescence analysis. Reactivation of samples was performed for 72 h in a growth chamber at 10 °C and 100 μmol m^{-2} s^{-1} photosynthetic photon flux density (PPFD) for a daily 12 h photoperiod and moistened twice a day with mineral water. These conditions mimicked the environmental conditions accompanying high water availability corresponding

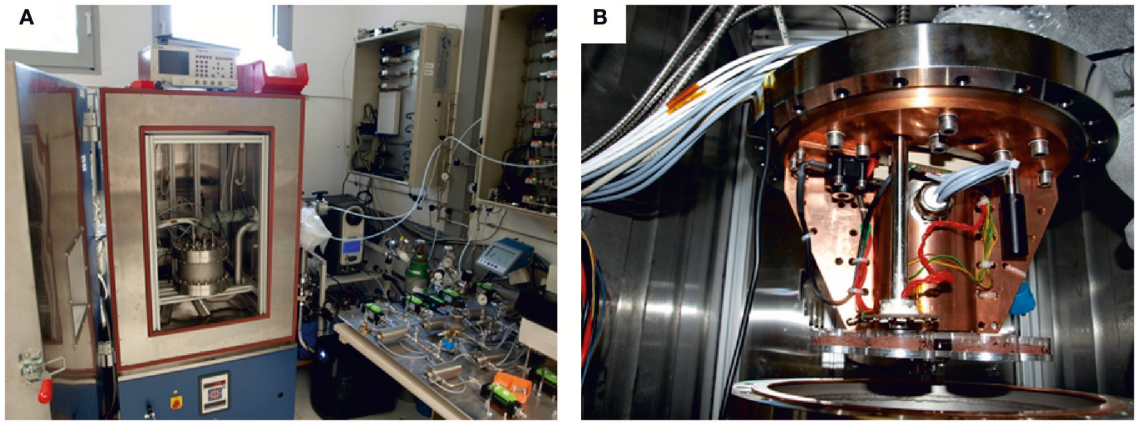

FIGURE 2 | Mars Simulation Facility at DLR. **(A)** Closed experiment chamber. **(B)** Opened experiment at DLR-chamber.

TABLE 1 | Experimental conditions used in the Mars Simulation Facility (MSF) of the DLR Institute of Planetary Research in Berlin in comparison to Mars surface conditions.

Ranges of experimental and environmental parameters	Mars-like conditions in the lab	Mars conditions
Relative humidity	0.1–75%	0–100% (at soil near saturation according to Harri et al., 2014)
Pressure	750 Pa	680–790 Pa (Hassler et al., 2013)
Temperature	(night −50°C to day +20°C), simulation of equatorial to mid latitude regions	Mean value (−55°C, −130°C at the poles to +27°C at the equatorial regions)
Atmospheric gas composition	CO_2 (95%), N_2 (4%), O_2 (0.15%)	CO_2 (95.97%), N_2 (1.89%), Argon (1.93%), O_2 (0.15%), (de Vera et al., 2014)
Radiation	Xe-UV (2,200 to 2,200 nm)	Solar radiation (>200 nm) (Schuerger et al., 2003; de Vera et al., 2014)

to physiological activity such as early morning dew formation, low temperatures, and low light conditions (Lange et al., 1970). Chlorophyll *a* fluorescence of re-activated samples was measured with a photosynthesis yield analyzer (Mini-PAM, Walz GmbH, Germany) as described by Sancho et al. (2007).

Epifluorescence and Confocal Laser Scanning Microscopy

Changes in cell viability and metabolic activity of *C. gyrosa* exposed to simulated Mars conditions were assessed by epifluorescence and confocal laser scanning microscopy (CLSM). Before observation, the lichen samples were rehydrated with mineral water and reactivated for 12 h at 10°C. Subsequently, samples were incubated for an additional period of 24 h in a Sanyo MLR-351 plant growth chamber under environmental parameters consisting of 21°C, 60–70% relative humidity, and 12 h dark/12 h illumination with 250 μmol m^{-2} s^{-1} photosynthetically active radiation. Thin sections (80–100 μm) of re-activated lichen samples were prepared with a vibratome and immediately visualized using a Zeiss Apotome epifluorescence microscope (Zeiss, Hamburg, Germany) with a HXP 120 lamp and an Axiocam 506 digital camera. The cube filters for epifluorescence were 38 HE GFP (excitation 450–490 nm and emission 500–550 nm) and cube 50 Cy5 (excitation 625–655 nm and emission 665–715 nm).

Thin sections from re-activated thallus samples for CLSM were stained with 25 μM of the fluorescent dye FUN-1® (Molecular Probes, Oregon, USA) in 2% glucose and 10 mM HEPES buffer (pH 7.0) and incubated at 25°C for 3 h. FUN-stained samples were then observed using a Zeiss LSM 7 DUO Confocal Microscope (Zeiss GmbH, Germany) with a 10X EC Plan-Neofluar objective. Images were acquired at eight bits with 1,024 × 1,024 pixels format using the 488 nm line of an argon ML laser as the only excitation source and a mean beam splitter of 488/561. Emission bands for each channel were 505–550 nm (for green), 581–620 nm (for red), and 672–758 nm (for blue). Image stacks were taken through the z axis at 4 μm intervals through the whole section and analyzed with ZEN 2011 software (Zeiss GmbH, Germany). Images were obtained by combining the three fluorescence signals.

Field Emission Scanning Electron Microscopy

To accurately assess thallus anatomy and morphological changes in *C. gyrosa* samples exposed to simulated Mars conditions, field emission scanning electron microscopy (FESEM) with energy dispersive X-ray spectroscopy (EDS) was conducted. Before FESEM examinations, thin sections of the reactivated thallus samples were fixed with 2.5% glutaraldehyde in 0.1 M cacodylate-buffer (pH 7.4) at 4°C for 2 h, washed three times in cacodylate-buffer for 5 min per wash period, and post-fixed in 1% osmium tetroxide for 1 h at 4°C. The samples were

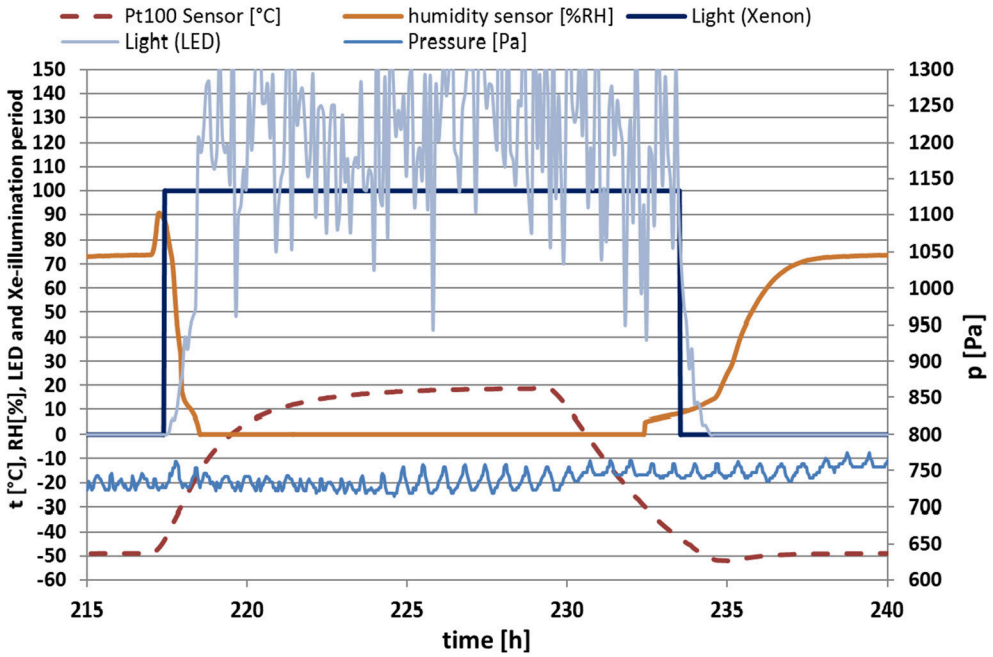

FIGURE 3 | Mars-like environmental conditions [temperature (*t*), relative humidity (RH), illumination period (by LED and Xenon) and pressure (*p*)] of a selected exemplary temporal section extracted from the 30 day data set of the Mars simulation experiment.

then dehydrated by subsequent serial dilutions in ethanol and acetone and then dried in a critical point drying device (Leica EM CPD300) at 34.5°C. Finally, the fixed lichen samples were sputter-coated with a thin gold film and observed with an FEI Teneo FESEM (FEI Company, Eindhoven, The Netherlands) using the secondary electron detection mode with an acceleration voltage of 5 kV for ultra-high resolution images and 10 kV for elemental microanalysis and mapping.

DNA-Based Analyses

Polymerase chain reaction (PCR) analyses were performed to verify deoxyribonucleic acid (DNA) damage by both random amplification of polymorphic DNA (RAPD) fingerprinting and single gene amplifications. DNA was extracted from rehydrated lichen samples using the Nucleospin Plant kit (Macherey-Nagel, Düren, Germany) following the protocol optimized for fungi. Amplification of the internal transcribed spacer (ITS) regions and the large and small subunits ribosomal RNA genes were performed using BioMix (BioLine GmbH, Luckenwalde, Germany) after adding 5 pmol of each primer and 20 ng of template DNA at final volume of 25 µl. The amplification was carried out using a MyCycler Thermal Cycler (Bio-Rad Laboratories GmbH, Munich, Germany) equipped with a heated lid. Conditions for rDNA regions amplification and primer sequences are reported in **Tables 2**, **3**, respectively. For the mycobiont, the RAPD protocol of Selbmann et al. (2011) was applied. For RAPD of the *C. gyrosa* photobiont, the OPA 13 primer (**Table 3**) was used and conditions for amplification included several steps: (i) a denaturation step at 94°C for 4 min; (ii) denaturation at 96°C for 30 s; (iii) annealing at 49°C for 60 s; and (iv) extension at 72°C for 30 s. The final three steps were repeated 40 times with a final extension at 72°C for 6 min. Band intensity was measured and compared using Image J software, version 1.45 (Schneider et al., 2012).

Pyrolysis-Gas Chromatography/Mass Spectrometry (Py-GC/MS)

Chemical analyses of lichen thalli were carried out by direct pyrolysis-gas chromatography/mass spectrometry (Py-GC/MS) using a double-shot pyrolyser (Frontier Laboratories, model 2020i) attached to a GC/MS Agilent 6890N as described in Miller et al. (2016). One milligram each of *C. gyrosa* samples from the control, niche-led conditions, and exposed-to-full UV sets were placed in small crucible capsules and introduced into a pre-heated micro-furnace at 500°C for 1 min. The volatile pyrolysates were then directly injected into the GC/MS for analysis. The gas chromatograph was equipped with a HP-5ms-UI, low polar-fused silica (5%-phenyl-methylpolysiloxane) capillary column of 30 m × 250 µm × 0.25 µm film thickness. The oven temperature was held at 50°C for 1 min and then increased to 100°C at 30°C min^{-1}, from 100 to 300°C at 10°C min^{-1}, and then stabilized at 300°C for 10 min. The carrier gas was helium at a controlled flow of 1 ml min^{-1}. The detector was an Agilent 5973 mass selective detector, and mass spectra were acquired at 240°C under electron impact (70 eV of energy). Masses were scanned from m/z 40–600. Each sample was pyrolyzed twice without perceptible differences between the chromatograms of the same sample. Compound assignment was achieved via comparison with already published data or stored in digital libraries (NIST and Wiley libraries).

TABLE 2 | Amplification conditions.

Samples	DNA region	Primers	First denaturation	Denaturation	Annealing	Extension	Final extension
					35 cycles		
Mycobiont	ITS (700 bp)	ITS5-ITS4	95°C for 2 min	95°C for 30 s	55°C for 30 s	72°C for 30 s	72°C per 5 min
Mycobiont	LSU (1,200 bp)	ITS5-LR5	95°C for 3 min	95°C for 45 s	52°C for 30 s	72°C for 3 min	72°C per 7 min
Mycobiont	LSU (2,000 bp)	ITS5-LR7	95°C for 3 min	95°C for 45 s	52°C for 30 s	72°C for 3 min	72°C per 7 min
Photobiont	SSU (1,000 bp)	NS1-NS2	94°C for 3 min	94°C for 45 s	55°C for 1 min	72°C for 3 min	72°C for 5 min
Photobiont	SSU (2,000 bp)	NS1-NS4	94°C for 3 min	94°C for 45 s	55°C for 1 min	72°C for 3 min	72°C for 5 min
Photobiont	SSU (3,000 bp)	NS1-18L	94°C for 3 min	94°C for 45 s	55°C for 1 min	72°C for 3 min	72°C for 5 min

TABLE 3 | Primer sequences.

Primer	Sequence (5′->3′)	References
ITS4	TCCTCCGCTTATTGATATGC	White et al., 1990
ITS5	GGAAGTAAAAGTCGTAACAAGG	White et al., 1990
LR5	TCCTGAGGGAAACTTCG	Vilgalys and Hester, 1990
LR7	TACTACCACCAAGATCT	Vilgalys and Hester, 1990
NS1	GTAGTCATATGCTTGTCTC	White et al., 1990
NS2	GGCTGCTGGCACCAGACTTGC	White et al., 1990
NS4	CTTCCGTCAATTCCTTTAAG	White et al., 1990
18L	CACCYACGGAAACCTTGTTACGACTT	Hamby et al., 1988
$(GGA)_7$	GGA GGA GGA GGA GGA GGA GGA	Kong et al., 2000
OPA 13	CAGCACCCAC	Ho et al., 1995

RESULTS AND DISCUSSION

Mars-Like Conditions

Before examining and analyzing the results, it has to be clarified that Mars-like conditions in reference to our present work means that we cannot simulate the reduced Martian gravity and direct exposure to heavy radiation particles in the laboratory; these conditions are expected to happen on the surface of Mars because of the lack of a protective global magnetic field; however, by simulating Mars-like niche conditions we are approaching conditions with reduced radiation (that could be expected in micro-fissures and micro-caves close to the surface of Mars) or reduced sunlight intensity caused by dust in the atmosphere.

PSII Activity During the Exposure to Simulated Mars-Like Conditions

Photosynthetic activity measurements were executed in 30 min steps. The yield-value dropped from 0.35 down to approximately 0 for all samples within the first hour of the experiment. Over the remaining experimental period, the photosynthetic activity of all samples ranged from very low to non-existent (**Figure 4**). Although the photosynthetic light reaction was measured before and after the experiment, it can be concluded that *C. gyrosa* was not photosynthetically active during the Mars exposure experiment. The lichen therefore coped with Mars-like conditions by entering a dormant stage and would not be able to survive on Mars in the long-term in the absence of photosynthetic activity.

PSII Activity Before and After the Exposure to Simulated Mars-Like Condition0073

The PSII was measured as the maximum QY for the different set of samples before exposure to simulated Mars-like conditions and showed a homogeneous tendency without significant differences between them (**Figure 5**). However, after exposure to the Mars-like environment, the mean values showed differences over a range of 20% for both sample sets, including the control set (Cg9–Cg12, **Figure 5**). These differences were higher than those of the second control set (Cg13–Cg16) with 0.5%.

These results indicate that a simulated Mars-like environment with attenuated niche-like conditions and full impact of Mars UV radiation (full UV) did not significantly affect the photosynthetic activity of the re-activated *C. gyrosa*. In other words, the photosynthetic activity of the lichen thalli recovered efficiently after re-activation (rehydration after exposure to Mars-like conditions).

Morphology and Cell Viability After Exposure to Simulated Mars-Like Conditions

Chlorophyll autofluorescence monitored by epifluorescence microscopy for evaluating cell viability of the photobiont showed slight differences in the red light emission (chlorophyll autofluorescence) among the three sets of samples (**Figure 6**). The *C. gyrosa* thalli exposed to niche-led conditions exhibited red fluorescence similar to the control samples (**Figures 6A,B**). In samples fully exposed to UV radiation, algal cells were less abundant, and almost no autofluorescence was observed in zones occupied by algal clusters (**Figure 6C**). This indicates an irradiation-induced degradation of chlorophyll or an inefficient reactivation of lichen physiological processes after rehydration. However, minimal red fluorescence was recorded in the algal layer (**Figure 6D**).

The FUN-1 stain was used for detecting the presence of metabolically active fungal cells by CLSM due to intracellular processing of the vacuolar dye (red fluorescence). Algal cells could also be observed and identified by recording their autofluorescence signal in the blue channel (**Figure 7**). CLSM analyses of the lichen photobiont were in line with the epifluorescence-monitored chlorophyll autofluorescence. Living algal cells (with intense blue fluorescence) were more abundant

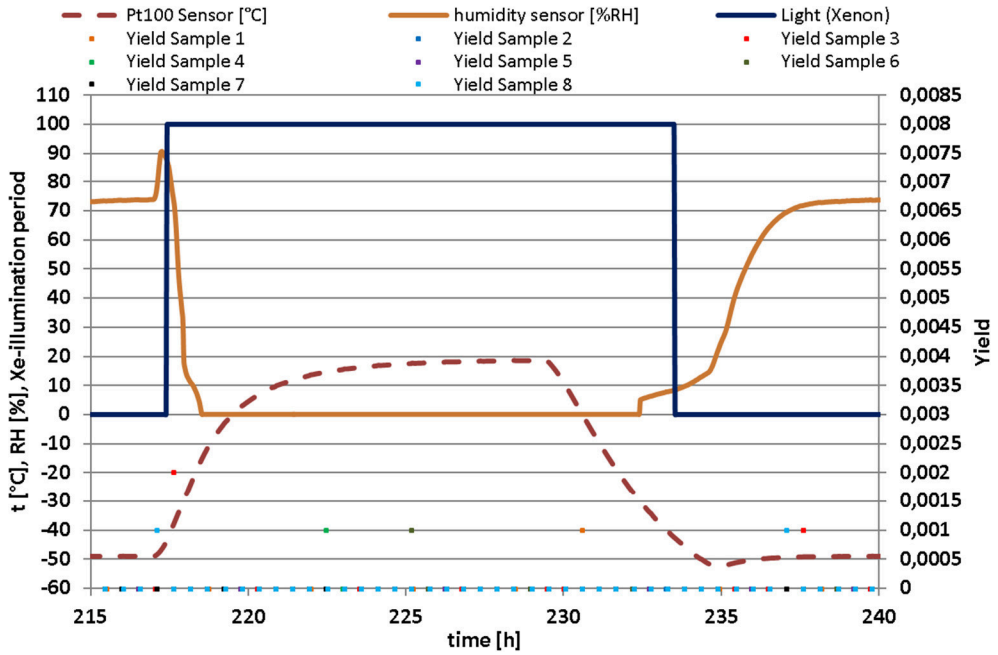

FIGURE 4 | Measurements of photosynthesis activity of eight samples. The photosynthesis activity is shown by the Yield values under Mars-like environmental conditions [temperature (*t*), relative humidity (RH), illumination period by Xenon-lamp] of a selected exemplary temporal section extracted from the 30 day data set of the Mars simulation experiment. No effective photosynthetic activity was measured during the simulation.

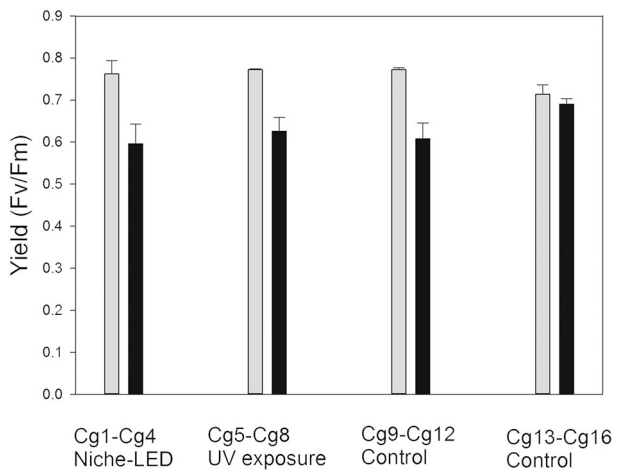

FIGURE 5 | Photosynthetic performance of photosystem II (PSII) by chlorophyll *a* fluorescence: Before exposure (light gray) and after Mars simulation experiment (dark gray).

in the control (**Figure 7A**) and samples exposed to niche-led conditions (**Figure 7B**) than to full UV (**Figure 7C**). The latter samples showed clear asymmetry of the algal layer in the thin lichen cross-sections as intense chlorophyll autofluorescence was intermixed with faded blue fluorescent cells (**Figure 7C**). Concerning the mycobiont, similar levels of metabolization of the FUN-1 stain yielding green fluorescent hyphae with clear red fluorescent vacuoles were observed in the control and irradiated samples, particularly in the proximity of the algal layer, suggesting metabolically active fungal cells (**Figures 7A,B**). Green fluorescent hyphae without red structures were particularly observed in the innermost medullary part of the lichen, pointing to a lack of viability in these regions.

FESEM of the thin lichen sections used for assessing thallus structural changes and damage to cell walls revealed differences among the three set of samples (**Figure 8**). The control sample showed the characteristic *C. gyrosa* thallus structure with the algal layer composed of photobiont cells arranged in clusters (**Figure 8A**) and a medulla with loosely interwoven fungal hyphae (**Figure 8B**). Both control and niche-led samples showed good anatomical preservation of the algal clusters in addition to the individual cells (**Figure 8C**). In addition, the medulla did not seem to be structurally affected and consisted of interlaced hyphae with numerous voids (**Figure 8D**), indicating that the niche-like exposure conditions did not disturb either the lichen thallus structure or the morphology. Interestingly, FESEM examinations revealed highly mineral-encrusted hyphae in all samples, predominantly in the inner medullary structure (**Figure 8E**). According to crystal shape and EDS analyses, this mineral is consistent with whewellite (calcium oxalate monohydrate), an insoluble organic salt secreted by the cells for several purposes, including calcium regulation, protection, and structural strengthening (Giordani et al., 2003). Whewellite crystals are widespread among organisms and have been reported on stone surfaces that were densely colonized by lichens (Pereira de Oliveira et al., 2011). Extracellularly deposited whewellite-crystals were also observed by Meeßen et al. (2013),

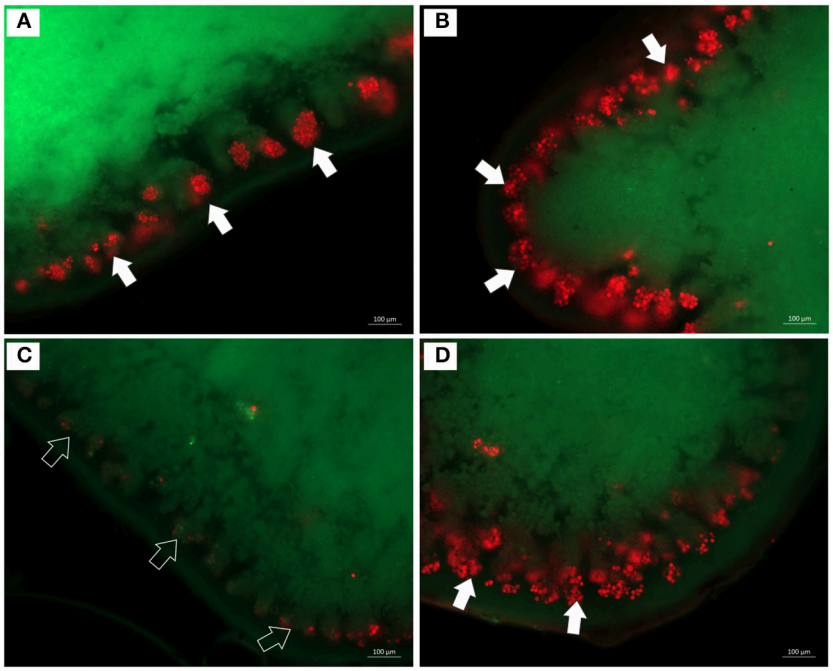

FIGURE 6 | Epifluorescence microscopy images of thin sections of *C. gyrosa* lichen thalli before **(A)**, and after exposure to niche-led conditions **(B)**, and to full UV radiation **(C,D)**. Red color represents chlorophyll autofluorescence from algal cells (white arrows). In samples fully exposed to UV radiation **(C,D)**, almost no autofluorescence was observed in zones occupied by algal clusters (black arrows).

Böttger et al. (2014), and De la Torre et al. (2017) on *C. gyrosa* medullary hyphae.

On the other hand, the asymmetry observed by CLSM relating to the numbers and distribution of algal cells throughout the lichen thalli of the full UV exposed samples was clearly detected by FESEM. **Figure 8F** shows part of a lichen thallus with disrupted photobiont cells in the zones occupied by algal clusters, whereas other parts of the same thin section showed well-preserved algal cells (**Figure 8G**). The loose inner medulla of the niche-led samples (**Figure 8C**) contrasted with the tightly packed fungal cells of the full UV exposed samples conglutinated with extracellular cementing substances, particularly in the proximity of the algal layer (**Figure 8H**). Taken together, these data indicate that *C. gyrosa* samples exposed to full UV radiation show a slight delay in physiological activity recovery after rehydration in comparison to the lichen thalli exposed to niche-led conditions. In a review by Holzinger and Karsten (2013) about desiccation tolerance of aeroterrestrial algae, it was reported that green algae rapidly reduced photosynthetic activities during desiccation but recover quickly after rehydration. Similarly, Aubert et al. (2007) showed that samples of the lichen *X. elegans* in high mountain environments instantly recovered respiration after hydration and both photobiont and mycobiont cells did not suffer irreversible desiccation-induced damage.

DNA Integrity Evaluation

DNA integrity was assessed by amplifying three different genes both for the mycobiont and photobiont and also by using a fingerprinting analysis to analyze whole genome integrity. PCR-stop assays are a powerful method for evaluating DNA damage since lesions block the progression of DNA polymerase (Kumar et al., 2004; Trombert et al., 2007), and long amplicons have a higher likelihood of undergoing DNA damage than short PCR amplicons (Rudi et al., 2010). In addition, in genomic PCR fingerprinting that amplifies short genomic DNA portions, PCR band intensity mainly decreased in the highest molecular weight fragments in single-gene PCR (Atienzar et al., 2002; Atienzar and Jha, 2006). Amplicons were obtained both for ITS and large subunit (LSU) regions of the mycobiont (**Figure 9A**). These approaches have been applied to dried *Cryomyces antarcticus* colonies exposed to UV irradiation (Selbmann et al., 2011) and then successfully applied under both simulated space- and Mars conditions-, ionizing radiation-, and alpha particles-exposed samples of the same fungus (Onofri pers. com.; Pacelli et al., 2017a,b,c). A reduction of amplicon intensity was observed with increasing genetic marker length. Nevertheless, DNA was still intact and perfectly detectable at the highest molecular weight band (2,000 bases). Single gene amplifications of photobiont DNA (**Figure 9B**) revealed that DNA was amplified at both 1,000 and 2,000 bases. We could not obtain a PCR product (band) for the longest length tested (3,000 bases).

RAPD profiles of samples under Mars-like conditions were identical to those of both the mycobiont and photobiont since no band disappearance was observed; the whole genome was conserved (**Figure 10**). For DNA analyses, the photobiont was the most affected by Martian conditions, showing a reduction

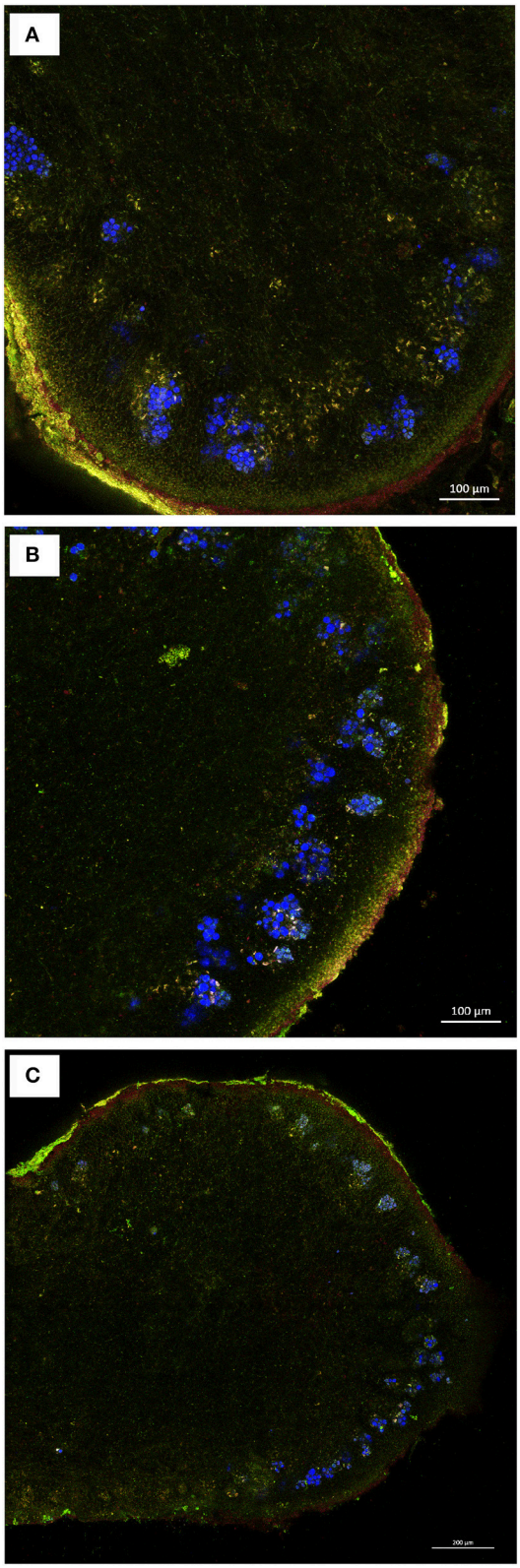

FIGURE 7 | CLSM images of FUN-1 stained thin sections of *C. gyrosa* lichen thalli before **(A)**, and after exposure to niche-led conditions **(B)**, and to full UV radiation **(C)**. The FUN-1 stain yielding green fluorescent hyphae with red fluorescent vacuoles represent metabolically active hyphae, which are particularly observed in the proximity of the algal clusters. Blue cells represent chlorophyll autofluorescence. Green fluorescent hyphae without red structures, indicating lack of viability, are observed in the innermost medullary part of the lichen fully exposed to UV radiation **(C)**.

up to 50% for the maximum gene length (**Figure 10B**), while the mycobiont DNA was perfectly detectable at every examined gene length (**Figure 10A**). Notably, in our experiments DNA could be easily extracted and detected even after being exposed to Mars-like conditions. The low temperatures in space was shown to reduce DNA breaks by half compared to ambient Earth temperatures (Lindahl, 1993), and the dry space environment was shown to preserve DNA (Lyon et al., 2010). Furthermore, it has been already reported that the low temperatures and dry conditions on Mars may preserve DNA in a better way in the long-term than do the conditions on Earth (Kanavarioti and Mancinelli, 1990; Sephton, 2010). Other studies on *C. antarcticus* DNA damage after exposure to the Martian atmosphere similarly demonstrated that fungal DNA was not affected and remained perfectly detectable by PCR (Pacelli et al., 2017b).

Analytical Pyrolysis (Py-GC/MS)

The GC/MS total ion chromatograms (TIC) of the pyrolysates of the three sets of samples are shown in **Figure 11**. They were very similar and consisted mainly of furanes, furfural, and methyl derivatives of these compounds. They were polysaccharide-derived xyloses and hexoses which constituted about 95% of the lichen molecular composition according to Schellekens et al. (2009). These compounds were also found by analytical pyrolysis to be common products of metabolic lichen thalli activities (Saiz-Jimenez et al., 1991). The most abundant compound of the three TICs was levoglucosan (peak 25, **Figure 11**), which is a six carbon ring structure formed from the carbohydrate (such as starch or cellulose) pyrolysis. One of the differences observed in the chromatograms was the presence of L-arabinopyranose in the full UV-irradiated lichens (peak 26, **Figure 11C**). This was a furan-related aldopentose, which is found in nature as a component of biopolymers such as hemicellulose. Neophytadiene, a marker of chlorophyll in algae and cyanobacteria (Saiz-Jimenez et al., 1990), was present in all of the samples (peak 27, **Figure 11**). Its relative abundance decreased in the fully UV-irradiated lichens (**Figure 11C**); nevertheless, in the latter case, the peak was partially masked by L-arabinopyranose (peak 26).

A series of sterols and terpenes were identified in all the TICs (from min 22 to 28). Our results revealed a mixture of C_{28-30} sterols (peaks 37–41 and 43–46, **Figure 11**), which included ergosterol acetates, ergostanol, stigmastan-3,5-dien, and β-sitosterol. They were plant cell membrane components and were lichen secondary metabolites, which have been widely studied due to their medical and pharmaceutical applications. Ergosterol is regarded as the typical membrane constituent of fungi and serves as a bioregulator of membrane fluidity, asymmetry, and

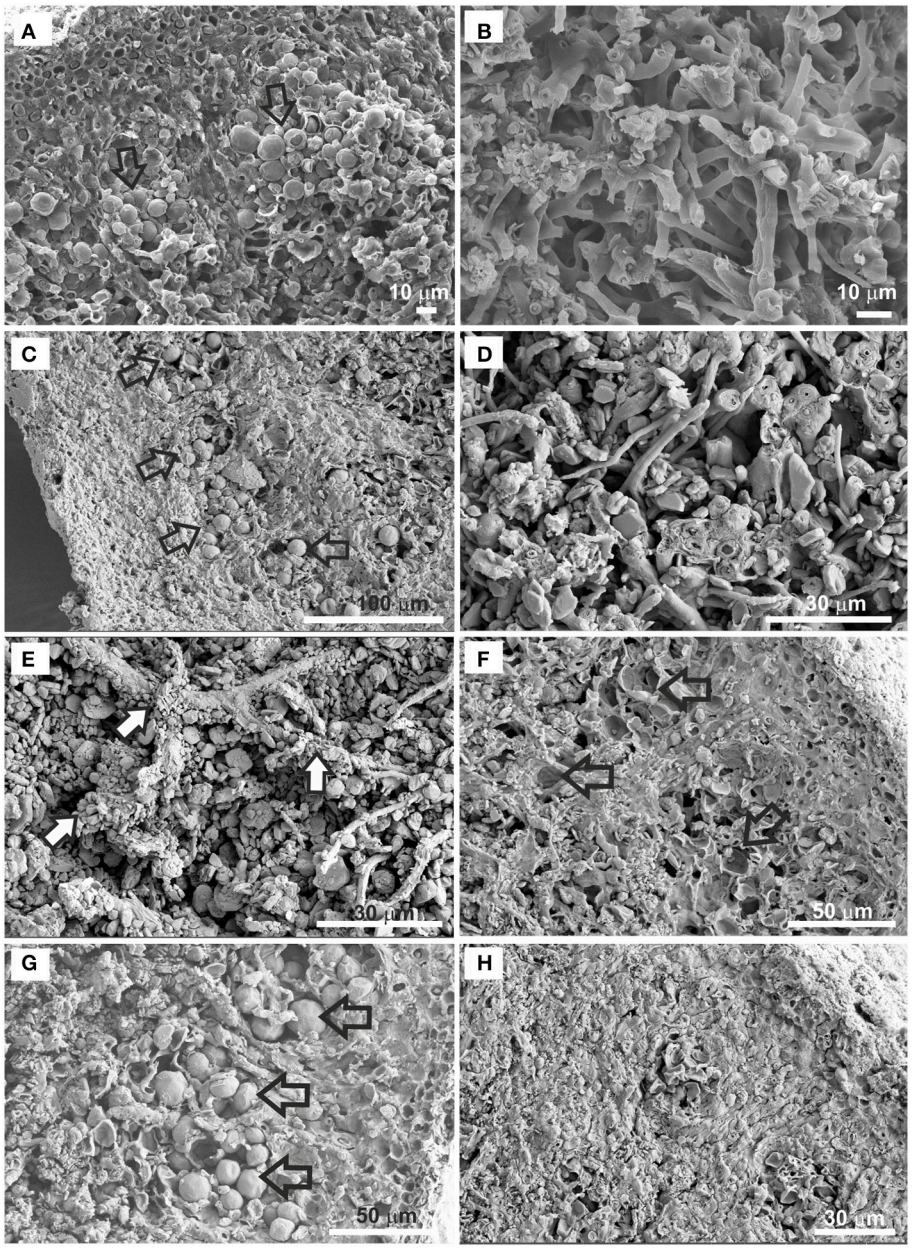

FIGURE 8 | FESEM images of *C. gyrosa* thin sections before **(A,B)**, and after exposure to niche-led conditions **(C–E)**, and to full UV radiation **(F–H)**. The control sample shows photobiont cells arranged in clusters (**A**, arrows), and the medulla with loosely interwoven fungal hyphae **(B)**. The samples exposed to niche-led conditions show good anatomical preservation of the algal clusters (**C**, arrows) and of the lichen medulla **(D)**. Highly mineral-encrusted hyphae (**E**, white arrows) were observed in all samples. Disrupted photobiont cells (**F**, arrows), as well as well-preserved algal cells (**G**, arrows) are observed in the full UV exposed samples. Tightly packed fungal cells are observed for the full UV exposed samples **(H)**.

integrity. Sufficient ergosterol content is necessary for fungal cell growth and normal membrane function. The TIC of the niche-led samples showed a relative increase in the presence of sterols (**Figure 11B**), while a clear decrease is observed for the full UV-irradiated samples (**Figure 11C**). Taking into account that the fluidity of biological membranes is influenced by the amount of sterols (Russel, 1989), this result could indicate surface damage to the membrane resulting from high UV radiation doses. Furthermore, the decrease in the relative abundance of β-sitosterol of the full UV-irradiated samples (**Figure 11C**) could be due to its dehydration and subsequent transformation into stigmasta-3,5-diene (León-Camacho et al., 2004). In line with the previous findings, D-α-Tocopherol (vitamin E; Peak 42), a key lipid-soluble antioxidant in membranes (Munne-Bosch and Alegre, 2002), was found solely in the control sample (**Figure 11A**). Fatty acids (FAs) are homologous and typically

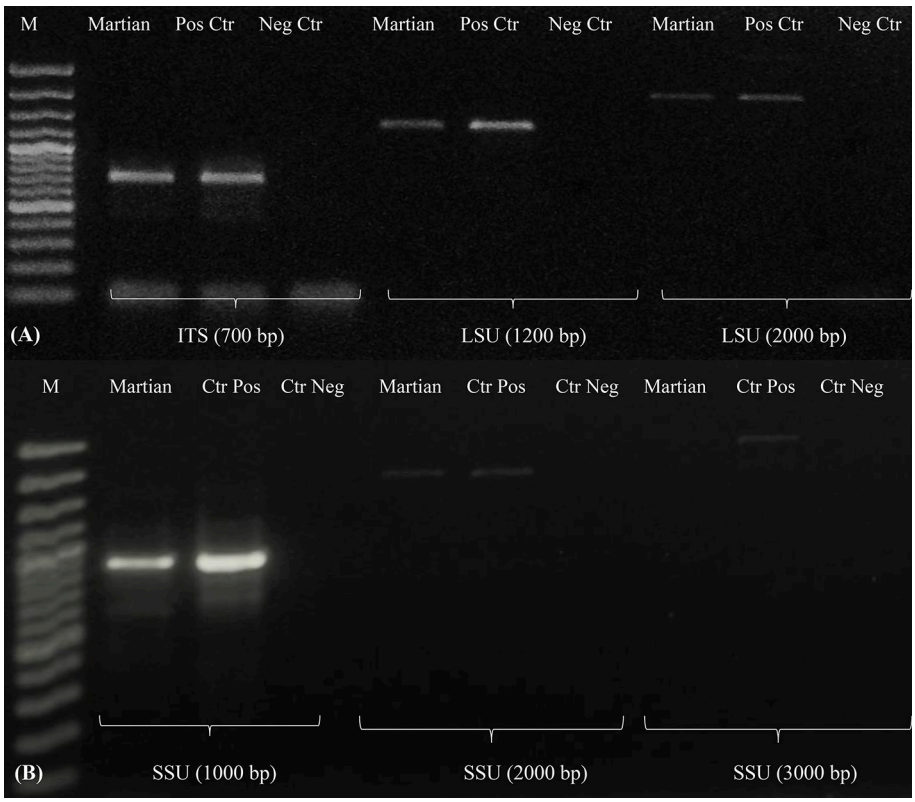

FIGURE 9 | Single gene amplification of *C. gyrosa* mycobiont **(A)** and photobiont **(B)**. Gene length as reported in **Table 2**. MW, DNA ladder; Martian, Martian conditions; CTR Pos, Untreated Control; CTRL Neg, PCR Negative Control.

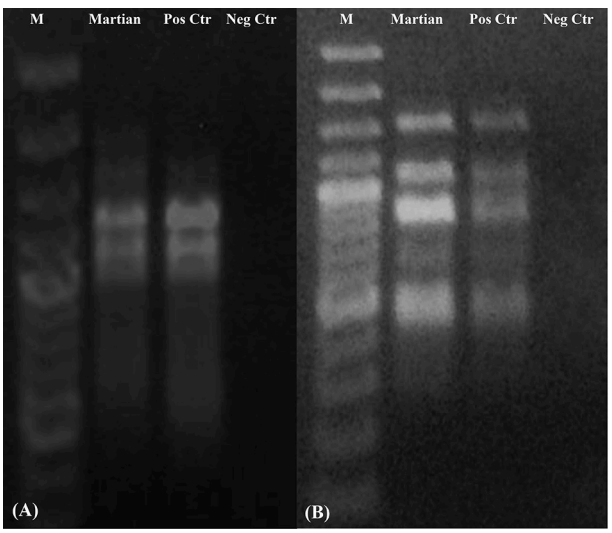

FIGURE 10 | RAPD profile of *C. gyrosa* mycobiont **(A)** and photobiont **(B)**. Samples correspondence as reported in **Figure 9**.

found in the molecular composition of lichens. Nevertheless, only pentanoic, palmitic, and linoleic acids are detected in the TICs of the lichens (peaks 2, 28, and 29, respectively). The low FA abundance was due to the incompatibility with the apolar columns used in GC and to secondary reactions that occur at the elevated temperatures applied during the pyrolysis (Dignac et al., 2006). A few nitrogen (N)-containing compounds were detected among the pyrolisates (peaks 23, 30, and 34; **Figure 11**), which were probably derived from peptides. Their decline in the full UV-irradiated lichens could indicate the use of N-precursors to sustain the synthesis of N-containing compounds under stress conditions. These results show that analytical pyrolysis is a valuable tool for assessing alterations in lichens' chemical composition. For instance, specific compounds could be used as biomarkers of cell membrane damage. There are several main advantages of analytical pyrolysis use in for astrobiology: (i) easy sample preparation (drying and milling); (ii) fast analysis time; (iii) very high reproducibility; and (iv) only small amount of sample is required (0.5–5 mg).

CONCLUSIONS

Our multidisciplinary approach allowed us to assess the viability, structure, DNA integrity, and chemical composition of the lichen *C. gyrosa* after exposure to simulated Mars conditions. Although the lichen samples did not have the capability to be photosynthetically active during the 30-day

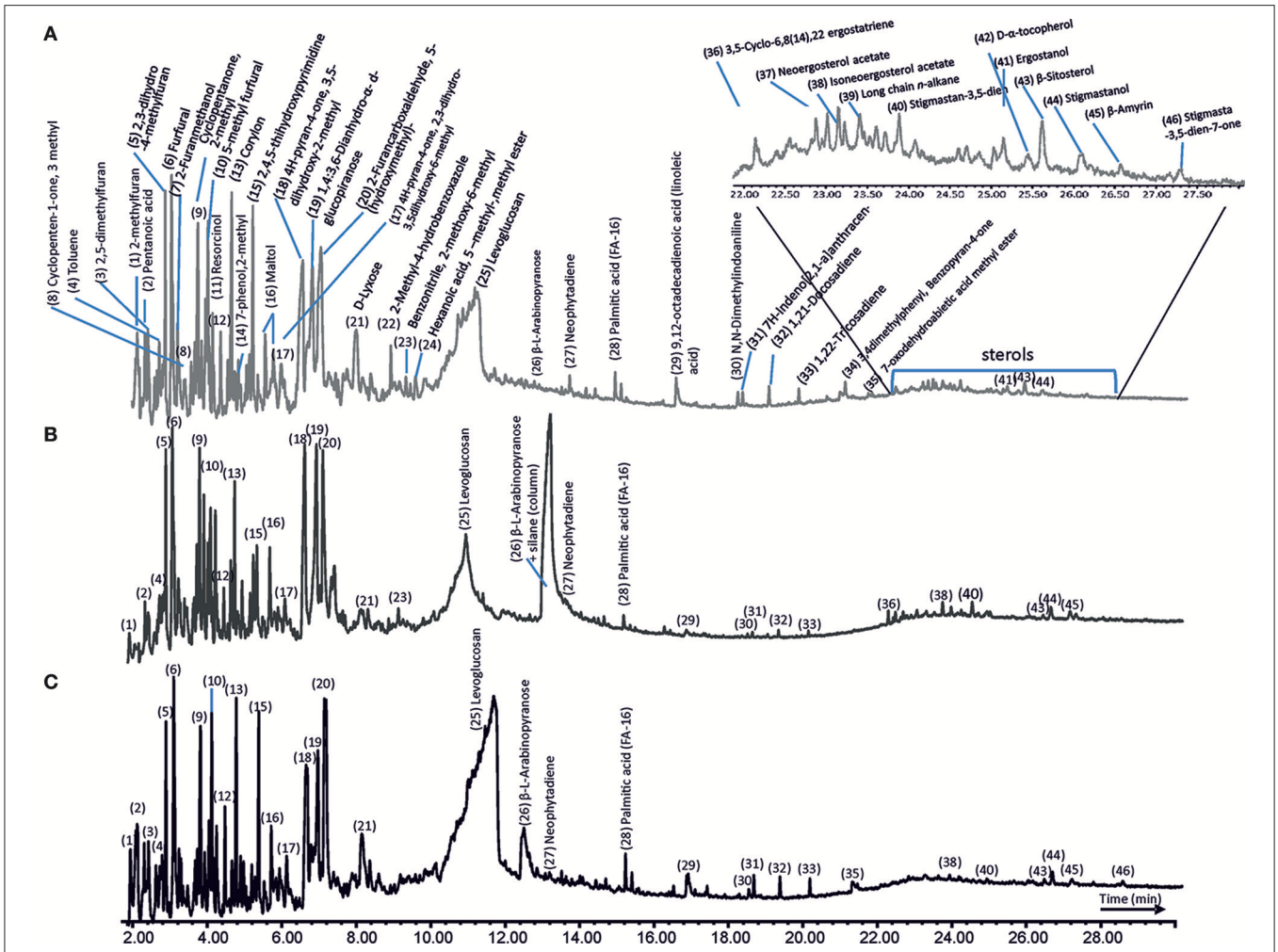

FIGURE 11 | Analytical pyrolysis (Py-GC/MS) at 500°C of the *C. gyrosa* lichen thalli before **(A)**, and after exposure to niche-led conditions **(B)**, and to full UV radiation **(C)**.

exposure to the Mars-like environment, their photosynthetic activity efficiently recovered after re-activation of the lichen thalli. However, microscopic examination revealed a slight delay in the recovery of *C. gyrosa* after exposure to full UV conditions in comparison to the lichen thalli exposed to niche-led conditions. Good anatomical preservation of the algal clusters and fungal hyphae from the medulla indicated that the niche-led exposure conditions did not disturb either lichen thalli structure or morphology. No DNA damage was observed in the fungal component, while the amplicon for the algal component disappeared after exposure to simulated Mars conditions, suggesting that the photobiont is the most affected component after exposure to simulated conditions. Analytical pyrolysis revealed a similar composition for the UV- and non-irradiated lichens, which were dominated by the typical cell wall constituents. Nevertheless, the changes in the relative abundance of specific sterols in the lichens exposed to full UV conditions indicate that the UV irradiation induced injury to the lichen membranes.

We showed by experimental means that the surface of Mars would be harmful for the tested lichen *C. gyrosa*; therefore, the surface of Mars would not be a habitable place for *C. gyrosa*. In contrast, niches on Mars close to the surface, in which the organism is protected against UV-radiation, might be retreat areas for this lichen. It means that we have to clearly differentiate between the Martian surface (not habitable), the subsurface (potentially habitable), and niches near the surface (partially habitable in fissures, cracks, and micro-caves in rocks, de Vera et al., 2014).

AUTHOR CONTRIBUTIONS

RT: coordinated the complete study, and determined the chlorophyll a-fluorescence. AM: provided several analysis-methods: CLMS (Confocal-Laser-Scanning Microscopy), Epifluorescence and FESEM/Field Emission Scanning Microscopy), and TEM (Transmission Electron Microscopy). JR: provided the analytical pyrolysis (Py-GC/MS) methodology.

CP: provided the DNA integrity evaluation (RAPD and PCR methods). SO: coordinated and supervised the DNA integrity evaluation (RAPD and PCR methods). LG: selected the lichen sample (field campaigns) and supervised the writing of the manuscript. BC: provided the CLMS analysis. AL: provided the technical control of the Mars Simulation Chamber at DLR-Berlin. DW: prepared the biological samples for the simulation test and evaluated the results. JV: coordinated and supervised the Mars simulation test.

ACKNOWLEDGMENTS

The authors acknowledge the Spanish Ministry of Economy, Industry and Competitiveness (MINECO, project SUBLIMAS ESP2015-69810-R). AM and JR thank the MINECO for the *Juan de la Cierva–Incorporación* (IJCI-2014-20443) and *Ramón y Cajal* (RYC-2014-16338) post-doctoral contracts, respectively. The authors are grateful to Dr. Ronald Charles Wolf for English improvement. CP and SO thank ASI grant BIOMEX-MCF n. 2013-063-R.0.

REFERENCES

Atienzar, F. A., and Jha, A. N. (2006). The random amplified polymorphic DNA (RAPD) assay and related techniques applied to genotoxicity and carcinogenesis studies: a critical review. *Mutat. Res.* 613, 76–102. doi: 10.1016/j.mrrev.2006.06.001

Atienzar, F. A., Venier, P., Jha, A. N., and Depledge, M. H. (2002). Evaluation of the random amplified polymorphic DNA (RAPD) assay for the detection of DNA damage and mutations. *Mut. Res.* 521, 151–163. doi: 10.1016/S1383-5718(02)00216-4

Aubert, S., Juge, C., Boisson, A.-M., Gout, E., and Bligny, R. (2007). Metabolic processes sustaining the reviviscence of lichen *Xanthoria elegans* in high mountain environments. *Planta* 226, 1287–1297. doi: 10.1007/s00425-007-0563-6

Böttger, U., Meeßen, J., Martinez-Frias, J., Hübers, H.-W., Rull, F., Sánchez, F. J., et al. (2014). Raman spectroscopic analysis of the calcium oxalate producing extremotolerant lichen *Circinaria gyrosa*. *Int. J. Astrobiol.* 13, 19–27. doi: 10.1017/S1473550413000293

Braovaca, S., Tamburinib, D., JacquelineŁucejko, J., McQueena, C., Kutzkea, H., and Colombi, M. P. (2016). Chemical analyses of extremely degraded wood using analytical pyrolysis and inductively coupled plasma atomic emission spectroscopy. *Microchem. J.* 124, 368–379. doi: 10.1016/j.microc.2015.09.016

Crespo, A., and Barreno, E. (1978). Sobre las comunidades terrícolas de líquenes vagantes Sphaerothallio, *Xanthoparmelion vagantis* al. Nova. *Acta Bot. Malac.* 4, 55–62.

De la Rosa, J. M., Gonzalez-Perez, J. A., Hatcher, P. G., Knicker, H., and Gonzalez-Vila, F. J. (2008). Determination of refractory organic matter in marine sediments by chemical oxidation, analytical pyrolysis and solid-state ^{13}C nuclear magnetic resonance spectroscopy. *Eur. J. Soil Sci. Soc.* 59, 430–438. doi: 10.1111/j.1365-2389.2007.00979.x

De la Rosa, J. M., González-Vila,; F. J., López-Capel, E., Manning, D. A. C., Knicker, H., and González-Pérez, J. A. (2009). Structural properties of non-combustion-derived refractory organic matter which interfere with BC quantification. *J. Anal. Appl. Pyrol.* 85, 399–407. doi: 10.1016/j.jaap.2008.11.019

De la Torre, R., Miller, A. Z., Cubero, B., Martín-Cerezo, M. L., Raguse, M., and Meeßen, J. (2017). The effect of high-dose ionizing radiation on the astrobiological model lichen *Circinaria gyrosa*. *Astrobiology* 17, 145–153. doi: 10.1089/ast.2015.1454

De la Torre, R., Sancho, L. G., Horneck, G., de los Ríos, A., Wierzchos, J., Olsson-Francis, K., et al. (2010). Survival of lichens and bacteria exposed to outer space conditions – results of the Lithopanspermia experiments. *Icarus* 208, 735–748. doi: 10.1016/j.icarus.2010.03.010

De los Ríos, A., Ascaso, C., Wierzchos, J., and Sancho, L. G. (2009). "Space flight effects on lichen ultrastructure and physiology," in *Symbioses and Stress. Cellular Origin, Life in Extreme Habitats and Astrobiology,* Vol 17, eds J. Seckbach and M. Grube (Dordrecht: Springer). doi: 10.1007/978-90-481-9449-0_30

de Vera, J.-P., Schulze-Makuch, D., Khan, A., Lorek, A., Koncz, A., Möhlmann, D., et al. (2014). Adaptation of an Antarctic lichen to Martian niche conditions can occur within 34 days. *Planet. Space Sci.* 98, 182–190. doi: 10.1016/j.pss.2013.07.014

Dignac, M. F., Houot, S., and Derenne, S. (2006). How the polarity of the separation column may influence the characterization of compost organic matter by pyrolysis-GC/MS. *J. Anal. Appl. Pyrol.* 75, 128–139. doi: 10.1016/j.jaap.2005.05.001

Gausla, Y., and Ustvedt, E. M. (2003). Is parietin a UV-B or a blue-light screening pigment in the lichen *Xanthoria parietina*? *Photochem. Photobiol. Sci.* 2, 424–432. doi: 10.1039/b212532c

Giordani, P., Modenesi, P., and Tretiach, M. (2003). Determinant factors for the formation of the calcium oxalate minerals, weddellite and whewellite, on the surface of foliose lichens. *Lichenologist* 35, 255–270. doi:10.1016/S0024-2829(03)00028-8

Hamby, R. K., Sims, L., Issel, L., and Zimmer, E. (1988). Direct ribosomal RNA sequencing: optimization of extraction and sequencing methods for work with higher plants. *Plant Mol. Biol. Rep.* 6, 175–192. doi: 10.1007/BF02669591

Harri, A. M., Genzer, M., Kemppinen, O., Gomez-Elvira, J., Haberle, R., Polkko, J., et al. (2014). Mars science laboratory relative humidity observations: initial results. *J. Geo Phys. Res. Planets* 119, 2132–2147. doi: 10.1002/2013JE004514

Hassler, D. M., Zeitlin, C., Wimmer-Schweingruber, R. F., Ehresmann, B., Rafkin, S., Eigenbrode, J. L., et al. (2013). Mars' surface radiation environment measured with the Mars Science Laboratory's curiosity rover. *Science* 343:1244797. doi: 10.1126/science.1244797

Hense, B. A., Gais, P., Jütting, U., Scherb, H., and Rodenacker, K. (2008). Use of fluorescence information for automated phytoplankton investigation by image analysis. *J. Plankton Res.* 30, 587–606. doi: 10.1093/plankt/fbn024

Ho, C. L., Phang, S. M., and Pang, T. (1995). Molecular characterisation of *Sargassum polycystum* and *S.* siliquosum (Phaeophyta) by polymerase chain reaction (PCR) using random amplified polymorphic DNA (RAPD) primers. *J. Appl. Phycol.* 7, 33–41. doi: 10.1007/BF00003547

Holzinger, A., and Karsten, U. (2013). Desiccation stress and tolerance in green algae: consequences for ultrastructure, physiological, and molecular mechanisms. *Front. Plant Sci.* 4:327. doi: 10.3389/fpls.2013.00327

Horneck, G. (1993). Responses of *Bacillus subtilis* spores to space environment: results from experiments in space. *Orig. Life Evol. Biosph.* 23, 37–52. doi: 10.1007/BF01581989

Horneck, G., Bücker, H., and Reitz,. G. (1994). Long-term survival of bacterial spores in space. *Adv. Space Res.* 14, 41–45. doi: 10.1016/0273-1177(94)90448-0

Horneck, G., Bücker, H., Reitz, G., Requardt, H., Dose, K., Martens, K. D., et al. (1984). Life sciences: microorganisms in the space environment. *Science* 225, 226–228. doi: 10.1126/science.225.4658.226

Horneck, G., Rettberg, P., Reitz, G., Wehner, J., Eschweiler, U., Strauch, K., et al. (2001). Protection of bacterial spores in space, a contribution to the discussion on Panspermia. *Orig. Life Evol. Biosph.* 31, 527–547. doi: 10.1023/A:1012746130771

Jönsson, K. I., Rabbow, E., Schill, R. O., Harms-Ringdahl, M., and Rettberg, P. (2008). Tardigrades survive exposure to space in low Earth orbit. *Curr. Biol.* 18, 729–731. doi: 10.1016/j.cub.2008.06.048

Kanavarioti, A., and Mancinelli, R. L. (1990). Could organic matter have been preserved on Mars for 3.5 billion years? *Icarus* 84:196–202. doi: 10.1016/0019-1035(90)90165-6

Kong, L., Dong, J., and Hart, G. E. (2000). Characteristics, linkage-map positions, and allelic differentiation of *Sorghum bicolor* (L.) Moench DNA simple-sequence repeats (SSRs). *Theor. Appl. Genet.* 101, 438–448. doi: 10.1007/s001220051501

Kumar, A., Tyagi, M. B., and Jha, P. N. (2004). Evidences showing ultraviolet-B radiation induced damage of DNA in cyanobacteria and its detection by PCR assay. *Biochem. Biophys. Res. Commun.* 318, 1025–1030. doi: 10.1016/j.bbrc.2004.04.129

Lange, O. L., Schulze, E. D., and Koch, W. (1970). Experimentellökologische untersuchungen an flechten der Negev-Wüste.III: CO_2-gaswechsel und wasserhaushalt von krustenflechten am natürlichen standort während der sommerlichen trockenperiode. *Flora* 159, 525–533.

Lee, J. G., Lee, C. G., Kwag, J. J., Buglass, A. J., and Lee, G. H. (2005). Determination of optimum conditions for the analysis of volatile components in pine needles by double-shot pyrolysis-gas chromatography-mass spectrometry. *J. Chromatogr. A* 1089, 227–234. doi: 10.1016/j.chroma.2005.06.060

León-Camacho, M., Alvarez Serrano, M., and Graciani Constante, E. (2004). Formation of stigmasta-3,5-diene in olive oil during deodorization and/or physical refining using nitrogen as stripping gas. *Grasas Aceites* 55, 227–232.

Lindahl, T. (1993). Instability and decay of the primary structure of DNA. *Nature* 362, 709–715. doi: 10.1038/362709a0

Lorek, A., and Koncz, A. (2013). "Simulation and measurement of extraterrestrial conditions for experiments on habitability with respect to Mars," in *Habitability of Other Planets and Satellites,* eds J.-P. de Vera and J. Seckbach (Dordrecht: Springer Netherlands), 145–162.

Lyon, D. Y., Monier, J. M., Dupraz, S., Freissinet, C., Simonet, P., and Vogel, T. M. (2010). Integrity and biological activity of DNA after UV exposure. *Astrobiology* 10, 285–292. doi: 10.1089/ast.2009.0359

MacGillivray, T., and Helleur, R. (2001). Analysis of lichens under environmental stress using TMAH thermochemilysis-gas chromatography. *J. Anal. Appl. Pyrol.* 58–59, 465–480. doi: 10.1016/S0165-2370(00)00205-9

Meeßen, J., Backhaus, T., Brandt, A., Raguse, M., Böttger, U., de Vera, J. P., et al. (2017). The effect of high-dose ionizing radiation on the isolated photobiont of the astrobiological model lichen *Circinaria gyrosa*. *Astrobiology* 17, 154–162. doi: 10.1089/ast.2015.1453

Meeßen, J., Sánchez, F. J., Brandt, A., Balzer, E. M., de la Torre, R., Sancho, L. G., et al. (2013). Extremotolerance and resistance of lichens: comparative studies on five species used in astrobiological research. I. Morphological and anatomical characteristics. *Orig. Life Evol. Biosph.* 43, 283–303. doi: 10.1007/s11084-013-9337-2

Miller, A. Z., De la Rosa, J. M., Jiménez-Morillo, N. T., Pereira, M., González-Pérez, J. A., Calaforra, J. M., et al. (2016). Analytical pyrolysis and stable isotope analyses reveal past environmental changes in coralloid speleothems from Easter Island (Chile). *J. Chromatogr. A* 1461, 144–152. doi: 10.1016/j.chroma.2016.07.038

Munne-Bosch, S., and Alegre, L. (2002). The function of tocopherols and tocotrienols in plants. *Crit. Rev. Plant Sci.* 21, 31–57. doi: 10.1080/0735-260291044179

Nguyen, K. H., Chollet-Krugler, M., Gouault, N., and Tomasi, S. (2013). UV-protectant metabolites from lichens and their symbiotic partners. *Nat. Prod. Rep.* 30, 1490–1508. doi: 10.1039/c3np70064j

Onofri, S., de la Torre, R., de Vera, J. P., Ott, S., Zucconi, L., Selbmann, L., et al. (2012). Survival of rock-colonizing organisms after 1.5 years in outer space. *Astrobiology* 12, 508–516. doi: 10.1089/ast.2011.0736

Osticioli, I., Mascalchi, M., Pinna, D., and Siano, S. (2013). "Potential of chlorophyll fluorescence imaging for assessing bio-viability changes of biodeteriogen growths on stone monuments," in *Proceedings SPIE 8790, Optics for Arts, Architecture, and Archaeology IV* (Bellingham, WA), 879003. doi: 10.1117/12.2020563

Pacelli, C., Selbmann, L., Moeller, R., Zucconi, L., Fujimori, A., and Onofri, S. (2017a). Cryptoendolithic Antarctic black fungus *Cryomyces antarcticus* irradiated with accelerated helium ions: survival and metabolic activity, DNA and ultrastructural damage. *Front. Microbiol.* 8:2002. doi: 10.3389/fmicb.2017.02002

Pacelli, C., Selbmann, L., Zucconi, L., De Vera, J. P., Rabbow, E., Horneck, G., et al. (2017b). BIOMEX experiment: ultrastructural alterations, molecular damage and survival of the fungus *Cryomyces antarcticus* after the Experiment Verification Tests. *Origins Life Evol. B* 47, 187–202. doi: 10.1007/s11084-016-9485-2

Pacelli, C., Selbmann, L., Zucconi, L., Raguse, M., Moeller, R., Shuryak, I., et al. (2017c). Survival, DNA integrity, and ultrastructural damage in antarctic cryptoendolithic eukaryotic microorganisms exposed to ionizing radiation. *Astrobiology* 17, 126–135. doi: 10.1089/ast.2015.1456

Pereira de Oliveira, B., De la Rosa, J. M., Miller, A. Z., Saiz-Jimenez, C., Gómez-Bolea, A., Sequeira Braga, M. A., et al. (2011). An integrated approach to assess the origins of black films on a granite monument. *Environ. Earth Sci.* 63, 1677–1690. doi: 10.1007/s12665-010-0773-2

Rettberg, P., Eschweiler, U., Strauch, K., Reitz, G., Horneck, G., Wanke, H., et al. (2002). Survival of microorganisms in space protected by meteorite material: results of the experiment EXOBIOLOGIE of the PERSEUS mission. *Adv. Space Res.* 30, 1539–1545. doi: 10.1016/S0273-1177(02)00369-1

Richardson, D. H. S. (1992). *Pollution Monitoring with Lichens.* Slough: Richmond Publishing.

Rikkinen, J. (1995). "What's behind the pretty colours? A study on the photobiology of lichens," in *Bryobrothera,* Vol. 4, ed T. Koponen (Helsinki: The Finnish Bryological Society), 41–56. doi: 10.2307/3244316

Rudi, K., Hagen, I., Johnsrud, B. C., Skjefstad, G., and Tryland, I. (2010). Different length (DL) qPCR for quantification of cell killing by UV-induced DNA damage. *Int. J. Environ. Res. Public Health* 7, 3376–3381. doi: 10.3390/ijerph7093376

Russel, N. J. (1989). "Structural and functional role of lipids," in *Microbial Lipids*, eds C. Ratledge and S. G. Wilkinson (New York, NY: Academic Press), 279–349.

Saiz-Jimenez, C., Garcia-Rowe, J., Garcia del Cura, M. A., Roekens, E., and van Grieken, R. (1990). Endolithic cyanobacteria in Maastricht limestone. *Sci. Total Environ.* 94, 209–220. doi: 10.1016/0048-9697(90)90171-P

Saiz-Jimenez, C., Grimalt, J., Garcia-Rowe, J., and Ortega-Calvo, J. J. (1991). Analytical pyrolysis of lichen thalli. *Symbiosis* 11, 313–326.

Sánchez, F. J., Mateo-Martí, E., Raggio, J., Meeßen, J., Martínez-Frías, J., Sancho, L. G., et al. (2012). The resistance of the lichen *Circinaria gyrosa* (nom. *provis*.) towards simulated Mars conditions – a model test for the survival capacity of an eukaryotic extremophile. *Planet. Space Sci.* 72, 102–110. doi: 10.1016/j.pss.2012.08.005

Sancho, L. G., de la Torre, R., Horneck, G., Ascaso, C., de Los Rios, A., Pintado, A., et al. (2007). Lichens survive in space: results from the 2005 LICHENS experiment. *Astrobiology* 7, 443–454. doi: 10.1089/ast.2006.0046

Sancho, L. G., Schroeter, B., and del Prado, R. (2000). Ecophysiology and morphology of the globular erratic lichen *Aspicilia fruticulosa* (Eversm.) FLAG. From Central Spain. New aspects in cryptogamic research. *Bibl. Lichenol.* 75, 137–147.

Schellekens, J., Buurman, P., and Pontevedra-Pombal, X. (2009). Selecting parameters for the environmental interpretation of peat molecular chemistry - a pyrolysis-GC/MS study. *Org. Geochem.* 40, 678–691. doi: 10.1016/j.orggeochem.2009.03.006

Schneider, C. A., Rasband, W. S., and Eliceiri, K. W. (2012). NIH Image to ImageJ: 25 years of image analysis. *Nat. Methods* 9, 671–675. doi: 10.1038/nmeth.2089

Schreiber, U., Bilger, W., and Neubauer, C. (1994). "Chlorophyll fluorescence as a non-intrusive indicator for rapid assessment of *in vivo* photosynthesis," in *Ecophysiology of Photosynthesis, Ecological Studies,* Vol. 100, eds E.-D. Schulze and M. M. Caldwell (Berlin: Springer-Verlag), 49–70.

Schuerger, A. C., Mancinelli, R. L., Kern, R. G., Rothschild, L. J., and McKay, C. P. (2003). Survival of endospores of *Bacillus subtilis* on spacecraft surfaces under simulated martian environments: implications for the forward contamination of Mars. *Icarus* 165, 253–276. doi: 10.1016/S0019-1035(03)00200-8

Selbmann, L., Isola, D., Zucconi, L., and Onofri, S. (2011). Resistance to UV-B induced DNA damage in extreme-tolerant cryptoendolithic Antarctic fungi: detection by PCR assays. *Fungal Biol.* 115, 937–944. doi: 10.1016/j.funbio.2011.02.016

Sephton, M. A. (2010). Organic geochemistry and the exploration of Mars. *J. Cosmol.* 5, 1141–1149.

Sohrabi, M., Stenroos, S., Myllys, L., Søchting, U., Ahti, T., and Hyvönen, J. (2013). Phylogeny and taxonomy of the 'manna lichens'. *Mycol. Progress* 12, 231–269. doi: 10.1007/s11557-012-0830-1

Spribille, T., Tuovinen, V., Resl, P., Vanderpool, D., Wolinski, H., Aime, M. C., et al. (2016). Basidiomycete yeasts in the cortex of ascomycete macrolichens. *Science* 353, 488–492. doi: 10.1126/science.aaf8287

Stojanovic, I.Ž., Radulovic, N. S., Mitrovic, T. L., Stamenkovic, S. M., and Stojanovic, G. S. (2011). Volatile constituents of selected *Parmeliaceae lichens. J. Serb. Chem. Soc.* 76, 987–994. doi: 10.2298/JSC101004087S

Treshow, M., and Anderson, K. (1989). *Plant Stress from Air Pollution*. New York, NY: Wiley.

Trombert, A., Irazoqui, H., Martín, C., and Zalazar, F. (2007). Evaluation of UV-C induced changes in *Escherichia coli* DNA using repetitive extragenic palindromic–polymerase chain reaction (REP–PCR). *J. Photochem. Photobiol.* 89, 44–49. doi: 10.1016/j.jphotobiol.2007.08.003

Vilgalys, R., and Hester, M. (1990). Rapid genetic identification and mapping of enzymatically amplified ribosomal DNA from several *Cryptococcus* species. *J. bacterial.* 172, 4238–4246. doi: 10.1128/jb.172.8.4238-4246.1990

White, T. J., Bruns, T., Lee, S. J. W. T., and Taylor, J. L. (1990). "Amplification and direct sequencing of fungal ribosomal RNA genes for phylogenetics," in *PCR Protocols: A Guide to Methods and Applications*, eds M. A. Innis, D. H. Gelfand, J. J. Sninsky, and T. J. White (San Diego, CA: Academic Press), 315–322.

Conflict of Interest Statement: The authors declare that the research was conducted in the absence of any commercial or financial relationships that could be construed as a potential conflict of interest.

frontiers in Microbiology

ORIGINAL RESEARCH
published: 12 September 2017
doi: 10.3389/fmicb.2017.01709

Silicates Eroded under Simulated Martian Conditions Effectively Kill Bacteria—A Challenge for Life on Mars

Ebbe N. Bak[1], Michael G. Larsen[1], Ralf Moeller[2], Silas B. Nissen[1], Lasse R. Jensen[1], Per Nørnberg[1], Svend J. K. Jensen[3] and Kai Finster[1,4]*

[1] Department of Bioscience, Aarhus University, Aarhus, Denmark, [2] Space Microbiology Research Group, Institute of Aerospace Medicine, German Aerospace Center (DLR), Cologne, Germany, [3] Department of Chemistry, Aarhus University, Aarhus, Denmark, [4] Stellar Astrophysics Center, Department of Physics and Astronomy, Aarhus University, Aarhus, Denmark

The habitability of Mars is determined by the physical and chemical environment. The effect of low water availability, temperature, low atmospheric pressure and strong UV radiation has been extensively studied in relation to the survival of microorganisms. In addition to these stress factors, it was recently found that silicates exposed to simulated saltation in a Mars-like atmosphere can lead to a production of reactive oxygen species. Here, we have investigated the stress effect induced by quartz and basalt abraded in Mars-like atmospheres by examining the survivability of the three microbial model organisms *Pseudomonas putida*, *Bacillus subtilis,* and *Deinococcus radiodurans* upon exposure to the abraded silicates. We found that abraded basalt that had not been in contact with oxygen after abrasion killed more than 99% of the vegetative cells while endospores were largely unaffected. Exposure of the basalt samples to oxygen after abrasion led to a significant reduction in the stress effect. Abraded quartz was generally less toxic than abraded basalt. We suggest that the stress effect of abraded silicates may be caused by a production of reactive oxygen species and enhanced by transition metal ions in the basalt leading to hydroxyl radicals through Fenton-like reactions. The low survivability of the usually highly resistant *D. radiodurans* indicates that the effect of abraded silicates, as is ubiquitous on the Martian surface, would limit the habitability of Mars as well as the risk of forward contamination. Furthermore, the reactivity of abraded silicates could have implications for future manned missions, although the lower effect of abraded silicates exposed to oxygen suggests that the effects would be reduced in human habitats.

Keywords: habitability, erosion, reactive oxygen species, forward contamination, stress factors, saltation, toxicity, microorganisms

OPEN ACCESS

Edited by:
Daniela Billi, Università degli Studi di Roma Tor Vergata, Italy

Reviewed by:
Aude Picard, Harvard University, United States
Timothy Ferdelman, Max Planck Institute for Marine Microbiology, Germany

****Correspondence:***
Ebbe N. Bak
ebbe.bak@bios.au.dk

Specialty section:
This article was submitted to Extreme Microbiology, a section of the journal Frontiers in Microbiology

Received: *30 June 2017*
Accepted: *23 August 2017*
Published: *12 September 2017*

Citation:
Bak EN, Larsen MG, Moeller R, Nissen SB, Jensen LR, Nørnberg P, Jensen SJK and Finster K (2017) Silicates Eroded under Simulated Martian Conditions Effectively Kill Bacteria—A Challenge for Life on Mars. Front. Microbiol. 8:1709. doi: 10.3389/fmicb.2017.01709

INTRODUCTION

An in-depth understanding of the interaction between the Martian surface environment and living cells is essential for assessment of the habitability of Mars, the risk of forward contamination and the hazards associated with manned missions. The Martian surface temperatures vary from −150° to 20°C, and the surface pressure is usually 4–10 mbar (Millour et al., 2015). Consequently, the

Martian surface is extremely arid and even if liquid water is present, the water activity is likely too low to support life (Martin-Torres et al., 2015; Ojha et al., 2015). While such an arid, cold, low-pressure environment often is not detrimental for desiccation tolerant, dormant cells and spores, the radiation on the Martian surface can be highly damaging (Hansen et al., 2009; Johnson et al., 2011). The solar irradiation flux on Mars is about 40% of the irradiation on Earth, but, the thin atmosphere and the sparse ozone layer (Lefevre et al., 2008) result in a substantially higher UVB and UVC radiation than on Earth (Cockell et al., 2000). Schuerger et al. (2003) demonstrated that 15 min of exposure to Mars-like UV radiation sterilized monolayers of *Bacillus subtilis* spores. The effect of UV radiation is, however, reduced dramatically when cells and spores are shielded by a thin layer of dust or a few layers of dead cells (Mancinelli and Klovstad, 2000; Diaz and Schulze-Makuch, 2006; de La Vega et al., 2007; Paulino-Lima et al., 2010). The flux of ionizing radiation from the sun and galactic cosmic rays are three orders of magnitude higher on the Martian surface as compared to the surface of Earth due to the thin Martian atmosphere and the absence of a global magnetic field (Hassler et al., 2014). Nevertheless, ionizing radiation from the sun only poses a minor challenge for *B. subtilis* and *D. radiodurans*, and a cover that would protect against UV radiation would also shield from the charged particles in the solar wind (Tuleta et al., 2005; Paulino-Lima et al., 2011). Protection against galactic cosmic rays, mainly high-energy particles, requires much thicker shielding. However, the flux to the Martian surface would only cause a half-life of *B. subtilis* spores within the order of thousands of years (Moeller et al., 2010; Hassler et al., 2014). In summary, the Martian surface does not generally allow life to proliferate, but may not pose an immediate threat to dormant cells.

The Martian soil is dominated by silicate minerals (Bish et al., 2013) primarily produced by physical abrasion of olivine basalts (Morris et al., 2004; Gunnlaugsson et al., 2009). The soil and dust particles are produced by meteor impacts and by wind-driven saltation through repetitive low-energy collisions (Kok et al., 2012). A recent study showed that silicates exposed to simulated wind-driven saltation in a Mars-like atmosphere could lead to a production of reactive oxygen species (ROS) including hydrogen peroxide (H_2O_2) and hydroxyl radicals (·OH) (Bak et al., 2017). A production of ROS from abraded silicates may explain the oxidative capabilities of the Martian soil as observed by the Viking Biological Experiments (Klein, 1978) and may cause oxidative stress for living cells. Based on these observations, we hypothesized that wind abraded silicates on Mars may pose an additional stress factor for living cells.

To test our hypothesis, we conducted a series of experiments in which cell suspensions of *Pseudomonas putida*, *B. subtilis* and *D. radiodurans* were exposed to quartz and basalt samples abraded by simulated wind-driven saltation in Mars-like atmospheres. The exposure experiments were conducted without exposing the abraded material to oxygen to simulate the *in situ* conditions for indigenous organisms and a scenario of forward contamination. Furthermore, we investigated the effect of secondary exposure to air to simulate the environment inside a human habitat. *Pseudomonas putida* is a common soil bacterium, which can withstand some level of oxidative stress (Kim and Park, 2014). The endospores of *B. subtilis* and cells of *D. radiodurans* have been reported to be highly resistant against a range of stress factors including desiccation, chemical oxidative stress (Melly et al., 2002; Slade and Radman, 2011) and ionizing radiation (Anderson et al., 1956; Moeller et al., 2008). Furthermore, they have been used to study the effects of exposure to a Mars-like environment including the impact of UV and ionizing radiation (Diaz and Schulze-Makuch, 2006; de La Vega et al., 2007; Moeller et al., 2010; Kerney and Schuerger, 2011). The resistance of *B. subtilis* to abraded silicates was further investigated by testing a range of mutant strains lacking specific spore components, which previously have been found to be related to resistance against oxidizing agents (Setlow, 2014). *Bacillus sp.* spores are of particular interest and concern, as they are common contaminants in cleanrooms used for assembly of spacecraft (Puleo et al., 1977; La Duc et al., 2009; Smith et al., 2017) and thus likely agents of forward contamination.

MATERIALS AND METHODS

Simulated Saltation of Silicates

Quartz sand samples were prepared by sieving commercially available quartz (Merck, Cat. No. 1.07536) to obtain the 125–1,000 μm fraction. The quartz sand was washed and dried to remove small particles and finally divided into 10 g aliquots using a Fritsch Rotary cone samples divider. The same procedure was used to produce 10 g basalt aliquots based on olivine basalt that was collected in Gufunes on Iceland (64°08′22.18″N, 21°47′21.27″W) and crushed. The mineral composition of the same batch of crushed basalt was reported in Bak et al. (2017). The samples were transferred to about 20 cm long and 3 cm wide quartz ampoules with rounded ends (**Figure 1A**). One end of the ampoules was extended by a narrow quartz inlet tube that allowed connection to a vacuum system. The ampoules were evacuated to <0.12 mbar and filled with 8 ± 0.2 mbar of a Mars-like atmosphere composed of 95% CO_2 (>99.9% purity, AGA, Denmark) and 5% of a custom made gas mixture (>99% purity, Air Liquid, Denmark) to give a final composition of 95% CO_2, 3% N_2, 1.75% Ar, 0.15% O_2 and 0.1% CO, which is similar to the composition of the Martian atmosphere (Mahaffy et al., 2013). The pressure was monitored with a Pfeiffer TPR 265 Pirani gauge for $p < 1$ mbar and a Pfeiffer APR 250 Pirani gauge for $p > 1$ mbar. The ampoules were sealed by melting off the narrow inlet tubes. Wind-driven saltation was simulated by mounting the ampoules in a turning wheel running at 30 rpm (**Figure 1B**). This set-up caused the silicate samples to fall from one end of the ampoules to the other once per second, which mimics the repeated low energy impacts that are characteristic for saltation (Merrison, 2012). The samples were tumbled for 63 days, which led to a considerable abrasion of the material resulting in an increase of the specific surface area of 3.44 and 0.76 $m^2\ g^{-1}$ for the quartz and the basalt samples, respectively (Bak et al., 2017). Some of the abraded samples were suspended in 10 ml of water followed by overnight drying at 60°C, which has been shown to neutralize the potential for production of ROS (Bak et al., 2017).

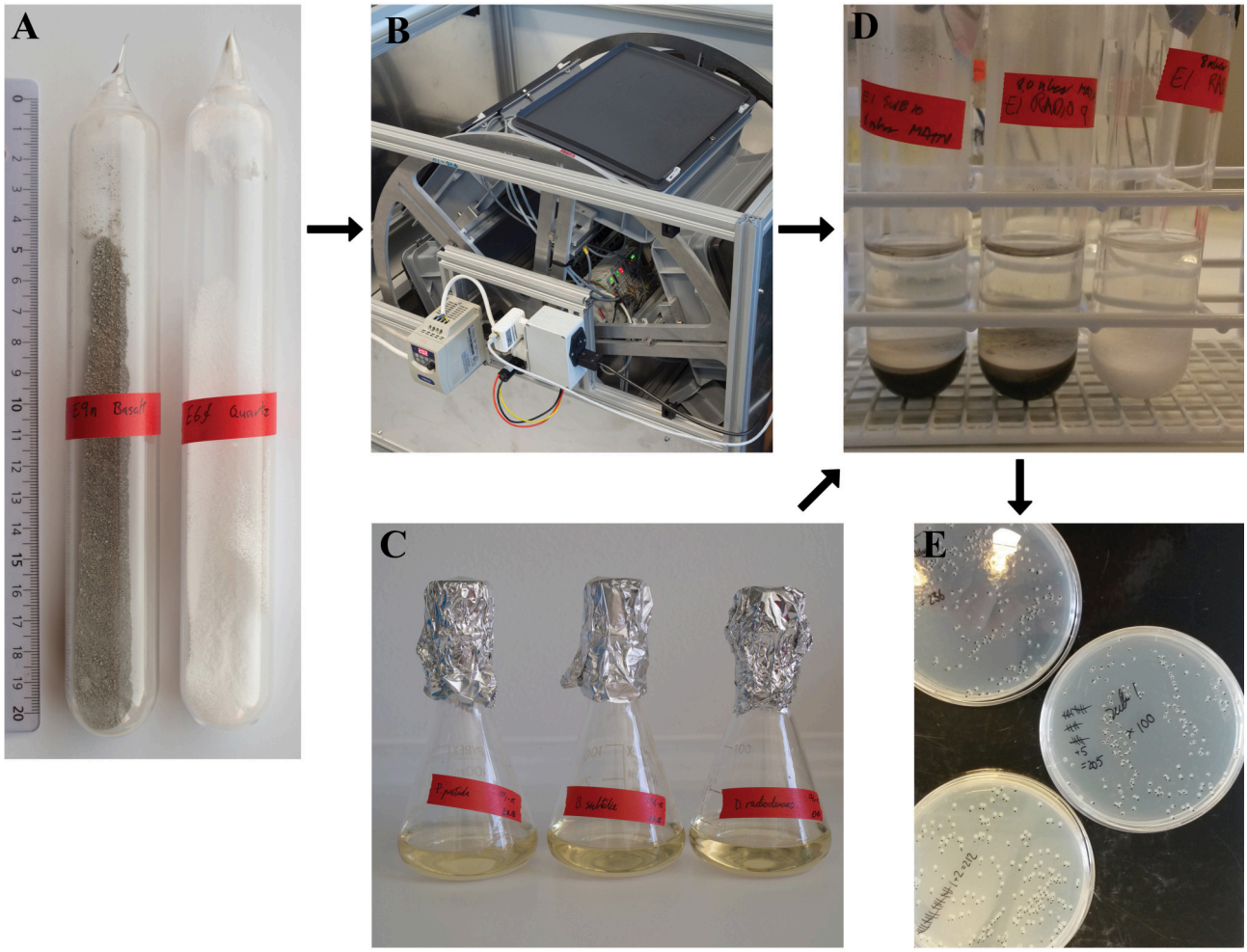

FIGURE 1 | (A) Sealed quartz ampoules with basalt (left) and quartz sand (right). **(B)** Turning wheel running at 30 rpm. The ampoules were fixed inside the gray boxes. **(C)** Media inoculated with cell cultures. **(D)** Abraded silicate samples mixed with washed cell cultures. **(E)** Agar plates with colonies of the tested bacteria.

These samples were used as negative controls and are hereafter referred to as inactivated samples.

Preparation of Cell Suspensions

The bacterial strains used in this study are listed in **Table 1**. *Pseudomonas putida* mt-2 KT2440, *Bacillus subtilis* 168 and *Deinococcus radiodurans* R1 were obtained from the German Collection of Microorganisms and Cell Cultures GmbH (DSMZ, Braunschweig, Germany) as DSM6125, DSM402 and DSM20539, respectively. Stock cultures of all strains were stored as aliquots in 15% glycerol at -80°C. The following growth media and buffer solutions were used: Lysogeny Broth (LB) medium [10 g NaCl, 10 g tryptone (Fluka) and 5 g yeast extract (Merck) per liter, pH adjusted to 7]; Nutrient Broth (NB) medium (Scharlau) and phosphate buffered saline (PBS) (8 g NaCl, 0.2 g KCl, 1.44 g Na_2HPO_4 and 0.24 g KH_2PO_4 per liter, pH adjusted to 7.3). For preparation of agar plates the liquids were supplemented with 1.5% w/w of bacteriological agar. All chemicals were of analytical grade and acquired from commercial suppliers. MilliQ water was used for all solutions. *P. putida* cultures were grown in 100 ml Erlenmeyer flasks containing 30 ml of medium composed of 20% LB-medium and 80% PBS. *Bacillus subtilis* and *D. radiodurans* were grown under the same condition, but in a medium composed of 20% NB-medium and 80% PBS (**Figure 1C**). Pre-cultures were prepared from frozen stocks and incubated at room temperature (21–23°C) on a shaker at 120 rpm. The optical density (OD) was measured after ~24 h at 600 nm and the equivalent of 1 ml of $OD_{600} = 0.1$ was transferred to fresh medium and incubated under identical conditions. The survival experiments were carried out with cultures that were harvested in the late exponential growth phase (after 10–12 h for *P. putida* and *B. subtilis* and 17–19 h for *D. radiodurans*) and in the stationary phase (after 118–120 h for all species), see Figure S1. The purity of the cultures was checked by microscopy.

Prior to the survival tests, the cultures were centrifuged at 4,696 × g for 5 min. in 50 ml sterile Falcon tubes. The supernatant was discarded and the pellet was resuspended in 30 ml PBS. This washing procedure was done twice.

TABLE 1 | Bacterial strains used in this study.

Strain	Genotype and/ or phenotype[a]	Source (References)
***Pseudomonas putida* STRAIN**		
DSM6125	Wild type (mt-2 KT2440)	DSMZ[b]
***Deinococcus radiodurans* STRAIN**		
DSM20539 (type strain)	Wild type (R1)	DSMZ
***Bacillus subtilis* STRAINS**		
DSM402	Wild type (168)	DSMZ
PS832	Wild type parent of PS356	P. Setlow (Slieman and Nicholson, 2001)
PY79 (PE594)	Wild type parent of PE277, PE618, PE620, and PE1720, prototroph	P. Eichenberger (Raguse et al., 2016)
PE277	*safA::tet*, Tet^R	P. Eichenberger (Raguse et al., 2016)
PE618	*cotE::cat*, Cm^R	P. Eichenberger (Raguse et al., 2016)
PE620	*cotX cotYZ::neo*, Neo^R	P. Eichenberger (Raguse et al., 2016)
PE1720	*safA::tet*, Tet^R *cotE::cat*, Cm^R	P. Eichenberger (Raguse et al., 2016)
PS356	*sspA sspB*	P. Setlow (Mason and Setlow, 1986)

The corresponding spore deficiency for the B. subtilis mutants can be found in ***Table 2****.*
[a]Cm^R: chloramphenicol (5 μg/ml), Neo^R: neomycin (10 μg/ml), Tet^R: tetracycline (10 μg/ml).
[b]German Collection of Microorganisms and Cell Cultures GmbH (Braunschweig, Germany).

All *Bacillus subtilis* strains used for the spore resistance experiments were congenic to their respective wild-type strain. Spores were obtained by cultivation under vigorous aeration in double-strength liquid Schaeffer sporulation medium (Schaeffer et al., 1965) under identical conditions for each strain, purified and stored as described by Nicholson and Setlow (1990). When appropriate, chloramphenicol (5 μg/ml), neomycin (10 μg/ml), or tetracycline (10 μg/ml) was added to the medium (**Table 1**). Spore preparations consisted of single spores with no detectable clumps, and were free (>99%) of growing cells, germinated spores and cell debris, as seen in the phase-contrast microscope (Nagler et al., 2014).

Exposure of Bacteria to Abraded Silicates

The cell and spore suspensions were adjusted to $\sim 10^6$ colony forming units (CFU)/ml in PBS. For the experiments conducted in air to simulate the effect of abraded silicates inside a human habitat, the ampoules were opened by scoring and breaking of the narrow neck and the abraded silicate samples left exposed to ambient air. After 5 min exposure to ambient air, the silicate samples were mixed with the cell suspensions at a mass ratio of 1:2 (**Figure 1D**). The resulting slurries were vortexed and placed on a shaker at 120 rpm. Control samples were prepared in the same manner by mixing the inactivated silicate samples with the cell suspensions at a 1:2 mass ratio followed by vortexing and shaking. Experiments that were conducted under anoxic conditions to simulate the *in situ* conditions on the Martian surface were executed in the same way as the samples exposed to air except that the cell suspension were flushed with N_2 (>99.9% purity, AGA, Denmark) prior to use to remove dissolved oxygen and that the ampoules and silicate samples were handled in a N_2–flushed glove box. A minimum of three samples tumbled in separate ampoules were prepared for each treatment, which forms the basis for the calculated standard error of mean (SEM). All samples were exposed to air when the first subsamples were taken for plating after 15 min.

Survival Assay

The initial CFU count for each cell suspension in PBS was determined by plating in triplicates. The number of CFU was determined after 0.25, 1, 2.5, 5, and 24 h for the cell suspensions with the abraded silicates, the corresponding oxic and anoxic PBS controls as well as for the control samples with inactivated silicates. To determine the surviving fraction of cells after a given exposure time, the samples were vortexed and serial dilutions of the subsamples were plated. The survival of *D. radiodurans* and *B. subtilis* 168 was evaluated by plating on NB-plates while LB-plates were used to evaluate the survival of *P. putida* and the other *B. subtilis* strains. The plates were incubated at 30°C, and the number of colonies was determined after at least 1 day of incubation for *P. putida* and *B. subtilis* and after 2 days for *D. radiodurans* (**Figure 1E**). The number of colonies did not change considerably after extended incubation time. The surviving fraction was calculated as the mean number of CFU relative to the starting concentration. 100 μl of the cell suspension was streaked onto each plate giving a level of detection (LOD) of 10 CFU ml^{-1} for undiluted samples. Samples with a surviving fraction below the LOD was plotted as having a CFU count equal to the LOD. For statistical comparison, we performed unpaired *t*-tests on the log-transformed CFU counts assuming unequal variances. We had a minimum of three biological replicates for each treatment and used a significance threshold of $p < 0.05$.

pH Measurements

Inactivated quartz and basalt samples as well as abraded samples that had not been exposed to water were mixed with PBS at a 1:2 mass ratio in triplicates. The pH was measured using a glass pH electrode (Mettler Toledo Inlab® Expert Pro-ISM) with a Mettler Toledo Seven Compact pH meter after 24 h.

RESULTS

The number of CFU of *P. putida* harvested during exponential growth increased in the PBS controls as well as in the controls with inactivated silicates (**Figure 2A**). The abraded silicates caused a significant decrease in the number of CFU as compared to the inactivated controls with an about 99% decrease with quartz and to a concentration below the LOD with basalt ($p < 0.001$, $n \geq 3$). Stationary phase cultures of *P. putida* cells were not affected by abraded quartz while abraded basalt killed approximately 99% of the cells within 24 h (**Figure 2B**), and thus caused a significant decrease in the viability as compared to the inactivated basalt ($p = 0.008$, $n \geq 3$).

Microscopic examination showed that the *B. subtilis* cultures harvested in the exponential growth phase were dominated by

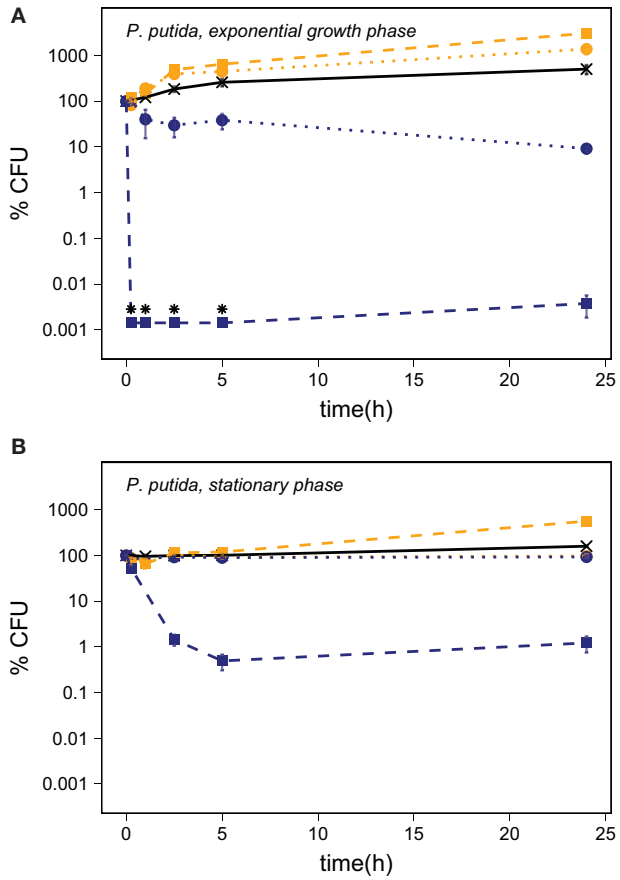

FIGURE 2 | The percentage of CFU of *P. putida* harvested in the exponential growth phase **(A)** and in the stationary phase **(B)** in a PBS control (—X—) and after addition of abraded quartz (·· ●· ·) and basalt (– –■– –) relative to the starting concentration of ~10^6 CFU/ml. The survival of *P. putida* is shown for experiments with inactivated silicates (orange) and abraded silicates kept anoxic (blue). The error bars show the SEM, and the asterisks indicate that the number of CFU was below the LOD.

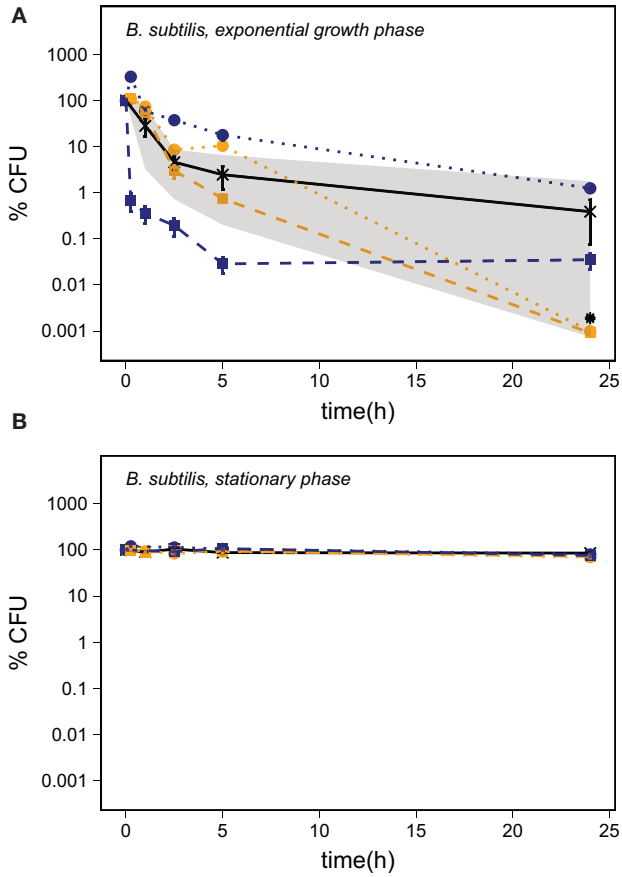

FIGURE 3 | The percentage of CFU of *B. subtilis* harvested in the exponential growth phase **(A)** and in the stationary phase **(B)** in a PBS control (—X—) and after addition of abraded quartz (·· ●· ·) and basalt (– –■– –) relative to the starting concentration of ~10^6 CFU/ml. The minimum and maximum number of CFU in the PBS control replicates are marked by the gray area. The survival of *B. subtilis* is shown for experiments with inactivated silicates (orange) and abraded silicates kept anoxic (blue). The error bars show the SEM, and the asterisks indicate that the number of CFU was below the LOD.

vegetative cells with no endospores observed. *B. subtilis* harvested in the stationary phase was a mixture of free endospores, endospores encapsulated by mother cells and vegetative cells without endospores. A *Bacillus subtilis* culture harvested in the stationary phase and heated to 80°C for 10 min showed a decrease to 64 ± 6% of the CFU counts before heating (average ± SEM, $n = 3$), which is in good agreement with the observed proportion of endospores. Cells of *B. subtilis* harvested in the exponential growth phase showed a substantial decrease in CFU even in the PBS control (**Figure 3A**). There was a faster decrease in the number of CFU in samples supplemented with abraded basalt, but the response did not differ significantly from the PBS control after 24 h of exposure ($p = 0.70$, $n \geq 3$). The final concentration of CFU in experiments conducted with stationary phase cultures was 65-85% of the starting concentration for all treatments including the PBS control (**Figure 3B**).

Most of the *B. subtilis* wild-type and mutant strains showed a change in the number of CFU of less than 50% of the starting concentration following all treatments (**Table 2**). The only exception was PS356, which showed a decrease in the number of CFU for all treatments. This indicates that while small acid-soluble spore proteins (SASP) do not seem to be important for the resistance toward abraded basalt, they are generally important for spore survival. None of the strains had a significantly lower number of CFU after exposure to basalt as compared to both the PBS and the inactivated basalt controls ($p \geq 0.06$, $n = 3$, for all strains).

The number of *D. radiodurans* CFU grown from exponential growth phase cells did not change significantly in the PBS and the quartz samples within 24 h of exposure (**Figure 4A**) ($p \geq 0.14$, $n \geq 4$). Samples exposed to abraded basalt showed the same trend as *P. putida* with an increase in the CFU number in inactivated samples and a decrease to below the LOD in activated samples ($p < 0.001$, $n \geq 3$). Inactivated basalt did not have a considerable effect on the number of CFU of stationary phase cells while activated basalt led to a decrease in CFU number to below the

TABLE 2 | The percentage of CFU of *B. subtilis* spores relative to the starting concentration following exposure to PBS, inactivated basalt and basalt for 24 h.

Strain	Gene deficiency	Spore deficiency	% CFU after 24 h		
			PBS	Inactivated basalt	Basalt
PE594 (wt)	none	none	82 ± 7	76 ± 3	73 ± 5
PE620	*cotX*, *cotYZ*	Crust	113 ± 8	64 ± 4	64 ± 2
PE618	*cotE*	Outer coat	75 ± 7	92 ± 5	97 ± 5
PE277	*safA*	Inner coat	55 ± 3	75 ± 2	59 ± 7
PE1720	*cotE*, *safA*	Inner and outer spore coat	82 ± 2	113 ± 4	63 ± 5
PS832 (wt)	none	none	111 ± 5	73 ± 2	87 ± 17
PS356	*sspA sspB*	Major α- and β-type SASP	36 ± 11	25 ± 4	40 ± 2

The basalt was kept anoxic. The results are the average of three replicates ± SEM. PE594 is the wild-type of the other PE strains while PS832 is the wild-type of the PS356 strain.

LOD, although slower than for cells in the exponential growth phase (**Figure 4B**).

Silicate samples exposed to oxygen following the abrasion showed a lower effect on the viability of *P. putida* and *D. radiodurans* as compared to the effects of samples kept anoxic, with the exception of *D. radiodurans* harvested in the exponential growth phase and exposed to abraded quartz (**Table 3**). The CFU counts were in general lower than the CFU counts obtained from corresponding inactivated samples, but never decreased to below the LOD.

Addition of abraded quartz to PBS did not affect the initial pH of 7.3 ± 0.1 while addition of abraded basalt led to an increase in pH to 8.2 ± 0.1. The inactivated controls showed the same pH effect as the abraded silicates that had not been exposed to water.

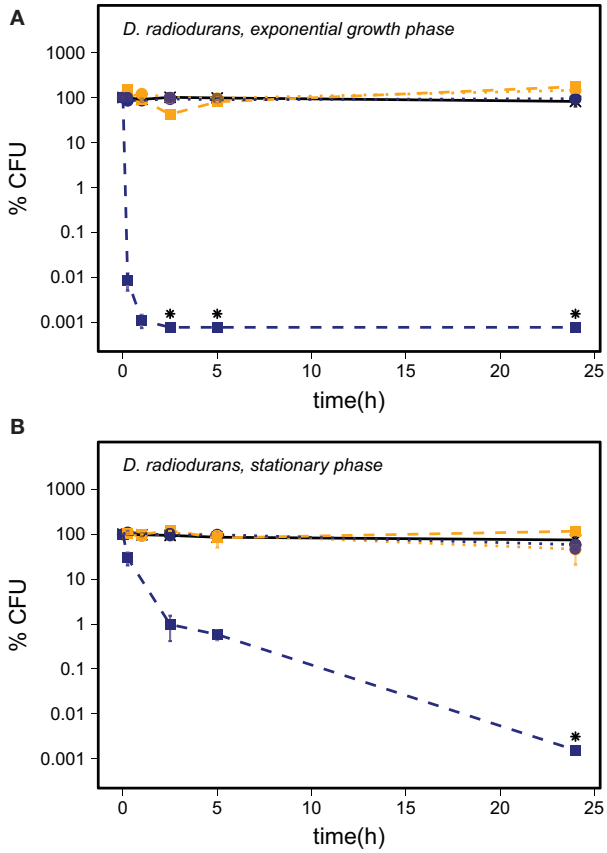

FIGURE 4 | The survival of *D. radiodurans* harvested in the exponential growth phase **(A)** and in the stationary phase **(B)** in the PBS control (—X—) and after addition of abraded quartz (·· ● ··) and basalt (– –■– –) relative to the starting concentration of ~10^6 CFU/ml. The survival of *D. radiodurans* is shown for experiments with inactivated silicates (orange) and abraded silicates kept anoxic (blue). The error bars show the SEM, and the asterisks indicate that the number of CFU was below the LOD.

DISCUSSION

Cells exposed to abraded silicates experience a range of potential stresses including anoxia, starvation, pH changes and ROS. The combined effect of these factors had a detrimental effect on vegetative cells as clearly seen by the experiments with abraded basalt. By including PBS controls with each experiment, we could isolate the effect of starvation and anoxia. Changes in the number of CFU due to adhesion of cells to the silicate particles or growth stimulated by supply of micronutrient should depend on the mineral composition and thus be independent of whether the samples had been inactivated or not. The inactivated silicate controls could therefore be used to account for potential effects of adhesion, supply of micronutrients as well as pH changes, which were found to be unaffected by the inactivation process. Thus, by comparing the effects of abraded silicates to the corresponding inactivated controls, we could elucidate the effects of ROS produced by the abraded silicates as well as possible direct effects of reactive surface sites produced during abrasion.

Viability of Bacteria in PBS and Inactivated Silicate Controls

Each of the PBS controls shown in **Figures 2–4** present the average of five cell cultures of which some were prepared in oxic PBS and some were prepared in anoxic PBS. We did not observe any effect of the presence of oxygen in the PBS controls and thus conclude that the oxygen regime did not directly affect the survival of the cells. Starvation, as it was induced by transferring cells from nutrient rich growth medium to PBS, affected the three bacterial species in different ways.

The increased number of CFU for exponential growth phase *P. putida* cells in PBS and in suspensions with inactivated silicate samples could partly be explained by cell division combined with a reduction in cell size. This is supported by a reduced average forward scatter and SYTO9 intensity over time (Figure S2), which reflect the overall cell size and the DNA content, respectively. Furthermore, *Pseudomonas putida* KT2440, which is identical to *P. putida* mt-2 with the exception of the presence of the TOL plasmid in mt-2 (Nakazawa, 2002), is known to accumulate

TABLE 3 | The relative number of CFU 24 h after addition of abraded quartz or basalt (average % of initial concentration ± SEM).

Species	Phase when harvested	PBS control	Inactivated quartz	Quartz exposed to air	Quartz kept anoxic	Inactivated basalt	Basalt exposed to air	Basalt kept anoxic
P. putida	Exponential growth	503 ± 116	3,070 ± 480	77 ± 27	9.2 ± 1.9	1,380 ± 340	634 ± 48	below LOD
	Stationary	158 ± 7	97 ± 7	156 ± 63	93 ± 6	561 ± 35	288 ± 38	1.2 ± 0.5
B. subtilis	Exponential growth	0.39 ± 0.31	below LOD	below LOD	1.2 ± 0.2	below LOD	0.026 ± 0.005	0.035 ± 0.013
	Stationary	85 ± 6	70 ± 2	66 ± 5	80 ± 3	72 ± 8	69 ± 2	76 ± 7
D. radiodurans	Exponential growth	82 ± 19	145 ± 29	30 ± 4	94 ± 7	174 ± 15	12 ± 4	below LOD
	Stationary	74 ± 12	46 ± 26	71 ± 8	58 ± 13	116 ($n = 1$)	15 ± 12	below LOD

*A part of the data is shown as end-points in **Figures 2–4**.*

large amount of polyhydroxyalkanoate (PHA) (Follonier et al., 2011). Accumulated PHA by *P. putida* mt-2 in our experiments could have provided an energy and carbon source for the additional cell divisions. The large increase in CFU number after addition of abraded basalt could indicate that growth was further enhanced by micronutrients supplied by the basalt. However, the increase in the number of CFU in the samples with inactivated quartz as compared to the PBS control remains unexplained.

The number of CFU of *B. subtilis* harvested in the exponential growth phase and transferred to PBS ranged from below the LOD to about 2% of the starting concentration after 24 h (**Figure 3A**). Microscopic inspection of the cells revealed that the *B. subtilis* cells became motile toward the end of the exponential growth phase and started to form endospores at the transition to the stationary phase. *Bacillus subtilis* 168 has not been shown to produce PHA (Singh et al., 2009) and, while some strains of *B. subtilis* can accumulate glycogen during sporulation with media containing *e.g.* xylose, (Kiel et al., 1994), there are no indications that *Bacillus subtilis* 168 would have accumulated storage compounds in our experiments. The sequential response to nutrient limitation with transformation into a motile stage followed by sporulation in combination with a lack of energy reserves and a sudden change to nutrient-free PBS may explain the lethal effect of starvation. The varying number of CFU after 24 h could be the result of a small but variable number of endospores in the cell suspension.

The moderate increase in the number of CFU of D. radiodurans harvested in the exponential growth phase in the inactivated silicate control samples could be due to ongoing cell division and/or separation of cell aggregates.

The Stress Effect of Abraded Quartz

Abraded quartz did not have a considerable effect on the survival of cells harvested in the stationary phase but killed up to 91% of *P. putida* cells harvested during exponential growth (**Table 3**). Previous studies have shown that the addition of abraded quartz would have caused a release of about 9 μM ·OH and 31 μM H_2O_2 (Bak et al., 2017). This ROS production may be the cause of the observed effect as H_2O_2 can damage cells directly by e.g., oxidation of [4Fe-4S] clusters of dehydratases (Jang and Imlay, 2007) and mononuclear iron enzymes (Anjem and Imlay, 2012) and indirectly by production of ·OH by reactions with transition metal ions through Fenton (i.e., $H_2O_2 + Fe^{2+} \rightarrow OH^- + \cdot OH + Fe^{3+}$) and Fenton-like reactions (Prousek, 2007). Hydroxyl radicals react with most organic compounds at diffusion limited rates (Buxton et al., 1988) and can lead to e.g., DNA damage (Bjelland and Seeberg, 2003) and damage of cell membranes by initiating lipid peroxidation (Buege and Aust, 1978).

The bacteria used in our assays are accustomed to some level of oxidative stress as ROS constantly are produced intracellularly by adventitious reduction of molecular oxygen by reduced redox enzymes (Seaver and Imlay, 2004; Korshunov and Imlay, 2010). For *E. coli* it has been shown that these processes lead to an intracellular H_2O_2 concentration of about 50 nM H_2O_2 (Imlay, 2013) and that the production rate is equal to the influx of H_2O_2 when extracellular H_2O_2 concentrations were about 200 nM (Seaver and Imlay, 2001). An extracellular concentration of about 31 μM H_2O_2 following addition of abraded quartz would thus significantly increase the oxidative stress inside the cells. The increased oxidative stress would, however, not necessarily result in reduced survival as *P. putida*, *B. subtilis* as well as *D. radiodurans* possess a range of detoxification mechanisms.

Our test organisms can produce catalases and peroxidases and thereby effectively decompose H_2O_2 (Inaoka et al., 1999; Slade and Radman, 2011; Kim and Park, 2014; Svenningsen et al., 2015). Furthermore, all three species possess manganese and manganese complexes which increase the resistance to oxidative stress by scavenging O_2^- and H_2O_2 and thus counteract protein damage (Inaoka et al., 1999; Horsburgh et al., 2002; Daly et al., 2010; Banh et al., 2013). Manganese can also replace iron in mononuclear enzymes (Anjem et al., 2009) which neutralizes this potential cause of Fenton-like reactions (Anjem and Imlay, 2012). Especially *D. radiodurans* is known to accumulate high concentrations of manganese, which is linked to their extreme radiation resistance (Daly et al., 2004, 2010). Also, *Deinococcus radiodurans* cells contain carotenoids, which function as antioxidants (Tian et al., 2007).

Despite this array of defense mechanisms, the cells may acquire DNA damage by oxidative stress. The vegetative cells of *P. putida*, *B. subtilis,* and *D. radiodurans* can counteract DNA damage by an array of DNA repair mechanisms (Slade and Radman, 2011; Lenhart et al., 2012; Mielecki et al., 2013) and especially *D. radiodurans* can withstand high degrees of DNA damage due to effective protection of the DNA repair proteins by manganese complexes (Daly et al., 2010). Even though *B. subtilis* endospores do not actively maintain the DNA while dormant, they are highly resistant to H_2O_2 due to the combined effect of shielding by the spore coat (Riesenman and Nicholson, 2000), low permeability of the compact inner membrane (Cortezzo and Setlow, 2005) and stabilization of DNA by α/β-type small acid soluble spore proteins (Setlow and Setlow, 1993) and dipicolinic acid (Setlow et al., 2006).

It has been shown that *P. putida* cells can survive exposure to 4 and 50 mM H_2O_2 in exponential phase and stationary phase, respectively (Klotz and Anderson, 1994) and the viability of *D. radiodurans* is unaffected by exposure to up to 10 mM H_2O_2 (Tian et al., 2007). Likewise, vegetative cells of *B. subtilis* are not affected by addition of 100 μM H_2O_2 (Hartford and Dowds, 1994) and endospores can resist up to 1.5 M H_2O_2 (Melly et al., 2002). As the expected H_2O_2 production from the abraded silicates is orders of magnitude lower than the H_2O_2 concentrations previously shown to affect the viability of *P. putida*, the observed effect on survival cannot be explained by H_2O_2 release. The production of ·OH from abraded quartz, however, may be responsible for the observed effects. The high reactivity of ·OH toward most organic compounds makes it virtually impossible for the cells to counteract the direct effects of ·OH.

The Stress Effect of Abraded Basalt

Exposure to abraded basalt effectively killed both exponential growth and stationary phase cells of *P. putida* and *D. radiodurans* (**Figures 2**, **4**). The low effect of the corresponding inactivated control samples suggests that the low viability is caused by a production of ROS from the abraded basalt samples. In a previous study, basalt samples did not lead to production of H_2O_2 in water, which is surprising as a fraction of the abraded material originated from abrasion of the quartz ampoules (Bak et al., 2017). It was suggested that the absence of H_2O_2 may be due to the presence of transition metal ions e.g., iron in the basalt, which could catalyze the breakdown of H_2O_2. This would entail a production of highly reactive ·OH, which may explain the greater toxicity of basalt. The significantly lesser effect of abraded basalt exposed to oxygen (**Table 3**) supports this hypothesis as e.g., Fe^{2+} could become oxidized by oxygen, which would counteract Fenton reactions.

Spore resistance of *B. subtilis* to abraded silicates could not be attributed to any specific spore components, as the tested mutants in general showed the same high level of resistance to abraded basalt as the wild-type strains. Based on previous studies it has been suggested that the resistance of *B. subtilis* spores to oxidizing agents is related to enzymes in the outer layers, spore coat proteins, low permeability of the compact, inner membrane and the presence of α- and β-SASPs (Setlow, 2014). While we have tested the role of the spore crust, the spore coat and α- and β-SASPs individually, we cannot exclude that the resistance is due to a combination of a range of factors for which none of the tested components are essential. If ·OH was the main agent for oxidative damage caused by abraded basalt, then lipid peroxidation could be the main cause of the effects observed with vegetative cells. In this case, we would expect the spore resistance of *B. subtilis* to be at least partly attributed to the spore layers shielding the cell membranes. This was partly tested with the mutant lacking the spore crust and the mutants lacking either the inner or the outer or both layers of the spore coat (**Table 2**). These mutants did, however, all maintain some parts of the outer layers of the spore, which may have been sufficient to shield the outer membrane.

The Stress Effect of Wind-Abraded Silicates on Mars

Our results show that the toxicity of abraded silicates is strongly influenced by the mineralogy and secondary exposure to oxygen. The Martian soil is mainly composed of basaltic material of which the crystalline fraction is dominated by plagioclase feldspar, olivine and augite (Bish et al., 2013). This is similar to the composition of the basaltic material used in this study (Bak et al., 2017). Furthermore, under Martian *in situ* conditions the abraded basalt would only be exposed to the 10^{-5} bar oxygen present in the Martian atmosphere, which equals the oxygen concentration used for the simulated Martian atmosphere. Thus, abraded basalt that was not secondarily exposed to oxygen is the most realistic analog of the Martian soil investigated in this study. Interestingly, these samples also showed the strongest detrimental effect on survival of our test organisms.

Our exposure experiments were conducted in aqueous solution. Therefore, cells exposed to Martian soil as a result of e.g., forward contamination would not initially be exposed to the effects examined here. All known lifeforms do, however, require water for metabolic activity and ultimately to proliferate, in which case the stress effects of abraded silicates would apply. This could be circumvented by e.g., *B. subtilis* which in the form of endospores were largely unaffected by abraded silicates. Upon initial exposure to water the endospore would not be affected by the abraded silicates, and at the time of sporulation we would expect a much lower stress effect, if any, as shown by our experiments with inactivated basalt. Recent studies suggest annual formation of thin films of water on Mars at the northern water ice annulus (Kereszturi and Appere, 2014) and possibly more widespread night-time transient liquid brines caused by uptake of water vapor by deliquescent salts (perchlorates) in the soil (Martin-Torres et al., 2015). It is possible that reactive, abraded silicates accumulate in dry periods and are allowed to react periodically and locally when water is available. Abraded silicates have been found to form covalent bonds with atmospheric methane in a dry state (Jensen et al., 2014; Bak et al., 2016). Similar reactions may occur between abraded silicates and cells in a dry state, which could pose an additional challenge for life. This, however, was not

investigated in the present study and awaits therefore further exploration.

The reactivity of the Martian soil is also pertinent in relation to the risk of manned missions. Freshly produced silicate dust has for long been known to cause serious health problems within the mining industry (Fubini and Hubbard, 2003), and during the Apollo missions the astronauts were complaining about respiratory irritation due to inhalation of Lunar dust brought into the spacecraft (Cain, 2010). This is partly related to physical irritation caused by inhalation of particles, but also due to production of ROS (Fubini and Hubbard, 2003; Wallace et al., 2009). The results of our experiments indicate that the reactivity of abraded silicates could be even more problematic in the dry, almost anoxic atmosphere of Mars. However, this stress effect would likely be lower inside a human habitat as secondary exposure to air led to a considerable decrease in toxicity. As shown with inactivated basalt, the effect was further reduced by exposing the abraded material to water, which could be used as simple detoxification measures.

The dramatic effects of abraded basalt on the survival of *P. putida,* and the highly radiation resistant *D. radiodurans* suggest that the Martian surface is even more hostile to terrestrial organisms than previously thought. This should lower the risk of forward contamination but may also add to the hazards encountered by future manned missions. We have not determined the cause(s) behind the toxicity of abraded silicates but put forward the hypothesis that the toxicity is the result of a production of H_2O_2, which through Fenton-like reactions facilitated by transition metal ions in the basalt led to the formation of highly reactive ·OH. We propose that organisms isolated from spacecraft assembly clean rooms should be examined with respect to their resistance toward exposure to abraded silicates for a better assessment of the risk of forward contamination.

AUTHOR CONTRIBUTIONS

The study was conceived by EB, SJ, PN, and KF. EB and LJ made a pilot study for the survival assay. The experiments with *B. subtilis* mutant strains were conducted by ML and RM and the rest of the survival experiments were performed by EB. SN conducted the flow cytometry analyses. The manuscript was written by EB and KF with input from ML, SN, LJ, RM, SJ, and PN.

FUNDING

This research was financially supported by the Danish Council for Independent Research, Natural Sciences (ref. 09-066733). RM was supported by DLR grant DLR-FuE-Projekt ISS LIFE, Programm RF-FuW, Teilprogramm 475.

ACKNOWLEDGMENTS

We would like to thank J. J. Iversen for construction of the tumbling system, J. C. Kondrup for making the ampoules and B. Rasmussen for preparation of the quartz and basalt samples. The authors thank Andrea Schröder for her technical assistance during parts of this work and acknowledge Peter Setlow and Patrick Eichenberger for their generous donation of the *Bacillus subtilis* mutant strains. Also, we will like to thank Nanna Svenningsen for providing the *Pseudomonas putida* culture. Flow cytometry was performed at the FACS Core Facility, Aarhus University, Denmark.

SUPPLEMENTARY MATERIAL

The Supplementary Material for this article can be found online at: http://journal.frontiersin.org/article/10.3389/fmicb.2017.01709/full#supplementary-material

REFERENCES

Anderson, A. W., Nordan, H. C., Cain, R. F., Parrish, G., and Duggan, D. (1956). Studies on a radio-resistant micrococcus. 1. Isolation, morphology, cultural characteristics, and resistance to gamme radiation. *Food Technol.* 10, 575–578.

Anjem, A., and Imlay, J. A. (2012). Mononuclear iron enzymes are primary targets of hydrogen peroxide stress. *J. Biol. Chem.* 287, 15544–15556. doi: 10.1074/jbc.M111.330365

Anjem, A., Varghese, S., and Imlay, J. A. (2009). Manganese import is a key element of the OxyR response to hydrogen peroxide in *Escherichia coli*. *Mol. Microbiol.* 72, 844–858. doi: 10.1111/j.1365-2958.2009.06699.x

Bak, E. N., Jensen, S. J. K., Nornberg, P., and Finster, K. (2016). Methylated silicates may explain the release of chlorinated methane from Martian soil. *Earth Planet Sci Lett.* 433, 226–231. doi: 10.1016/j.epsl.2015.10.044

Bak, E. N., Zafirov, K., Merrison, J. P., Jensen, S. J. K., Nørnberg, P., Gunnlaugsson, H. P., et al. (2017). Production of reactive oxygen species from abraded silicates. Implications for the reactivity of the martian soil. *Earth Planet Sci Lett.* 473C, 113–121. doi: 10.1016/j.epsl.2017.06.008

Banh, A., Chavez, V., Doi, J., Nguyen, A., Hernandez, S., Ha, V., et al. (2013). Manganese (Mn) oxidation increases intracellular Mn in Pseudomonas putida GB-1. *PLoS ONE* 8:e77835. doi: 10.1371/journal.pone.0077835

Bish, D. L., Blake, D. F., Vaniman, D. T., Chipera, S. J., Morris, R. V., Ming, D. W., et al. (2013). X-ray diffraction results from mars science laboratory: mineralogy of rocknest at gale crater. *Science* 341:1238932. doi: 10.1126/science.1238932

Bjelland, S., and Seeberg, E. (2003). Mutagenicity, toxicity and repair of DNA base damage induced by oxidation. *Mutat. Res.* 531, 37–80. doi: 10.1016/j.mrfmmm.2003.07.002

Buege, J. A., and Aust, S. D. (1978). Microsomal lipid peroxidation. *Meth. Enzymol.* 52, 302–310. doi: 10.1016/S0076-6879(78)52032-6

Buxton, G. V., Greenstock, C. L., Helman, W. P., and Ross, A. B. (1988). Critical-review of rate constants for reactions of hydrated electrons, hydrogen-atoms and hydroxyl radicals (.Oh/.O−) in aqueous-solution. *J. Phys. Chem. Ref. Data.* 17, 513–886. doi: 10.1063/1.555805

Cain, J. R. (2010). Lunar dust: the Hazard and astronaut exposure risks. *Earth Moon Planets* 107, 107–125. doi: 10.1007/s11038-010-9365-0

Cockell, C. S., Catling, D. C., Davis, W. L., Snook, K., Kepner, R. L., Lee, P., et al. (2000). The ultraviolet environment of mars: biological implications past, present, and future. *Icarus* 146, 343–359. doi: 10.1006/icar.2000.6393

Cortezzo, D. E., and Setlow, P. (2005). Analysis of factors that influence the sensitivity of spores of *Bacillus subtilis* to DNA damaging chemicals. *J. Appl. Microbiol.* 98, 606–617. doi: 10.1111/j.1365-2672.2004.02495.x

Daly, M. J., Gaidamakova, E. K., Matrosova, V. Y., Kiang, J. G., Fukumoto, R., Lee, D. Y., et al. (2010). Small-molecule antioxidant

proteome-shields in deinococcus radiodurans. *PLoS ONE* 5:e12570 doi: 10.1371/journal.pone.0012570

Daly, M. J., Gaidamakova, E. K., Matrosova, V. Y., Vasilenko, A., Zhai, M., Venkateswaran, A., et al. (2004). Accumulation of Mn(II) in, *Deinococcus radiodurans* facilitates gamma-radiation resistance. *Science* 306, 1025–1028. doi: 10.1126/science.1103185

de La Vega, U. P., Rettberg, P., and Reitz, G. (2007). Simulation of the environmental climate conditions on martian surface and its effect on *Deinococcus radiodurans*. *Adv. Space Res.* 40, 1672–1677. doi: 10.1016/j.asr.2007.05.022

Diaz, B., and Schulze-Makuch, D. (2006). Microbial survival rates of *Escherichia coli* and *Deinococcus radiodurans* under low temperature, low pressure, and UV-Irradiation conditions, and their relevance to possible martian life. *Astrobiology* 6, 332–347. doi: 10.1089/ast.2006.6.332

Follonier, S., Panke, S., and Zinn, M. (2011). A reduction in growth rate of Pseudomonas putida KT2442 counteracts productivity advances in medium-chain-length polyhydroxyalkanoate production from gluconate. *Microb. Cell Fact.* 10, 25–35. doi: 10.1186/1475-2859-10-25

Fubini, B., and Hubbard, A. (2003). Reactive oxygen species (ROS) and reactive nitrogen species (RNS) generation by silica in inflammation and fibrosis. *Free Radic. Bio. Med.* 34, 1507–1516. doi: 10.1016/S0891-5849(03)00149-7

Gunnlaugsson, H. P., Rasmussen, H., Madsen, M. B., and Nornberg, P. (2009). New analysis of the Mossbauer spectra of olivine basalt rocks from Gusev crater on Mars. *Planet. Space Sci.* 57, 640–645. doi: 10.1016/j.pss.2008.09.009

Hansen, A. A., Jensen, L. L., Kristoffersen, T., Mikkelsen, K., Merrison, J., Finster, K. W., et al. (2009). Effects of long-term simulated martian conditions on a freeze-dried and homogenized bacterial permafrost community. *Astrobiology* 9, 229–240. doi: 10.1089/ast.2008.0244

Hartford, O. M., and Dowds, B. C. (1994). Isolation and characterization of a hydrogen peroxide resistant mutant of *Bacillus subtilis*. *Microbiology* 140(Pt 2), 297–304. doi: 10.1099/13500872-140-2-297

Hassler, D. M., Zeitlin, C., Wimmer-Schweingruber, R. F., Ehresmann, B., Rafkin, S., Eigenbrode, J. L., et al. (2014). Mars' surface radiation environment measured with the mars science laboratory's curiosity rover. *Science* 343:1244797. doi: 10.1126/science.1244797

Horsburgh, M. J., Wharton, S. J., Karavolos, M., and Foster, S. J. (2002). Manganese: elemental defence for a life with oxygen. *Trends Microbiol.* 10, 496–501. doi: 10.1016/s0966-842x(02)02462-9

Imlay, J. A. (2013). The molecular mechanisms and physiological consequences of oxidative stress: lessons from a model bacterium. *Nat. Rev. Microbiol.* 11, 443–454. doi: 10.1038/nrmicro3032

Inaoka, T., Matsumura, Y., and Tsuchido, T. (1999). SodA and manganese are essential for resistance to oxidative stress in growing and sporulating cells of *Bacillus subtilis*. *J. Bacteriol.* 181, 1939–1943.

Jang, S. J., and Imlay, J. A. (2007). Micromolar intracellular hydrogen peroxide disrupts metabolism by damaging iron-sulfur enzymes. *J. Biol. Chem.* 282, 929–937. doi: 10.1074/jbc.M607646200

Jensen, S. J. K., Skibsted, J., Jakobsen, H. J., ten Kate, I. L., Guimlaugsson, H. P., Merrison, J. P., et al. (2014). A sink for methane on Mars? The answer is blowing in the wind. *Icarus* 236, 24–27. doi: 10.1016/j.icarus.2014.03.036

Johnson, A. P., Pratt, L. M., Vishnivetskaya, T., Pfiffner, S., Bryan, R. A., Dadachova, E., et al. (2011). Extended survival of several organisms and amino acids under simulated martian surface conditions. *Icarus* 211, 1162–1178. doi: 10.1016/j.icarus.2010.11.011

Kereszturi, A., and Appere, T. (2014). Searching for springtime zonal liquid interfacial water on Mars. *Icarus* 238, 66–76. doi: 10.1016/j.icarus.2014.05.001

Kerney, K. R., and Schuerger, A. C. (2011). Survival of *Bacillus subtilis* endospores on ultraviolet-irradiated rover wheels and mars regolith under simulated martian conditions. *Astrobiology* 11, 477–485. doi: 10.1089/ast.2011.0615

Kiel, J. A. K. W., Boels, J. M., Beldman, G., and Venema, G. (1994). Glycogen in *Bacillus-Subtilis* - molecular characterization of an operon encoding enzymes involved in glycogen biosynthesis and degradation. *Mol. Microbiol.* 11, 203–218. doi: 10.1111/j.1365-2958.1994.tb00301.x

Kim, J., and Park, W. (2014). Oxidative stress response in *Pseudomonas putida*. *Appl. Microbiol. Biot.* 98, 6933–6946. doi: 10.1007/s00253-014-5883-4

Klein, H. P. (1978). Viking biological experiments on mars. *Icarus* 34, 666–674. doi: 10.1016/0019-1035(78)90053-2

Klotz, M. G., and Anderson, A. J. (1994). The role of catalase isozymes in the culturability of the root colonizer *Pseudomonas-Putida* after exposure to hydrogen-peroxide and antibiotics. *Can. J. Microbiol.* 40, 382–387. doi: 10.1139/m94-062

Kok, J. F., Parteli, E. J. R., Michaels, T. I., and Karam, D. B. (2012). The physics of wind-blown sand and dust. *Rep. Prog. Phys.* 75:106901. doi: 10.1088/0034-4885/75/10/106901

Korshunov, S., and Imlay, J. A. (2010). Two sources of endogenous hydrogen peroxide in *Escherichia coli*. *Mol. Microbiol.* 75, 1389–1401. doi: 10.1111/j.1365-2958.2010.07059.x

La Duc, M. T., Osman, S., Vaishampayan, P., Piceno, Y., Andersen, G., Spry, J. A., et al. (2009). Comprehensive census of bacteria in clean rooms by using DNA microarray and cloning methods. *Appl. Environ. Microb.* 75, 6559–6567. doi: 10.1128/AEM.01073-09

Lefevre, F., Bertaux, J. L., Clancy, R. T., Encrenaz, T., Fast, K., Forget, F., et al. (2008). Heterogeneous chemistry in the atmosphere of Mars. *Nature* 454, 971–975. doi: 10.1038/nature07116

Lenhart, J. S., Schroeder, J. W., Walsh, B. W., and Simmons, L. A. (2012). DNA repair and genome maintenance in *Bacillus subtilis*. *Microbiol. Mol. Biol. R.* 76, 530–564. doi: 10.1128/MMBR.05020-11

Mahaffy, P. R., Webster, C. R., Atreya, S. K., Franz, H., Wong, M., Conrad, P. G., et al. (2013). Abundance and isotopic composition of gases in the martian atmosphere from the curiosity rover. *Science* 341, 263–266. doi: 10.1126/science.1237966

Mancinelli, R. L., and Klovstad, M. (2000). Martian soil and UV radiation: microbial viability assessment on spacecraft surfaces. *Planet. Space Sci.* 48, 1093–1097. doi: 10.1016/S0032-0633(00)00083-0

Martin-Torres, F. J., Zorzano, M. P., Valentin-Serrano, P., Harri, A. M., Genzer, M., Kemppinen, O., et al. (2015). Transient liquid water and water activity at Gale crater on Mars. *Nat. Geosci.* 8, 357–361. doi: 10.1038/ngeo2412

Mason, J. M., and Setlow, P. (1986). Essential role of small, acid-soluble spore proteins in resistance of *Bacillus subtilis* spores to UV light. *J. Bacteriol.* 167, 174–178. doi: 10.1128/jb.167.1.174-178.1986

Melly, E., Cowan, A. E., and Setlow, P. (2002). Studies on the mechanism of killing of *Bacillus subtilis* spores by hydrogen peroxide. *J. Appl. Microbiol.* 93, 316–325. doi: 10.1046/j.1365-2672.2002.01687.x

Merrison, J. P. (2012). Sand transport, erosion and granular electrification. *Aeolian Res.* 4, 1–16. doi: 10.1016/j.aeolia.2011.12.003

Mielecki, D., Saumaa, S., Wrzesinski, M., Maciejewska, A. M., Zuchniewicz, K., Sikora, A., et al. (2013). *Pseudomonas putida* AlkA and AlkB proteins comprise different defense systems for the repair of alkylation damage to DNA - *In vivo*, *In vitro*, and *In silico* Studies. *PLoS ONE* 8:e76198. doi: 10.1371/journal.pone.0076198

Millour, E., Forget, F., Spiga, A., Navarro, T., Madeleine, J.-B., Montatobe, L., et al. (2015). *The Mars Climate Database (MCD Version* 5.2).

Moeller, R., Rohde, M., and Reitz, G. (2010). Effects of ionizing radiation on the survival of bacterial spores in artificial martian regolith. *Icarus* 206, 783–786. doi: 10.1016/j.icarus.2009.11.014

Moeller, R., Setlow, P., Horneck, G., Berger, T., Reitz, G., Rettberg, P., et al. (2008). Roles of the major, small, acid-soluble spore proteins and spore-specific and universal DNA repair mechanisms in resistance of *Bacillus subtilis* spores to ionizing radiation from x rays and high-energy charged-particle bombardment. *J. Bacteriol.* 190, 1134–1140. doi: 10.1128/JB.01644-07

Morris, R. V., Klingelhofer, G., Bernhardt, B., Schroder, C., Rodionov, D. S., de Souza, P. A., et al. (2004). Mineralogy at Gusev crater from the Mossbauer spectrometer on the Spirit rover. *Science* 305, 833–836. doi: 10.1126/science.1100020

Nagler, K., Setlow, P., Li, Y. Q., and Moeller, R. (2014). High salinity alters the germination behavior of bacillus subtilis spores with nutrient and nonnutrient germinants. *Appl. Environ. Microb.* 80, 1314–1321. doi: 10.1128/AEM.03293-13

Nakazawa, T. (2002). Travels of a Pseudomonas, from Japan around the world. *Environ. Microbiol.* 4, 782–786. doi: 10.1046/j.1462-2920.2002.00310.x

Nicholson, W. L., and Setlow, P. (1990). "Sporulation, germination, and outgrowth," in *Molecular Biological Methods for Bacillus*, eds C. R. Harwood and S. M. Cutting (Sussex: John Wiley and Sons), 391–450.

Ojha, L., Wilhelm, M. B., Murchie, S. L., McEwen, A. S., Wray, J. J., Hanley, J., et al. (2015). Spectral evidence for hydrated salts in recurring slope lineae on Mars. *Nat. Geosci.* 8, 829–832. doi: 10.1038/ngeo2546

Paulino-Lima, I. G., Janot-Pacheco, E., Galante, D., Cockell, C., Olsson-Francis, K., Brucato, J. R., et al. (2011). Survival of *Deinococcus radiodurans* against laboratory-simulated solar wind charged particles. *Astrobiology* 11, 875–882. doi: 10.1089/ast.2011.0649

Paulino-Lima, I. G., Pilling, S., Janot-Pacheco, E., de Brito, A. N., Barbosa, J., Leitao, A. C., et al. (2010). Laboratory simulation of interplanetary ultraviolet radiation (broad spectrum) and its effects on *Deinococcus radiodurans*. *Planet. Space Sci.* 58, 1180–1187. doi: 10.1016/j.pss.2010.04.010

Prousek, J. (2007). Fenton chemistry in biology and medicine. *Pure Appl. Chem.* 79, 2325–2338. doi: 10.1351/pac200779122325

Puleo, J. R., Fields, N. D., Bergstrom, S. L., Oxborrow, G. S., Stabekis, P. D., and Koukol, R. C. (1977). Microbiological profiles of viking spacecraft. *Appl. Environ. Microb.* 33, 379–384.

Raguse, M., Fiebrandt, M., Denis, B., Stapelmann, K., Eichenberger, P., Driks, A., et al. (2016). Understanding of the importance of the spore coat structure and pigmentation in the *Bacillus subtilis* spore resistance to low-pressure plasma sterilization. *J. Phys. D Appl. Phys.* 49:285401. doi: 10.1088/0022-3727/49/28/285401

Riesenman, P. J., and Nicholson, W. L. (2000). Role of the spore coat layers in *Bacillus subtilis* spore resistance to hydrogen peroxide, artificial UV-C, UV-B, and solar UV radiation. *Appl. Environ. Microb.* 66, 620–626. doi: 10.1128/AEM.66.2.620-626.2000

Schaeffer, P., Millet, J., and Aubert, J. P. (1965). Catabolic repression of bacterial sporulation. *P. Natl. Acad. Sci. U.S.A.* 54:704. doi: 10.1073/pnas.54.3.704

Schuerger, A. C., Mancinelli, R. L., Kern, R. G., Rothschild, L. J., and McKay, C. P. (2003). Survival of endospores of *Bacillus subtilis* on spacecraft surfaces under simulated martian environments: implications for the forward contamination of Mars. *Icarus* 165, 253–276. doi: 10.1016/S0019-1035(03)00200-8

Seaver, L. C., and Imlay, J. A. (2001). Hydrogen peroxide fluxes and compartmentalization inside growing *Escherichia coli*. *J. Bacteriol.* 183, 7182–7189. doi: 10.1128/JB.183.24.7182-7189.2001

Seaver, L. C., and Imlay, J. A. (2004). Are respiratory enzymes the primary sources of intracellular hydrogen peroxide? *J. Biol. Chem.* 279, 48742–48750. doi: 10.1074/jbc.M408754200

Setlow, B., and Setlow, P. (1993). Binding of small, acid-soluble spore proteins to DNA plays a significant role in the resistance of *Bacillus subtilis* spores to hydrogen peroxide. *Appl. Environ. Microbiol.* 59, 3418–3423.

Setlow, B., Atluri, S., Kitchel, R., Koziol-Dube, K., and Setlow, P. (2006). Role of dipicolinic acid in resistance and stability of spores of *Bacillus subtilis* with or without DNA-protective alpha/beta-type small acid-soluble proteins. *J. Bacteriol.* 188, 3740–3747. doi: 10.1128/JB.00212-06

Setlow, P. (2014). "Spore resistance properties," in *The Bacterial Spore: From Molecules to Systems*, eds P. Eichenberger and A. Driks (Washington, DC: American Sociaty for Microbiology), 201–215. doi: 10.1128/microbiolspec.TBS-0003-2012

Singh, M., Patel, S. K. S., and Kalia, V. C. (2009). *Bacillus subtilis* as potential producer for polyhydroxyalkanoates. *Microb. Cell Fact.* 8:38. doi: 10.1186/1475-2859-8-38

Slade, D., and Radman, M. (2011). Oxidative stress resistance in deinococcus radiodurans. *Microbiol. Mol. Biol. R.* 75, 133–191. doi: 10.1128/MMBR.00015-10

Slieman, T. A., and Nicholson, W. L. (2001). Role of dipicolinic acid in survival of *Bacillus subtilis* spores exposed to artificial and solar UV radiation. *Appl. Environ. Microb.* 67, 1274–1279. doi: 10.1128/AEM.67.3.1274-1279.2001

Smith, S. A., Benardini, J. N., Anderl, D., Ford, M., Wear, E., Schrader, M., et al. (2017). Identification and characterization of early mission phase microorganisms residing on the mars science laboratory and assessment of their potential to survive mars-like conditions. *Astrobiology* 17, 253–265. doi: 10.1089/ast.2015.1417

Svenningsen, N. B., Perez-Pantoja, D., Nikel, P. I., Nicolaisen, M. H., de Lorenzo, V., and Nybroe, O. (2015). *Pseudomonas putida* mt-2 tolerates reactive oxygen species generated during matric stress by inducing a major oxidative defense response. *BMC Microbiol.* 15:202. doi: 10.1186/s12866-015-0542-1

Tian, B., Xu, Z. J., Sun, Z. T., Lin, J., and Hua, Y. J. (2007). Evaluation of the antioxidant effects of carotenoids from *Deinococcus radiodurans* through targeted mutagenesis, chemiluminescence, and DNA damage analyses. *Biochim. Et Biophys. Acta Gen. Subjects* 1770, 902–911. doi: 10.1016/j.bbagen.2007.01.016

Tuleta, M., Gabla, L., and Szkarlat, A. (2005). Low-energy ion bombardment of frozen bacterial spores and its relevance to interplanetary space. *Europhys. Lett.* 70, 123–128. doi: 10.1209/epl/i2004-10471-3

Wallace, W. T., Taylor, L. A., Liu, Y., Cooper, B. L., McKay, D. S., Chen, B. W., et al. (2009). Lunar dust and lunar dust stimulant activation and monitoring. *Meteorit. Planet. Sci.* 44, 961–970. doi: 10.1111/j.1945-5100.2009.tb00781.x

Conflict of Interest Statement: The authors declare that the research was conducted in the absence of any commercial or financial relationships that could be construed as a potential conflict of interest.

frontiers in Microbiology

ORIGINAL RESEARCH
published: 17 October 2017
doi: 10.3389/fmicb.2017.02002

Cryptoendolithic Antarctic Black Fungus *Cryomyces antarcticus* Irradiated with Accelerated Helium Ions: Survival and Metabolic Activity, DNA and Ultrastructural Damage

Claudia Pacelli[1], Laura Selbmann[1], Ralf Moeller[2], Laura Zucconi[1], Akira Fujimori[3] and Silvano Onofri[1]*

[1] Department of Ecological and Biological Sciences, University of Tuscia, Viterbo, Italy, [2] German Aerospace Center, Institute of Aerospace Medicine, Radiation Biology Department, Space Microbiology Research Group, Cologne, Germany, [3] National Institute of Radiological Sciences, Research Center for Charged Particle Therapy, Chiba, Japan

OPEN ACCESS

Edited by:
Andreas Teske, University of North Carolina at Chapel Hill, United States

Reviewed by:
Issay Narumi, Toyo University, Japan
Isao Yumoto, National Institute of Advanced Industrial Science and Technology, Japan

***Correspondence:**
Laura Selbmann
selbmann@unitus.it

Specialty section:
This article was submitted to Extreme Microbiology, a section of the journal Frontiers in Microbiology

Received: *29 June 2017*
Accepted: *28 September 2017*
Published: *17 October 2017*

Citation:
Pacelli C, Selbmann L, Moeller R, Zucconi L, Fujimori A and Onofri S (2017) Cryptoendolithic Antarctic Black Fungus Cryomyces antarcticus Irradiated with Accelerated Helium Ions: Survival and Metabolic Activity, DNA and Ultrastructural Damage. Front. Microbiol. 8:2002. doi: 10.3389/fmicb.2017.02002

Space represents an extremely harmful environment for life and survival of terrestrial organisms. In the last decades, a considerable deal of attention was paid to characterize the effects of spaceflight relevant radiation on various model organisms. The aim of this study was to test the survival capacity of the cryptoendolithic black fungus *Cryomyces antarcticus* CCFEE 515 to space relevant radiation, to outline its endurance to space conditions. In the frame of an international radiation campaign, dried fungal colonies were irradiated with accelerated Helium ion (150 MeV/n, LET 2.2 keV/μm), up to a final dose of 1,000 Gy, as one of the space-relevant ionizing radiation. Results showed that the fungus maintained high survival and metabolic activity with no detectable DNA and ultrastructural damage, even after the highest dose irradiation. These data give clues on the resistance of life toward space ionizing radiation in general and on the resistance and responses of eukaryotic cells in particular.

Keywords: cosmic rays, extremophiles, extremotolerance, fungi, HZE particles, He^{2+} ions, space radiation environment

INTRODUCTION

In looking for life on other planets, a robust and detailed understanding of the limits of radiation resistance of Earth extremophiles is extremely important. Indeed, beyond the shielding influence of Earth's magnetic field and atmosphere, strong ionizing radiations pervade the space environment, representing the major hazard for microbial survival, persistence of detectable biosignatures, and operation of spacecraft equipment (Dartnell, 2011). GCR, SEP, and trapped energetic particles in a planetary magnetic field are natural sources of radiation in space. Although only 1% of GCRs is composed by particles of high (H) charge (Z) and high energy (E) (HZE), i.e., He and Fe ions, the

Abbreviations: CFU, colony-forming units; GCR, galactic cosmic radiation; HIMAC, Heavy Ion Medical Accelerator in Chiba; HZE, high atomic charge and energy; LET, linear energy transfer; MEA, malt extract agar; NIRS, National Institute of Radiological Sciences; PCR, polymerase chain reaction; PMA-qPCR, Propidium MonoAzide-quantitative polymerase chain reaction; RAPD, random amplified polymorphic DNA; SPE, solar energetic particle events; TEM, transmission electron microscopy; XTT, colorimetric assay of cellular viability with 2,3-*bis*(2-methoxy-4-nitro-5-sulfophenyl)-5- [(phenylamino) carbonyl]-2H-tetrazolium hydroxide.

HZE particles are considered one of the major damage for microorganisms accidentally traveling in space (Durante and Cucinotta, 2011). Being high-LET (linear energy transfer) radiation, they cause densely packed lesions characterized by locally multiplied damaged types and sites, which are known to be the major causes of the lethal and mutagenic effects of ionizing radiation (Goodhead, 1994, 1999; Sutherland et al., 2000). The real effect of HZE on microorganisms is still unknown since during the previous space exposure experiments microorganisms were exposed and survived to non-ionizing parameters only (Rabbow et al., 2012, 2015).

In that contest, the STARLIFE-irradiation campaign (2013–2015) aimed to study the responses of astrobiological model microorganisms to increased doses of ionizing radiation and heavy ions, mimicking representatives of the GCR, never tested before. The dose rates used in the experiments were higher than those of natural GCR (Moeller et al., 2017).

Our model organism was the Antarctic cryptoendolithic black fungus *Cryomyces antarcticus* CCFEE 515, previously selected for astrobiological experiments for assessing the habitability of Mars, the likelihood of Lithopanspermia, i.e., the possible transfer of life via meteorites (Mileikowsky et al., 2000; Clark, 2001; Nicholson, 2009), and for the astronauts and planetary space protection (Hawrylewicz et al., 1962; Rummel, 2001; Nicholson et al., 2009; Horneck et al., 2010). In a space experiment the fungus has already survived 18 months real space exposition and Martian simulated conditions (Onofri et al., 2012, 2015).

Cryomyces antarcticus was isolated from the McMurdo Dry Valleys in Antarctica, considered as Mars analog due to cold temperatures, dryness and high UV irradiation (Selbmann et al., 2005; Onofri et al., 2012).

In the frame of STARLIFE experiments *C. antarcticus* has already shown a high resistance to gamma radiation up to 55.61 kGy (Co^{60}) in dried condition (Pacelli et al., 2017b).

In a separate experiment the fungus has also demonstrated to tolerate densely (deuterons, ^{2}H up 1,500 Gy) and sparsely (X-rays up to 300 Gy) ionizing radiation in physiological condition (Pacelli et al., 2017a). In this experiment *C. antarcticus* has been tested, with other astrobiological models, with accelerated Helium (150 MeV/nucleon) up to 1 kGy, as part of space-relevant ionizing radiations tested in the STARLIFE irradiation campaign (Moeller et al., 2017). Alpha particles are able to originate a high LET and a consequent higher direct biological effect (Cordero, 2017). The fungal response, after exposure in dried condition, was assessed by (i) cultivation test (CFU number), (ii) membrane damage assessment (PMA-qPCR), (iii) metabolic activity (XTT assay), (iv) DNA integrity (single gene PCRs and fingerprinting analysis), and (v) ultrastructural damage (TEM analysis).

MATERIALS AND METHODS

Samples Preparation and Exposure Conditions

Cryomyces antarcticus CCFEE 515, an Antarctic cryptoendolithic black yeast-like micro-colonial fungus, was isolated from sandstone rock collected at Linnaeus Terrace (McMurdo Dry Valleys, Southern Victoria Land) by S. Onofri during the Antarctic expedition 1980-81. Samples were prepared as follows: cell suspensions (1,000 CFU) were spread on Petri dishes of MEA medium (malt extract, powdered 30 g/L; peptone 5 g/L; agar 15 g/L; Applichem, GmbH). Fungal colonies were incubated at 15°C for 3 months and dried under laminar flow in a sterile cabinet. Colonies were irradiated with accelerated helium ion (150 MeV/n, LET 2.2 keV/μm) doses (ranging from 50 to 1,000 Gy), at the HIMAC facility at the NIRS in Japan: the doses were 50, 100, 500, and 1,000 Gy. Controls (0 Gy) were kept in the lab at room temperature.

Dose rates used in this study were far beyond those that reach Mars' surface and objects in outer space to simulate doses that organisms would receive over extended periods of time (Moeller et al., 2017; Verseux et al., 2017). All tests were performed in triplicate.

Survival Assessment

Cultivation Test

Microorganism survival was determined by measuring colony forming ability as percentages of CFU. Three of the treated colonies were re-hydrated for 72 h in 1 mL of physiological solution (NaCl 0.9%); 0.1 mL (1,000 cells/mL) of the suspension was spread on Petri dishes supplemented with MEA (five replicates). Dishes were incubated at 15°C for 3 months and developing colonies were counted. Means and standard deviations were calculated. Statistical analyses were performed by one-way analysis of variance (ANOVA) and pair wise multiple comparison procedure (Tukey test, Box et al., 1978), carried out using the statistical software SigmaStat 2.0 (Jandel, United States).

Membrane Damage Assessment

Quantitative PCR after treatment with PMA was performed to assess the membrane integrity for the all irradiation doses.

After 3 days of re-hydration, PMA (Biotium, Hayward, CA, United States) at a final concentration of 200 μM was added to colonies for 1 h. PMA penetrates only damaged membrane cells, crosslinks to DNA after light exposure and thereby prevents PCR. DNA extraction, purification and quantitative PCR, used to quantify the number of fungal Internal Transcribed Spacer (ITS) ribosomal DNA fragments present in both PMA treated and non-treated samples, were performed according to Onofri et al. (2012). Before qPCR, DNAs were quantified and normalized at same concentration (2 ng/mL) using Qubit dsDNA HS Assay Kit (Life Technologies, United States). All tests were performed in triplicate.

Determination of Metabolic Activity by XTT Assay

Colorimetric assay of cellular viability, namely XTT assay, was performed according to the protocol in Kuhn et al. (2003). The XTT is converted to a colored formazan in the presence of cell metabolic activity. After irradiation, colonies of *C. antarcticus* were re-hydrated in 1 mL of Malt Extract (30 gr/L). After 10 days, fungal cells were washed, suspended in phosphate-buffered saline (PBS) and placed into 96 well plates, three wells for each condition. The XTT assay was performed adding

54 μL XTT (10 mg/ml)/menadione (2 mM) to each well. Plates were covered with foil and incubated, in agitation, at room temperature (24°C). Formazan product in the supernatant was detected by measuring the optical density at 492 nm (Labsystem Multiskan, Franklin, MA, United States) after 2, 3, 4, and 12 h of incubation.

DNA Integrity Assessment

DNA Extraction, Single Gene PCR Reactions, and RAPD Analysis

DNA was extracted from colonies using Nucleospin Plant kit (Macherey-Nagel, Düren, Germany) following the protocol optimized for fungi (Selbmann et al., 2014).

Internal Transcribed Spacer and Small Subunit region (SSU) were amplified using BioMix (BioLine GmbH, Luckenwalde, Germany) adding 5 pmol of each primer and 2 ng of template DNA at final volume of 25 μL. The amplification was carried out using MyCycler Thermal Cycler (Bio-Rad Laboratories GmbH, Munich, Germany) equipped with a heated lid. The fungal rDNA regions were amplified using ITS4, ITS5, LR5, and LR7 and amplification conditions are as reported in Selbmann et al. (2011). Band intensities were measured and compared by using Image J software (Schneider et al., 2012). The whole genome was analyzed through fingerprinting analysis (Random Amplified Polymorphic DNA, RAPD protocol) and was performed using GGA_7 primer according to Selbmann et al. (2011).

Primers specification as follows: ITS4 (TCCTCCGCTTA TTGATATGC, White et al., 1990); ITS5 (GGAAGTAAAAGT CGTAACAAGG, White et al., 1990); LR5 (TCCTGAGGGA AACTTCG, Vilgalys and Hester, 1990); LR7 (TACTACCACC AAGATCT, Vilgalys and Hester, 1990); $(GGA)_7$ (GGA GGA GGA GGA GGA GGA GGA, Kong et al., 2000).

Ultrastructural Damage Assessment

After re-hydration, controls and colonies irradiated with medium and maximum irradiation dose (500 and 1,000 Gy) were prepared for TEM.

Colonies were treated with 5% glutaraldehyde/cacodylate sucrose buffer 0.1 M (pH 7.2) for 12 h at 4°C, washed three times in the same buffer for 1 h each at 4°C and fixed with 1% OsO_4 + 0.15% ruthenium red in 0.1 M cacodylate buffer (pH 7.2) for 3 h at 4°C. Samples were washed in distilled water (two times for 30 min at 4°C), treated with 1% uranyl acetate in distilled water for 1 h at 4°C and washed in distilled water (two times, 30 min at 4°C). Samples were then dehydrated in ethanol solutions: 30, 50, 70% (15 min each, at room temperature) and 100% ethanol (1 h at room temperature); then, they were infiltrated in mixtures of ethanol 100%: LR White resin (Agar Scientific) (2:1 for 3 h; 1:1 for 3 h, 1:2 overnight), in rotator, at 4°C. The final step of the infiltration process was performed in pure resin for 36 h. Samples were then embedded in pure resin in gelatine capsules at 48–52°C for 2 days and blocks were cut by a Reichert-Jung E Ultracut ultramicrotome equipped with diamond knife. Ultrathin sections (60–80 nm) were collected on copper grids and stained with uranyl acetate and lead citrate; then they were observed with JEOL 1200 EX II Transmission Electron Microscope. The images have been acquired using a Veleta CCD camera (Olympus Soft Imaging Solutions).

RESULTS

Survival Assessment

Cultivation Test

Survival was not affected after irradiation at 50 Gy (**Figure 1**). From 100 Gy onward, a progressive increase of mortality was recorded with the increasing of irradiation doses; yet, *C. antarcticus* retained the colony-forming ability after all treatments and 65% of vitality with the respect to the laboratory control was still maintained at the highest dose applied (1,000 Gy).

Metabolic Activity

The XTT results demonstrated a decrease in *C. antarcticus* metabolic activity, with the increasing of helium ions irradiation doses (**Figure 2**). This substance is cleaved to formazan by the succinate dehydrogenase system of the mitochondrial respiratory chain. Only living cells, possessing an intact

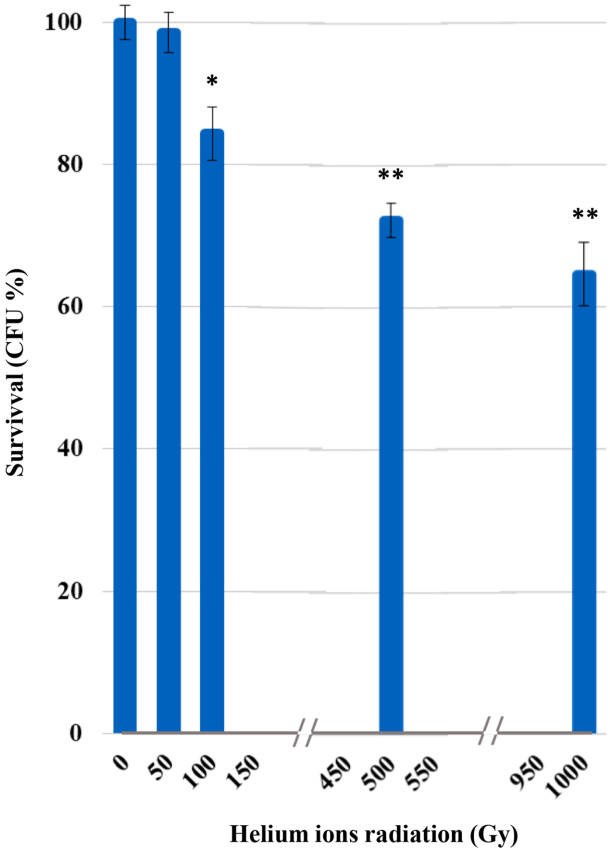

FIGURE 1 | Cultivation test after helium ions radiation: percentages of *Cryomyces antarcticus* CFU after 50, 100, 500, and 1,000 Gy. Data were normalized with the control. Significant differences were calculated by Tukey test with $*p > 0.05$; and $**p > 0.001$.

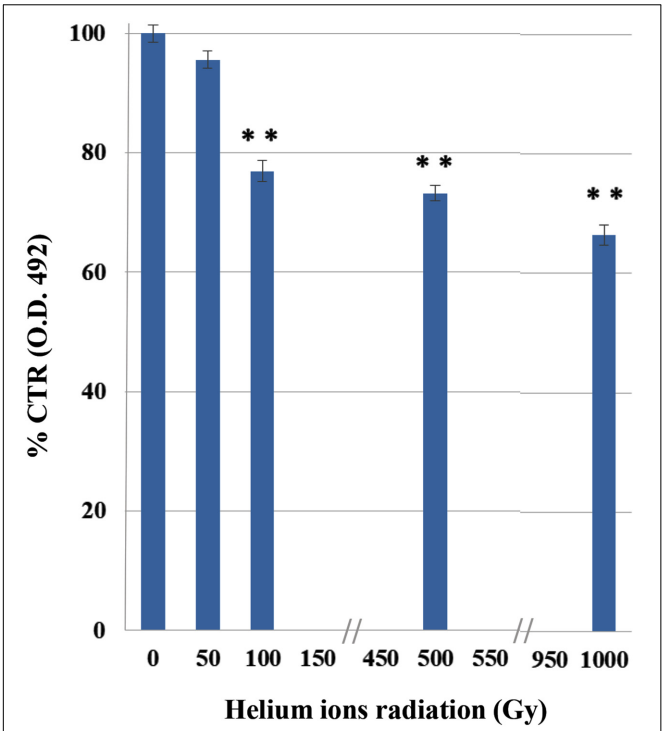

FIGURE 2 | Effects of irradiation on metabolic activity of *C. antarcticus* cells by XTT assay after helium ions radiation. O.D. 492 nm, optical density at 492 nm. Data were normalized with the control. Significant differences were calculated by Tukey test with $^{**}p > 0.001$.

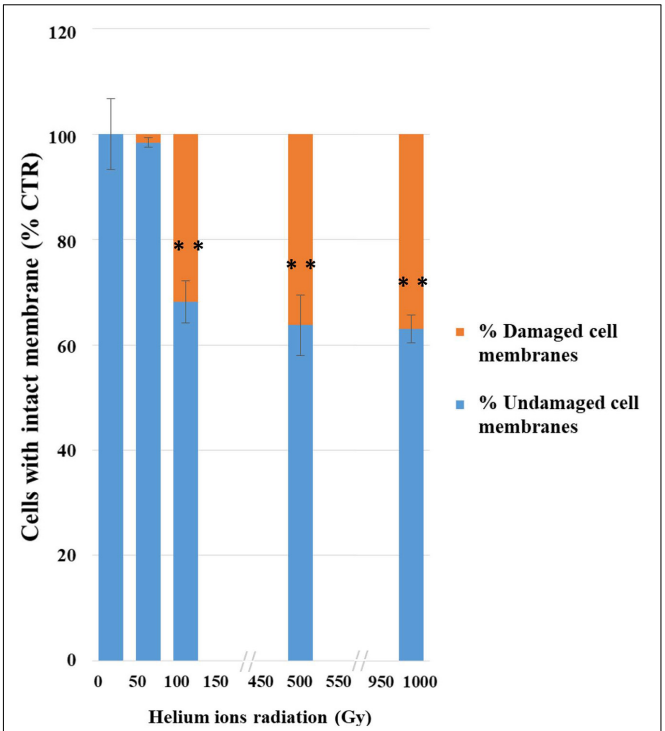

FIGURE 3 | Results of PMA assay coupled with qPCR after helium ions radiation: 50, 100, 500, and 1,000 Gy. The graph shows percentages of *C. antarcticus* cells with intact membrane, normalized with the control. Percentages of *C. antarcticus* cells with damaged membrane (Red), and corresponding percentages of cells (Blue) with intact membrane. Significant differences were calculated by Tukey test with $^{**}p > 0.001$.

mitochondrial membrane and also an intact cell membrane, do have active dehydrogenase. The first significant reduction was measured at 100 Gy (77%). However, 66% of metabolic activity compared to the laboratory control is still maintained at the highest doses, confirming the cultivation tests results and showing a good preservation of cell machinery after treatments.

Membrane Damage Assessment

The integrity of plasma membranes in irradiated cells was assessed by using qPCR after treatments with PMA; this molecule penetrates cells with compromised plasma membranes and inhibit DNA amplification.

This analysis also revealed a progressive damage with the increasing of treatments (**Figure 3**); no significant damage was present after the lowest treatment (50 Gy) and 68% damaged cells were recorded at 100 Gy. Besides up to 63% of cells still maintained membrane integrity after the highest dose (1,000 Gy).

DNA Integrity Assessment

Amplicons were obtained both for ITS and for ITS-LSU regions, fragments of 700, 1,600, and 2,000 bp of *C. antarcticus* DNA respectively, after irradiation treatments (**Figures 4A–C**). All bands were well-preserved in 700, 1,600, and 2,000 bp gene length; the gel analyses, performed with ImageJ Software, for all of them measured 100% relative density of the band till the highest irradiation dose. The RAPD profiles were preserved in all the conditions tested (**Figure 4D**). A reduction of band intensity in 1 kGy irradiated samples was visible for the band round 1,000 bp while the highest molecular weight (MW) bands were maintained. This is difficult to explain since the highest MW bands (about 2,200 bp) of the RAPD profiles would have disappeared first in case of DNA damage (Atienzar et al., 2002); moreover, in the single gene amplification, band intensity was maintained even for DNA amplicons of 2,000 bp. In the overall, results indicate that these kinds of treatments did not cause any detectable damage to the fungal DNA, at least with the techniques here used; unfortunately, for organisms with such a thick cell wall other procedures, theoretically more appropriate to reveal DNA damage as the comet assay, are not applicable.

The possible mutational burden gained by the fungus after irradiation was studied by amplicon sequencing. The electropherograms appeared perfectly preserved with no single mutation detectable (data not shown).

Ultrastructural Damage Assessment

Despite the dehydration treatments, control cells were perfectly preserved (**Figures 5A,B**), with well-organized cytoplasm and cell membrane integrity (**Figure 5A**, right black arrow). Nucleus and vacuole (**Figure 5A**, black arrow) were well-visible.

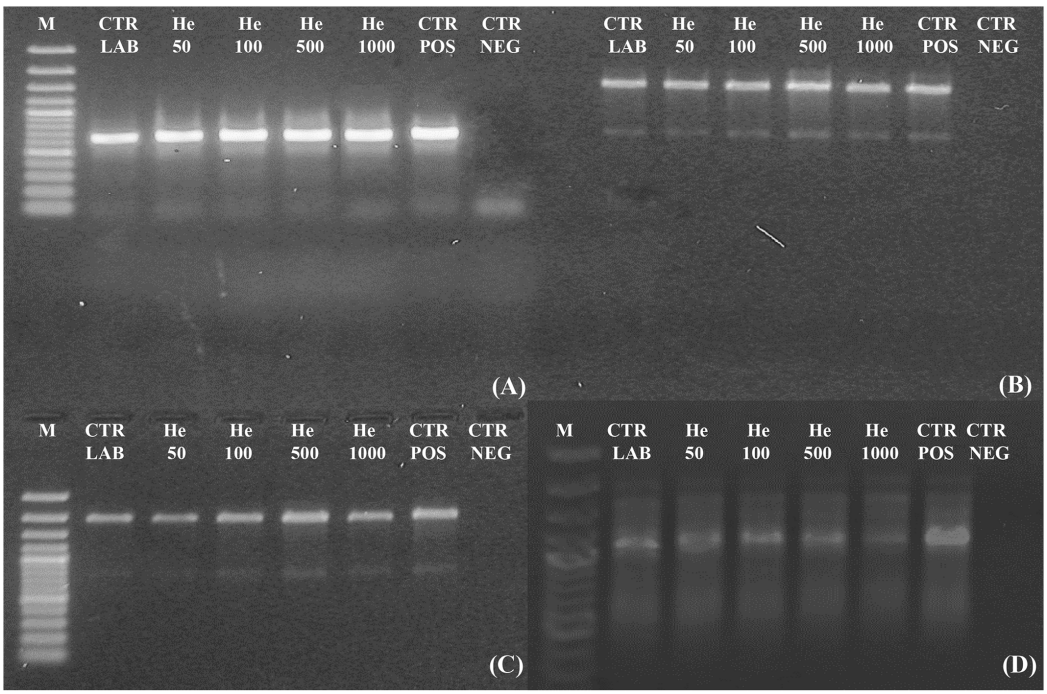

FIGURE 4 | Assessment of the DNA integrity on *C. antarcticus* single gene PCR **(A)** 700 bp; **(B)** 1,600 bp; **(C)** 2,000 bp and **(D)** genomic DNA damage as revealed by RAPD assay. **M**: DNA ladder, **POS CTR**: fresh colonies, **NEG CTR**: PCR negative control.

Even samples treated with 500 Gy were rather well-preserved (**Figures 5C–F**). Cell membranes were always maintained (**Figures 5C–F**, black arrows) except for cell on the right, **Figure 5D**, white arrow, where also cytoplasm organization was lost; organelles as nuclei, vacuoles and lipid bodies were also visible in most of the cells (**Figures 5C,D**, black arrow).

Membrane integrity and cytoplasm organization were maintained also at the highest dose of 1,000 Gy (**Figures 5G,H** black arrows), while plasmolysis and amorphous cytoplasm are evident in the cell documented in **Figure 5G**, white arrow. These results support data recorded with cultivation test, proving that a very good vitality was maintained even at the highest dose applied.

DISCUSSION

Given past and present interest of the Space Agencies in the long-term effects of ionizing radiation on survival, it is surprising that relatively few studies have been addressed to this issue. Helium ions inducing a high-linear energy transfer (LET) are of special interest for their potential biological action. Efforts have been played not only to elucidating fundamental radiobiological mechanisms, but also to applied aspects such as radiation therapy and human exposure to radiation during space flight. In this study we investigated the responses of a eukaryotic model, the fungus *C. antarcticus*, after irradiation with accelerated helium (high-energy particles), as space-relevant radiation. Helium nuclei are densely ionizing radiation sources (high LET radiation) and are of special concern as major source of radiation exposure in outer space (Horneck, 1994). In particular, ions of cosmic radiation are used to set the ultimate limit on (micro-)organisms survival in space (Horneck et al., 1994).

HZE particles (heavy ions) are the biologically most effective component of GCR; doses applied in this experiment are very high even compared to real space, where a putative organism should be exposed over extended periods of time to receive a comparable dose. One kGy of helium radiation corresponds to an average of approximately 2.0×10^5 He ions (Verseux et al., 2017). As measured during several space missions, for instance during the LDEF mission (Horneck et al., 1994), fluence was very low, around 6×10^{-5} particles/year-μm^2; as a consequence, they would not represent the major danger for a putative microorganism in space (Horneck et al., 2010).

Despite their high potential danger, alpha particles are more easily screened that other harmful radiation as beta or, even more, gamma radiation. The very thick and strongly melanized cell wall of our model organism may have represented an effective barrier for stopping He nuclei, even associated to high LET. In fact, no reduction of survival, metabolic activity or even cell with damaged membrane was detected at 50 Gy. Survival, PMA, and XTT tests gave a progressive reduction at the other irradiation doses. We assume that the first dose was not that high for our test organism to cause appreciable damage. The effect of treatments on the cells was progressively higher, and comparable among different tests, at 100, 500, and 1,000 Gy.

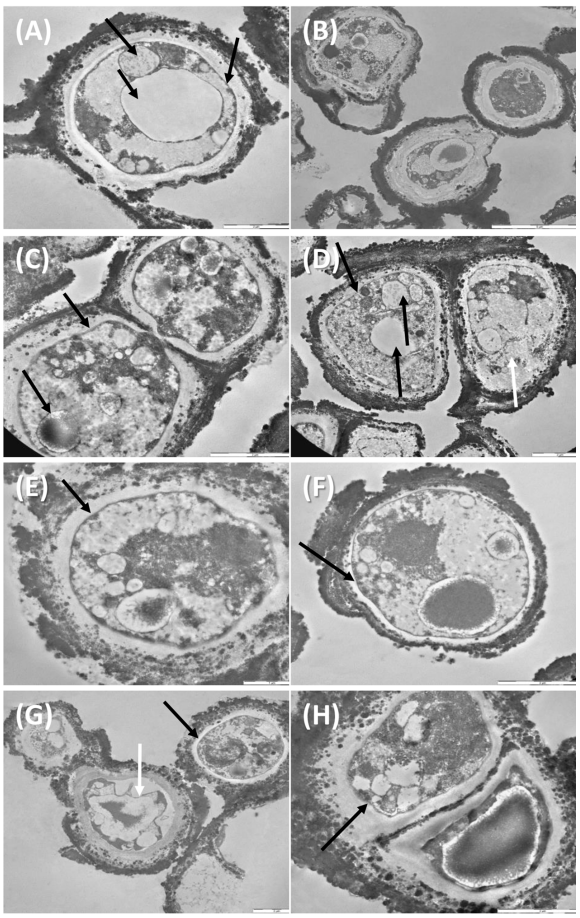

FIGURE 5 | TEM observations of *C. antarcticus*: Control **(A**,**B)**; 500 Gy treatments, **(C–F)** cell membrane and organelles are perfectly preserved (black arrows, **C–F**), damaged membrane (white arrow, **D**); 1,000 Gy treatments **(G**,**H)** plasmolysis and amorphous cytoplasm (white arrow, **G**) well-preserved membrane (black arrow, **G,H**).

This may justify the high survival and metabolic activity observed even at the maximum dose tested in the experiment where still 64% of living cells and 66% of metabolic activity were maintained, respectively.

Accordingly, still 63% of cells with intact membrane were present after PMA-qPCR assay at the highest irradiation dose (1,000 Gy). A general good membrane integrity was also observed with TEM; cell membrane was mostly preserved even at high doses applied while damages were visible in some cells at 1,000 Gy treatment in terms of membrane integrity and cytoplasm preservation (**Figure 5**). As reviewed by Horneck et al. (1994), DNA double-strand breaks (DSBs) are the most severe type of damage induced by HZE particles in microorganisms, as determined in cells of *Escherichia coli*, *Deinococcus radiodurans,* and *Bacillus subtilis*. Nevertheless, DNA damage was not detectable at all in our model *C. antarcticus*; single gene amplifications were successful even at highest dose and longest gene sequences tested; accordingly, the fingerprinting profiles were perfectly maintained (**Figure 4**).

These results were consistent with the other STARLIFE models as the cyanobacterium *Chroococcidiopsis* sp. and the lichen *Circinaria gyrosa* that also survived the treatment (de la Torre et al., 2017; Verseux et al., 2017). *C. antarcticus* has been extensively tested for its resistance to the space-relevant radiation (Onofri et al., 2012, 2015; Pacelli et al., 2016, 2017b). However, the tolerance mechanisms of this astrobiological model to outer space environmental stresses are still poorly understood but they could be related to its ability to survive desiccation. In fact, during anhydrobiosis, a state of metabolic inactivity after desiccation (Kranner et al., 2008), radiolysis of intracellular water, that is the most significant source of hazardous reactive oxygen species (Kovács and Keresztes, 2002), does not occur or is almost absent.

This radio-resistance of cells in a dry state was previously observed in bacteria as *Deinococcus radiodurans* (Bauermeister et al., 2011) and *Halobacterium salinarum* (Leuko et al., 2015; Leuko and Rettberg, 2017; Verseux et al., 2017) and was also addressed to reduced number of reactive oxygen species, and lower rates of harmful chemical reactions, when cells are in a dry state (Bauermeister et al., 2011).

In our study, the fungal DNA remained perfectly detectable even after exposure to 1 kGy of He^{2+} ions. These results are consistent with what previously observed when the fungus was treated with gamma-ionizing radiation (Pacelli et al., 2017b) and to other factors encountered in space and under Mars-like conditions (Pacelli et al., 2016). The DNA detectability after radiation treatments was reported for other microorganisms tested in the frame of STARLIFE project (Verseux et al., 2017). Those findings are relevant to search-for life missions on Mars, confirming this molecule as putative biosignature since its presence provides unequivocal proof of present or recently past life even if, it must be taken into account, that extracellular DNA may be bound to minerals or destroyed once hydrated (Aerts et al., 2014; Mojarro et al., 2017). Life detection missions to Mars focus on detecting biomarkers as evidence for extant or extinct life (Parnell et al., 2007; De Vera et al., 2012). The surface of Mars is continuously exposed to high levels of cosmic radiation, which could be deleterious for both microorganisms survival and persistence of molecular biosignatures such as DNA (Dartnell et al., 2007). Being amplified even after helium ions and ionizing radiation (Pacelli et al., 2017b; Verseux et al., 2017), we largely demonstrated that DNA has a high intrinsic stability and that it could be account as biosignature.

Even if space radiation is quite more complex and cannot be fully simulated on Earth, these results may help us to better understand the effects of helium ions radiation in future astrobiological simulation and real exposure experiments on fungal models and eukaryotic cells in general. This approach will more precisely elucidate the effects of space radiation on fungal resistance and aid in developing personalized radiological countermeasures for astronauts in the frame of planetary protection.

AUTHOR CONTRIBUTIONS

CP, SO, and LS designed the study. CP, RM, and AF performed the experiment. CP, SO, LS, and LZ analyzed and interpreted the data. CP wrote a first draft of the manuscript, which was corrected, revised and approved by all authors.

FUNDING

CP, SO, LS, and LZ were supported by BIOMEX MCF Experiment on ISS for tracking biosignatures on Martian and Lunar rocks analogs and E-GEM GeoMicrobiology for Space Exploration grants. AF and RM – MEXT Grant-in-Aid for Scientific Research on Innovative Areas "Living in Space" (Grant Numbers: 15H05935, 15K21745). RM – was supported by the DLR grant FuE-Projekt "ISS LIFE" (Programm RF-FuW, Teilprogramm 475).

ACKNOWLEDGMENTS

We would like to thank to the Italian Space Agency (ASI) for co-funding the research (BIOMEX MCF and E-GEM GeoMicrobiology for Space Exploration grants), the Italian National Program of Antarctic Researches (PNRA) and Italian National Antarctic Museum "Felice Ippolito" for funding the collection of Antarctic samples and preservation of strains in the CCFEE. We also would like to thank the HIMAC facility at the NIRS in Chiba, Japan to perform the irradiation. The authors thank Andrea Schröder for her technical assistance during parts of this work.

REFERENCES

Aerts, J. W., Röling, W. F., Elsaesser, A., and Ehrenfreund, P. (2014). Biota and biomolecules in extreme environments on Earth: implications for life detection on Mars. *Life* 4, 535–565. doi: 10.3390/life4040535

Atienzar, F. A., Venier, P., Jha, A. N., and Depledge, M. H. (2002). Evaluation of the random amplified polymorphic DNA (RAPD) assay for the detection of DNA damage and mutations. *Mutat. Res.* 521, 151–163. doi: 10.1016/S1383-5718(02)00216-4

Bauermeister, A., Moeller, R., Reitz, G., Sommer, S., and Rettberg, P. (2011). Effect of relative humidity on *Deinococcus radiodurans*' resistance to prolonged desiccation, heat, ionizing, germicidal, and environmentally relevant UV radiation. *Microb. Ecol.* 61, 715–722. doi: 10.1007/s00248-010-9785-4

Box, G. E., Hunter, W. G., and Hunter, J. S. (1978). *Statistics for Experimenters: An Introduction to Design, Data Analysis, and Model Building*, Vol. 1. New York, NY: Wiley.

Clark, B. C. (2001). Interplanetary interchange of bioactive material: probability factors and implications. *Orig. Life Evol. Biosph.* 31, 185–197. doi: 10.1023/A:1006757011007

Cordero, R. J. (2017). Melanin for space travel radioprotection. *Environ. Microbiol.* 19, 2529–2532. doi: 10.1111/1462-2920.13753

Dartnell, L. (2011). Biological constraints on habitability. *Astron. Geophys.* 52, 1.25–1.28. doi: 10.1111/j.1468-4004.2011.52125.x

Dartnell, L. R., Desorgher, L., Ward, J. M., and Coates, A. J. (2007). Martian sub-surface ionising radiation: biosignatures and geology. *Biogeosciences* 4, 455–492. doi: 10.5194/bg-4-545-2007

de la Torre, R., Miller, A. Z., Cubero, B., Martín-Cerezo, M. L., Raguse, M., and Meeßen, J. (2017). The effect of high-dose ionizing radiation on the astrobiological model lichen *Circinaria gyrosa*. *Astrobiology* 17, 145–153. doi: 10.1089/ast.2015.1454

De Vera, J. P., Boettger, U., de la Torre Noetzel, R., Sánchez, F. J., Grunow, D., Schmitz, N., et al. (2012). Supporting Mars exploration: BIOMEX in Low Earth Orbit and further astrobiological studies on the Moon using Raman and PanCam technology. *Planet. Space Sci.* 74, 103–110. doi: 10.1016/j.pss.2012.06.010

Durante, M., and Cucinotta, F. A. (2011). Physical basis of radiation protection in space travel. *Rev. Mod. Phys.* 83, 1245–1281. doi: 10.1103/RevModPhys.83.1245

Goodhead, D. T. (1994). Initial events in the cellular effects of ionizing radiations: clustered damage in DNA. *Int. J. Radiat. Biol.* 65, 7–17. doi: 10.1080/09553009414550021

Goodhead, D. T. (1999). Mechanisms for the biological effectiveness of high-LET radiations. *J. Radiat. Res.* 40, 1–13. doi: 10.1269/jrr.40.S1

Hawrylewicz, E., Gowdy, B., and Ehrlich, R. (1962). Micro-organisms under a simulated Martian environment. *Nature* 193, 497. doi: 10.1038/193497a0

Horneck, G. (1994). HZE particle effects in space. *Acta Astronaut.* 32, 749–755. doi: 10.1016/0094-5765(94)90170-8

Horneck, G., Bücker, H., and Reitz, G. (1994). Long-term survival of bacterial spores in space. *Adv. Space Res.* 14, 41–45. doi: 10.1016/0273-1177(94)90448-0

Horneck, G., Klaus, D. M., and Mancinelli, R. L. (2010). Space microbiology. *Microbiol. Mol. Biol. Rev.* 74, 121–156. doi: 10.1128/MMBR.00016-09

Kong, L., Dong, J., and Hart, G. E. (2000). Characteristics, linkage-map positions, and allelic differentiation of *Sorghum bicolor* (L.) Moench DNA simple-sequence repeats (SSRs). *Theor. Appl. Genet.* 101, 438–448. doi: 10.1007/s001220051501

Kovács, E., and Keresztes, A. (2002). Effect of gamma and UV-B/C radiation on plant cells. *Micron* 33, 199–210. doi: 10.1016/S0968-4328(01)00012-9

Kranner, I., Beckett, R., Hochman, A., and Nash, T. H. III (2008). Desiccation-tolerance in lichens: a review. *Bryologist* 111, 576–593. doi: 10.1639/0007-2745-111.4.576

Kuhn, D. M., Balkis, M., Chandra, J., Mukherjee, P. K., and Ghannoum, M. A. (2003). Uses and limitations of the XTT assay in studies of *Candida* growth and metabolism. *J. Clin. Microbiol.* 41, 506–508. doi: 10.1128/JCM.41.1.506-508.2003

Leuko, S., Domingos, C., Parpart, A., Reitz, G., and Rettberg, P. (2015). The survival and resistance of *Halobacterium salinarum* NRC-1, *Halococcus hamelinensis*, and *Halococcus morrhuae* to simulated outer space solar radiation. *Astrobiology* 15, 987–997. doi: 10.1089/ast.2015.1310

Leuko, S., and Rettberg, P. (2017). The effects of HZE particles, γ and X-ray radiation on the survival and genetic integrity of *Halobacterium salinarum* NRC-1, *Halococcus hamelinensis*, and *Halococcus morrhuae*. *Astrobiology* 17, 110–117. doi: 10.1089/ast.2015.1458

Mileikowsky, C., Cucinotta, F. A., Wilson, J. W., Gladman, B., Horneck, G., Lindegren, L., et al. (2000). Natural transfer of viable microbes in space, part 1: from Mars to Earth and Earth to Mars. *Icarus* 145, 391–427. doi: 10.1006/icar.1999.6317

Moeller, R., Raguse, M., Leuko, S., Berger, T., Hellweg, C. E., Fujimori, et al. (2017). STARLIFE—an international campaign to study the role of galactic cosmic radiation in astrobiological model systems. *Astrobiology* 17, 101–109. doi: 10.1089/ast.2016.1571

Mojarro, A., Ruvkun, G., Zuber, M. T., and Carr, C. E. (2017). Nucleic acid extraction from synthetic mars analog soils for in situ life detection. *Astrobiology* 17, 747–760. doi: 10.1089/ast.2016.1535

Nicholson, W. L. (2009). Ancient micronauts: interplanetary transport of microbes by cosmic impacts. *Trends Microbiol.* 17, 243–250. doi: 10.1016/j.tim.2009.03.004

Nicholson, W. L., Schuerger, A. C., and Race, M. S. (2009). Migrating microbes and planetary protection. *Trends Microbiol.* 17, 389–392. doi: 10.1016/j.tim.2009.07.001

Onofri, S., de la Torre, R., de Vera, J. P., Ott, S., Zucconi, L., Selbmann, L., et al. (2012). Survival of rock-colonizing organisms after 1.5 years in outer space. *Astrobiology* 12, 508–516. doi: 10.1089/ast.2011.0736

Onofri, S., de Vera, J. P., Zucconi, L., Selbmann, L., Scalzi, G., Venkateswaran, K. J., et al. (2015). Survival of antarctic cryptoendolithic fungi in simulated martian

conditions on board the international space station. *Astrobiology* 15, 1052–1059. doi: 10.1089/ast.2015.1324

Pacelli, C., Bryan, R. A., Onofri, S., Selbmann, L., Shuryak, I., and Dadachova, E. (2017a). Melanin is effective in protecting fast and slow growing fungi from various types of ionizing radiation. *Environ. Microbiol.* 19, 1612–1624. doi: 10.1111/1462-2920.13681

Pacelli, C., Selbmann, L., Zucconi, L., de Vera, J. P., Rabbow, E., Horneck, G., et al. (2016). BIOMEX experiment: ultrastructural alterations, molecular damage and survival of the fungus *Cryomyces antarcticus* after the Experiment Verification Tests. *Orig. life. Evol. Biosph.* 47, 187–202. doi: 10.1007/s11084-016-9485-2

Pacelli, C., Selbmann, L., Zucconi, L., Raguse, M., Moeller, R., Shuryak, I., et al. (2017b). Survival, DNA integrity, and ultrastructural damage in Antarctic cryptoendolithic eukaryotic microorganisms exposed to ionizing radiation. *Astrobiology* 17, 126–135. doi: 10.1089/ast.2015.1456

Parnell, J., Cullen, D., Sims, M. R., Bowden, S., Cockell, C. S., Court, R., et al. (2007). Searching for life on Mars: selection of molecular targets for ESA's aurora ExoMars mission. *Astrobiology* 7, 578–604. doi: 10.1089/ast.2006.0110

Rabbow, E., Rettberg, P., Barczyk, S., Bohmeier, M., Parpart, A., Panitz, C., et al. (2012). EXPOSE-E: an ESA astrobiology mission 1.5 years in space. *Astrobiology* 12, 374–386. doi: 10.1089/ast.2011.0760

Rabbow, E., Rettberg, P., Barczyk, S., Bohmeier, M., Parpart, A., Panitz, C., et al. (2015). The astrobiological mission EXPOSE-R on board of the International Space Station. *Int. J. Astrobiol.* 14, 3–16. doi: 10.3389/fmicb.2017.01533

Rummel, J. D. (2001). Planetary exploration in the time of astrobiology: protecting against biological contamination. *Proc. Natl. Acad. Sci. U.S.A.* 98, 2128–2131. doi: 10.1073/pnas.061021398

Schneider, C. A., Rasband, W. S., and Eliceiri, K. W. (2012). NIH Image to ImageJ: 25 years of image analysis. *Nat. Methods* 9, 671–675. doi: 10.1038/nmeth.2089

Selbmann, L., de Hoog, G. S., Mazzaglia, A., Friedmann, E. I., and Onofri, S. (2005). Fungi at the edge of life: cryptoendolithic black fungi from Antarctic desert. *Stud. Mycol.* 51, 1–32.

Selbmann, L., Isola, D., Egidi, E., Zucconi, L., Gueidan, C., de Hoog, G. S., et al. (2014). Mountain tips as reservoirs for new rock-fungal entities: *Saxomyces* gen. nov. and four new species from the Alps. *Fungal Divers.* 65, 167–182. doi: 10.1007/s13225-013-0234-9

Selbmann, L., Isola, D., Zucconi, L., and Onofri, S. (2011). Resistance to UV-B induced DNA damage in extreme-tolerant cryptoendolithic Antarctic fungi: detection by PCR assays. *Fungal Biol.* 115, 937–944. doi: 10.1016/j.funbio.2011.02.016

Sutherland, B. M., Bennett, P. V., Sidorkina, O., and Laval, J. (2000). Clustered damages and total lesions induced in DNA by ionizing radiation: oxidized bases and strand breaks. *Biochemistry* 39, 8026–8031. doi: 10.1021/bi9927989

Verseux, C., Baqué, M., Cifariello, R., Fagliarone, C., Raguse, M., Moeller, R., et al. (2017). Evaluation of the resistance of *Chroococcidiopsis* spp. to sparsely and densely ionizing irradiation. *Astrobiology* 17, 118–125. doi: 10.1089/ast.2015.1450

Vilgalys, R., and Hester, M. (1990). Rapid genetic identification and mapping of enzymatically amplified ribosomal DNA from several *Cryptococcus* species. *J. Bacteriol.* 172, 4238–4246. doi: 10.1128/jb.172.8.4238-4246.1990

White, T. J., Bruns, T., Lee, S., and Taylor, J. (1990). "Amplification and direct sequencing of fungal ribosomal RNA genes for phylogenetics," in *PCR Protocols: A Guide to Methods and Applications*, eds N. Innis, D. Gelfand, J. Sninsky, and T. White (Cambridge, MA: Academic Press), 315–322.

Conflict of Interest Statement: The authors declare that the research was conducted in the absence of any commercial or financial relationships that could be construed as a potential conflict of interest.

frontiers in Microbiology

METHODS
published: 15 August 2017
doi: 10.3389/fmicb.2017.01533

EXPOSE-R2: The Astrobiological ESA Mission on Board of the International Space Station

Elke Rabbow[1], Petra Rettberg[1], Andre Parpart[1], Corinna Panitz[2], Wolfgang Schulte[3], Ferdinand Molter[3], Esther Jaramillo[4], René Demets[5], Peter Weiß[6] and Rainer Willnecker[6]*

[1] Institute of Aerospace Medicine, Radiation Biology, German Aerospace Center, Cologne, Germany, [2] Institute of Pharmacology and Toxicology, Uniklinik RWTH Aachen, Aachen, Germany, [3] OHB System AG, Wessling, Germany, [4] RUAG Schweiz AG, RUAG Space, Zürich, Switzerland, [5] European Space Research and Technology Centre, European Space Agency, Noordwijk, Netherlands, [6] Microgravity User Support Center, German Aerospace Center, Cologne, Germany

OPEN ACCESS

Edited by:
Andreas Teske, University of North Carolina at Chapel Hill, United States

Reviewed by:
Issay Narumi, Toyo University, Japan
Luke McKay, Montana State University, United States

***Correspondence:**
Elke Rabbow
elke.rabbow@dlr.de

Specialty section:
This article was submitted to Extreme Microbiology, a section of the journal Frontiers in Microbiology

Received: *28 April 2017*
Accepted: *28 July 2017*
Published: *15 August 2017*

Citation:
Rabbow E, Rettberg P, Parpart A, Panitz C, Schulte W, Molter F, Jaramillo E, Demets R, Weiß P and Willnecker R (2017) EXPOSE-R2: The Astrobiological ESA Mission on Board of the International Space Station. Front. Microbiol. 8:1533. doi: 10.3389/fmicb.2017.01533

On July 23, 2014, the Progress cargo spacecraft 56P was launched from Baikonur to the International Space Station (ISS), carrying EXPOSE-R2, the third ESA (European Space Agency) EXPOSE facility, the second EXPOSE on the outside platform of the Russian Zvezda module, with four international astrobiological experiments into space. More than 600 biological samples of archaea, bacteria (as biofilms and in planktonic form), lichens, fungi, plant seeds, triops eggs, mosses and 150 samples of organic compounds were exposed to the harsh space environment and to parameters similar to those on the Mars surface. Radiation dosimeters distributed over the whole facility complemented the scientific payload. Three extravehicular activities later the chemical samples were returned to Earth on March 2, 2016, with Soyuz 44S, having spent 588 days in space. The biological samples arrived back later, on June 18, 2016, with 45S, after a total duration in space of 531 days. The exposure of the samples to Low Earth Orbit vacuum lasted for 531 days and was divided in two parts: protected against solar irradiation during the first 62 days, followed by exposure to solar radiation during the subsequent 469 days. In parallel to the space mission, a Mission Ground Reference (MGR) experiment with a flight identical Hardware and a complete flight identical set of samples was performed at the premises of DLR (German Aerospace Center) in Cologne by MUSC (Microgravity User Support Center), according to the mission data either downloaded from the ISS (temperature data, facility status, inner pressure status) or provided by RedShift Design and Engineering BVBA, Belgium (calculated ultra violet radiation fluence data). In this paper, the EXPOSE-R2 facility, the experimental samples, mission parameters, environmental parameters, and the overall mission and MGR sequences are described, building the background for the research papers of the individual experiments, their analysis and results.

Keywords: astrobiology, ground simulation, survival, UV, vacuum, extra-terrestrial UV radiation, temperature, space missions

INTRODUCTION

Space environment provides a variety of environmental extreme parameters that up to date cannot be simulated on ground. In particular the combination of low pressure, temperature oscillations, short wavelength UV (ultraviolet) and the complex cosmic ionizing radiation is only available in space and provides a research environment for astrobiology that resembles other solar system bodies and moons closer than laboratories on Earth can. One of the first opportunities for astrobiological samples to be exposed to space conditions was provided by Apollo 16 on its round trip to moon in 1972 (Bucker et al., 1973, 1974). Since Apollo, a variety of international astrobiological exposure experiments utilizing the space UV regime with short wavelength <295 nm cut off by the ozone layer on Earth, the ionizing radiation climate consisting of combinations of protons, electrons, and HZE [High Z (= atomic number) Energy] particles and microgravity were performed on retrievable and non-retrievable satellites as well as on space stations, developed by Space Agencies in United States, Europe, and Russia and reviewed in several papers (Taylor et al., 1974; Horneck, 1998a; Horneck et al., 2010; Raggio et al., 2011). Retrievable experiment platforms in Low Earth Orbit (LEO) allowing the postflight analysis of the experiments on ground were accommodated, e.g., on (i) space shuttles, as the German Exposure tray mounted 1983 on the cold plate of the cargo bay of Spacelab SL1 (Horneck et al., 1984a) and 1993 of Spacelab D2 (Horneck et al., 1996), (ii) retrievable free-flying satellites like the NASA Long Duration Exposure Facility (LDEF, 1984–1990) with the German Exostack (Horneck et al., 1994), the ESA (European Space Agency) Exobiology Radiation Assembly (ERA) flown 1992–1993 on the EUropean REtrievable CArrier (EURECA) (Horneck et al., 1995; Baglioni et al., 2007) and the satellites Bion-9 (Cosmos-2044, 1989), Bion-10 (1992/93), Bion-11 (1996) (Kuzicheva and Gontareva, 2003), Bion-M1 (2013) and five ESA BIOPAN missions (1994–2007) flown with Russian Foton satellites (Demets et al., 2005), (iii) space stations like the exposure platforms on Russian space missions that included the space stations Salyut-7 and MIR, the French "Exobiologie" experiment flown 1999 on the Russian MIR station (Rettberg et al., 2002) and the BIORISK canisters on the International Space Station (ISS) from IBMP/Roscosmos (2005–2009). Recently, non-retrievable free flying carriers of the CubeSat series equipped with *in situ* measurement systems like the NASA O/OREOS mission[1] (Woellert et al., 2011) indicate a new era of future active astrobiological experiments.

Access to space and its environment provides the opportunity to investigate the effects of extreme environmental conditions on life, supporting research on resistance strategies and underlying metabolic mechanisms, on the astrobiological questions of the origin and evolution of life, the limits of life and the habitability of other solar system bodies and the possible distribution of life beyond Earth. Many biological samples were exposed in astrobiological space missions, from microorganisms to small animals, lichen, and plant seeds (Horneck et al., 1984b, 2010; Horneck and Brack, 1992; Horneck, 1998b; Sancho et al., 2007; Jonsson et al., 2008). Focus was laid on the exploration of the lithopanspermia scenario, a hypothetic natural way of interplanetary transfer of life (Nicholson et al., 2000; Horneck et al., 2001; de La Torre et al., 2010; Raggio et al., 2011). Access to space also increases our knowledge on the interstellar, cometary, and planetary chemistry and its role in the origin of life (Kuzicheva and Gontareva, 2001, 2002; Cottin et al., 2008) and on the chemical modification, evolution, survival, and destruction of complex organics like polycyclic aromatic hydrocarbons, fullerenes and complex aromatic networks in outer space (Ehrenfreund and Foing, 1997). Recently, beginning in 2008, three consecutive astrobiological exposure missions were conducted on the ISS, carrying biological and chemical samples alike to space in the retrievable ESA multiuser exposure facilities EXPOSE (Rabbow et al., 2012, 2015).

THE EXPOSE-R2 FACILITY HARDWARE

The design of EXPOSE is based on the heritage of the Space Shuttle missions SL1 and D2 exposure platforms and ERA of the EURECA mission (Rabbow et al., 2009). ESA initiated the ERA Follow-on Scientific Study under ESA Contract no. 8116/88/F/BZ (SC) (Horneck et al., 1988) and as consequence developed the ESA-EXPOSE multiuser exposure facilities for long-term exposure of international and interdisciplinary experiments to the space environment on the outside of the ISS. The facility was designed following the scientific requirements to provide access to space environment, in particular (i) different UV regimes with respect to wavelength spectrum (i.e., Space, Mars) and transmitted irradiance (attenuation), (ii) space vacuum or other planetary atmospheres and pressures, (iii) temperature oscillation, with (iv) constant real time monitoring, and (v) telemetry of the environmental conditions and the facility health and status. In addition EXPOSE was required to facilitate long duration exposure in space for as many samples of different sizes as possible and the return of the samples to ground for analysis.

The EXPOSE core flight hardware (HW) was a box-shaped structure of 480 mm × 390 mm area and 140 mm height, and a mass of approximately 44 kg. It was equipped with four UV sensors (CUV 280 sensor, OEC GmbH, Germany), one on each corner of EXPOSE. In addition, one radiometer (Dexter 6M Thin Film Based Thermopile Detector) monitored the full solar electromagnetic spectrum[2]. A temperature sensor at the Reference Point of the core HW initiated the survival

Abbreviations: EGSE, Electrical Ground Support Equipment; ERA, Exobiology Radiation Assembly; ESA, European Space Agency; EURECA, European Retrievable Carrier; EVA, extravehicular activity, spacewalk; FOV, field of view; Gy, gray; HW, hardware; ISS, International Space Station; LDEF, Long Duration Exposure Facility; LEO, Low Earth Orbit; MgF_2, magnesium fluoride; MGR, Mission Ground Reference, Mission parallel Ground simulation; MUSC, Microgravity User Support Center; O/OREOS, Organism/Organic Exposure to Orbital Stresses; Pa, Pascal; PI, principal investigator; ppm, parts per million; PSI, Planetary and Space Simulation Facilities at DLR, Cologne, Germany; TLD, thermoluminescence dosimeter; UV, ultraviolet.

[1]http://ooreos.engr.scu.edu/dashboard.htm

[2]http://wwwsolar.nrl.navy.mil/solar_spectra.html

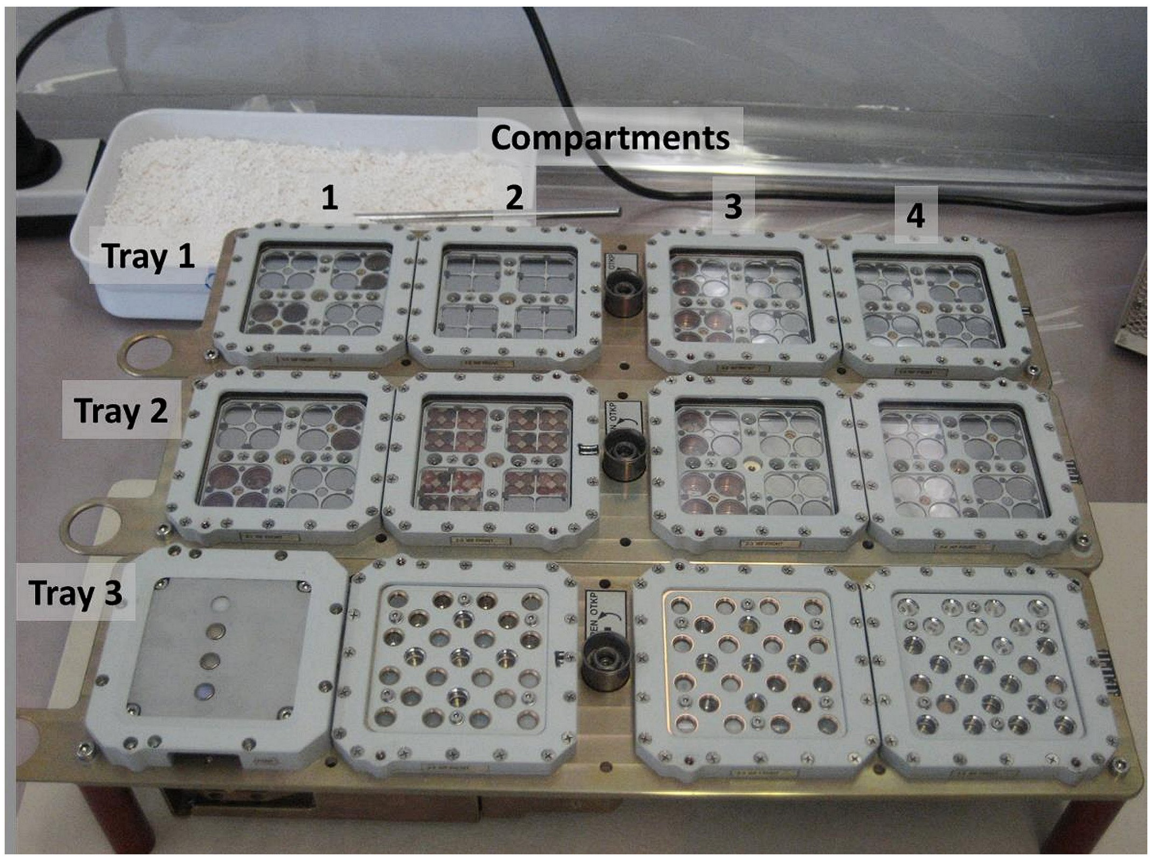

FIGURE 1 | EXPOSE-R2 flight trays with all experiments integrated. Top to bottom: Trays 1, 2, 3; left to right: compartments 1, 2, 3, and 4. Valves and earrings are on the left side. Bottom left compartment with the active radiation measurement instrument R3D. The earrings were intended to secure the trays during EVAs. Credit: DLR.

heaters at temperatures below −25°C to keep EXPOSE electronics operating. Three trays were inserted into the upper part of the box-shaped structure. Each tray measured 466 mm × 120 mm × 72 mm (length × width × height). The final mass of each tray was 5–5.5 kg. Four rectangular cavities of 77 mm × 83 mm and 33.5 mm depth, called compartments, accommodated stacks of two or three sample carriers. Each tray was equipped with a venting line connecting the compartments with the tray's valve (originally designed by Phitec, Switzerland). Valves opening and closing was commanded from ground. On the bottom side of trays 1 and 2, three temperature sensors were attached (type S 651 PDX 24 B by MINCO Europe, France). On the bottom of tray 3, two Minco sensors as in trays 1 and 2 were attached, and one AD590 sensor by Analog Devices. Plugs connected the trays with auxiliary electronics in the bottom part of the box-like structure. Together with the adapters for attachment to the external ISS platform on the Russian Zvezda Module it was called "monoblock."

The here described EXPOSE-R2 mission was the third EXPOSE mission, reusing the monoblock from EXPOSE-R, the first mission on the URM-D platform outside of the Russian Zvezda module, flown from March 2009 to February 2011. After 682 days exposure to the LEO environment, the complete EXPOSE-R facility was returned into the ISS, but only the three trays loaded with the scientific samples were returned to Ground at the end of the 833 days mission. The monoblock with the UV and radiation sensors, electronics and heaters remained stored inside the ISS. Therefore, the UV sensors could not be re-calibrated. An overview of the EXPOSE-R mission (Rabbow et al., 2015) and results of the experiments are presented in the same special issue of the International Journal of Astrobiology (Volume 14, Issue 1, 2015).

The compartments of each tray were numbered starting at the valve side of the tray and—for EXPOSE-R and -R2—the earring intended to secure the trays during extravehicular activities (EVAs) (**Figure 1**). An overview of the EXPOSE-E mission in 2008 and results of the experiments are presented in a special collection of Astrobiology 2012. EXPOSE-R2 environmental and status data were collected every 10 s and stored as well as down linked as telemetry. Data of the mission were made available to the investigators and the public on the MUSC (Microgravity User Support Center) web page[3] and used for the mission parallel Mission Ground Reference (MGR) experiments in the Planetary

[3]http://www.musc.dlr.de/expose-r-2/

and Space Simulation Facilities (PSI) at DLR (German Aerospace Center) in Cologne, Germany[4].

The biological samples were accommodated in stacks of two or three sample carriers into the compartments of the trays 1 and 2. Depending on the type, the sample carriers provided space for 64 samples of 7 mm diameter and 10 mm height (**Figure 2**) or for 16 samples of maximum 12 mm diameter and 4 mm height (for three layers, **Figure 3**) or 6 mm height (for two layers) in sample wells. The chemical samples in 25 individual sample containers called "cells" were integrated in two stacked sample carrier layers each in three compartments of tray 3 (**Figure 4**). This stacked conformation of the sample carriers allowed a completely identical exposure of all samples in one compartment to the space conditions except solar UV radiation. Only the samples in the top carriers were irradiated while the sample in the lower carriers were completely shaded, providing the respective in-flight dark controls. Each sample hole of the 16-well biological sample carriers was covered with an individual 2 mm thick magnesium fluoride (MgF_2) (tray 1) or quartz (tray 2) sample window. On top of each carrier, filter frames with two layers of selected cut off and neutral density (ND) filters were accommodated to attenuate the solar UV radiation. MgF_2 glassware allowed transmission of extraterrestrial short wavelength UV radiation with wavelength >120 nm and was accommodated in tray 1 (MolTech GmbH, Germany). For the simulation of a Mars-like UV spectrum with wavelength >200 nm in tray 2, quartz windows and filters were complemented by long pass cut off filters of approximately 50% transmission at 216 nm (MolTech GmbH, Germany; coated by ThinFilmPhysics, Switzerland). Individual wavelength independent UV attenuation for the EXPOSE-R2 samples was achieved by additional 0.1 or 0.001% transmission ND filters made of MgF_2 or quartz, respectively (MolTech GmbH, Germany; coated by ThinFilmPhysics, Switzerland). Each compartment was covered by an 8 mm thick optical MgF_2 (tray 1) or quartz (tray 2) top window (MolTech GmbH, Germany).

Tray 3 sample cells screwed into the sample carriers of the chemical experiment were individually closed by 1 mm thick MgF_2 windows to minimize UV transmission loss. The compartments accommodating the astrochemical experiment P.S.S. were closed by the upper sample carriers themselves. Top windows and the tray 3 upper carriers were sealed gas tight to the trays with window frames and O-rings screwed to the structure with 25 screws each. Only the first compartment of tray 3 was not connected to the venting line. This compartment was powered for the insertion of the active dosimetry instrument R3D-R2, a radiation sensor package for UV and ionizing radiation measurements. While the dosimeter was secured in the compartments also by a respective window frame, it was not sealed.

[4]http://www.dlr.de/spacesim

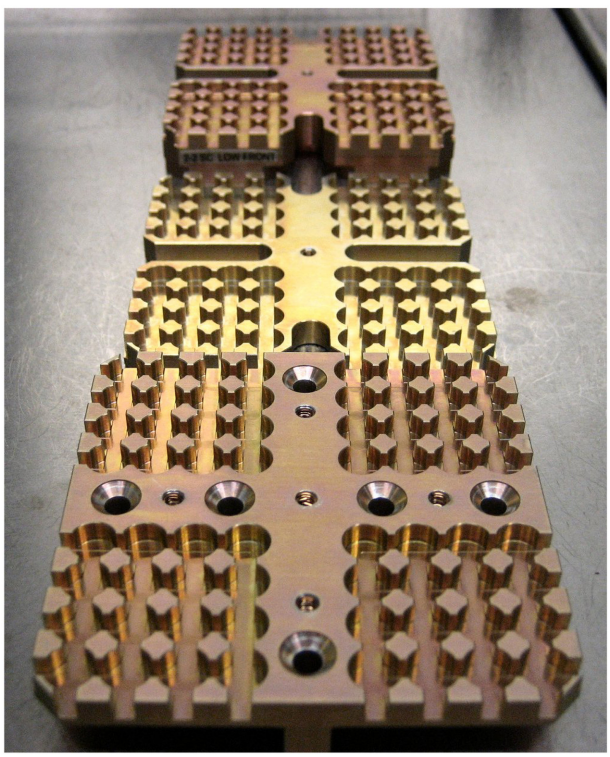

FIGURE 2 | Sixty-four-well sample carrier 2-2, three layers, from top to bottom: low, intermediate, and up carrier. Credit: DLR.

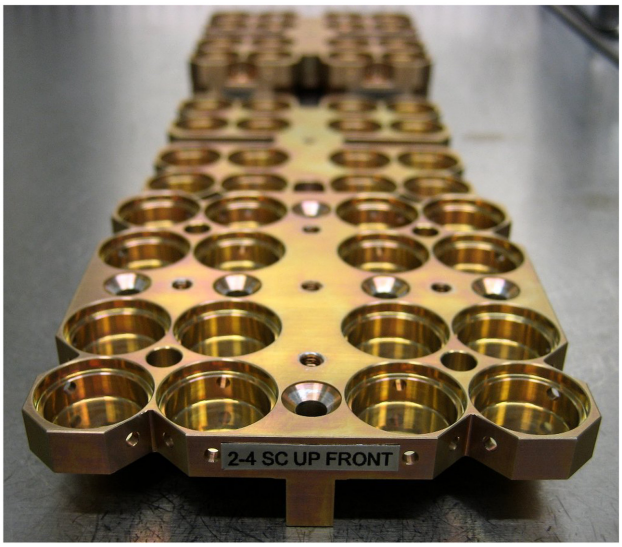

FIGURE 3 | Design of 16-well sample carriers 2-4 with three layers: top, middle, and bottom, marked up, intermediate, and low. Credit: DLR.

EXPOSE-R2 MISSION GROUND REFERENCE HARDWARE

In parallel to the space mission, an MGR experiment was performed at DLR, Cologne, Germany, using its PSI. A mission similar set of trays was provided to accommodate and expose a full flight parallel set of samples to simulated space parameters

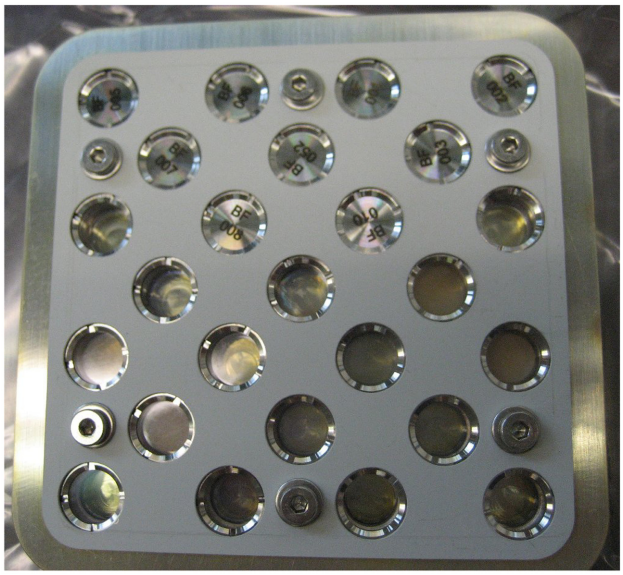

FIGURE 4 | Design of 25 cell top carrier of tray 3 P.S.S. experiment. Credit: Cottin, LISA.

as similar to those experienced by the flight samples in space as was technically feasible. The MGR trays were identical to the flight trays except that they were not powered. Therefore, they were not equipped with temperature sensors, the valves were operated manually and no active dosimeter R3D-R2 was foreseen, leaving the respective compartment 3-1 empty.

THE ASTROBIOLOGICAL EXPERIMENTS ON EXPOSE-R2

For the EXPOSE-R2 mission, three international experiments proposed in response to the ESA ILSRA 2009 Announcement of Opportunity were selected: two biological experiments BIOMEX [principal investigator (PI) J.-P. de Vera, DLR, Berlin, Germany] and BOSS (PI P. Rettberg, DLR, Cologne, Germany) and the organic chemical experiment P.S.S. (PI H. Cottin, LISA, Paris, France). In addition, the Russian biological experiment BIODIVERSITY was provided by IBMP, Moscow (Russia). Results of the experiments are expected to be published in Frontiers in Microbiology under the Research Topic Title: Habitability Beyond Earth and in an upcoming special collection of Astrobiology. The three ESA experiments were accommodated in three compartments each, while two compartments were allocated to the IBMP experiment. The remaining active compartment was reserved for the R3D-R2 instrument. The experiments, investigators, affiliations, countries, and the respective flown samples are collected in **Table 1**. The final numbers of samples per experiment are summarized in **Table 2**. The distribution of the experiments in EXPOSE-R2 is shown in **Figure 5** and an overview of the optical filters is given in **Figure 6**. All compartments except the active and completely separate R3D-R2 compartment in tray 3 were connected to the venting line of the respective trays, therefore open to the atmospheric conditions outside of the tray via the valve.

All biological samples were provided by the investigators and accommodated into the sample carriers by MUSC, DLR, Cologne. The chemical samples were provided already mounted in their sample carriers by the PI. The biological experiments BIOMEX, BOSS, and BIODIVERSITY exposed one set of their samples to LEO space conditions in tray 1 and another set to simulated Mars conditions in tray 2. Therefore partly identical samples were accommodated in tray 1 underneath short wavelength transparent MgF_2 windows and filter combinations and evacuated to space vacuum, and in tray 2 covered with window and filter combinations adjusting the LEO extraterrestrial UV spectrum to a Mars-like spectrum with wavelengths >200 nm and a Mars simulating atmosphere. All passive radiation dosimeters were either stacked into special holes in the 64-well upper sample carriers (DEPTH DOSE) or provided in aluminum holders ready for integration underneath each sample carrier stack on the bottom of the compartments (PDP). The PPO UV dosimeters were stacked into special holes in the filter frames and covered by additional 0.1 MgF_2 ND filter. With the support of the Payload Developer OHB and ESA, the three trays were fully loaded with all sample carriers and closed on June 12, 2014 in nitrogen atmosphere at the DLR premises in Cologne. The inner nitrogen gas in tray 2 was exchanged with a Mars like gas mixture composed of 95.55% CO_2, 2.70% N_2, 1.60% Ar, 0.15% O_2, ∼370 ppm H_2O (Praxair Deutschland GmbH) at a pressure of 980 Pa in the PSI at DLR, Cologne on July 2, 2014.

EXPOSE-R2 MGR SET-UP

For the MGR, a mission identical set of samples was accommodated in three ground trays. As for flight, the trays were closed with the appropriate glassware and inner gas: MgF_2 glassware and nitrogen gas at ambient pressure for tray 1 and 3 and quartz glassware and Mars gas and pressure for tray 2. The trays were accommodated on a special temperature controlled interface and connected to the vacuum facility PSI 2. For the MGR environmental exposure conditions simulating those experienced by the flight experiment were provided, except for UV < 200 nm, microgravity, and ionizing radiation. For the entire MGR duration pressure and atmospheric composition, temperature fluctuations, and UV 200–400 nm radiation were applied similar to the space flight experiment as far as technically possible. Because the UV sensors on the EXPOSE-R monoblock reused for EXPOSE-R2 never returned to ground for inspection and recalibration, the spectral UV irradiances and fluences were calculated by RedShift for the individual flight samples, using the UV sensor data to verify the underlying models. Final total fluences per compartment were simulated on ground with a SOL 2000 solar simulator (Dr. Hönle GmbH, Germany). The PSI facilities

TABLE 1 | List of EXPOSE-R2 experiments, investigators, and samples.

Experiment	Investigator	Affiliation	Samples
BIOMEX 1	D. Billi	University of Roma 2, Italy	*Chroococcidiopsis* CCMEE 029
BIOMEX 2	N. Kozyrovska	Kyiv, Ukraine	*Paenibacillus* and *Kombucha*
BIOMEX 3	S. Onofri	University Tuscia, Viterbo, Italy	*Cryomyces antarcticus*
BIOMEX 4	Th. Leya	Fraunhofer IBMT, Potsdam, Germany	*Chlamydocapsa* CCCryo 101-99 and *Nostoc commune* CCCryo 231-06
BIOMEX 5	R. de la Torre	INTA, Madrid, Spain	*Circinaria gyrosa*
BIOMEX 6	N. Feyh	TU Berlin, Germany	Biofilm
BIOMEX 7	P. Rettberg	DLR, Cologne, Germany	*Deinococcus radiodurans*
BIOMEX 8	S. Ott	University of Düsseldorf, Germany	Pigments and *Buellia frigida*
BIOMEX 9	B. Huwe	University of Potsdam, Germany	*Grimmia sessitana*
BIOMEX 10	D. Wagner	AWI Potsdam, Germany	*Methanosarcina* sp.
BIOMEX 11	C. Cockell	University of Edinburgh, Scotland, United Kingdom	*Gloeocapsa* OU20
BOSS 1	P. Rettberg (PI)	DLR, Cologne, Germany	*Deinococcus geothermalis*, biofilms and planktonic
BOSS 2	C. Cockell	University of Edinburgh, Scotland, United Kingdom	*Gloeocapsa* OU 20 biofilm
BOSS 3	S. Leuko H. Stan-Lotter	DLR, Cologne, Germany University of Salzburg, Austria	*Halomonas* salina, *Halococcus morrhuae salinarum* biofilms, planktonic and mixture of both
BOSS 4	K. Venkateswaran	JPL, Pasadena, United States	*Bacillus horneckiae*, spores
BOSS 5	D. Billi	University of Roma 2, Italy	*Chroococcidiopsis*, 029 and 057 biofilms and planctonic
BIODIVERSITY 1	V. Sychev (PI)	IBMP, Moscow, Russia	Variety of bacteria, fungi, plant seeds
BIODIVERSITY 2	O. Gusev	National Institute of Agrobiological Sciences, Tsukuba, Japan	*Anhydrobiotic chironomid* larvae
BIODIVERSITY 3	M. Sugimoto	Okayama University, Japan	*Hordeum vulgare* and *Brachypodium distachyon*
BIODIVERSITY 4	Th. Zierold	Naturkundemuseum Chemnitz, Germany	*Triops cancriformis* on clay in Finoplast
P.S.S. 1	H. Cottin (PI)	LISA, Paris, France	Chemical samples (comets, Titan, Mars)
P.S.S. 2	C. Szopa	LATMOS, Versailles, France	Chemical samples (Titan)
P.S.S. 3	M. Bertrand	CBM, Orléans, France	Chemical samples (meteorites)
P.S.S. 4	M. Dobrijevic	Observatoire de Bordeaux, France	Biochips
P.S.S. 5	A. Elsaesser	Leiden Observatory, Leiden, Netherlands	Chemical samples (interstellar medium)
P.S.S. 6	G. Baratta	Catania Observatory, Catania, Italy	Chemical samples (comets, graphite)
PDP, BIOCHIP, DEPTH DOSE	T. Berger	DLR, Cologne, Germany	TLDs
R3D-R2	T. Dachev	SRTI-BAS, Sofia, Bulgaria	Active instrument
PPOs	R. Demets	ESA-ESTEC, Noordwijk, Netherlands	PPO passive UV dosimeters

TABLE 2 | Amount of samples in EXPOSE-R2.

Experiment	Samples accommodated
BIOMEX	256
BOSS	128
BIODIVERSITY	224
P.S.S.	150
PDP, DEPTH DOSE	46
PPO	24
Total	828

were also extensively used during the pre-flight experiment verification tests and science verification tests to select and verify the most suitable test candidates and experimental set up.

MISSION SEQUENCE

On July 8, 2014, the three flight trays, sealed and packed in soft pouches and equipped with shock detectors and temperature loggers, were transported in a temperature controlled transport container via Munich and Moscow to Baikonur where they arrived July 23, 2014. Temperature and shock limits were not exceeded during transport. In Baikonur, the trays were accommodated into 56P Progress and launched successfully in the night of July 23, 2014 to the ISS. After docking on July 24, the trays were stored inside the ISS. On August 6, the three trays were inspected by the crew, integrated into the monoblock from EXPOSE-R stored on the ISS (**Figure 7**) and nominal function was confirmed. The now complete EXPOSE-R2 was covered and remained inside ISS until Aleksandr Skvortsov and Oleg Artemyev installed the complete facility on the URM-D platform

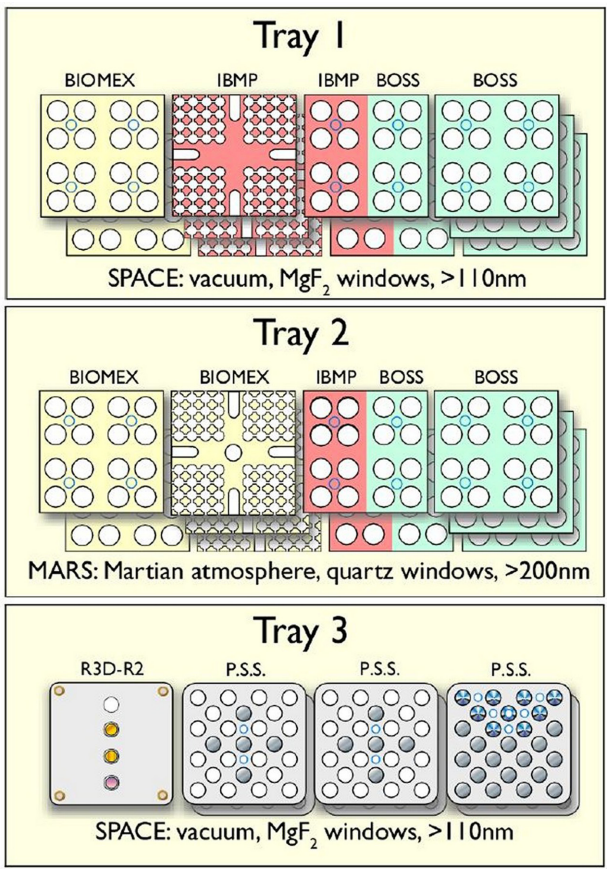

FIGURE 5 | Experiments as accommodated for flight in EXPOSE-R2. Credit: René Demets, ESA.

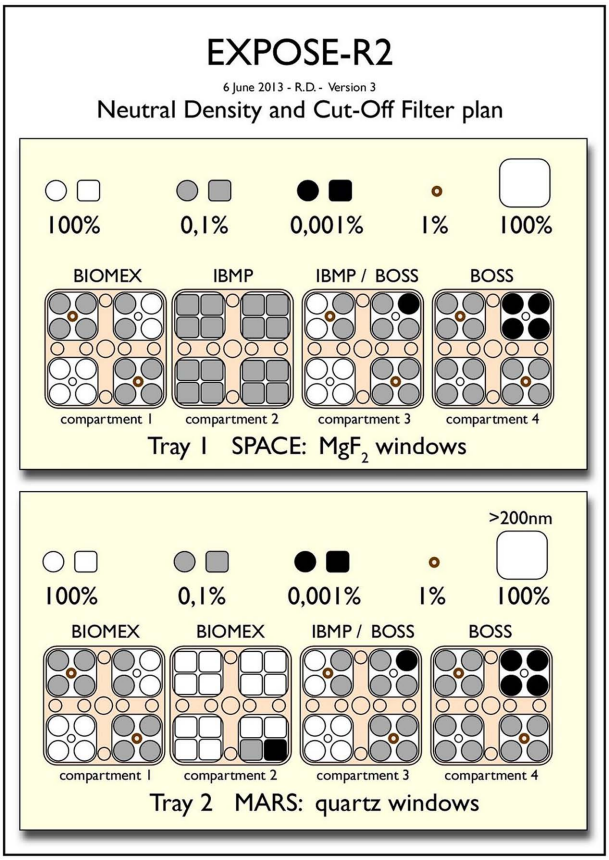

FIGURE 6 | Filter frame with integrated optical filters for trays 1 and 2. In the top left and bottom right quarters, PPO stacks covered by small round neutral density filters are integrated (brown circles). Credit: René Demets, ESA.

outside the Zvezda module during EVA-39 on August 18, 2014. On August 20, 2014, valves 1 and 3 of the still covered EXPOSE-R2 were opened by telecommand by Mission Control Center Moscow (MCC-M) marking the start of the vacuum exposure period of the experiment. Data transfer and R3D-R2 functionality were tested. While valve 1 at tray 1 functioned flawlessly, resulting in telemetry data confirming status open, valve 3 of tray 3 telemetry confirmed movement of the valve, but not to the final full open position. Status telemetry nevertheless confirmed valve 3 open and the baroswitches a decrease inside both trays 1 and 3. Therefore, final status "open and evacuated" was confirmed for both trays. Tray 2 remained closed to keep the simulated Mars atmosphere and 980 Pa pressure inside. During the following 62 days EXPOSE-R2 underwent a period of outgassing while protected against solar irradiation by its sun shield. This novel element in the mission operations was introduced after the EXPOSE-R mission, when several optical windows had acquired a discoloration (and thus a loss of transmission) during the spaceflight. The causative factor appeared to be the release of off gassing products from the facility itself and its test samples, which were subsequently photo-processed by solar UV at the inner window surfaces into a thin, semi-opaque contamination layer. To mitigate this unwanted effect on EXPOSE-R's successor -R2, the outgassing period in space was inserted to remove all volatiles suspected as cause for the window contamination. To avoid overheating of the electronics in this temporary thermally non-optimal configuration, EXPOSE-R2 had to be shut off. No temperature data became available for this period, but Feeder B was programmed to keep EXPOSE-R2 at a temperature above −25°C. After the dark evacuation period for trays 1 and 3 for 62 days, Commander Max Suraev and Alexander Samokutyaev removed the cover from the EXPOSE-R2 trays during EVA-40 (**Figure 8**) on October 22, 2014, starting the UV exposure of the experiments. Power was switched on October 23, 2014 and data were regularly received by telemetry confirming nominal status of EXPOSE-R2.

EXPOSE-R2 was programmed to collect environmental data every 10 s from the six temperature sensors, the four UV sensors, the radiometer, and the R3D-R2 experiment, complemented by health data and status data of the three valves. Data were downlinked regularly to MUSC, DLR via MCC-M. All data were archived, analyzed, and provided to the PIs on an ftp server. They were visualized on the interactive DLR-MUSC webpage (see text footnote 2). During the entire mission, no off-nominal event occurred.

FIGURE 7 | The EXPOSE-R2 trays integrated into the EXPOSE-R monoblock inside the ISS. Credit ESA, ROSCOSMOS.

On January 11, 2016, R3D-R2 power off and trays 1 and 3 valves closure commands were sent by MCC-M and acknowledged by EXPOSE-R2. Data received confirmed that the valve of tray 1 was closed, but the valve of tray 3 was not closed. After repeat of the command, EXPOSE-R2 data confirmed execution of the command to close valve 3. Data were thoroughly analyzed by OHB and MCC-M with the agreed conclusion that valve 3 was closed, capturing the space vacuum inside the tray as in tray 1 after 509 days of evacuation to space. After another month, during EVA-42 on February 3, 2016, Yuri Malenchenko and Sergej Volkov returned the complete EXPOSE-R2 facility into the ISS via the PIRS module, ending a total space exposure duration on the URM-D platform of 534 days and full LEO UV radiation for 469 days (ca. 16 months).

Later on ground during tray 3 inspection, it was confirmed that tray 3 valve was not closed properly. Hence, the tray most likely was re-pressurized in an unforeseen, uncontrolled way in the PIRS module on February 3, 2016, ending a 532 days vacuum period for tray 3.

Tray 3 Return to Ground

Before return to ground, EXPOSE-R2 was stored for 28 days inside the ISS until on March 2, 2016, tray 3 touched down at Karaganda on-board the 44S return capsule at an outside temperature around −3°C. It was packed in a pouch and transport container with temperature and shock monitoring and returned via helicopter to the city of Zhezkazgan in Kazakhstan, from there by plane to Moscow and Munich and finally by car to DLR, Cologne where it arrived in the morning of March 7, at 8:00 h. A first inspection confirmed that shock and temperature limits were not exceeded. Already in Moscow, inspection of the tray 3 baroswitch indicated an inner tray pressure >10,000 Pa, confirming the misgivings of a premature and uncontrolled pressurization of the tray at the end of EVA-42 during return into the ISS. Nevertheless, the valve closed signal retrieved by telemetry was confirmed by tray 3 Electrical Ground Support Equipment (EGSE). After thorough investigation, the reason for the ambivalent information was attributed to a fault in a micro-switch operation.

On March 8, 2016, tray 3 was imported into the anaerobic workbench flooded with nitrogen at ambient pressure at DLR, Cologne. The R3D-R2 instrument was disassembled from compartment 1. When the window frames could be removed from the P.S.S. top carriers and the carriers removed from the tray without previously operating the valve, it was confirmed once more that the tray was already pressurized. The carriers were transferred into a glass desiccator capturing the nitrogen gas. The R3D-R2 instrument was exported from the workbench, inspected, packed, and returned by courier. R3D-R2 arrived safely at the investigators premises on March 16th, 2016. The PDP passive dosimeters were also exported from the workbench and directly handed over to the investigator. P.S.S. carriers were removed from the glass desiccator inside the workbench, sealed into plastic bags inside the nitrogen flooded anaerobic workbench

FIGURE 8 | EXPOSE-R2 uncovered in space. The EXPOSE-R monoblock was reused but refurbished with three new trays carrying the samples of the EXPOSE-R2 mission. Credit ESA, ROSCOSMOS.

at DLR and returned hand-carried together with additional 5°C constant temperature MGR P.S.S. carriers to the PI on March 14, 2016 by CNES.

After de-integration of a part of the P.S.S. sample cells by the PI, the flight P.S.S. carriers with remaining sample cells returned once more to DLR on June 7 for short storage and transportation support to Co-investigators in Berlin. After 22 days storage under nitrogen gas in the anaerobic workbench, the P.S.S. carriers were transported together with the BIOMEX carrier stack of compartment 2 of tray 2 to Berlin on June 29, 2016 upon request of the PIs (see below).

Trays 1 and 2 Return to Ground

After EVA-42 the remaining two trays were stored in orbit until June 18 for a total of 136 days when they returned to ground with Soyuz 45S. Both trays were stored for return in the cargo compartment underneath the seats of the crew in the Soyuz capsule. Tray 1 was inverted, i.e., with the top window oriented in the same direction as the main g-vector, while tray 2 was oriented in with top windows facing away for g-vector. The latter orientation accelerated the sample toward their carriers. Regardless of the orientation, all samples remained unaffected inside their individual sample wells. The Soyuz capsule landed on June 18, 2016 in Kazakhstan. Temperature at landing site was a sunny 25°C. Similar to tray 3, the trays were packed into bags and transported to Moscow where they arrived on June 19. The first postflight inspection confirmed all valves closed and nominal low inner pressure. The trays were flown to Munich arriving on June 21 and driven by car in the cooling transportation container at 15°C to DLR, Cologne, where they arrived Wednesday, June 22. Shock and temperature limits were not exceeded. After close inspection, both trays were transferred into the anaerobic workbench with nitrogen gas for opening and disassembly of the sample carriers. In order to open the trays, they were equilibrated with ambient pressure nitrogen by opening the valves inside the nitrogen bench via the connected EGSE. All four top window frames and top windows of each tray were removed after unscrewing of the 25 screws attaching each window frame to the tray. Filter frames were unscrewed and removed. Finally, all carrier stacks were unscrewed, removed, and stacked in the original order in a sterile metal box that was used for export from the nitrogen work bench to a sterile biological safety cabinet. The PDP aluminum holders were removed from the bottom of the compartments, also exported from the workbench and directly handed over to the PI. Samples of the BIOMEX 10 experiment from GFZ Potsdam (previously AWI) were oxygen intolerant. Therefore, they were de-integrated from the sample carriers 2-2 directly inside the nitrogen filled anaerobic workbench and transferred into special anaerobic flasks before they were exported from the anaerobic workbench and returned to the investigator. BIOMEX 2 samples from Kyiv, Ukraine, BIOMEX 6 samples from TU Berlin, and BIOMEX 7 samples from DLR, Cologne were also de-integrated inside the workbench form carriers 2-2, exported via the airlock and

TABLE 3 | EXPOSE-R2 mission sequence durations overview.

Mission period	Duration
Inside ISS period launch to EVA-39	26 days
Dark evacuation period valve open to EVA-40	62 days
Valve open to valve closed	509 days
Outside space evacuation period	531 days
Outside data availability	468 days
Total vacuum period tray 3 (closure to PIRS)	532 days*
Total vacuum period tray 1	672 days
Mars gas period tray 2 after second closing	722 days
Outside UV irradiation period EVA-40 to EVA-42	469 days
Outside mission period EVA-39 to EVA-42	534 days
Post-outside storage in ISS tray 3	28 days
Post-outside storage in ISS trays 1 + 2	136 days
Total mission duration tray 3 launch to landing	588 days
Total mission duration trays 1 + 2 launch to landing	696 days

**With uncontrolled pressurization in PIRS.*

TABLE 4 | EXPOSE-R2 MGR sequence durations overview.

MGR period	Duration
Inside ISS period temperature simulation	26 days
Mission temperature simulation according to data	468 days
Total vacuum period MGR tray 3	566 days*
Total vacuum period MGR tray 1	672 days
Mars gas period MGR tray 2	722 days

**Nominal expected evacuation period.*

returned to the respective investigators, leaving the carriers 2-2 with the remaining BIOMEX 8 samples under anaerobic conditions inside the workbench where they were stored in a nitrogen equilibrated glass desiccator until return to the PI together with the stored remaining P.S.S. carriers on June 29, 2016. All other samples of trays 1 and 2 were de-integrated from the sample carriers under ambient but sterile conditions, packed and returned to the individual investigators. For details of Mission and MGR sequnce durations refer to **Tables 3**, **4** respectively. Results of the respective experiments are expected to be published in Frontiers in Microbiology under the Research Topic Title: Habitability Beyond Earth and in an upcoming special collection of Astrobiology.

MISSION ENVIRONMENTAL PARAMETER

Temperature Profile during Full Exposure Period

Lower limit of the temperature was determined by Feeder B and the associated heating system, preventing a temperature decrease below −20°C. Temperature data from the trays were not available until EXPOSE-R2 was powered after EVA-40 October 23, 2014. For the next 16 months, data were regularly downlinked every month to MUSC via the MCC-M. Highest temperature measured

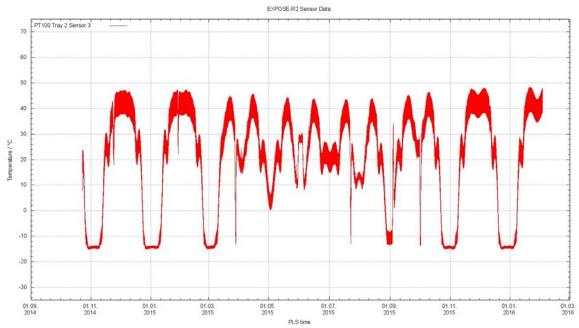

FIGURE 9 | Overview of the EXPOSE-R2 tray temperature profiles for tray 2 temperature sensor 3 and the respective mission period from October 23, 2014 to February 2, 2016 when EXPOSE-R2 was powered and data available. Credit OHB.

during the mission was 57.98°C at tray 3 compartment 4. Lowest temperature of −20.9°C was detected by the temperature sensor of tray 3 compartment 2. In general, compartments closer to the ISS, i.e., measured by temperature sensors 1-3, 2-3, and 3-3, experienced the higher temperatures during warm periods and were not as cold as compartments facing space during cold periods. A temperature plot for tray 2 temperature sensor 3 for the respective mission period from October 23, 2014 to February 2, 2016, is shown in **Figure 9**: a fast rhythm of temperature fluctuations of approximately 10°C in warm periods and a few degrees in cold periods with a periodicity of approximately 90 min according to day/night times of each orbit were overlaid by approximately 1 month cycles from cold periods reaching −20°C limited by the Feeder B heating system up to 50°C in warm periods. This slow rhythm was due to the changing position of the orbital plane of the ISS w.r.t the sun. From April 2015 to August 2015, these colder phases of the 1 month rhythm reached a minimum of only 0°C with most of the colder periods not decreasing below 20°C. Therefore, a total of 12 warm periods with temperatures of more than 30°C alternated with three cold periods with temperatures below −10°C before the April to August warm period and five periods with temperatures below −10°C after that period.

UV Irradiation

The total mission average UV-fluence values were calculated by RedShift. To calculate shadow maps for the upper side of EXPOSE-R2, ISS mission flight data of the ISS position in its orbit, ISS attitude, joint angles defining positions of solar arrays and radiators provided by DLR MUSC were used. Evolution of the ISS configuration (3D models), visiting spacecraft and the respective fields of view (FOV) were taken into account for the resulting total mission fluence data for each of the 12 compartments. The UV fluences for the individual compartments and experiments were determined with regard to the different sizes and heights of the samples, leading to different FOVs. As a compromise, the means of the corresponding individually determined FOVs of the samples per compartment were taken. Fluence values for the full spectrum of the extraterrestrial sun as

well as for different wavelength ranges were provided. Fluences for the wavelength range from 200 to 400 nm were applied to the respective compartments and experiments during the MGR; the highest fluence was 739 $MJm^{-2}{}_{200-400\ nm}$ at compartment 3-2, lowest fluence was 437 MJm^{-2} at compartment 2-1. Note that these fluences reflect the combination of the mean FOV of the samples of the individual compartments and the solar insolation variation over the EXPOSE-R2 surface.

The mean fluence for the biologically active wavelength rage of 200 to 400 nm calculated for EXPOSE-R2 was 536 ± 116 MJm^{-2}. The fluences per tray were similar for tray 1 (458 ± 32 $MJm^{-2}{}_{200-400\ nm}$) and tray 2 (492 ± 66 $MJm^{-2}{}_{200-400\ nm}$), due to the similar geometry of the samples and their FOV. For tray 3, the mean value was 731 ± 12 $MJm^{-2}{}_{200-400\ nm}$; sample geometry of tray 3 resulted in an increased FOV and therefore higher fluences compared to trays 1 and 2. Calculated UV data and the underlying model were verified using the UV data of the four UV sensors and the radiometer of the mission period between EVA-40 and EVA-42 when EXPOSE-R2 was powered and not covered. Calculations of the respective UV fluences at sample site underneath each individual optical filter combination for each individual (FOV) and taking into account the UV-attenuating effect of the window "contamination" (see below) together with further detailed information and results on the irradiation of EXPOSE-R2 are expected to be published in the upcoming special collection of Astrobiology by Beuselinck (in preparation).

Window Inspection

A first visual inspection of the top windows revealed a slight, light-brown discoloration on all MgF_2 windows of tray 1—referred to as "contamination" in accordance with a similar finding after the EXPOSE-R mission—while the quartz windows of tray 2 seemed clear, except the quartz window on compartment 2-3, also showing a light-brown discoloration. In all cases, the contamination seemed to be less than after the EXPOSE-R mission. This improvement can be attributed to three factors: 1. On EXPOSE-R2, the monoblock of EXPOSE-R was re-used, and had already undergone outgassing in space during its first mission; 2. The period of sun-exposure (with ensuing photoprocessing of volatile materials by solar light) was shorter on -R2 than on -R; 3. EXPOSE-R2 was subjected to an 8-week period of evacuation before solar irradiation was started (see above). Further results on the investigation of this phenomenon are expected to be published in the upcoming special collection of Astrobiology (Demets, in preparation). Data on the solar spectral UV and VIS irradiances from the active R3D-R2 experiment in compartment 3-1 measured every 10 s in addition to ionizing radiation were regularly downloaded together with all other science and status data and provided to the investigator. Publication of the results in the upcoming special collection of Astrobiology is expected by Schuster (in preparation).

Cosmic Radiation

Cosmic ionizing radiation experienced by EXPOSE-R2 was measure with passive detectors of the PDP and DEPTH DOSE experiments and the active R3D-R2 instrument. Additional thermoluminescence dosimeters (TLDs) were accommodated in some P.S.S. BIOCHIP cells. Preliminary averaged absorbed daily dose rates determined for the three essential components of the radiation field encountered at the orbit of the ISS were: (i) inner Radiation Belt (South Atlantic Anomaly protons) varying from 340 to 844 $\mu Gy\ d^{-1}$ due to altitudinal changes of the ISS, (ii) galactic cosmic rays (GCR) slowly moving up from 68 to 82 $\mu Gy\ d^{-1}$ due to the falling solar activity and rising GCR flux over the whole period, and (iii) outer Radiation Belt (electrons) peaking at 2960 $\mu Gy\ d^{-1}$ (Dachev et al., Results presented during the EXPOSE-R2 Postflight Review, ESTEC, December 2016) (Dachev et al., 2016).

The DOSIS-R2 passive TLDs of the PDP and DEPTH DOSE experiment were distributed over the whole facility in stacks in special cavities between the sample holes of the top UV-exposed sample carriers with very low shielding (down to a few $\mu m/cm^2$) and below the sample carrier stacks at the bottom of the compartments of all three trays. The total mission dose reached values up to 1 Gy (Berger et al., results presented during the EXPOSE-R2 Postflight Review, ESTEC, December 2016). Results are expected to be published in the upcoming special collection of Astrobiology by Berger (in preparation).

Space Vacuum

The atmospheric pressure outside of the ISS at the Zvezda module was not measured directly by EXPOSE-R2. The Russian agency RSC Energia determined the pressure varying between 1.33×10^{-3} and 1.33×10^{-4} Pa (10^{-5} and 10^{-6} mm of mercury). The lower pressure usually accounts for the Wake direction (the rear of the ISS relative to flight direction), the higher pressure for the Ram direction (the front of the ISS relative to flight direction).

THE EXPOSE-R2 MGR PERFORMANCE AND ENVIRONMENTAL PARAMETER

All four astrobiology experiments BOSS, BIOMEX, BIODIVERSITY, and P.S.S. participated in the MGR with a flight identical set of samples. The dosimetry experiments were not included in the MGR, because ionizing radiation was not an intended part of the mission simulation. Three ground trays identical to the flight trays with respect to the samples interface were loaded with the flight-identical set of samples and covered with flight-identical optical filtering systems. Inner tray gas and pressure was provided identical as for flight. All three trays were closed under nitrogen atmosphere and the captured nitrogen gas inside tray 2 was exchanged with Mars gas at a pressure of 980 Pa similar to the flight tray 2 with a delay of nearly months with respect to the flight trays end of August 2014. The two year EXPOSE-R2 MGR started with the accommodation of the three trays on the temperature controlled interface on August 28, 2014 and ended on August 16, 2016 with the removal of the trays from the temperature controlled interface of the PSI at DLR. Thereafter, all samples were de-integrated under sterile conditions and similar in sequence as the flight samples and distributed to the investigators for analysis. During the space

mission, all data were received in time and without major outages or data loss for the mission simulation.

Temperature Simulation

Automated temperature simulation for the three MGR trays on the temperature controlled interface started with application of transport temperatures where available with a delay of maximum 2 months due to data analysis and reformatting processes. As soon as environmental data measured and downlinked from EXPOSE-R2 in orbit became available, they were also analyzed and fed into the MGR simulation program of the PSI at DLR, Cologne, controlling the on ground MGR tray temperature simulation according to the data frequency in 10 s steps. After return of the flight trays into the ISS, a Zvezda inner temperature data profile was provided by MCC-M and applied to the MGR samples. Transport data of tray 3 return and trays 1 and 2 return were simulated individually after the appropriate simulated delay times to mimic as best as possible the different flight trays return dates and situations. Flight trays temperatures and MGR temperatures measured at the tray structure (as in flight) deviated by maximum 2°C.

Vacuum Simulation

On October 15, 2014, MGR trays 1 and 3 were attached to the PSI vacuum facilities and evacuated, simulating the opening of the valves of the respective trays in space and marking the start of the space exposure simulation. Final pressure values of the MGR trays 1 and 3 varied between 1×10^{-5} and 6×10^{-5} Pa, depending on the simulation temperature. The premature pressurization due to the malfunction of the flight tray 3 valve before return of the trays into the ISS was not simulated. Instead, upon request of the PI, the nominal mission vacuum duration was simulated and the valve of the MGR tray 3 was closed and the tray re-pressurization in nitrogen performed after a total of 672 days.

UV Irradiation Simulation

As in space, all three MGR trays remained covered light tight for 62 days after evacuation. Thereafter, calculated total mission UV fluences for each compartment provided by RedShift for the wavelengths 200 to 400 nm determined the total MGR simulation irradiation fluences applied using the solar simulator SOL2000 (Dr. Hönle GmbH). The lamps continuous spectrum with wavelengths >200 nm was measured with a calibrated Bentham 150 spectroradiometer (Gigahertz, Türkenfeld, Germany) at the top of the EXPOSE-R2 MGR trays. The MGR compartments were irradiated on ground individually with the same UV fluences for the wavelength range 200–400 nm as determined for the space borne facility. An overview of the EXPOSE-R2 mission and MGR sequence durations with respect to exposure parameters are given in **Tables 3**, **4**, respectively.

CONCLUSION

EXPOSE-R2 accommodating four astrobiological experiments (BOSS, BIOMEX, BIODIVERSITY, and P.S.S.), the passive dosimeters and the active dosimeter R3D-R2 was launched to the ISS on July 23, 2014. It was installed on the external URM-D platform of the Zvezda module on August 18, 2014. Following a 2-month dark evacuation phase, the experiments were exposed to UV for 469 days until February 3, 2016, when the complete facility was returned into the ISS. The three trays were downloaded with Soyuz in 2 steps due to limited download capacities: Tray 3 returned to ground on March 2, 2016, trays 1 and 2 on June 18th, 2016. The EXPOSE monoblock originating from the EXPOSE-R mission again remained stored on board of the ISS for possible further use. During the exposure period, trays 1 and 3 were open to space vacuum and extraterrestrial solar UV radiation >120 nm, while tray 2 kept an inner artificial Mars atmosphere at 1000 Pa pressure and admitted a Mars UV spectrum with wavelengths >200 nm. The mission was carried out in compliance with the requirement of all experiments for (i) space exposure duration of minimum 12 months to maximum 18 months, (ii) storage time after final integration of all samples in the sample carriers until upload of maximum 6 months, (iii) storage on the ISS prior to the space exposure, and (iv) after space exposure of maximum 6 months and v) de-integration until hand over of the samples to the scientists of several weeks. For the complete storage and transportation times, all three experiments requested monitored and controlled temperatures of preferred ambient 20°C with a minimum of 4°C and a maximum of 30°C. During the exposure period, requested upper temperature limits was 60°C. All temperature limits were met. Temperatures experienced on the ISS ranged from −20.9 to 58.0°C, without any individual temperature peak as during the EXPOSE-E mission. In contrast to the two previous EXPOSE missions, no data were lost or corrupted apart from some individual time points.

The selection of appropriate samples, the development of sample design and preparation and the definition of exposure limits were supported by the preflight tests performed in space simulation facilities. In addition, the complete integrated experiment set up for a full mission parallel MGR provided (i) complementing data for comparison and discrimination of effects induced by space parameters, (ii) corrective approaches for the mission simulation experiment as for the P.S.S. experiment in case of off nominal events during the mission, and (iii) a backup in case of major malfunctions or loss of experiments. In general, access to space simulation facilities increases experiment space for increased sample numbers exposed to space conditions, even if they are just simulated, thus providing a valuable additional experiment environment.

Nevertheless, access to space remains irreplaceable for astrobiological investigations and the quest for the limits of life. The complex combination of environmental conditions in space cannot be accurately simulated. Solar simulators can only approximate the short wavelength solar extraterrestrial UV spectrum; simulation of its combination with other space parameters is even less accurate. Therefore, access to space missions for experiments exposing samples to space conditions outside of a spacecraft and with that, outside of Earths protecting atmosphere, ozone layer and—if possible—magnetosphere for prolonged exposure durations remains important.

Though the EXPOSE-R2 mission was an overall success, several issues for improvement for future space missions were identified:

- UV dosimetry. The unavailability of the UV sensors for re-calibration was known in advance. Therefore, UV calculation was procured from the beginning of the EXPOSE-R2 mission, using the UV data only for verifying purposes. Nevertheless, reliable UV fluence measurements are necessary for analysis and interpretation of the data retrieved from the biological and chemical samples.
- Shadowing. Complex carriers like the ISS are by themselves shadow casting obstacles for solar radiation exposure experiments mounted on its external platforms. This leads to a gradient in the insolation over the whole exposure area and to sometimes unexpected shadowing of certain areas (Beuselinck, personal communication) that should be avoided as much as possible.
- Pressure. Pressure data were provided by the Russian operations team, but were not measured at the EXPOSE-R2 facility. For experiments utilizing space vacuum, a pressure detection system at facility site or—preferable—at sample site should be obvious.
- Safety. Safety concerns are a major issue on manned spacecraft. As consequence, selection of test systems is constricted to those that proof to not pose possible hazards to the crew. The accommodation of facilities like EXPOSE on unmanned free flying satellites would reduce the risk of safety problems, provide faster access to space and to a wider range of orbits or even interplanetary routes.

Multiuser exposure facility like EXPOSE are both, a constraint and a benefit for science. While on one side, the experiments accommodated together on one facility by nature have to agree on a common space mission scenario in particular with respect to mission duration, on the other side, the simultaneous exposure allows comparison of results and common use of data as for example those derived from the dosimetry experiments and a higher visibility of the mission.

AUTHOR CONTRIBUTIONS

ER, PR, AP, and CP contributed to the scientific support, accommodation, and MGR of EXPOSE-R2. WS, FM, and EJ contributed in all HW and operation design and information aspects. RD was Mission science responsible, PW and RW contributed with Mission operations and respective Information. All authors provided Information in their field to the manuscript and proof read.

FINAL REMARKS AND ACKNOWLEDGMENTS

After all flight and MGR samples of the EXPOSE-R2 mission were distributed, the era of astrobiological exposure experiments on EXPOSE facilities preliminarily ended.

Three EXPOSE missions have successfully been flown with exposure durations between 1.5 and 2 years in orbit. EXPOSE-R and EXPOSE-R2 impressively demonstrated the reusability of the facility's monoblock and fast turnover time between the two missions.

Exposing several hundred to more than a thousand biological and chemical samples and dosimeters of the respective astrobiological experiments, the three EXPOSE missions leave a huge amount of data. The success of the missions can be evaluated by the two special issues already published for the EXPOSE-E mission (Astrobiology, Volume 12, No 5, 2012) and for the EXPOSE-R mission (International Journal of Astrobiology, Volume 14, Issue 1, 2015). Published results of the individual experiments and investigators of the EXPOSE-R2 mission described here are expected online in Frontiers in Microbiology under the upcoming Research Topic titled "Habitability Beyond Earth" and in an upcoming special collection of Astrobiology online and in print. For these publications, this article is meant as background information on the mission itself and the complimenting MGR.

The authors would like to express their special thanks to ESA for providing the flight opportunity and all HW of the EXPOSE-R2 mission and MGR, as already for the previous EXPOSE missions and for supporting the operation under the respective MUSC contracts. Thanks go also to the payload developer OHB with all subcontractors for the always constructive and friendly teamwork and the PIs with their investigator groups for working out all sample related issues. Without the dedication and space enthusiasm of all, the mission would not have been possible.

REFERENCES

Baglioni, P., Sabatini, M., and Horneck, G. (2007). "Astrobiological experiments in low earth orbit: facilities, instrumentation, and results," in *Complete Course in Astrobiology*, eds G. Horneck and P. Rettberg (Berlin: Wiley-VCH), 273–320.

Bucker, H., Horneck, G., Allkofer, O. C., Bartholoma, K. P., Beaujean, R., Cuer, P., et al. (1973). The biostack experiment on Apollo 16. *Life Sci. Space Res.* 11, 295–305.

Bucker, H., Horneck, G., Wollenhaupt, H., Schwager, M., and Taylor, G. R. (1974). Viability of *Bacillus subtilis* spores exposed to space environment in the M-191 experiment system aboard Apollo 16. *Life Sci. Space Res.* 12, 209–213. doi: 10.1016/B978-0-08-021783-3.50033-7

Cottin, H., Coll, P., Coscia, D., Fray, N., Guan, Y. Y., Macari, F., et al. (2008). Heterogeneous solid/gas chemistry of organic compounds related to comets, meteorites, Titan, and Mars: laboratory and in lower Earth orbit experiments. *Adv. Space Res.* 42, 2019–2035. doi: 10.1016/j.asr.2007.09.017

Dachev, T. P., Tomov, B. T., Matviichuk, Y. N., Dimitrov, P. G., and Bankov, N. G. (2016). High dose rates obtained outside ISS in June 2015 during SEP event. *Life Sci. Space Res.* 9, 84–92. doi: 10.1016/j.lssr.2016.03.004

de La Torre, R., Sancho, L. G., Horneck, G., De Los Rios, A., Wierzchos, J., Olsson-Francis, K., et al. (2010). Survival of lichens and bacteria exposed to outer space conditions - Results of the *Lithopanspermia* experiments. *Icarus* 208, 735–748. doi: 10.1016/j.icarus.2010.03.010

Demets, R., Schulte, W., and Baglioni, P. (2005). The past, present and future of BIOPAN. *Adv. Space Res.* 36, 311–316. doi: 10.1016/j.asr.2005.07.005

Ehrenfreund, P., and Foing, B. H. (1997). Fullerenes in space. *Adv. Space Res.* 19, 1033–1042. doi: 10.1016/S0273-1177(97)00350-5

Horneck, G. (1998a). Biological monitoring of radiation exposure. *Adv. Space Res.* 22, 1631–1641. doi: 10.1016/S0273-1177(99)00028-9

Horneck, G. (1998b). Exobiological experiments in earth orbit. *Adv. Space Res.* 22, 317–326.

Horneck, G., and Brack, A. (1992). Study of the origin, evolution and distribution of life with emphasis on exobiology experiments in earth orbit. *Adv. Space Biol. Med.* 2, 229–262. doi: 10.1016/S1569-2574(08)60023-4

Horneck, G., Bucker, H., Dose, K., Martens, K. D., Bieger, A., Mennigmann, H. D., et al. (1984a). Microorganisms and biomolecules in space environment experiment ES 029 on Spacelab-1. *Adv. Space Res.* 4, 19–27.

Horneck, G., Bucker, H., and Reitz, G. (1994). Long-term survival of bacterial spores in space. *Adv. Space Res.* 14, 41–45. doi: 10.1016/0273-1177(94)90448-0

Horneck, G., Bucker, H., Reitz, G., Requardt, H., Dose, K., Martens, K. D., et al. (1984b). Life sciences: microorganisms in the space environment. *Science* 225, 226–228.

Horneck, G., Cadet, J., Dose, K., Fritz-Niggli, H., and Kiefer, J. (1988). *ERA Follow-on Scientific Study: Perspectives of Exobiological and Radiation Biological Research by use of Free-flying Carriers in Earth Orbit.* Final Report ESA-SC. Paris: European Space Agency.

Horneck, G., Eschweiler, U., Reitz, G., Wehner, J., Willimek, R., and Strauch, K. (1995). Biological responses to space: results of the experiment "Exobiological Unit" of ERA on EURECA I. *Adv. Space Res.* 16, 105–118. doi: 10.1016/0273-1177(95)00279-N

Horneck, G., Klaus, D. M., and Mancinelli, R. L. (2010). Space microbiology. *Microbiol. Mol. Biol. Rev.* 74, 121–156. doi: 10.1128/MMBR.00016-09

Horneck, G., Rettberg, P., Rabbow, E., Strauch, W., Seckmeyer, G., Facius, R., et al. (1996). Biological dosimetry of solar radiation for different simulated ozone column thicknesses. *J. Photochem. Photobiol. B* 32, 189–196. doi: 10.1016/1011-1344(95)07219-5

Horneck, G., Rettberg, P., Reitz, G., Wehner, J., Eschweiler, U., Strauch, K., et al. (2001). Protection of bacterial spores in space, a contribution to the discussion on Panspermia. *Orig. Life Evol. Biosph.* 31, 527–547. doi: 10.1023/A:1012746130771

Jonsson, K. I., Rabbow, E., Schill, R. O., Harms-Ringdahl, M., and Rettberg, P. (2008). Tardigrades survive exposure to space in low Earth orbit. *Curr. Biol.* 18, R729–R731. doi: 10.1016/j.cub.2008.06.048

Kuzicheva, E. A., and Gontareva, N. B. (2001). Study of the peptide prebiotic synthesis in context of exobiological investigations on earth orbit. *Adv. Space Res.* 28, 713–718. doi: 10.1016/S0273-1177(01)00325-8

Kuzicheva, E. A., and Gontareva, N. B. (2002). Prebiotic synthesis of nucleotides at the earth orbit in presence of lunar soil. *Adv. Space Res.* 30, 1525–1531. doi: 10.1016/S0273-1177(02)00367-8

Kuzicheva, E. A., and Gontareva, N. B. (2003). Exobiological investigations on Russian spacecrafts. *Astrobiology* 3, 253–261. doi: 10.1089/15311070376901635 2

Nicholson, W. L., Munakata, N., Horneck, G., Melosh, H. J., and Setlow, P. (2000). Resistance of *Bacillus* endospores to extreme terrestrial and extraterrestrial environments. *Microbiol. Mol. Biol. Rev.* 64, 548–572. doi: 10.1128/MMBR.64.3.548-572.2000

Rabbow, E., Horneck, G., Rettberg, P., Schott, J. U., Panitz, C., L'afflitto, A., et al. (2009). EXPOSE, an astrobiological exposure facility on the international space station - from proposal to flight. *Orig. Life Evol. Biosph.* 39, 581–598. doi: 10.1007/s11084-009-9173-6

Rabbow, E., Rettberg, P., Barczyk, S., Bohmeier, M., Parpart, A., Panitz, C., et al. (2012). EXPOSE-E: an ESA astrobiology mission 1.5 years in space. *Astrobiology* 12, 374–386. doi: 10.1089/ast.2011.0760

Rabbow, E., Rettberg, P., Barczyk, S., Bohmeier, M., Parpart, A., Panitz, C., et al. (2015). The astrobiological mission EXPOSE-R on board of the International Space Station. *Int. J. Astrobiol.* 14, 3–16. doi: 10.1017/S1473550414000202

Raggio, J., Pintado, A., Ascaso, C., De La Torre, R., De Los Rios, A., Wierzchos, J., et al. (2011). Whole lichen thalli survive exposure to space conditions: results of Lithopanspermia experiment with *Aspicilia fruticulosa*. *Astrobiology* 11, 281–292. doi: 10.1089/ast.2010.0588

Rettberg, P., Eschweiler, U., Strauch, K., Reitz, G., Horneck, G., Wanke, H., et al. (2002). Survival of microorganisms in space protected by meteorite material: results of the experiment 'EXOBIOLOGIE' of the PERSEUS mission. *Adv. Space Res.* 30, 1539–1545. doi: 10.1016/S0273-1177(02)00369-1

Sancho, L. G., De La Torre, R., Horneck, G., Ascaso, C., De Los Rios, A., Pintado, A., et al. (2007). Lichens survive in space: results from the 2005 LICHENS experiment. *Astrobiology* 7, 443–454. doi: 10.1089/ast.2006.0046

Taylor, G. R., Spizizen, J., Foster, B. G., Volz, P. A., Bücker, H., Simmons, R. C., et al. (1974). A descriptive analysis of the Apollo 16 microbial response to space environment experiment. *BioScience* 24, 505–511. doi: 10.2307/1296886

Woellert, K., Ehrenfreund, P., Ricco, A. J., and Hertzfeld, H. (2011). Cubesats: cost-effective science and technology platforms for emerging and developing nations. *Adv. Space Res.* 47, 663–684. doi: 10.1016/j.asr.2010.10.009

Conflict of Interest Statement: The authors declare that the research was conducted in the absence of any commercial or financial relationships that could be construed as a potential conflict of interest.

frontiers in Microbiology

ORIGINAL RESEARCH
published: 15 September 2017
doi: 10.3389/fmicb.2017.01680

On the Stability of Deinoxanthin Exposed to Mars Conditions during a Long-Term Space Mission and Implications for Biomarker Detection on Other Planets

Stefan Leuko[1], Maria Bohmeier[1], Franziska Hanke[2], Ute Böettger[2], Elke Rabbow[1], Andre Parpart[1], Petra Rettberg[1] and Jean-Pierre P. de Vera[3]*

[1] German Aerospace Center, Research Group "Astrobiology", Radiation Biology Department, Institute of Aerospace Medicine, Köln, Germany, [2] German Aerospace Center, Institute of Optical Sensor Systems, Berlin, Germany, [3] German Aerospace Center, Institute of Planetary Research, Berlin, Germany

Outer space, the final frontier, is a hostile and unforgiving place for any form of life as we know it. The unique environment of space allows for a close simulation of Mars surface conditions that cannot be simulated as accurately on the Earth. For this experiment, we tested the resistance of *Deinococcus radiodurans* to survive exposure to simulated Mars-like conditions in low-Earth orbit for a prolonged period of time as part of the Biology and Mars experiment (BIOMEX) project. Special focus was placed on the integrity of the carotenoid deinoxanthin, which may serve as a potential biomarker to search for remnants of life on other planets. Survival was investigated by evaluating colony forming units, damage inflicted to the 16S rRNA gene by quantitative PCR, and the integrity and detectability of deinoxanthin by Raman spectroscopy. Exposure to space conditions had a strong detrimental effect on the survival of the strains and the 16S rRNA integrity, yet results show that deinoxanthin survives exposure to conditions as they prevail on Mars. Solar radiation is not only strongly detrimental to the survival and 16S rRNA integrity but also to the Raman signal of deinoxanthin. Samples not exposed to solar radiation showed only minuscule signs of deterioration. To test whether deinoxanthin is able to withstand the tested parameters without the protection of the cell, it was extracted from cell homogenate and exposed to high/low temperatures, vacuum, germicidal UV-C radiation, and simulated solar radiation. Results obtained by Raman investigations showed a strong resistance of deinoxanthin against outer space and Mars conditions, with the only exception of the exposure to simulated solar radiation. Therefore, deinoxanthin proved to be a suitable easily detectable biomarker for the search of Earth-like organic pigment-containing life on other planets.

Keywords: Raman spectroscopy, *Deinococcus radiodurans*, deinoxanthin, Mars

OPEN ACCESS

Edited by:
Baolei Jia,
Chung-Ang University, South Korea

Reviewed by:
James A. Coker,
University of Maryland University College, United States
Haitham Sghaier,
Centre National des Sciences et Technologies Nucléaires, Tunisia

****Correspondence:***
Stefan Leuko
stefan.leuko@dlr.de

Specialty section:
This article was submitted to Extreme Microbiology, a section of the journal Frontiers in Microbiology

Received: *23 May 2017*
Accepted: *21 August 2017*
Published: *15 September 2017*

Citation:
Leuko S, Bohmeier M, Hanke F, Böttger U, Rabbow E, Parpart A, Rettberg P and de Vera J-PP (2017) On the Stability of Deinoxanthin Exposed to Mars Conditions during a Long-Term Space Mission and Implications for Biomarker Detection on Other Planets. Front. Microbiol. 8:1680. doi: 10.3389/fmicb.2017.01680

INTRODUCTION

The search for evidence of extant or extinct life on Mars by *in situ* investigations began in 1976 with the landing of the Viking spacecraft (Klein, 1999) and continues today with the curiosity rover investigating whether life was ever present on Mars. The climatic history of Mars can be divided into three main eras, beginning with a water-rich epoch (Noachian; <3.95–3.7 billion years),

followed by a cold and semi-arid period (Hesperian; 3.7–2.9 billion years) and transitioning into present-day arid and cold desert conditions (Amazonian; 3.1 billion years to present) (Fairén et al., 2010). Concerning the habitability of Mars, these eras also represent three stages of habitability (Fairén et al., 2010). The Noachian era may represent a potentially habitable epoch, when basic requirements for life as we know it, such as water and energy were present on Mars. The Hesperian era was possibly very challenging for life with liquid solutions evaporating and during the Amazonian era, the surface of Mars has become, except for some subsurface niches (de Vera et al., 2014; Schirmack et al., 2014), uninhabitable to life as we know it. Although there is no definitive proof that life existed on Mars, the possibility is intriguing and the search for signs of extinct or extant life is one of the main focuses of Astrobiologists.

Whenever life-forms were present in an environment, they often leave traces of their former presence in the form of biomarkers. A biomarker can be defined as a chemical species or pattern which is uniquely derived from a living organism (Edwards et al., 2014). Among the most widespread and stable bacterial biomarkers is the class of hopanes (Toporski and Steele, 2002), which are pentacyclic organic compounds found in bacterial membranes where they are used to control cell membrane permeability and aid in their adaptation to extreme environmental conditions (Edwards et al., 2011). Another important group of biomarkers are carotenoids, which can serve as accessory pigments in the light-harvesting complexes of photosynthetic organisms (Tian and Hua, 2010) or scavenge reactive oxygen species like singlet oxygen ($^1O_2$) and peroxyl radicals in non-phototrophic (Armstrong, 1997; Stahl and Sies, 2003; Slade and Radman, 2011). Carotenoids protect DNA from oxidative damage (Shahmohammadi et al., 1998), proteins from carbonylation (Tian et al., 2009), and membranes from lipid peroxidation (Sy et al., 2015). Previous research reports that the ability of oxygen quenching increases with the number of double bonds in the carotenoid molecule, yet quenching varies with chain length, structure, and functional groups (Hirayama et al., 1994). Conjugated keto groups and the presence of a cyclopentane ring increase quenching, while hydroxy, epoxy, and methoxy groups show lesser effects (Hirayama et al., 1994).

Currently, there are two well-established methods to detect and identify carotenoids; the first is detection and separation by HPLC (Tian et al., 2007) and the second is Raman spectroscopy. Raman spectroscopy is a spectroscopic technique used to observe vibrational, rotational, and other low-frequency modes in a molecule. It measures the spectrum of light scattered from a sample, which is irradiated with a monochromatic source in the visible, near-infrared, or UV region (Marshall et al., 2007). Carotenoids are π-electron-conjugated carbon chain molecules and are similar to polyenes with regard to their structure and optical properties (Marshall et al., 2007). Their strong color is due to an allowed π–π* transition that occurs in the visible region of the electromagnetic spectrum (Marshall et al., 2007). Carotenoids have two strong Raman bands due to in-phase ν_1(C=C) and ν_2(C–C) stretching vibrations of the polyene chain and a medium intensity feature due to in-plane rocking modes of CH_3 groups attached to the polyene chain coupled with C–C bonds (Gill et al., 1970; Vítek et al., 2009). Because the Raman spectrum results from laser excitation giving rise to a series of characteristic bands in the range of 100–3,500 cm^{-1}, the molecular signatures of biomolecules and minerals occur simultaneously in the same analytical interrogation process (Edwards et al., 2014).

One non-photosynthetic bacterium of significant astrobiological interest, *Deinococcus radiodurans*, is brightly colored due to the expression of six carotenoid pigments related to β-carotene, the dominant of which is deinoxanthin (Saito et al., 1998; Ji, 2010; Dartnell and Patel, 2014). Disrupting the synthesis pathway of deinoxanthin by a knock-out of the phytoene synthase *crtB* gene results in a colorless mutant which is more susceptible to oxidative DNA-damaging agents than the wild-type (Zhang et al., 2007). *D. radiodurans* is well known for its extreme resistance against prolonged desiccation, UV and ionizing radiation, oxidative stress, as well as genotoxic chemicals (Battista, 1997; Cox and Battista, 2005; Bauermeister et al., 2012). In particular, the high tolerance against ionizing radiation is perplexing, as there are no naturally occurring environments known that result in exposure exceeding 260 mGy per year (Ghiassi-nejad et al., 2002), making it unlikely that a species evolved mechanisms to protect itself against high dose ionizing radiation (Cox and Battista, 2005). A likely explanation for this extreme radiation tolerance has been suggested by Mattimore and Battista (1996), where the authors proposed that the radiation resistance is a consequence of an adaptation to prolonged desiccation, for example, desiccation, similar to γ-irradiation, introduces many DNA double-strand breaks into the genome of *D. radiodurans* (Cox and Battista, 2005). Alternatively, the radiation resistance may have evolved as an adaptation to permafrost or semi-frozen conditions where background radiation-induced DNA damage is accumulated or to high natural ionizing radiation levels in manganese-rich marine sediments (Richmond et al., 1999; Sghaier et al., 2007; Slade and Radman, 2011).

This resistance against desiccation and radiation makes *D. radiodurans* of high astrobiological interest to investigate the possibility of survival on arid planets such as Mars.

Presently, the International Space Station (ISS) is orbiting Earth in low-Earth orbit (LEO), providing scientists a unique opportunity to study the responses of terrestrial organisms to the space environment. Environmental parameters surrounding the ISS – such as vacuum (between10^{-3} and 10^{-4} Pa), intense solar, and cosmic radiation, as well as temperature extremes severely impact the survival of microorganisms (Horneck et al., 2012; Wassmann et al., 2012; Kawaguchi et al., 2013). Due to its resistance against radiation and desiccation, the resistance and response of *Deinococcus* spp. to simulated (Kawaguchi et al., 2013) or real space conditions (Dose et al., 1995) has been previously investigated. In the frame of the EXPOSE-R2 space mission (see Rabbow et al., 2017), *D. radiodurans* was exposed to simulated Mars conditions in LEO for 1.5 years as part of the Biology and Mars experiment (BIOMEX). For an in-depth description and goals of the BIOMEX investigations please refer to de Vera et al. (2012). Here we report on the stability and detectability of the biomarker deinoxanthin with Raman spectroscopy, the survival of *D. radiodurans*, and the

genetic integrity of the 16S rRNA gene following exposure to Mars conditions, utilizing the space environment for a realistic simulation.

MATERIALS AND METHODS

Cultivation

Deinococcus radiodurans DSM46620 was obtained from the Deutsche Sammlung von Mikroorganismen und Zellkulturen (DSMZ, Braunschweig, Germany). *D. radiodurans* Δ*crtB* was a kind gift from Prof. Chengxian Fang (College of Life Sciences, Wuhan University, Wuhan, China; Zhang et al., 2007). Both strains were routinely cultured in 2× TGY medium, composed of (per liter) 10 g tryptone, 6 g yeast extract, and 2 g d-glucose monohydrate, pH 7.2. For solid medium, 15 g/L agar was added to the nutrient solution before autoclaving. Organisms were cultured in 50 mL medium at 30°C, shaking at 200 × *g* for 2 days.

Sample Preparation

After reaching late exponential phase (OD_{600nm} ∼1.0), samples were centrifuged for 15 min at 3,000 × *g* at 4°C and the resulting pellet was washed with 25 mL 1× phosphate-buffered saline (PBS), pH 7.4. Samples were centrifuged again for 15 min at 3,000 × *g* at 4°C and the resulting pellet was re-suspended in 3 mL 1× PBS. The cell concentration was determined in a Thoma Cell Counter and a working stock of 5×10^8 cells/mL was prepared. Forty microliters of this solution was spotted onto quartz disks (ϕ9 mm, 1 mm thickness, 63.61 mm^2 area) resulting in a final concentration of 2×10^7 cells/disk. To evaluate possible beneficial effects of embedding cells in sulfatic Mars regolith simulant [S-MRS, composition and Raman spectroscopic properties of the simulant are described in detail by Böttger et al. (2012)], 10 mg/mL was added to the working solution. After this, the mixture was vortexed (Biovendis, IKA MS3 basic) for 10 s at full speed (3,000 × *g*) before each sample withdrawal to ensure comparable S-MRS distribution, and 40 μL was spotted onto quartz disks as described above. A detailed size distribution of the employed S-MRS is given by Baqué et al. (2015). The quartz disks were dried overnight in a clean safety workbench at room temperature (∼22°C and ∼40% relative humidity). All exposure experiments presented in this work have been conducted with desiccated organisms as described above.

Electron Microscopy

To analyze the distribution of the simulated Mars regolith on the quartz disks, electron microscopy images were obtained. Samples were prepared as described above and 10 disks were evaluated with a Hitachi TM3000 Tabletop microscope with an acceleration voltage of 15 kV. Energy dispersive spectroscopy (EDS) analysis was performed with the program Quantax70 (Bruker).

Extraction of Deinoxanthin

Cell extracts from *D. radiodurans* containing deinoxanthin were obtained according to a modified protocol of Lemee et al. (1997). Briefly, cells were grown until late-exponential phase (OD_{600nm} ∼1.0) and harvested by centrifugation for 20 min at 4,000 × *g*. Forty grams of cell pellet was mixed with 200 mL methanol containing 0.3 g of 2,6-di-*t*-*butyl*-*p*-cresol (BHT) as antioxidant, homogenized by adding 5 g of sterilized glass beads and vortexed for 10 min at 3,000 × *g*. The sample was then centrifuged for 10 min at 10,000 × *g* and the supernatant removed. This process was repeated four times until the pellet lost all visible color. Supernatants from this process were pooled and then concentrated via evaporation at 50°C for 24 h. Forty microliters was spotted onto similar quartz disks as previously described and the samples were dried overnight in a clean safety workbench at room temperature in darkness.

Pre-flight Ground Tests

To determine the feasibility of the proposed experiments in space and to optimize sample preparation and analysis, three ground experiments were conducted before the mission, two experiment verification tests (EVTs) and one science verification test (SVT). The tested parameters for the EVTs were as follows: monochromatic UV-$C_{(254nm)}$ radiation (NN 8/15; Heraeus Noblelight, Hanau, Germany) with fluences of 0, 10, 100, 1,000, and 10,000 J/m^2, and temperatures of −25 and +65°C for 1 h, respectively. A second EVT investigated the effects of simulated solar radiation (achieved with a Wolfram halide lamp with a spectral irradiance in the range of 200–400 nm; Dr. Hoenle AG, Germany) with the following fluences: 0, 1.5×10^3, 1.5×10^4, 1.5×10^5, 5.0×10^5, and 8×10^5 kJ/m^2, respectively. The SVT consisted of the following parameters: Simulated Martian atmosphere (95.55% CO_2, 2.70% N_2, 1.60% Ar, 0.15% O_2, ∼370 ppm H_2O, pressure 10^3 Pa; Praxair Deutschland GmbH) for 38 days with exposure to a simulated solar irradiation fluence of 1.5×10^6 kJ/m^2. To further simulate the space experiment conditions, samples were placed in three different compartments, which were stacked as: top (t) compartment, where samples were exposed to the full solar radiation spectra, middle (m) and bottom (b) where no solar radiation could penetrate the samples. This arrangement was also employed for the flight and a detailed description of the hardware is given by Rabbow et al. (2012).

Flight Preparation and Mission Ground Reference (MGR) Preparation

Flight, MGR, and laboratory control samples were prepared from the same starting cultures. Flight and MGR samples were accommodated in the sample trays as described for the SVT test and laboratory controls were stored in the laboratory under ambient conditions (∼22°C and ∼40% relative humidity) in darkness until the flight sample returned. For flight samples, sample trays were accommodated in Tray II of the EXPOSE-R2 mission. Tray II was hermetically closed, evacuated, and flooded with 980 Pa pressure Mars gas (described above), and covered by a quartz window with transmission of solar electromagnetic radiation of $\lambda > 200$ nm, similar to the spectrum expected on the Martian surface. To attenuate the total mission UV fluence, samples were additionally covered with quartz neutral density filter (0.001% transmission). These filters were employed due to the results obtained during preliminary experiments (detailed in

the results section). An identical arrangement of samples was used for the MGR experiment.

Flight Parameters and Conditions

Samples were transported to Baikonur and launched on 23 August 2014 with the 56P Progress rocket. EXPOSE-R2 was installed on the URM-D platform on Svezda module on 18 August 2014 during the EVA-39 by Aleksandr Skvortsov and Oleg Artemyev. The cover, protecting samples from solar radiation before the start of the exposure period, was removed on 22 October 2014. Samples were outside the ISS for 534 days and exposed to solar radiation for 469 days. During the EXPOSE-R2 experiment, the height of the ISS varied between 398 and 417 km above Earth[1]. Over the duration of the mission, the upper surface of the sample trays was exposed to 549.88 MJ/m^2 of solar radiation (200–400 nm). Due to the previously mentioned neutral density filters, the samples in the top layer were exposed to a fluence of 5.54 kJ/m^2. The trays were returned to the interior of the ISS on 03 February 2016 and the BIOMEX trays arrived back on Earth on 18 June 2016 with the Soyuz 45S rocket. The total mission duration was 696 days from launch to return to ground. An identical arrangement of samples was used for the MGR experiment. During the MGR, the environmental data of the flight unit (e.g., temperature profile and UV exposure) were followed with a time-delay of 2 months within DLR's Planetary and Space simulation facilities (Rabbow et al., 2016). Additional laboratory control samples from the same batch of bacteria were stored in the dark in a desiccator under ambient conditions in the laboratory until the end of the mission and analyzed in parallel to the flight samples.

Sample Analysis

Raman Spectroscopy

After exposure to stress conditions, the detectability of deinoxanthin was determined by Raman spectroscopy. Sample disks were placed under a Raman Microscope (WITec), equipped with a 532 nm laser. Spectra were routinely obtained by employing 3.02 mW of laser power. Line scans were performed using the 10× optical objective and measured over a predetermined distance (10 μm) with 50 spectra accumulated with an integration time of 2 s. Each sample was analyzed by five line scans where the area of analysis was randomly chosen, resulting in a total of 250 scans per sample. Following the line scans, area scans were performed over a square of 50 × 50 μm^2, divided into 25 lines per image with 25 points for each line measured and with 2 s integration time. All spectra (875 in total) were evaluated against predetermined quality criteria (**Figure 6**).

Survival

Following evaluation by Raman spectroscopy, the survival by cultivation was assessed by determining the number of colony forming units (CFUs). To remove cells from the quartz disks, the samples on the disks were coated with 30 μL 10% (w/v) polyvinylalcohol (PVA) and dried in a sterile safety cabinet at room temperature over-night. The solidified PVA was gently removed with flame-sterilized forceps and transferred into 500 μL 1× PBS (pH 7.4) buffer. This procedure was repeated three times with samples being stored at 4°C. Disks were inspected under the microscope (×60 magnification) to confirm that no residual samples were left. To investigate survival, 20 μL of a dilution series from the recovered samples was plated onto 2× TGY medium and incubated for up to 1 week at 30°C and evaluated daily for growth. The survival rate was calculated as relative survival after exposure to space conditions (N) compared with the untreated laboratory control (N_0).

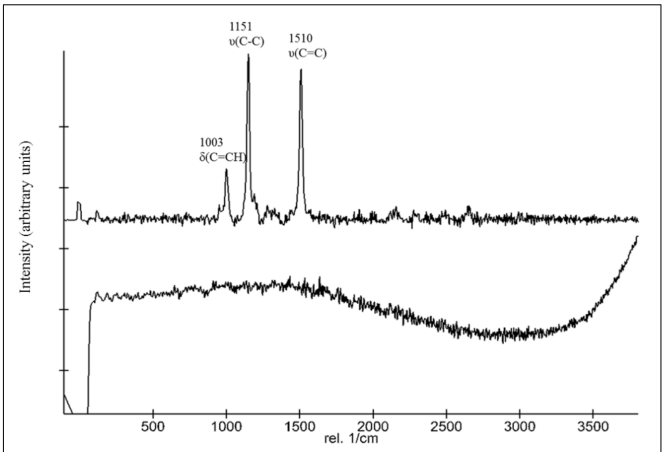

FIGURE 1 | Comparison of Raman spectra of *D. radiodurans* and the Δ*crtB* mutant. The top spectrum was obtained from *D. radiodurans* and the bottom spectrum from the Δ*crtB* strain. The top spectrum shows the distinctive 1,003, 1,151, and 1,510 cm^{-1} peaks of deinoxanthin.

Integrity of 16S rRNA Gene

DNA from all samples was extracted using the XS-buffer method as previously described by Tillett and Neilan (2000), purified with a standard PCI (25:24:1) protocol, precipitated with ice-cold isopropanol and washed twice with 75% EtOH, and air-dried for 15 min. DNA was re-suspended in 30 μL dH_2O and the concentration was determined with a Nanodrop spectrophotometer (Thermo Scientific, Wilmington, MA, United States) and 10 ng was routinely used as template for quantitative PCR (qPCR). Quantitative PCR was performed following exposure to space conditions and simulated Mars conditions by employing the forward primer Drad16S_F1 (5′-TTTATGGAGAGTTTGATCCTG-3′) and the reverse primer Drad16S_R1502 (5′-AAAGGAGGTGATCCAACC-3′) resulting in a 1,501 bp product. Primers were designed based on the available type strain sequence. Amplifications were performed in an Opticon2 system (BioRad) using the PeqLab KAPA Sybr FAST Kit. Thermal cycling conditions were: Initial denaturation at 94°C for 3 min, followed by 40 cycles of denaturation at 94°C for 30 s, primer annealing at 60°C for 20 s, and strand extension at 72°C for 90 s. The standard curve was calculated on the basis of a 16S rRNA gene product obtained from serial diluted (1:10; 1:100; 1:1.000; and 1:10.000), isolated DNA, obtained from a freshly grown WT culture. Melting curve analysis (0.2°C s^{-1}) and agarose gel electrophoresis (2% agarose)

[1]http://www.heavens-above.com/IssHeight.aspx

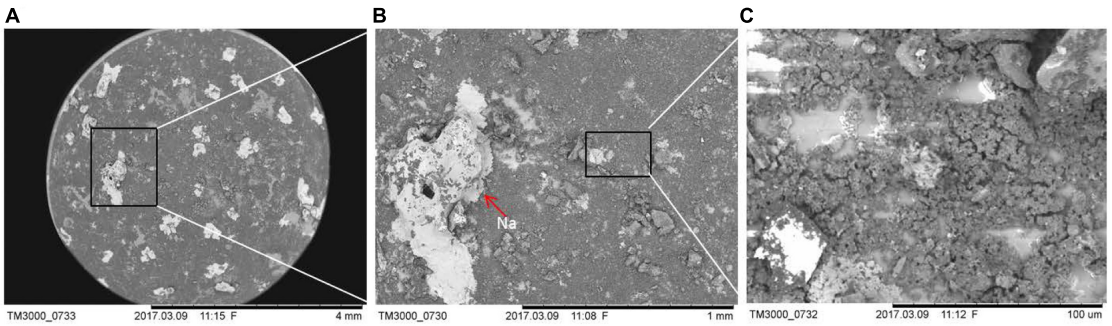

FIGURE 2 | Electron microscopic evaluation of the distribution of the simulated Mars regolith on the quartz sample disks. Image **(A)** was taken with ×25, **(B)** with ×1,000, and **(C)** with ×1,500 magnification, respectively. Elementary analysis was conducted by EDS.

revealed single amplicons for all samples (data not shown). The amplification efficiency (E) was calculated from the slope of the standard curve using the formula: $E(\%) = 10^{(-1/\text{slope})} - 1$ (Bustin et al., 2009). PCR efficiency and correlation coefficient for the standard curve were 81% and $r^2 = 0.998$, respectively. Resulting values from the qPCR runs were converted to relative lesion frequencies per 1.501 kB (∼1.5 kB) DNA by application of the Poisson distribution (lesions/amplicon $= -\ln(A_t/A_0)$, where A_t represents the amplification of treated samples and A_0 is the amplification of untreated controls) as previously described (Hunter et al., 2010).

RESULTS

The suitability of Raman spectroscopy to detect carotenoids is well established. **Figure 1** shows representative stacked Raman spectra from the two strains employed in this study. The spectra of the WT contain major features at approximately 1,003, 1,151, and 1,510 cm^{-1}. The bands at 1,510 and 1,152 cm^{-1} are due to in-phase C=C (ν_1) and C–C stretching (ν_2) vibrations of the polyene chain in carotenoids. Additionally, in-plane rocking modes of CH_3 groups attached to the polyene chain coupled with C–C bonds occurred in the 1,003 cm^{-1} region. The spectra obtained for the Δ*crtB* strain show no distinctive features or peaks, confirming a lack of deinoxanthin or any other Raman active compound under the tested conditions (**Figure 1**). No significant interference by the S-MRS was detected.

To evaluate if *D. radiodurans* and the Δ*crtB* mutant are suitable candidates for the scientific questions asked by the BIOMEX proposal, several ground tests were conducted. In particular, the stability of deinoxanthin as a biomarker was of higher interest than the survival of the cells. Evaluations of the surface properties of the dried samples combined with the simulated Mars regolith revealed inhomogenic coverage of the quartz disks with cracks within the layers (**Figure 2**). Experiment verification tests were designed to evaluate if the tested organism survive extreme environments such as radiation, desiccation, and vacuum as foreseen in the space experiment. A SVT was designed to simulate the complete mission in a shorter timeframe on Earth, to evaluate if the chosen organism has the potential of survival, and as a rehearsal for the procedures and logistics. The first EVT focused on the survivability of both strains exposed to monochromatic UV-$C_{(254nm)}$ radiation as well as temperature extremes as they may occur during the space experiment and the results are given in **Figure 3**. The second EVT focused on the survival following exposure to simulated polychromatic solar UV radiation with the biologically deleterious spectral irradiance calculated between 200 and 400 nm and results are presented in **Figure 4**. The survival of *D. radiodurans* and the Δ*crtB* mutant displayed a dose-dependent decrease of survival when exposed to germicidal UV-$C_{(254nm)}$ radiation. A reduction of survival by three orders of magnitude was observed when both strains where exposed to high/low temperature. The addition of simulated Martian soil showed no significant positive or detrimental effect on the survival of both strains under the chosen conditions. Following all exposure experiments, the detectability of the deinoxanthin was evaluated and is shown in **Figure 3B**. No reduction or shifts in the Raman signal were observed following the described treatment. Similar to exposure to UV-C radiation, exposure to the simulated solar spectrum lead to a dose-dependent decrease in survival and growth was undetected in the timeframe used following exposure up to 8×10^5 kJ/m^2 (**Figure 4B**). Again, the addition of simulated Martian soil provided no additional protection. Compared to UV-$C_{(254nm)}$ radiation, deinoxanthin is strongly susceptible to simulated polychromatic radiation (**Figure 4B**). Although the cells survived simulated polychromatic light up to 1.5×10^4 kJ/m^2, the previously seen signature peaks of deinoxanthin were no longer detectable by Raman spectroscopy following exposure to 1.5×10^3 kJ/m^2 and higher.

Results from the science verification test (SVT) are given in **Figure 5**. It is evident from the results that cells in the top layer (exposed to the full solar spectrum), did not survive. This could also be confirmed by the Raman spectra which show no characteristic Raman signals of the WT (**Figure 5B**). Organisms in the middle and bottom compartment without any exposure to UV radiation survived without any significant loss in viability and deinoxanthin was easily detected. For the reason that both, the cell survival and the Raman signature, are highly affected by polychromatic light, we chose a strong neutral density filter (0.001% T), to reduce the fluence over the duration of the

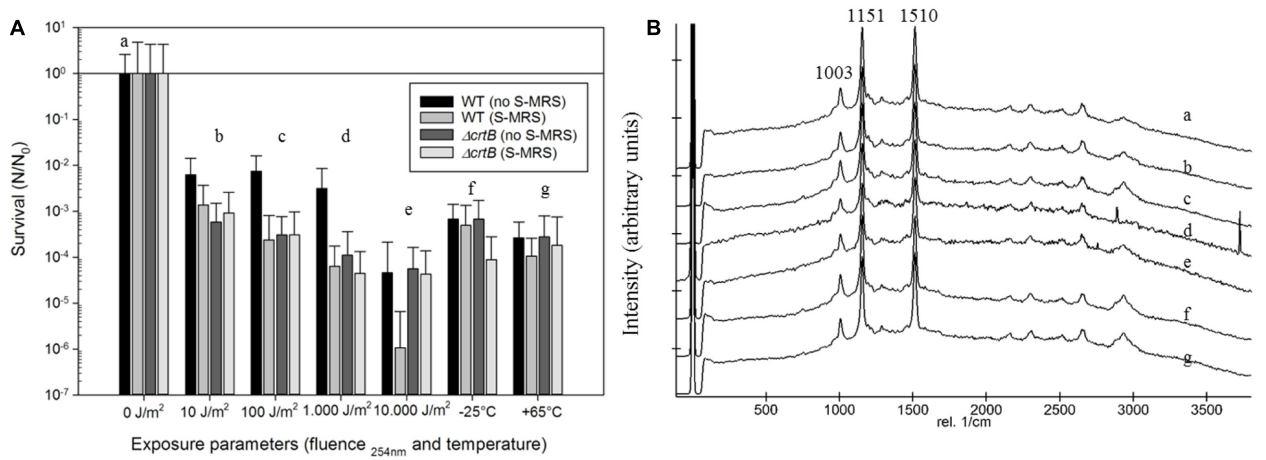

FIGURE 3 | (A) Survival of *D. radiodurans* and the Δ*crtB* strain following exposure with or without the protection of simulated Martian regolith to UV-C_{254nm} radiation, different temperatures, and simulated Mars-like solar radiation. The survival is given by the quotient N/N_0, where N_0 is the number of colonies of the non-treated samples and N that of the exposed samples to the different experimental conditions. **(B)** Stacked Raman spectra from *D. radiodurans* exposed in the presence of regolith following respective treatments. Small letters (a–g) correspond to the treatment in **(A)**.

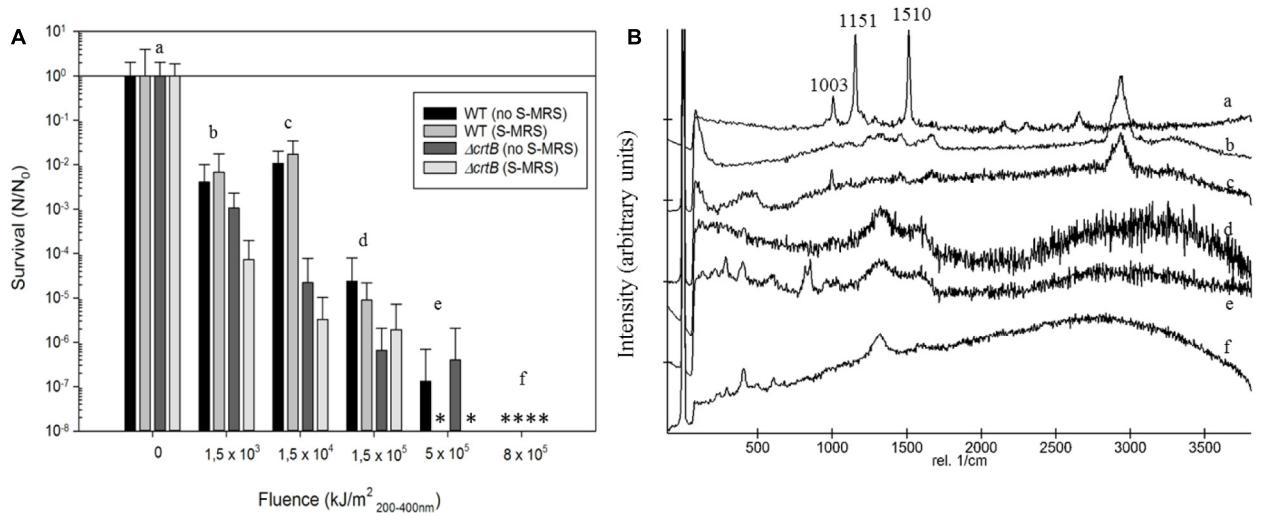

FIGURE 4 | (A) Survival of *D. radiodurans* and the Δ*crtB* strain following exposure to simulated solar radiation up to 8×10^5 kJ/m^2. * indicates that no survival was observed. The survival is given by the quotient N/N_0, where N_0 is the number of colonies of the non-treated samples and N that of the exposed samples to the different experimental conditions. **(B)** Stacked Raman spectra from *D. radiodurans* exposed with regolith following respective treatments. Small letters (a–f) correspond to treatment in **(A)**.

mission. Following the previously mentioned measured fluences, samples were exposed to 5.54 kJ/m^2 solar radiation (200–400 nm) during the duration of the mission.

Following the return of the samples and the arrival in the laboratory, survival was evaluated immediately and Raman spectra were obtained from all samples. *D. radiodurans* grows best between 30 and 37°C, with a doubling time of 1.5–3 h (Cox and Battista, 2005). Unfortunately, no survival was observed for either the WT or the Δ*crtB* mutant, even after prolonged incubation for up to 3 weeks at 30°C. Given roughly 21× longer to grow than a strain maintained under laboratory conditions, we believe that the probability of observing growth from the cells exposed to space conditions is very low. Expectedly, evaluation of the 16S rRNA integrity revealed that the 16S rRNA gene suffered severe damage during this process. Results from the laboratory control show that the prolonged desiccation and storage resulted in an 81% chance of a lesion within the 16S rRNA gene, without being exposed to solar radiation or other detrimental factors (**Table 1**). The stability of deinoxanthin was investigated by Raman spectroscopy and accumulated spectra were divided into four different classes (**Figure 6**). Spectra of classes 1 and 2 show a strong signal/low noise ratio with the

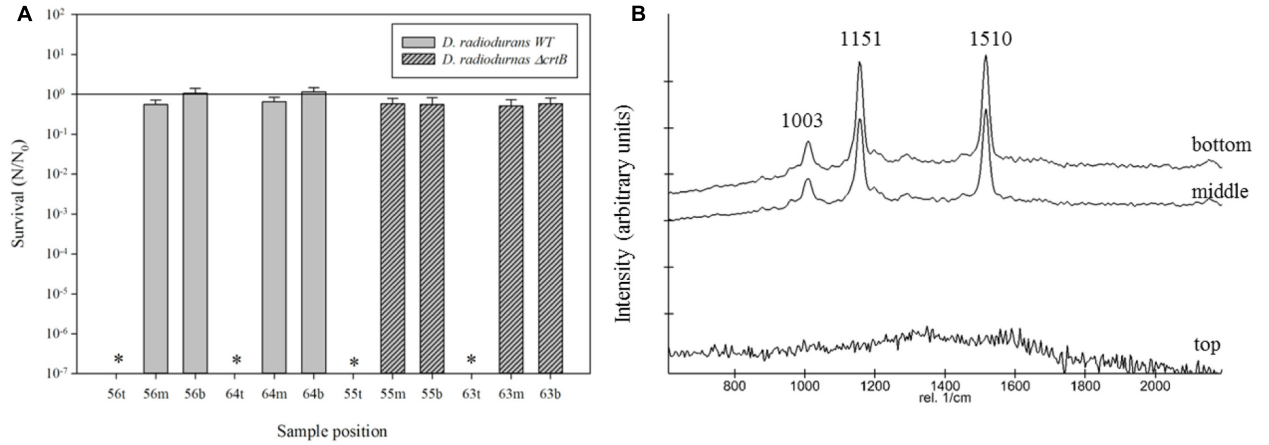

FIGURE 5 | (A) Survival of *D. radiodurans* and Δ*crtB* with regolith from the science verification test (SVT). *Indicates that no survival was observed. **(B)** Stacked Raman spectra from samples exposed to solar irradiance (top), and no irradiance (middle and bottom).

three characteristic peaks dominating the spectra. Class 3 spectra have a medium signal/noise ration with the peaks fading. Class 4 spectra are classified by a weak signal/noise ratio with the peak at 1,003 cm^{-1} scarcely detectable. Results of this evaluation are given in **Figure 7**. For all flight and MGR samples, 875 spectra were obtained and evaluated separately. Samples exposed to solar radiation lost the deinoxanthin signal almost completely, with samples exposed in the space mission marginally better preserved than samples from the MGR (**Figure 7**). Samples not exposed to solar radiation revealed strong deinoxanthin signals, both after spaceflight and ground simulation. It is interesting to note that the signal from the laboratory control (kept in dark) appears to be significantly weaker (44.1% class 1 spectra, compared to 96.7% class 1 spectra from the ISS bottom sample) compared to spectra from samples not exposed to solar radiation during the space mission. To investigate if deinoxanthin is resistant to detrimental environmental conditions when not protected by the cell, it was extracted from cell homogenate, using methanol and BHT, and the resulting concentrated sample was exposed to UV-C radiation, vacuum, and different temperature extremes (**Figure 8**). Exposure to heat, (+90°C) for 24 h, resulted in a visible quality loss of the spectrum. All other tested factors did not influence the quality of the obtained spectra significantly.

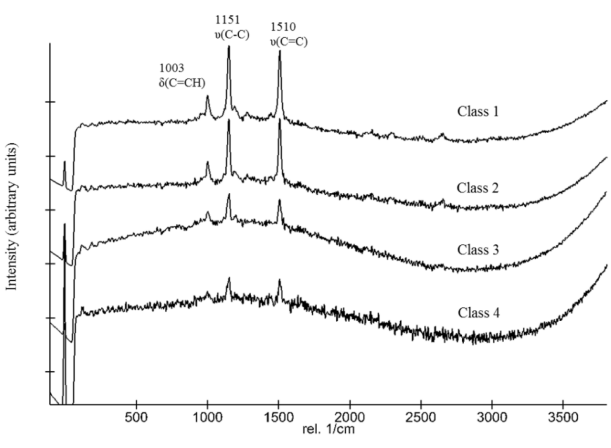

FIGURE 6 | Categorization of spectra and classification in different classes.

TABLE 1 | Relative lesion frequency in the 16S rRNA gene fragment (1.5 kb) calculated against DNA extracted from freshly grown *D. radiodurans*.

Sample location	Relative lesion frequency (%)	Sample location	Relative lesion frequency (%)
LC WT	81 (±2)	LC Δ*crtB*	76 (±5)
ISS WT_t	100	ISS Δ*crtB*_t	100
ISS WT_m	100	ISS Δ*crtB*_m	65 (±3)
ISS WT_b	94 (±6)	ISS Δ*crtB*_b	70 (±2)
MGR WT_t	100	MGR Δ*crtB*_t	100
MGR WT_m	93 (±5)	MGR Δ*crtB*_m	83 (±6)
MGR WT_b	89 (±1)	MGR Δ*crtB_b*	81 (±3)

Sample location indicates whether samples were exposed to outer space (ISS) or part of the mission ground reference (MGR). LC denotes a laboratory control from the same batch that was sent to the ISS. Lowercase t, m, and b describe the sample position within the tray as follows: t, top; m, middle; and b, bottom. Only the top samples were exposed to solar radiation.

DISCUSSION

The BIOMEX was aimed at exposing different extremophilic organisms and potential biomarkers to Martian-like conditions in LEO, being simulated in one of the trays as part of the EXPOSE-R2 mission. Here we report the results of the survival and genetic integrity of *D. radiodurans* and the Δ*crtB* mutant and the stability and detectability of deinoxanthin following the exposure. The main focus of this work was to determine the stability of deinoxanthin and the possibility of this molecule to be a useful biomarker to detect life on other planets. Although both strains survived the preliminary tests relatively well, except intense

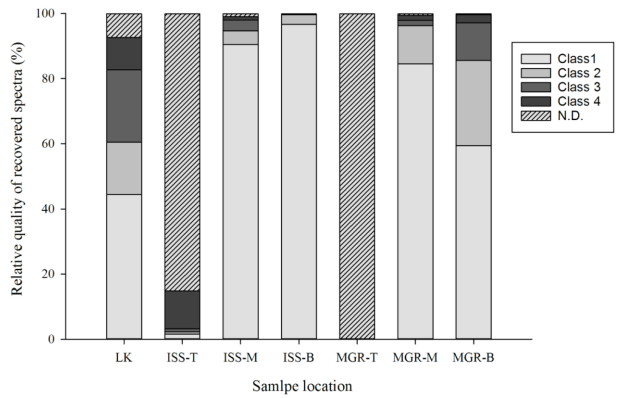

FIGURE 7 | Evaluation of the deinoxanthin signal intensity according to the defined classes (**Figure 6**) following ground simulations and samples exposed to outer space conditions during the EXPOSE-R2 mission. N.D. denotes that no signal could be determined. Eight hundred and seventy-five spectra were evaluated for each bar and scored according to the previously determined signal class (**Figure 6**). Sample location indicates whether samples were exposed to outer space (ISS) or part of the mission ground reference (MGR). LK denotes a laboratory control from the same batch that was sent to the ISS. T, M, and B describe the sample position within the tray as follows: T, top; M, middle; and B, bottom. Only the top samples were exposed to solar radiation.

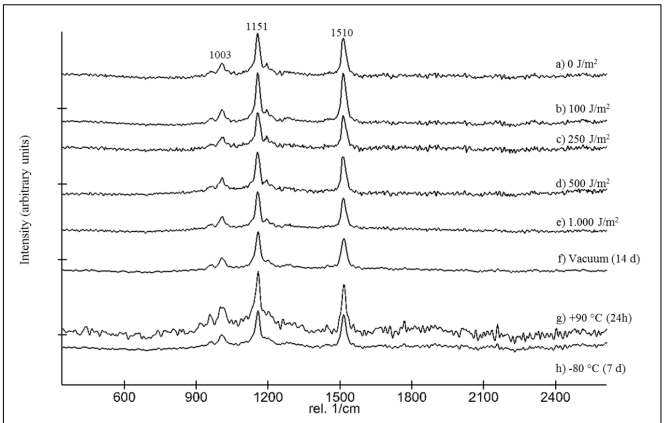

FIGURE 8 | Stacked Raman spectra showing the effect of UV-C_{254nm} radiation up 1,000 J/m^2 (a–e), vacuum (f), as well as +90°C (g) and –80°C (h) to MeOH/BHT extracted cell homogenate of *D. radiodurans*.

exposure to solar radiation, we were not able to recover colony-forming units from any of the samples, not even the laboratory control. It is well established that *D. radiodurans* is desiccation resistant (Cox and Battista, 2005; Bauermeister et al., 2011); however, desiccation for 17 months without protective substances such as glucose and storage in a non-oxidizing atmosphere such as argon lead to a lethal amount of DNA double-strand breaks as previously reported by Dose et al. (1995). Similar to these results, storage of dried *D. radiodurans* and the Δ*crtB* mutant strain in the dark under ambient laboratory conditions lead to an 81% chance of a lesion within the 16S rRNA gene (**Table 1**). Exposure to extraterrestrial Mars-like solar UV radiation led to a 100% probability of a lesion (**Table 1**). The addition of the simulated Martian regolith did not improve the survivability of the strains, although a beneficial effect has been previously reported (Pogoda de la Vega et al., 2007); however, our results suggest that a long-term storage of cells embedded in the dust has a detrimental effect on the cells. A possible explanation for this conundrum may be that UVR-induced radicals form in Mars substrates (Shkrob et al., 2010), which might be mimicked by the employed S-MRS and therefore may affect the survivability (Meeßen et al., 2015). It has previously been reported that even multilayers of cells act as a protective barrier for the cells underneath (Kawaguchi et al., 2013); here, however, the impact of prolonged desiccation was sufficient to kill the cells even without exposure to solar radiation.

The picture is different when investigating the stability and detectability of deinoxanthin by Raman spectroscopy. Carotenoids serve as accessory pigments to increase the efficiency of photosystems but are also synthesized by many non-photosynthetic bacteria as they function as efficient scavengers of ROS (Dartnell et al., 2012). It has previously been shown that deinoxanthin is particularly effective in scavenging H_2O_2 and singlet oxygen, performing better than other carotenes or xanthophylls (Tian et al., 2007; Dartnell et al., 2012). Furthermore, deinoxanthin is also remarkably stable when not inside the cell, compared to other possible biomarkers such as DNA, which is more vulnerable against radiation when not protected by the cell (Leuko et al., 2011). The abilities of Raman spectroscopy to detect biomarkers such as carotenoids from samples collected in remote and extreme areas such as the Atacama Desert, Death Valley, volcanic rocks, or Antarctica have been extensively tested and verified (Edwards et al., 2005; Jorge Villar et al., 2006; Vítek et al., 2010; Winters et al., 2013). It was also shown that carotenoid signatures can be recovered from cryptochasmoendoliths, preserved microbial filaments, and relict sedimentary structures (Edwards et al., 2007). However, we also know from previous research that carotenoids are vulnerable toward oxidation and photodecomposition (Vítek et al., 2014). The detrimental effect of solar radiation on pigmentation is well established and has been previously investigated for *Cyanophora paradoxa* (Häder and Häder, 1989) or for corals (Brown and Dunne, 2008). This photodegradation is primarily caused by the UV-A part of the solar spectrum (Kumar et al., 2015); however, a destruction of Raman biosignatures is also commissioned by high doses of ionizing radiation (Dartnell et al., 2012) and γ-irradiation (Meeßen et al., 2017). The detrimental effect of radiation has also been demonstrated by previous space missions to LEO, where Cockell et al. (2011) report the complete disappearance of previous β-carotene Raman signatures from several phototrophic organisms. Over the history of Mars, galactic cosmic radiation and solar cosmic rays played an important role in the degradation of organic molecules near the planetary surface, should they have ever been present (Vítek et al., 2014). Calculations by Pavlov et al. (2012) suggest that organic molecules with masses greater than 100 amu (atomic mass unit) would be destroyed in less than 1 billion years in the top 5 cm of Martian regolith (Vítek et al., 2014). Furthermore, analysis by Raman spectroscopy of Martian meteorites, e.g., MIL03346 which belongs to the nakhlite group, failed to identify

any biological signature (Wang et al., 2015). However, only a diminutive amount of Martian meteorites has been analyzed, so future research may reveal signs of biological life in a meteorite.

Our results presented here suggest that 1.5 years exposure to the Mars-like solar UV spectrum is already sufficient to degrade deinoxanthin beyond detectability with Raman spectroscopy, at the investigated total fluence. To search for signs of extinct life on the surface of Mars seems therefore pointless; however, below the surface the picture may be completely different. Protected from the most detrimental environmental source, radiation, signs of earlier life may still be preserved. Caves, or other subterranean cavities, can be suspected on other planets and in particular Moon or Mars show clear photographic evidence of lave tube caves (Boston et al., 2003).

In this study we showed the successful detection of the carotenoid deinoxanthin following exposure to Mars conditions for 1.5 years simulated in space when protected from solar radiation. Even though some signals were recovered from samples exposed to solar radiation, the vast majority of carotenoids were degraded beyond detectability by Raman spectroscopy. All other tested space relevant conditions, such as temperature oscillations, vacuum, or a Martian atmosphere, had no detectable effect on the molecule. Future missions are planned to investigate caves on Mars and by extending our search for life on Mars to the subsurface, we certainly would increase our chances to find traces of extant or extinct life on our neighbor planet.

AUTHOR CONTRIBUTIONS

SL and MB performed the experimental setup and the survival assays; SL, MB, UB, FH, and J-PdV performed Raman spectroscopic analysis; ER and AP conducted the MGR experiments; AP conducted Electron microscopy. SL, MB, FH, UB, ER, AP, PR, and J-PdV helped with data interpretation, scientific guidance, and preparation of the manuscript.

ACKNOWLEDGMENT

The authors thank the European Space Agency for the flight opportunity and would like to acknowledge the support of ESA (special thanks to René Demets) and of the MUSC team.

REFERENCES

Armstrong, G. A. (1997). Genetics of eubacterial carotenoid biosynthesis: a colorful tale. *Annu. Rev. Microbiol.* 51, 629–659. doi: 10.1146/annurev.micro.51.1.629

Baqué, M., Verseux, C., Böttger, U., Rabbow, E., De Vera, J. P., and Billi, D. (2015). Preservation of biomarkers from cyanobacteria mixed with Mars like regolith under simulated Martian atmosphere and UV flux. *Orig. Life Evol. Biosph.* 46, 289–310. doi: 10.1007/s11084-015-9467-9

Battista, J. R. (1997). Against all odds: the survival strategies of *Deinococcus radiodurans*. *Annu. Rev. Microbiol.* 51, 203–224. doi: 10.1146/annurev.micro.51.1.203

Bauermeister, A., Hahn, C., Rettberg, P., Reitz, G., and Moeller, R. (2012). Roles of DNA repair and membrane integrity in heat resistance of *Deinococcus radiodurans*. *Arch. Microbiol.* 194, 959–966. doi: 10.1007/s00203-012-0834-x

Bauermeister, A., Moeller, R., Reitz, G., Sommer, S., and Rettberg, P. (2011). Effect of relative humidity on *Deinococcus radiodurans* 'resistance to prolonged desiccation, heat, ionizing, germicidal, and environmentally relevant UV radiation. *Microb. Ecol.* 61, 715–722. doi: 10.1007/s00248-010-9785-4

Boston, P. J., Frederick, R. D., Welch, S. M., Werker, J., Meyer, T. R., Sprungman, B., et al. (2003). Human utilization of subsurface extraterrestrial environments. *Gravit. Space Res. Bull.* 16, 121–131.

Böttger, U., de Vera, J. P., Fritz, J., Weber, I., Hübers, H. W., and Schulze-Makuch, D. (2012). Optimizing the detection of carotene in cyanobacteria in a Martian regolith analogue with a Raman spectrometer for the ExoMars mission. *Planet Space Sci.* 60, 356–362. doi: 10.1016/j.pss.2011.10.017

Brown, B. E., and Dunne, R. P. (2008). Solar radiation modulates bleaching and damage protection in a shallow water coral. *Mar. Ecol. Prog. Ser.* 362, 99–107. doi: 10.3354/meps07439

Bustin, S. A., Benes, V., Garson, J. A., Hellemans, J., Huggett, J., Kubista, M., et al. (2009). The MIQE guidelines: minimum information for publication of quantitative real-time PCR experiments. *Clin. Chem.* 55, 611–622. doi: 10.1373/clinchem.2008.112797

Cockell, C. S., Rettberg, P., Rabbow, E., and Francis-Olsson, K. (2011). Exposure of phototrophs to 548 days in low Earth orbit: microbial selection pressure in outer space and on early earth. *ISME J.* 5, 1671–1682. doi: 10.1038/ismej.2011.46

Cox, M. M., and Battista, J. R. (2005). *Deinococcus radiodurans* – the consummate survivor. *Nat. Rev. Microbiol.* 3, 882–892. doi: 10.1038/nrmicro1264

Dartnell, L. R., Page, K., Jorge-Villar, S. E., Wright, G., Munshi, T., Scowen, I. J., et al. (2012). Destruction of Raman biosignatures by ionizing radiation and the implications for life detection on Mars. *Anal. Bioanal. Chem.* 403, 131–144. doi: 10.1007/s00216-012-5829-6

Dartnell, L. R., and Patel, M. R. (2014). Degradation of microbial fluorescence biosignatures by solar ultraviolet radiation on Mars. *Int. J. Astrobiol.* 13, 112–123. doi: 10.1017/S1473550413000335

de Vera, J. P., Boettger, U., de la Torre Noetzel, R., Sánchez, F. J., Grunow, D., Schmitz, N., et al. (2012). Supporting Mars exploration: BIOMEX in low Earth orbit and further astrobiological studies on the Moon using Raman and PanCam technology. *Planet. Space Sci.* 74, 103–110. doi: 10.1016/j.pss.2012.06.010

de Vera, J.-P., Schulze-Makuch, D., Khan, A., Lorek, A., Koncz, A., Möhlmann, D., et al. (2014). Adaptation of an Antarctic lichen to Martian niche conditions can occur within 34 days. *Planet. Space Sci.* 98, 182–190. doi: 10.1016/j.pss.2013.07.014

Dose, K., Bieger-Dose, A., Dillmann, R., Gill, M., Kerz, O., Klein, A., et al. (1995). Era-experiment "Space Biochemistry". *Adv. Space Res.* 16, 119–129. doi: 10.1016/0273-1177(95)00280-R

Edwards, H. G. M., Herschy, B., Page, K., Munshi, T., and Scowen, I. J. (2011). Raman spectra of biomarkers of relevance to analytical astrobiological exploration: hopanoids, sterols, and steranes. *Spectrochim. Acta A.* 78, 191–195. doi: 10.1016/j.saa.2010.09.020

Edwards, H. G. M., Hutchinson, I. B., Ingley, R., and Jehlička, J. (2014). Biomarkers and their Raman spectroscopic signatures: a spectral challenge for analytical astrobiology. *Philos. Trans. R. Soc. A.* 372:20140193. doi: 10.1098/rsta.2014.0193

Edwards, H. G. M., Jorge Villar, S. E., Pullan, D., Hargreaves, M. D., Hofmann, B. A., and Westall, F. (2007). Morphological biosignatures from relict fossilized sedimentary geological specimens: a Raman spectroscopic study. *J. Raman Spectrosc.* 38, 1352–1361. doi: 10.1002/jrs.1775

Edwards, H. G. M., Moody, C. D., Jorge Villar, S. E., and Wynn-Williams, D. D. (2005). Raman spectroscopic detection of key biomarkers of cyanobacteria and lichen symbiosis in extreme Antarctic habitats: evaluation for Mars lander missions. *Icarus* 174, 560–571. doi: 10.1016/j.icarus.2004.07.029

Fairén, A. G., Davila, A. F., Lim, D., Bramall, N., Bonaccorsi, R., Zavaleta, J., et al. (2010). Astrobiology through the ages of Mars : the study of terrestrial analogues to understand the habitability of Mars. *Astrobiology* 10, 821–843. doi: 10.1089/ast.2009.0440

Ghiassi-nejad, M., Mortazavi, S. M. J., Cameron, J. R., Niroomand-rad, A., and Karam, P. A. (2002). Very high background radiation areas of Ramsar, Iran:

preliminary biological studies. *Health Phys.* 82, 87–93. doi: 10.1097/00004032-200201000-00011

Gill, D., Kilponen, R. G., and Rimai, L. (1970). Resonance Raman scattering of laser radiation by vibrational modes of carotenoid pigment molecules in intact plant tissue. *Nature* 39, 371–386. doi: 10.1038/227743a0

Häder, D. P., and Häder, M. A. (1989). Effects of solar and artificial radiation on motility and pigmentation in *Cyanophora paradoxa*. *Arch. Microbiol.* 152, 453–457. doi: 10.1007/BF00446928

Hirayama, O., Nakamure, K., Hamada, S., and Kobayasi, Y. (1994). Singlet oxygen quenching ability of naturally occurring carotenoids. *Lipids* 29, 149–150. doi: 10.1007/BF02537155

Horneck, G., Moeller, R., Cadet, J., Douki, T., Mancinelli, R. L., Nicholson, W. L., et al. (2012). Resistance of bacterial endospores to outer space for planetary protection purposes – experiment PROTECT of the EXPOSE-E mission. *Astrobiology* 12, 445–456. doi: 10.1089/ast.2011.0737

Hunter, S. E., Jung, D., Di Giulio, R. T., and Meyer, J. N. (2010). The qPCR assay for analysis of mitochondrial DNA damage, repair, and relative copy number. *Methods* 51, 444–451. doi: 10.1016/j.ymeth.2010.01.033

Ji, H. F. (2010). Insight into the strong antioxidant activity of Deinoxanthin, a unique carotenoid in *Deinococcus radiodurans*. *Int. J. Mol. Sci.* 11, 4506–4510. doi: 10.3390/ijms11114506

Jorge Villar, S. E., Edwards, H. G. M., and Benning, L. G. (2006). Raman spectroscopic and scanning microscopic analysis of a novel biological colonisation of volcanic rocks. *Icarus* 184, 158–169. doi: 10.1016/j.icarus.2006.04.009

Kawaguchi, Y., Yang, Y., Kawashiri, N., Shiraishi, K., Takasu, M., Narumi, I., et al. (2013). The possible interplanetary transfer of microbes: assessing the viability of *Deinococcus* spp. under the ISS environmental conditions for performing exposure experiments of microbes in the Tanpopo mission. *Orig. Life Evol. Biosph.* 43, 411–428. doi: 10.1007/s11084-013-9346-1

Klein, H. P. (1999). Did Viking discover life on Mars? *Orig. Life Evol. Biosph.* 29, 625–631. doi: 10.1023/A:1006514327249

Kumar, B. N. V., Kampe, B., Rösch, P., and Popp, J. (2015). Characterization of carotenoids in soil bacteria and investigation of their photodegradation by UVA radiation via resonance Raman spectroscopy. *Analyst* 140, 4584–4593. doi: 10.1039/C5AN00438A

Lemee, L., Peuchant, E., and Clerc, M. (1997). Deinoxanthin: a new carotenoid isolated from *Deinococcus radiodurans*. *Tetrahedron* 53, 919–926. doi: 10.1016/S0040-4020(96)01036-8

Leuko, S., Neilan, B. A., Burns, B. P., Walter, M. R., and Rothschild, L. J. (2011). Molecular assessment of UVC radiation-induced DNA damage repair in the stromatolitic halophilic archaeon, *Halococcus hamelinensis*. *J. Photochem. Photobiol.* 102, 140–145. doi: 10.1016/j.jphotobiol.2010.10.002

Marshall, C. P., Leuko, S., Coyle, C. M., Walter, M. R., Burns, B. P., and Neilan, B. A. (2007). Carotenoid analysis of halophilic archaea by resonance Raman spectroscopy. *Astrobiology* 7, 631–643. doi: 10.1089/ast.2006.0097

Mattimore, V., and Battista, J. R. (1996). Radioresistance of *Deinococcus radiodurans*: functions necessary to survive ionizing radiation are also necessary to survive prolonged desiccation. *J. Bacteriol.* 178, 633–637. doi: 10.1128/jb.178.3.633-637.1996

Meeßen, J., Backhaus, T., Brandt, A., Raguse, M., Böttger, U., de Vera, J. P., et al. (2017). The effect of high-dose ionizing radiation on the isolated photobiont of the astrobiological model lichen *Circinaria gyrosa*. *Astrobiology* 17, 154–162. doi: 10.1089/ast.2015.1453

Meeßen, J., Wuthenow, P., Schille, P., Rabbow, E., de Vera, J.-P. P., and Ott, S. (2015). Resistance of the lichen *Buellia frigida* to simulated space conditions during the pre-flight tests for BIOMEX-viability assay and morphological stability. *Astrobiology* 15, 601–615. doi: 10.1089/ast.2015.1281

Pavlov, A. A., Vasilyev, G., Ostryakow, V. M., Pavlov, A. K., and Mahaffy, P. (2012). Degradation of the organic molecules in the shallow subsurface of Mars due to irradiation by cosmic rays. *Geophys. Res. Lett.* 39:L13202. doi: 10.1029/2012GL052166

Pogoda de la Vega, U., Rettberg, P., and Reitz, G. (2007). Simulation of the environmental climate conditions on martian surface and its effect on *Deinococcus radiodurans*. *Adv. Space Res.* 40, 1672–1677. doi: 10.1016/j.asr.2007.05.022

Rabbow, E., Parpart, A., and Reitz, G. (2016). The planetary and space simulation facilities at DLR Cologne. *Microgr. Sci. Technol.* 28, 215–229. doi: 10.1007/s12217-015-9448-7

Rabbow, E., Rettberg, P., Barczyk, S., Bohmeier, M., Parpart, A., Panitz, C., et al. (2012). EXPOSE-E: an ESA astrobiology mission 1.5 years in space. *Astrobiology* 12, 374–386. doi: 10.1089/ast.2011.0760

Rabbow, E., Rettberg, P., Parpart, A., Panitz, C., Schulte, W., Molter, F., et al. (2017). EXPOSE-R2: the astrobiological ESA mission on board of the international space station. *Front. Microbiol.* 8:1533. doi: 10.3389/fmicb.2017.01533

Richmond, R. C., Sridhar, R., Zhou, Y., and Daly, M. J. (1999). Physico-chemical survival pattern for the radiophile *D. radiodurans*: a polyextremophile model for life on Mars. *SPIE* 3755, 210–222. doi: 10.1117/12.375078

Saito, T., Ohyama, Y., Ide, H., Otha, S., and Yamamoto, O. (1998). A carotenoid pigment of the radioresistant bacterium *Deinococcus radiodurans*. *Microbios* 95, 79–90.

Schirmack, J., Böhm, M., Brauer, C., Löhmannsröben, H.-G., de Vera, J.-P., Möhlmann, D., et al. (2014). Laser spectroscopic real time measurements of methanogenic activity under simulated Martian subsurface analogue conditions. *Planet. Space Sci.* 98, 198–204. doi: 10.1016/j.pss.2013.08.019

Sghaier, H., Narumi, I., Satoh, K., Ohba, H., and Mitomo, H. (2007). Problems with the current deinococcal hypothesis: an alternative theory. *Theory Biosci.* 126, 43–45. doi: 10.1007/s12064-007-0004-x

Shahmohammadi, H. R., Asgarani, E., Terato, H., Saito, T., Ohyama, Y., Gekko, K., et al. (1998). Protective role of bacterioruberin and intracellular KCl in the resistance of *Halobacterium salinarum* against DNA-damaging agents. *J. Radiat. Res.* 39, 251–262. doi: 10.1269/jrr.39.251

Shkrob, I. A., Chemerisov, S. D., and Marin, T. W. (2010). Photocatalytic decomposition of carboxylated molecules on light exposed martian regolith and its relation to methane production on Mars. *Astrobiology* 10, 425–435. doi: 10.1089/ast.2009.0433

Slade, D., and Radman, M. (2011). Oxidative stress resistance in *Deinococcus radiodurans*. *Microbiol. Mol. Biol. Rev.* 75, 133–191. doi: 10.1128/MMBR.00015-10

Stahl, W., and Sies, H. (2003). Antioxidant activity of carotenoids. *Mol. Aspects Med.* 24, 345–351. doi: 10.1016/S0098-2997(03)00030-X

Sy, C., Dangles, O., Borel, P., and Caris-Veyrat, C. (2015). Interactions between carotenoids from marine bacteria and other micronutrients: impact on stability and antioxidant activity. *Mar. Drugs* 13, 7020–7039. doi: 10.3390/md13117020

Tian, B., and Hua, Y. (2010). Carotenoid biosynthesis in extremophilic *Deinococcus-Thermus* bacteria. *Trends Microbiol.* 18, 512–520. doi: 10.1016/j.tim.2010.07.007

Tian, B., Sun, Z., Shen, S., Wang, H., Jiao, J., Wang, L., et al. (2009). Effects of carotenoids from *Deinococcus radiodurans* on protein oxidation. *Lett. Appl. Microbiol.* 49, 689–694. doi: 10.1111/j.1472-765X.2009.02727.x

Tian, B., Xu, Z., Sun, Z., Lin, J., and Hua, Y. (2007). Evaluation of the antioxidant effects of carotenoids from *Deinococcus radiodurans* through targeted mutagenesis, chemiluminescence, and DNA damage analysis. *Biochim. Biophys. Acta* 1770, 902–911. doi: 10.1016/j.bbagen.2007.01.016

Tillett, D., and Neilan, B. A. (2000). Xanthogenate nucleic acid isolation from cultured and environmental cyanobacteria. *J. Phycol.* 35, 1–8. doi: 10.1046/j.1529-8817.2000.99079.x

Toporski, J., and Steele, A. (2002). "The relevance of bacterial biomarkers in astrobiological research," in *Proceedings of the Second European Workshop on Exo/Astrobiology*, Vol. SP-518 (Noordwijk: European Space Agency).

Vítek, P., Edwards, H. G. M., Jehlička, J., Ascaso, C., de los Ríos, A., Valea, S., et al. (2010). Microbial colonization of halite from the hyper-arid Atacama desert studied by Raman spectroscopy. *Philos. Trans. R. Soc. A* 368, 3205–3221. doi: 10.1098/rsta.2010.0059

Vítek, P., Jehlička, J., Edwards, H. G. M., Hutchinson, I., Ascaso, C., and Wierzchos, J. (2014). Miniaturized Raman instrumentation detects carotenoids in Mars-analogue rocks from the Mojave and Atacama deserts. *Philos. Trans. R. Soc. A.* 372:20140196. doi: 10.1098/rsta.2014.0196

Vítek, P., Osterrothová, K., and Jehlička, J. (2009). Beta-carotene – A possible biomarker in the Martian evaporitic environment: Raman micro-spectroscopic study. *Planet. Space Sci.* 57, 454–459. doi: 10.1016/j.pss.2008.06.001

Wang, A., Korotev, R. L., Jolliff, B. L., and Ling, Z. (2015). Raman imaging of extraterrestrial materials. *Planet. Space Sci.* 112, 23–34. doi: 10.1177/0003702817721715

Wassmann, M., Moeller, R., Rabbow, E., Panitz, C., Horneck, G., Reitz, G., et al. (2012). Survival of spores of the UV-resistant *Bacillus subtilis* strain MW01 after exposure to Low-Earth Orbit and simulated Martian conditions: data from the space experiment ADAPT on EXPOSE-E. *Astrobiology* 12, 498–507. doi: 10.1089/ast.2011.0772

Winters, Y. D., Lowenstein, T. K., and Timofeeff, M. N. (2013). Identification of carotenoids in ancient salt from Death Valley, Saline Valley, and Searles Lake, California, using laser Raman spectroscopy. *Astrobiology* 13, 1065–1080. doi: 10.1089/ast.2012.0952

Zhang, L., Yang, Q., Luo, X., Fang, C., Zhang, Q., and Tang, Y. (2007). Knockout of *crtB* and *crtI* gene blocks the carotenoid biosynthetic pathway in *Deinococcus radiodurans* R1 and influences its resistance to oxidative DNA-damaging agents due to change of free radicals scavenging ability. *Arch. Microbiol.* 188, 411–419. doi: 10.1007/s00203-007-0262-5

Conflict of Interest Statement: The authors declare that the research was conducted in the absence of any commercial or financial relationships that could be construed as a potential conflict of interest.

frontiers in Microbiology

ORIGINAL RESEARCH
published: 28 April 2017
doi: 10.3389/fmicb.2017.00671

The Impact of Space Flight on Survival and Interaction of *Cupriavidus metallidurans* CH34 with Basalt, a Volcanic Moon Analog Rock

*Bo Byloos[1,2], Ilse Coninx[1], Olivier Van Hoey[3], Charles Cockell[4], Natasha Nicholson[4], Vyacheslav Ilyin[5], Rob Van Houdt[1], Nico Boon[2] and Natalie Leys[1]**

[1] Microbiology Unit, Belgian Nuclear Research Centre, SCK•CEN, Mol, Belgium, [2] Center for Microbial Ecology and Technology, Ghent University, Ghent, Belgium, [3] Research in Dosimetric Applications, Belgian Nuclear Research Centre, SCK•CEN, Mol, Belgium, [4] UK Centre for Astrobiology, School of Physics and Astronomy, University of Edinburgh, Edinburgh, UK, [5] Institute of Medical and Biological Problems of Russian Academy of Sciences, Moscow, Russia

Microbe-mineral interactions have become of interest for space exploration as microorganisms could be used to biomine from extra-terrestrial material and extract elements useful as micronutrients in life support systems. This research aimed to identify the impact of space flight on the long-term survival of *Cupriavidus metallidurans* CH34 in mineral water and the interaction with basalt, a lunar-type rock in preparation for the ESA spaceflight experiment, BIOROCK. Therefore, *C. metallidurans* CH34 cells were suspended in mineral water supplemented with or without crushed basalt and send for 3 months on board the Russian FOTON-M4 capsule. Long-term storage had a significant impact on cell physiology and energy status (by flow cytometry analysis, plate count and intracellular ATP measurements) as 60% of cells stored on ground lost their cell membrane potential, only 17% were still active, average ATP levels per cell were significantly lower and cultivability dropped to 1%. The cells stored in the presence of basalt and exposed to space flight conditions during storage however showed less dramatic changes in physiology, with only 16% of the cells lost their cell membrane potential and 24% were still active, leading to a higher cultivability (50%) and indicating a general positive effect of basalt and space flight on survival. Microbe-mineral interactions and biofilm formation was altered by spaceflight as less biofilm was formed on the basalt during flight conditions. Leaching from basalt also changed (measured with ICP-OES), showing that cells release more copper from basalt and the presence of cells also impacted iron and magnesium concentration irrespective of the presence of basalt. The flight conditions thus could counteract some of the detrimental effects observed after the 3 month storage conditions.

Keywords: microbe-mineral interactions, space flight, *Cupriavidus metallidurans* CH34, basalt, FOTON

OPEN ACCESS

Edited by:
Daniela Billi,
University of Rome Tor Vergata, Italy

Reviewed by:
James F. Holden,
University of Massachusetts Amherst, USA
Kai Waldemar Finster,
Aarhus University, Denmark

***Correspondence:**
Natalie Leys
natalie.leys@sckcen.be

Specialty section:
This article was submitted to Extreme Microbiology, a section of the journal Frontiers in Microbiology

Received: *06 February 2017*
Accepted: *31 March 2017*
Published: *28 April 2017*

Citation:
Byloos B, Coninx I, Van Hoey O, Cockell C, Nicholson N, Ilyin V, Van Houdt R, Boon N and Leys N (2017) The Impact of Space Flight on Survival and Interaction of Cupriavidus metallidurans CH34 with Basalt, a Volcanic Moon Analog Rock. Front. Microbiol. 8:671. doi: 10.3389/fmicb.2017.00671

INTRODUCTION

Microorganisms can interact with rocks and minerals to enhance leaching of elements for sustaining their survival and growth. They can impact rock and mineral weathering through production of organic acids and other ligands, which in turn impact mineral solubility, denudation, and speciation (Dong, 2010). These microbe-mineral interactions are in fact essential for soil

formation through biotransformation, biochemical cycling, and bioweathering (Gadd, 2010). In addition, they can be useful for and have already been applied in industry. For example, acidophilic iron- and sulfur oxidizing bacteria are used in biomining applications to oxidize copper and gold sulfidic bonds in order to solubilize and recover the economically interesting metals from the ores (Ubaldini et al., 2000). These interactions can also lead to the formation of biofilm communities on the mineral surface, in which members will be protected from harsh environments (Harrison et al., 2005).

Microbe-mineral interactions have also become of interest for space exploration missions. At the moment, human presence in space needs to be fully supported from Earth. To reduce the costs and the dependency for supplies from Earth for future more distant space missions, current research is investigating if supplies can be generated from endogenous material on planets and asteroids, such as the regolith and rocks. Microorganisms can be used in this process of *in-situ* resource utilization (ISRU) to extract useful elements that could be applied as fertilizers in a life support system and in the formation of fertile soil for plant cultivation (Cockell, 2010).

Since space conditions have been shown to cause many changes in bacterial physiology, including changes in motility and biofilm formation (Brown et al., 2002; Leys et al., 2004; Horneck et al., 2010; Leroy et al., 2010; Kim et al., 2013), these conditions may also influence microbe-mineral interactions as microgravity eliminates mass-driven convection and only diffusion can impact element release and availability as well as alter microbe-mineral contact (Jánosi et al., 2002). To evaluate the possibility of microbe-based ISRU, the potential impact of space environmental conditions such as microgravity and radiation on microbe-mineral interactions need to be studied.

Our study aimed at investigating the influence of space conditions on these microbe-mineral interactions, by testing the impact of space flight conditions on the survival and biofilm formation of the bacterium *Cupriavidus metallidurans* CH34 in mineral water supplemented with basalt. *C. metallidurans* is a motile β-proteobacterium that is found in the natural communities of basaltic rock (Sato et al., 2004). Furthermore, the interaction of type strain CH34 with basalt has already been studied and indicated that stress and starvation responses are triggered in the presence of basalt (Bryce et al., 2016) and that strain CH34 can sequester iron from basalt to sustain its growth (Olsson-Francis et al., 2010). In addition, type strain CH34 has been used previously as test organism to investigate bacterial behavior in space (Leys et al., 2009).

Thus, in order to prepare for a potential future feasibility studies of the biomining process in space (the ESA BIOROCK experiment), here preliminary tests were performed to assess the impact of flight conditions on an inactive bacterial inoculum, and its interactions with basalt rock. Therefore, *C. metallidurans* CH34 was stored in mineral water supplemented with basaltic rock and send on board of the FOTON-M4 capsule for 3 months. After flight, cell survival, physiology, biofilm formation, and the elements leaching from basalt were investigated.

MATERIALS AND METHODS

Strain and Media Composition

Cupriavidus metallidurans type strain CH34 (Mergeay et al., 1985) was cultivated at 30°C on a shaker in dark, aerobic conditions in a Tris buffered mineral (284 MM) medium containing 2 g/l sodium gluconate (Merck) as sole and more selective carbon source (Mergeay et al., 1985). The composition of the mineral water (Chaudfontaine, Belgium) used for cell's suspensions is given in **Table 1**, according to manufacturer's analysis. Cultivable bacteria were enumerated as CFUs on R2A medium (2% agar; Thermo Scientific, Belgium) and 284 MM agar (2% agar). R2A medium is a general medium used to plate out environmental samples taken from drinking water or aqueous environments (Reasoner and Geldreich, 1985).

Basalt Composition

Basalt, an igneous volcanic rock, was used as analog to the basalt rock that is found on the Mare regions of the Moon which have a low Ti content (Anand et al., 2012). The basalt was taken from the mid-ocean ridge close to the Eyjafjallajökull volcano in Iceland. The composition of this basalt is given in **Table 2**.

Flight Setup

Three independent cultures of *C. metallidurans* CH34 were grown to stationary phase ($OD_{600\ nm} \sim 1$), cells were harvested and washed three times with 10 mM $MgSO_4$ and re-suspended in mineral water (10^9 cells/ml, $OD_{600\ nm} = 1$). Five milliliters of this cell suspension was transferred to silicone cryogenic vials (VWR international, Belgium) and supplemented with or without 10 w/v % basalt, which was crushed to 1–2 mm in size, washed in deionized water and heat sterilized beforehand. A control without cells containing only water and basalt was also prepared. Two replicate sets were prepared: one for flight and one for ground control.

The prepared cryogenic vials were wrapped with parafilm to secure the caps. Active temperature loggers (Smartbuttons, ACR systems, Canada) were added to the packages as well as passive radiation sensors [Thermoluminescence detectors (TLDs) and optically stimulated luminescence detectors (OSLDs); (Goossens et al., 2006; Vanhavere et al., 2008)] to monitor the temperature

TABLE 1 | Composition of Chaudfontaine mineral water.

Composition	mg/l
HCO_3	305
Ca	65
Na	44
SO_4	40
Cl	35
Mg	18
K	2.5
F	0.4
NO_3	<0.1
pH	7.6
Dry weight (Total suspended solid; 180°C)	385

TABLE 2 | Composition of basaltic rock used in the experiment.

%		ppm	
SiO_2	51.1	Nb	0.7
Al_2O_3	15.16	Zr	46.8
FeO	9.53	Y	25.1
MgO	8.87	Sr	64
CaO	12.36	Rb	0.5
Na_2O	1.76	Zn	79.4
K_2O	0.05	Cu	95.3
TiO_2	0.91	Ni	131.6
MnO	0.18	Cr	351.1
P_2O_5	0.08	V	301.4
Sum	100	Ba	2.5
Lost on ignition (LOI)	−0.47	Sc	47.6

changes and the total radiation dose cumulated over the duration of the experiment.

The complete flight package was kept in the dark at ambient temperature (22.9 ± 1.8°C, **Figure 1A**) before and during transport from SCK•CEN (Mol, Belgium) to Moscow (Russia). It left SCK•CEN on 28th of June 2014, 3 weeks before the launch of the FOTON-M4 capsule. Ten days before launch, the samples were transported from Moscow (Russia) to the launch site (Baikonour, Kazakhstan), and put in the capsule 1 day before launch on July 18, 2014 (**Figure 1D**). Samples were kept at lower temperature during this transport (7.8 ± 3.9°C, **Figure 1A**). Inside the FOTON M4 capsule the experiment was kept at ambient temperature (17.6 ± 2.5°C, **Figure 1A**). The FOTON M4 capsule flew at 575 km altitude, with a 64.9° inclination in Low-Earth orbit and returned to Earth on September 1, 2014. Samples were returned from the landing site to Moscow at which temperatures were again low (7 ± 0.5°C). Samples then returned to SCK•CEN (Mol, Belgium) on September 30, 2014, while at ambient temperature (22.4 ± 2.1°C). The parallel ground control was kept at SCK•CEN at ambient temperature during the complete time period (22.9 ± 3°C, **Figure 1B**). Total radiation dose absorbed in water for the flight samples was measured and was 20.1 ± 1.47 mGy over the whole experiment duration. For the ground experiments the total dose was 1.2 ± 0.02 mGy.

To test the influence of temperature and storage conditions, a post-flight control ground experiment with and without basalt was performed. The cell suspensions and basalt were exactly prepared as mentioned in Section Flight Setup. Cryo tubes were placed in an incubator and the temperature profile of the flight experiment was simulated. At the end, the samples were analyzed exactly as described for the flight experiment (Section Post-flight Analysis). Data from this experiment is showed as "T ground" conditions in the results. The temperature profile is shown in **Figure 1C**. The data from these stimulated flight temperatures samples are used in the further results part of this paper.

Post-flight Analysis

After return to SCK•CEN, the samples were kept at ambient temperature and processed for analysis. Liquid was aspirated and 1 ml of this solution was transferred to sterile tubes for the following analyses: (1) two hundred microliters was used to estimate the number of viable cells by plating a serial dilution on R2A and 284 MM agar, (2) two hundred microliters was used for flow cytometry analysis, ATP and PHB measurements and (3) six hundred microliters was used to measure pH. The remaining 4 ml of the solution was used for ICP-OES analysis (see Section ICP-OES).

Contamination was revealed on the counting agar plates of the flight samples both on 284 MM and R2A in a level to 10^4–10^5cells/ml, as colonies visually different from CH34 were present until these dilutions. The cause of this contamination is unclear. No contaminations were found in the parallel ground control set, which was prepared and analyzed at the same time.

Sonication

After liquid aspiration, a piece of the basalt was aseptically removed from the tubes and analyzed with Scanning Electron Microscopy (see Section SEM). Next, 5 ml filtered mineral water was added and the solution was probe sonicated for 3 min at 20 kHz, 4 W at low-intensity to release the biofilm and intact cells from the biofilm from the basalt. The protocol for sonication was determined before the flight experiment based on previously described protocols (Kobayashi et al., 2009) and was found to be optimal at the conditions described above. After sonication, the solution was again analyzed as described in the post-flight analysis.

Flow Cytometry

Samples were stained and analyzed with flow cytometry to analyze physiology and impact of space flight conditions on the CH34 cells. This was done according to the optimized procedures, described in Buysschaert et al. (2016), Van Nevel et al. and SLMB recommendation for characterizing drinking water communities (SLMB, 2012; Van Nevel et al., 2013; Buysschaert et al., 2016). Cell suspensions were diluted 10,000 times in 0.2 μm filtered Evian mineral water, as this gave the lowest background fluorescence. Next, the different dyes were added and cell suspensions were incubated at 35°C. The tested dyes include $DiBAC_4(3)$ (Sigma Aldrich, U.S.A.), cFDA (Sigma Aldrich, U.S.A.), SYBR Green (Sigma Aldrich), and PI (Sigma Aldrich). The different dye concentrations and incubations times are shown in **Table 3**. Work solutions were all prepared in DMSO and kept at 4°C. These were prepared from stock solutions in DMSO kept at −20°C. For cFDA and $DiBAC_4(3)$ cells were centrifuged and washed with Evian water before analyzing the samples with flow cytometry to eliminate background signals from the staining solution. For the other dyes, stained cell solutions were analyzed directly after incubation and the cells were not washed.

Stained bacterial suspensions were analyzed on an Accuri C6 (BD, Erembodegem) with a blue (488 nm, 20 mW) and red (640 nm, 14.7 mW) laser which was calibrated according to the manufacturer's recommendation. Standard optical filters were used and included FL-1 (530/30 nm), FL-2 (585/40 nm), and FL-3 (670 LP) for the blue laser and FL-4 (675/25 nm) for the red laser. The dyes $DiBAC_4(3)$, cFDA, and SYBR

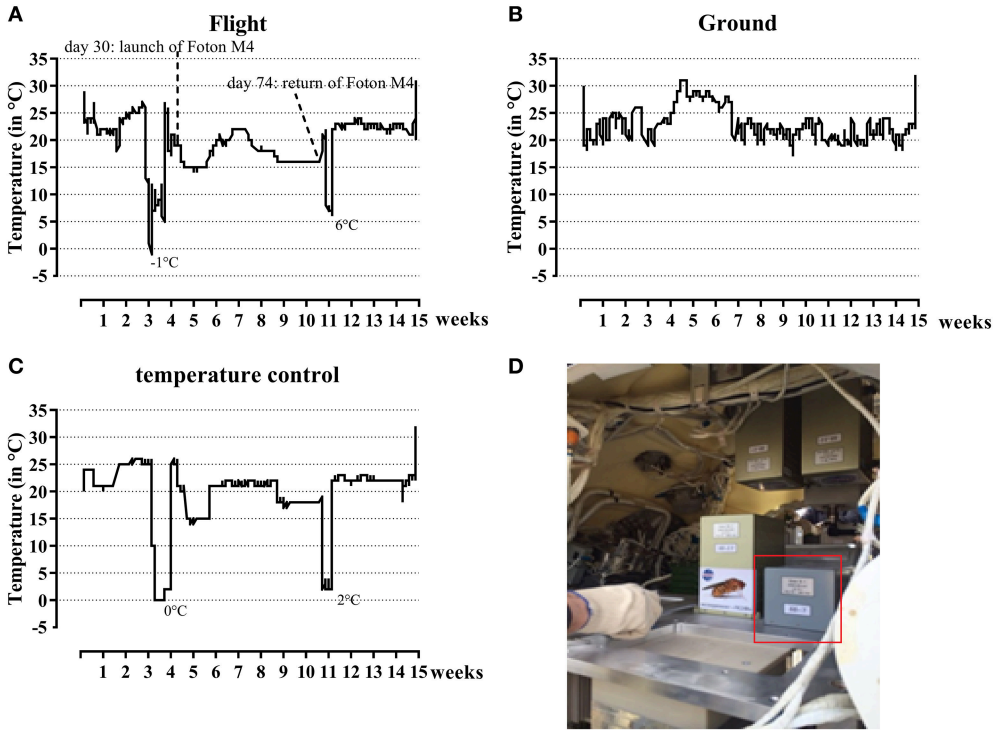

FIGURE 1 | Temperature profiles during the flight experiment and simulated control experiment and its setup in the FOTON capsule. Both during flight **(A)** and ground **(B)** temperature profiles were determined. The temperature profile for the flight experiment was later on simulated **(C)** to determine the effect of these changes on the results. The experiment as set-up in the FOTON capsule is circled in red **(D)**.

TABLE 3 | Used dyes for flow cytometer analysis, incubation times and concentration.

Stain	Analysis (<2,000 events/μl)	Incubation (35°C)	Final concentration	Excitation (nm)/Emission (nm)
SYBR Green (SG)	All cells	13 min	1x	497/520
Propidium iodide (PI)	Permeabilized cells	13 min	0.2 μM	533/617
5(6)-Carboxyfluorescein diacetate (cFDA)	Active cells	20 min	10 μM	488/515
Bis(1,3-dibutylbarbituric acid) trimethine oxonol [$DiBAC_4(3)$]	Membrane polarization and potential	20 min	5 μM	490/520

Green were all detected with FL-1, PI was detected on FL-3. A quality control with 6 and 8 peaks fluorescent beads (by manufacturer BD, Erembodegem) and cleaning cycle was performed prior to experiments to assess both the accuracy (bead count and position) and the cleanliness of the machine. Samples were analyzed using the Accuri C6 software (version 1.0.264.21). The flow files were uploaded to FlowCyte database (FR-FCM-ZYZQ).

The different dyes are used to test for different physiological parameters and determine the effect of the flight conditions on CH34. Sybr Green (SG) was used to stain all cells as this stain can enter both intact and damaged cells independent from their physiological state. SG enters the cells in both permeabilizated and non-permeabilizated cells due to its positive charge which allows it to pass it through the membrane (Veal et al., 2000; Berney et al., 2007, 2008). $DiBAC_4(3)$ staining allows differentiating between cells with an intact membrane potential and normal polarization and cells which have a depolarized membrane or lost membrane function as $DiBAC_4(3)$ can only enter the latter due to its anionic structure. Once in the cell it binds to positively charged proteins or hydrophobic regions. No binding of $DiBAC_4(3)$ with outer membrane structures is observed. Increased depolarization of the membrane also causes more influx of $DiBAC_4(3)$ while hyperpolarization causes a decrease in influx and thus fluorescence (Berney et al., 2008; Muller and Nebe-Von-Caron, 2010; Sträuber and Müller, 2010). cFDA staining can passively enter cells and is metabolized by esterase enzymes in the cytoplasm to its fluorescent product cFluorescein (cF) that accumulates in the cytoplasm and is thus an indicator for enzymatic cell activity. Negative charges present in cF ensures that it is better retained in the cell, avoiding leakage of the product as well as reducing

background signal by unspecific binding (Sträuber and Müller, 2010).

SEM

To obtain an idea about cell morphology and biofilm structure Scanning Electron Microscopy (SEM) was performed. Five microliters of the solution as well as a piece of basalt was taken and transferred to a 0.2 μm filter (Milipore) and fixed two times with fixation solution [3% gluteraldehyde (w/v) in 0.15 M cacodylate solution, pH 7.6] in filter holders. Between each fixation step, the membrane was left to dry for 20 min at room temperature. Afterwards the filter surface was washed three times with the wash solution (0.15 M cacodylate solution). Next, filter holders were wrapped with parafilm and stored overnight at 4°C to let the filters dry. The next day, the filter surface was rinsed with ethanol, in ascending concentrations (30, 50, 70, 90, 95, 100% v/v), once for each concentration. Between each step the filters were left to dry for 10 min. The final rinsing with 100% ethanol was done three times. To dry the surface completely, the ethanol solution was replaced with hexamethyldisilazane (HMDS), and the filters were again rinsed three times, with 10 min of incubation between each step. Next, the filters were air-dried in a desiccator for storage. For visualization, these filters were taped onto an aluminum stub using carbon tape and coated with gold particles using the ScanCoat machine (2 × 300 ms, 6–8 mbar argon; 50 mA plasma tension). They were directly thereafter visualized with the JEOL JSM6610LV SEM Microscope with a W filament.

Intracellular ATP

To measure intracellular ATP levels the BIOTHEMA intracellular ATP kit HS was used and adapted from the manufacturer's protocol for smaller volumes. Cell suspensions were diluted 1/100 and 25 μl of this dilution was added in a cuvette. Twenty-five microliters of ATP eliminating agent was added and the cuvette was left to incubate for 10 min to degrade all the extracellular ATP. Twenty-five microliters of cell lysis "extractant BS" was added to the cell solution, vortexed and immediately thereafter 200 μl "ATP reagent HS" was added. Luminescence was measured immediately after (Kikkoman Lumitester c-100). Five microliters of a 100 nmol/l ATP standard was added as an internal control and light emission (luminescence) was measured again. From the overall amount of ATP (in pmol) measured in the samples, i.e., the value I, then the average intracellular ATP concentration per cell was calculated as follows:

$$\frac{\left(\frac{I_{sample}}{I_{standard+sample}-I_{sample}}\right)}{\textit{total cell count (with SG in flow) in measured sample}}$$

Intracellular PHB

To measure intracellular PHB levels, a Nile Red staining protocol was developed, based on the work of Degelau et al. (1995), for *C. metallidurans* CH34 and adapted to our test conditions. Nile red binds selectively to non-polar lipid droplets inside cells and can be used to detect the presence of storage lipids (PHA/PHB) via fluorescence spectrophotometry (Greenspan and Fowler, 1985; Johnson and Spence, 2010). A Nile red working solution (200 mg/l) was prepared from a 1 g/l Nile red stock solution in DMSO, stored at −20°C. Ten microliters of the cell solution was diluted in 100 μl sterile Evian mineral water in a micro titer plate (MTP). Five microliters of the work solution was added and the MTP was incubated for 30 min at 30°C. Water without cells but with dye was used as a negative control and water without cells and without dye was used for background correction (blanco). Afterwards fluorescence of the lipid-bound Nile red was determined with a Thermo Scientific™ Fluoroskan Ascent™ Microplate Fluorometer. Nile red solution has an excitation peak at 544 nm and an emission peak at 590 nm. The normalized amount of intracellular PHB per cell was then calculated with following formula:

$$\frac{\frac{(FI_{590\ nm,\ 10\ \mu l\ sample}-FI_{590\ nm,\ negative\ control}-FI_{590\ nm,\ blanco})}{OD_{600\ nm}}}{\textit{total cell count (with SG) in measured sample}}$$

ICP-OES

At the end of the experiment, the in-organic element concentrations in the water were measured to compare changes in water chemistry induced by the rocks and cells during the experiment. Four milliliters of the supernatant from the vials without basalt fragments was taken from the tubes and centrifuged (10,000 × g; 15 min, 20°C) to pellet the cells. This supernatant was then filtered through a 0.22 μm filter to remove particles and 20 μl of 70% nitric acid was added before final inorganic element concentrations in the cell-free supernatant were determined by ICP-OES (Inductively Coupled Plasma Optical Emission Spectroscopy). Details on the wavelengths used for ICP-OES analysis are provided in **Supplementary Table S1**. For concentrations below the detection limit, values were changed to zero and analyzed in the subsequent statistical analysis as such.

Statistical Analysis

For the statistical analysis of the data the GraphPad Prism (version 7.0) software package was used. For all the data of the cell suspension, normal distribution was assumed, while homogeneity of variances was tested with Levene's test and a two-tailed, one way ANOVA was used with Tukey *post-hoc* testing (alpha = 0.05). *P*-values of the statistical analysis are mentioned in **Supplementary Table S2**.

RESULTS

The Effect of Space Flight and Basalt on Cell Survival and Physiology

Effect of Space Flight on Cultivability

To assess cell viability and cultivability after space flight, a serial dilution of the cell suspensions was plated on R2A and 284 MM agar (**Figures 2A,B** respectively). Cultivability significantly decreased ($p < 0.0001$) in the space flight experiment, compared to the initial cell number, irrespective of the presence of basalt, leading to 50% of the population remaining cultivable. Statistical analysis have been summarized in **Table 4**. A greater loss of cultivability was observed for the

ground experiment with only 1 and 0.1% of the population still being cultivable, with and without basalt, respectively. These results indicated that cultivability decreased significantly less during space flight compared to the ground control and that the presence of basalt positively affected cultivability of the ground control.

Effect of Space Flight on Physiology

The impact of space flight conditions and the presence of basalt on physiological changes within the cells were analyzed with flow cytometry by staining with specific functional dyes. The total cell numbers, measured with SYBR Green (SG), decreased slightly but significantly in samples without basalt ($p < 0.0002$) compared to the initial cell number as well as in the ground sample with basalt ($p < 0.0336$). When ground and flight samples were compared, flight samples with basalt significantly differed from the ground samples ($p < 0.003$, **Figure 2C**). When intact cell numbers were compared (by measuring SG positive cells when stained with both SG and PI, **Figure 2D**) to the initial setup (with 99% of the population intact in the initial setup) only the flight sample without basalt differs significantly, containing 60% intact cells ($p < 0.0001$). In addition, these samples also were significantly different from the flight samples with basalt (86%) ($p < 0.0001$) and ground with and without basalt (90%; $p < 0.0001$). Permeabilizated fractions (measuring the PI positive cells when stained with both SG and PI, **Figure 2E**) increased significantly in all test conditions ($p < 0.0001$) compared to the initial (contained 1% permeabilizated cells). Both flight conditions with and without basalt and ground control without basalt contained more permeabilizated cells then the ground with basalt, which only contained 5% permeabilizated cells. The number of cells stained with $DIBAC_4(3)$ (**Figure 2F**), related to cells that lost their membrane potential, significantly increased ($p < 0.0014$) in all conditions compared to the initial amount in the initial culture (3%). Less membrane potential-defected cells were observed in the flight samples with basalt (16%) significantly differing ($p < 0.0078$) from the ground samples and flight samples without basalt, indicating that the presence of basalt and flight conditions reduced the number of cells that lost their membrane potential. Cell activity measurements, with cFDA (**Figure 2G**) showed that the number of active cells in the flight experiment with basalt did not significantly differ ($p > 0.1647$) from the initial setup (35%), in contrast to the other samples ($p < 0.0095$) with decreased numbers of active cells. Basalt also increased the number of active cells in the flight sample with basalt (26%) compared to other conditions.

Effect of Space Flight on Energy Status

Intracellular ATP was measured to determine the energy status of the cells (**Figure 2H**). When ATP levels were compared with the initial culture ($p << 0.0001$), ATP levels decreased 3-fold in the stored cells in water, in all conditions. Flight had a significant effect ($p < 0.0439$) on ATP levels with flight samples containing more ATP/cell then the ground samples. Basalt did not impact ATP levels, neither for ground nor flight samples. In addition, the energy stock of the cells was estimated by measuring PHB content (**Figure 2I**). The PHB content per cell significantly increased after the 3 months of storage of the cells in water ($p < 0.005$), in all conditions, compared to the initial culture and on average doubling PHB concentration. No significant difference ($p > 0.0792$) was seen between ground and flight samples except for the ground samples without basalt ($p < 0.0376$) which contained more PHB then the ground and flight samples with basalt.

The Effect of Basalt and Space Flight on Biofilm Formation

SEM Microscopy

SEM analysis showed biofilm formation on basalt under flight conditions and in the ground control experiment, although the biofilm formed during flight conditions was less developed (**Figure 3**). On the ground the basalt surface is completely covered with biofilm cells, while for the flight samples some basalt surface can still be seen (**Figure 3**, flight). The level of biofilm formation in the ground control samples is comparable to that observed in preflight preparation experiments with the same setup (showed in **Supplementary Figure S1**).

Effect of Space Flight on Cultivability of Biofilm Cells

When biofilm cells were cultured on R2A and 284 MM agar (**Figures 4A,B** respectively), the viable count for flight was significantly higher ($p < 0.0058$) than the ground samples. The number of cultivable cells in the biofilm fraction was also 1–1.4 log lower than in the planktonic cell fraction, indicating a significant impact ($p < 0.0003$) of the biofilm mode of growth on cultivability.

Effect of Space Flight on Physiology of Biofilm Cells

The total biofilm cell number was significantly lower ($p < 0.0004$; **Figure 4C**) in the flight samples compared to the ground. Flight samples also contained significantly more permeabilizated cells ($p > 0.004$; **Figure 4E**) and less intact cells ($p > 0.0001$; **Figure 4D**). No significant differences were observed for activity (**Figure 4G**) and membrane potential (**Figure 4F**) between flight and ground conditions.

Effect of Space Flight on Energy Status of Biofilm Cells

No significant difference was observed between the intracellular ATP levels nor the PHB content of biofilm cells from the flight and ground experiment (**Figure 4H**). In contrast, the ATP content of the biofilm cells is 10x lower than the ATP content ($p < 0.0006$) of the planktonic cells while the intracellular PHB content does not significantly differ from the planktonic cells in suspension (**Figure 4I**).

The Effect of Basalt on Element Release

ICP-OES was performed to quantify magnesium, aluminum, calcium, iron, copper, and phosphate in solution and to evaluate the possible impact of CH34 cells on the leaching of elements from basalt (**Figure 5**). The long-term storage of basalt in mineral water did not significantly impact the concentration of any of the five tested elements, except for calcium. Water with basalt, both from flight and ground contained significantly less

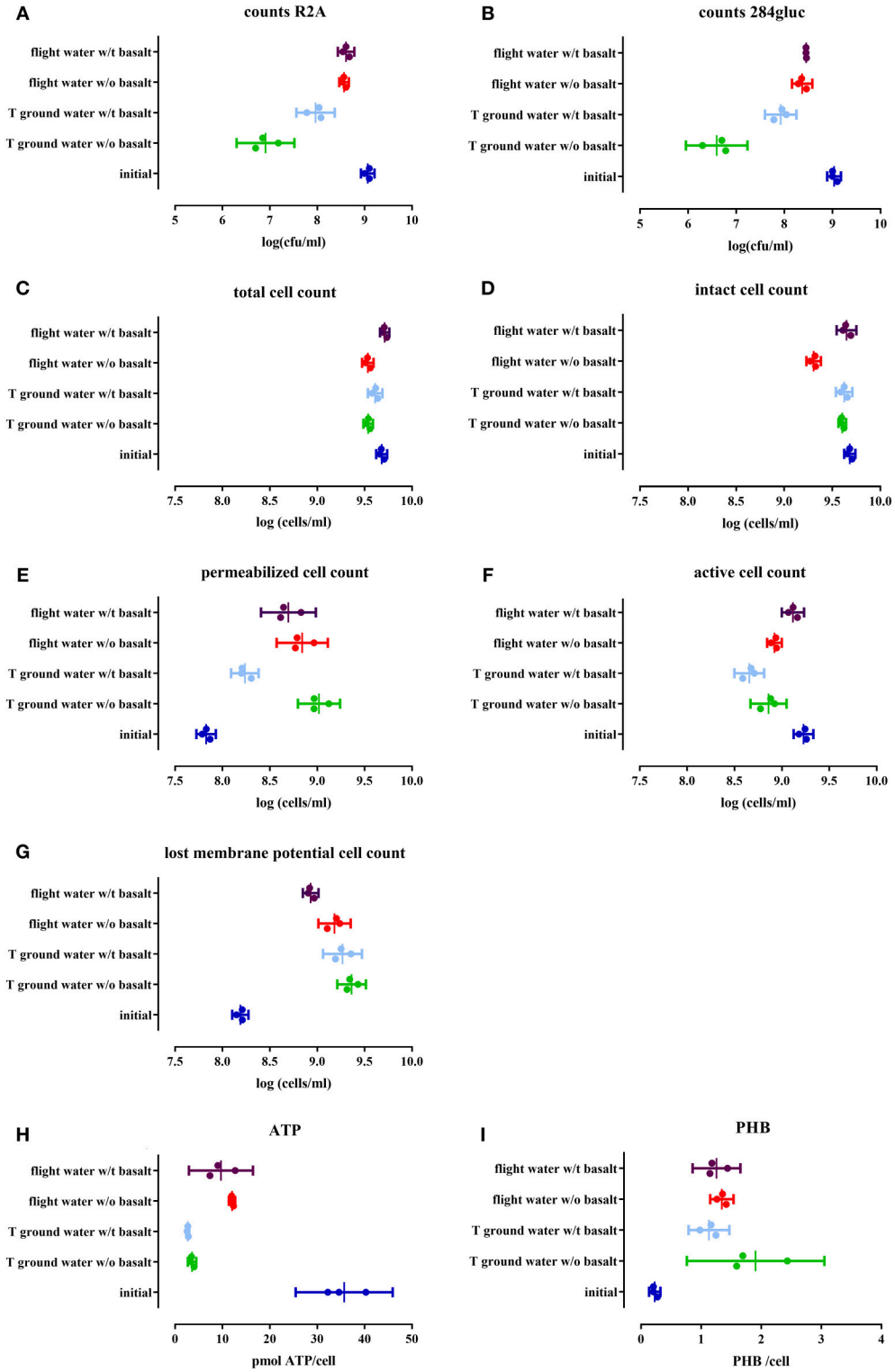

FIGURE 2 | Cell physiology, cultivability, ATP and PHB levels of an initial stationary phase culture of CH34 cells stored in mineral water with (indicated with w/t) and without (w/o) basalt, analyzed after the three month flight experiment and after the control temperature ground experiment. All replicates are represented by a dot; the mean is indicated as a line as well as the 95% confidence interval between the brackets. For the statistical analysis, one way ANOVA was used with Tukey post testing (alpha = 0.05), *p*-values as well as significance are reported in **Table 4** and in **Supplementary Table S2**. Samples were plated on R2A **(A)** and 284 MM **(B)** to determine cultivability of CH34. The total cells number (SG) **(C)** as well as the number of intact cells (SGPI) **(D)**, permeabilizated (SGPI) **(E)**, active (cFDA) **(F)**, and cells which have lost their membrane potential [$DIBAC_4(3)$] **(G)** were measured. ATP **(H)** and PHB **(I)** content of the cells was also measured.

TABLE 4 | Summarizing table of the results for the different parameters of the planktonic cell fraction as well as the statistical significance (*P*-value), cultivability decrease and percentages of the population measured with flow cytometry.

Parameter	Condition	Amount	Significance	*P*-value	Amount
Cultivability	Initial	9 log = 100%	Ground	<0.0001	95% log decrease
			Flight	0.0162	50% log decrease
	Flight		Ground	0.0025	90% decrease
	Basalt		Ground	<0.0001	90% log decrease
Total cell count	Initial		Ground	0.0336	
			Flight w/o basalt	0.0002	
	Flight		Ground	0.0185	
			Flight w/t basalt	<0.0001	
	Basalt		Ground	0.0247	
			Flight	<0.0001	
Intact	Initial	99%	Flight w/o basalt	<0.0001	60%
	Flight	73%	Flight w/o basalt	<0.0001	60%
	Basalt	86%	Flight w/o basalt	<0.0001	60%
Permeabilized	Initial	1%	Ground	0.0014	15%
			Flight	<0.0001	17%
	Flight	17%	Ground	0.0078	15%
			Flight w/t basalt	0.0006	10%
	Basalt	6%	Ground w/t basalt	<0.0001	4%
Active	Initial	35%	Ground	<0.0001	16%
			Flight w/o basalt	0.0003	24%
	Flight	24%	Ground	0.0013	16%
			Flight w/t basalt	<0.0001	25%
	Basalt	18%	Ground	0.0073	16%
			Flight	0.0095	25%
Lost membrane potential	Initial	3%	Ground	<0.0001	56%
			Flight	<0.0001	30%
	Flight	30%	Ground	0.0251	56%
			Flight w/t basalt	0.0003	17%
	Basalt	27%	Flight w/t basalt	0.0029	17%
ATP	Initial		Flight	<0.0001	
			Ground	<0.0001	
	Flight		Ground	0.0439	
PHB	Initial		Ground	0.005	
			Flight	0.002	
	Flight		Flight w/t basalt	0.0376	
	Basalt		Ground w/t basalt	0.0135	

calcium compared to the start ($p < 0.0225$), indicating that basalt triggered a calcium complexation and removal from the water. The presence of CH34 cells impacted these concentrations: in the ground experiments there was more magnesium found in the water with cells with basalt compared to samples from the ground without cells with basalt ($p < 0.0275$) and the start of the experiment ($p < 0.0181$). No significant difference could be seen for magnesium in the flight samples compared to the ground samples. This is also the case for iron where samples from the ground samples contained significantly more iron compared to the condition without cells ($p < 0.0254$) and with and without basalt ($p < 0.0468$). Next, both ground and flight samples with basalt with cells contained significantly more copper than with basalt but without cells ($p < 0.0013$) and with cells but without basalt ($p < 0.006$). Flight and ground samples were however not significantly different from one another for copper ($p > 0.5597$). For calcium, only the cells from the flight experiment without basalt were significantly different from the other conditions ($p < 0.0251$), not showing any calcium complexation because basalt was not present in the samples. Phosphate concentrations in the ground and flight samples without basalt were significant higher than the conditions which contained basalt with ($p < 0.0004$) and without cells ($p < 0.0491$).

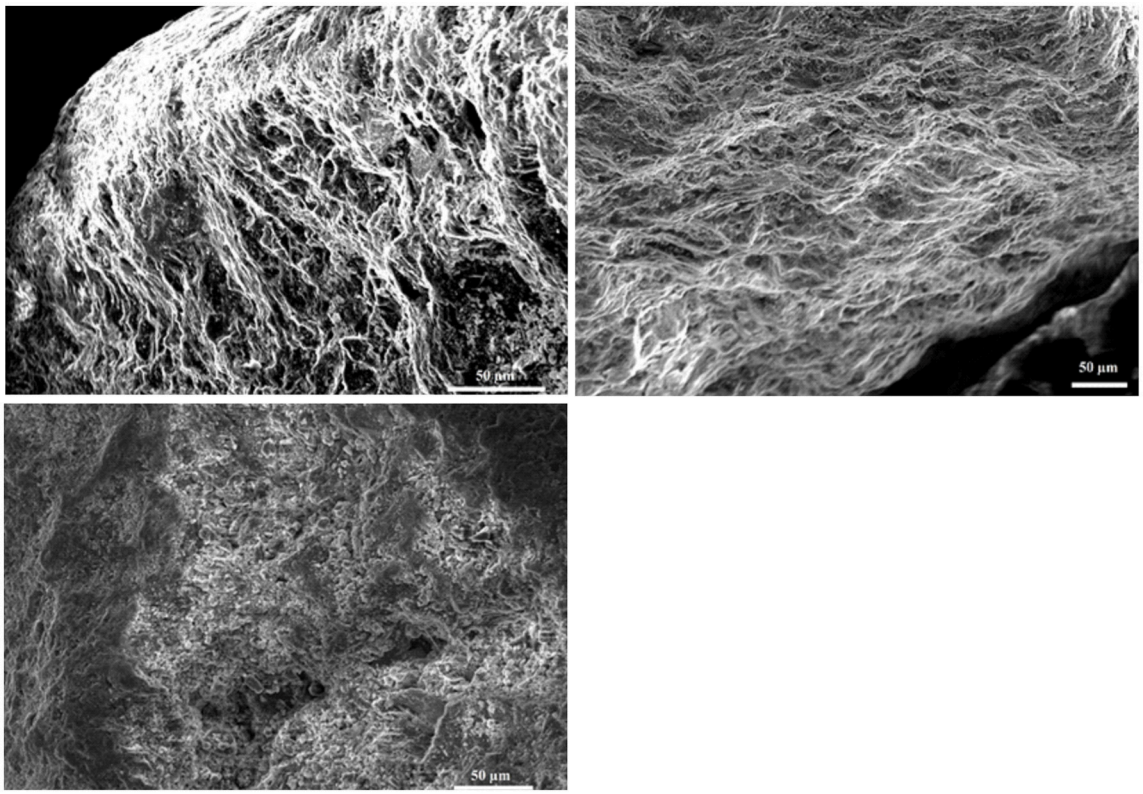

FIGURE 3 | Images obtained by SEM microscopy. Upper left is a SEM image of basalt from the flight experiment and upper right a SEM image of basalt from the ground experiment. The control, lower right, is a SEM picture of the basalt after the 3 month experiment where no cells have been added and the surface of the basalt can be seen. Both in ground and flight experiment, biofilm covers the basalt surface. For the flight, less thick biofilm is seen as the surface is still visible and the biofilm does not cover the whole surface such as seen in the ground picture.

DISCUSSION

To evaluate the effect of space flight conditions on the survival of *C. metallidurans* CH34, a 3-month space flight experiment on board the Russian FOTON-M4 capsule was conducted with cells suspended in mineral water. In addition, the effect of the presence of basalt and biofilm formation on basalt was scrutinized.

As expected, long-term storage had a significantly detrimental effect on physiology and cultivability of CH34 cells. Both flight and ground samples with and without basalt had lower cultivability, less ATP and more PHB per cell compared to the beginning of the experiment, and in addition contained more permeabilizated cells and cells that have lost their membrane potential.

Decreased cultivability, but no decline in total cell numbers, indicates that the cells surviving in these oligotrophic conditions transition into a more dormant state. This is already been shown in other experiments in similar oligotrophic conditions (Kell et al., 1998; Oliver, 2005). Both the presence of basalt and flight conditions had a positive effect, lessening the impact of the survival conditions, where 10% of the culture was cultivable with basalt and 50% in flight in contrast to 0.1% in the ground experiment.

The energy status of these cells was also assessed by analyzing the ATP and PHB content, as in CH34 most of its stored energy is in the formation of polyhydroxybuterates (PHB) (Sato et al., 2004; Janssen et al., 2010; Budde et al., 2011). When ATP levels were compared to the start, these were significantly lower and PHB significantly increased compared to the starting conditions. The CH34 cells thus reduce their "immediate operational" energy levels (ATP) but increase their energy storage levels (PHB) when put in these survival conditions. Space flight conditions seem to counteract this decrease in ATP content, while basalt limited the PHB accumulation of the cells.

The drop in cultivability thus coincides with a 3-fold decrease in energy levels (measured ATP), and a 2-fold increase in energy stock levels (PHB) over the 3 months flight experiment. Previous studies show that cells accumulate PHB in nutrient poor environments in mineral water (Kadouri et al., 2005). Although, not investigated here, PHB accumulation could result from metabolic redirecting of proteome or lipid cellular fractions seen in closely related *Ralstonia eutropha* H12 (Brigham et al., 2010; Sharma et al., 2016); cryptic growth as more permeabilizated cells are seen in these conditions (McAlister et al., 2002); usage of leached byproducts of the plastic tubes (Jones et al., 2003) or residual organic fractions still present on the basalt. Other

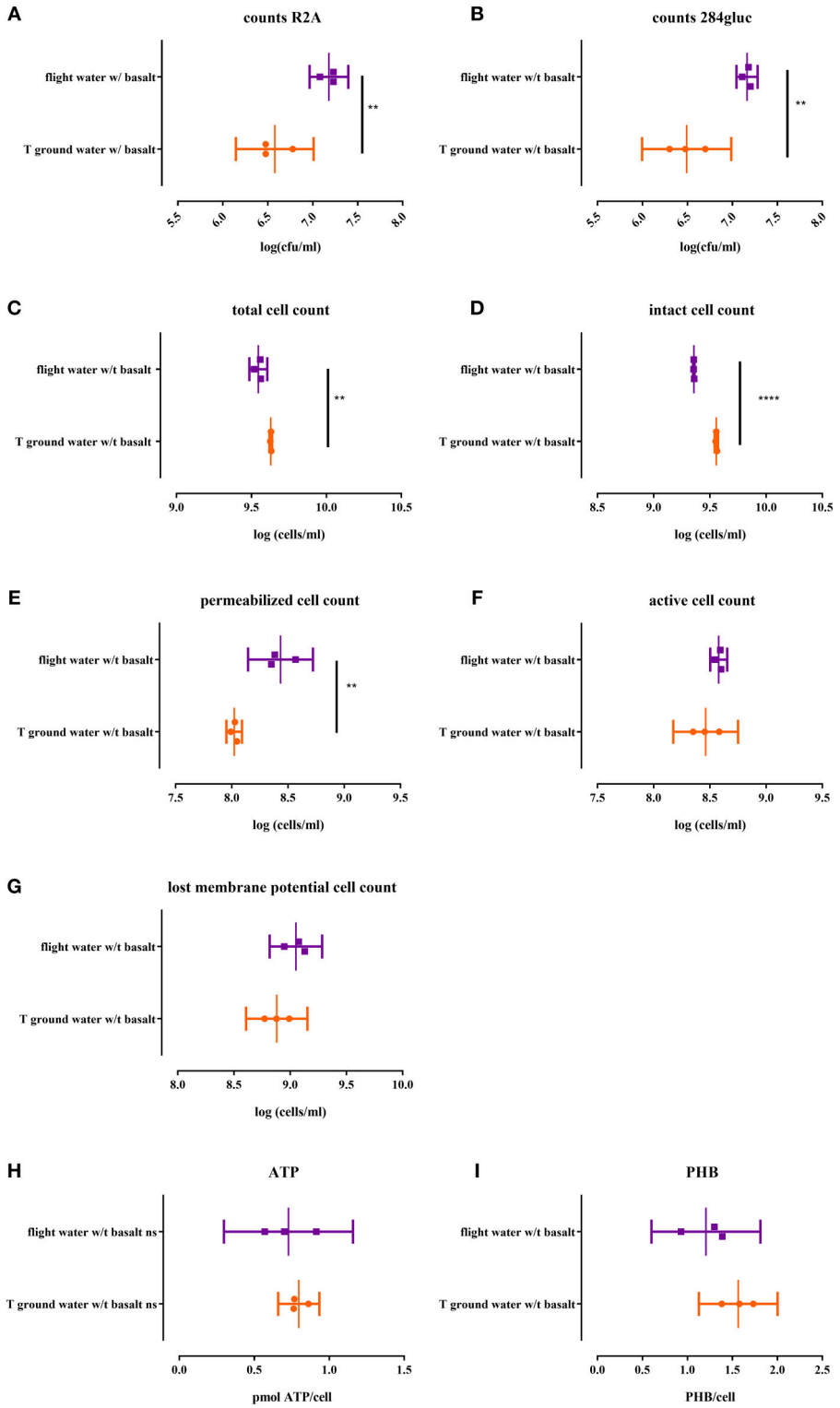

FIGURE 4 | Cell physiology, cultivability ATP and PHB levels of the CH34 biofilm fraction after sonication of both flight and ground samples with basalt, analyzed after the three month flight experiment. All replicates are represented by a dot; the mean is indicated as a line as well as the 95% confidence interval between brackets. For the statistical analysis, one way ANOVA was used with Tukey post testing (alpha = 0.05). Significances are indicated with (*) (with: $^{**}p < 0.01$ and $^{****}p < 0.0001$). *P*-values as well as significance are also reported in **Supplementary Table S2**. Samples were plated on R2A **(A)** and 284 MM agar **(B)** to determine cultivability of CH34 biofilm cells. The total cells number (SG) **(C)** as well as the number of intact cells (SGPI) **(D)**, permeabilizated (SGPI) **(E)**, active (cFDA) **(G)** and cells which have lost their membrane potential [$DIBAC_4(3)$] **(F)** were measured. ATP **(H)** and PHB **(I)** content of the cells was also measured.

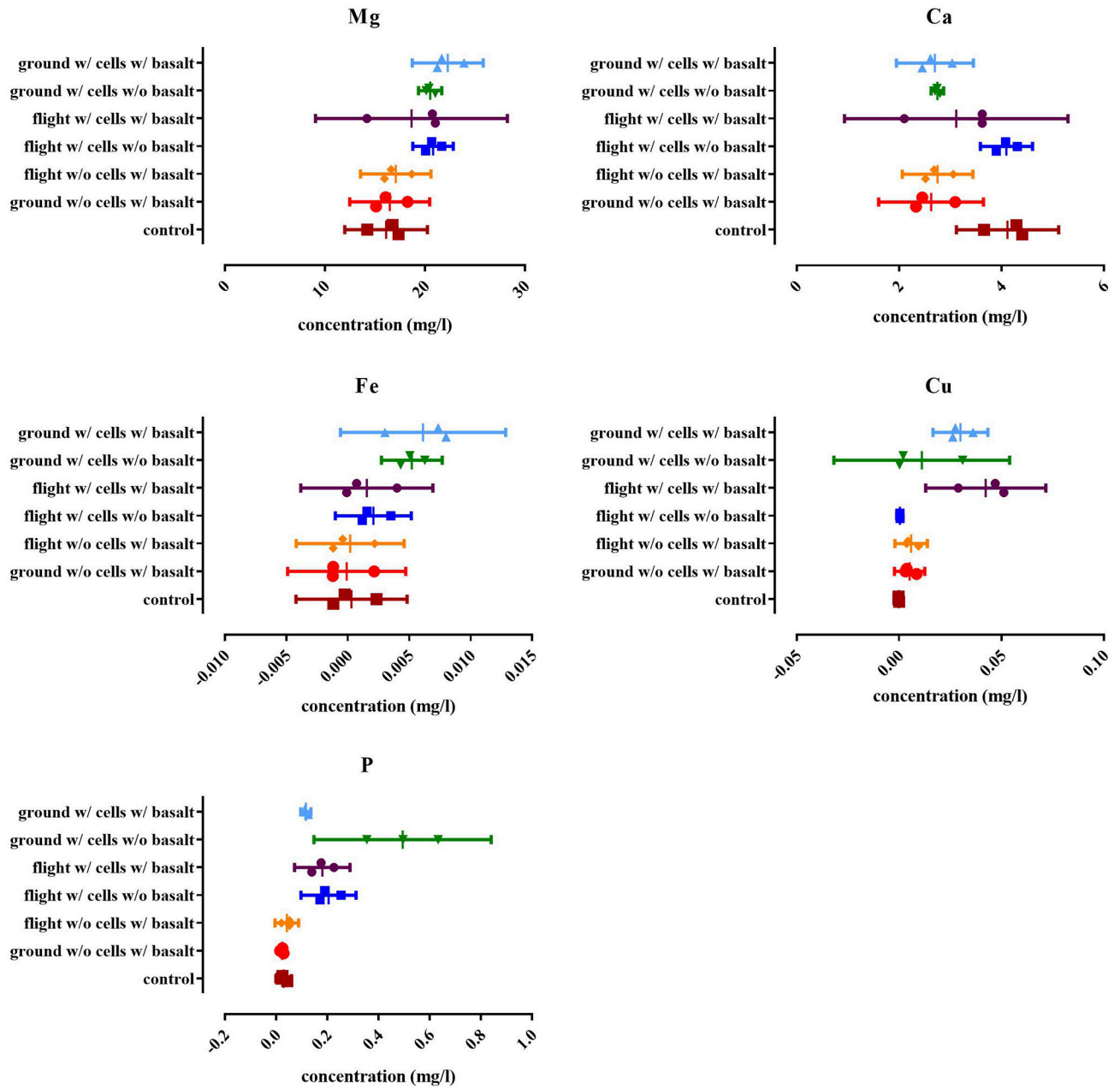

FIGURE 5 | Results of the ICP-OES analysis for the magnesium (Mg), total phosphate (P), calcium (Ca), iron (Fe), and copper (Cu) content expressed as the concentration in the suspension (in mg/l). The "control" is the concentration of the respective elements in the water used at the start of the experiment. All replicates are represented by a dot, the mean is indicated as well as the 95% confidence interval. For the statistical analysis, one way ANOVA was used with Tukey post testing (alpha = 0.05), *p*-values as well as significance are reported in **Supplementary Table S2**.

factors such as exposure to stress conditions (Povolo and Casella, 2000; Rojas et al., 2011) and phosphate limitation (Shang et al., 2003; Budde et al., 2011) can trigger PHB accumulation as well. It has also been shown that PHB utilization during starvation conditions results in metabolic activity and cultivability (James et al., 1999; Trevors, 2011; Najdegerami et al., 2012). PHB accumulation on the other hand can result in loss of cultivability which is also seen in our results (Holmquist and Kjelleberg, 1993).

Flight conditions and basalt had a positive impact on physiology, counteracting some of the detrimental storage effects. Cells in the flight conditions with basalt contained the highest amount of total, intact and active cells while fewer cells lost their membrane potential. In addition, samples containing basalt, both on ground and in flight, contained less cells which were permeabilizated or lost their cell membrane potential and had higher total and intact fractions. In summary, fewer cells lose

their cell membrane potential, more are active and keep a higher ATP level and lower PHB level resulting in higher cultivability. It has been seen before, in other experiments, with actively growing cells in culture medium, that indeed space flight can have a significant impact on physiology, predominately due to microgravity effects. It was shown that bacteria have increased metabolic activity, higher biomass, and produce more secondary metabolites in these conditions allowing growth (Leys et al., 2004; Nickerson et al., 2004; Mastroleo et al., 2009; Taylor, 2015). For cells tested in survival conditions, *Ralstonia pickettii,* starting from a 10^5 cells/ml in water, showed a higher cell break down and autolysis rate in simulated microgravity compared to normal gravity after 14 days in this survival setup (Baker and Leff, 2004).

Space flight conditions have an impact on the bacterial cell physiology, which in turn can have an impact on microbial rock weathering and biofilm formation to maximize survival. Biofilm formation was different in flight and ground conditions, observed using SEM pictures. A clear biofilm was formed in ground conditions but this is not the case in the flight experiment in which the biofilm was shown to be less developed and differently structured. When total cell numbers were determined there was also a significant difference between ground and flight samples indicating that in flight fewer cells were present in the biofilm. This contrary to some papers where biofilm formation increased in space flight conditions (McLean et al., 2001). Cells present in the biofilm during flight also show different physiology traits, as more were permeabilizated, less intact, but more cultivable. In biofilm cells, ATP content or PHB content did not differ between ground and flight samples. Flight thus impacts the number of cells which transition into the biofilm state which increases cultivability but more cells are permeabilizated and less are intact. It was also observed that cells in the biofilm had significant less PHB then cells in suspension, indicating that part of the PHB may have been directed toward biofilm formation. It was already reported that PHB utilization could promote colonization and biofilm formation in nutrient poor environments, as it promotes motility and viability of these cells (Tribelli and López, 2011)

For the elemental analysis, basalt had an effect on calcium removal from the water, irrespectively of the presence of cells and both in ground and flight experiments, probably due to complexation on basalt (Stockmann et al., 2011). Also when adding cells, calcium is removed from the water even in samples without basalt, indicating that cells can take up calcium in this condition. This was also observed for phosphate as concentrations were lower, both in ground and flight experiments, with basalt, while without basalt more phosphate was remaining in suspension. Cells released more magnesium and iron with and without basalt in the ground samples while water from the flight experiment contained less of these elements, showing that cells keep more of these elements intracellularly in these conditions, irrespective of the presence of basalt. Copper is released from the basalt in the presence of cells both in flight and ground, thus cells having a positive impact on copper release from basalt.

Our results indicate that in general flight conditions as well as basalt had a positive effect on survival, counteracting some of the detrimental effects of inoculum storage in water. Cells were more cultivable, contained more ATP and more cells were present which were intact and active while fewer cells lost their membrane potential. This changes cellular physiology. Cells will thereby not as easily transition into a more "dormant" state and start forming a biofilm on basalt. With this experiment, we provide for the first time results for the combined effect of space flight conditions and the presence of basalt on survival in water. We could also show that in space cells form slightly less biofilm and so that there is an impact of space flight conditions on microbe-mineral interactions. As these experiments were performed with limited amount of samples and ground and flight samples were prepared separately, batch specific changes may have occurred. It is clear however that this preliminary experiment is only the very first step and much more is still to be tested and learned. Results presented here are preliminary results and more (long lasting) experiments are needed to draw definite conclusions. Nevertheless, this research may hopefully open the door for future studies and potentially applications of microbe-mineral interactions in space and even on Earth.

AUTHOR CONTRIBUTIONS

BB performed the analysis after flight except for ICP-OES and radiation sensor read-out. ICP-OES was performed by NN and CC. IC prepared the flight setup and prepared the package before send-off. OV provided the radiation sensors included in the flight setup as well as read-out and data analysis. VI was responsible for incorporating the flight setup within Russian spaceflight experiment "MIKROB." BB, IC, OV, NN, VI, CC, RV, NB, and NL helped with data interpretation, scientific guidance, and preparation of the manuscript.

ACKNOWLEDGMENTS

This work was supported by the European Space Agency (ESA-PRODEX), Belgian Science Policy (BELSPO) through the E-GEM/BIOROCK project and the Inter-University Attraction Pole (IUAP) "μ-manager" funded by the Belgian Science Policy (BE, 305 P7/25)(BB). We thank Kai Finster and CC for the coordination of the BIOROCK project, and VI for incorporating biomaterial within Russian spaceflight experiment "MIKROB." The authors would also like to thank the people of the microbiology unit at SCK-CEN and the IMBP institute for all the support and help during pre-and post-flight analysis and preparations.

SUPPLEMENTARY MATERIAL

The Supplementary Material for this article can be found online at: http://journal.frontiersin.org/article/10.3389/fmicb.2017.00671/full#supplementary-material

Supplementary Figure S1 | Scanning Electron Microscopy (SEM) image of basalt after preflight preparatory experiment with the same setup as the flight experiment.

Supplementary Table S1 | Wavelengths used for ICP-OES analysis.

Supplementary Table S2 | Statistical analysis of the planktonic, biofilm fractions as well as for the ICP-OES analysis.

REFERENCES

Anand, M., Crawford, I. A., Balat-Pichelin, M., Abanades, S., Van Westrenen, W., Péraudeau, G., et al. (2012). A brief review of chemical and mineralogical resources on the Moon and likely initial *in situ* resource utilization (ISRU) applications. *Planet. Space Sci.* 74, 42–48. doi: 10.1016/j.pss.2012.08.012

Baker, P. W., and Leff, L. (2004). The effect of simulated microgravity on bacteria from the Mir space station. *Microgravity Sci. Technol.* 15, 35–41. doi: 10.1007/BF02870950

Berney, M., Hammes, F., Bosshard, F., Weilenmann, H.-U., and Egli, T. (2007). Assessment and interpretation of bacterial viability by using the LIVE/DEAD BacLight Kit in combination with flow cytometry. *Appl. Environ. Microbiol.* 73, 3283–3290. doi: 10.1128/AEM.02750-06

Berney, M., Vital, M., Hülshoff, I., Weilenmann, H.-U., Egli, T., and Hammes, F. (2008). Rapid, cultivation-independent assessment of microbial viability in drinking water. *Water Res.* 42, 4010–4018. doi: 10.1016/j.watres.2008.07.017

Brigham, C. J., Budde, C. F., Holder, J. W., Zeng, Q., Mahan, A. E., Rha, C., et al. (2010). Elucidation of β-oxidation pathways in *Ralstonia eutropha* H16 by examination of global gene expression. *J. Bacteriol.* 192, 5454–5464. doi: 10.1128/JB.00493-10

Brown, R. B., Klaus, D., and Todd, P. (2002). Effects of space flight, clinorotation, and centrifugation on the substrate utilization efficiency of *E. coli*. *Microgravity Sci. Technol.* 13, 24–29. doi: 10.1007/BF02881678

Bryce, C. C., Le Bihan, T., Martin, S. F., Harrison, J. P., Bush, T., Spears, B., et al. (2016). Rock geochemistry induces stress and starvation responses in the bacterial proteome. *Environ. Microbiol.* 18, 1110–1121. doi: 10.1111/1462-2920.13093

Budde, C. F., Riedel, S. L., Willis, L. B., Rha, C., and Sinskey, A. J. (2011). Production of poly (3-hydroxybutyrate-co-3-hydroxyhexanoate) from plant oil by engineered *Ralstonia eutropha* strains. *Appl. Environ. Microbiol.* 77, 2847–2854. doi: 10.1128/AEM.02429-10

Buysschaert, B., Byloos, B., Leys, N., Van Houdt, R., and Boon, N. (2016). Reevaluating multicolor flow cytometry to assess microbial viability. *Appl. Microbiol. Biotechnol.* 100, 9037–9051. doi: 10.1007/s00253-016-7837-5

Cockell, C. S. (2010). Geomicrobiology beyond earth: microbe-mineral interactions in space exploration and settlement. *Trends Microbiol.* 18, 308–314. doi: 10.1016/j.tim.2010.03.005

Degelau, A., Scheper, T., Bailey, J., and Guske, C. (1995). Fluorometric measurement of poly-β hydroxybutyrate in *Alcaligenes eutrophus* by flow cytometry and spectrofluorometry. *Appl. Microbiol. Biotechnol.* 42, 653–657. doi: 10.1007/BF00171939

Dong, H. (2010). Mineral-microbe interactions: a review. *Front. Earth Sci. China* 4, 127–147. doi: 10.1007/s11707-010-0022-8

Gadd, G. M. (2010). Metals, minerals and microbes: geomicrobiology and bioremediation. *Microbiology* 156, 609–643. doi: 10.1099/mic.0.037143-0

Goossens, O., Vanhavere, F., Leys, N., De Boever, P., O'sullivan, D., Zhou, D., et al. (2006). Radiation dosimetry for microbial experiments in the International Space Station using different etched track and luminescent detectors. *Radiat. Prot. Dosimetry* 120, 433–437. doi: 10.1093/rpd/nci652

Greenspan, P., and Fowler, S. D. (1985). Spectrofluorometric studies of the lipid probe, nile red. *J. Lipid Res.* 26, 781–789.

Harrison, J., Turner, R., Marques, L., and Ceri, H. (2005). A new understanding of these microbial communities is driving a revolution that may transform the science of microbiology. *Am. Sci.* 93, 508–515. doi: 10.1511/2005.56.977

Holmquist, L., and Kjelleberg, S. (1993). Changes in viability, respiratory activity and morphology of the marine *Vibrio* sp. strain S14 during starvation of individual nutrients and subsequent recovery. *FEMS Microbiol. Ecol.* 12, 215–223. doi: 10.1111/j.1574-6941.1993.tb00034.x

Horneck, G., Klaus, D. M., and Mancinelli, R. L. (2010). Space microbiology. *Microbiol. Mol. Biol. Rev.* 74, 121–156. doi: 10.1128/MMBR.00016-09

James, B. W., Mauchline, W. S., Dennis, P. J., Keevil, C. W., and Wait, R. (1999). Poly-3-hydroxybutyrate in *Legionella pneumophila*, an energy source for survival in low-nutrient environments. *Appl. Environ. Microbiol.* 65, 822–827.

Jánosi, I. M., Czirók, A., Silhavy, D., and Holczinger, A. (2002). Is bioconvection enhancing bacterial growth in quiescent environments? *Environ. Microbiol.* 4, 525–531. doi: 10.1046/j.1462-2920.2002.00328.x

Janssen, P. J., Van Houdt, R., Moors, H., Monsieurs, P., Morin, N., Michaux, A., et al. (2010). The complete genome sequence of *Cupriavidus metallidurans* strain CH34, a master survivalist in harsh and anthropogenic environments. *PLoS ONE* 5:e10433. doi: 10.1371/journal.pone.0010433

Johnson, I., and Spence, M. (2010). *The Molecular Probes Handbook: A Guide to Fluorescent Probes and Labeling Technologies.* Carlsbad, CA: Life Technologies Corporation.

Jones, R. M., Britt-Compton, B., and Williams, P. A. (2003). The naphthalene catabolic (nag) genes of *Ralstonia* sp. strain U2 are an operon that is regulated by NagR, a LysR-type transcriptional regulator. *J. Bacteriol.* 185, 5847–5853. doi: 10.1128/JB.185.19.5847-5853.2003

Kadouri, D., Jurkevitch, E., Okon, Y., and Castro-Sowinski, S. (2005). Ecological and agricultural significance of bacterial polyhydroxyalkanoates. *Crit. Rev. Microbiol.* 31, 55–67. doi: 10.1080/10408410590899228

Kell, D. B., Kaprelyants, A. S., Weichart, D. H., Harwood, C. R., and Barer, M. R. (1998). Viability and activity in readily culturable bacteria: a review and discussion of the practical issues. *Antonie van Leeuwenhoek* 73, 169–187. doi: 10.1023/A:1000664013047

Kim, W., Tengra, F. K., Young, Z., Shong, J., Marchand, N., Chan, H. K., et al. (2013). Spaceflight promotes biofilm formation by *Pseudomonas aeruginosa*. *PLoS ONE* 8:e62437. doi: 10.1371/journal.pone.0076106

Kobayashi, H., Oethinger, M., Tuohy, M. J., Procop, G. W., and Bauer, T. W. (2009). Improved detection of biofilm-formative bacteria by vortexing and sonication: a pilot study. *Clin. Orthop. Relat. Res.* 467, 1360–1364. doi: 10.1007/s11999-008-0609-5

Leroy, B., Rosier, C., Erculisse, V., Leys, N., Mergeay, M., and Wattiez, R. (2010). Differential proteomic analysis using isotope-coded protein-labeling strategies: comparison, improvements and application to simulated microgravity effect on *Cupriavidus metallidurans* CH34. *Proteomics* 10, 2281–2291. doi: 10.1002/pmic.200900286

Leys, N., Hendrickx, L., De Boever, P., Baatout, S., and Mergeay, M. (2004). Space flight effects on bacterial physiology. *J. Biol. Regul. Homeost. Agents* 18, 193–199.

Leys, N., Baatout, S., Rosier, C., Dams, A., S'heeren, C., Wattiez, R., et al. (2009). The response of *Cupriavidus metallidurans* CH34 to spaceflight in the international space station. *Antonie Van Leeuwenhoek* 96, 227–245. doi: 10.1007/s10482-009-9360-5

Mastroleo, F., Van Houdt, R., Leroy, B., Benotmane, M. A., Janssen, A., Mergeay, M., et al. (2009). Experimental design and environmental parameters affect *Rhodospirillum rubrum* S1H response to space flight. *ISME J.* 3, 1402–1419. doi: 10.1038/ismej.2009.74

McAlister, M., Kulakov, L., O'hanlon, J., Larkin, M., and Ogden, K. L. (2002). Survival and nutritional requirements of three bacteria isolated from ultrapure water. *J. Ind. Microbiol. Biotechnol.* 29, 75–82. doi: 10.1038/sj.jim.7000273

McLean, R. J., Cassanto, J. M., Barnes, M. B., and Koo, J. H. (2001). Bacterial biofilm formation under microgravity conditions. *FEMS Microbiol. Lett.* 195, 115–119. doi: 10.1111/j.1574-6968.2001.tb10507.x

Mergeay, M., Nies, D., Schlegel, H., Gerits, J., Charles, P., and Van Gijsegem, F. (1985). *Alcaligenes eutrophus* CH34 is a facultative chemolithotroph with plasmid-bound resistance to heavy metals. *J. Bacteriol.* 162, 328–334.

Muller, S., and Nebe-Von-Caron, G. (2010). Functional single-cell analyses: flow cytometry and cell sorting of microbial populations and communities. *FEMS Microbiol. Rev.* 34, 554–587. doi: 10.1111/j.1574-6976.2010.00214.x

Najdegerami, E. H., Tran, T. N., Defoirdt, T., Marzorati, M., Sorgeloos, P., Boon, N., et al. (2012). Effects of poly-β-hydroxybutyrate (PHB) on Siberian sturgeon (*Acipenser baerii*) fingerlings performance and its gastrointestinal tract microbial community. *FEMS Microbiol. Ecol.* 79, 25–33. doi: 10.1111/j.1574-6941.2011.01194.x

Nickerson, C. A., Ott, C. M., Wilson, J. W., Ramamurthy, R., and Pierson, D. L. (2004). Microbial responses to microgravity and other low-shear environments. *Microbiol. Mol. Biol. Rev.* 68, 345–361. doi: 10.1128/MMBR.68.2.345-361.2004

Oliver, J. D. (2005). The viable but nonculturable state in bacteria. *J. Microbiol.* 43, 93–100.

Olsson-Francis, K., VAN Houdt, R., Mergeay, M., Leys, N., and Cockell, C. S. (2010). Microarray analysis of a microbe-mineral interaction. *Geobiology* 8, 446–456. doi: 10.1111/j.1472-4669.2010.00253.x

Povolo, S., and Casella, S. (2000). A critical role for aniA in energy-carbon flux and symbiotic nitrogen fixation in *Sinorhizobium meliloti*. *Arch. Microbiol.* 174, 42–49. doi: 10.1007/s002030000171

Reasoner, D., and Geldreich, E. (1985). A new medium for the enumeration and subculture of bacteria from potable water. *Appl. Environ. Microbiol.* 49, 1–7.

Rojas, L. A., Yáñez, C., González, M., Lobos, S., Smalla, K., and Seeger, M. (2011). Characterization of the metabolically modified heavy metal-resistant *Cupriavidus metallidurans* strain MSR33 generated for mercury bioremediation. *PLoS ONE* 6:e17555. doi: 10.1371/journal.pone.0017555

Sato, Y., Nishihara, H., Yoshida, M., Watanabe, M., Rondal, J. D., and Ohta, H. (2004). Occurrence of hydrogen-oxidizing *Ralstonia* species as primary microorganisms in the Mt. Pinatubo volcanic mudflow deposits. *Soil Sci. Plant Nutr.* 50, 855–861. doi: 10.1080/00380768.2004.10408546

Shang, L., Jiang, M., and Chang, H. N. (2003). Poly (3-hydroxybutyrate) synthesis in fed-batch culture of *Ralstonia eutropha* with phosphate limitation under different glucose concentrations. *Biotechnol. Lett.* 25, 1415–1419. doi: 10.1023/A:1025047410699

Sharma, P. K., Fu, J., Spicer, V., Krokhin, O. V., Cicek, N., Sparling, R., et al. (2016). Global changes in the proteome of *Cupriavidus necator* H16 during poly-(3-hydroxybutyrate) synthesis from various biodiesel by-product substrates. *AMB Expr.* 6, 36. doi: 10.1186/s13568-016-0206-z

SLMB (2012). *Determining the Total Cell Count and Ratios of High and Low Nucleic Acid Content Cells in Freshwater Using Flow Cytometry*. Bern: Federal Office of Public Health.

Stockmann, G. J., Wolff-Boenisch, D., Gislason, S. R., and Oelkers, E. H. (2011). Do carbonate precipitates affect dissolution kinetics? 1: basaltic glass. *Chem. Geol.* 284, 306–316. doi: 10.1016/j.chemgeo.2011.03.010

Sträuber, H., and Müller, S. (2010). Viability states of bacteria specific mechanisms of selected probes. *Cytometry Part A* 77, 623–634. doi: 10.1002/cyto.a.20920

Taylor, P. W. (2015). Impact of space flight on bacterial virulence and antibiotic susceptibility. *Infect. Drug Resist.* 8:249. doi: 10.2147/IDR.S67275

Trevors, J. (2011). Viable but non-culturable (VBNC) bacteria: Gene expression in planktonic and biofilm cells. *J. Microbiol. Methods* 86, 266–273. doi: 10.1016/j.mimet.2011.04.018

Tribelli, P. M., and López, N. I. (2011). Poly(3-hydroxybutyrate) influences biofilm formation and motility in the novel Antarctic species *Pseudomonas extremaustralis* under cold conditions. *Extremophiles* 15, 541–547. doi: 10.1007/s00792-011-0384-1

Ubaldini, S., Veglio, F., Beolchini, F., Toro, L., and Abbruzzese, C. (2000). Gold recovery from a refractory pyrrhotite ore by biooxidation. *Int. J. Miner. Process.* 60, 247–262. doi: 10.1016/S0301-7516(00)00019-3

Van Nevel, S., Koetzsch, S., Weilenmann, H.-U., Boon, N., and Hammes, F. (2013). Routine bacterial analysis with automated flow cytometry. *J. Microbiol. Methods* 94, 73–76. doi: 10.1016/j.mimet.2013.05.007

Vanhavere, F., Genicot, J. L., O'sullivan, D., Zhou, D., Spurný, F., Jadrníčková, I., et al. (2008). DOsimetry of BIological EXperiments in SPace (DOBIES) with luminescence (OSL and TL) and track etch detectors. *Radiat. Meas.* 43, 694–697. doi: 10.1016/j.radmeas.2007.12.002

Veal, D., Deere, D., Ferrari, B., Piper, J., and Attfield, P. (2000). Fluorescence staining and flow cytometry for monitoring microbial cells. *J. Methods* 243, 191–210. doi: 10.1016/S0022-1759(00)00234-9

Conflict of Interest Statement: The authors declare that the research was conducted in the absence of any commercial or financial relationships that could be construed as a potential conflict of interest.

Advantages of publishing in Frontiers

OPEN ACCESS
Articles are free to read for greatest visibility and readership

FAST PUBLICATION
Around 90 days from submission to decision

HIGH QUALITY PEER-REVIEW
Rigorous, collaborative, and constructive peer-review

TRANSPARENT PEER-REVIEW
Editors and reviewers acknowledged by name on published articles

Frontiers
Avenue du Tribunal-Fédéral 34
1005 Lausanne | Switzerland

Visit us: www.frontiersin.org
Contact us: info@frontiersin.org | +41 21 510 17 00

REPRODUCIBILITY OF RESEARCH
Support open data and methods to enhance research reproducibility

DIGITAL PUBLISHING
Articles designed for optimal readership across devices

FOLLOW US
@frontiersin

IMPACT METRICS
Advanced article metrics track visibility across digital media

EXTENSIVE PROMOTION
Marketing and promotion of impactful research

LOOP RESEARCH NETWORK
Our network increases your article's readership